A thesis entitled

NATURAL AND ARTIFICIAL DIAGENESIS OF COAL MACERALS

by

JAMES ALLAN, B.Sc., M.Sc.

Submitted to the University of Newcastle upon Tyne

for the degree of Doctor of Philosophy.

Organic Geochemistry Unit,
Department of Geology.

March, 1975.

To:

Christine

Anna

and Jane

Contents

Abstract

Non-condensed structures in vitrinites and sporinites, prepared from high- to medium-volatile bituminous coals, have been studied both by extraction and degradation. Additionally, seven concentrates of alginites, resinites and cutinite were studied.

Analyses of extractable vitrinite and sporinite alkanes showed that their yields increased markedly between 83.3% and 83.9% $C_{vitrinite}$ (d.a.f.), and reached maximum values at 85.4% $C_{vitrinite}$ (d.a.f.). n-Alkane distributions showed increasingly lower average molecular weights with increasing rank, and the CPI's (n-C_{23} to n-C_{33}) decreased to almost unity at 83.9% $C_{vitrinite}$ (d.a.f.). This occurred while individual homologues progressively increased in concentration. Pyrolytic and oxidative degradation of the extracted and saponified maceral residues showed that n-alkyl chains with more than 20 carbon atoms, attached peripherally to the "kerogens", generally had even-dominated distributions. Thus, during natural diagenesis of these materials, the generation of long-chain n-alkanes showing an even-carbon-number preference may be the cause of the observed decreasing CPI values.

The branched/cyclic alkanes of vitrinites and sporinites also showed progressive distributional changes with increasing rank, manifested by relative decreases in the yields of polycycloalkanes and increases in the yields of lower molecular weight constituents, particularly the C_{14} to C_{20} acyclic isoprenoid alkanes.

Hopane-type triterpanes with 27, 29, 30 and 31 carbon atoms have been identified among the higher molecular weight constituents, and gc retention data suggest a remarkable constancy in the distributions of these compounds between the two macerals. Pyrolysis showed that further quantities of these compounds could be produced after extraction of the macerals.

The extractable alkanes of alginites and cutinite were also composed of complex mixtures of normal and branched/cyclic alkanes, and iso- and anteiso-alkanes were identified in one alginite fraction. Resinite alkanes were unique in type, showing restricted gc distributions confined generally to the sesqui- and diterpane regions.

Small yields of carboxylic acids were obtained by saponification of both extracts and residues. Fatty acids from all the macerals except resinite contained palmitic and stearic acids as prominent constituents, and, in general, the distributions of fatty acids could not be related to those of the alkanes obtained by extraction or pyrolysis. Carboxylic acids from resinites were again unique in type, and analysis of these compounds from one of the resinites has shown that they consist of diterpenoid acids, including agathic acid, pimaric acid and isomers, and dehydroabietic acid.

Straight-chain, saturated α, ω-dicarboxylic acids, with up to 28 carbon atoms, were found only in alginite and cutinite. These macerals were deposited in more fresh-water environments than vitrinite and sporinite, and the presence of dicarboxylic acids in fossil lipid mixtures may be indicative of an early phase of aerobic decomposition during diagenesis.

Oxidative degradation of extracted and saponified sporinite, alginite and cutinite residues showed that polymethylene chains in the "kerogens" generally contained up to 15 carbon atoms; although chains with up to 24 carbon atoms were detected. In sporinites, the amounts decreased with increasing rank, and were scarcely detectable above *ca.* 85% $C_{vitrinite}$ (d.a.f.). Loss of these linear structures at higher ranks may be associated with the approaching coalification break of sporinites in medium- to low-volatile bituminous coals.

Acknowledgements

I wish to thank Dr. A.G. Douglas for his guidance, interest and encouragement throughout this project, and for his advice during the writing of this thesis. In a similar capacity, I am indebted to Dr. D.G. Murchison for his assistance in the field of coal petrology, and also for his critical appraisal of the thesis.

I also wish to thank Dr. B.S. Cooper for the many hours spent in discussions developing concepts and ideas which arose during the course of this work, and for his enthusiastic interest in the project as a whole.

I wish to acknowledge the generous assistance of the many members of the National Coal Board who arranged for the collection of many of my samples, and also to thank Dr. I. Rolfe and Dr. B. van der Weide for providing samples of torbanite.

I am also indebted to Dr. J.M. Jones and Mr. E. Scott for unveiling the mysteries of reflectance microscopy, Mr. F. Goodarzi and Mr. P.J. Grantham whose respective fields of work have contributed towards a better understanding of the results of this project, and to Mrs. A. Summerbell, Mr. K. Hall, Miss J. Gilliland and Mr. C. Laidler for their many and varied technical skills and assistance throughout the course of my work.

I would like to thank Dr. D. Hunneman, Dr. W. Scott and Dr. W. Henderson for their help in obtaining mass spectra of many of my samples, and particularly Dr. G. Eglinton for making available to me the mass spectrometric facilities in the Organic Geochemistry Unit at the University of Bristol.

Finally, I wish to thank all those other members of the Organic Geochemistry Unit, past and present, who have given help and advice at all times.

The work was supported by a maintenance grant from the Natural Environment Research Council.

Introduction

There have been two major coal-forming periods in the history of the Earth since the development of an extensive land flora. The first and more extensive period began in the Carboniferous and terminated during Permian times. At the present time Permo-Carboniferous coals are dominantly bituminous to anthracitic in rank. A subordinate period of coal formation occurred during Eocene to Pliocene times, and these deposits are generally lignites to brown coals at the present time. Coals are known to occur in all geological periods from the Devonian to the Pleistocene however, and their geographical distribution is reviewed by Francis (1961).

It is widely accepted that there is a continuous series of materials extending from peats to anthracites via brown and bituminous coals. Chemical progression along the series is marked by, among other things, increasing carbon contents and increasing calorific values. This process of coalification is basically controlled by the geological factors of time, temperature and pressure, although the relative importance of these is subject to dispute. However the maturation of sedimentary kerogens is generally believed to be temperature-rather than pressure-controlled (Philippi, 1969), and it seems not unreasonable to suppose that coalification is similarly controlled.

Many of the world's major coalfields were formed by successive peat accumulations in paralic basins. Evidence of palaeogeography is provided by transgressive marine sediments intercalated in coal measures. However paralic basins are not prerequisites for the eventual formation of coal. Many environments exist where peat can accumulate, but preservation is perhaps more important. Inland limnic basins are equally suitable, provided that subsidence and sedimentation operate together to ensure burial of peat layers by impervious layers of sediment. Prolonged aerial exposure leads to oxidation, decomposition and dispersal of organic debris.

Most coal seams have accumulated *in situ* and the coal is often a member of a cyclothemic series of sediments. They may be underlain by seat-earths in which roots are often well preserved, and overlain by roof-shales rich in fossilized plant structures. Sandstones may separate successive roof-shales and seat-earths but where subsidence is sufficiently extensive clear-water limestones may be developed.

Plant debris undergoes microbiological degradation in peats. The degree of degradation is controlled by the nature and level of the swamp waters. The more oxidative the environment the greater the decomposition. Fungal remains in coals testify to aerobic conditions. However the morphological humification of cellular structures indicate basically stagnant conditions. Once an accumulated peat layer is inundated and sealed under a layer of sediment, microbiological activity will rapidly cease and the peat becomes subject to geochemical alteration.

Bituminous coal is composed of a variety of microscopically-identifiable components termed macerals, which occur in definite interassociations termed microlithotypes. The macroscopically-recognizable constituents of banded coals are called lithotypes. These terms are based on the Stopes-Heerlan classification adopted in Europe (ICCP, 1963).

Macerals are grouped into three types: vitrinite, exinite and inertinite, each of which contains more than one constituent. Vitrinite is the most abundant component of most banded authochthonous coals, and is derived from woody tissues. Two types are distinguished. Collinite is botanically structureless while telinite shows variably-preserved cellular structure. Cell cavities are filled often with collinite, occasionally with resinite. ~~Collinite~~ Telinite is thought to have formed by mummification of wood under stagnant conditions. The structureless form of ~~telinite~~ collinite has led to the suggestion that it may be formed from dopplerite or some gelification of decayed wood. The fact that ~~telinite~~ collinite can occur as fissure infills certainly suggests some period of at least semifluidity.

The origin of vitrinite has been variously ascribed to cellulose and lignin, but in reviewing the subject van Krevelen (1963) suggests that attempting a distinction may be fruitless as both lignins and cellulose, with protein, are each capable of producing humic degradation products under suitable conditions. In a later review article Cooper and Murchison (1969) state that vitrinite is the product of degradation of lignin, cellulose and nitrogen-containing compounds.

A number of macerals, known as fusinite, semifusinite, micrinite and sclerotinite, are classified in the inertinite group because of their inert behaviour on heating. They exhibit higher reflectivity than a corresponding vitrinite. Fusinite and semifusinite are undoubtedly derived from wood as cellular structures are preserved. Unlike vitrinite however cell cavities are either empty or filled with mineral matter. Fusinite is formed under much drier conditions than vitrinite, and is considered to have been formed at a relatively higher temperature with a concomitantly higher carbon content. Semifusinite appears intermediate in appearance between vitrinite and fusinite, suggesting that the latter two macerals are the end members of a continuous series of preservational conditions.

Micrinite is generally considered to be of aerobic origin, and despite lack of botanical structure it has been considered to be derived from woody material which has undergone extensive degradation (van Krevelen, 1961). Stach (1968) considers massive micrinite to be inert detrital plant material while granular micrinite, through common association with microspores, may be derived from protoplasm. Sclerotinite is a minor coal constituent and is of fungal origin.

The exinite group of macerals has four constituents: sporinite, cutinite, resinite, and alginite, of self-evident derivation. They all exhibit lower reflectivity than a corresponding vitrinite. On carbonisation they give high tar yields and leave little coke. Sporinite is generally the most abundant exinite in authochthonous coals. Although flattened parallel to the bedding the resilience of spore exines often leads to good morphological preservation, making these macerals valuable in stratigraphic correlations of coals and sediments. Whole spore assemblages can be distinctive, and have proved valuable in palaeoecological studies (Smith, 1962). Cutinite and resinite are generally minor constituents of coals, but accumulations of cuticles are known, producing the foliaceous so-called paper coals. Alginite is unusual in authochthonous coals but can be concentrated in drift deposits of torbanite (boghead coal), where it is often associated with other detrital vegetable and mineral matter. Exinites are derived from aliphatic-rich plant constituents and hence have a higher hydrogen content than other associated macerals. In industrial carbonisation processes they are the major contributors to tar and gas production.

The respective macerals are quite distinctive in bituminous coals, but as coalification advances through to anthracite they become more similar to each other in their optical, and presumably chemical, properties as individual morphological identity is lost.

Distinctive associations of macerals can be recognized in the microscopic examination of banded bituminous coals. By definition these microlithotypes must occur in bands of at least 50 microns width (ICCP, 1963). Vitrite, fusite and sporite are monomaceralic microlithotypes, classified on the basis of $\geq$ 95% purity of their respective macerals. Clarite (vitrinite + exinite), durite (inertinite + exinite) and vitrinertite (vitrinite + inertinite) consist of at least 95% of two macerals, the proportion of each being greater than that of other constituents. Clarodurite and duroclarite are microlithotypes in which components of all three maceral groups occur in greater than 5% amounts. The distinction between the two is dependent on whether vitrinite exceeds inertinite or *vice versa*.

Microlithotypes are finally grouped into four lithotypes, which are the visible constituents of coal. They are vitrain, fusain, clarain and durain. Vitrain is black, hard and lustrous, clean to the touch, and occurs in bands and lenses. Fusain on the other hand is often very friable and usually occurs in lensoid form. It resembles charcoal in appearance. Clarain is also black and shiny but contains very fine dull striations by which it is distinguished from vitrain. Durain is often mat black and very hard, and resembles carbonaceous shale. This lithotype generally has a higher mineral matter content than the others and can grade laterally into cannel or boghead coals, or carbonaceous shale.

The diagenesis of coals is called coalification. Carbon, hydrogen and oxygen are basic elements of all living organisms, and concomitantly of coal. Nitrogen and sulphur together generally account for no more than 2% of most coals. The major effect of coalification is an increase of carbon content at the expense of all other elements, while the main products are water, methane and carbon dioxide. The atomic H/C vs. O/C diagram, introduced by van Krevelen (1950), presents coalification in a graphical manner. The above atomic ratios of vitrinites of increasing rank produce a curving line trending towards the origin of the graph, the so-called vitrinisation band. The course of vitrinisation involves initially the basic chemical process of dehydration, followed by decarboxylation and demethanation. Compilations of data of all macerals allow each group to be plotted on coalification diagrams, thus clearly demonstrating the convergent compositions of individual types as coalification advances (Dormans *et al.*, 1957; van Krevelen, 1961, 1963).

A variety of other parameters are employed, other than elemental compositions, to delineate rank. They include moisture content, volatile matter content, calorific value and reflectance. These are generally applied to vitrite or vitrinite because the wide occurrence of this material makes it useful for correlation purposes. The optimum rank ranges for the use of these parameters have been outlined by Teichmuller and Teichmuller (1968). Reflectance is useful in its own right as the technique may be applied to vitrinite particles which occur in a wide variety of sediments other than coal. As organic matter is a very sensitive indicator of geothermal conditions, observable changes occur in the reflectance of vitrinite before inorganic matter shows any diagenetic alteration.

It has long been established that coal progressively increases in rank with depth in a given vertical profile (Hilt's Law), unless local igneous effects have been operative. The agents responsible are temperature, pressure and geological time. Maximum palaeotemperatures and the time-span of the heating are considered of prime importance in the maturation of all sedimentary organic matter, and the inter-relationship of rank with time and temperature has been presented graphically by Karweil (1955). The effect of overburden or tectonic pressure is considered to be relatively unimportant in promoting chemical changes, but may contribute to the organisation of a layered structure with coalification.

Coal is a chemically-complex heterogeneous material and a wide variety of scientific techniques have been employed to elucidate structural parameters and the changes which occur during coalification. The majority of such work has been done on vitrinite because of the ease of obtaining high purity concentrates.

Dryden (1963) has comprehensively reviewed the qualitative and quantitative results of many chemical and physical investigations of the macerals, and combined the data into numerical parameters with which any proposed bituminous coal structure must comply. Dryden tabulates carbon content, volatile matter, hydrogen distributions, aromatic carbon distributions, aromatic nuclei configurations, oxygen distributions, free radical contents and aromaticities for two vitrinites of 82.5 and 90.0% C(d.a.f), respectively. Exinite and micrinite data, where known, are correlated with vitrinite.

Given (1960) proposed a dihydroanthracene-based structure for a vitrinite of 82% C, with aromatic nuclei linked essentially by single methylene bridges. This was later modified by replacing dihydroanthracene with dihydrophenanthrene structures (Given, 1961), because NMR investigations of vacuum distillates of coals failed to indicate isolated methylene bridges in the structures (Brown *et al.*, 1960; Brown & Ladner, 1960). Earlier, Montgomery *et al.* (1956), had noted a predominance of phenanthrene over anthracene nuclei in coal oxidation products.

The three-dimensional complexity of Given's structural model readily explains why coal shows a disordered structure, but it can only be regarded as representing an average molecular unit because coal contains significant proportions of both smaller and larger condensed aromatic units (Dryden, 1963). Advancing coalification causes an increase in aromaticity and development of orientated stacks of aromatic clusters.

X-ray diffraction analyses of coals have provided an insight into the physical structure, resulting in the recognition of three basic structural stages of coalification (Hirsch, 1954; Brown & Hirsch, 1955; Carts *et al.*, 1956). High-volatile bituminous coals have an "open structure" built up of cross-linked aromatic clusters showing no preferred orientation. Medium- to low-volatile bituminous coals pass through a "liquid structure" where cross-linking systems are broken down and aromatic clusters achieve some orientation. Low-volatile bituminous to anthracitic coal develops an "anthracitic" structure where strong preferred orientation of clusters build up and cross-linking material is lost. The clusters do not themselves increase significantly in size, but are orientated into crystallites or lamellae of increasing dimensions. Interestingly a recent investigation of sedimentary kerogens by high-resolution electron microscopy has shown that both naturally- and artificially-metamorphosed kerogens undergo a similar attainment of order without growth of individual aromatic clusters (Oberlin *et al.*, 1974).

The aromaticity of macerals increases with rank, except for fusinite which has a fairly constant composition. High-volatile bituminous exinites have a much lower aromaticity than corresponding vitrinites, which in turn are less aromatic than corresponding micrinites. At a rank of *ca.* 93% C complete aromaticity of all macerals is attained (van Krevelen, 1963). While the chemical processes taking place to attain complete aromaticity may be the same in all macerals, they must clearly operate at different relative rates in order to achieve the same end-point at similar ranks.

The aliphatic structures in coal contain the greater part of the hydrogen present up to low-volatile bituminous rank. Drydon quotes an

H_{ar}/H_{al} average ratio of 0.54 for a vitrinite containing 90% C (d.a.f.), with ca. 23% of this occurring in methyl groups. Most of the remaining aliphatic hydrogen is generally considered to be in alicyclic/hydro-aromatic structures, as shown in Given's molecular model of vitrinite. Certainly oils obtained by hydrogenolysis and low-temperature carbon-isation tars contain high proportions of cyclic compounds, although compositions vary widely with the petrology and rank of the parent coal. Reviewing available data from chemical and spectroscopic analyses, Francis (1961) concludes that much of the aliphatic part of the vitrinite structures are actually hydroaromatic, existing as highly substituted ring systems.

The problem of the origin of petroleum has stimulated extensive research into the geological fate of organic matter which is deposited in sedimentary rocks. That petroleum is basically of organic origin is currently generally accepted because of the biological affinities or properties exhibited by some petroleum constituents. Optical activity has been observed in petroleum distillates (Hills & Whitehead, 1966), C^{13}/C^{12} carbon isotope ratios often more closely resemble those of biological systems than of inorganic carbonates (Silverman, 1967), and a wide variety of biological structures have been detected (e.g. porphyrins, isoprenoid alkanes and cyclic terpenoids).

Petroleum generation is considered to be an essentially temperature-controlled reaction, the hydrocarbon components being derived from the lipid components of kerogen (Philippi, 1969). The geothermal conditions required for petroleum formation have been delineated (Pusey, 1973).

The constitution of kerogen has been widely investigated by chemical and spectroscopic methods, but the generally amorphous nature of the material renders microscopic petrographic evaluation unrewarding.

Nevertheless, recognizable organic detritus can be found in kerogens, although the amounts are usually small. Knowledge of the organic input of kerogens is desirable in relating source materials to geochemical products. In a recent investigation of petroleum hydrocarbon distributions, Philippi (1974) considers the relative contributions of terrestrial and marine organic matter as important controls.

An investigation carried out in this laboratory (Powell, 1969) related the compositions of organic extracts of a variety of Carboniferous sedimentary rocks to the visible petrographic organic composition. The sediments ranged from fresh water to marine-deposited. A surprisingly good quantitative correlation was found between extractabilities and the amounts of terrestrial organic matter (macerals), irrespective of depositional environment. The rank of the samples was also found to be an important control.

This thesis is concerned with the organic geochemistry of coal macerals, both from the point of view of maceral structures and the potential of terrestrial organic detritus to contribute to sedimentary hydrocarbons. A series of vitrinite and exinite concentrates were prepared from bituminous coals of ranks ranging from 77.1 to 86.6% $C_{vit.}$ (d.a.f.). The exinite concentrates were predominantly sporinite. In order to compare individual macerals within the exinite group, concentrates of alginite, resinite and cutinite were also examined, although these were of lower rank than the sporinites.

Infra-red spectra were recorded before chemical work began, and the samples were then extracted thoroughly for the examination of soluble hydrocarbons and fatty acids. The maceral "kerogens" were further analysed by controlled degradations. All extracted samples were saponified to remove bound fatty acids and alcohols. Selected samples from each maceral group were subsequently pyrolysed in an autoclave under low-temperature, inert conditions (275° and 375°C). Qualitative and quantitative examinations of the pyrolysates were carried out. In addition, selected exinite residues were oxidatively degraded with alkaline potassium permanganate and the acid products were examined.

The degradative work carried out is considered to affect basically the non-condensed structures in coals, i.e. those parts of the structure often referred to in the literature as "amorphous material" or "disordered carbon". Furthermore, the pyrolytic conditions employed were relatively mild and may simulate reactions which would occur during natural diagenesis. At all stages of the work microscopic examinations were carried out in order to evaluate the effects of the chemical work on the physical appearances and optical properties of the macerals.

Chapter 1

Samples: their origin, method of concentration and
petrographic and elemental analyses of
the maceral concentrates.

Infra-red spectroscopy of the maceral concentrates.

Samples

Vitrinite and Sporinite

The samples used in this investigation were of English and Scottish origin. The rank range represented extends from high-volatile bituminous into medium-volatile bituminous coals. Availability of suitable materials was the major factor in sample selection. As far as possible, both vitrains and spore-rich durains were collected together from vertically-adjacent horizons within individual seams to minimise vertical and lateral environmental variations. Eleven concentrates of both vitrinite and sporinite were eventually prepared. One vitrinite, from Westfield Opencast, and one sporinite, from Donibristle, have no corresponding sporinite or vitrinite respectively.

Prior to maceral concentration, selected blocks of vitrain and durain were examined microscopically by incident white light and ultraviolet radiation to determine the petrological constitution of the samples. To this end, specimens were mounted in resin and relief-polished on rotating alumina laps. Techniques of block-making and polishing are given in a later section. Microscopic examination ensured that only materials containing the highest proportions of the desired macerals were ultimately selected for maceral concentration. This was found to be especially important when dealing with durains in which the content of sporinite was highly variable.

The following descriptions of individual samples are a compilation of data from the examination of a number of polished specimens from each seam, and do not represent petrographic seam profiles. The following headings give seam names where known, with localities in parentheses.

Seam unknown (Westfield Opencast, Fife)

A number of durains and cannels were collected from this site, but were found upon examination to contain insufficient quantities of sporinite to make concentration viable. Samples of vitrain were also collected from which a vitrinite concentrate was prepared.

The Westfield coals occur in an isolated basin approximately 1000m. in diameter which is fault-bounded on the northern side. The coal seams are of exceptional thickness in the centre of the basin and generally thin out towards the edges. It is thought that movement on the north-bounding fault could be responsible for development of the basin contemporaneously with peat accumulation (Blenkinsop, 1973).

Seam unknown (Donibristle, Fife)

A sample of a spore-rich durain from Donibristle was supplied by a local museum. The sample was unjointed, and the material used was cut from the inner portion of the block to minimise any effects of contamination and oxidation which might have occurred during the long period of storage in the museum. The coal was brown in colour with a rather granular appearance, reflecting the high content of megaspores which it contained.

Microscopical examination showed that the sporinite content was dominated by abundant thick-walled megaspores, dark-grey in colour but showing orange/gold internal reflections. They were generally fragmented and compressed so that the original internal cavities were distinguishable either as dark lines or as fine bands of granular micrinite. The spores were mainly in a matrix of fusinite with lesser amounts of semifusinite. Quartz was often associated with inertinite. A few stringers of vitrinite occurred within the durain, sufficient for a reflectivity determination to be made. Pyrite was present to a small extent in small rounded grains.

High Hazles

Samples of High Hazles coals of variable ranks were collected from three localities, and were examined as individual samples. The localities were Gedling, in Nottinghamshire, and Warsop and Whitwell, in Derbyshire. Durains from Warsop and Whitwell were dominantly durite, with bands of very spore-rich material. Crassispores and megaspores predominated, often showing good morphology. Sporinite was present in a matrix of fusinite and semifusinite, with granular micrinite in association with some spores. The Whitwell sample graded occasionally into clarodurite. Resinite and pyrite were minor components of both.

Durain from Gedling was also mainly durite, but graded occasionally through clarodurite to duroclarite. The sporinite content of this sample was much lower than in the other two, but there were some local concentrations of crassi- and tenuispores. These generally showed rather poor morphology and often appeared corroded. The disseminated megaspores were better preserved, and spore-coat ornamentation could be seen. Large lenses of fusinite in this sample sometimes showed excellent "bogenstruktur".

Shallow (Lea Hall, Staffordshire)

Durain from the Shallow seam was almost exclusively composed of durite, with high local concentrations of crassispores in a matrix of fusinite and semifusinite. Inertinite-rich durite also occurred in which the sporinite content was very low. Occasional transitions to clarodurite occurred, and these bands contained little sporinite. Megaspores, usually fragmented, occurred throughout the durite and were sometimes locally concentrated. Granular micrinite was associated with some of these. Large spore-free lenses of fusinite were present in the durite. Resinite and pyrite were minor constituents.

Clowne (Whitwell, Derbyshire)

Durain from the Clowne seam was composed of durite and claro-durite. The total sporinite content of the two microlithotypes was not high, apart from some local concentrations in narrow laminae. Microspores were both thin- and thick-walled, sometimes appearing rather corroded. Megaspores were disseminated throughout, usually fragmented and showing internal reflections through the dark grey body colour. Fusinite and semifusinite were the major components of the durite along with lesser vitrinite and micrinite in the claro-durite. Resinite was a minor constituent.

Pyrite was abundant in the Clowne durain, occurring as small discrete globules and as large aggregates. The Clowne seam has a marine roof, characterised by the presence of *Lingula sp.*, (Spink and Ford, 1968). This could lead to strong reducing conditions within the original peat (Francis, 1961; Williams and Keith, 1963), and the observed high pyrite content is probably a reflection of intense anaerobic bacterial activity.

Deep Hard (Babbington, Nottinghamshire)

Durain from the Deep Hard seam was composed of durite of rather uniform appearance, with an estimated content of sporinite of about 50% in the richer bands. Crassispores were dominant in a matrix of fusinite and semifusinite. Elongate lenses of fusinite occurred showing good "bogenstruktur". Megaspores were dispersed throughout the durite and were usually fragmented. In the lesser compressed megaspores, the internal cavities were filled with microspores and inertinite, or granular micrinite if they were not ruptured. Resinite was a minor component.

Beeston (Peckfield, Yorkshire)

This durain contained numerous laminae of almost pure sporinite consisting of masses of microspores compressed to the extent that outlines of individual spores were often indistinct. Less spore-rich bands were composed dominantly of sporinite and semifusinite, with occasional fine stringers of vitrinite. Megaspores occurred throughout, but were often indistinct in the spore-rich bands. Inner cavities were filled with granular micrinite when the spores were unbroken. Both resinite and pyrite were seen in only trace quantities in this durain.

Barnsley (Dinnington, Yorkshire)

Durain from the Barnsley seam was composed of durite, clarodurite and duroclarite, the former being the most predominant microlithotype. The sporinite content was not high and varied between the microlithotypes. Crassi- and tenuispores were present, but megaspores were not abundant and were usually fragmented. Sporinite occurred in a matrix of fusinite and semifusinite in durite, with increasing amounts of vitrinite in the other microlithotypes. Lamellae and lenses of pure fusinite were seen in durite. Resinite was only a minor constituent, as was pyrite.

Parkgate (Houghton Main, Yorkshire)

This durain was composed mostly of durite which had a highly-variable, but often low, sporinite content. Crassispores predominated over tenuispores. Megaspores were not common, and were dispersed throughout the durite. The sporinite was light grey in colour and showed variations in shade and relief, testifying to the higher rank of this coal. The durite was composed of fusinite and semifusinite along with the sporinite, with some micrinite usually in association with the sporinite. Resinite and pyrite were minor constituents.

Silkstone (Cortonwood, Yorkshire)

Durain from the Silkstone seam had a high sporinite content in the durite, with variations in the sporinite content producing a banded appearance when viewed microscopically. Spores were light grey in colour and showed variable relief. Crassispores were more abundant than tenuispores. Megaspores occurred throughout, usually fragmented and infilled with spore-rich durite. Sporinite was found in a matrix of semifusinite and micrinite in the durite, with vitrinite lamellae producing gradations to clarodurite. Resinite was only identified in trace quantities.

Alginite

Three torbanites have been used as a source of the exinite maceral alginite. Microscopical examination of the samples showed that all three had a high content of alginite and variable traces of vitrinite, inertinite and sporinite, along with variable amounts of argillaceous material. Because of the inherently high algal content of the torbanites, the samples were not pre-treated in any way to remove contaminants.

The origin of torbanites has been a matter of much discussion in the past and a number of theories have been proposed for the origin of the microscopically-observable "yellow bodies" (Bertrand and Renault, 1892a, 1892b; Jeffrey, 1909; Conacher, 1917). An algal origin is now generally accepted, the actual alga found in many torbanites being closely related to the extant form *Botryococcus braunii* (Blackburn and Temperley, 1936). The torbanites used in this work were from Scotland, South Africa and Australia.

Scottish torbanite (Torbanehill, Scotland)

Torbanehill, near Bathgate, is the type locality for torbanite which, along with associated oil shales, was the source material for a once-flourishing shale-oil industry.

Alginite was the major component of the torbanite, along with minor amounts of fusinite, semifusinite, vitrinite and sporinite. These contaminating macerals usually occurred as small angular fragments dispersed throughout the mass, but occasional larger cellular fragments of semifusinite and stringers of vitrinite were seen. Interstices between algal masses were infilled with mineral matter. Pyrite occurred in only trace quantities.

Torbanehill torbanite is of Carboniferous age, occurring within a sequence where the autochthonous bright coals have achieved bituminous rank (Millais and Murchison, 1969). It is thought to have originated through extensive algal growth in fresh water pools and lakes within the coal-forming swamps. Occasional teeth, spines and scales of fresh water fish have been found. Water level within the pools would presumably be maintained by rainfall and influx of surface waters percolating through the surrounding peat, which would act as a filter removing much coarse plant debris (MacGregor, 1938). Under quiet conditions, the slow movement of water would in itself inhibit the transport of all but the finest material. Nutrient supply would be in the form of dissolved mineral matter. Algal growth took place in the upper aerated layers of the pools, dead algal material sinking to form a rich sapropel, as well as accumulating around the pool margins.

Australian torbanite (Hartley Vale, New South Wales)

The Australian torbanite appeared quite strongly compressed and was very rich in alginite. There were however numerous fine stringers of fusinite, semifusinite and vitrinite, plus occasional microspores. Argillaceous material infilled spaces between the algae, although this appeared to be small in quantity.

The origin and distribution of New South Wales torbanites have been thoroughly investigated (Dulhunty, 1942, 1944). Numerous lenticular deposits occur within Coal Measure sequences of Permian age. The algae proliferated in isolated pools marginally-located within the coal-forming swamps. Water was probably supplied by seasonal torrential streams draining adjacent upland areas which would percolate through the accumulating peats and supply nutrients necessary for algal growth.

South African torbanite (Leslie, Transvaal)

This sample appeared microscopically to be almost pure alginite, with only occasional minute fragments of possible inertinite. Microspores were also present in trace quantities only. The alginite was quite strongly compressed and there was little visible evidence of interstitial argillaceous material. Pyrite was quite common, sometimes occurring as small ovoid nodules. Uncompressed individual algae were seen in these nodules, indicating syngenetic pyrite formation in unconsolidated sediment, possibly as a result of bacterial activity. The torbanite is of Permian age. No information is currently available to the author on the distribution of South African torbanites, but it seems likely that they originated in conditions similar to those described previously for other torbanites.

Resinite

Three samples of resinite have been used in this work. The concentrates were all of high purity, having been isolated from lignites. Unfortunately they are of very low rank but it is hoped to show essential constitutional differences between resinite and other members of the exinite maceral group. In a strict sense, the samples used here should properly be regarded as intermediate products in an incipient stage of coalification.

Yallourn resin (Victoria, Australia)

A sample of Yallourn resin, already isolated, was available in this Department. It was a brownish, opaque, brittle material occurring as lumps up to about 2cm across. It is found as pockets, and bands, within extensive lignite deposits (Francis, 1961) of Oligocene age (Thomas, 1969). Microscopically it appeared very homogeneous, but showed internal oriented bubbles and cracks which are probable indicators of the material having flowed.

A significant contributor to the Yallourn lignite deposits is closely related to *Agathis australis*, which is known to produce at least five constitutionally-different resins (Thomas, 1969). In view of the size of the lumps of this sample and of its flow structures, bled resin is a probable source material.

Yallourn resin is very similar to amber, kauri and copal in elemental composition (Francis, 1961), indicating that the material has undergone little coalification.

Bitterfeld resin (Germany)

Bitterfeld resin was a brownish, hard, translucent material, which occurs in Tertiary lignite deposits (Murchison and Jones, 1963). No information is available to the author upon its mode of occurrence within the lignites or upon its parent plant material. Microscopically it was a homogeneous material with no internal structures.

Maghara resin (Sinai)

Maghara resin occurs as ovoid lenses and cell infillings in a lignitous coal of Liassic age (Powell Duffryn Tech. Serv. Rpt., 1963), the lenses being of sufficient size for the resin to be isolated macroscopically. The resin content of the whole coal was about 4.0%, and the dominant microlithotype was clarite. The resin itself was a brown, hard, translucent substance which was homogeneous microscopically.

Cutinite

Cutinite is the fourth constituent of the exinite maceral group and occurs as a minor constituent of many coals. It is rarely found in any abundance however, and only one sample, from the Indiana (USA) paper coal, was available to the author. This coal was discovered in Indiana in 1958. The seam was approximately 18" thick at outcrop, the upper 6" being very rich in leaf cuticles and spores embedded in vitrinitic attritus. Oxidation and mechanical weathering of the matrix had left almost pure cuticular material (Guennel and Neavel, 1959). The coal was of low rank and produced a high yield of tar, gas and oil upon distillation because of the high exinite content (Neavel and Miller, 1960).

The high exinite content was clearly observable when the coal was examined microscopically. Sporinite was present in only minor quantities. The vitrinitic material was of very low reflectance and showed strong rectilinear patterns of desiccation cracks. Much of the coal had a rather dirty amorphous appearance.

In view of the friable nature of the available sample, isolation of pure cutinite was straightforward.

Maceral Concentration

Sporinite

The problem of separating sporinite from bituminous coal was reviewed and studied by the author in an earlier project (Allan, 1970), where small quantities of coal were used. The method used was to suspend crushed durain in solutions of zinc chloride of variable density to concentrate sporinite (Dormans *et al.*, 1953). The specific gravities of coal macerals vary between the maceral groups, and also vary within each group with rank (ICCP, 1963). These variations are shown in Fig. 1. The differences between exinites and the other maceral groups are sufficiently great, up to low-volatile bituminous rank, for effective separation of exinite.

Difficulties are encountered at higher ranks where the specific gravities of sporinite and vitrinite converge. At this stage of coalification ($C_{vit.}$ *ca.* 87% d.a.f.) exinite undergoes a coalification break (Stach, 1953), the reflectance of sporinite increases rapidly and it becomes indistinguishable from vitrinite. The change in appearance of sporinite is accompanied by the evolution of considerable quantities of methane. Once sporinite has undergone this transformation, spores cannot be retrieved from coals even by maceration techniques (Stach, 1968).

Zinc chloride solution has been used successfully as a heavy, separatory liquid, after extensive crushing of spore-rich durain in a ball mill (Dormans *et al.*, 1953). Zinc chloride is very soluble in water (432 gms/100 mls cold water) and a specific gravity of 1.30 is readily attainable. Furthermore it is easily removed from the coal after use by washing. Alternative separatory liquids, such as Thoulet's solution, become strongly adsorbed on to coal and are therefore unsatisfactory, while organic liquids could not be used since partial extraction of the samples would have occurred. Although

FIG.I. VARIATION OF SPECIFIC GRAVITIES OF MACERALS WITH RANK

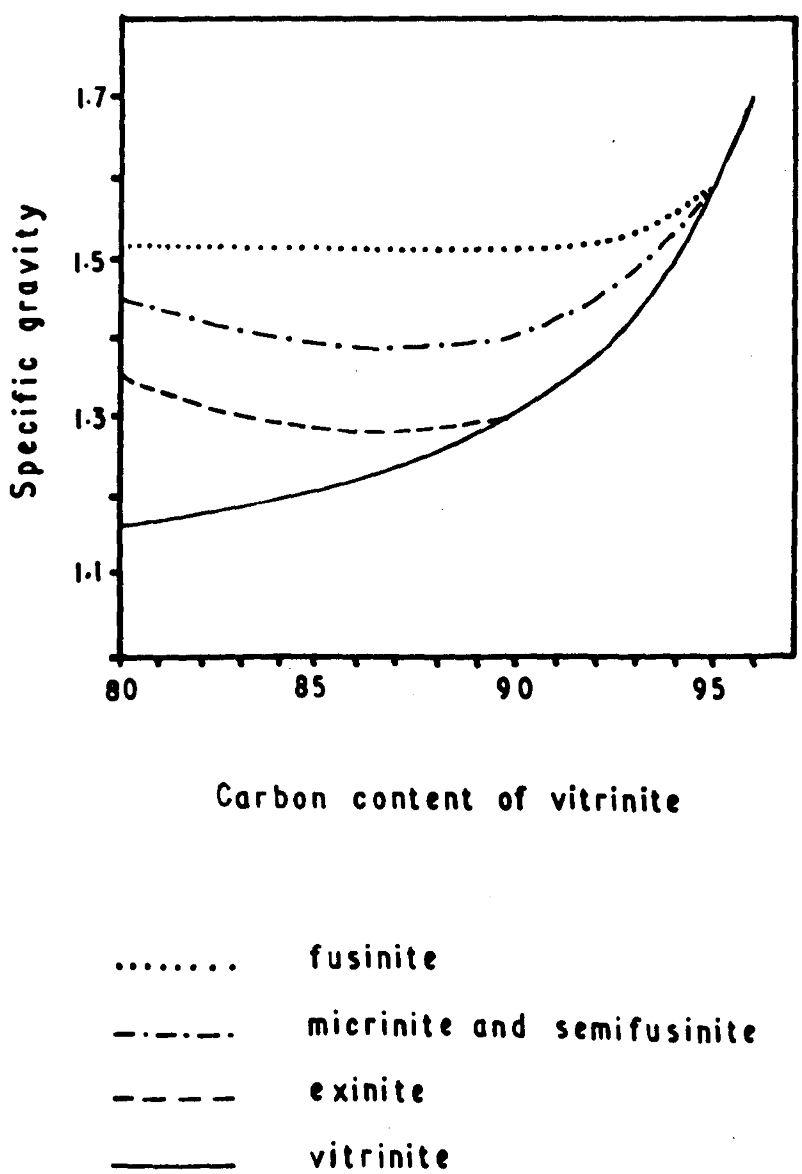

suspension in heavy liquids is adequate for separation of exinites from other macerals, it is not viable as a method for concentrating one exinite component from other members of the group. Thus it is essential that the required component, in this case sporinite, occurs in great excess over other exinite macerals in the starting materials. The samples of durain used in this work all fulfilled this criterion. Resinite occurred in nearly all the samples, but always as a minor component. Neither cutinite nor alginite were observed in any of the selected durains.

A second contributory factor towards a successful concentration of sporinite is the manner in which the durain is crushed prior to the heavy liquid separation. Despite earlier work in which coal was ground for long periods in a ball mill, it has been found that controlled crushing of the initial material, together with constant fractionation by size can lead to substantial increases in the sporinite content of certain fractions. In fact, one sporinite concentrate of high purity has been produced by crushing alone (Allan, 1970).

The components of coal vary in their hardness, and sporinite is one of the most resilient macerals. Sequential crushing and sieving will preferentially break up and remove the more friable components from the whole coal, and they will tend to concentrate in the finest fractions. The tougher spore exines will be slowly freed from the coal matrix, and their degree of fragmentation will be less than for the other macerals. Thus they will become relatively more concentrated in the coarser fractions. The final consideration here is that a high degree of particle homogeneity must be achieved to effect final adequate concentration. This can be followed during the separation process by microscopical examination under high magnification.

The following is an outline of the final method employed in sporinite concentrations. It is emphasized however that each sample of coal must be treated individually. This applies especially to the stepwise float/sink separations. Microscopical examination of the product and an estimation of its composition is a useful guide to the next logical step.

Method

The outer edges of the blocks of durain were removed with a rotary saw and contaminating bands of vitrain and clarain were also cut out. The blocks were then broken down into 1 to 1½ inch lumps. These were examined and any that contained visible vitrain and/or clarain were discarded. As vitrinite has a specific gravity fairly close to that of sporinite, it was considered advisable to remove as much vitrinite as possible in the early stages. The remaining material chosen for concentration was washed ultrasonically in methanol for 10 minutes to remove any surface organic contamination due to handling, storage, etc. During the following separation procedure, strict precautions were taken to ensure that the samples were kept free from organic contaminants.

Durain was crushed in a disc mill for 10 seconds (TEMA Machinery Ltd) and sieved through a B.S. 120 mesh sieve on an automatic shaker (Endecott Test Sieve Shaker). Material greater than 120 mesh size was returned to the mill with a further aliquot of fresh durain. The -120 mesh material was sieved to pass 240 mesh, and collected. The fraction greater than 240 mesh was returned to the disc mill. Each crushing period, of fresh material with admixed sieved material, was limited to 10 seconds to prevent excessive pulverisation of the spore exines. This process was continued until all the material passed through the 240 mesh sieve.

A problem was encountered in sieving the powder through the 240 mesh sieve. It rapidly became blocked with adherent powder unless very small quantities were used. Because large quantities of material required sieving (up to 1 Kg. per sample), it was clearly impracticable to use the automatic shaker. To overcome the problem the 240 mesh sieve was mounted centrally, with a receiver underneath, on a gramophone turntable, using a rubber mat to prevent slipping. Two soft brushes (fine copper wire and bristle) were clamped above the sieve so that they just contacted its surface as it was rotated, and they were so arranged that any powder on the sieve was continually swept across the surface. The resulting sieving action was found to be quite rapid and reasonably efficient. Practice determined the length of time necessary for each aliquot to be treated in this way. If brushing was continued for too long the larger particles were pushed through, thus distorting the sieve and rendering the process inefficient.

Early in the project it was considered desirable to sieve the -240 fraction through a B.S. 400 mesh sieve. Much of the fusinite and semifusinite in the durains was rapidly pulverised to this size in the disc mill. Sieving through a 400 mesh should relatively remove some of this material, and enrich the coarser grade in the required components. Furthermore, early difficulties were encountered in wetting very finely-powdered durain which rendered sink/float separations in the zinc chloride solution ineffective, because of rapid flocculation. This became less of a problem if the -400 mesh powder was first removed. Consequently, three samples were concentrated using powder treated in this way, but final yields of concentrate were small. Obviously much sporinite was discarded in the -400 mesh fraction, although relatively more inertinite was removed. Once the wetting problem was overcome (see below), the remainder of the durains were only sieved down to -240 mesh.

Microscopical examination of sieved fractions

The constitution of the various sieved fractions was monitored by visual examination under high magnification. Fractions of +120 mesh were composed of dominantly heterogeneous particles, with spores contaminated with, or enclosed in, other macerals. The -120 +240 mesh fractions still showed a high degree of heterogeneity of particles, although some fragments, especially of megaspores, were relatively clean. At -240 mesh, many particles were monomaceralic. Fragments of spore exines occurred quite free of other adherent material or with partial rims of attached vitrinite and inertinite. Granular micrinite in spore cavities was not removed by this process, but amounts of this maceral were small. At this stage the material was ready for heavy liquid separations.

Sink/float separation

Solutions of zinc chloride were made up to specific gravities of 1.25 and 1.30 respectively. They were acidified with a few drops of concentrated hydrochloric acid to prevent precipitation of insoluble zinc hydroxide.

20 gm aliquots of sample were dispersed into 100 mls of zinc chloride solution of S.G. 1.30. This was rapidly and effectively achieved using a high-speed, motor-driven propeller. The powder was settled onto the surface of the liquid in a centrifuge tube, the propeller created a vortex in the liquid and the powder was impelled through the blades to become quickly dispersed. The problem of flocculation was not encountered at all using this method. The suspension was centrifuged at 2500 r.p.m. for 15 minutes. The "floats" layer and all the liquid (which usually contained a relatively small proportion of suspended material) were decanted into a Buchner funnel and filtered. The zinc chloride was recovered and the residue was washed thoroughly with acidified water. The collected "floats" were

dried at $60^{o}C$.

Microscopical examination of these fractions showed a partial removal of much of the inertinites and the retention of pure spore fragments, spore fragments with attached macerals, vitrinitic particles and some inertinites in the free state. The "sinks" from this step were discarded. The amounts of retained material from this step varied greatly between samples.

The recovered, dried material was then suspended in a solution of S.G. 1.25. Initially, an intermediate separation using a solution of S.G. 1.275 was employed, but fractionation of the material was not generally improved by this treatment and the step was omitted. The samples were repeatedly processed in solutions of S.G. 1.25 until the amount of "sinks" became minimal. The number of steps required to achieve this varied between samples.

The constitution of the concentrate was determined by qualitative microscopic examination. Usually, it was found that much contaminating material was still attached to the exine fragments, either as partial rims or enclosed within the inner cavities of spores. Material attached peripherally was removed by further grinding in the disc mill for 5 to 10 seconds, followed by successive treatments in liquid of 1.25 specific gravity until the amount of "sinks" again became minimal. Successive crushings and suspensions, with constant monitoring of the product microscopically, were continued until the concentration of sporinite did not significantly increase any further. The limitations of the process are the relative inefficiency of the sink/float technique and the inability of the crushing process to achieve complete particle purity. The former would probably be improved by decreasing the ratio of powder to liquid when carrying out the specific gravity separations and the latter by decreasing the particle size of the starting material. Time however becomes a limiting factor when a number of large samples required processing.

Nevertheless, using the above procedure, concentrations of sporinite of 90 to 95% purity were obtained from low rank bituminous coals. Difficulties seemingly increased directly with the rank of the coal, and a concentrate of about 77% purity only was obtained from Parkgate durain, one of the higher rank samples.

Quantitative examination of the concentrates (Table 1) was undertaken microscopically, using the automatic point-count method. A 500 point count was done on a relief-polished block, under oil immersion, at a magnification of x500. This has an accuracy of ±2-3% (ICCP, 1963). Full details of the concentrations are given in the experimental section.

Vitrinite

Vitrinite concentrates were produced by hand-picking of vitrain bands lying in close contact with the durains used for sporinite concentrations. The vitrain bands were initially removed from the coal using a vibrating engraver (Burgess Model VT 62 Electric Engraver). This was very successful in view of the brittle nature of vitrain. Selective hand-picking of the resulting fragments ensured that good concentrates of vitrinite were produced.

After cleaning the fragments for organic analysis, they were crushed in a disc mill to pass a B.S. 100 mesh sieve. Maceral analyses were again done by point-counting over 500 points. In nearly all samples a high petrographic purity was found, the major contaminants being inertinites (Table 1). However, the Beeston concentrate contained *ca.* 5% sporinite, which was considered unacceptable for the project. It was therefore ground to pass a B.S. 240 mesh sieve, and suspended in zinc chloride solution of S.G. 1.25. The suspension was centrifuged at 2500 r.p.m. for 15 minutes, the resulting "floats" layer and supernatant liquid decanted, and the "sinks" were recovered. After washing and drying, analysis showed that much of the sporinite had been removed.

Other exinite macerals

Three alginites, three resinites and one cutinite have also been used in this work, as discussed earlier in this chapter. The isolation of these samples has been detailed in the discussion upon the origin and occurrence of the source materials.

The petrographic analyses of all the maceral concentrates obtained are given in Table 1.

Maceral analysis

Petrographic analyses of the maceral concentrates are shown in Table 1. All were made by the point-count method, using 500 points. Vitrinite and sporinite counts were carried out using incident white light only, but alginites were examined under both visible and ultraviolet radiation. The exinitic content of these concentrates was determined under ultraviolet radiation, while the non-exinitic constituents were determined under white light.

The resinite concentrates were all of high petrographic purity when examined microscopically, probably in the order of 99% pure, and it was considered unnecessary to carry out point-counts for them. The sample of cutinite was also petrographically very pure, with only trace quantities of visible vitrinite and sporinite along with some pyrite and clay minerals. Consequently this sample was also not point-counted.

Elemental analysis

Ultimate and proximate analyses (Table 2) of vitrinites,

Table 1: Petrographic analyses of maceral concentrates

Vitrinite concentrates	Vitrinite %	Exinite %	Inertinite %
Westfield	95.5	0.8: sporinite	3.7: dominantly granular micrinite
High Hazles (Gedling)	93.5	1.6: sporinite	4.9: granular micrinite > fusinite
Clowne*	92.7	1.0: sporinite	6.2: granular micrinite
Shallow	91.5	0.9: sporinite	7.6: granular micrinite
High Hazles (Warsop)	97.0	0.7: sporinite > resinite	2.3: semifusinite and fusinite
Deep Hard	90.3	2.0: sporinite	7.7: micrinite > fusinite
High Hazles (Whitwell)	97.0	0.2: sporinite	2.8: dominantly semi-fusinite
Beeston	93.9	0.5: sporinite	5.6: dominantly gran-ular micrinite
Barnsley	89.1	0.3: sporinite	10.6: dominantly micrinite
Parkgate	96.0	2.2: sporinite	1.8: semifusinite > micri-nite > fusinite
Silkstone*	94.5	1.1: sporinite	4.2: micrinite > fusin-ite > semifusinite

* Pyrite counted to less than 1%.

Alginite concentrates	Alginite %	Sporinite %	Inertinite %	Vitrinite %	Mineral matter %
Scotland	90.8	0.4	4.9	3.0	0.9
South Africa	95.5	tr.	0.3	none	4.2
New South Wales	93.0	0.3	3.1	2.1	1.5

tr. Sporinite observed in this sample but no particles were traversed during the point count.

Table 1 (cont'd.)

Sporinite** concentrates	Sporinite %	Vitrinite %	Inertinite %
Donibristle	95.6	1.0	3.4: fusinite
High Hazles (Gedling)	94.3	0.4	5.3: micrinite > fusinite
Clowne	91.2	0.4	8.4: semifusinite and micrinite
Shallow	88.1	1.4	10.5: semifusinite > micrinite
High Hazles (Warsop)	94.6	0.2	5.2: semifusinite and micrinite
Deep Hard	93.0	tr.	7.0: micrinite and fusinite
High Hazles (Whitwell)	94.3	0.2	5.5: dominantly semi-fusinite
Beeston	94.3	0.3	5.4: fusinite and micrinite
Barnsley	89.7	1.1	9.2: semifusinite > micrinite
Parkgate	77.5	2.0	20.5: semifusinite > micrinite + fusinite
Silkstone	89.7	1.0	9.3: micrinite and fusinite

** Resinite is a trace component of most of these samples.

tr. Vitrinite was observed in this sample but no particles were traversed during the point count.

Table 2: Ultimate and proximate analyses of the maceral concentrates

	Ultimate analysis				Proximate analysis	
	C	H	S	N+O	Volatile matter	Fixed carbon
	% (d.a.f.)				% (d.a.f.)	
Vitrinite						
High Hazles (Gedling)	77.1	4.9	0.8	17.2	50.75	49.25
Westfield	77.2	4.8	0.5	17.5	52.5	47.5
Clowne	77.5	5.1	1.5	15.9	48.6	51.4
Shallow	77.7	5.2	0.8	16.3	46.8	53.2
High Hazles (Warsop)	79.6	5.4	0.9	14.1	43.6	56.4
Deep Hard	81.9	4.4	0.5	13.2	52.4	47.6
High Hazles (Whitwell)	82.3	5.0	1.1	11.6	46.0	54.0
Beeston	83.3	5.1	1.1	10.5	48.3	51.7
Barnsley	83.9	5.1	0.9	10.1	47.8	52.2
Parkgate	85.4	5.3	1.0	8.3	46.8	53.2
Silkstone	86.6	5.5	1.0	6.9	47.0	53.0
Sporinite						
Donibristle	78.5	7.5	0.9	13.1	81.8	18.2
High Hazles (Gedling)	80.9	7.0	1.1	11.0	65.6	34.4
Clowne	81.1	7.1	1.2	10.6	65.1	34.9
Shallow	80.6	6.7	1.2	11.5	63.1	36.9
High Hazles (Warsop)	82.2	6.8	1.4	9.6	71.1	28.9
Deep Hard	83.3	6.8	0.8	9.1	70.4	29.6
High Hazles (Whitwell)	83.0	7.4	1.3	8.3	76.7	23.3
Beeston	81.6	6.8	1.0	10.6	68.8	31.2
Barnsley	84.2	6.9	0.9	8.0	70.5	29.5
Parkgate		n.d.			n.d.	
Silkstone	87.1	6.4	0.4	6.1	56.5	43.5

Table 2 (cont'd.)

	Ultimate analysis				Proximate analysis	
	C	H	S	N+O	Volatile matter	Fixed carbon
	% (d.a.f.)				% (d.a.f.)	
Alginite*						
Scotland	82.8	10.8	0.4	6.0	97.8	2.2
South Africa	80.5	11.1	0.8	7.6	100.0	-
New South Wales	84.0	10.7	0.5	4.8	98.8	1.2
Resinite						
Yallourn[1]	79.1	10.1	n.d.	n.d.	n.d.	
Bitterfeld[2]	79.7	10.0	n.d.	n.d.	100.0	-
Maghara	n.d.				n.d.	
Cutinite						
Indiana[3]	74.7	8.1	0.2	17.0	94.8	5.2

* Samples demineralised prior to analysis.

1 Francis (1961)

2 Murchison and Jones (1963)

3 Neavel and Miller (1960)

n.d. not determined.

d.a.f. All analyses have been corrected to a dry, ash-free basis.

sporinites and demineralised alginites were done commercially* but the results for the resinite and cutinite samples have been quoted from the literature, where available.

Reflectance

The reflectivities of the vitrinite concentrates were determined by 50 rotational measurements, and calculated against calibrated glass standards. The results, shown in Table 3, are given as mean maximum reflectances ($\bar{R}_{max}$). Also shown in the table are the reflectivities of vitrinite particles or stringers associated with the alginite and cutinite samples. These are given as mean reflectances ($\bar{R}$), determined without rotation of the microscope stage.

Table 3: Vitrinite reflectance of maceral sources

Sample	$\bar{R}_{max}$
Westfield	0.47
High Hazles (Gedling)	0.51
Shallow	0.56
Clowne	0.60
High Hazles (Warsop)	0.62
Deep Hard	0.63
Beeston	0.64
High Hazles (Whitwell)	0.68
Barnsley	0.91
Silkstone	1.04
Parkgate	1.12
	$\bar{R}$
Indiana cutinite	0.42 (20 readings)
Scottish torbanite	0.27 (31 readings)
New South Wales torbanite	0.18 (20 readings)
South African torbanite	n.d.

n.d. not determined.

* United Analysts Ltd.

Infra-red spectroscopy

Infra-red spectroscopy is a technique standardly employed in coal analysis, despite the difficulties involved in obtaining good spectra. Spectra are obtained mostly in the 2.5 to 15 micron range (4000 to 670 wavenumbers).

A number of techniques are available for obtaining coal spectra. Thin sections, although difficult to prepare because of the friable nature of coal, have been employed. Alternatively, powdered samples can be mulled with agents such as "Nujol" and hexachlorobutadiene, although such materials themselves absorb characteristically in the 2.5 to 15 micron range. A commonly used method is the halide disc technique, where the powdered sample is mixed with KBr or KCl and pressed into a translucent disc. The main problems in making discs are achieving sufficiently fine particle size and the elimination of water. In a thorough qualitative and quantitative investigation a combination of techniques is desirable.

Previous work

The first extensive investigation of coals by infra-red spectroscopy (Cannon and Sutherland, 1945a, 1945b) used thin sections (0.01 mm thick). Since then, much information has become available on coals and macerals (Gordon *et al.*, 1952; Friedel and Pelipetz 1953; Bergmann *et al.*, 1954; van Vucht *et al.*, 1955; Monnot and Ladam, 1955; Friedel and Queiser, 1956; van Krevelen and Schuyer, 1957; Roy, 1957; Brooks *et al.*, 1958a; Murchison, 1966; Ratajczak, 1968; Millais and Murchison, 1969), coal extracts (Orchin *et al.*, 1951; Kirby *et al.*, 1954; Roy, 1957; den Hertog and Berkowitz, 1958; Brown, 1959), changes during coalification (Cannon, 1953; Brown 1955a; Brown and Hirsch, 1955; Kinney and Douchette, 1958; Bent and Brown, 1961), as well as detailed work on the assignments of specific adsorptions to coal structures. Excellent reviews on infra-red spectroscopy in coal research have been given by Tschamler and de Ruiter (1963) and Friedel (1966).

Vitrinite

Vitrinite is the maceral most extensively studied by infra-red spectroscopy, presumably because of the ease with which high-purity concentrates can be attained throughout a wide rank range.

In the present project a representative selection of vitrinite concentrates was examined, using the halide disc technique. The samples used were the Clowne, Shallow, High Hazles (Whitwell), Barnsley, Parkgate and Silkstone vitrinites. The spectra are shown in Fig. 2. The differences in the spectra were generally of differing intensities rather than of changing absorption frequencies. There was a general broad region of absorption decreasing from 4000 to 2000 cm^{-1} which has been ascribed to electronic scattering by the vitrinite particles in the halide disc (Friedel, 1966) and/or structureless absorption (Brown, 1955a) due to the growth of "graphitic-type" structures. Superimposed on this absorption in the lower-rank samples was a strong band centered at 3300 cm^{-1} due to hydrogen-bonded -OH groups, and distinct bands at 2920 and 2860 cm^{-1} due to aliphatic C-H absorptions (Bellamy, 1964; Friedel and Queiser, 1956; Kinney and Douchette, 1958; Brooks *et al.*, 1958a; Tschamler and de Ruiter, 1963; Friedel, 1966). A shoulder on the 2920 cm^{-1} band at 2950 cm^{-1} has been assigned to $-CH_3$ groups (Friedel, 1966). In the spectra of the Barnsley, Parkgate and Silkstone vitrinites, the absorption at 3300 cm^{-1} was much reduced in intensity, although it may be partially obscured by increasing general absorption in this region. Also the 2860 cm^{-1} band in the Parkgate sample was only discernible as a shoulder on the 2920 cm^{-1} band. The shoulder at 2950 cm^{-1} was not apparent which would indicate a reduction of $-CH_3$ groups.

The broad absorption at 3300 cm^{-1} due to hydrogen-bonded -OH

FIG. 2. INFRA-RED SPECTRA OF VITRINITES

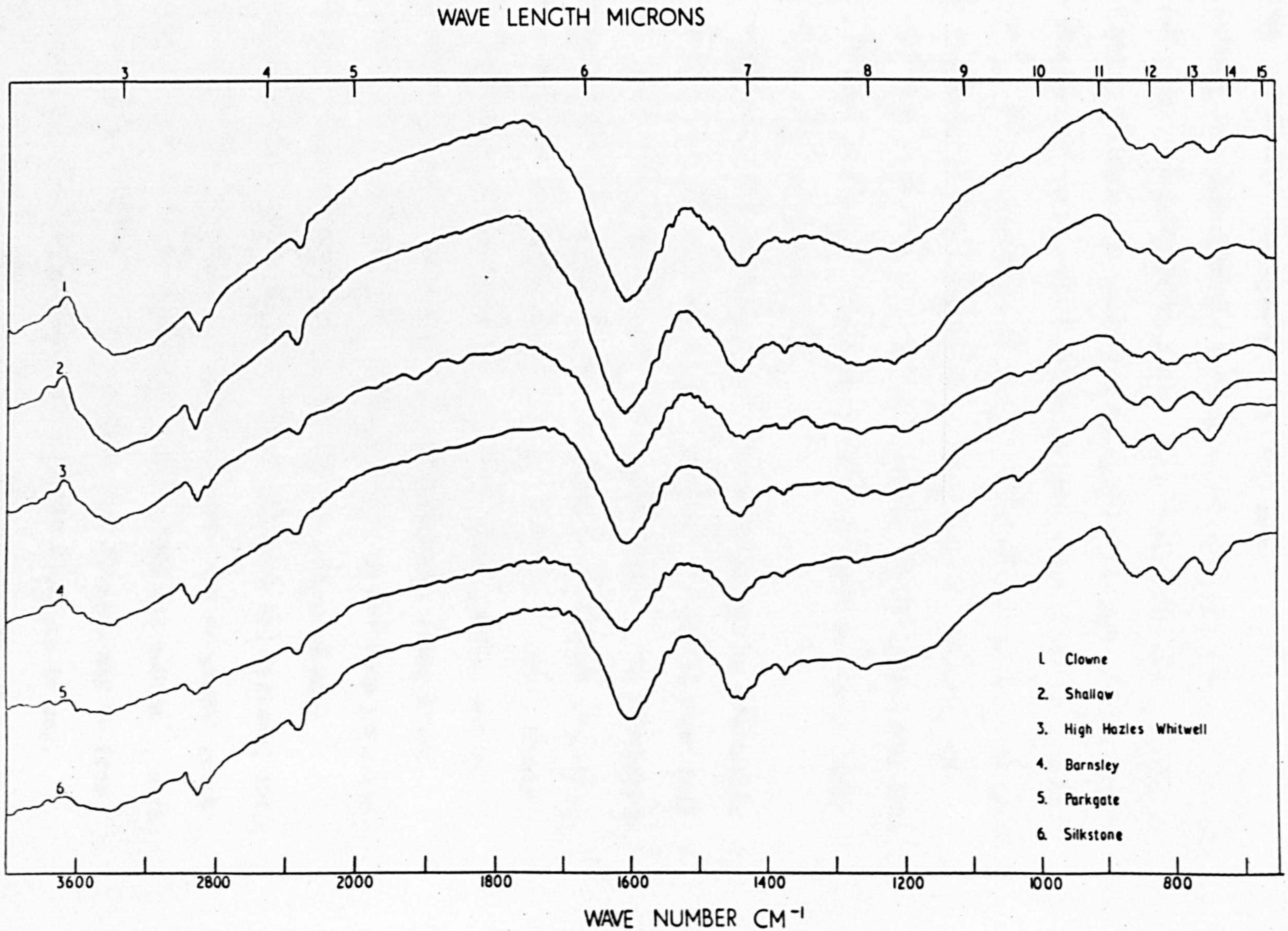

groups can be only attributed in part to the vitrinites. It has been shown that grinding of pure KBr produces a strong absorption at this wavelength, attributed to $KBr-H_2O$ groups, the intensity of the absorption being directly related to the time of grinding (Friedel and Retcofsky, 1963; Friedel, 1966). Only under the most stringent conditions of preparation can this be at best reduced. Other spurious absorptions due to $KBr-H_2O$ bonding may occur at 2040 cm^{-1} and 1630 cm^{-1}. Within the scope of this work it was not considered necessary to attempt elimination of these absorptions. However, the fact that the absorption at 3300 cm^{-1} decreased with increasing rank of the samples would indicate that it was certainly in part a function of the vitrinite structure.

In all the samples investigated, there was a strong absorption band centered at 1610 cm^{-1} which is a constant feature of many coal spectra, but which is the source of much discussion. The absorption has been variously assigned in part to aromatic C=C bonds in polynuclear condensed ring systems (Kinney and Douchette, 1958; Brooks *et al.*, 1958a; Cannon and Sutherland, 1945b; Brown, 1955a) and to conjugated oxygenated systems (Friedel and Queisor, 1956; Given and Peover, 1958; Fujii, 1963). More recently it has been proposed that this absorption may be partly due to the growth of non-crystalline graphitic structures in coals (Friedel and Carlson, 1971; Friedel and Carlson, 1972). The infra-red spectrum of ground graphite shows a broad area of absorption between 1800 and 900 cm^{-1}, with peaks at 1590 and 1360 cm^{-1}. Yet another contribution may be from carboxylate ions chemically-bound to inorganic elements in coal (Brooks *et al.*, 1958a). Finally, $KBr-H_2O$ absorption can enhance the total intensity of the 1610 cm^{-1} band when spectra are recorded through KBr discs, unless rigorous drying precautions are taken (Durie *et al.*, 1967; Friedel and Retcofsky, 1963).

A number of weak-intensity absorption bands occurred in the vitrinites, mostly seen as shoulders only, at about 1560, 1542, 1508 and 1490 cm^{-1}, which may be assigned to aromatic C=C absorptions.

A medium-intensity absorption band at 1450 cm^{-1} and weak-intensity absorption band at 1380 cm^{-1} are due to aliphatic C-H bonds (Brown, 1955a; Friedel and Queiser, 1956; Brooks *et al.*, 1958a; Kinney and Douchette, 1958; Bent and Brown, 1961; Friedel, 1966). The weakness of the 1380 cm^{-1} band has been interpreted as showing a paucity of $-CH_3$ groups (Friedel and Queiser, 1956; Brooks *et al.*, 1958a; Bent and Brown, 1961). The relative intensities of these absorptions were almost constant throughout the rank range investigated.

A broad band of absorption, generally of rather weak intensity, between 1300 and 1000 cm^{-1} is generally assigned to various C-O functions, although specific assignments are difficult, owing to the diffuse nature of the absorption (Cannon and Sutherland, 1945b; Brown, 1955a; Friedel and Queiser, 1956; Roy, 1957).

Absorption bands due to aromatic groups occurred in the 900 to 700 cm^{-1} region of the spectra. All the vitrinites showed three weak absorptions occurring at 860, 815 and 750 cm^{-1}. In the lower-rank samples, the 815 cm^{-1} band was slightly stronger than the other two, but at the higher-rank end of the series the bands were of approximately equivalent intensities. These bands have been interpreted both as a mean spectrum of polynuclear condensed aromatic systems (van Vucht *et al.*, 1955), and specific substitutional configurations on single benzene rings (Friedel and Queiser, 1956).

Sporinite

The samples used in the infra-red investigation of sporinites were concentrates from the Donibristle, Clowne, Shallow, High Hazles (Whitwell), Barnsley, Parkgate and Silkstone seams (Fig. 3).

FIG. 3. INFRA-RED SPECTRA OF SPORINITES

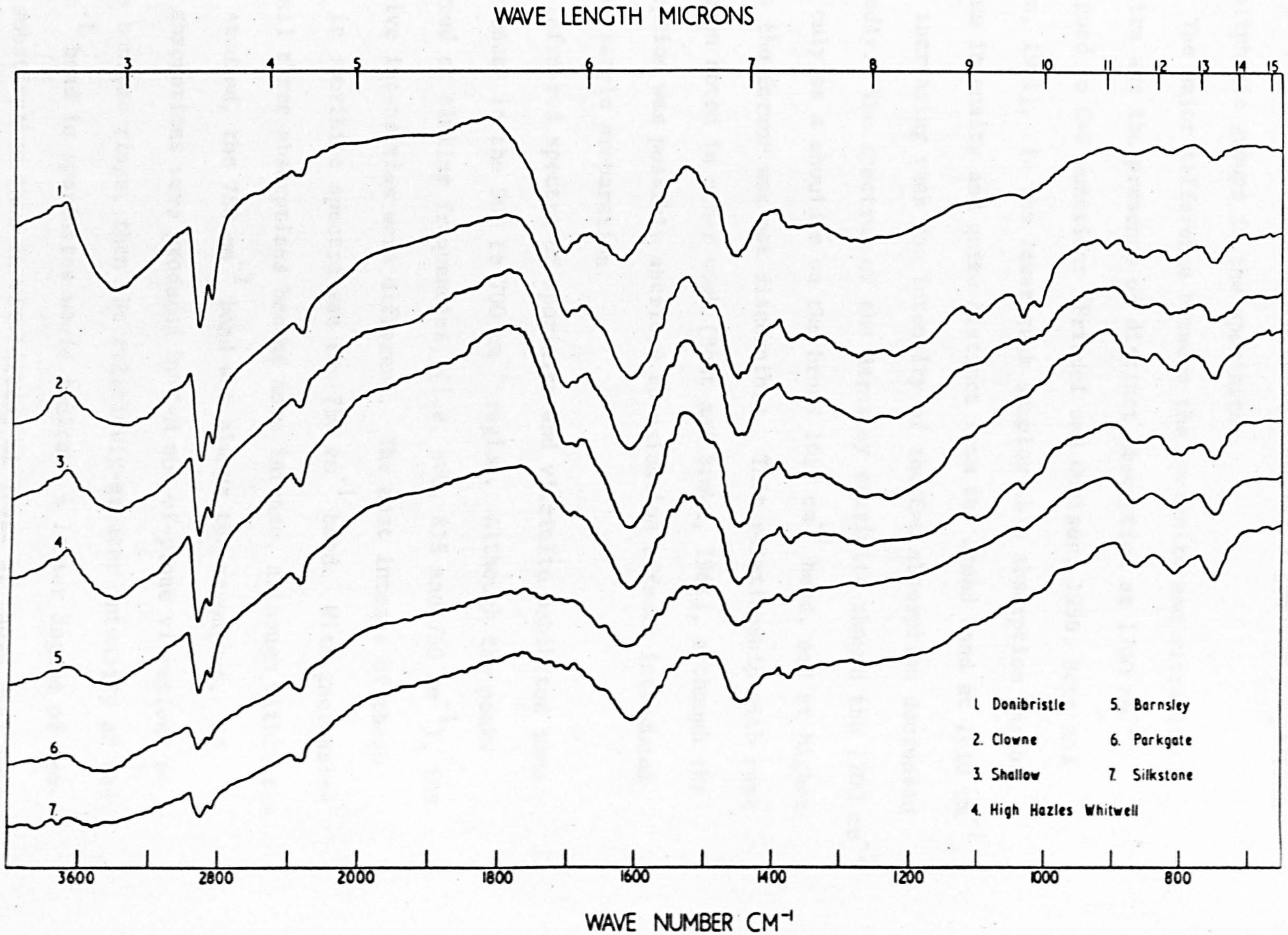

The spectra obtained ~~showed~~ a great similarity to the corresponding vitrinite spectra. Aliphatic C-H absorptions at 2920 and 2860 cm^{-1} were more intense than in the vitrinites, especially in the lower-rank samples, which could indicate a greater proportion of aliphatic groups in the sporinites.

The major difference between the sporinite and vitrinite spectra was the presence of distinct absorption at 1700 cm^{-1}, assigned to C=O functions (Friedel and Queiser, 1956; Bent and Brown, 1961). In the lower rank samples this absorption was of medium intensity and quite distinct from the broad band at 1610 cm^{-1}. With increasing rank the intensity of the C=O absorption decreased markedly. The spectrum of the Barnsley sporinite showed the 1700 cm^{-1} band only as a shoulder on the broad 1610 cm^{-1} band, and at higher ranks the former was not discernible. This relationship with rank has been noted in other work (Bent and Brown, 1961), although the absorption was possibly ascribed to oxidation effects introduced during sample preparation.

Infra-red spectra of sporinite and vitrinite exhibited some differences in the 900 to 700 cm^{-1} region. Although the peaks occurred at similar frequencies, (i.e. 860, 815 and 750 cm^{-1}), the relative intensities were different. The most intense of these peaks in sporinite spectra was the 750 cm^{-1} band. With increasing rank all three absorptions became more intense, although within the range studied, the 750 cm^{-1} band was always the strongest. If these absorptions were produced by C-H out-of-plane vibrations on single benzene rings, then the relatively-greater intensity of the 750 cm^{-1} band in sporinites would indicate a lesser degree of aromatic substitution than in vitrinites, at least at these rank levels.

<u>Resinite</u>

Infra-red spectra of the three resinites were obtained (Fig. 4) and were quite different to those of vitrinite and sporinite, most notably in the absence of any absorption at *ca.* 1600 cm^{-1}. However, the samples used all were below bituminous rank, and the spectra of resinites of bituminous coals do show this absorption (Murchison, 1966).

The resinites used in this work all showed strong- to medium-intensity absorptions at 2920, 2860, 1460 and 1375 cm^{-1}, due to aliphatic C-H bonding, but there was little evidence of aromatic structures. Bitterfeld resinite produced a weak absorption band at 888 cm^{-1}, and Maghara resinite produced a weak band at 812 cm^{-1}. Both of these absorptions may possibly be due to aromatic structures.

Strong-intensity C=O absorption in the 1740 to 1700 cm^{-1} region was present in all three spectra. In the spectrum of Maghara resinite this absorption was resolved into two peaks at 1698 cm^{-1}, possibly -COOH absorption (Brooks *et al.*, 1958a), and at 1723 cm^{-1}, with a shoulder at 1735 cm^{-1}. The 1735 cm^{-1} absorption may be ascribed to ester groups, while the 1723 cm^{-1} band may be due to aldehyde or ketone functions. Bitterfeld resinite produced maximum absorption at 1735 cm^{-1}, with a shoulder at 1720 cm^{-1}. Yallourn resinite showed a broad undifferentiated band of absorption in this region with a maximum at 1720 cm^{-1}.

The three resinites also exhibited more or less complex patterns of absorption between 1250 and 1000 cm^{-1} which can probably be ascribed to C-O groups and -OH functions. Strict allocations of these absorption bands would require elucidation by specific chemical and infra-red work.

Bitterfeld resinite produced only a very weak absorption due to -OH functions in the region of the spectrum above 3000 cm^{-1}, whereas the other two samples exhibited broad bands with maxima close to 3440 cm^{-1}.

FIG. 4. INFRA-RED SPECTRA OF RESINITES AND CUTINITE

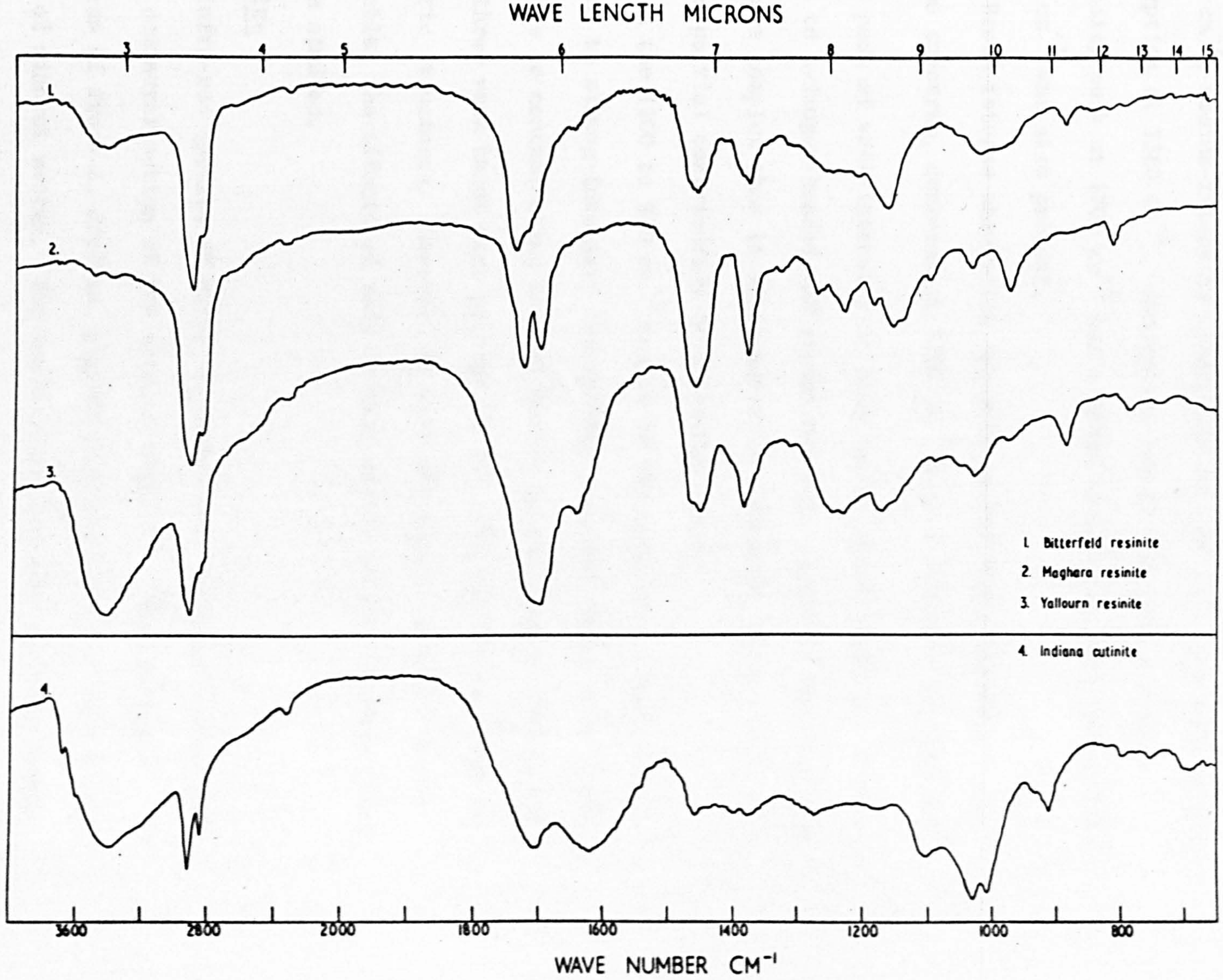

Cutinite

The sample of Indiana cutinite produced an infra-red spectrum (Fig. 4) rather similar to those of low-rank sporinites. Aliphatic C-H bonding was indicated by strong absorption bands at 2920 and 2860 cm^{-1}, medium-intensity absorption at 1460 cm^{-1} and weak-intensity absorption at 1380 cm^{-1}. Absorption due to C=O gave a strong-intensity peak at 1705 cm^{-1} and a broad absorption band centered at 1620 cm^{-1} was also present.

Broad intense absorption occurred at the short-wavelength end of the spectrum, centered at 3400 cm^{-1} with a shoulder at 3600 cm^{-1} and a peak of weak-intensity at 3680 cm^{-1}. These bands are attributed to hydrogen-bonded -OH groups and this region of the spectrum was more complex than in other macerals. However, there was probably a partial contribution from $KBr-H_2O$ bonds.

In the 1100 to 900 cm^{-1} region of the spectrum, a number of medium- to strong-intensity absorptions occurred, which were probably due to contaminating mineral matter in the sample. Below 900 cm^{-1} three weak bands were present at 797, 752 and 692 cm^{-1} due to aromatic structures. However, as only one sample of cutinite was available, the effects of rank in this region of the spectrum could not be studied.

Alginite

Infra-red spectra of three alginites were recorded before and after demineralisation of the samples (Fig. 5). The infra-red spectrum of fresh S. African alginite indicated very little evidence of mineral matter. The spectrum of the demineralised sample showed only minor differences in the loss of weak-intensity absorptions between 1120 and 925 cm^{-1}

The spectra of New South Wales and Scottish alginites originally showed intense absorption bands in the range 1250 to 750 cm^{-1},

FIG. 5. INFRA-RED SPECTRA OF ALGINITES

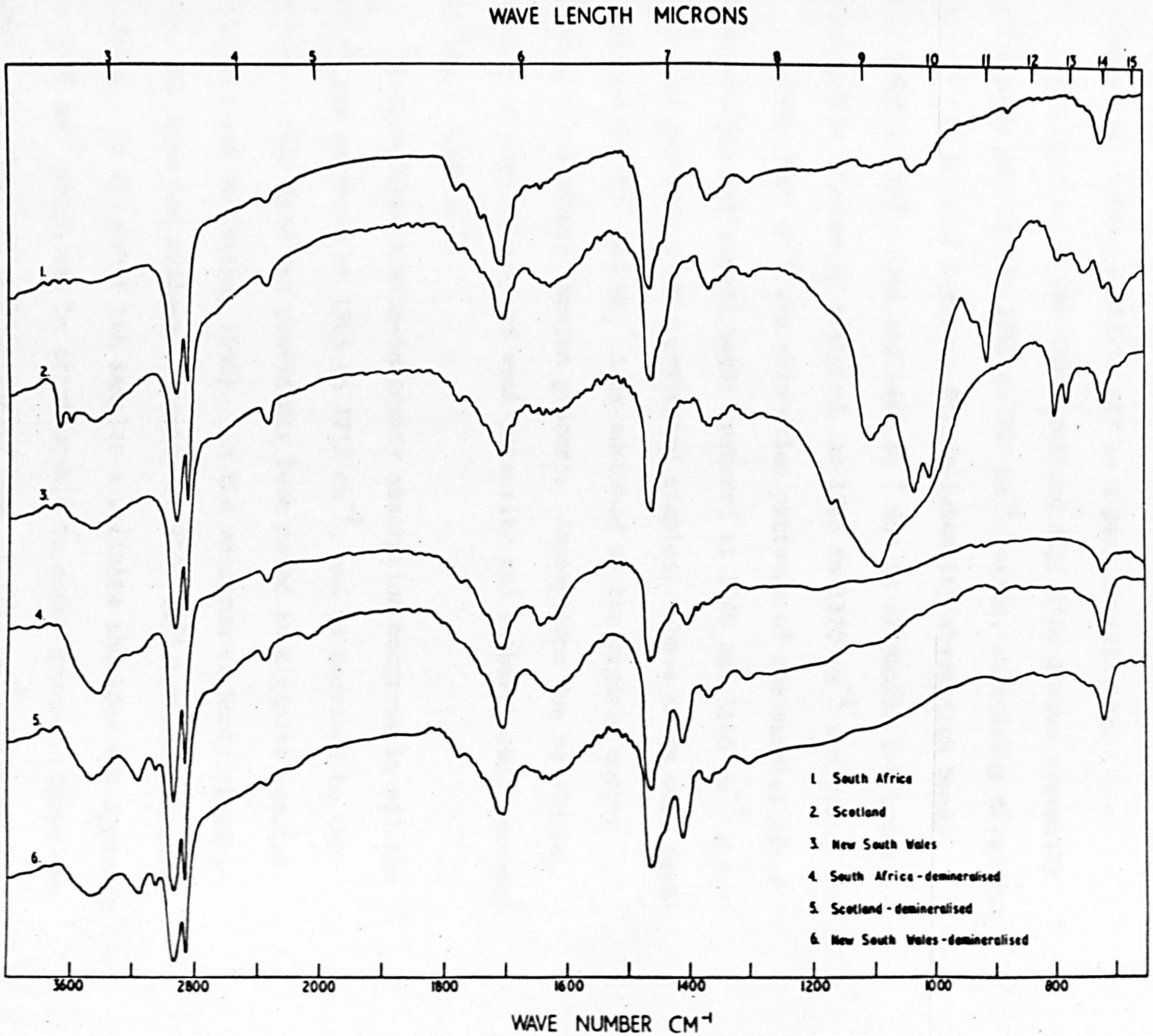

ascribed to inorganic material. These bands were not present in the spectra of the demineralised samples. The absorptions ascribed to mineral matter in fresh Scottish alginite corresponded closely with the spectrum of kaolinite (Millais and Murchison, 1969). The mineral matter absorptions in New South Wales alginite were less definitive, although illite may be a part contributor.

The spectra of the demineralised alginites showed virtually no absorptions in the 1250 to 750 cm^{-1} region, indicating effective removal of mineral matter. Strong-intensity absorption bands occurred at 2920, 2860 and 1460 cm^{-1} due to aliphatic C-H bonds. Absorption, similarly assigned, at 1365 to 1370 cm^{-1} was weak.

Above 3000 cm^{-1} the absorption patterns of the samples after demineralisation showed bands centered at 3040 and 3160 cm^{-1} which were not apparent in the untreated samples. These bands were probably due to $-OH^-$ and NH_4^+ ions adsorbed by the organic matter during the demineralisation process. Absorptions due to -OH in untreated samples were of weak-intensity and rather broad, centered at about 3460 cm^{-1}.

Rather broad medium-intensity absorption occurred in all the alginites centered at 1705 to 1710 cm^{-1}, and is ascribed to C=O groups. This band has previously been noted in alginite spectra (Millais and Murchison, 1969). In the spectrum of Scottish alginite the band had maximum intensity at 1703 cm^{-1} but was otherwise diffuse. In the other two samples a definite shoulder was apparent at 1735 cm^{-1} which may be attributable to ester groups. There was also a superimposed weak-intensity band at 1775 cm^{-1} which is of unknown derivation.

Only Scottish alginite showed an absorption band near 1600 cm^{-1}, which was observed in all the spectra of vitrinite and sporinite. In this sample the maximum absorption was at 1625 cm^{-1} and the band was of weak-intensity. Assignments of this band have been previously discussed. The other two alginites showed more specific absorptions, although very weak, between 1660 and 1630 cm^{-1}, which may be assigned to C=C functions. These differences may be attributable to the samples being of lower rank, but the rank differences are small. Generally, however, there was little evidence of unsaturated bonds in the spectra, other than a very weak band at 880 cm^{-1} in New South Wales alginite and at 895 cm^{-1} in Scottish alginite.

A medium-intensity absorption band at 720 cm^{-1} was common to all three samples. In view of the lack of evidence for aromatic functions and the strong absorptions at other wavenumbers for aliphatic C-H, this band is probably due to $-(CH_2)_n$-chains, where $n \geq 4$ (Nakanishi, 1964).

The presence of carbonyl absorptions in the alginites is thus now a common factor of all the low-rank exinite macerals examined and is the most notable difference between the exinite and vitrinite maceral groups. Modern resins are known to contain variable proportions of acidic and neutral material which is susceptible to polymerisation when deposited in a sediment (Thomas, 1969; Brooks and Steven, 1967). The polymerisation of acid- and ester-containing materials has been variously proposed for the origin of sporinite (Brooks and Shaw, 1968a), cutinite (Neavel and Miller, 1960) and alginite (Dulhunty, 1944). Infra-red spectroscopy of these macerals certainly indicated the presence of carbonyl functions at low rank levels, and, in the case of sporinite, a reduction of these groups with increasing coalification.

Spurious absorptions in the infra-red spectra of the three alginites were noted after demineralisation. There was a medium-intensity band at 1410 cm^{-1} which may be attributed to NH_4^+ or CO_3^{--} ions (Nakanishi, 1964). In view of other weaker spurious absorptions between 3300 and 3000 cm^{-1}, adsorption of NH_4^+ during demineralisation was the more likely source. Continued washing of one sample by refluxing in hot water reduced the intensity of the 1410 cm^{-1} band, but failed to eliminate it. Washing with hot dilute hydrochloric acid followed by hot water effected the removal of the spurious bands between 3300 and 3000 cm^{-1}. The lower (1410 cm^{-1}) band was again relatively weaker in intensity and had shifted to 1405 cm^{-1}. It would seem that the presumed NH_4^+ ions were strongly adsorbed on the organic matter and rather vigorous treatment would be required to remove them. This would introduce the risk of chemical alteration of the organic matter.

Experimental

Sporinite concentration

The method employed to produce sporinite-rich concentrates from selected durains has been outlined earlier in this chapter. The complete experimental details of the separations are given in Table 4. Each sample was fractionated once by a density separation in zinc chloride solution of S.G. 1.30 to produce "floats" and "sinks" fractions. This step was identical for each sample and, as such, has been omitted from Table 4, where it is understood that the detailed separations in zinc chloride solution of S.G. 1.25 follow the separation at S.G. 1.30.

Preparation of samples for microscopical examination

The constitutions of the various sieved fractions, of the products of the successive heavy liquid separations, and of the final maceral concentrates were determined by microscopical examination. Samples were mounted in Bakelite resin and first ground on wet 220- and 600-grades carborundum paper, successively. This was followed by relief-polishing on rotating "Selvyt" cloth laps, using successively 5/20, 3/50 and "Gamma" polishing alumina.

When a rapid cursory examination was required, a portion of sample was mixed on a microscope slide with melted "Santolite" resin (m.p. 62°C). This solidifies immediately on cooling, and can be rapidly relief-polished in a similar manner to Bakelite resin.

Microscopical examinations were carried out under oil immersion (R.I. immersion oil 1.516). If point-counts were being carried out, a magnification of x500 was used. In other cases where only a visual check was required, a magnification of x200 was used.

Infra-red spectroscopy

Infra-red spectra were recorded using a Hilger and Watts Infrascan Mk. 2 H900 Recording Infra-red Spectrophotometer. The recording

Table 4: Experimental details for the sink/float concentration of sporinites

Sample	Size (B.S. mesh)	Weight (gm.)	Fractionation at S.G. 1.25* No. of steps:	Details	Final wt.** (gm.)
Donibristle	-240 to + 400	n.d.	1:	concentrate of high purity achieved immediately.	40.0
High Hazles (Gedling)	-240 to +400	352	2:	only 19 gm. "floats" obtained from first separation and "sinks" re-separated to recover a further 2.5 gm.	21.5
High Hazles (Warsop)	-240	*ca.* 1000	4:	successive separations carried out without further crushings.	70.0
High Hazles (Whitwell)	-240	*ca.* 1000	5:	successive separations carried out without further crushings	60.0
Clowne	-240	*ca.* 1000	2:	most material lost at first separation, as "sinks".	27.0
Shallow	-240	*ca.* 1000	1:	concentrate of high purity achieved immediately	55.0
Deep Hard	-240	900	8:	"floats" re-ground in disc mill after steps 1, 4 and 5 because of particle heterogeneity.	65.0
Beeston	-240	700-800	4:	successive separations carried out without further crushings.	56.0
Barnsley	-240	*ca.* 1000	3:	successive separations carried out without further crushings.	46.0
Silkstone	-240 to +400	399	9:	"floats" re-ground in disc mill after steps 3, 5, 6 and 7 because of particle heterogeneity.	41.1
Parkgate	-240	*ca.* 1000	7:	much difficulty found with this sample in removing inertinite. It appeared to flocculate but this was not confirmed by microscopy. After 7th step little sample left and process discontinued, but poor concentrate obtained. No further crushings were carried out as contaminating inertinite was in a free state mainly.	17.0

* The sink/float separations were constantly monitored by microscopical examination to determine if further crushing of samples was required to achieve particle homogeneity, or if contaminants were in a free state.

** Maceral analyses of all concentrates are given in Table 1.

chart was linear in wavenumbers between 4000 and 600 cm^{-1}. A transmission scale of 1:1 was used, with energy range 1 and a scan time of 8 minutes. Selected ranges of some spectra were also recorded with a transmission scale of 5:1 and energy range 2. The 1603 cm^{-1} absorption band of polystyrene film was used as a wavenumber standard.

The spectra were recorded using maceral dispersions in KBr discs, pressed under 15 tons/sq. in. for 10 minutes, the die being attached to a vacuum pump. For vitrinites and sporinites, a ratio of 1 mg. of maceral to 250 mg. of KBr was used, the two being ground in an agate mortar to achieve an intimate mix. The ratio for resinites, alginite and cutinite was 3 mg. maceral to 250 mg. KBr. The KBr was used directly from an oven maintained at *ca.* 120°C.

Demineralisation of alginites

The three alginite samples were demineralised by sequential digestion with hydrochloric and hydrofluoric acids (Forsman and Hunt, 1958). Digestion in hot concentrated HCl was carried out for 2 hours followed, after filtration and washing, with two 7 hr. periods of digestion with hot 40% HF. Following neutralisation of excess HF, samples were filtered and washed with hot 50% HCl and saturated NH_4OH solution to remove fluorides. Final washings with water were followed by oven-drying at *ca.* 45° under vacuum for 24 hours.

Chapter 2

Organic extraction of the maceral concentrates: aliphatic hydrocarbons.

Introduction

Extraction with organic solvents was the first step in the chemical investigation of the maceral concentrates. Although there are specific solvents which will dissolve large proportions of vitrinite and sporinite particularly, the resultant extracts closely resemble the original maceral in many respects, and there is little apparent direct information to be gained from them. One of the basic objects of this work was to study individual macerals both from the point of view of their respective structures as components of coal and also as organic constituents of sedimentary rocks, using the modern analytical techniques available to the organic geochemist. Conseqnently, common organic solvents were used for the extractions, but as later degradative work was to be carried out the extractions were run for considerable periods of time to remove as much as possible of the soluble organic matter, in the accepted sense of the term. The extracted residues could then be regarded as individual contributors to sedimentary kerogens of terrigenous origin, and the results obtained from the degradations could be interpreted with respect to changes occurring in the maceral matrices during diagenesis and also to changes which might occur in terrestrially-derived kerogens in sedimentary rocks.

Extraction

The vitrinite and exinite maceral concentrates were exhaustively extracted with an azeotropic mixture of chloroform, acetone and methanol (47%, 30% and 23% respectively) to provide total organic extracts. The extracts of vitrinites, sporinites and cutinite were black, tarry gums, those of alginites were brown gums, while resinites yielded red to brown viscous liquids. The yields of extracts varied considerably between macerals, and for vitrinites and sporinites they also varied with rank. Extractibilities are given in Table 5. There was no definite correlation between extractibility and rank, although in general terms it showed an overall decrease with increasing rank (Fig. 6). This is partly in agreement with Dryden (1963) who reviewed data on coal extractibility. For benzene-type solvents he concluded that there was a rapid decline in extractibility above 88.9% C, but at lower ranks no definite relationship existed. For pyridine-type solvents it decreased at the high rank end of the coalification series, while at lower ranks yields were variable. These generalisations would seem to be more applicable to vitrinite than sporinite with respect to the samples used in the present work.

An investigation of coals from the Saar district of Germany showed a direct relationship between rank and diethyl ether extracts, with yields reaching a maximum at a rank of *ca*. 30% volatile matter (Leythaeuser and Welte, 1969). This is at a rank equivalent to *ca*. 86% C in vitrinite on a dry, ash-free (d.a.f.) basis. However coal is a chemically-complex material and many non-specific solvents will produce an extract that is not representative of the whole of the coal structure. Hence relationships between extractibility and rank should be viewed with some care.

Table 5 shows that there was considerable variation of extractibilities of the alginites, resinites and cutinite. The latter sample produced an extract of a similar order to that of a low rank sporinite. Alginites yielded very low amounts, while resinites proved to be exceptionally soluble.

The fractionation scheme used to isolate aliphatic hydrocarbons and carboxylic acids from the total extracts is shown in Fig. 7. Complete experimental details are given at the end of the relevant chapters.

Table 5: Yields of organic extracts from the maceral concentrates

	Extractibility (mg/gm)
Vitrinite	
High Hazles Gedling	91.3
Westfield	100.6
Clowne	145.3
Shallow	147.5
High Hazles Warsop	130.4
Deep Hard	95.2
High Hazles Whitwell	111.2
Beeston	169.6
Barnsley	108.7
Parkgate	20.8
Silkstone	24.3
Sporinite	
Donibristle	44.5
High Hazles Gedling	63.3
Clowne	55.0
Shallow	55.6
High Hazles Warsop	41.5
Deep Hard	39.5
High Hazles Whitwell	48.4
Beeston	40.1
Barnsley	51.3
Parkgate	36.2
Silkstone	41.5
Alginite	
Scotland	5.9
South Africa	3.2
New South Wales	15.6
Resinite	
Yallourn	856.8
Bitterfeld	345.7
Maghara	535.1
Cutinite	
Indiana	79.6

FIG. 6. YIELDS OF ORGANIC EXTRACTS FROM VITRINITES AND SPORINITES

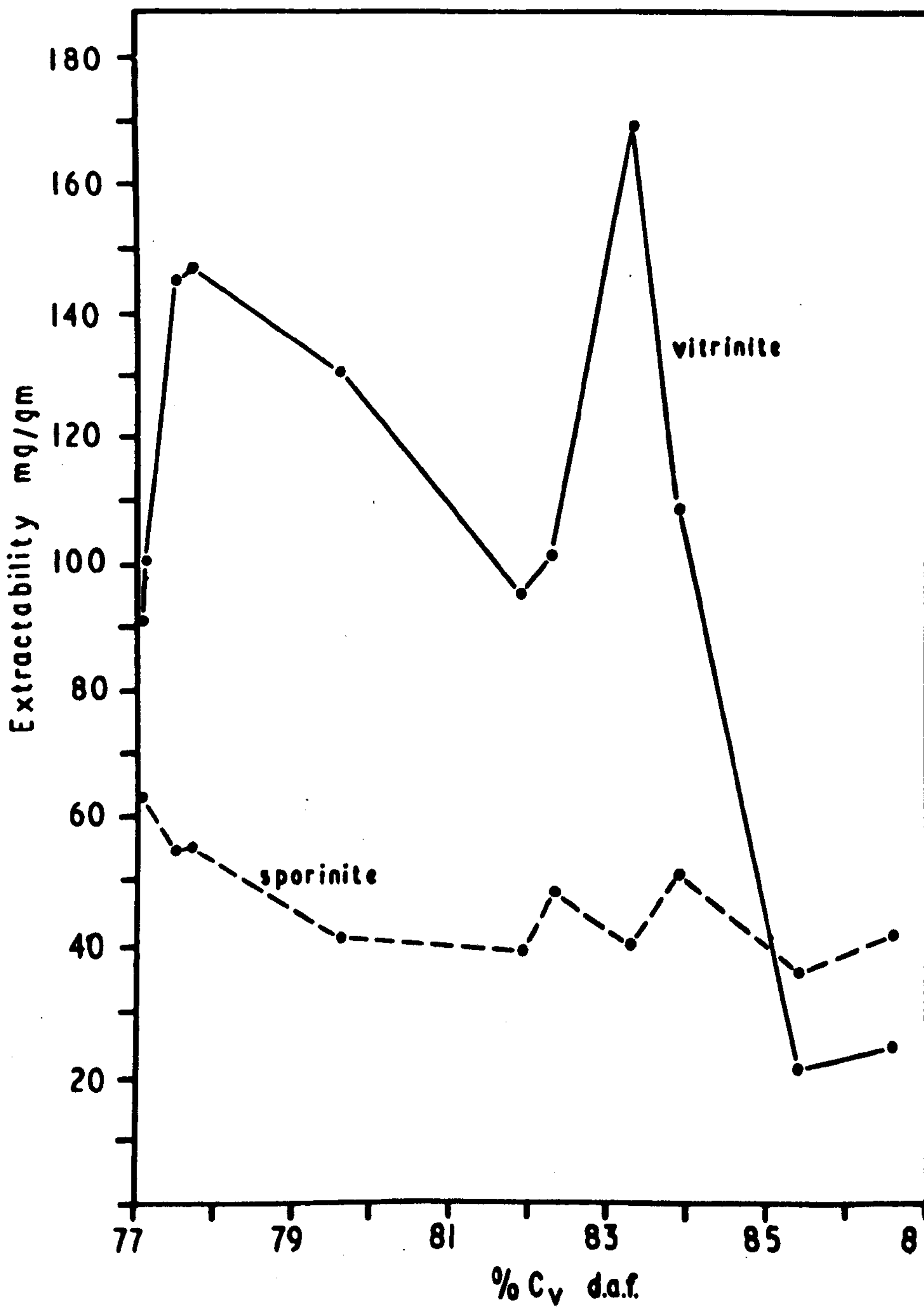

Fig. 7: Flow diagram for the extraction of maceral concentrates

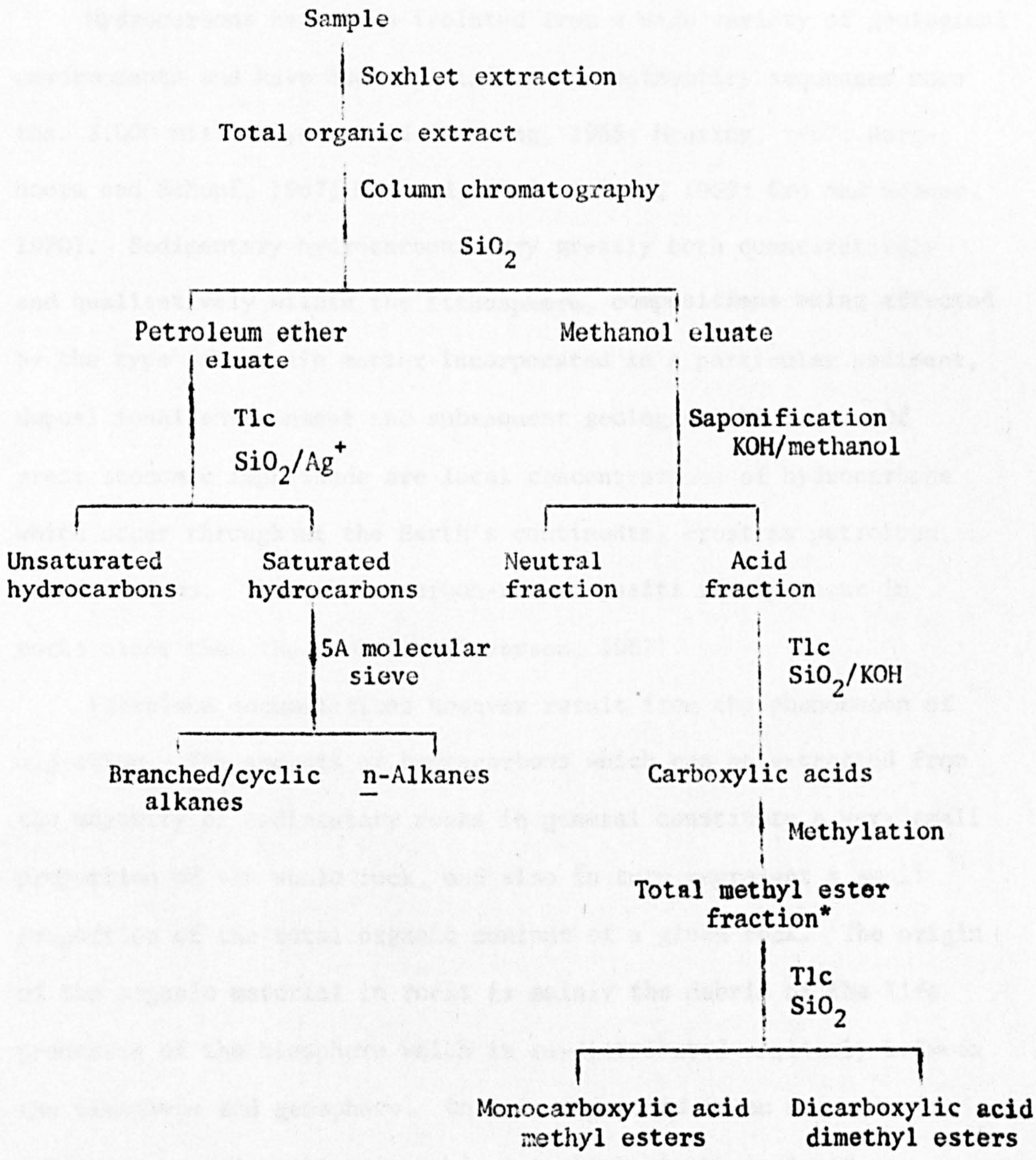

* The treatment of the total methyl ester fraction of resinite extracts differed from that for the other maceral extracts; full details are given in the relevant experimental section.

Hydrocarbons

Introduction

Hydrocarbons have been isolated from a wide variety of geological environments and have been identified in sedimentary sequences more than 3,000 million years old (Hoering, 1965; Hoering, 1967; Barghoorn and Schopf, 1967; MacLeod, 1968; Calvin, 1969; Oro and Nooner, 1970). Sedimentary hydrocarbons vary greatly both quantitatively and qualitatively within the lithosphere, compositions being affected by the type of organic matter incorporated in a particular sediment, depositional environment and subsequent geological history. Of great economic importance are local concentrations of hydrocarbons which occur throughout the Earth's continental crust as petroleum accumulations. These hydrocarbon-rich deposits rarely occur in rocks older than the Cambrian (Leverson, 1967).

Petroleum accumulations however result from the phenomenon of migration. The amounts of hydrocarbons which can be extracted from the majority of sedimentary rocks in general constitute a very small proportion of the whole rock, and also in turn represent a small proportion of the total organic content of a given rock. The origin of the organic material in rocks is mainly the debris of the life processes of the biosphere which is re-distributed variously between the biosphere and geosphere. Once incorporated in an accumulating sediment, organic matter is subject to both biochemical and geochemical degradation, the former terminating when the sediment is sufficiently buried to produce a sterile environment. The ultimate products of geochemical action are considered to be methane and a metamorphosed residue which is ingested into the mantle.

The origin of sedimentary hydocarbons is a subject of great interest in organic geochemistry. As investigations continue, it is becoming apparent that many plants and animals biosynthesize aliphatic hydrocarbons, but the proportion produced is usually only a small part of the total lipid fraction of a particular organism. Thus there will be a direct input of hydrocarbons into sedimentary sequences which contain organic debris, but of these a variable proportion may be chemically and biochemically degraded in the early stages of sedimentation. However, sediments can often produce hydrocarbons, both naturally, and artificially in the laboratory, in quantities vastly in excess of the amount of the original hydrocarbon input. Therefore other sources must exist in the organic material that are capable of generating hydrocarbons under geological conditions.

The aliphatic hydrocarbons in many living organisms have been investigated and certain broad distributional patterns are apparent, although by no means definitive. As this thesis is concerned with the organic geochemistry of coal macerals, it will be apposite to consider briefly the occurrence of hydrocarbon types in biological materials that become incorporated into coals.

Hydrocarbons have been isolated from the surface waxes of many higher land plants. Waxes occur as surface coatings of the leaves, flowers, seeds and stems of most plants and they generally consist of a complex mixture of aliphatic long-chain hydrocarbons, acids, alcohols, esters and related compounds (Douglas and Eglinton, 1966). Both straight- and branched-chain alkanes, and unsaturated hydrocarbons, have been isolated from various plant waxes. This has been the subject of much research and two comprehensive reviews on the distribution of alkanes are available (Eglinton and Hamilton, 1963; Douglas and Eglinton, 1966). In general, higher plant-wax n-alkanes exhibit a predominance of odd carbon-numbered chain lengths, with a large proportion of the total n-alkane fractions lying between n-C_{25}

and n-C_{35}. Within this range the dominant homologues often are n-C_{27}, n-C_{29}, n-C_{31} and n-C_{33}, while the even-carbon numbered homologues are usually minor components.

There are also reports available indicating the occurrence of generally smaller amounts of lower molecular weight n-alkanes in higher plant tissues. The leaves of *Trifolium pratense* contain n-alkanes in the n-C_{15} to n-C_{25} range which show only a slight predominance of odd-numbered homologues (Weenink, 1962), while the internal lipids of *Spinacia oleracea* leaves contain n-C_{28} to n-C_{33} n-alkanes showing a typical higher plant distribution but, in addition, smaller amounts of n-C_{16} to n-C_{28} n-alkanes which have a smooth distribution (Kaneda, 1969). Herbin and Robins (1969) have stated that where n-alkanes form only a small proportion of the lipids of leaf cuticular waxes, the preference of odd- over even-numbered homologues tends to disappear.

Tubers of *Dioscorea deltoidea* contain a low proportion of n-C_{19} to n-C_{35} n-alkanes in the external lipids which show an odd-dominated distribution between n-C_{22} and n-C_{29}, but the distributional maximum lies at n-C_{21}. The combined external and internal lipids have a maximum at n-C_{19} (Hardman and Brain, 1971). Analyses of the lipids of several woods have shown the occurrence of smooth distributions of n-alkanes up to n-C_{35} (Cocker and Shaw, 1963; Cocker *et al.*, 1965; Grice *et al.*, 1968), and typical odd-dominated higher n-alkane patterns with lesser amounts of lower molecular weight homologues showing smooth distributions (Del Castillo *et al.*, 1967).

The wax n-alkanes of many lower plants contain relatively high amounts of lower molecular weight n-alkanes in the n-C_{15} to n-C_{23} range which have almost smooth distributions (Stransky *et al.*, 1967).

Branched alkanes isolated from higher plants are usually present in small amounts compared to the n-alkanes. However, in the wax of *Plantago ovata* seeds the anteiso-C_{18} hydrocarbon was the most abundant single constituent and constituted 10% of the total hydrocarbon fraction (Gelpi *et al.*, 1969). Tobacco leaf wax has been shown to contain odd-numbered iso-alkanes in the C_{27} to C_{33} range with iso-C_{31} as the major component of the homology, as well as even-numbered anteiso-alkanes in the C_{28} to C_{34} range, with anteiso-C_{32} as the major component (Mold *et al.*, 1963).

Iso- and anteiso-alkanes are known to be present in a number of leaf waxes, and a number have been identified in the C_{13} to C_{33} range (Eglinton and Hamilton, 1967). In natural waxes it has been generally concluded that iso-alkanes contain an odd number of carbon atoms while anteiso-alkanes contain an even number (Wollrab *et al.*, 1967). Monomethyl-branched hydrocarbons, other than iso- or anteiso-alkanes, have also been identified in natural plant waxes (Stransky and Streibl, 1969).

Olefinic hydrocarbons also occur in plant lipids, the content varying between species and between individual plant parts. A review paper reports the occurrence of three types of olefins in plant waxes, namely straight-chain terminal, probable branched chain, and cis- disubstituted olefins (Stransky and Streibl, 1969). Acyclic isoprenoid alkenes, usually polyunsaturated, are known. Apple wax has been shown to contain the C_{15} alkene farnesene (Murray *et al.*, 1964), and squalene, or an isomer, was isolated from seeds of *Balanites* sp. (Hardman *et al.*, 1970). Alkenes of carotenoid-type can be isolated from many plants where they are components of the pigments of flowers and fruits. Carotenes, especially β-carotene, also occur in plant photosynthetic tissues.

Mono-, sesqui- and diterpenoid hydrocarbons are minor components of plant resins which are often minor constituents of coals.

The resins are composed of esters, acids, alcohols, aldehydes and hydrocarbons, but normal or simple branched hydrocarbons have not been identified (Thomas, 1969).

Lower organisms are also contributors to coals. Algae are common but usually minor autochthonous coal constituents. Occasionally, however, algal-rich coals are found, often in association with normal bright coals, and algae are also contributors to the organic matter of many oil shales. Bacteria and fungi must proliferate in coal-forming swamps, and although morphological remains rarely are preserved, the metabolic products of these organisms will be ubiquitous minor contributors to the organic debris. Fungal spores, sclerotia and hyphae have been identified in coal.

Of particular relevance to coal studies are the analyses of the hydrocarbons of the fresh water alga *Botryococcus braunii*. This organism exhibits two distinct physiological states. In the brown resting state, *ca*. 76% of the dry weight of the alga was composed of hydrocarbons, the bulk of which was composed of two isomeric, multibranched, polyunsaturated olefins of empirical formula $C_{34}H_{58}$, termed botryococcene and iso-botryococcene (Maxwell *et al*., 1968). A structure has recently been proposed for botryococcene (Cox *et al*., 1973). In the green growing state, *ca*. 20% of the dry weight of the alga was extractable as hydrocarbons, less than 5% of which were botryococcenes. Analysis of these hydrocarbons showed that three homologies were present, two of which were of the general formula C_nH_{2n-2} (5 compounds) and C_nH_{2n-4} (4 compounds) (Knights *et al*., 1970). Laboratory polymerisation of *Botryococcus* algae by exposure to the air produced a rubbery material rather like coorongite, the presumed precursor of many torbanites. This can occur in both the green and brown states of the alga. A recent proposition is that coorongite, and hence torbanite, is the result of the polymerisation of the alkenes of the green growing state (Cane and Albion, 1973).

Olefins have been reported in the lipid fractions of other algae. Mono- and polyunsaturated n-alkenes of C_{17}, C_{19} and C_{21} chain lengths have been identified from a variety of marine algae (Blumer *et al.*, 1970; Youngblood *et al.*, 1971). Mono- and di-enoic n-C_{15} and n-C_{17} hydrocarbons are quoted as being common constituents of many marine algae (Youngblood *et al.*, 1971).

Broad recurring patterns are distinguishable in the distributions of n-alkanes which have been isolated from algal sources. Both marine and fresh water algal n-alkanes often contain n-C_{15} or n-C_{17} as the major component of the homology (Clark, 1966; Oro *et al.*, 1967; Stransky *et al.*, 1968; Han *et al.*, 1968a; Winters *et al.*, 1969). The total range of n-alkanes is quite variable between genera, but when longer chain (i.e. higher than n-C_{23}) homologues are present there is no marked preference for odd- or even-numbered chain lengths (Clark, 1966). This is in direct contrast to the distributions found in higher plant waxes. Simple branched alkanes have also been reported from algal sources (Han *et al.*, 1968a; Stransky *et al.*, 1968; Han and Calvin, 1970).

Hydrocarbons have been isolated from bacteria and fungi. n-Alkanes extracted from waxes of fungal spores show distributions similar to those of higher plant waxes (Oro *et al.*, 1966; Laseter *et al.*, 1968). Branched chain hydrocarbons have also been reported as fungal lipid constituents (Weete, 1972). Bacterial hydrocarbons are often complex mixtures of normal, branched, saturated and unsaturated isomers (Weete, 1972). However, few analyses are available from which general deductions can be made. The n-alkanes of *Desulphovibrio desulphuricans* showed a smooth distribution in the C_{25} to C_{35} range with a maximum at n-C_{29} (Davis, 1968). However the relative compositions of cultured bacterial lipids can be affected by the nature of the culture medium (Tornabene *et al.*, 1967). In this respect, it has been demonstrated that the n-alkane patterns of higher plants may show variations between identical species collected at different localities (Stransky *et al.*, 1967). It has been suggested that photosynthetic and non-photosynthetic bacteria may show distributionally different n-alkane patterns (Han *et al.*, 1968b; Calvin, 1969).

Biological alkane patterns, generally of the predominantly odd higher plant type, can often be recognised in extracts of Recent sediments, older sediments which have had a mild thermal history, peats and low rank coals. As maturation proceeds the indigenous hydrocarbons become less dominant in the total distribution as a secondary generation of hydrocarbons proceeds, producing a decrease in the predominance of odd-numbered n-alkanes and in the average molecular weight of the hydrocarbon fractions.

Coal is a material sensitive to change under progressive diagenesis, and the hydrocarbon patterns obtainable from coals of various rank levels provide evidence of these changes. Hydrocarbons have been isolated from many brown coals which are of commercial interest because of the "montan wax" which can be extracted from them. The n-alkane constituents of montan waxes generally show a predominance of odd- over even-numbered carbon chains in the higher molecular weight range (Wollrab *et al.*, 1962; Maxwell, 1967; Wollrab and Streibl, 1969; Dungworth, 1972). n-Alkanes showing a smooth distribution in the n-C_{23} to n-C_{33} range were isolated from an unspecified montan wax (Edwards *et al.*, 1963) but the method of isolation of the wax was not given, and in view of the other evidence this result may be erroneous.

Branched and cyclic alkanes and unsaturated hydrocarbons have been reported as montan wax constituents. Cyclic di- and triterpenoid alkanes have been isolated from Czechoslovakian lignites (Maxwell, 1967) and from Bovey Tracey lignite (Dungworth, 1972), while simple branched alkanes have been reported from a Bohemian lignite (Wollrab and Streibl, 1969). Neither pristane nor phytane have been identified from soft brown coals but the presence of C_{15}, C_{18} and C_{19} acyclic isoprenoid hydrocarbons in low-temperature brown coal tar has been noted (Kochloefl *et al.*, 1963). Simple straight-chain olefins, of probable direct plant origin, in the range C_{11} to C_{40}, have been isolated from Bohemian lignite along with trace quantities of branched unsaturated hydrocarbons (Wollrab and Streibl, 1969).

During the course of progressive coalification from brown coal through bituminous coal to anthracite, thermal maturation produces quantitative and qualitative changes in the organic extracts of coals. In a study of Australian coals ranging from low (66.6% C d.a.f.) to high (95.7% C d.a.f.) rank, n-alkane distributions in the C_{23} to C_{33} range were found to become smoother and, at the same time, show a continuous decrease in the average molecular weight of the mixture (Brooks and Smith, 1967). The rate of change of the hydrocarbon distribution was greatest in the soft-brown to sub-bituminous range. The samples used in the investigation were of quite diverse origins, including fossil wood, pollen-rich coals, vitrains and whole coals. Nevertheless, the results indicated that processes do occur, probably essentially thermally-controlled, which lead to progressive alterations in n-alkane distributions.

In a study of German coals ranging in rank from sub-bituminous to medium-volatile bituminous, the yield and distribution of n-alkanes could again be related to the degree of coalification (Leythaeuser and Welte, 1969). The samples used were of whole coals and petrographic variations led to some variability in results. The authors' findings were that the alkane contents of the diethyl ether extracts decreased progressively as the rank increased. The predominance of odd-numbered n-alkanes, in the range n-C_{23} to n-C_{29}, also progressively decreased while a relatively greater proportion of the series occurred below n-C_{23}. At the highest ranks studied, some of the samples showed a reversal of the trend towards lower average molecular weight.

In contrast, the alkane contents of acetone/dichloromethane extracts of bituminous coals of N.E. England exhibited a marked maximum at 85.2% C (calculated from the reflectivity of the vitrain) (Cooper, 1973).

Much information is available in the literature on the hydrocarbon types that can be extracted from coals or macerals, but the majority of analyses have been made on individual samples. n-Alkanes have been identified in extracts of vitrinite (Halleux and de Greef, 1963; Powell, 1969; Allan, 1970), vitrain-rich whole coal (Ouchi and Imuta, 1963; Vahrman, 1970), and spore-rich exinite (Kroger *et al.*, 1964; Powell, 1969; Allan, 1970). Acyclic isoprenoid alkanes have been identified in a variety of coals (Leythaeuser and Welte, 1969; Birkofer and Pauly, 1969; Powell, 1969; Vahrman, 1970). A relationship has been shown to exist in Australian coals correlating the relative concentrations of pristane and phytane with rank (Brooks *et al.*, 1969). Iso-alkanes have also been identified as coal components (Birkofer and Pauly, 1969; Vahrman, 1972), along with cycloalkanes (Vahrman, 1972). Gas-chromatographic-mass spectrometric identification of triterpanes from a vitrinite-rich coal has been made (Birkofer and Pauly, 1969) and recently, adamantane was identified for the first time in a bituminous coal extract (Ouchi and Imuta, 1973).

Unsaturated aliphatic hydrocarbons are not often quoted as bituminous coal constituents but their occurrence has been noted (Kroger *et al.*, 1964; Powell, 1969). Alk-1-enes and alk-2-enes have been reported from one particular coal (Spence and Vahrman, 1965; Vahrman, 1970). The general distribution of the alkenes was said to be similar to the corresponding n-alkanes, although they occurred in very much smaller quantities.

Aromatic hydrocarbons usually occur in coal extracts to a much greater extent than aliphatic hydrocarbons. However the complexity of these fractions makes identifications difficult. Nevertheless alkylated mono- and di-cyclic aromatic compounds and unsubstituted polycyclic aromatics have been identified (Ouchi and Imuta, 1963; Halleux and de Greef, 1963; Kroger *et al.*, 1964; Birkofer and Pauly, 1969; Vahrman, 1972).

Few analyses of the hydrocarbons of algal coals are available. A Scottish torbanite, of high-volatile bituminous rank, contained n-alkanes in the n-C_{12} to n-C_{37} range showing a smooth distribution and a maximum at n-C_{20}. Pristane and phytane were identified as branched alkane components (Maxwell, 1967; Douglas *et al.*, 1969b).

Coorongite, an intermediate stage in the formation of torbanite, has been shown also to contain n-alkanes in the n-C_{14} to n-C_{27} range, and these also showed a smooth distribution. Pristane, phytane and the C_{18} acyclic isoprenoid alkane were also identified. Alkenes were present in the lipid fraction of the coorongite and an homology of n-alk-1-enes ranging from C_{16} to C_{28} was identified (Maxwell, 1967).

Results

Total alkanes

A fraction containing alkanes only (total alkanes) was isolated from each maceral extract, except Yallourn resinite, and was examined by gas chromatography. Vitrinite, sporinite, cutinite and alginite alkanes were further separated into normal and branched/cyclic alkanes by 5A molecular sieve. Quantitative data for maceral alkanes are given in Table 6.

Gas chromatographic (gc) analyses of the total alkanes from vitrinites (Figs. 8 and 8a) and sporinites (Figs. 9 and 9a) showed that they all contained alkanes generally in the range n-C_{15} to *ca.* n-C_{33}. However the experimental methods employed in this work produced losses of lower-boiling components below about C_{15}, so that the lower limits of these distributions were experimentally and not naturally produced. Therefore, quantitative comparisons of results below C_{15} cannot be made. n-Alkanes were apparent up to *ca.* n-C_{30} in the gc traces of the total alkanes, and they showed distributional changes with increasing rank of the samples. Branched and cyclic components occurred bimodally, mainly in the sterane/triterpane region and below C_{20}, and these compounds also showed changes with increasing rank. Pristane was the major single component of the total alkanes throughout most of the investigated rank range. The distributions of normal and branched/cyclic alkanes from all the macerals are individually discussed below in more detail.

The total alkanes of Indiana cutinite (Fig. 10) had a bimodal distribution due to the occurrence of two distinct ranges of branched and cyclic compounds. n-Alkanes were however apparent between n-C_{16} and n-C_{29}. Pristane was again a dominant component.

Alginite total alkanes (Fig 11) had dissimilar distributions

Table 6: Alkanes isolated from the maceral concentrates

	Total alkanes (mg/gm)	n-Alkanes (mg/gm)	Branched/cyclic alkanes (mg/gm)	Alkanes/Extract %	b/c / n Alkanes
Vitrinite					
High Hazles Gedling	0.11	0.02	0.10	0.12	6.12
Westfield	0.14	0.02	0.11	0.14	6.94
Clowne	0.79	0.10	0.58	0.36	4.88
Shallow	0.12	0.02	0.07	0.08	4.93
High Hazles Warsop	0.17	0.03	0.09	0.13	3.03
Deep Hard	0.23	0.04	0.16	0.24	3.72
High Hazles Whitwell	0.10	0.01	0.07	0.09	7.00
Beeston	0.38	0.07	0.26	0.23	3.64
Barnsley	1.06	0.42	0.58	0.98	1.37
Parkgate	1.11	0.58	0.44	5.24	0.75
Silkstone	0.69	0.34	0.29	2.82	0.84
Sporinite					
Donibristle	0.22	0.02	0.15	0.49	8.06
High Hazles Gedling	0.68	0.06	0.56	1.10	9.00
Clowne	1.26	0.17	0.82	1.36	4.88
Shallow	0.34	0.04	0.21	0.61	5.55
High Hazles Warsop	0.38	0.05	0.23	0.93	4.30
Deep Hard	0.92	0.14	0.57	2.33	3.95
High Hazles Whitwell	0.77	0.19	0.56	1.60	2.99
Beeston	0.80	0.08	0.58	1.99	7.25
Barnsley	2.98	0.91	1.35	5.81	1.48
Parkgate	3.46	0.66	1.97	9.55	2.97
Silkstone	2.53	0.97	1.27	6.10	1.30
Alginite					
Scotland	1.96	0.63	0.85	33.28	1.36
South Africa	0.44	0.04	0.31	13.77	7.85
New South Wales	4.41	1.25	2.45	28.34	1.96
Cutinite					
Indiana	0.23	0.05	0.14	0.29	2.80
Resinite					
Yallourn	n.d.	n.d.	n.d.	n.d.	n.d.
Bitterfeld	0.09	n.d.	n.d.	0.03	n.d.
Maghara	10.11	n.d.	n.d.	1.85	n.d.

n.d. not determined

Fig. 8. Total alkanes of vitrinites

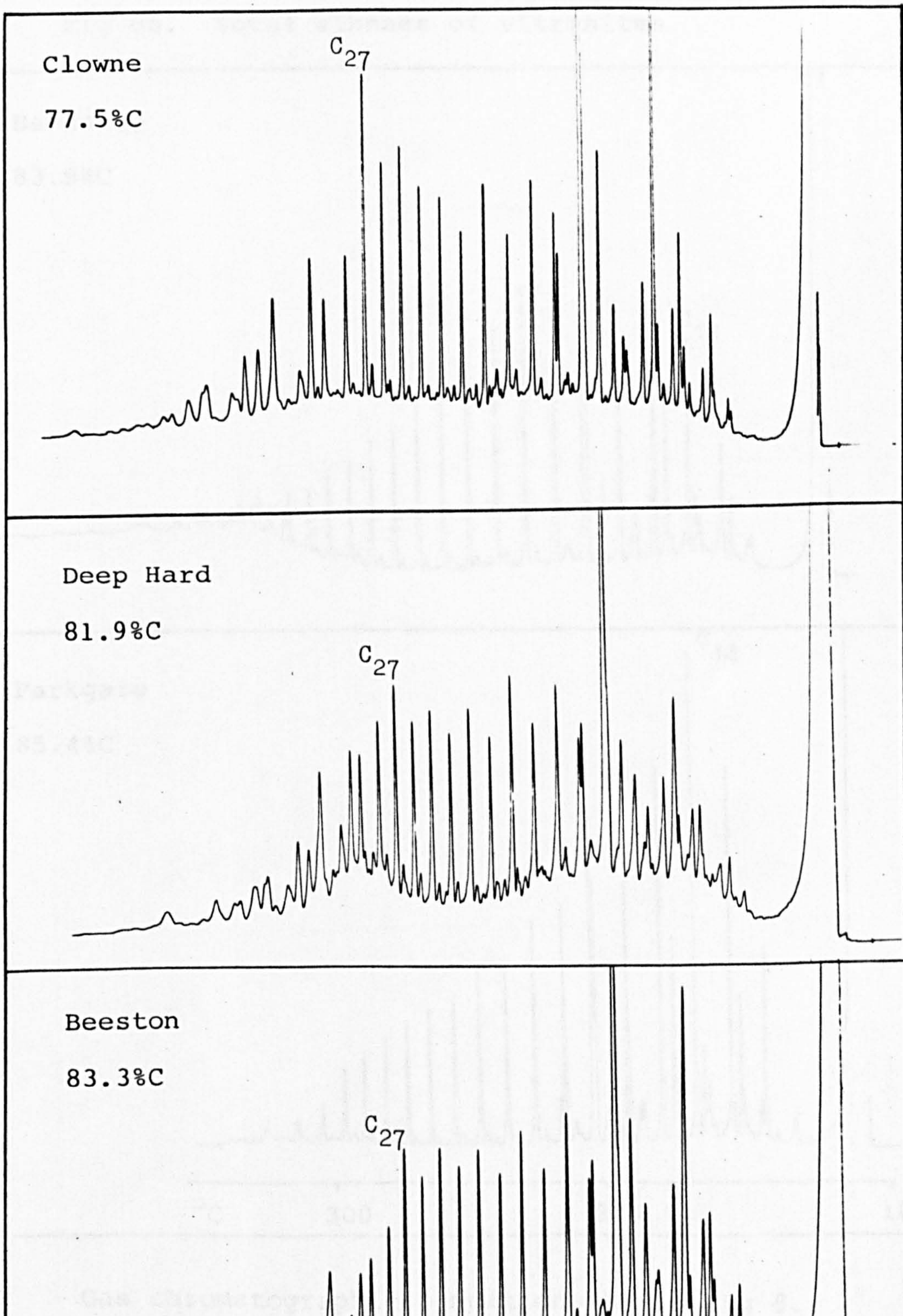

Gas chromatographic conditions: 20'x1/16"o.d. column containing 3% OV-1 on Varaport 30 (100-120 mesh); programmed 100-300°C at 4°/min; detector 290°; injector 300°; nitrogen 60 p.s.i.

Fig 8a. Total alkanes of vitrinites

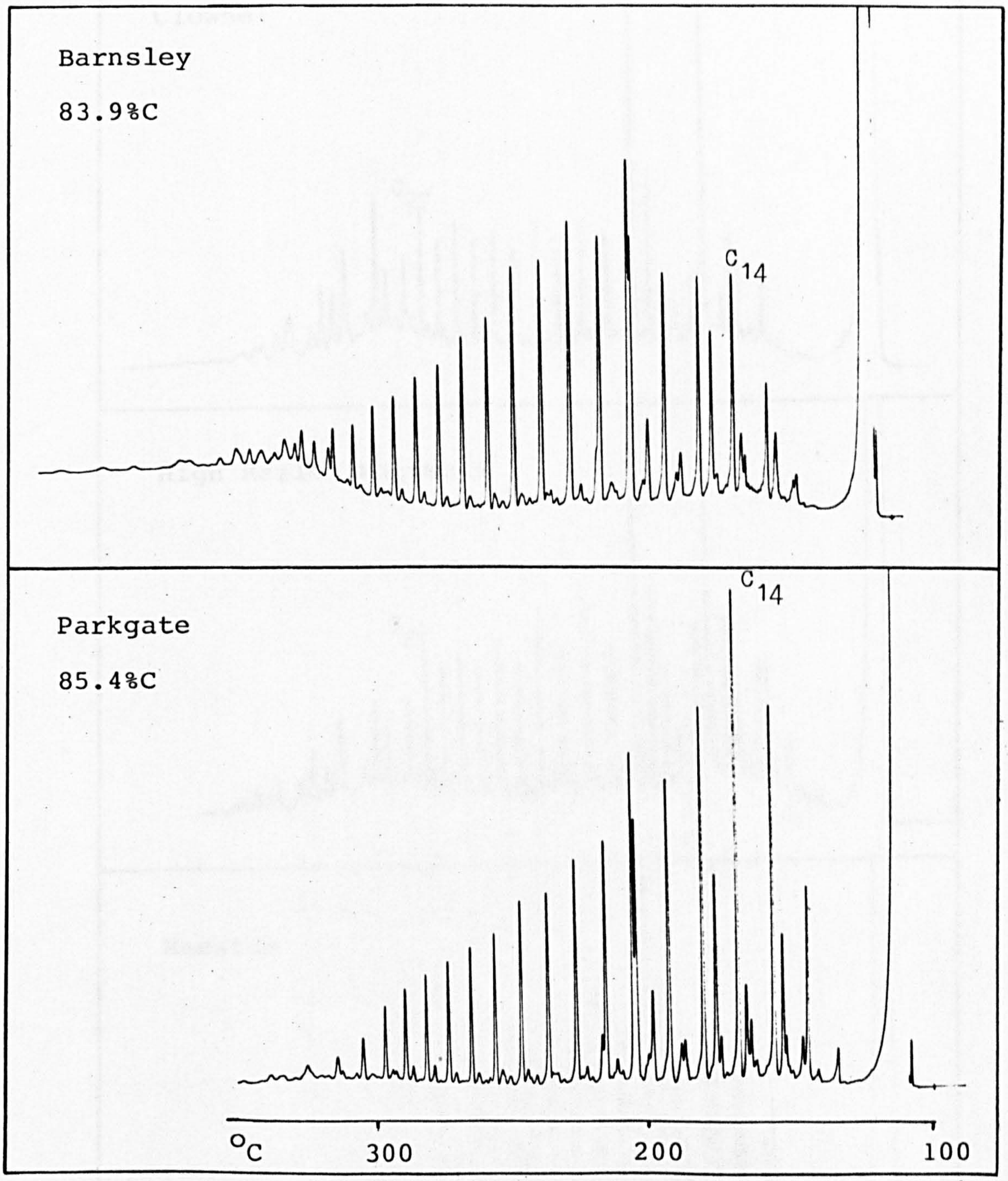

Gas chromatographic conditions as in Fig 8.

Fig. 9. Total alkanes of sporinites

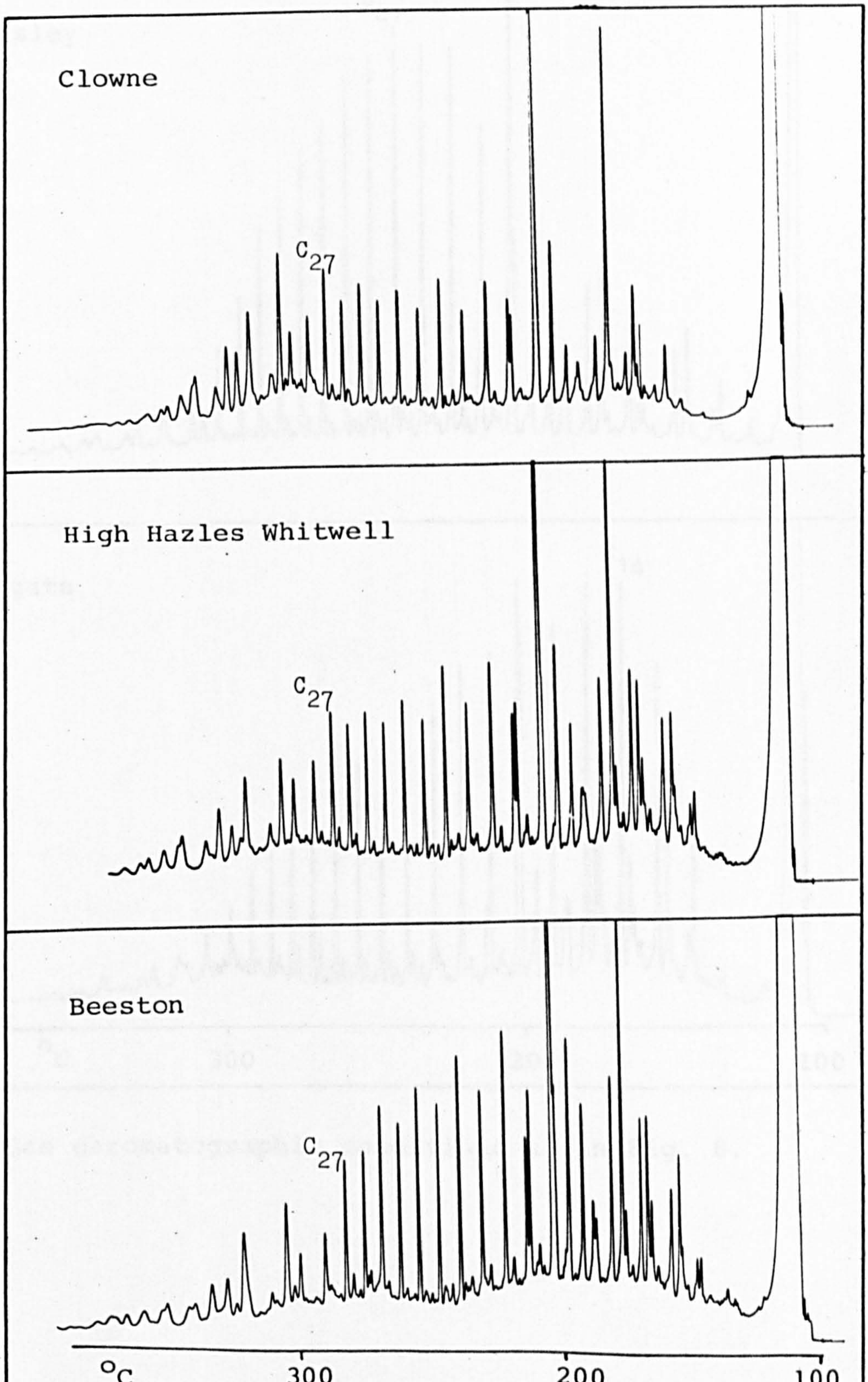

Gas chromatographic conditions as in Fig. 8.

Fig. 9a. Total alkanes of sporinites

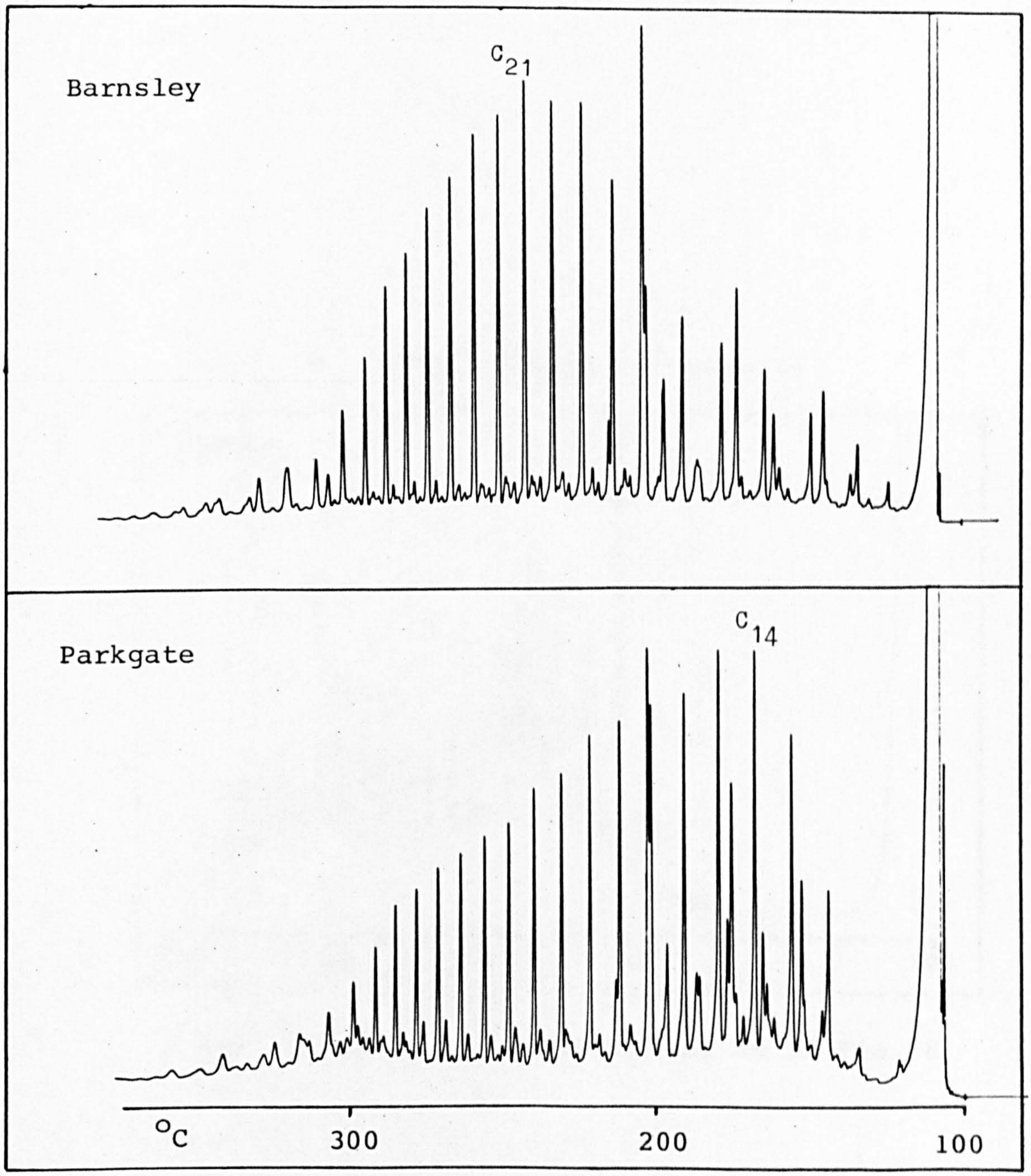

Gas chromatographic conditions as in Fig. 8.

Fig. 10. Total alkanes of cutinite

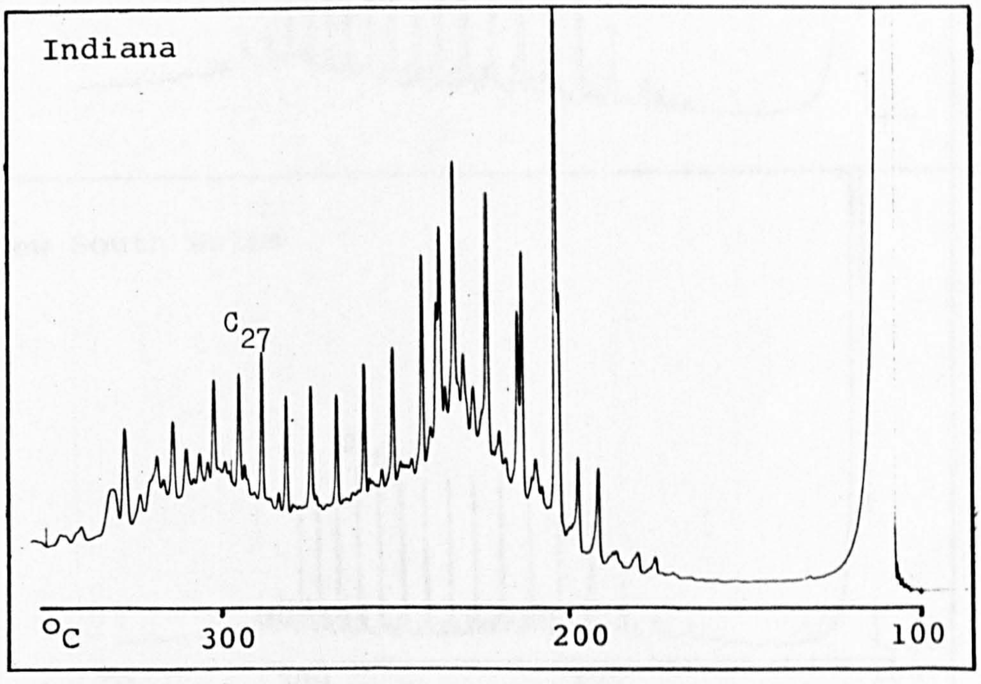

Gas chromatographic conditions as in Fig. 8.

Fig. 11. Total alkanes of alginites

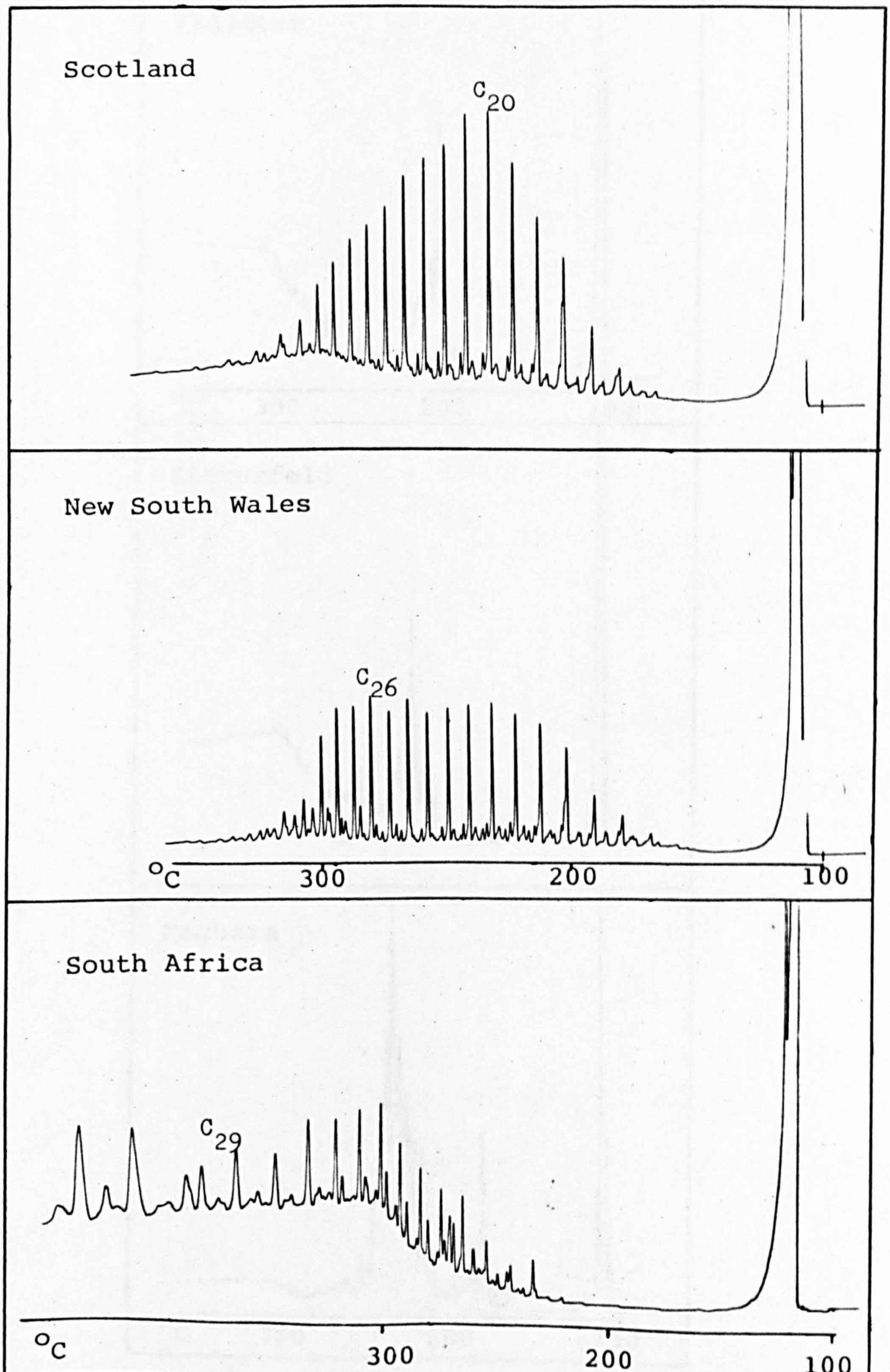

Gas chromatographic conditions as in Fig. 8, except for South African alginite where stationary phase was OV-101 (3%)

Fig. 12. Total hydrocarbons of Yallourn resinite and total alkanes of Bitterfeld and Maghara resinites

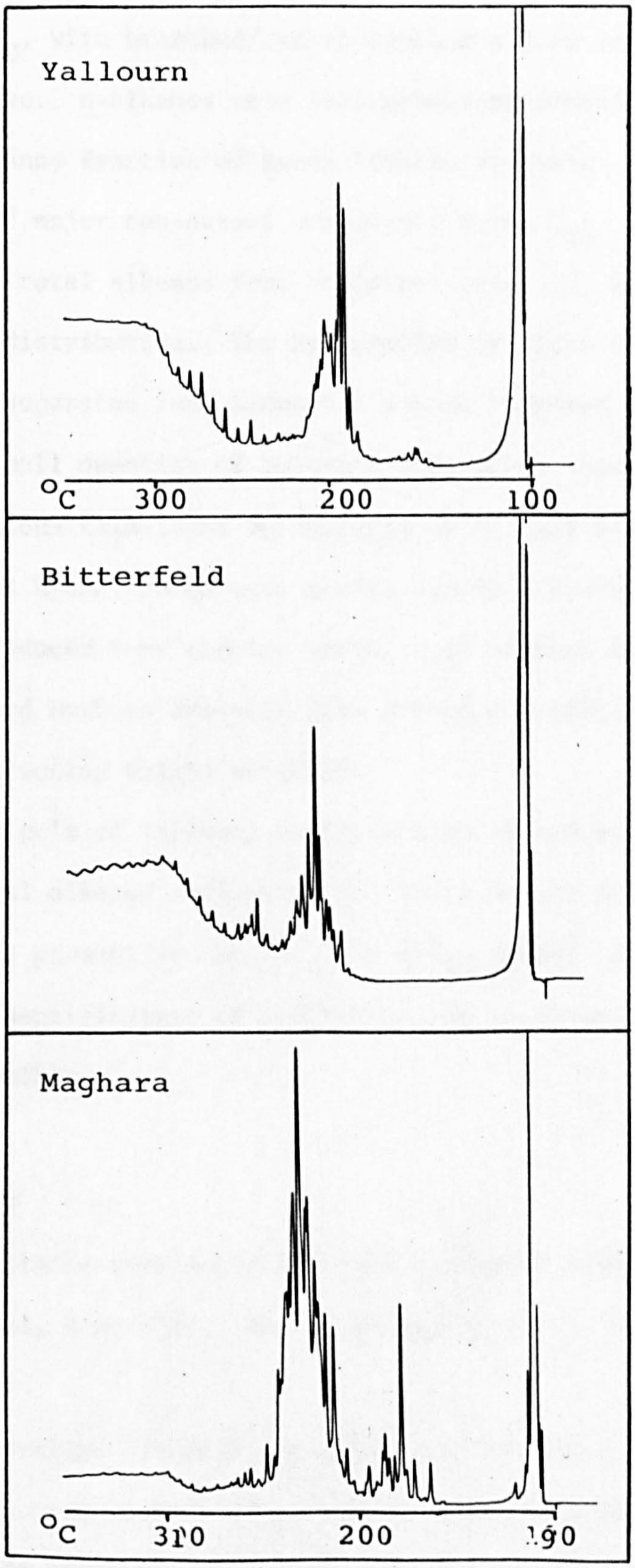

Gas chromatographic conditions: Yallourn-5'x1/8 "o.d. column containing 3% OV-101 on Varaport 30 (100-120 mesh) programmed 100-300°C at 6°/min; detector 300°; injector 300°; nitrogen 40 p.s.i; Bitterfeld and Maghara- as above except 6'x1/8" column programmed 90-310°C to those of vitrinite and sporinite. Scottish and New South Wales alginite alkanes were dominated by normal components between n-C_{15} and n-C_{30}, with branched/cyclic compounds also occurring throughout this range. n-Alkanes were less prominent constituents of the total alkane fraction of South African alginite, which produced a number of major non-normal components above C_{30}.

The total alkanes from resinites (Fig. 12) showed a third type of distribution. The hydrocarbon fraction of Yallourn resinite was not separated into saturated and unsaturated fractions because of the small quantity of material available. However analytical argentatious thin-layer chromatography of this sample showed that the total hydrocarbons were predominantly alkanes. All three resinites produced very complex mixtures of alkanes in the C_{16} to C_{22} range, and Maghara resinite also produced a small quantity of lower molecular weight material.

The gc's of Yallourn resinite total hydrocarbons and Bitterfeld total alkanes indicated that there may be small amounts of n-alkanes present in the n-C_{20} to n-C_{30} range. No previous reports of the identification of n-alkanes from resinites have been located by the author.

n-Alkanes

n-Alkanes were separated from the total alkane fractions of vitrinites, sporinites, alginites and cutinite, using 5A molecular sieve.

Generally, vitrinite n-alkane distributions (Figs. 13 and 13a) showing a predominance of odd-numbered homologues at lower ranks changed to ones that were much smoother at higher ranks. This is reflected in the carbon preference indices (CPI: Bray and Evans, 1961), measured in the range n-C_{23} to n-C_{33} and shown in Table 7,

Table 7: CPI* values of the maceral $\underline{n}$-alkanes

	CPI
Vitrinite	
High Hazles Gedling	1.56
Westfield	1.42
Clowne	1.28
Shallow	1.21
High Hazles Warsop	1.17
Deep Hard	1.21
High Hazles Whitwell	1.15
Beeston	1.20
Barnsley	1.08
Parkgate	1.04
Silkstone	1.07
Sporinite	
High Hazles Gedling	1.35
Donibristle	n.d.
Clowne	1.28
Shallow	1.14
High Hazles Warsop	1.05**
Deep Hard	1.17
High Hazles Whitwell	1.20
Beeston	1.18
Barnsley	1.04
Parkgate	1.04
Silkstone	1.02
Alginite	
Scotland	1.11
South Africa	1.26
New South Wales	1.14
Cutinite	
Indiana	1.12

* CPI's calculated by gc peak-height measurement in the range $\underline{n}$-C_{23} to $\underline{n}$-C_{33}.

n.d. not determined

** This value may be incorrect as the $\underline{n}$-alkane distribution obtained after treatment with 5A molecular sieve did not correspond to the apparent distribution in the total alkane chromatogram - there was an apparent reduction in the predominance of higher molecular weight odd-numbered homologues.

which can be seen to progressively decrease from 1.56 at low rank to almost unity at high rank. In the lower rank samples, n-C_{27} appeared as the major component, but with increasing coalification n-C_{21} became the major homologue. A general change was also evident in the average molecular weight distributions, which were predominantly high at lower ranks and predominantly low at higher ranks. In the two samples of highest rank, n-C_{16} and n-C_{19} were the major n-alkanes, but these lower molecular weight ranges are susceptible to preferential losses during laboratory procedures and the true maxima may be much lower. This preferential loss can be seen by comparing the n-alkane distribution of Parkgate vitrinite (Fig. 13a) with the apparent distribution of these components in the total alkane chromatogram (Fig. 8a) of the same sample.

Sporinite n-alkane distributions (Figs. 14 and 14a) showed changes of pattern with increasing rank generally similar to those observed in vitrinite n-alkanes. The major component changed from n-C_{29} at low rank to n-C_{21} at high rank, although these highest rank distributions have been severely affected by laboratory procedures (cf. Fig. 9a for the apparent distribution of n-alkanes in the total alkane chromatogram of Parkgate sporinite). The CPI values of the sporinite n-alkanes, again measured in the range n-C_{23} to n-C_{33}, changed from 1.35 at low rank to 1.02 at high rank, accompanied by a change to increasingly lower average molecular weight distributions.

n-Alkanes from the three alginites (Fig. 15) exhibited three different distributional patterns. South African alginite produced n-alkanes from n-C_{18} to n-C_{36}, with n-C_{27} and n-C_{29} as the dominant homologues. The remainder of the distribution showed a much more reduced preference for odd carbon-numbered homologues. Alginite from New South Wales yielded n-alkanes ranging from n-C_{17} to n-C_{33}

Fig. 13. n-Alkanes of vitrinites

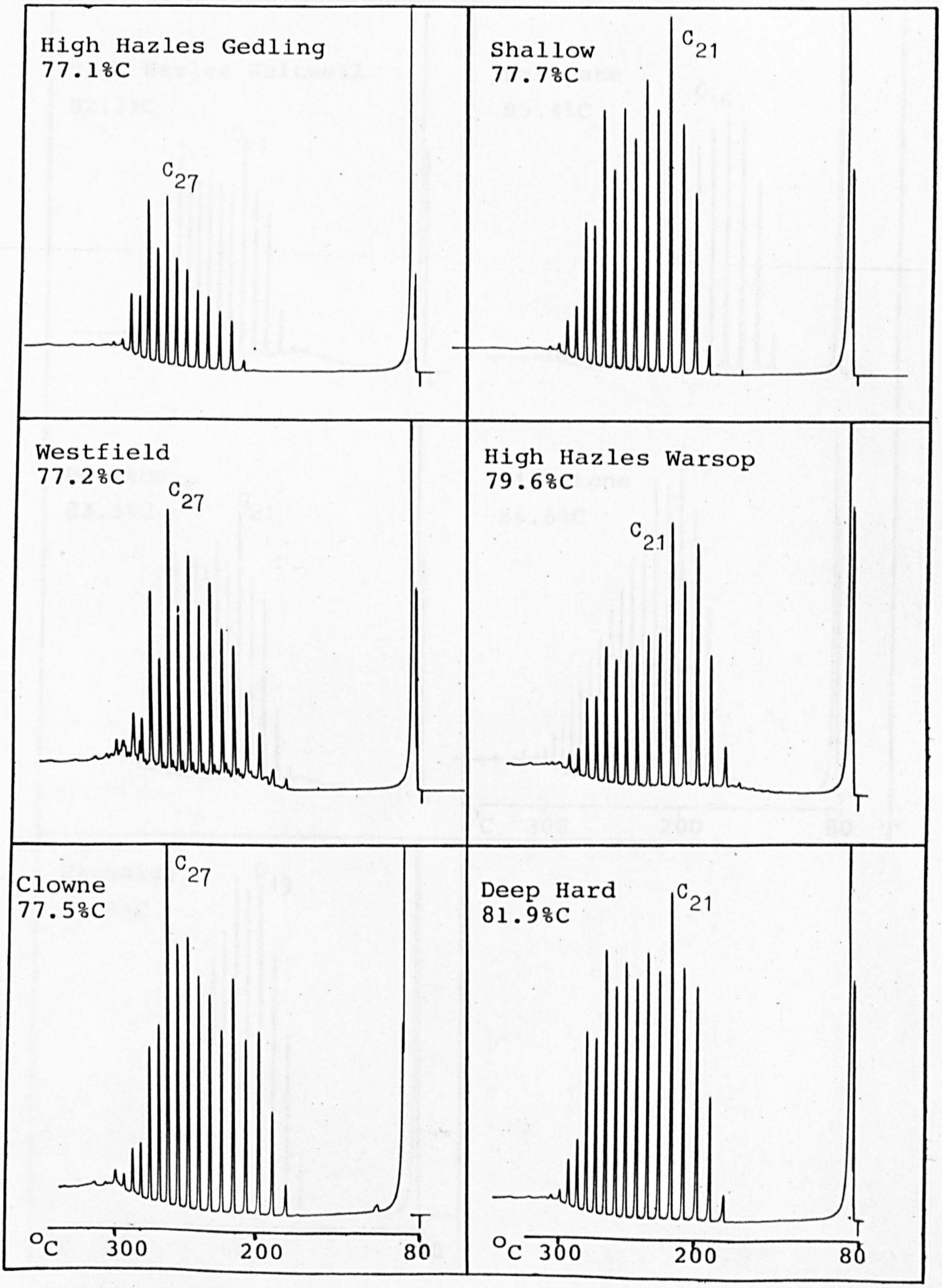

Gas chromatographic conditions: 5'x1/8" o.d. column containing 3% OV-101 on Varaport 30 (100-120 mesh); programmed 80-300°C at 6°/min; detector 300°; injector 300°; nitrogen 40 p.s.i.

Fig. 13a. n-Alkanes of vitrinites

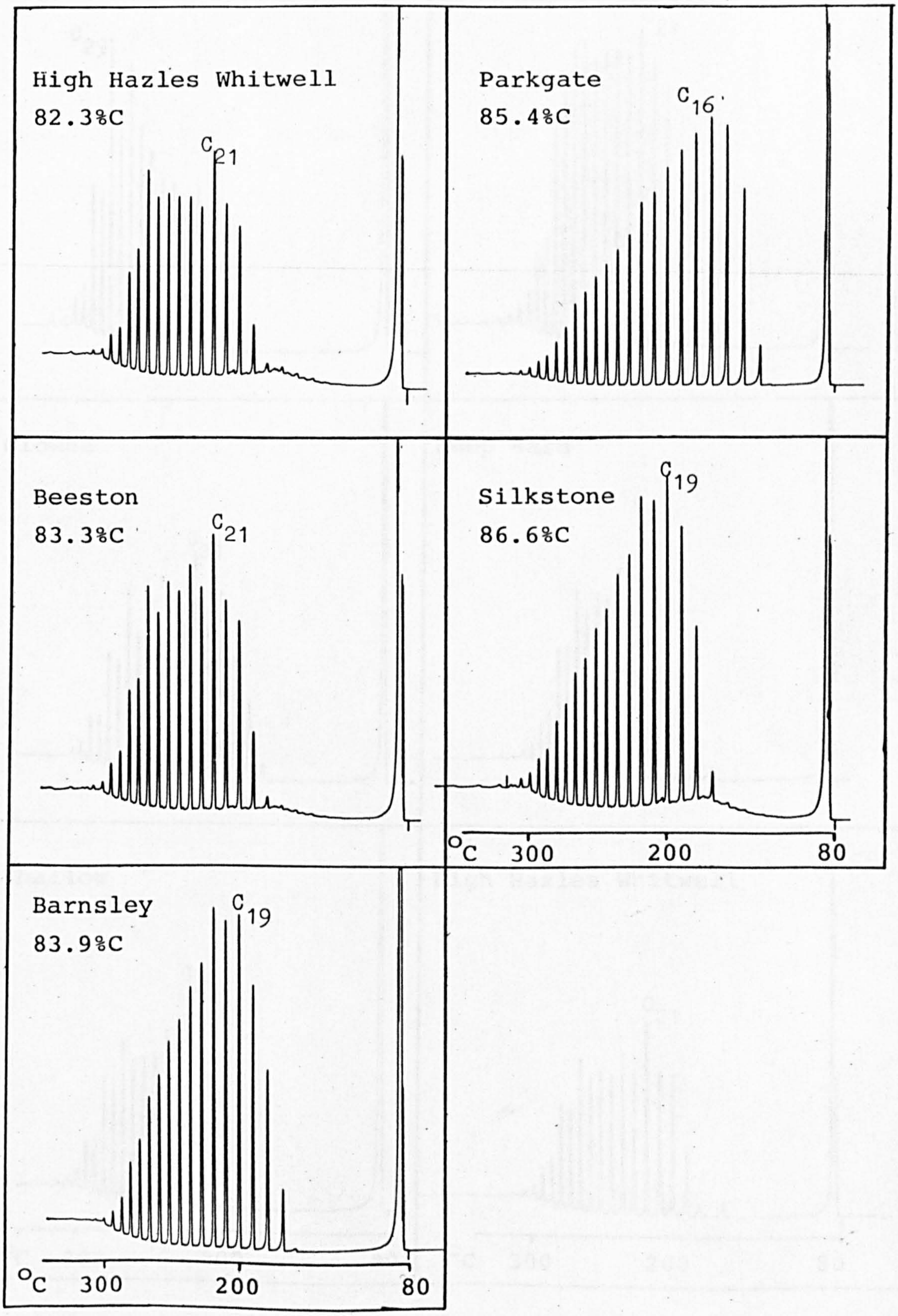

Gas chromatographic conditions as in Fig. 13.

Fig. 14. n-Alkanes of sporinites

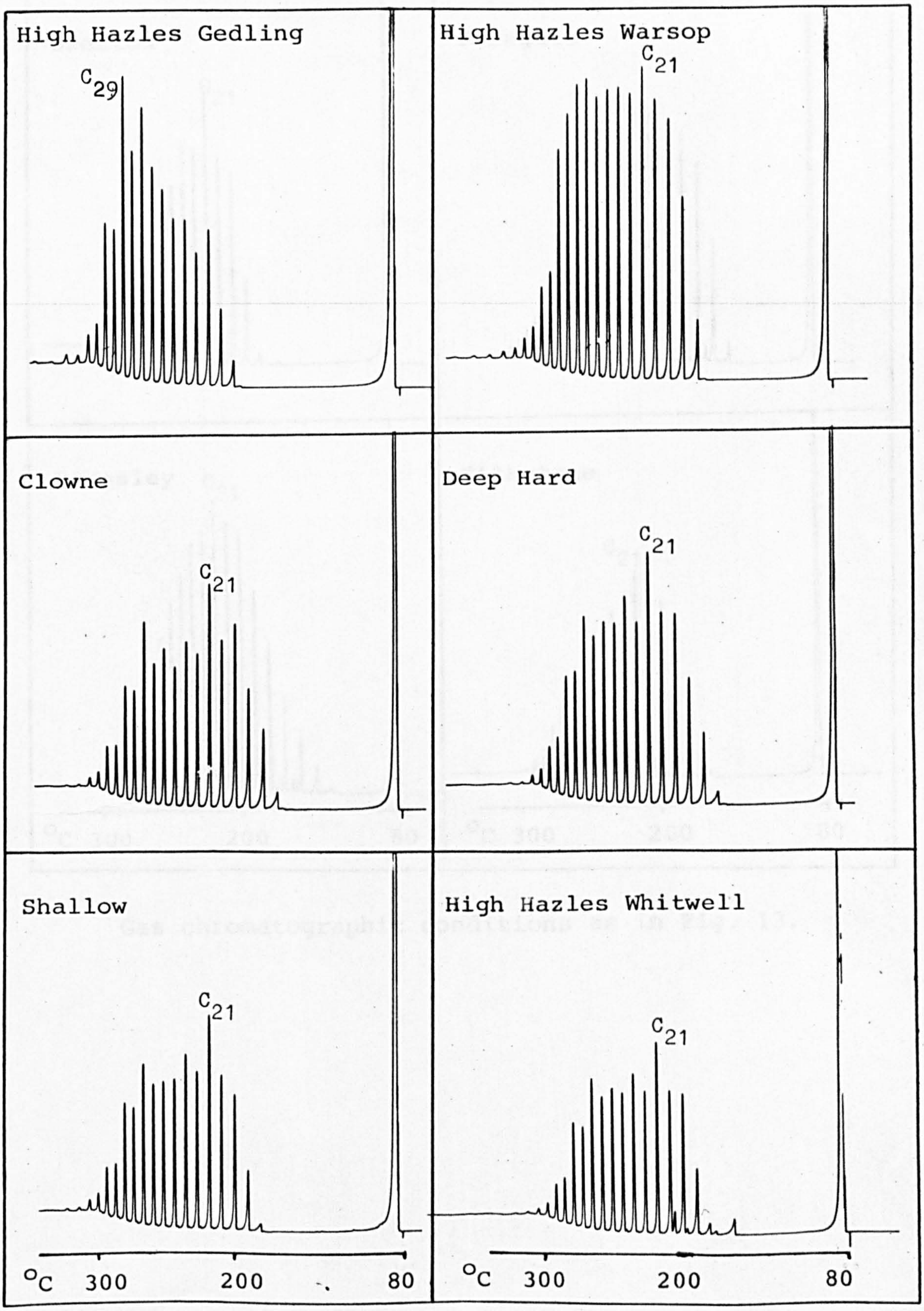

Gas chromatographic conditions as in Fig. 13.

Fig. 14a. n-Alkanes of sporinites

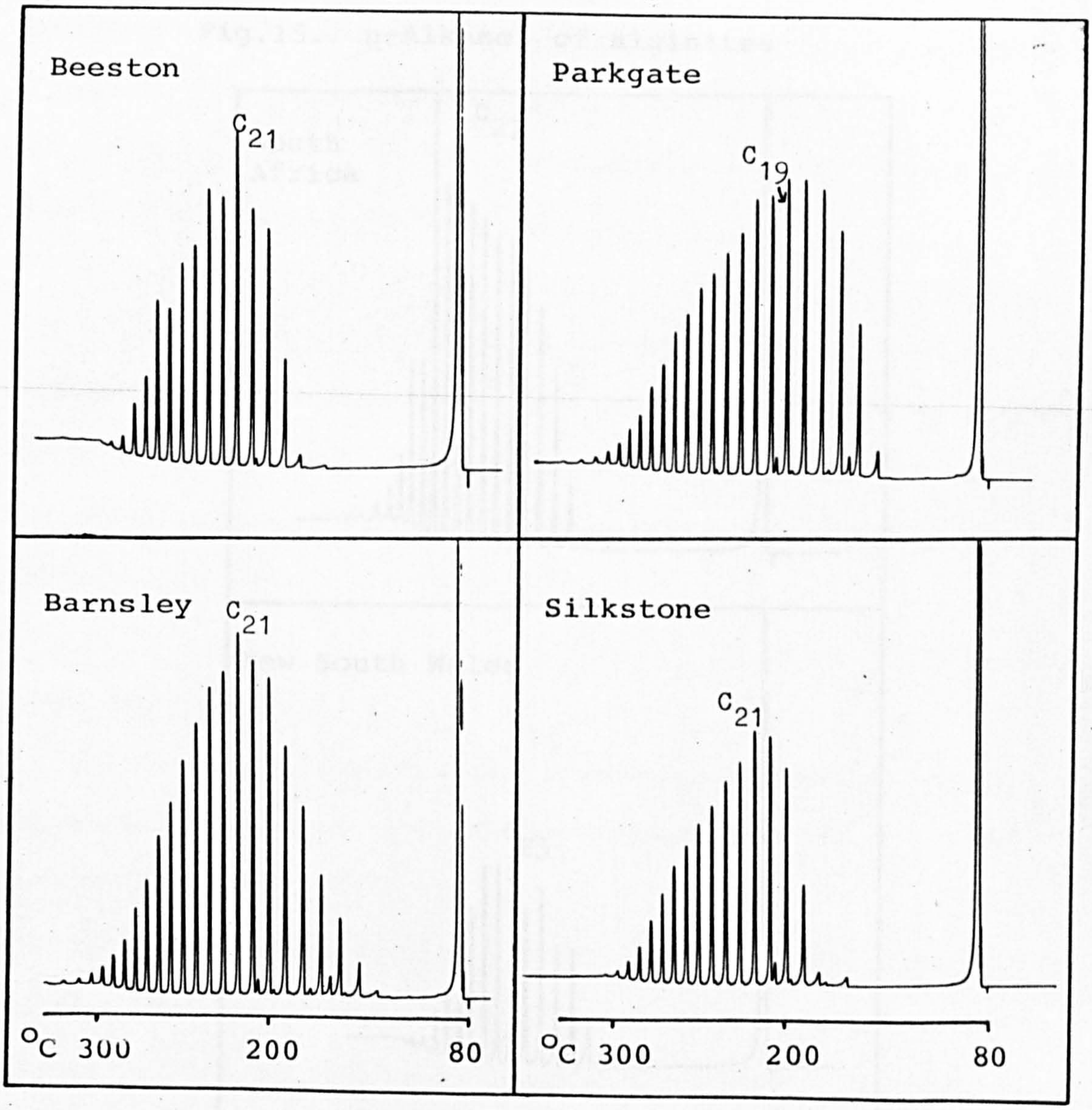

Gas chromatographic conditions as in Fig. 13.

Fig.15. n-Alkanes of alginites

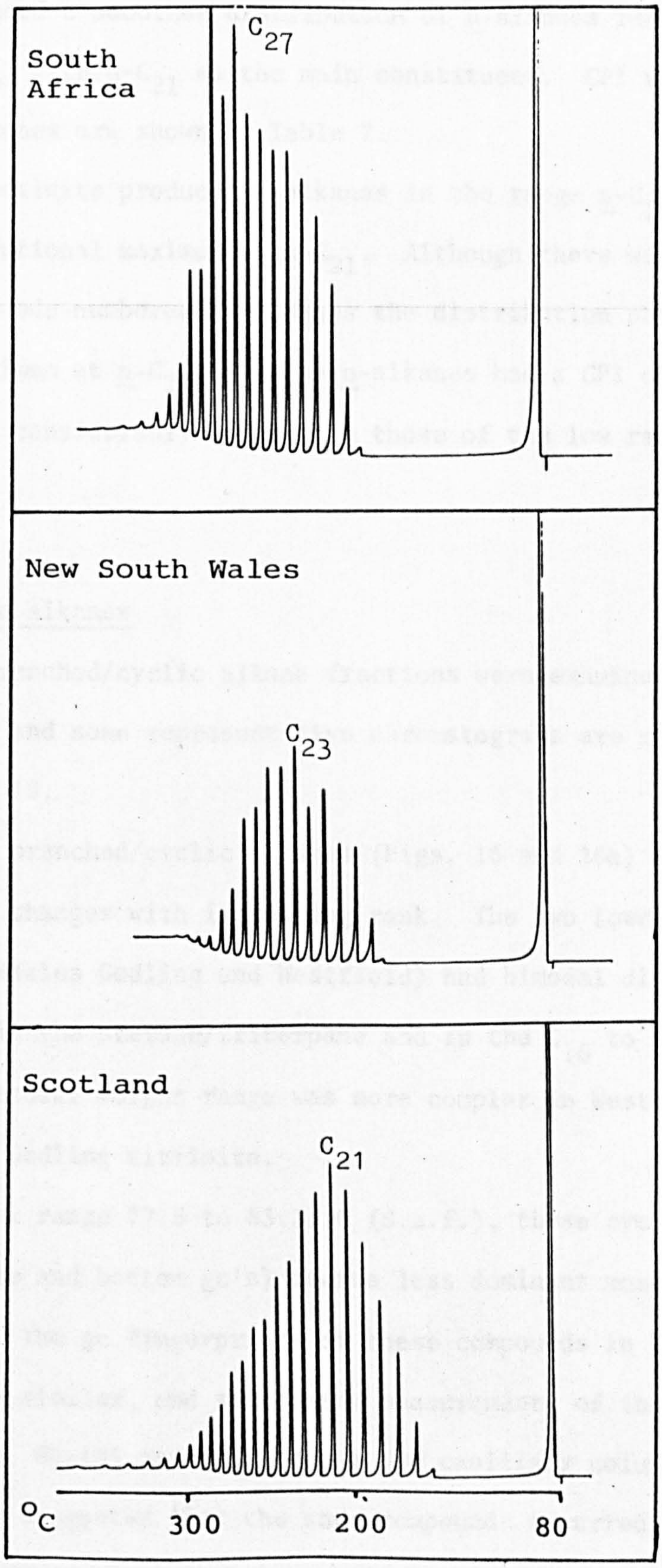

Gas chromatographic conditions as in Fig. 13.

with $\underline{n}$-C_{23} as the major component. This sample showed the greatest preference of odd-numbered members of all three alginites. Scottish alginite produced a smoother distribution of $\underline{n}$-alkanes ranging from $\underline{n}$-C_{15} to $\underline{n}$-C_{39}, with $\underline{n}$-C_{21} as the main constituent. CPI values for alginite $\underline{n}$-alkanes are shown in Table 7.

Indiana cutinite produced $\underline{n}$-alkanes in the range $\underline{n}$-C_{18} to $\underline{n}$-C_{35}, with a distributional maximum at $\underline{n}$-C_{21}. Although there was no major preference for odd-numbered homologues the distribution showed a subsidiary maximum at $\underline{n}$-C_{27}, and the $\underline{n}$-alkanes had a CPI of 1.12. This value was considerably lower than those of the low rank sporinites.

Branched/cyclic alkanes

All the branched/cyclic alkane fractions were examined by gas chromatography and some representative chromatograms are reproduced in Figs. 16 to 19.

Vitrinite branched/cyclic alkanes (Figs. 16 and 16a) showed distributional changes with increasing rank. The two lowest rank samples (High Hazles Gedling and Westfield) had bimodal distributions with material in the sterane/triterpane and in the C_{16} to C_{22} ranges. The higher molecular weight range was more complex in Westfield than in High Hazles Gedling vitrinite.

In the rank range 77.5 to 83.3% C (d.a.f.), these cycloalkanes (Fig. 16, middle and bottom gc's) became less dominant members of the fractions. The gc fingerprints of these compounds in this rank range were very similar, and subsequent measurements of their Kovats indices on 100m. OV-101 and 50m. Dexsil 300 capillary columns respectively strongly suggested that the same compounds occurred in each sample. Preliminary gc-ms work has confirmed that they included triterpanes of the hopane type, with 27 to 31 carbon atoms (but excluding the C_{28} triterpane). No identifications have yet been made on the compounds with more than 31 carbon atoms. C_{27}, C_{29}, C_{30} and C_{31} triterpanes have been identified by gc-ms in a French bituminous coal (Ensminger *et al.*, 1973), and these were also of the hopane type.

At ranks higher than 83.3% C (d.a.f.) the gc's indicated that there was a continual reduction in the relative concentrations of triterpanes with rank and a concomitant increase in the concentrations of material of lower molecular weight (Fig. 16a). Triterpane constituents did not disappear entirely however in the highest rank samples analysed.

Acyclic isoprenoid alkanes occurred throughout the rank range in vitrinite. Westfield and High Hazles Gedling vitrinite branched/cyclic alkanes contained the C_{18}, C_{19} and C_{20} acyclic isoprenoid alkanes but they were minor constituents compared to the higher molecular weight polycyclic material. With further coalification, they became major components of the branched/cyclic alkane fractions in which acyclic isoprenoids from C_{15} to C_{20} (with the possible exception of C_{17}) were found. In all samples analysed pristane was the dominant branched compound.

In general it could be seen that with increasing coalification there was a decrease in the average molecular weight distribution of compounds and a bimodal distribution at lower ranks slowly changed to a unimodal distribution at the highest ranks.

Branched/cyclic alkane fractions of sporinites (Figs. 17 and 17a) were generally similar to those of vitrinites. Donibristle sporinite was unusual however in that a greater part of the fraction occurred in the C_{16}-C_{22} region, but a secondary distributional maximum occurred in the sterane/triterpane region. High Hazles Gedling sporinite had a greater proportion of material in the higher molecular

Fig. 16. Branched/cyclic alkanes of vitrinites

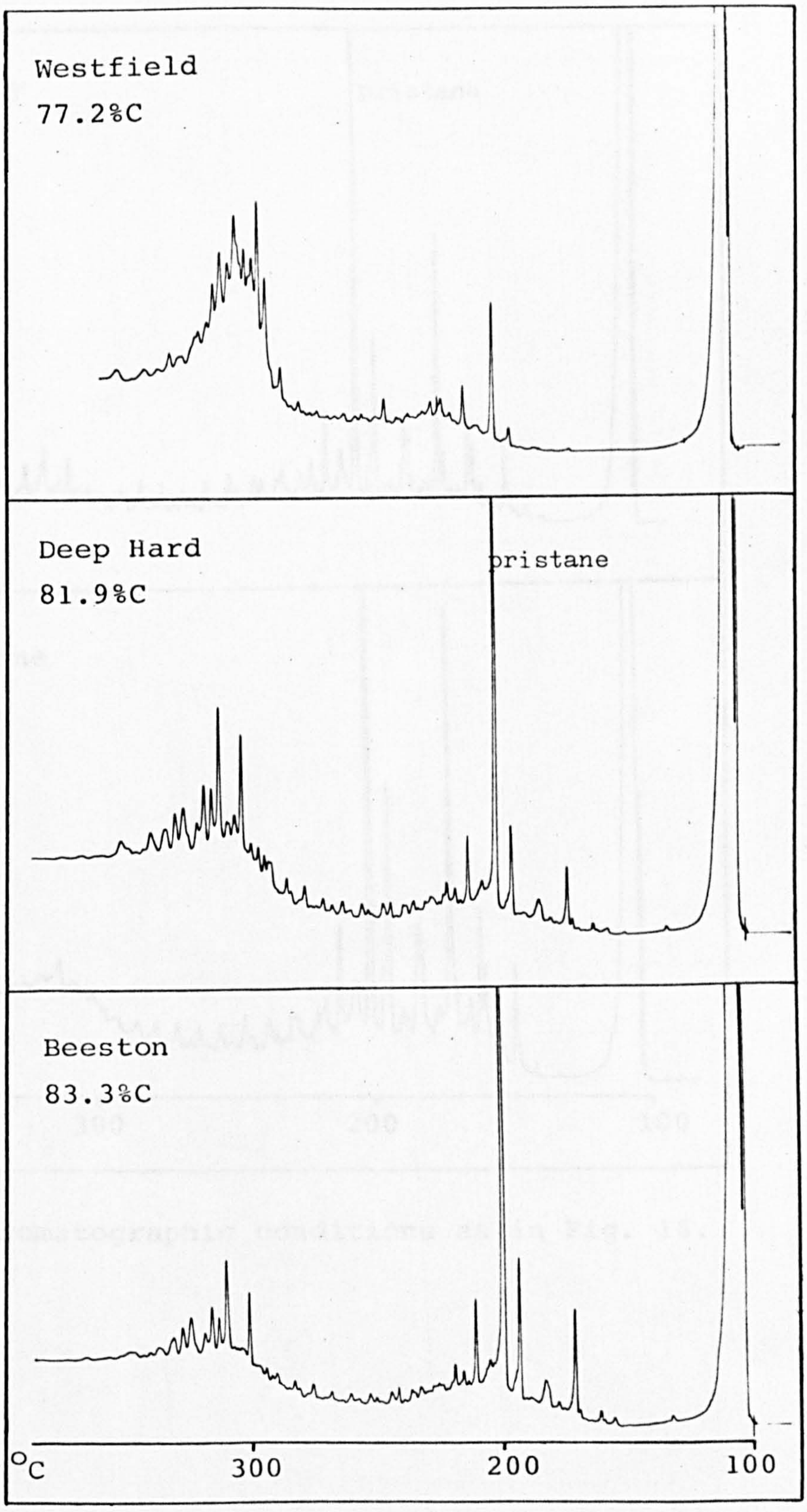

Gas chromatographic conditions: 10'x1/16"o.d. column containing 3% OV-101 on Varaport 30(100-120mesh); programmed 100-300°C at 4°/min; detector 300°; injector 300°; nitrogen 60p.s.i.

Fig. 16a. Branched/cyclic alkanes of vitrinites

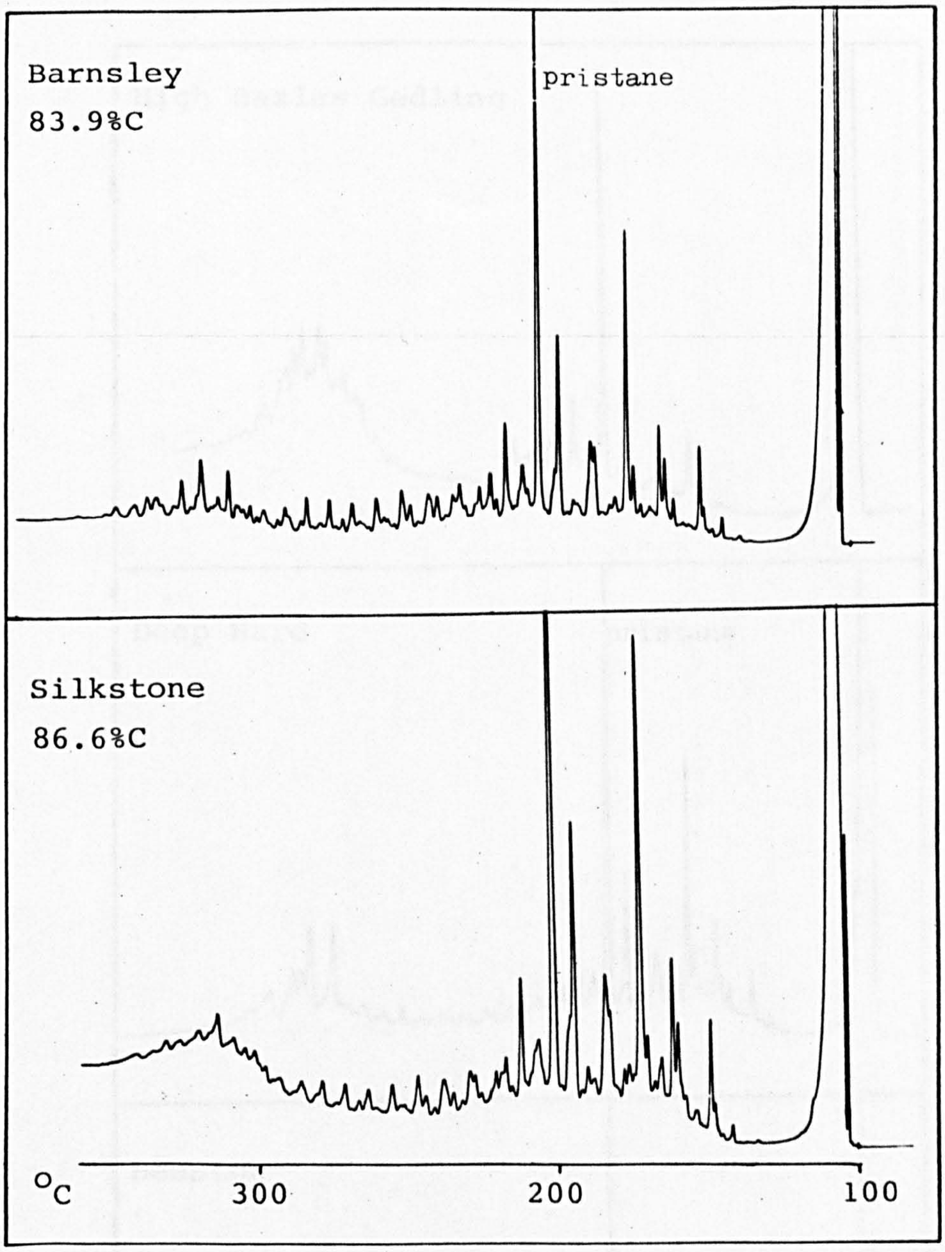

Gas chromatographic conditions as in Fig. 16.

Fig. 17. Branched/cyclic alkanes of sporinites

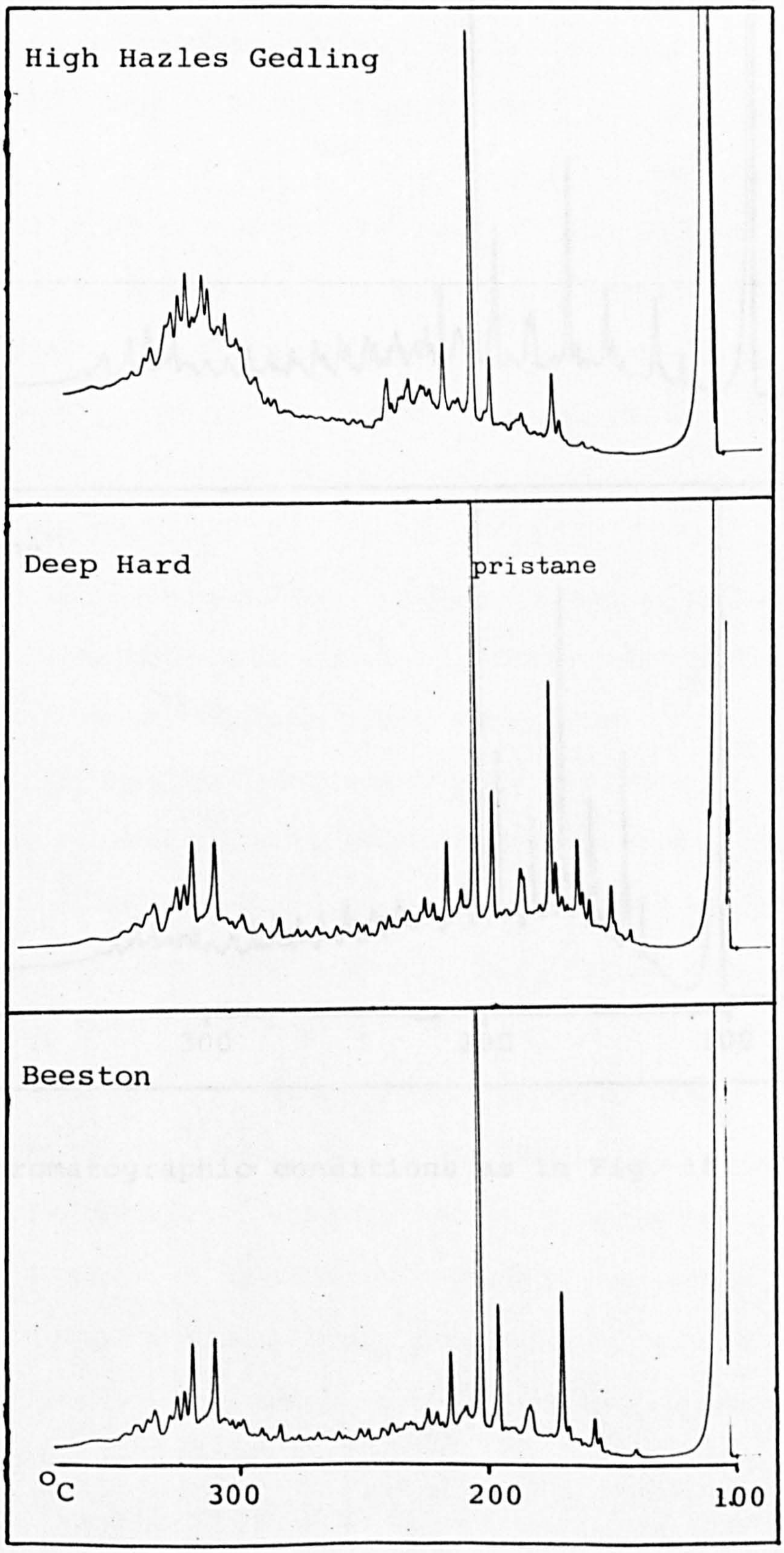

Gas chromatographic conditions as in Fig. 16.

Fig. 17a. Branched/cyclic alkanes of sporinites

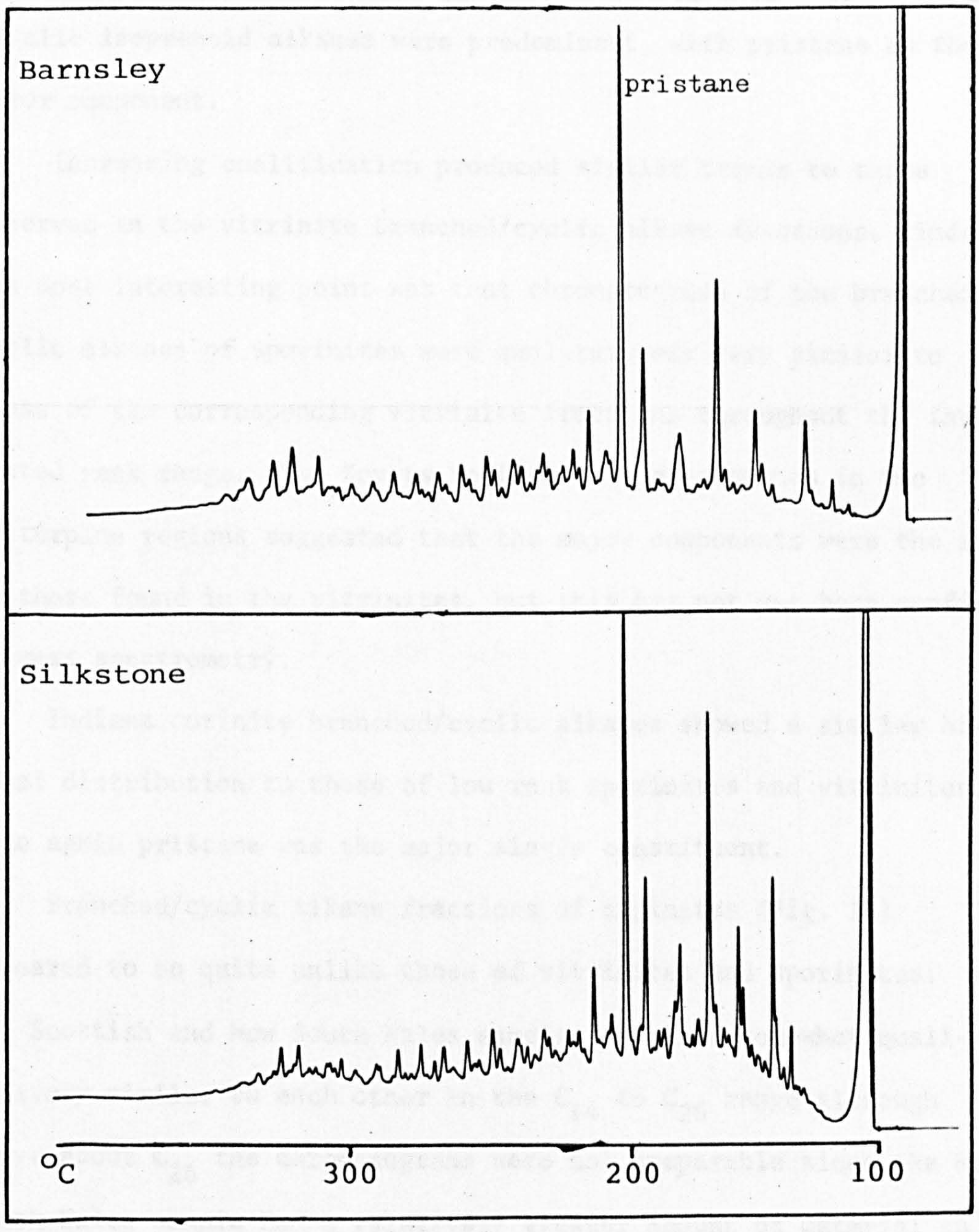

Gas chromatographic conditions as in Fig. 16.

weight range, and in the C_{16}-C_{22} region the C_{16}, C_{18}, C_{19} and C_{20} acyclic isoprenoid alkanes were predominant, with pristane as the major component.

Increasing coalification produced similar trends to those observed in the vitrinite branched/cyclic alkane fractions. Indeed, the most interesting point was that chromatograms of the branched/cyclic alkanes of sporinites were qualitatively very similar to those of the corresponding vitrinite fractions throughout the investigated rank range. The Kovats indices of the compounds in the triterpane regions suggested that the major components were the same as those found in the vitrinites, but this has not yet been confirmed by mass spectrometry.

Indiana cutinite branched/cyclic alkanes showed a similar bimodal distribution to those of low rank sporinites and vitrinites. Once again pristane was the major single constituent.

Branched/cyclic alkane fractions of alginites (Fig. 18) appeared to be quite unlike those of vitrinites and sporinites. The Scottish and New South Wales samples appeared somewhat qualitatively similar to each other in the C_{14} to C_{26} range although above about C_{26} the chromatograms were not comparable since the New South Wales sample had a relatively greater amount of material in this range than the Scottish sample. Both fractions were exceptionally complex throughout, and packed column gc suggested that at least three homologies were present. Pristane was present in both samples. South African alginite branched/cyclic alkanes showed a different distribution in that most of the fraction occurred above C_{27}, with smaller amounts only in the C_{16} to C_{27} range. It was however as equally complex a mixture as those isolated from the other alginites.

The Scottish alginite branched/cyclic alkanes were analysed on

Fig. 18. Branched/cyclic alkanes of alginites

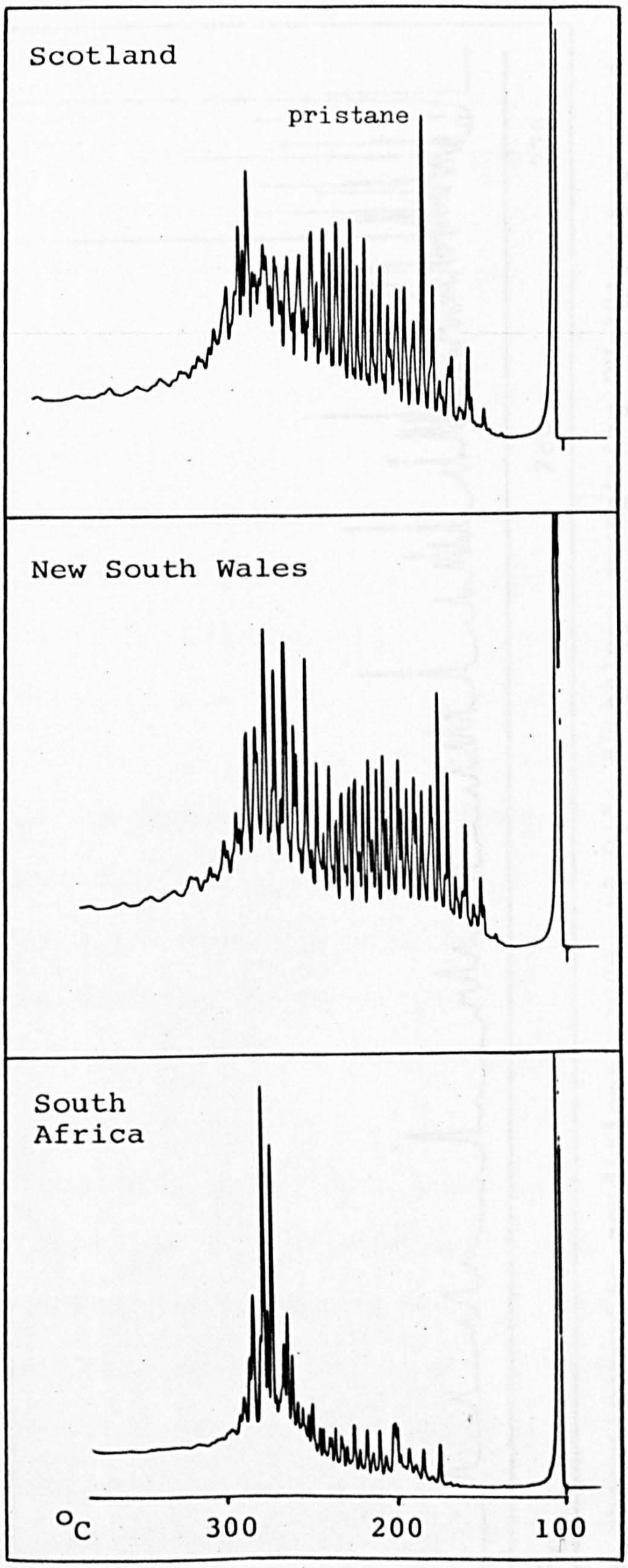

Gas chromatographic conditions: 5'x1/8"o.d. column containing 3% OV-101 on Varaport 30(100-120 mesh); programmed 100-300°C at 6°/min; detector 300°; injector 300°; nitrogen 40 p.s.i.

Fig. 19. Capillary gas chromatogram of branched/cyclic alkanes of Scottish alginite

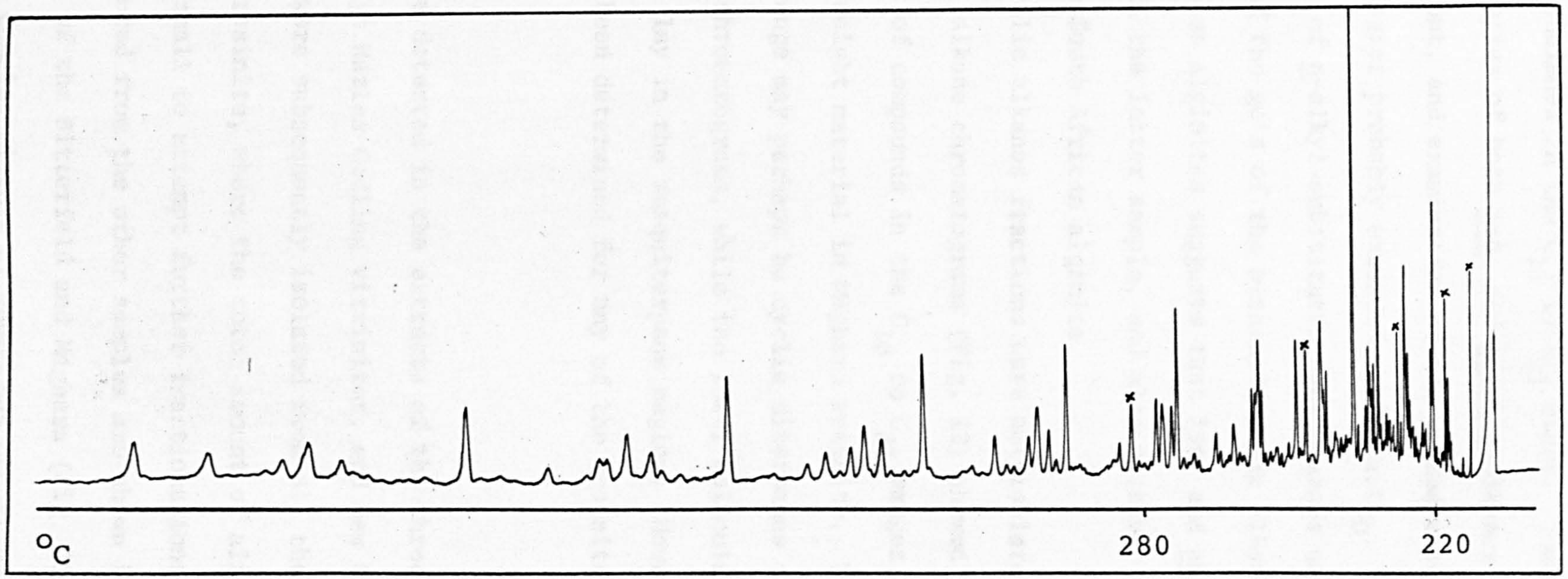

Gas chromatographic conditions: 100m. x0.01"o.d. column containing OV-101; programmed 220-280^oC at 2^o/min, with an initial hold for 20 mins at 220^o; detector 300^o; injector 300^o; nitrogen 15 p.s.i. n-Alkanes co-injected with the sample as shown: n-C_{12}, n-C_{14}, n-C_{16}, n-C_{18}, and n-C_{20}.

a high resolution capillary column (Fig. 19), and coinjected with iso- and anteiso-alkanes in the C_{15} to C_{22} range, and n-alkyl-substituted cyclohexanes in the C_{15} to C_{21} range. The results indicated that homologies of both iso- and anteiso-alkanes in the C_{15} to C_{24} were present, and examination of the packed column gc's shows that these homologies probably extended up to *ca.* C_{30}. The evidence for the presence of n-alkyl-substituted cyclohexanes was equivocal. The similarity of the gc's of the branched/cyclic alkanes of Scottish and New South Wales alginites suggests that iso- and anteiso-alkanes may be present in the latter sample, and also possibly relatively small amounts in South African alginite.

Branched/cyclic alkanes fractions were not isolated for resinites. The total alkane chromatograms (Fig. 12) showed highly complex mixtures of compounds in the C_{16} to C_{22} ranges, with some lower molecular weight material in Maghara resinite. The material in the C_{16}-C_{22} range may perhaps be cyclic diterpanes from their position in the chromatograms, while the lower molecular weight Maghara material lay in the sesquiterpane region. However no structures have been determined for any of the resinite compounds.

Alkenes

Alkenes were detected in the extracts of the three resinites, Westfield and High Hazles Gedling vitrinites, and New South Wales alginite. They were subsequently isolated from all these samples except Yallourn resinite, where the total amount of aliphatic hydrocarbons was too small to attempt further fractionations. The yields of alkenes recovered from the other samples are shown in Table 8.

Gc analysis of the Bitterfeld and Maghara (Fig. 20) resinite alkenes showed a complex mixture of compounds occurring in the sesqui- and diterpene regions of the chromatogram, paralleling the

Table 8: Alkenes isolated from the maceral concentrates

	Alkenes (mg/gm)	$\frac{\text{Alkenes}}{\text{Extract}}$ %
Resinite		
Bitterfeld	0.04	0.01
Maghara	7.31	1.34
Vitrinite		
Westfield	0.06	0.06
High Hazles Gedling	0.02	0.02
Alginite		
New South Wales	0.06	0.36

alkane constituents of these macerals.

Gc analysis of the two vitrinite alkene fractions (Fig. 21, top and middle chromatograms) indicated the presence in each of what appeared to be a dominating homologous series of compounds and a more complex region, probably of cyclic material, distributed about the C_{30} region. Westfield vitrinite yielded an homology in the C_{19} to C_{43} range with a smooth distribution and a marked maximum at C_{28}. In High Hazles Gedling vitrinite, an homology was confined to the C_{20} to C_{30} range, again with a smooth distribution and a maximum at C_{28}.

New South Wales alginite alkenes (Fig. 21, bottom chromatogram) were also dominated by an homologous series of compounds, ranging from C_{16} to C_{29}. In contrast to the vitrinites, this distribution had a maximum at C_{18} and in the higher molecular weight range (C_{24} to C_{29}) showed a predominance of even- over odd-numbered chain lengths. Above C_{25} other non-homologous material was present in lesser amounts.

Hydrogenation of New South Wales alginite and Westfield vitrinite alkenes converted the predominant homologies to n-alkanes (confirmed as such by coinjection of standards), indicating that the original compounds were n-alkenes.

Fig. 20. Alkenes of Maghara resinite

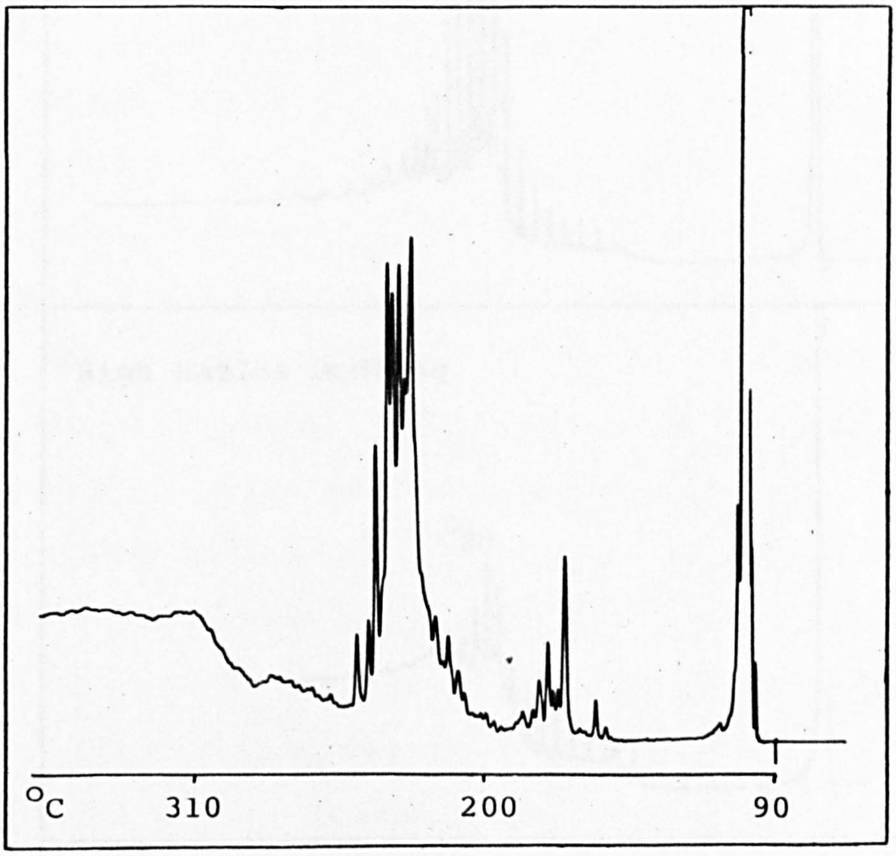

Gas chromatographic conditions as in Fig. 12
for Maghara resinite alkanes.

Fig. 21. Alkenes of vitrinite and alginite

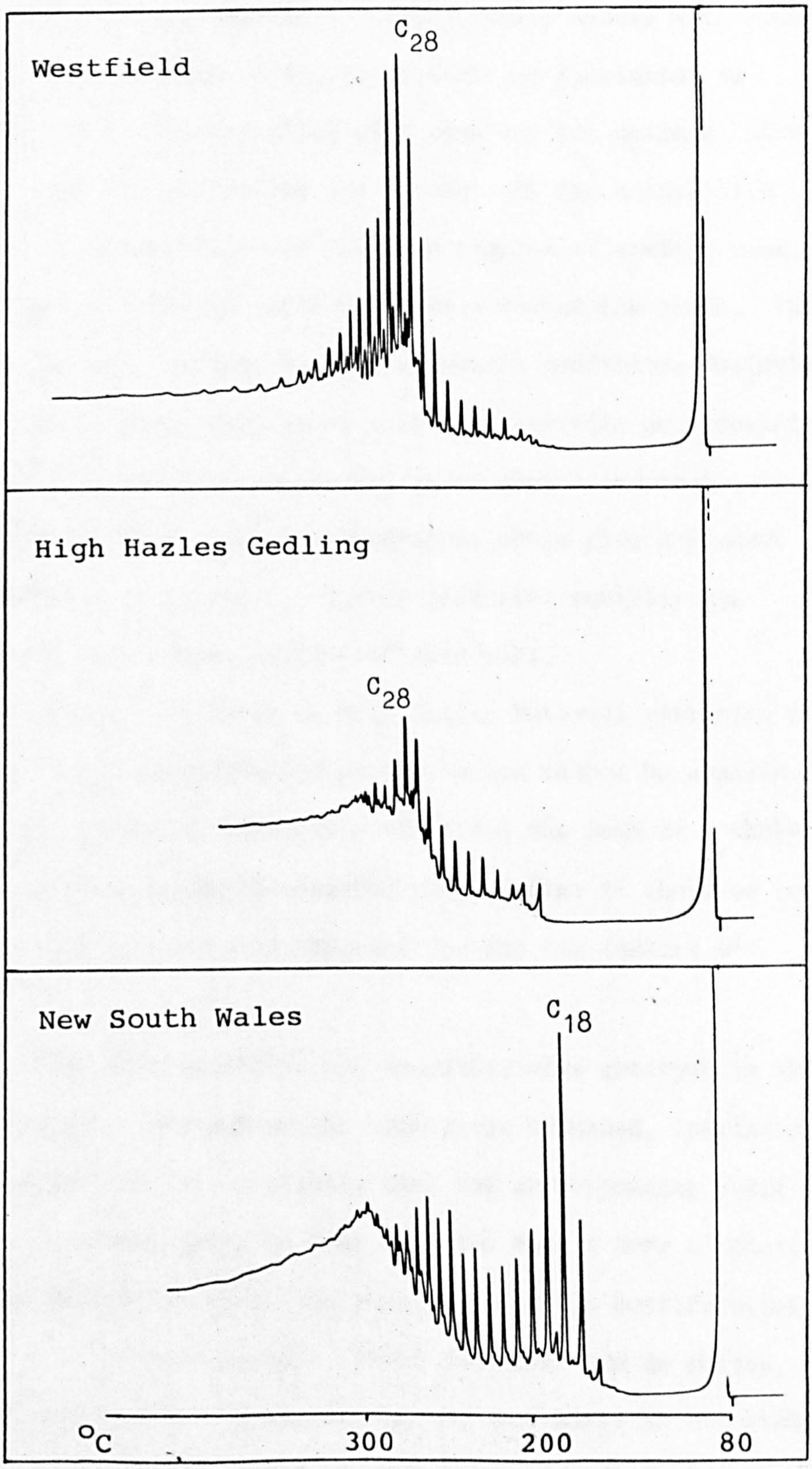

Gas chromatographic conditions: 5'x1/8"o.d. column containing 3% OV-101 on Varaport 30 (100-120 mesh); programmed 80-300°C at 6°/min; detector 300°; injector 300°; nitrogen 40 p.s.i.

Discussion

Saturated hydrocarbons were isolated from all the maceral concentrates except Yallourn resinite. Yields varied widely with maceral type and also with rank in the vitrinites and sporinites as depicted in Fig. 22. The variation with rank was not uniform however. Both vitrinite and sporinite from the Clowne coal had anomalously large amounts of alkanes relative to other samples of similar rank, whereas High Hazles Whitwell vitrinite gave a rather low yield. The Clowne values probably reflect the environmental conditions following deposition of the peat precursor, as both the vitrinite and sporinite were anomalous. As the peat was buried under marine sediments, decomposition under highly anaerobic conditions could give a product relatively enriched in hydrogen. Strong bacterial activity was indicated by the high pyrite content of this coal.

The low content of alkanes in High Hazles Whitwell vitrinite was not reflected in the corresponding sporinite and cannot be explained therefore as environmental conditions affecting the seam as a whole. Microscopically this vitrinite appeared very similar to those of the other samples, and no reason is apparent for its low content of alkanes.

Alkane yields from vitrinite and sporinite were greatest in the higher rank samples. Throughout the rank range examined, sporinite yielded a greater quantity of alkanes than the corresponding vitrinite. It has long been accepted that exinites have a more aliphatic structure than vitrinites up to the rank level of the coalification break (Boyer *et al.*, 1961; Francis, 1961; Tschamler and de Ruiter, 1966). The higher content of alkanes in the sporinites is acceptable on this basis provided that complete extraction had taken place. There is perhaps the possibility that in two different structural matrices the ability of a solvent to penetrate them may be variable,

FIG.22. YIELDS OF TOTAL ALKANES FROM VITRINITES AND SPORINITES

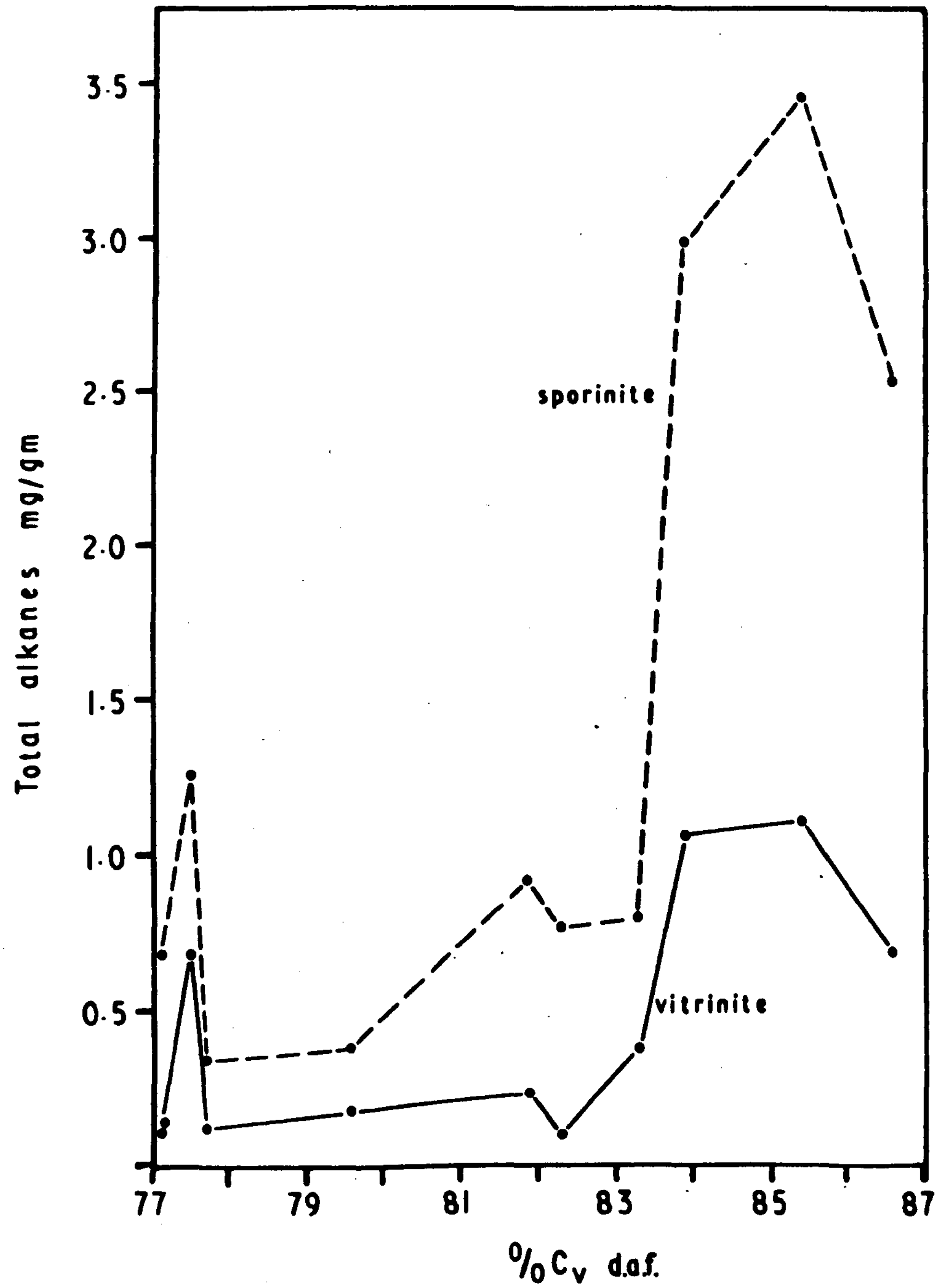

and hence the meaning of "total extraction" may also be variable.

The other exinite macerals investigated showed a wide divergence in the amounts of alkanes they contained (Table 6). Surprisingly, the richest of all the samples was Maghara resinite, which yielded more than twice the amount of alkanes than the next richest sample (New South Wales alginite). Conversely, the other two resinites provided exceptionally low, but comparable, amounts of alkanes. However resinite hydrocarbons were rather unique in type when compared to those of the other macerals, and would not give rise to the usual n-alkane-dominated hydrocarbon patterns associated with many sedimentary rocks (Meinschein, 1961; Martin *et al.*, 1963). They must therefore be considered as minor contributors to sedimentary hydrocarbons.

The three alginite samples produced widely differing amounts of alkanes and the highest value exceeded those of the richest sporinites. It is difficult however to generalise upon the role of algae as geological hydrocarbon sources from these results, as the phenomenon of torbanite formation is presently linked only to one specific alga. Clearly however this particular material has the potential to produce large amounts of hydrocarbons during maturation. The three alginites had carbon contents between 80.5% and 84.0% C (d.a.f.), and the yields of alkanes may be partly dependent on rank and partly on the relative states of reduction of the accumulating algal detritus. However, Brooks and Smith (1967) showed that the rate of change of alkane distributions of coals, and hence, presumably, of rate of production, was greatest in the sub-bituminous to high-volatile bituminous rank range. Samples of alginites of higher rank would be required to investigate more thoroughly their potential for generating alkanes.

The CPI values of the n-alkanes (measured above n-C_{23}) of vitrinites and sporinites decreased to almost unity with increasing coalification (Fig. 23). This trend has also been demonstrated in other studies (Brooks and Smith, 1967; Leythaeuser and Welte, 1969; Cooper, 1973). In the present investigation data showed that the CPI decrease was caused by a continued relative increase in concentration of each n-alkane in the n-C_{23} to n-C_{33} range. Individual n-alkane concentrations are listed in Tables 9 and 10.

In vitrinites, each alkane in the n-C_{20} to n-C_{29} range increased in concentration up to a rank of 83.9% C (d.a.f.) while n-C_{30} and n-C_{31} increased up to 86.6% C (d.a.f.) (Figs. 24 and 25). At a rank of 83.9% C the CPI had decreased to 1.08. In sporinites, n-alkanes in the n-C_{19} to n-C_{30} range increased in concentration up to a rank of 86.6% C (d.a.f.), although n-C_{31} reached a maximum concentration at a lower rank of 83.9% C (d.a.f.). The CPI's of the sporinite n-alkanes at these rank levels were close to unity. It can be seen therefore that the mechanism of CPI decrease is dominated by the generation of long-chain hydrocarbons, and not by degradation of the pre-existing patterns.

It is not possible, with this data, to determine the distribution of the alkanes that were actually being generated. If they had a CPI of unity and were produced in sufficiently large amounts they would dilute the pre-existing pattern to produce a smooth distribution. On the other hand, if n-alkanes with a CPI of less than unity were produced, the same effect would be achieved. However it might then be expected that even-dominated n-alkane distributions would occur commonly in nature. In fact, such distributions are rare, although some have been found (Albaiges and Torradas, 1974; Cooper, 1973; Grantham, 1974; Welte and Waples, 1973).

In a study of the changes in the distributions of n-alkanes with depth in the Green River shale, Robinson *et al.*, (1965), postu-

FIG. 23. VARIATION OF CPI OF n-ALKANES OF VITRINITE AND SPORINITE WITH RANK

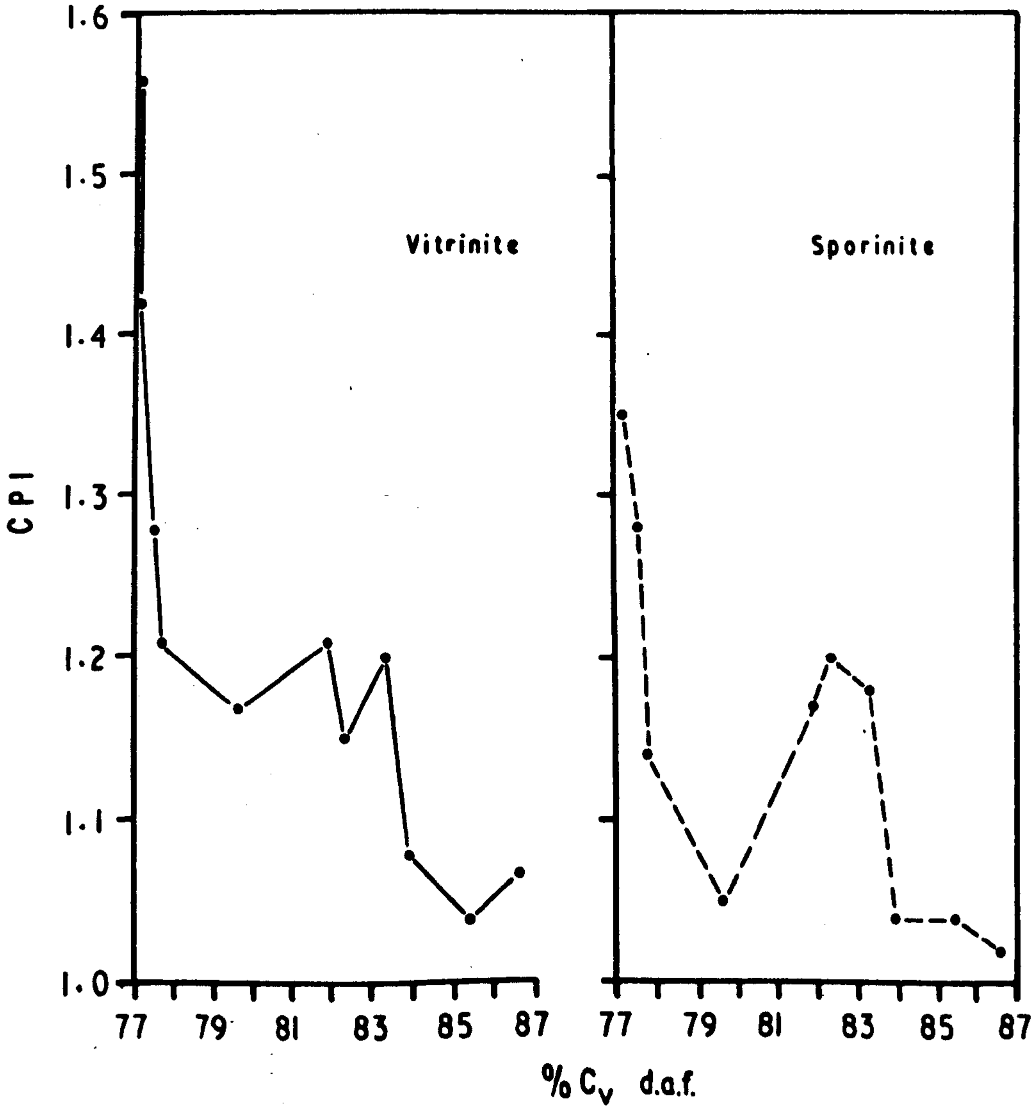

Table 9: Concentrations of n-alkanes isolated from vitrinites (mg/gm x 10^{-3})

n-Alkane carbon no.	High Hazles Gedling	Westfield	Clowne	Shallow	High Hazles Warsop	Deep Hard	High Hazles Whitwell	Beeston	Barnsley	Parkgate	Silkstone
17	-	-	1.0	-	0.6	0.4	-	0.4	25.0	55.0	21.0
18	-	0.1	9.6	0.2	2.0	1.8	0.2	2.3	37.0	55.1	33.2
19	-	0.4	6.5	1.0	3.7	3.4	0.7	5.6	46.1	47.5	39.5
20	0.1	0.7	9.6	1.4	3.2	3.6	0.9	6.2	45.2	42.0	36.6
21	0.7	1.1	8.4	2.0	4.1	4.7	1.1	8.1	46.9	39.8	37.3
22	0.9	1.3	6.5	1.5	2.3	3.6	0.8	6.6	39.2	32.5	30.4
23	1.1	1.7	7.8	1.6	2.3	3.9	0.9	7.2	36.1	29.2	28.1
24	1.2	1.5	8.4	1.3	2.2	3.5	0.9	6.5	31.5	26.1	23.9
25	1.5	1.9	9.6	1.5	2.1	3.7	0.9	6.7	28.3	23.0	21.5
26	1.6	1.4	9.4	1.1	1.9	3.3	0.9	5.8	23.5	19.7	17.7
27	2.8	2.2	13.0	1.4	2.1	3.9	1.0	6.6	20.3	16.8	15.8
28	1.7	0.9	6.4	0.8	1.3	2.6	0.6	3.7	14.1	11.8	11.7
29	2.4	1.6	5.5	0.8	1.2	2.6	0.5	3.3	10.6	8.4	9.4
30	0.9	0.4	1.9	0.3	0.4	1.0	0.2	1.4	5.1	5.1	5.8
31	0.9	0.4	1.6	0.2	0.2	0.7	0.1	0.9	2.3	3.6	4.1

Table 10: Concentrations of n-alkanes isolated from sporinites (mg/gm x 10^{-3})

n-Alkane carbon no.	High Hazles Gedling	Clowne	Shallow	High Hazles Warsop	Deep Hard	High Hazles Whitwell	Beeston	Barnsley	Parkgate	Silkstone
17	-	6.3	0.2	1.0	4.4	1.6	0.7	49.1	56.8	8.5
18	-	9.6	1.2	2.8	7.8	7.1	3.6	64.8	58.8	47.3
19	0.7	14.8	2.7	4.0	11.7	14.9	7.9	82.6	58.8	102.0
20	2.1	13.5	3.1	4.3	11.8	15.3	8.7	86.7	55.7	117.1
21	4.2	18.0	4.3	4.8	15.4	20.5	11.2	94.0	54.8	120.0
22	3.6	12.3	3.2	4.3	11.2	15.1	9.0	83.6	48.1	104.9
23	4.4	13.2	3.5	4.4	12.8	16.9	9.3	79.9	43.7	95.4
24	4.5	11.1	3.0	4.4	11.1	14.9	7.3	70.5	39.8	84.1
25	4.8	12.5	2.9	4.3	11.1	15.3	6.7	60.6	36.6	75.6
26	5.8	11.2	2.9	4.5	10.1	14.4	5.1	50.0	31.4	65.1
27	7.4	14.5	3.2	4.4	11.2	16.2	5.4	40.7	27.8	54.8
28	6.1	8.8	2.3	3.9	7.8	10.9	2.7	28.8	21.1	41.5
29	8.1	8.9	2.4	3.3	7.4	11.2	1.8	21.4	16.3	28.3
30	3.8	4.0	1.1	1.4	3.4	4.8	0.5	12.5	10.4	15.1
31	3.9	3.6	1.0	1.0	2.7	3.9	0.1	8.4	7.2	7.6

FIG. 24. VARIATION OF CONCENTRATION OF ODD-NUMBERED n-ALKANES OF VITRINITE WITH RANK

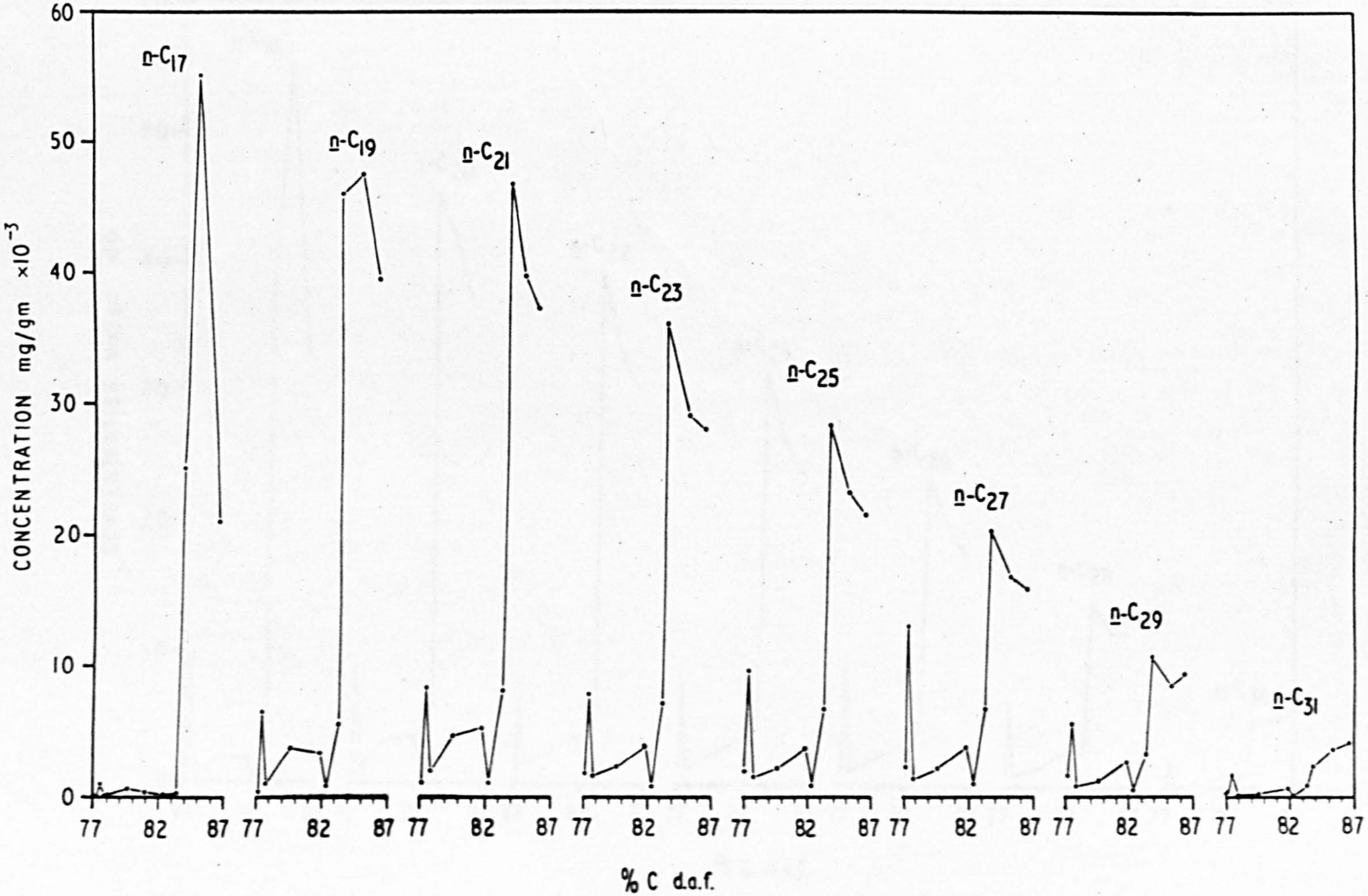

FIG. 25. VARIATION OF CONCENTRATION OF EVEN-NUMBERED n-ALKANES OF VITRINITE WITH RANK

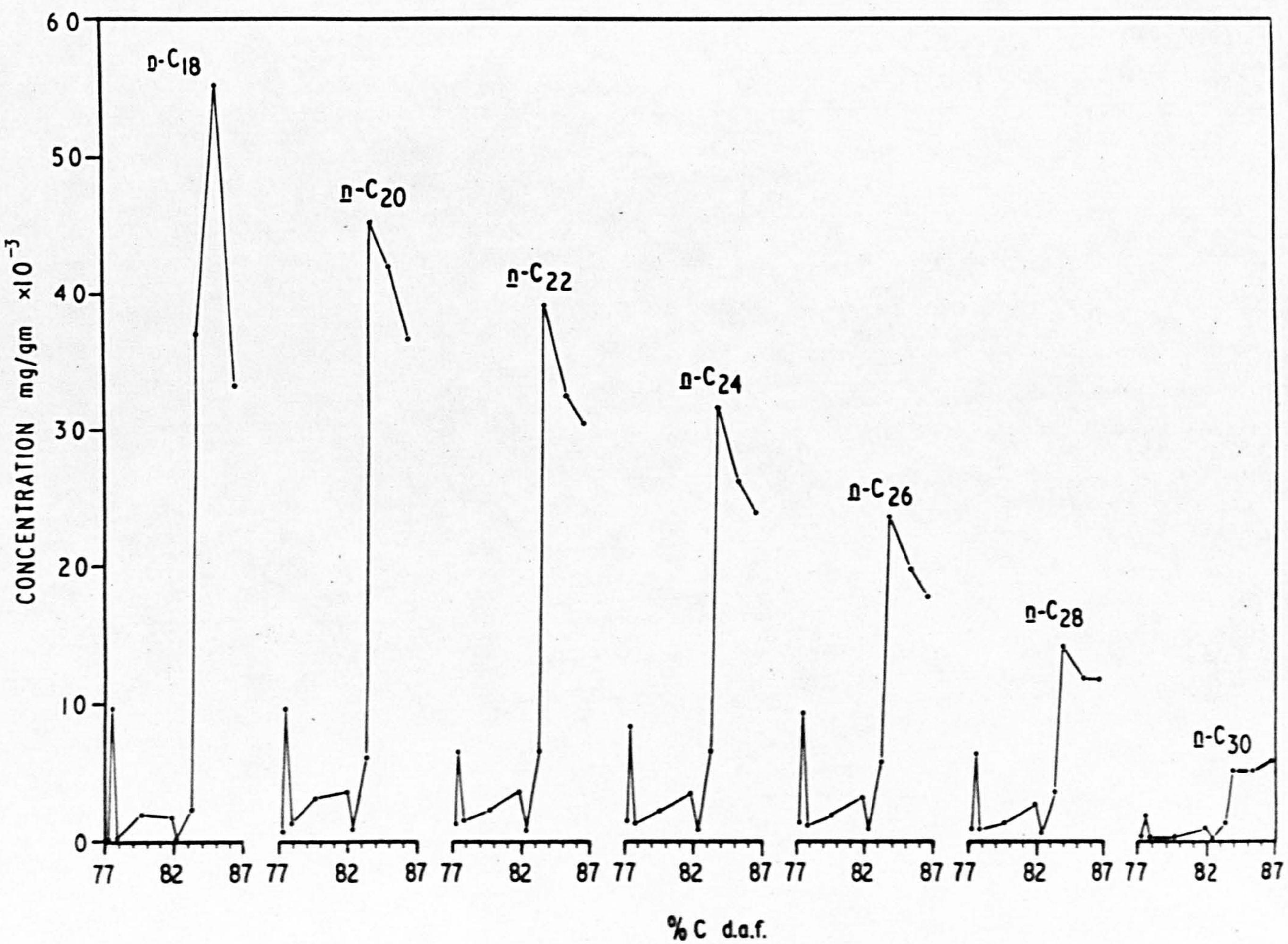

lated that the observed changes could be explained by the generation of even-dominated n-alkanes. It will be shown later (Chapter 4) that pyrolysis of the extracted vitrinite and sporinite residues, under mild conditions, produced even-dominated distributions of n-alkanes. However the fact that natural even-dominated distributions are rare has to be explained.

The relative proportions of the vitrinite n-alkanes lying above and below n-C_{23} (Fig. 26), changed markedly at the point where the higher n-alkanes showed maximum concentrations. At lower ranks, more than 60% by weight of the n-alkane fractions lay above n-C_{23} (with the exception of High Hazles Warsop vitrinite). At the point where the CPI was reduced to 1.08 and the higher n-alkanes showed their highest concentrations (i.e. Barnsley vitrinite), only *ca.* 40% of the whole fraction lay above n-C_{23}. This relationship was more tenuous in sporinites where the level of maximum higher (i.e. greater than n-C_{23}) n-alkane concentration was at a higher rank than in vitrinites. However the trend towards lower average molecular weights with increasing rank was still found (Fig. 26).

The foregoing evidence indicates that the distribution of n-alkanes in vitrinites and sporinites may have been dependent on processes which produced two distinct effects at different stages during coalification. Initially the trend towards decreasing CPI's and increasing higher n-alkane contents must have been a stage whereby alkanes were being generated from, possibly, the kerogenic matrices of the macerals, without undergoing extensive concomitant fragmentation to shorter chain lengths. Figs. 24 and 25 show that the rate of increase in concentration of individual homologues was slow up to a rank of 83.3% C (d.a.f.), but accelerated rapidly between 83.3% and 83.9% C (d.a.f.), and then the concentrations began to decline. However the amounts of total n-alkanes continued to increase

FIG.26. RELATIVE DECREASE OF $+\underline{n}-C_{23}$ $\underline{n}$-ALKANES OF VITRINITE AND SPORINITE WITH RANK

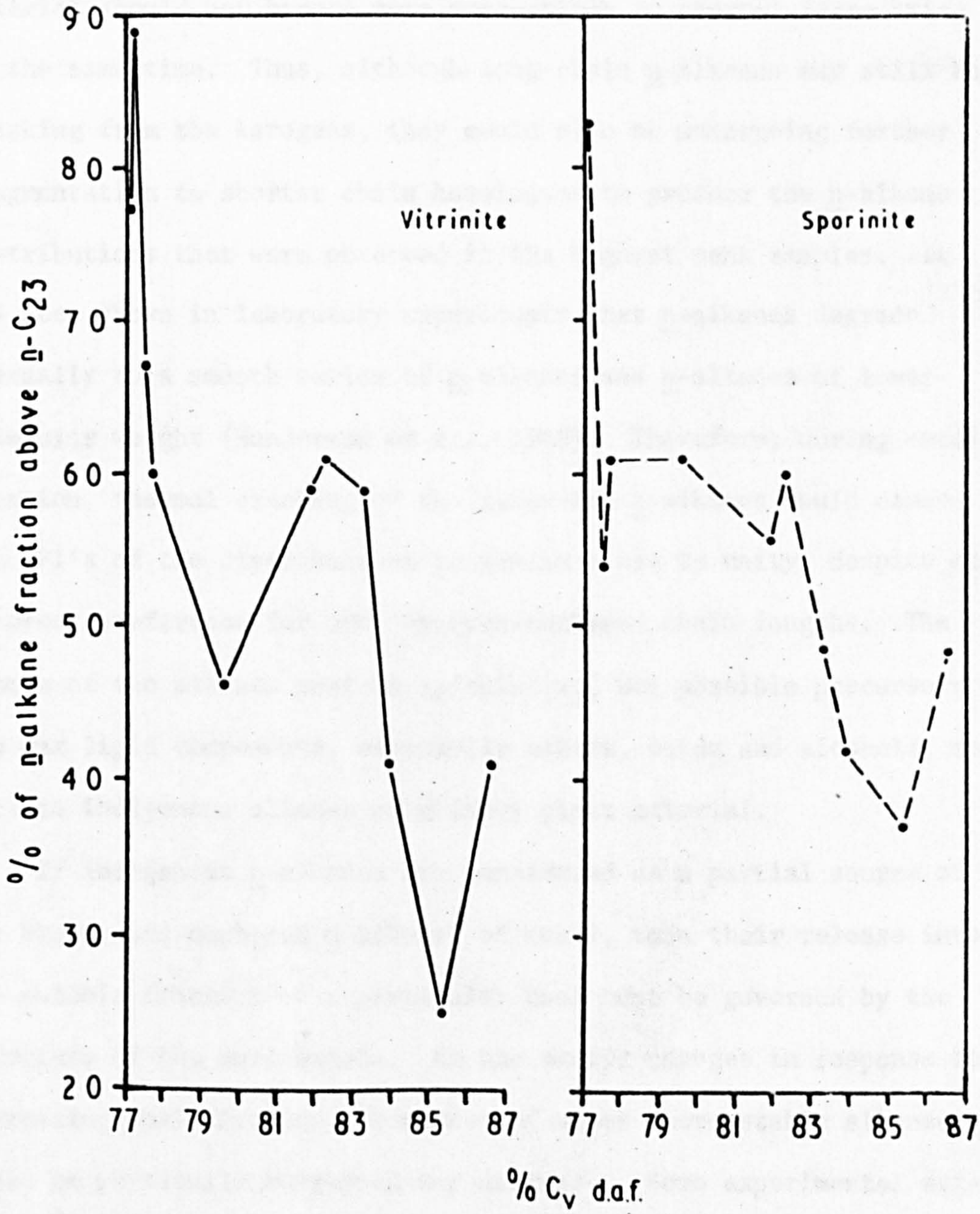

above this rank, and increasing amounts of the lower molecular weight constituents began to appear in the extracts. If the insoluble matrices of the macerals were showing a greater response to the prevailing geothermal conditions above a rank of 83.3% C (d.a.f.) by the thermal cracking of greater quantities of alkyl chains from the kerogens, then there is no *a priori* reason why the already-soluble material should not become more susceptible to thermal degradation at the same time. Thus, although long-chain n-alkanes may still be cracking from the kerogens, they could also be undergoing further fragmentation to shorter chain homologues to produce the n-alkane distributions that were observed in the highest rank samples. It has been shown in laboratory experiments that n-alkanes degrade thermally to a smooth series of n-alkanes and n-alkenes of lower molecular weight (Henderson *et al.*, 1968). Therefore, during coalification, thermal cracking of the generated n-alkanes would cause the CPI's of the distributions to remain close to unity, despite any inherent preference for odd- or even-numbered chain lengths. The source of the alkanes must be speculative, but possible precursors are wax lipid components, especially esters, acids and alcohols, as well as indigenous alkanes of primary plant material.

If indigenous n-alkanes are considered as a partial source of the higher odd-numbered n-alkanes of coals, then their release into the soluble fraction of a particular coal must be governed by the structure of the coal matrix. As the matrix changes in response to increasing coalification the number of sites where stable alkanes could be physically entrapped may decrease. Some experimental evidence has been advanced to show that the order of removal of hydrocarbons from coal by solvent extraction was governed by the molecular size and shape of the hydrocarbons (Vahrman, 1970) and that complete removal, especially of n-alkanes, required a considerable period of time.

Fat and wax esters are possible hydrocarbon precursors which occur in abundance in nature. In Recent sediments however the extractable content of these materials is generally low compared to the input (Abelson, 1963). This has been used as an argument for either their rapid incorporation into the insoluble fraction of the organic matter, or their equally rapid biological degradation by micro-organisms. Undoubtedly both of these factors are applicable to variable extents.

Wax esters contain straight-chain aliphatic carboxylic acids and alcohols with chain lengths of the alkyl moieties usually in the C_{20} to C_{34} range (Mazliak, 1969). They show a strong predominance of even-carbon-numbered chain lengths. They are not found in any great quantity, if at all, in bituminous coal extracts however (Brooks and Smith, 1969). If, therefore, these compounds are present in bituminous coals, they must either be bound in such a way to the matrix that hydrolysis of the ester linkage is insufficient to release the moieties, or hydrolysis may have taken place naturally to leave the moieties individual linked to the matrix, possibly through terminal oxygen functions or C-C linkages. Infra-red studies (previous chapter) showed that carbonyl groups were present in exinites almost to medium-volatile bituminous rank, but were not detectable in the vitrinites. This may be a reflection of the greater lipid input into exinites.

The production of alkanes by the decarboxylation of fatty acids has been postulated as an organic geochemical process (Cooper and Bray, 1963; Jurg and Eisma, 1970; Kvenvolden, 1966, 1970), and laboratory studies have indicated that thermal treatment of esters, and sediments, can produce n-alkanes which, under suitable conditions, can show odd- or even-dominated or smooth distributions (Douglas et al., 1970b; Maxwell, 1967; Mitterer and Hoering, 1968; Connan, 1970;

Dungworth, 1972; Connan, 1973; Coates, 1973; Stanbridge, 1973; Esnault, 1973). In dealing specifically with coals Brooks and Smith (1969) have effectively demonstrated that extracted coal residue itself acts as a catalyst in the decarboxylation of even-numbered acids to produce odd-numbered n-alkanes. In addition they showed that, while simple thermal treatment of esters produced even-numbered alkenes from the alcohol moieties, addition of the extractable acetone-soluble branched and cyclic esters of coal converted the alkenes to alkanes.

If n-alkane generation and their subsequent thermal cracking were of sequential importance during coalification, it is difficult to explain why the two processes were more sharply delineated in vitrinites than in sporinites. This could be an environmental factor as the sporinites were isolated from durains and the vitrinites from vitrain. Durains often have a higher content of clay minerals than vitrains, and clay catalysis may have been of greater importance in the sporinites, influencing the rates and temperatures at which the reactions proceeded. It would be of interest to compare the n-alkane concentrations of sporinites isolated from clarains and durains to see if such factors do in fact have any detectable effect.

The composition of the branched/cyclic alkane fractions of vitrinite and sporinite also seemed to be dependent on rank. There is, therefore, a possibility that this part of the hydrocarbons, extractable from geological samples, could be used for maturation studies as are n-alkanes. Unfortunately, quantifying the data and identifying the constituent compounds is not as straightforward as it is for n-alkanes because of the wide diversity of compound types that are present in these fractions.

Three major progressive changes occurred with increasing coalification, manifested in the increase in amounts of acyclic C_{15} to C_{20} isoprenoid alkanes, the decrease in the amounts of polycyclic compounds of high molecular weight, and increasing complexity of the fractions as a whole below about C_{28}.

The concentrations of the C_{18}, C_{19} (pristane) and C_{20} (phytane) acyclic isoprenoid alkanes are shown in Table 11. Examination of the gc's of the total alkane fractions showed that the C_{15} and C_{16} isoprenoid compounds also increased in concentration with increasing coalification, but the absolute amounts of these two compounds have not been calculated because of their greater susceptibility to loss during analysis.

The variation of pristane:phytane ratios with increasing coalification was elucidated for a series of Australian coals (Brooks *et al.*, 1969), where it was found that the ratio increased to a maximum at a rank of *ca.* 83% C (d.a.f.), and subsequently decreased with further coalification. Pristane:phytane ratios from the results of the present investigation are given in Table 11. Fig. 27 shows that sporinites produced a trend substantially in agreement with the work of Brooks and co-workers. The vitrinite trend was more random. Furthermore, sporinites produced a higher maximum ratio than vitrinites. A variation such as this in a particular parameter which is being applied to the problem of geochemical maturation underlines the importance of gaining some knowledge of the composition of the organic matter which is being investigated.

Brooks *et al.*, demonstrated by thermal degradation experiments that phytanic acid is more likely than phytol to produce a dominance of pristane over phytane in sediments. The pristane:phytane ratios therefore may be used as an indicator of the relative degree of oxidation which has occurred in the early diagenesis of sediments. The mechanism of the generation of these alkanes, from the respective

Table 11: Concentrations of acyclic isoprenoid alkanes in vitrinites and sporinites (mg/gm x 10^{-3}), and pristane:phytane ratios

	C_{18}	C_{19}	C_{20}	C_{19}/C_{20}
Vitrinite				
High Hazles Gedling	-	0.53	0.18	2.94
Westfield	-	0.62	0.24	2.58
Clowne	4.50	42.00	4.20	10.00
Shallow	0.53	6.90	0.85	8.20
High Hazles Warsop	0.80	7.20	0.80	9.00
Deep Hard	0.45	5.00	0.75	6.67
High Hazles Whitwell	0.12	2.10	0.44	4.80
Beeston	0.40	5.90	0.70	8.43
Barnsley	2.40	14.60	2.40	6.08
Parkgate	5.90	21.80	3.30	6.61
Silkstone	2.60	11.90	1.60	7.44
Sporinite				
High Hazles Gedling	3.60	25.50	5.10	5.00
Clowne	9.90	72.80	7.10	10.25
Shallow	1.30	9.20	1.30	7.08
High Hazles Warsop	2.50	19.50	2.00	9.75
Deep Hard	5.90	43.20	4.10	10.54
High Hazles Whitwell	4.60	37.40	3.70	10.11
Beeston	6.40	46.80	4.40	10.64
Barnsley	10.30	45.50	5.80	7.84
Parkgate	14.90	54.50	9.10	5.99
Silkstone	7.90	37.50	4.50	8.33

FIG. 27. VARIATION OF PRISTANE/PHYTANE RATIOS OF VITRINITE AND SPORINITE WITH RANK

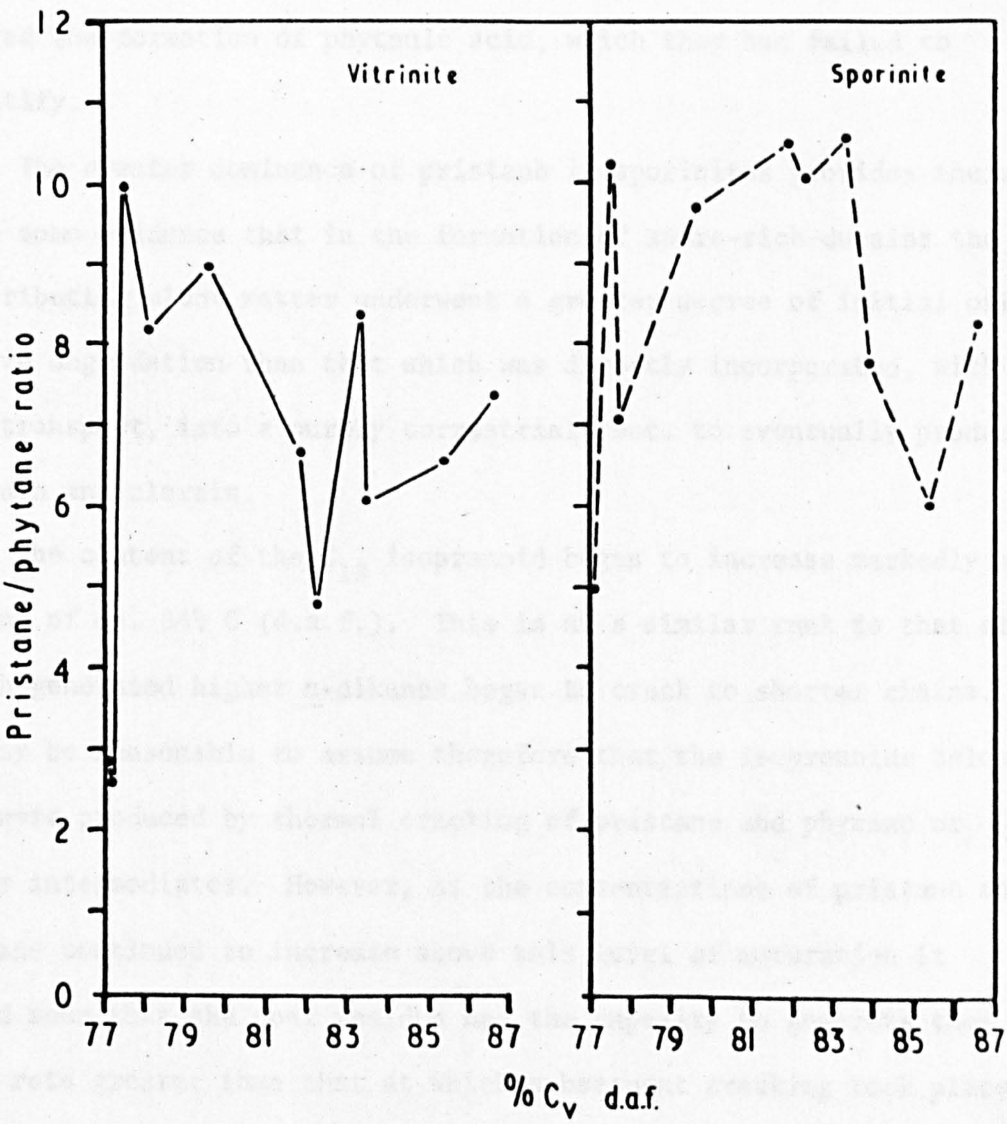

acid and alcohol precursor, is similar to that proposed by Brooks and Smith (1969) in their studies of n-alkane formation. In a recent study on the effect of laboratory thermal degradation of a Recent marine sediment, Ikan *et al.*, (1975), proposed two routes for the production of pristane from phytol, both requiring an oxidative step in the process. The suggested mechanisms were based on the analysis of the reaction products, but one proposed pathway required the formation of phytenic acid, which they had failed to identify.

The greater dominance of pristane in sporinites provides therefore some evidence that in the formation of spore-rich durains the contributing plant matter underwent a greater degree of initial oxidative degradation than that which was directly incorporated, without transport, into a purely terrestrial peat, to eventually produce vitrain and clarain.

The content of the C_{18} isoprenoid began to increase markedly at a rank of *ca.* 84% C (d.a.f.). This is at a similar rank to that at which generated higher n-alkanes began to crack to shorter chains. It may be reasonable to assume therefore that the isoprenoids below C_{19} were produced by thermal cracking of pristane and phytane or their intermediates. However, as the concentrations of pristane and phytane continued to increase above this level of maturation it would seem that the coal residue had the capacity to generate them at a rate greater than that at which subsequent cracking took place, at least to a rank of 85.4% C (d.a.f.). This is contrary to the behaviour of higher n-alkanes, which began to decrease in amounts at a rank of *ca.* 84% C (d.a.f.).

The thermal stability of hydrocarbons decreases as the size of the molecule increases. Hence, long-chain n-alkanes might be expected to crack to shorter-chain, more stable homologues. Furthermore, n-alkanes are less resistant to thermal breakdown than branched and cyclic alkanes, and so under purely thermal conditions pristane and phytane will be more stable than n-alkanes of corresponding chain lengths. However, if catalytic cracking is effective, isoprenoid alkanes, which contain tertiary carbon atoms, will be expected to crack much more readily than their corresponding n-alkanes (Gruse and Stevens, 1960).

Triterpanes became less dominant components of the branched/cyclic alkane fractions with increasing coalification. Consideration of gas chromatograms can be misleading however as such a decrease may only be an apparent one, caused by dilution of the fractions with increasing amounts of lower molecular weight material. However, if the relative amounts of the polycyclic alkanes in the chromatograms (Figs. 16, 16a, 17 and 17a) are considered along with concentrations of the branched/cyclic alkane fractions shown in Table 6, then it would seem that this diminution may, in fact, be a real trend.

The decrease in the triterpane content was accompanied by an increase in both the amount and complexity of compounds of lower molecular weight. In a study of Jurassic shales, cyclic alkanes containing up to three cyclohexane rings were found to be relatively more stable than tetra- and pentacyclic alkanes (Tissot *et al.*, 1971). Simulated progressive diagenesis of natural asphalts from the Aquitaine basin (France) and of Yallourn lignite (Australia) also confirmed that steranes and triterpanes decreased in concentration with increasing maturation of the sedimentary organic matter (Connan, 1972, 1973). The increasing predominance of compounds below about C_{28} in the vitrinite and sporinite branched/cyclic alkane fractions may have been due in part to the formation of cyclic material from the fragmented tetra- and pentacyclic alkanes. However an equally possible fate for these compounds may have been aromatisation. An increasing concentration of, probably, alkylcyclohexanes has been noted in the extracts of Northumberland coals of higher ranks (Jones and Cooper, 1970). They were presumed to be derived from the aliphatic bridging structures between aromatic centres in the coal matrix.

It is interesting to note that the increase in the complexity of these fractions began at about the same rank that higher n-alkanes reached maximum concentrations, i.e. when thermal cracking became a controlling factor in n-alkane distributions. As cracking produces radicals from which olefins may be formed, they may in part undergo isomerization and cyclisation under the influence of catalysts, and thus may have contributed to the branched and cyclic components (Henderson *et al.*, 1968).

The ratio of branched and cyclic to n-alkanes in vitrinite and sporinite extracts decreased greatly from low to high rank (Table 6). If extractable material reflects a qualitative picture of the type of aliphatic structures present in the maceral matrices, then one effect of coalification was that these aliphatic structures became more straight-chain in type as maturation proceeded. It must be borne in mind however that non-normal compounds have been thermo-catalytically produced from n-alkanes in laboratory experiments, as pointed out above.

Where sedimentary hydrocarbons are considered to have been derived from terrestrial organic matter, their source has often been attributed to wax-rich components (spores, pollen and cuticular material). It is therefore of interest to note that at ranks of 83.9% C (d.a.f.) and higher, the yields from sporinites were only three to four times greater than those of their corresponding vitrinites, and in each case the hydrocarbon distributions were like that of a mature oil. Clearly, vitrinitic material in sediments should not be disregarded as a potential hydrocarbon source. The qualitative similarity in the alkane distributions of the two macerals implies some degree of structural equivalence in those parts of the maceral kerogens which ultimately gave rise to hydrocarbons during coalification.

Continuing investigations of sedimentary hydrocarbons throughout the world are showing that their generation often occurred within a definite range of geothermal conditions. Pusey (1973) has stated that nearly all of the world's major oil deposits were formed within a "liquid window", which correlates depth of burial and geothermal gradient. The upper and lower temperature limits of this "window" are 132^{o}C and 66^{o}C respectively. Philippi (1965) concluded that oil generation in the Los Angeles and Ventura Basins (California) occurred at a temperature of not less than 115^{o}C, while Albrecht and Ourisson (1969) found that a temperature of 75^{o}C was sufficient to generate hydrocarbons in the Douala Basin (Cameroun).

A number of parameters, specified by physical examination of the host sedimentary rocks, have been used to define the conditions required for oil generation. The colour changes that organic matter undergoes during maturation have been used as an index (Correia, 1969; Staplin, 1969), while ESR studies of kerogen can be used to deduce palaeotemperatures (Pusey, 1973). Reflectivity measurements on vitrinite have received wide application in this field, the advantage being that very small particles can give accurate results and no separation of an organic fraction from the host rock is required. Hence oil and gas production can be related to coalification, and coal is a very sensitive indicator of geothermal changes.

The results of this investigation have shown that a ~~rapid~~ marked increase in the alkane content of sporinite and vitrinite occurred at a rank of 83.9% C (d.a.f.) (mean maximum reflectance, $\bar{R}_{max}$, 0.91%).

Qualitatively the n-alkane distributions were mature at this rank, (i.e. they had a CPI value near unity), and thereafter they showed a trend of decreasing average molecular weight (i.e. produced lighter fractions).

The geochemical zones of hydrocarbon generation have been outlined in other investigations using vitrinite reflectance. In the Atlantic Provinces of Canada, oil generation occurred between $\bar{R}$ 0.3 to 0.8%, followed by gasification at higher ranks (Hacquebard and Donaldson, 1970). A range of $\bar{R}$ from 0.5 to 1.35%, with the main phase occurring between 0.7 and 1.0%, was given in an investigation of the phases of oil generation (Vassoyevitch *et al.*, 1969), with gasification dominating above $\bar{R}$ 1.35%. Teichmuller (1971) delimited oil generation to between $\bar{R}$ 0.3 and 1.0% and gas generation to between $\bar{R}$ 0.7 and 2.0% for sedimentary basins in Germany, while in Australia the given limits were $\bar{R}$ 0.5 to 1.3% for oil and $\bar{R}$ > 1.3% for gas (Brooks, 1970; Shibaoka *et al.*, 1973).

These figures are at some variance with each other. If it is accepted that reflectivity is an absolute measurement, whether on vitrinites from Australian, European or North American sources, then other controlling factors must, in part, govern oil and gas genesis. The tectonic history of a sedimentary basin cannot be expressed simply in terms of a reflectivity measurement. The rate of heating, maximum temperature, time and pressure effects must be taken into account. Differences in rock facies can affect the rate of hydrocarbon generation (Powell and McKirdy, 1973), while the nature of the organic matter and its preservational history must themselves influence hydrocarbon production (Vassoyevitch *et al.*, 1969; Philippi, 1974). This latter fact is one which, seemingly, has often received scant attention.

Evidence for the presence of extractable olefinic hydrocarbons was obtained for Westfield and High Hazles Gedling vitrinites, New South Wales alginite and the three resinites. Alkenes have previously been isolated in a high-volatile bituminous coal (Spence and Vahrman, 1965) and Vahrman (1972) identified them as alk-1-enes and alk-2-enes. Trans-disubstituted and trisubstituted alkenes were reported in both High Hazles Gedling vitrinite and sporinite (Powell, 1969). In the present investigation alkenes have not been found in this sporinite.

The resinite alkenes were not identified structurally but n-alkenes were identified as the predominant compounds in unsaturated fractions of the vitrinites and alginite. The source of the vitrinite alkenes is problematical. The two possibilities are that they were either of direct plant origin or diagenetic products of maturation. In favour of the former source is the fact that they were of high molecular weight, but a predominance of odd chain lengths might have been expected in the n-alkene homologies (Stransky and Streibl, 1969). It is worth noting that they were only found in the two lowest rank samples.

In studies of simulated diagenesis, long-chain alcohols have been considered as a possible source of even-numbered long-chain n-alkanes (Brooks and Smith, 1969). The reaction produces an alkene with the same number of carbon atoms as the source alcohol. Pyrolysis experiments on geological samples can produce, under suitable conditions, alkene fractions which show a predominance of even-numbered alkenes (Douglas *et al.*, 1970b; Coates, 1973). Douglas *et al.* have discussed a number of reaction pathways whereby even- and odd-numbered alkenes may be formed. Henderson *et al.*, (1968) have shown that an n-alkane degraded thermally to homologous series of n-alkanes and n-alkenes of lower molecular weight and both series had smooth distributions. While such a process would produce a smooth distribution of olefins, the earlier discussion on n-alkane generation concluded that thermal cracking of long-chain hydrocarbons was not a significant process at low ranks.

By contrast, New South Wales alginite produced dominantly even-numbered n-alkenes, although the extractable n-alkanes of this sample had a CPI greater than unity. These olefins may therefore be of predominantly diagenetic origin, despite the low rank of the sample. Pyrolysis results of these and other macerals are discussed in Chapter 4.

The three resinite samples all yielded alkenes, considered to be probably sesqui- and diterpenes. Like resinite alkanes they were probably derived directly from oxygenated resin compounds by defunctionalisation. As many resin components contain one or more double bonds in the ring systems (Thomas, 1969) alkenes will be initially produced by dehydration or decarboxylation of the resin alcohols and acids. It is also known however that resin acids can undergo a diagenetic change whereby an aromatic and a saturated hydrocarbon of similar ring configurations are produced (Streibl and Herout, 1969). Terpenoids are also known to react with sulphur to produce aromatic hydrocarbons (Douglas and Mair, 1965). There is undoubtedly further scope for a detailed investigation of resinite hydrocarbons which, because of their relative high stability, may be of use both as biological markers and in the elucidation of diagenetic pathways during maturation.

Experimental

Prior to concentration and extraction of the macerals certain procedures were followed, routinely, to minimise the effects of contamination from the samples, solvents and apparatus.

Pre-cleaning of the durain samples has already been described (previous chapter). Torbanite samples were obtained as large unjointed lumps, from which the outer ½" to 1" layer was removed; they were then washed ultrasonically in methanol. Vitrain, resin and cutin samples could not be mechanically cleaned because of the small fragment sizes and were simply washed ultrasonically in methanol.

Vitrinite and alginite samples were crushed in a disc mill (TEMA) to pass 100 mesh. Resinite and cutinite samples were crushed in a mortar because of the small amount of material available. The resinites were crushed to pass 100 mesh but the cutinite proved to be a rather pliable material, and was finally extracted in a mildly disaggregated state.

All glassware was cleaned in chromic acid and/or washed ultrasonically in detergent, then rinsed in distilled water. All solvents, except diethyl ether and chloroform, were distilled in the laboratory through a 30 plate Oldershaw column.

Extraction

Macerals were extracted in a soxhlet apparatus with an azeotropic mixture of chloroform (47.0%), methanol (23.0%) and acetone (30.0%) using pre-cleaned thimbles. Extraction was considered complete when the residue, after subsequent ultrasonic extraction with the azeotropic mixture (1 hr.), yielded less than 1% by weight of the extract obtained by soxhlet extraction. Full data are given in Table 12.

Table 12: Analytical data for the extraction of the maceral concentrates

	Weight (gm)	Time (hr)	Total solvent volume (ml)	Weight of extract (gm)
Vitrinite				
High Hazles Gedling	23.1	232	1000	2.1097
Westfield	63.1	275	1600	6.3506
Clowne	43.8	1025	1800	6.3623
Shallow	65.0	1025	1900	9.5850
High Hazles Warsop	62.0	1025	1800	8.0859
Deep Hard	66.4	689	2400	6.3223
High Hazles Whitwell	61.6	1025	2100	6.8491
Beeston	26.0	683	2100	4.4088
Barnsley	9.9	562.5	900	1.0757
Parkgate	48.6	573	1200	1.0130
Silkstone	61.1	164	1200	1.4880
Sporinite				
Donibristle	40.0	102	1200	1.7807
High Hazles Gedling	21.5	228.5	1600	1.3394
Clowne	23.1	292	800	1.2708
Shallow	45.0	292	800	2.5041
High Hazles Warsop	45.0	292	800	1.8689
Deep Hard	57.9	306	1200	2.2849
High Hazles Whitwell	46.3	292	800	2.2410
Beeston	50.0	228.5	1600	2.0052
Barnsley	45.0	292	800	2.3088
Parkgate	14.2	204	800	0.5143
Silkstone	41.1	228.5	1600	1.7062
Alginite				
Scotland	53.0	117	400	0.3122
South Africa	50.4	117	400	0.1598
New South Wales	50.1	120	400	0.7800
Resinite				
Yallourn	18.3	48.5	800	15.6793
Bitterfeld	13.6	48.5	800	4.7016
Maghara	8.6	48.5	800	4.6022
Cutinite				
Indiana	16.0	384	2200	1.2729

Column chromatography

An aliquot of each extract was chromatographed on silica gel (BDH, 60-120 mesh) activated at *ca.* 120° for 1 hr. Columns were slurry-packed in petroleum ether and the extract, adsorbed on a small amount of silica gel from solution in methanol/chloroform, was added to the top of the column after washing the column with excess petroleum ether. Columns were eluted with petroleum ether followed by methanol. Weights of extract and silica gel used are shown in Table 13; the ratio of silica gel to extract was always ≳ 20:1.

Thin-layer chromatography

Petroleum ether eluates and the first 10 mls of each methanol eluate were monitored by analytical argentatious thin-layer chromatography (tlc), using a standard 1:1 mixture of octadecane and octadec-1-ene as reference compounds. Analytical plates, prepared by slurrying silica gel (Keiselgel G; 6 gms/plate) in a 5% $AgNO_3$ solution, coated to a thickness of 0.25 mm (Shandon spreader) and activated at *ca.* 120°, were developed in petroleum ether (b.p. 40-60°). After development they were sprayed with 50% sulphuric acid and charred for 10 min. at 250°C.

By comparison with the standards, all petroleum ether eluates were found to contain alkanes (Rf 0.8-0.9) and none were detected in the methanol eluates. Unsaturated compounds were detected in six samples, namely Westfield vitrinite (Rf 0.45-0.20), High Hazles Gedling vitrinite (Rf 0.45-0.20), New South Wales alginite (Rf 0.45-0.15), Bitterfeld resinite (Rf 0.51-0.08), Maghara resinite (Rf 0.65-0.08) and Yallourn resinite (Rf 0.43-0.00).

Alkane and alkene fractions were isolated from these samples, except Yallourn resinite, by preparative tlc, using plates coated to a thickness of 0.50 mm (10 gms silica gel/plate) and pre-cleaned

Table 13: Analytical data for the column chromatography of the maceral extracts

	Extract	SiO_2	Eluant volume Petroleum ether	Eluant volume Methanol	Eluate yield Petroleum ether	Eluate yield Methanol
	(gm)	(gm)	(ml)	(ml)	(mg)	(mg)
Vitrinite						
High Hazles Gedling	0.5624	20.0	30.0	150.0	0.8	267.7
Westfield	0.6351	20.0	30.0	100.0	2.6	279.6
Clowne	1.0333	20.0	30.0	200.0	5.6	442.1
Shallow	0.9937	20.0	30.0	200.0	0.8	394.8
High Hazles Warsop	1.2939	25.0	30.0	200.0	1.7	506.2
Deep Hard	0.8899	20.0	30.0	100.0	2.1	299.4
High Hazles Whitwell	1.1127	25.0	30.0	200.0	1.0	370.6
Beeston	0.7113	20.0	30.0	100.0	1.7	184.5
Barnsley	0.4902	20.0	30.0	200.0	4.8	243.1
Parkgate	0.3356	15.0	30.0	150.0	17.6	141.3
Silkstone	0.4960	20.0	30.0	100.0	14.0	107.3
Sporinite						
Donibristle	0.2671	26.0	30.0	100.0	1.2	177.5
High Hazles Gedling	0.2009	20.0	30.0	100.0	2.2	107.8
Clowne	0.5381	20.0	30.0	200.0	12.8	350.5
Shallow	0.8693	20.0	30.0	200.0	5.3	487.0
High Hazles Warsop	0.8433	20.0	30.0	200.0	7.8	440.4
Deep Hard	0.6440	20.0	30.0	100.0	15.5	282.9
High Hazles Whitwell	0.8320	20.0	30.0	200.0	13.3	338.9
Beeston	0.2052	20.0	30.0	200.0	4.0	166.5
Barnsley	0.7228	20.0	30.0	150.0	42.0	231.2
Parkgate	0.2189	15.0	30.0	100.0	20.9	109.4
Silkstone	0.2559	24.0	30.0	100.0	15.6	113.9
Alginite						
Scotland	0.0625	6.0	20.0	80.0	20.8	23.4
South Africa	0.0639	6.0	20.0	50.0	8.8	46.0
New South Wales	0.3900	20.0	30.0	100.0	112.2	115.7
Resinite						
Yallourn	1.3806	10.0	35.0	40.0	0.3	1256.5
Bitterfeld	0.7791	10.0	35.0	40.0	1.0	719.5
Maghara	0.8595	10.0	35.0	40.0	59.4*	425.4
Cutinite						
Indiana	0.5092	20.0	30.0	100.0	1.5	267.7

* Infra-red spectroscopy indicated that C=O groups were present in this fraction.

by development in ethyl acetate. After development in petroleum ether, plates were sprayed with Rhodamine G and examined under an ultraviolet lamp. Separated bands were marked and removed, and the hydrocarbons were recovered from the gel with petroleum ether (Table 14). Yallourn resinite hydrocarbons were not fractionated by preparative tlc because of the very small weight of material.

Molecular sieve

Total alkane fractions of all macerals, except resinite, were sub-divided into normal and branched/cyclic fractions by treatment with 5A molecular sieve (Union Carbide Int. Co.).

Sieving was carried out by boiling the fractions under reflux for 24 hrs in dry benzene with pre-extracted molecular sieve, activated at 300-400^{o}C, using a sieve to sample ratio of 100:1. The supernatant liquid, containing branched/cyclic alkanes, was then removed, the sieve was washed with fresh benzene, and the washings were combined with the branched/cyclic fraction. n-Alkanes were recovered by dissolving the sieve in 40% HF, under benzene. The aqueous phase was extracted with benzene (x3) after neutralisation of excess HF with boric acid solution. Data are given in Table 15.

Gas chromatography

Hydrocarbon fractions were analysed by temperature-programmed gas chromatography. In general, packed columns were used (*ca.* 400 to 800 plates/ft), with OV-1 and OV-101 silicone gums as stationary phases. Internal standards were used for compound identifications. In addition capillary columns (150,000 to 250,000 effective plates, measured at n-C_{34}) were employed to identify, by co-injection, acyclic isoprenoid alkanes and alginite iso- and anteiso-alkanes.

Table 14: Separation of alkanes and alkenes by preparative thin-layer chromatography

	Petroleum ether eluate (mg)	Alkanes (mg)	Alkenes (mg)
Vitrinite			
High Hazles Gedling	0.8	0.7	0.1
Westfield	2.6	1.8	0.4
Alginite			
New South Wales	112.2	110.5	1.4
Resinite			
Bitterfeld	1.0	0.2	0.1
Maghara*	59.4	15.9	11.5
Yallourn	0.3	n.d.	n.d.

* The petroleum ether eluate of this sample was shown to contain non-hydrocarbon material by infra-red spectroscopy (absorption band at 1704 cm^{-1}). The low recovery was because the material at the origin of the tlc plate was not recovered to remove the non-hydrocarbons.

n.d. Not fractionated because of the small quantity of material, but analytical tlc showed that both alkanes and alkenes were present in the petroleum ether eluate.

Table 15: Separation of normal and branched/cyclic alkanes by molecular sieve

	Total alkanes (mg)	n-Alkanes (mg)	Branched/cyclic alkanes (mg)
Vitrinite			
High Hazles Gedling	0.7	0.1	0.6
Westfield	1.8	0.2	1.4
Clowne	5.6	0.7	3.4
Shallow	0.8	0.1	0.5
High Hazles Warsop	1.7	0.3	0.9
Deep Hard	2.1	0.4	1.5
High Hazles Whitwell	1.0	0.1	0.7
Beeston	1.6	0.3	1.1
Barnsley	4.8	1.9	2.6
Parkgate	17.6	9.3	7.0
Silkstone	14.0	7.0	5.9
Sporinite			
Donibristle	1.2	0.1	0.8
High Hazles Gedling	2.2	0.2	1.8
Clowne	12.8	1.7	8.3
Shallow	5.3	0.6	3.3
High Hazles Warsop	7.8	1.1	4.7
Deep Hard	15.5	2.4	9.5
High Hazles Whitwell	13.3	3.2	9.6
Beeston	4.0	0.4	2.9
Barnsley	40.0	12.2	18.1
Parkgate	20.9	4.0	11.9
Silkstone	15.6	6.0	7.8
Alginite			
Scotland	18.5	5.9	8.0
South Africa	6.7	0.6	4.7
New South Wales	18.0	5.1	10.0
Cutinite			
Indiana	1.5	0.3	0.9

Pristane and phytane concentrations were obtained by co-injection of branched/cyclic fractions with an accurately-determined amount of n-hexadecane.

Infra-red spectroscopy

Infra-red spectra of alkanes from Barnsley and Parkgate vitrinites and Clowne, Barnsley and Parkgate sporinites had absorption bands at 2960-2965 ($-CH_3$), 2920-2925 ($-CH_2-$), 2850-2858 ($-CH_2-$), 1460-1465 ($-CH_3$, $-CH_2-$), and 1375-1378 cm^{-1} ($-CH_3$), with very weak absorption at 718-720 cm^{-1} ($-(CH_2)_n-$, where $n \geq 4$). Alginite branched/cyclic alkanes produced a much stronger 720 cm^{-1} absorption band than other macerals, indicating less cyclic material.

Spectra were run as thin films between NaCl discs (Hilger and Watts Infra-red Spectrometer), from 4000 to 650 cm^{-1}. The 1603 cm^{-1} absorption band of polystyrene was used as an internal standard.

Hydrogenation of alkenes

The alkene fractions isolated from Westfield vitrinite and New South Wales alginite were hydrogenated with hydrogen over palladium charcoal catalyst (ratio of catalyst to sample was 30:1) in ethyl acetate. Gas chromatography of the products on a 40m. capillary column, capable of resolving n-alkanes from their respective n-alk-1-enes, showed that the homologous series in the alkene fractions had been converted quantitatively to n-alkanes.

Chapter 3

Carboxylic acids from the maceral extracts and the extracted maceral residues.

Introduction

The distribution of oxygen in coals, especially vitrains, has been extensively investigated. The greater part of the oxygen content of bituminous vitrains is present as hydroxyl and carbonyl groups, with the remainder probably occurring mainly in heterocyclic and aromatic ether structures. Oxygen in carboxyl and methoxyl groups is considered to be negligible in high-volatile bituminous and higher rank coals (Blom *et al.*, 1957; van Krevelen, 1961; Francis, 1961; van Krevelen, 1963). The presence of saponifiable ester groups has been demonstrated in brown coals but they are rare in bituminous coals (Brooks and Smith, 1969).

Infra-red spectra of the bituminous vitrinites and sporinites used in this investigation showed some differences in oxygen function content. Spectra of the sporinites contained a carbonyl absorption band close to 1700 cm^{-1} which decreased in intensity with increasing coalification, and disappeared, or merged into a broad absorption area centered near 1600 cm^{-1}, at a rank of *ca.* 84% C (d.a.f.). Absorption at 1700 cm^{-1} was not observed in spectra of the vitrinites. As the sporinites contained less oxygen than the corresponding vitrinites, this could be indicative of a wide discrepancy in the relative abundances of -OH and C=O functional groups in the investigated high-volatile bituminous rank range (i.e. 77% to 84% C, d.a.f.).

In order to determine the presence of saponifiable ester groups in the macerals used in this investigation, both the methanol eluates from the column chromatography of total extracts and the extracted maceral residues were saponified with boiling methanolic KOH solution. Very small quantities of fatty acids were thus isolated from vitrinites, sporinites, alginites and cutinite. In addition, straight-chain α,ω-dicarboxylic acids were isolated from the alginites and the cutinite. Higher yields of carboxylic acids were isolated from the resinites, but these produced rather complex mixtures of probable cyclic diterpenoid acids and no simple fatty acids were found.

Results and Discussion

The yields of acidic saponification products isolated by tlc, and subsequently methylated, are given in Table 16. The results of the saponification of the three resinites, in which a different scheme of fractionation by tlc was employed (see experimental), are shown in Table 18.

Fatty acids

The highest yield of extractable fatty acids was obtained from the cutinite, but they accounted for only 0.01% by weight of the maceral. The yields from the sporinites and vitrinites were all very small, and showed no significant variations with rank. Sporinite yields ranged from 0.009% to 0.001%, while for vitrinites they varied between 0.008% and 0.001%. The lower limit of these values was at the limit of accuracy of measurement. Yields of a similar order were obtained from the alginites. In general, fatty acid yields from the extracted residues were lower than those from the extracts.

Gas chromatographic analyses of the fatty acid fractions (as methyl esters) from sporinite and vitrinite extracts showed broadly similar distribution patterns, and those shown in Fig. 28 are representative. Many, although not all, of the samples had a restricted range of n-acids, strongly even-dominated between n-C_{14} and n-C_{22}, with palmitic acid as the major straight-chain component. A non-normal component, present in all the fractions, was possibly methyl phytanate, by comparison of its retention data with that of the authentic compound. Only three extracts (Clowne vitrinite, High Hazles Whitwell vitrinite and Parkgate sporinite) produced detectable quantities of even-dominated long-chain n-fatty acids, extending up to n-C_{28}. A similar pattern of n-fatty acids was

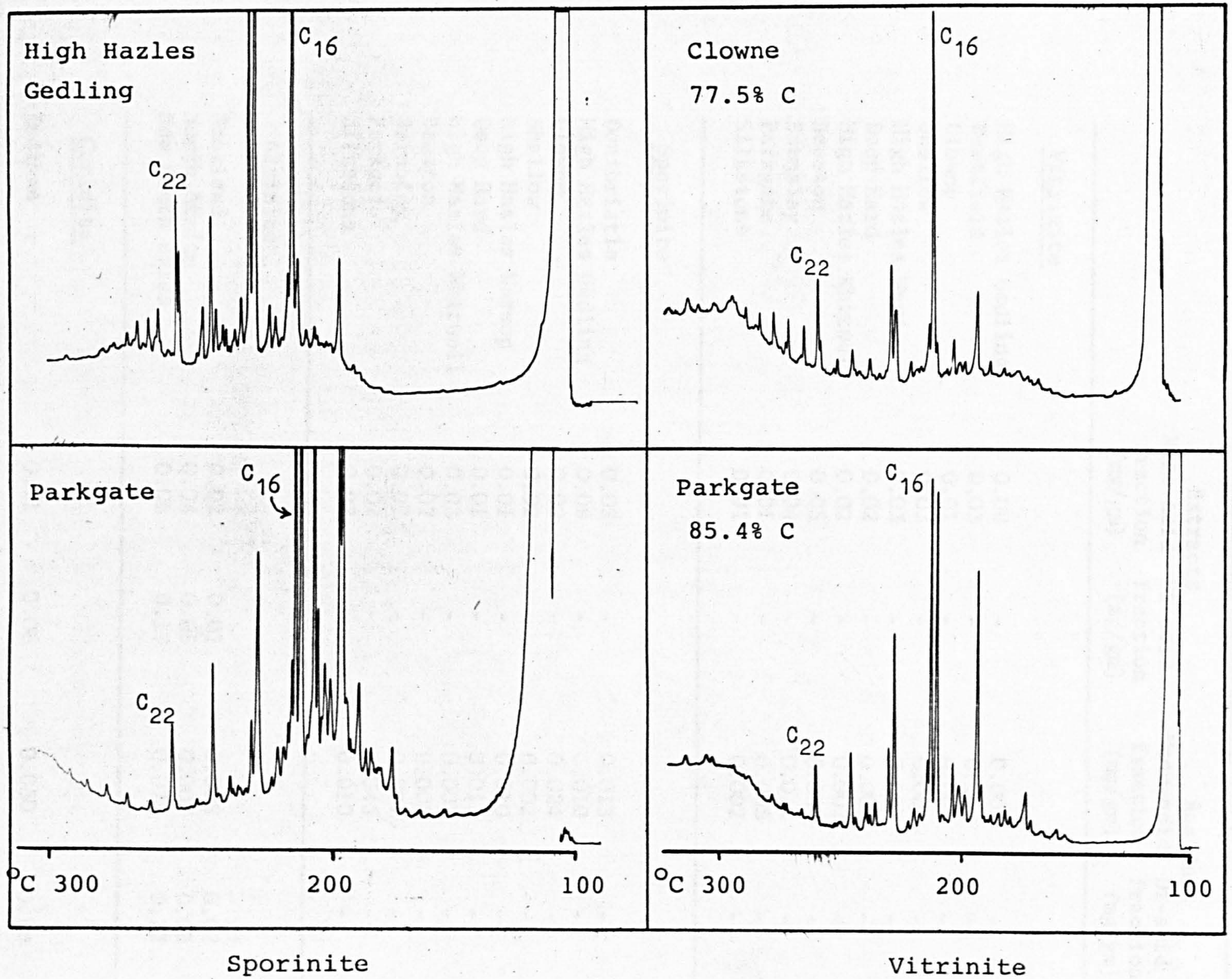

Fig. 28. Methyl esters of fatty acids of sporinite and vitrinite

Gas chromatographic conditions as in Fig. 8.

Table 16: Yields of mono- and dicarboxylic acids from maceral extracts and extracted residues (as methyl esters)

	Extracts Mono-acid fraction (mg/gm)	Extracts Di-acid fraction (mg/gm)	Residues Mono-acid fraction (mg/gm)	Residues Di-acid fraction (mg/gm)
Vitrinite				
High Hazles Gedling	0.08	-	0.009	-
Westfield	0.03	-	0.002	-
Clowne	0.01	-	0.005	-
Shallow	0.03	-	0.004	-
High Hazles Warsop	0.03	-	0.004	-
Deep Hard	0.02	-	0.002	-
High Hazles Whitwell	0.02	-	0.002	-
Beeston	0.05	-	0.004	-
Barnsley	0.04	-	0.012	-
Parkgate	0.01	-	0.005	-
Silkstone	0.01	-	0.002	-
Sporinite				
Donibristle	0.03	-	0.013	-
High Hazles Gedling	0.09	-	0.010	-
Clowne	0.02	-	0.024	-
Shallow	0.02	-	0.002	-
High Hazles Warsop	0.01	-	0.010	-
Deep Hard	0.01	-	0.011	-
High Hazles Whitwell	0.03	-	0.007	-
Beeston	0.02	-	0.008	-
Barnsley	0.02	-	0.007	-
Parkgate	0.02	-	0.043	-
Silkstone	0.02	-	0.010	-
Alginite				
Scotland	0.02	0.01	0.008	0.02
South Africa	0.04	0.05	0.002	0.09
New South Wales	0.06	0.19	0.075	0.12
Cutinite				
Indiana	0.11	0.06	0.030	0.90

isolated from High Hazles Gedling coal by Powell (1969).

Some of the extractable fatty acid mixtures contained variable amounts of branched/cyclic material, other than phytanic acid, while others contained virtually none. Where present with n-acids, this material was of low molecular weight (up to *ca.* C_{16}) and was very complex.

The distributions of fatty acids obtained from the extracted residues were generally similar to those obtained from the extracts, except that no n-fatty acids with chain lengths greater than 22 carbon atoms appeared to be present in any significant amount. A representative selection of chromatograms are shown in Fig. 29.

The extract and residue n-fatty acid distributions obtained in these analyses suggest that contamination from recent biological material has taken place. All but two of the original coal samples were collected underground in working deep mines, which are notoriously subject to percolating ground water. Although rigorous precleaning of all the samples was carried out prior to extraction, and strict precautions were observed to prevent laboratory contamination, this explanation remains a possibility, especially in view of the very low yields obtained.

On the other hand, the occurrence of lauric, palmitic and stearic acids in sporinite residues would not be unexpected in a structure composed, at least in part, of sporopollenin (Brooks and Shaw, 1968a), or in any other material which may have had, for example, a high glyceride input. However, these samples extended up to medium-volatile bituminous rank and the retention of such specific biological patterns is surprising, but interesting, if they are indigenous to the samples. Equally surprising, however, is the fact that the sporinites, supposedly rich in waxes, should not have yielded uniformly distinctive evidence of wax esters, especially in view of the

Fig. 29. Methyl esters of fatty acids of sporinite and vitrinite residues

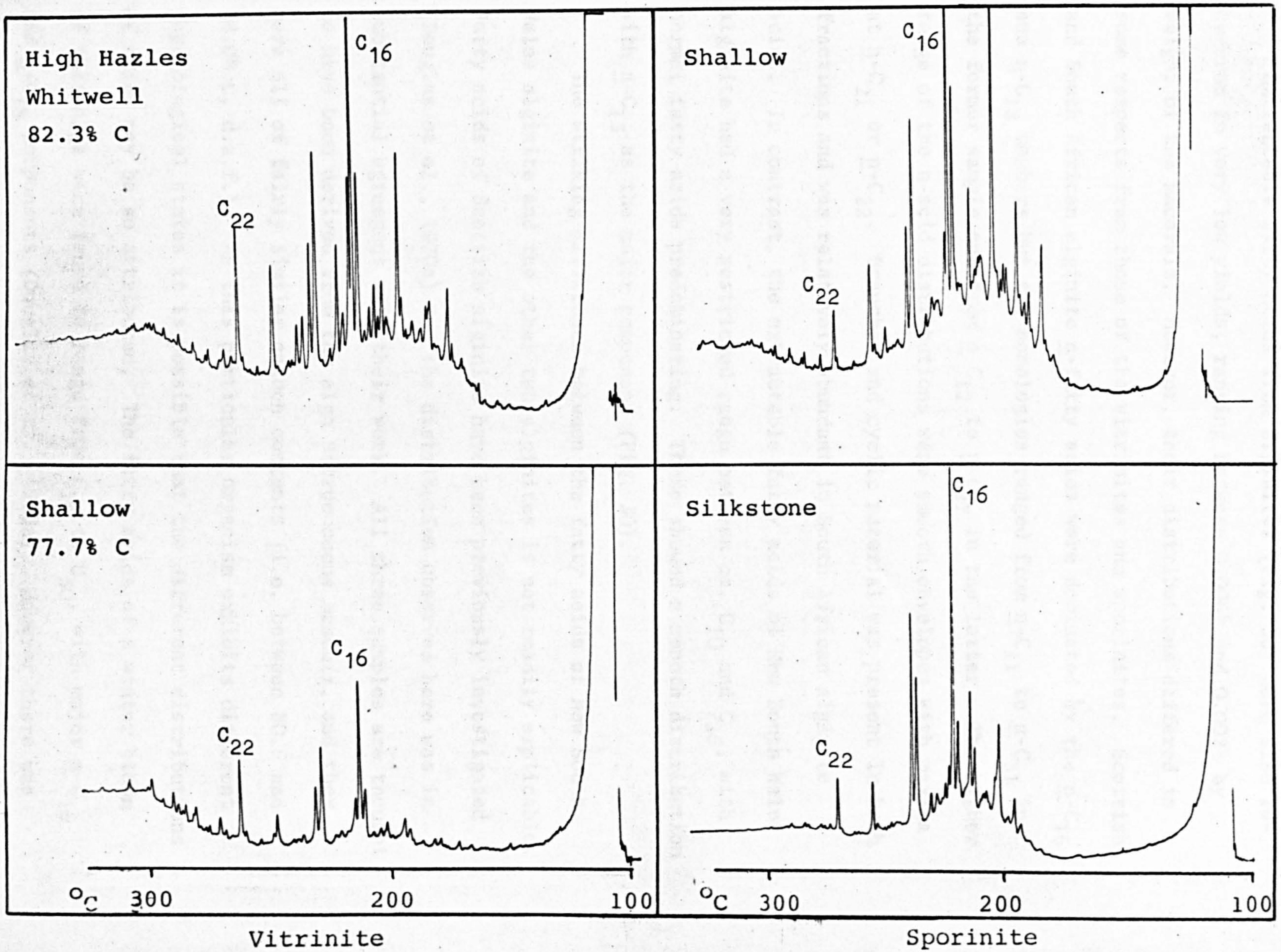

Gas chromatographic conditions as in Fig. 8.

extractable and pyrolytic alkane patterns produced by these macerals.

Extractable fatty acids from alginites (Fig. 30) were also recovered in very low yields, ranging between 0.006% and 0.002% by weight of the macerals. However, their distributions differed in some respects from those of the vitrinites and sporinites. Scottish and South African alginite n-fatty acids were dominated by the n-C_{16} and n-C_{18} members but the homologies ranged from n-C_{11} to n-C_{31} in the former sample and from n-C_{12} to n-C_{27} in the latter. The higher range of the n-acid distributions were smooth envelopes with maxima at n-C_{21} or n-C_{22}. Branched and cyclic material was present in both fractions and was relatively abundant in South African alginite acids. In contrast, the extractable fatty acids of New South Wales alginite had a very restricted range between *ca.* C_{10} and C_{15}, with normal fatty acids predominating. These showed a smooth distribution with n-C_{13} as the major component (Fig. 30).

The striking difference between the fatty acids of New South Wales alginite and the other two alginites is not readily explicable. Fatty acids of Scottish alginite have been previously investigated (Douglas *et al.*, 1970a) and the distribution observed here was in substantial agreement with their work. All three samples are thought to have been derived from the alga *Botryococcus braunii*, and they were all of fairly similar carbon contents (i.e. between 80.5 and 84.0% C, d.a.f.). As this particular organism exhibits different physiological states it is possible that the different distributions of acids may be so attributed. The fatty acids of a winter bloom of this alga were found to range from C_{14} to C_{30}, with major n-C_{16} and n-C_{18} components (Douglas *et al.*, 1969a). However there was little apparent structural difference in the microscopical appearance of the three materials. A point of interest is that the distribution of fatty acids isolated from New South Wales alginite

Fig. 30. Methyl esters of fatty acids of alginite

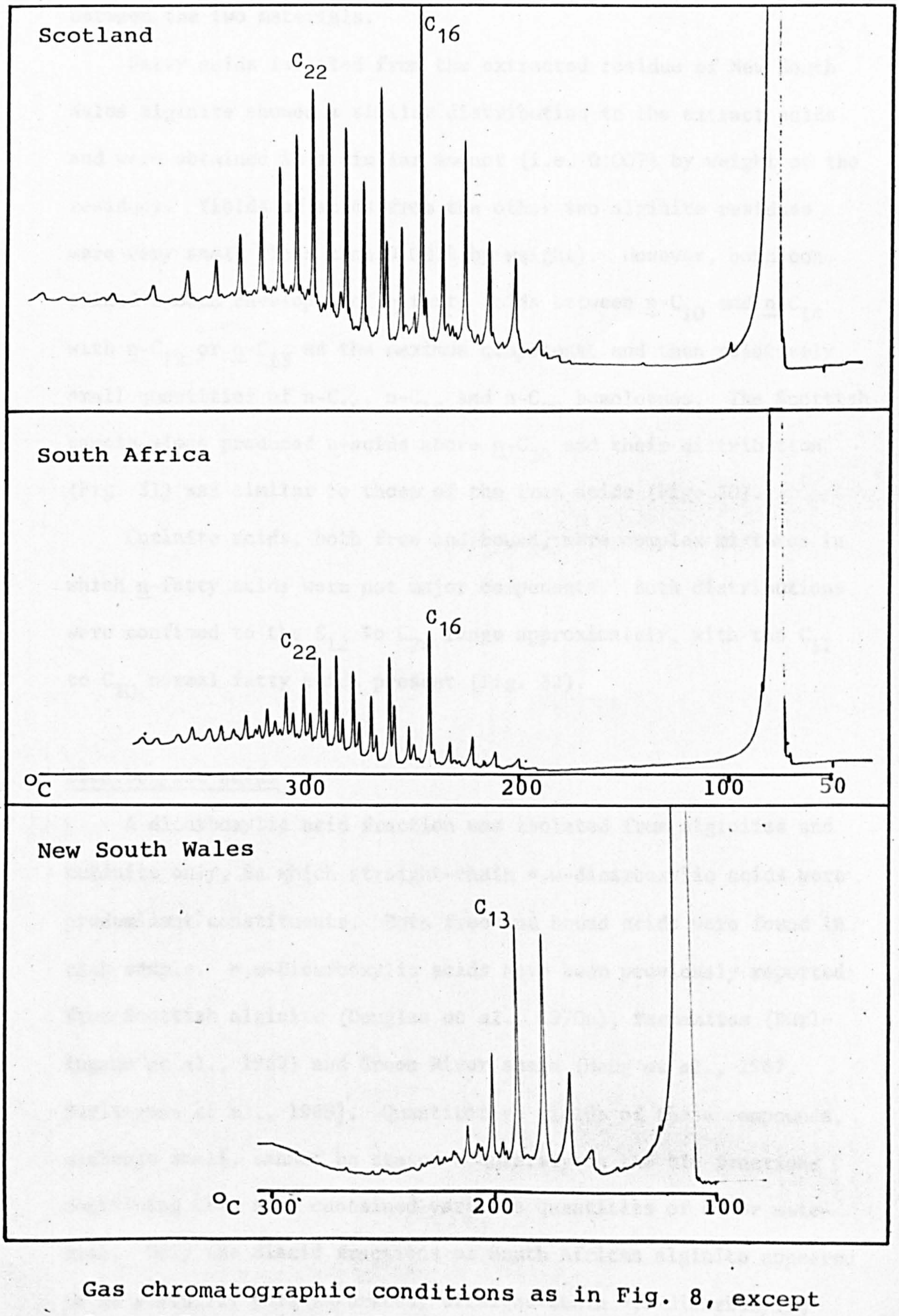

Gas chromatographic conditions as in Fig. 8, except Scottish and South African samples programmed 50-300°C, at 4°/min.

closely resembled those of *Tasmanites* from Alaska and Tasmania (Burlingame *et al.*, 1969), suggesting perhaps some relationship between the two materials.

Fatty acids isolated from the extracted residue of New South Wales alginite showed a similar distribution to the extract acids and were obtained in a similar amount (i.e. 0.007% by weight of the residue). Yields of acids from the other two alginite residues were very small (less than 0.001% by weight). However, both contained smooth envelopes of n-fatty acids between n-C_{10} and n-C_{14} with n-C_{12} or n-C_{13} as the maximum component, and then relatively small quantities of n-C_{16}, n-C_{18} and n-C_{20} homologues. The Scottish sample alone produced n-acids above n-C_{20} and their distribution (Fig. 31) was similar to those of the free acids (Fig. 30).

Cutinite acids, both free and bound, were complex mixtures in which n-fatty acids were not major components. Both distributions were confined to the C_{12} to C_{24} range approximately, with the C_{11} to C_{20} normal fatty acids present (Fig. 32).

Dicarboxylic acids

A dicarboxylic acid fraction was isolated from alginites and cutinite only, in which straight-chain α,ω-dicarboxylic acids were predominant constituents. Both free and bound acids were found in each sample. α,ω-Dicarboxylic acids have been previously reported from Scottish alginite (Douglas *et al.*, 1970a), *Tasmanites* (Burlingame *et al.*, 1969) and Green River shale (Haug *et al.*, 1967, Burlingame *et al.*, 1969). Quantitative yields of these compounds, although small, cannot be stated accurately as the tlc fractions containing them also contained variable quantities of other material. Only the diacid fractions of South African alginite appeared to be virtually pure saturated, straight-chain α,ω-dicarboxylic

Fig. 31. Methyl esters of fatty acids of alginite residues

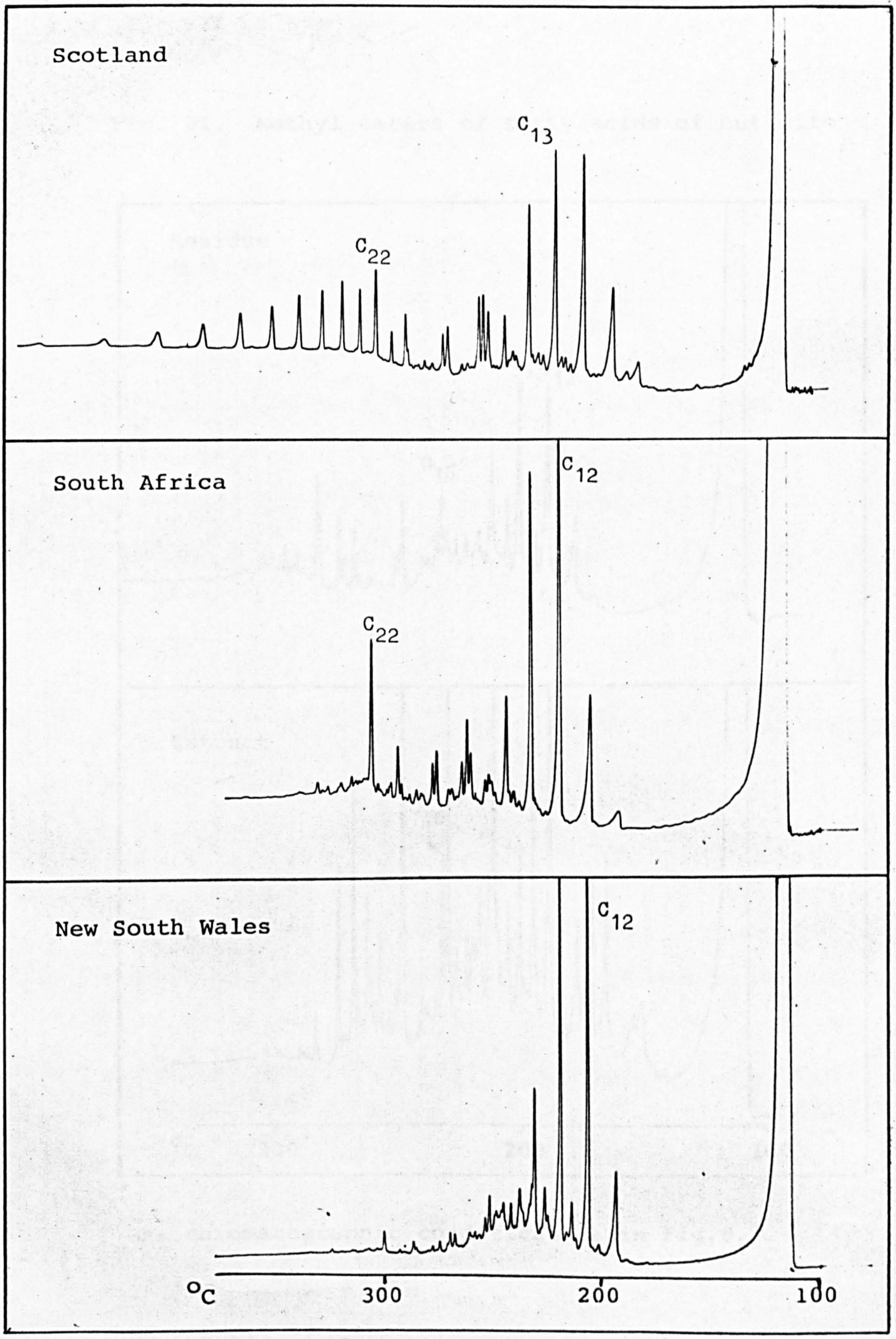

Gas chromatographic conditions as in Fig. 8.

Fig. 32. Methyl esters of fatty acids of cutinite

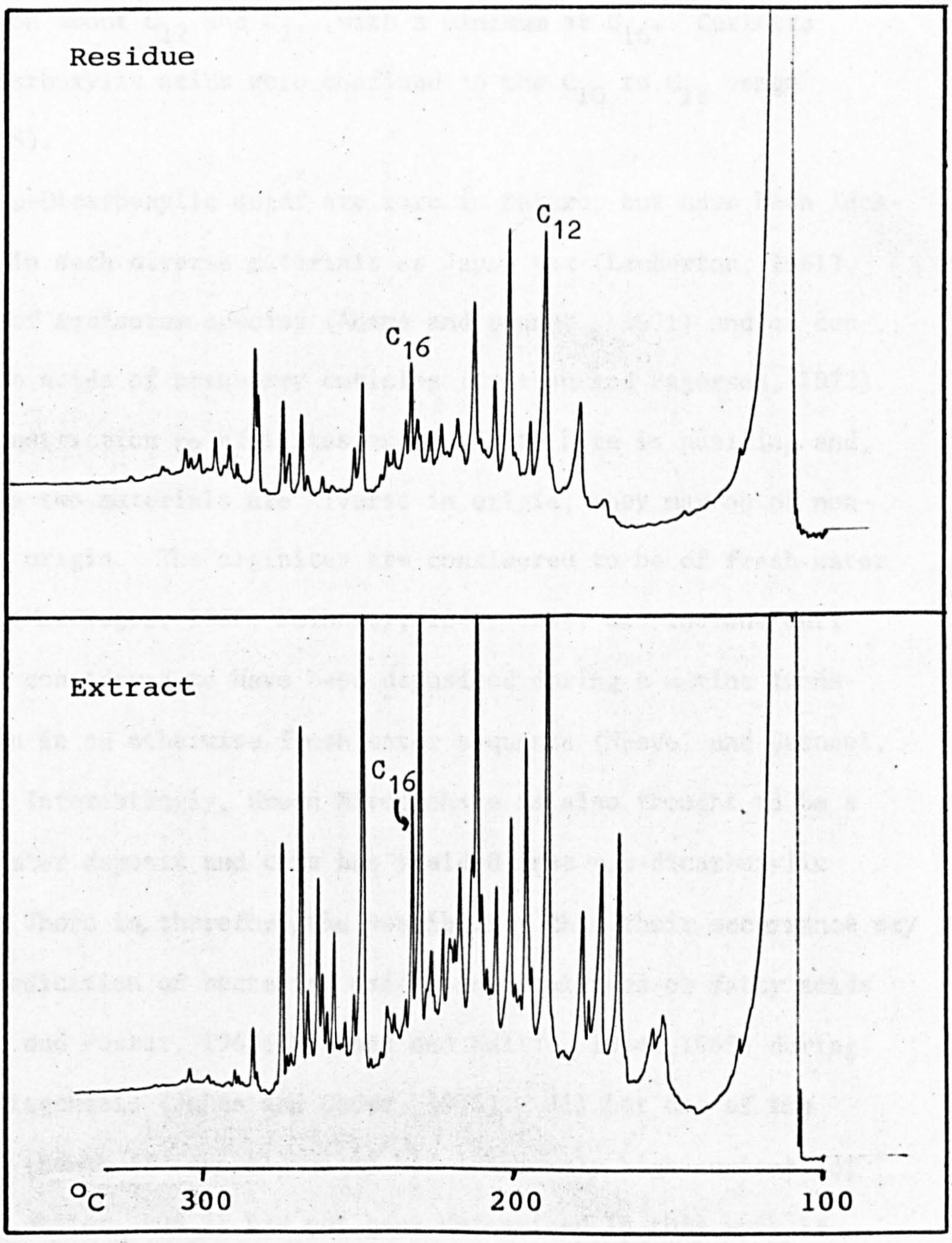

Gas chromatographic conditions as in Fig.8.

acids (Fig. 33).

The distributions of alginite α,ω-dicarboxylic acids showed minor variations between samples. They were generally confined to the C_9 to C_{27} range and usually showed smooth distributions with maxima varying between C_{12} and C_{16} (Figs. 33 and 34). The major exception was South African alginite which produced a bimodal distribution about C_{12} and C_{21}, with a minimum at C_{16}. Cutinite α,ω-dicarboxylic acids were confined to the C_{10} to C_{18} range (Fig. 35).

α,ω-Dicarboxylic acids are rare in nature, but have been identified in such diverse materials as Japan wax (Lamberton, 1961), spores of *Equisetum* species (Adams and Bonnet , 1971) and as constituent acids of cranberry cuticles (Croteau and Fagerson, 1972). Their restriction to alginites and cutinite here is puzzling and, as these two materials are diverse in origin, they may be of non-maceral origin. The alginites are considered to be of fresh water origin (MacGregor, 1938; Dulhunty, 1942, 1944) and Indiana cutinite is considered to have been deposited during a marine transgression in an otherwise fresh water sequence (Neavel and Guennel, 1960). Interestingly, Green River shale is also thought to be a fresh water deposit and this has yielded free α,ω-dicarboxylic acids. There is, therefore, the possibility that their occurrence may be an indication of bacterial oxidation of alkanes or fatty acids (Kester and Foster, 1963; McKenna and Kallio, 1964, 1965) during early diagenesis (Johns and Onder, 1975). All but one of the samples (South African alginite) had inherently high contents of mineral matter, and it has not been determined in this work if the diacids were combined with organic or inorganic material.

The structures of the α,ω-dicarboxylic acids of all the fractions were confirmed by combined gas chromatography-mass

Fig. 33. Dimethyl esters of α,ω-dicarboxylic acids of alginite

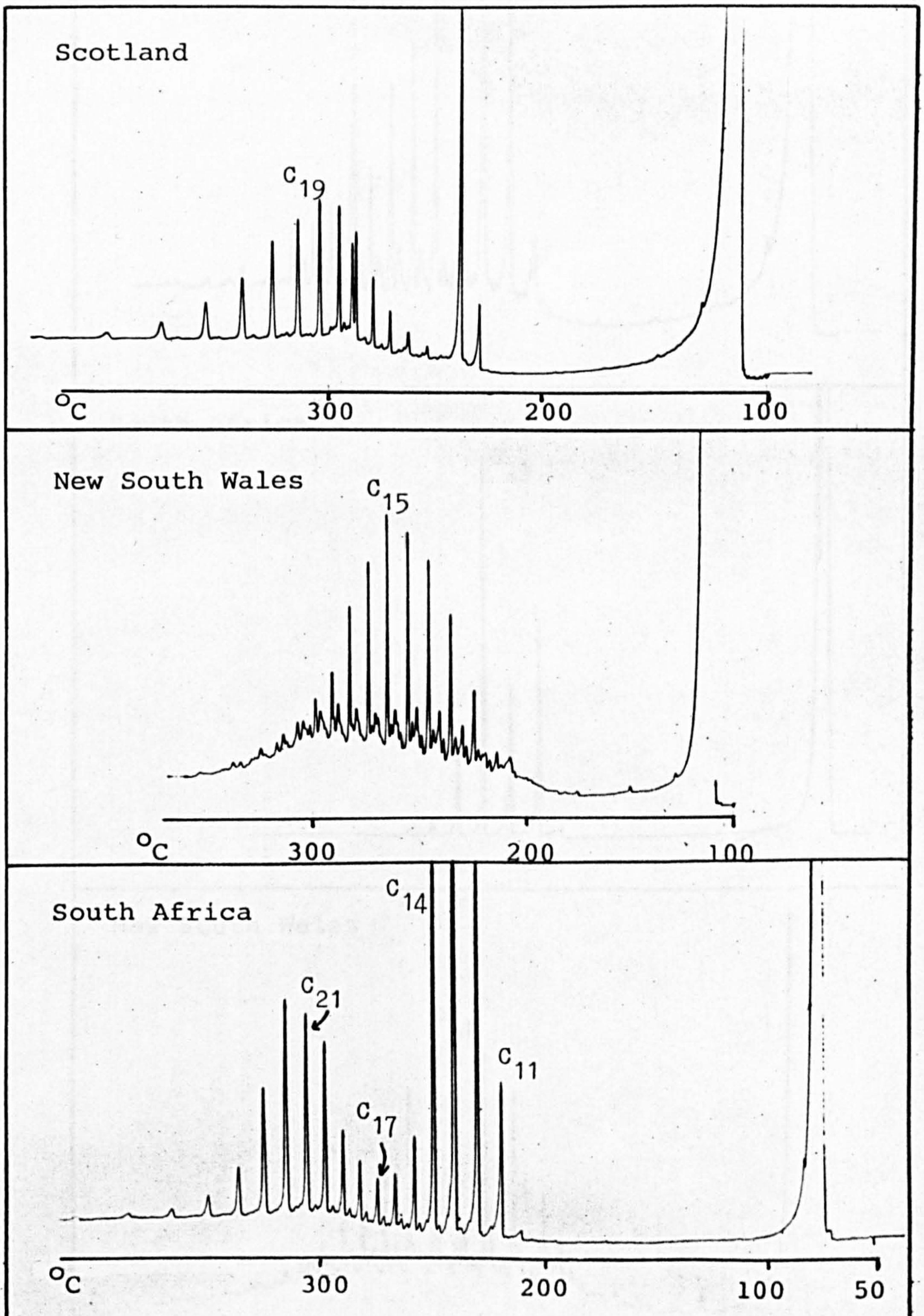

Gas chromatogaphic conditions as in Fig. 8, except South African alginite programmed 50-300°C at 4°/min.

Fig. 34. Dimethyl esters of α,ω-dicarboxylic acids of alginite residues

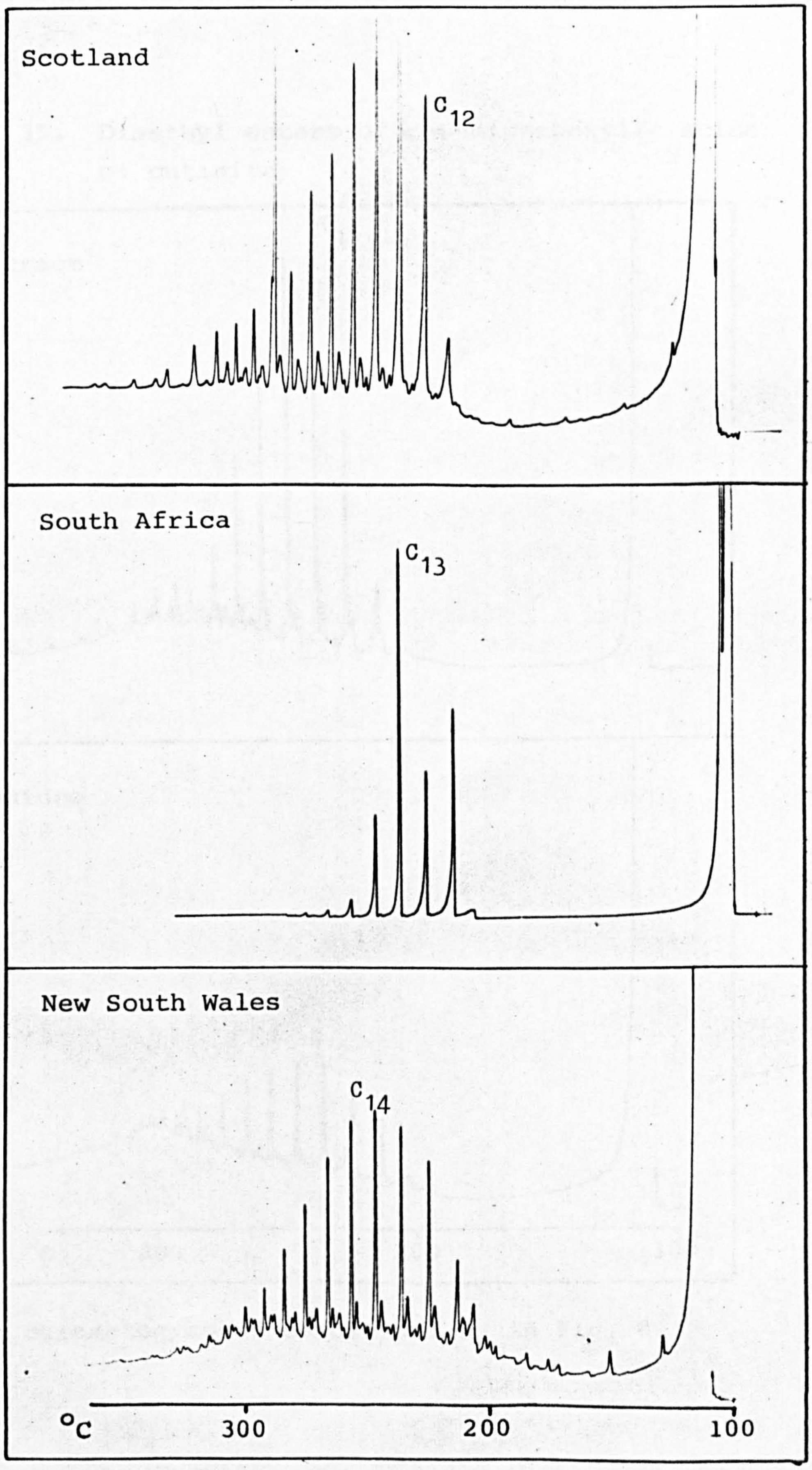

Gas chromatographic conditions as in Fig. 8.

Fig. 35. Dimethyl esters of α,ω-dicarboxylic acids of cutinite

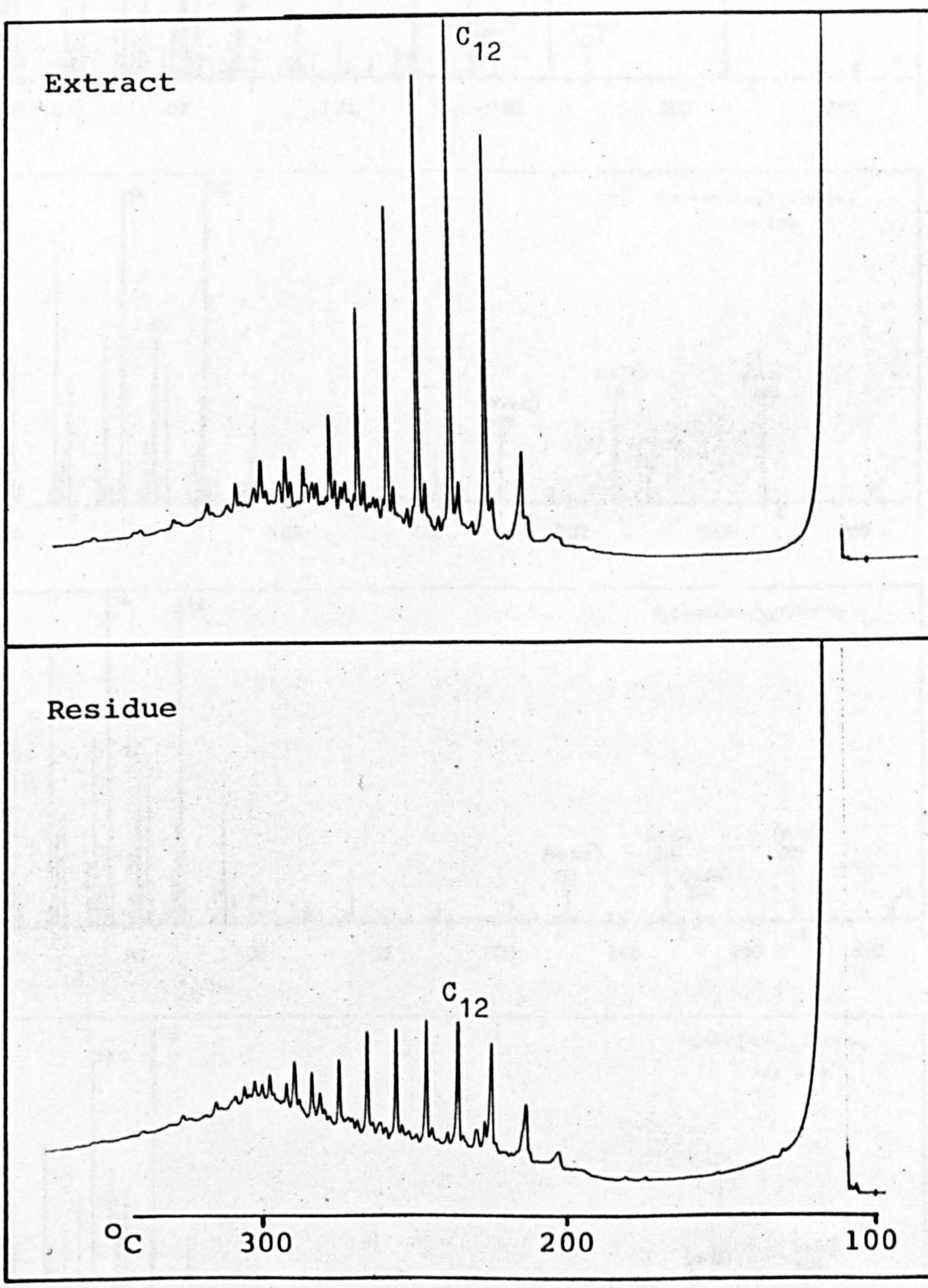

Gas chromatographic conditions as in Fig. 8.

Fig. 36. Mass spectra of dimethyl esters of free α,ω-dicarboxylic acids from South African alginite

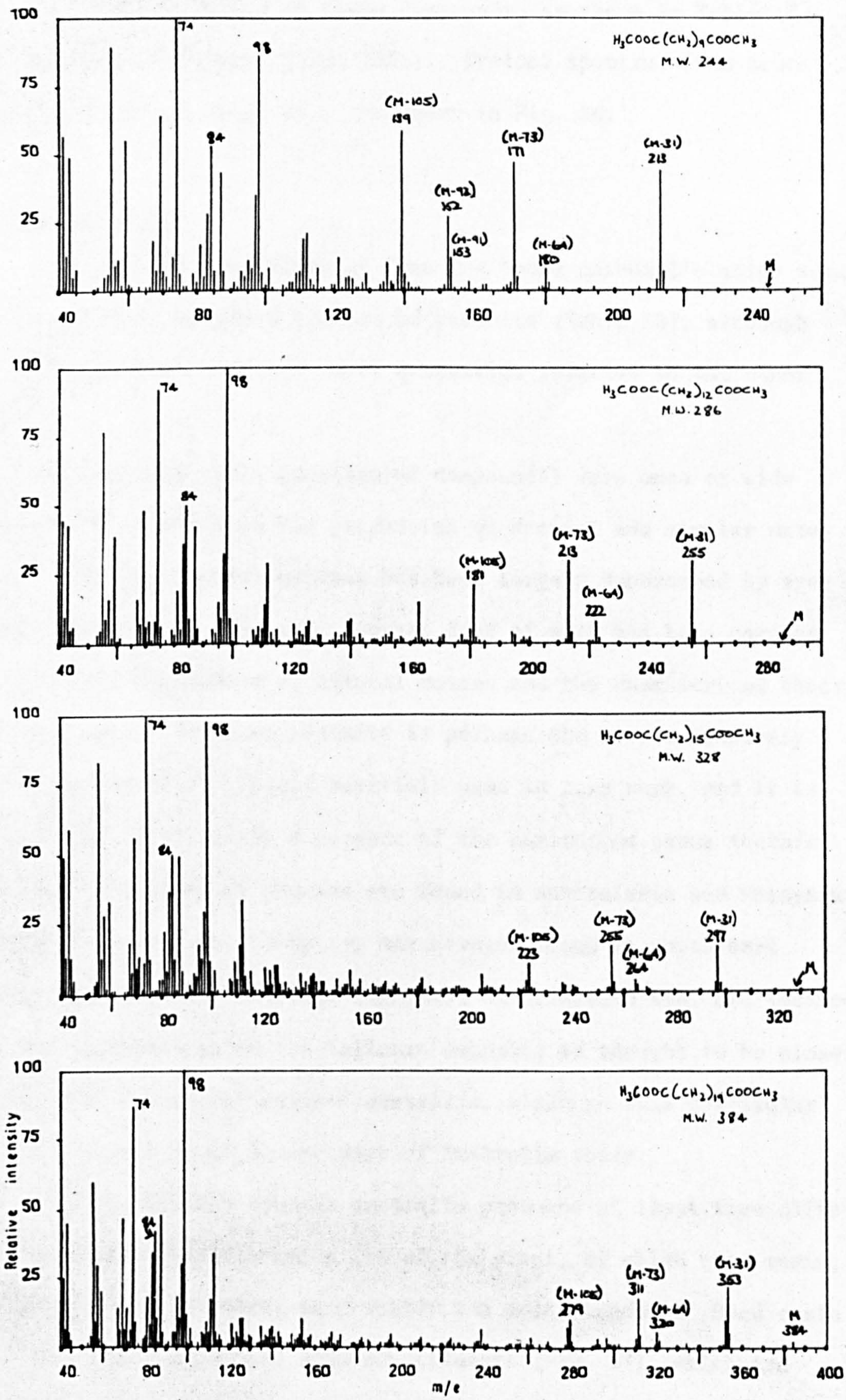

spectrometry, the spectra showing excellent correlations with the fragmentation patterns of these compounds, as shown in Table 17 (Ryhage and Stenhagen, 1959, 1965). Typical spectra, from South African alginite (Fig. 33), are shown in Fig. 36.

Resinite acids

Significant quantities of free and bound carboxylic acids were isolated from the three samples of resinite (Table 18), although Maghara resinite produced small quantities relative to the other two.

Resins (and their constituent compounds) were once of wide commercial interest in the production of varnish and similar materials, but the natural product has been largely superseded by synthetic materials. However, a great deal of work has been carried out on the composition of natural resins and the chemistry of their constituents. Yallourn resinite is perhaps the most extensively investigated of the fossil materials used in this work, and it is considered to be mainly a product of the coniferous genus *Agathis*, of which a variety of species are found in Australasia and Malaysia at the present time. They are not however found in south-east Australia where the Yallourn lignites, of Oligocene age, are located. A major contributor to the Yallourn deposits is thought to be closely-related to the extant *Agathis australis*, although this particular species is not found in any part of Australia today.

The present-day *Agathis australis* produces at least five different resins from different parts of the plant, of which bled resin, originating in the bark, is probably the most abundant. Bled resin has five major diterpene acid constituents (Fig. 37), which are agathic acid, <u>cis</u>- and <u>trans</u>-communic acids, sandaracopimaric acid and abietic acid (Thomas, 1966, 1969). The acids of the bled resins

Table 17: Mass spectral fragmentation patterns of the dimethyl esters of saturated, straight-chain α,ω-dicarboxylic acids: data from Ryhage and Stenhagen (1959, 1965)

m/e	Assignment	Comment
M	parent ion	often very small and may not be seen
M-31	loss of $-OCH_3$	all esters
M-60	" " $-COOCH_3$+H	short chain only
M-63	" " $-(OCH_3)_2$+H	short chain only
M-64	" " $-(OCH_3)_2$+2H	all esters except C_6 diacid ester
M-73	" " $-CH_2-COOCH_3$	all esters
M-91	" " $-COOCH_3+OCH_3$+H	((M-92) > (M-91) above C_9
M-92	" " $-COOCH_3+OCH_3$+2H	(
M-105	" " $-CH_2-COOCH_3+OCH_3$+H	increases after C_6
M-106	" " $-CH_2-COOCH_3+OCH_3$+2H	long chain only
27+(14)$_n$	probable hydrocarbon type	all esters
59+(14)$_n$	$H_3COOC-(CH_2)_n$	all esters
84	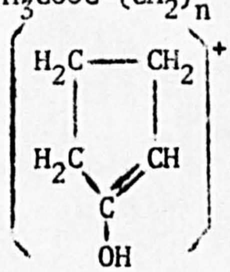	all esters
84+(14)$_n$	as above + $(CH_2)_n$	all esters
98	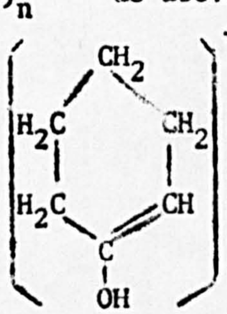 or 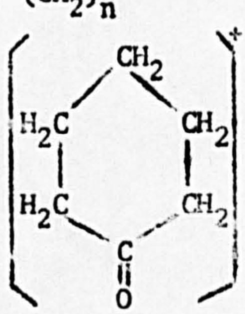	all esters, and is often the base peak

FIG. 37. MAJOR DITERPENOID ACID CONSTITUENTS OF BLED RESIN OF <u>AGATHIS AUSTRALIS</u>

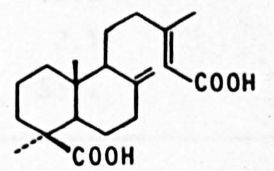

AGATHIC ACID

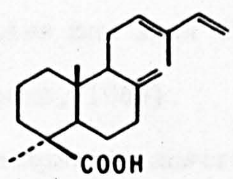

<u>trans</u>-COMMUNIC ACID

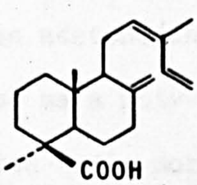

<u>cis</u>-COMMUNIC ACID

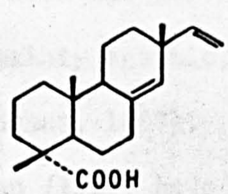

SANDARACOPIMARIC ACID

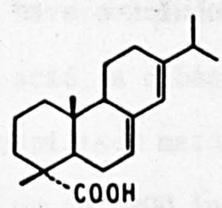

ABIETIC ACID

Table 18: Yields of carboxylic acids isolated from resinites (as methyl esters)

Sample	Extracts Wt. methyl esters recovered from tlc fractionation (mg/gm)	Residues Wt. methyl esters recovered from tlc fractionation (mg/gm)
Yallourn	25.5	13.6
Maghara	2.1	1.2
Bitterfeld	53.1	14.6

of other *Agathis* species may show differing constitutions (Carman and Dennis, 1964; Thomas, 1969).

Fresh resin from *Agathis australis* is almost completely soluble in acetone. Polymerisation in air takes place, initially fairly quickly, to produce an acetone-insoluble polymer which Carman and Cowley (1967) describe as a poly-communic acid with some communol units. Thus, deposited resin more than a few years old becomes depleted in communic acid and the acids of the remaining acetone-soluble portion are mainly agathic, abietic and sandaracopimaric acid (Gough, 1964; Thomas, 1969).

Brooks and Steven (1967) have investigated resinite from Yallourn lignite and have concluded that the basic structure is derived from agathic acid, a dibasic acid with C4 and C14 carboxyl substituents. The fossilised material is composed of oligomers with molecular weights of up to 1200 in which the C14 carboxyl group has been lost, and cross-linking has been achieved by double bond condensation. Some correlations have been attempted between fresh *Agathis* resins and fossil (i.e. Tertiary) resinites on the basis of chemical constitution, but only *A. ovata* has been definitely distinguished from *A. australis* so far in fossil samples (Thomas, 1969). However, Australian *Agathis* species of the present day do not contain abietic-type compounds, in contrast to species from New Zealand and Malaysia, and biogenetic differences such as this may aid correlative work (Thomas, 1969). At the present time, only one Miocene resinite from New Zealand shows a reasonable chemotaxonomic relationship with the living *A. australis*. Agathic and sandaracopimaric acids have been identified in this resinite, along with another major acidic component which may be abietic acid (Thomas, 1969).

The free and bound acids isolated in this work from the three resinites were methylated and fractionated by preparative tlc, which produced up to nine individual fractions (experimental data are given at the end of the chapter). Considerable simplification of the esters of the free acids was obtained, and Figs. 38 and 38a illustrate the gc's of the tlc bands separated from the total methyl ester fraction (Fig. 39) of Yallourn resinite. Mass spectra of many of the components of all three resinites have been obtained, but their complete interpretation is beyond the scope of the present investigation.

The mass spectra of many methyl esters of diterpenoid acids have been published in the literature, and a few of the spectra obtained from the Yallourn sample showed good correlations with some of the published data. Fig. 40 (A, B and C) shows the mass spectra of gc peaks 1, 2 and 3 of tlc band 2 (Fig. 38), and the mass spectrum (D) of authentic methyl 8, 15-isopimaradien-18-oate for comparison, provided by the Mass Spectrometry Data Centre, (MSDC) Aldermaston, Berkshire. All three compounds show a similar basic fragmentation pattern to that of the authentic compound, and are probably closely structurally-related to it. Their similarity of behaviour to tlc and gc support this. However, other isomers such as methyl 8, 15-pimaradien-18-oate and methyl 7, 15-isopimaradien-18-oate (MSDC)

Fig. 38. Methyl esters of tlc fractions of Yallourn resin acids

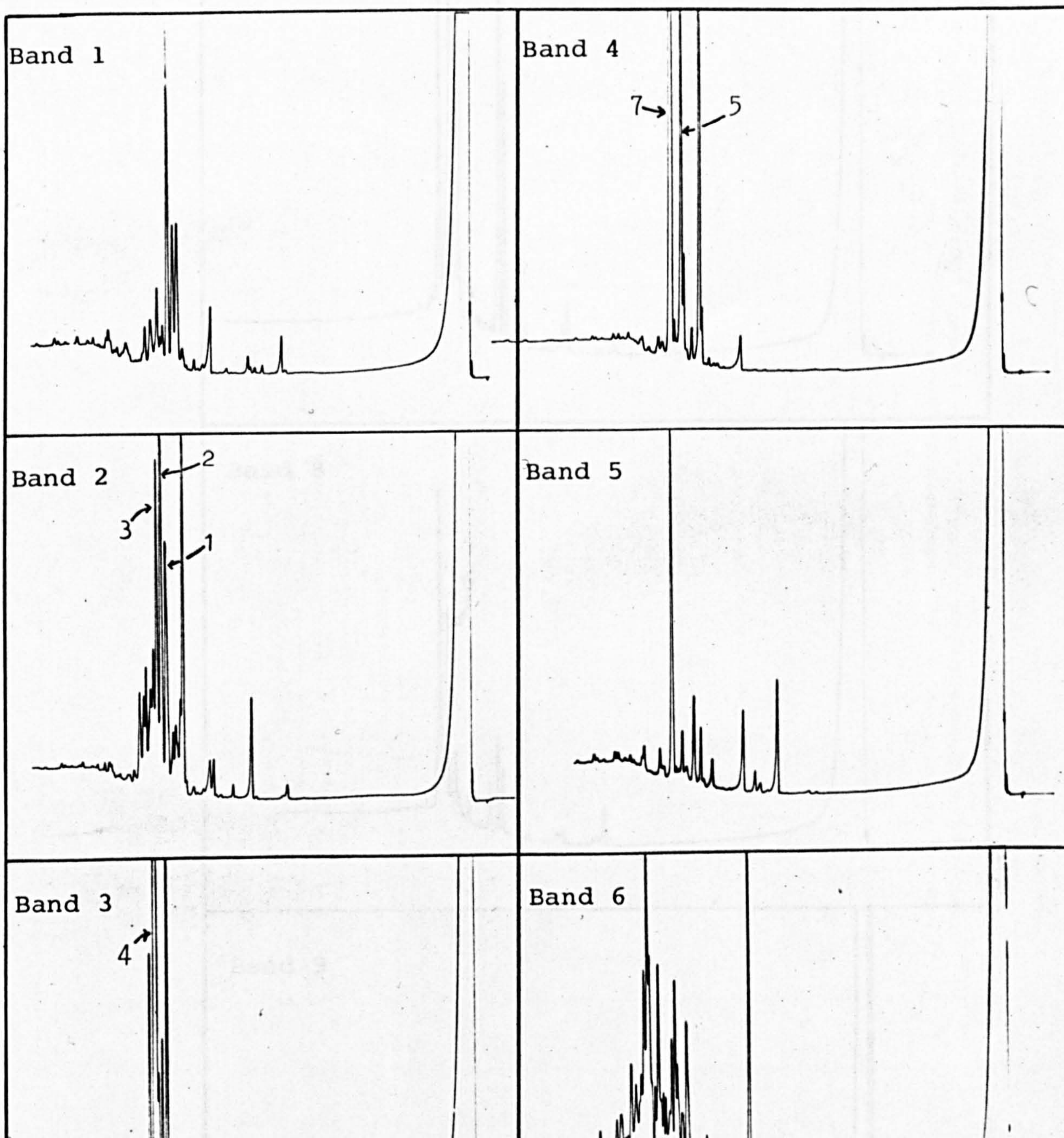

Gas chromatographic conditions as in Fig. 8.

Fig. 38a. Methyl esters of tlc fractions of Yallourn resin acids

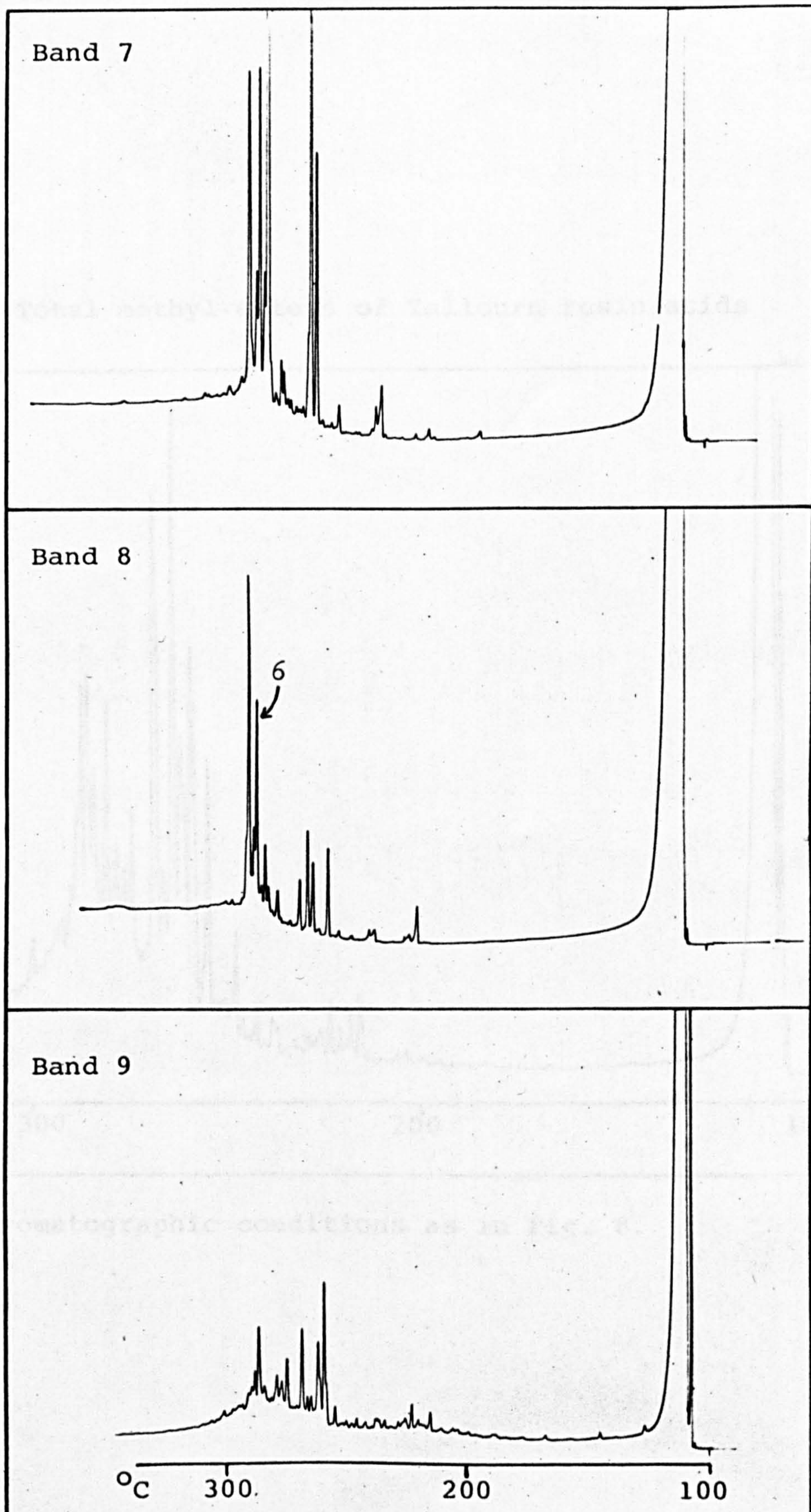

Gas chromatographic conditions as in Fig. 8.

Fig. 39. Total methyl esters of Yallourn resin acids

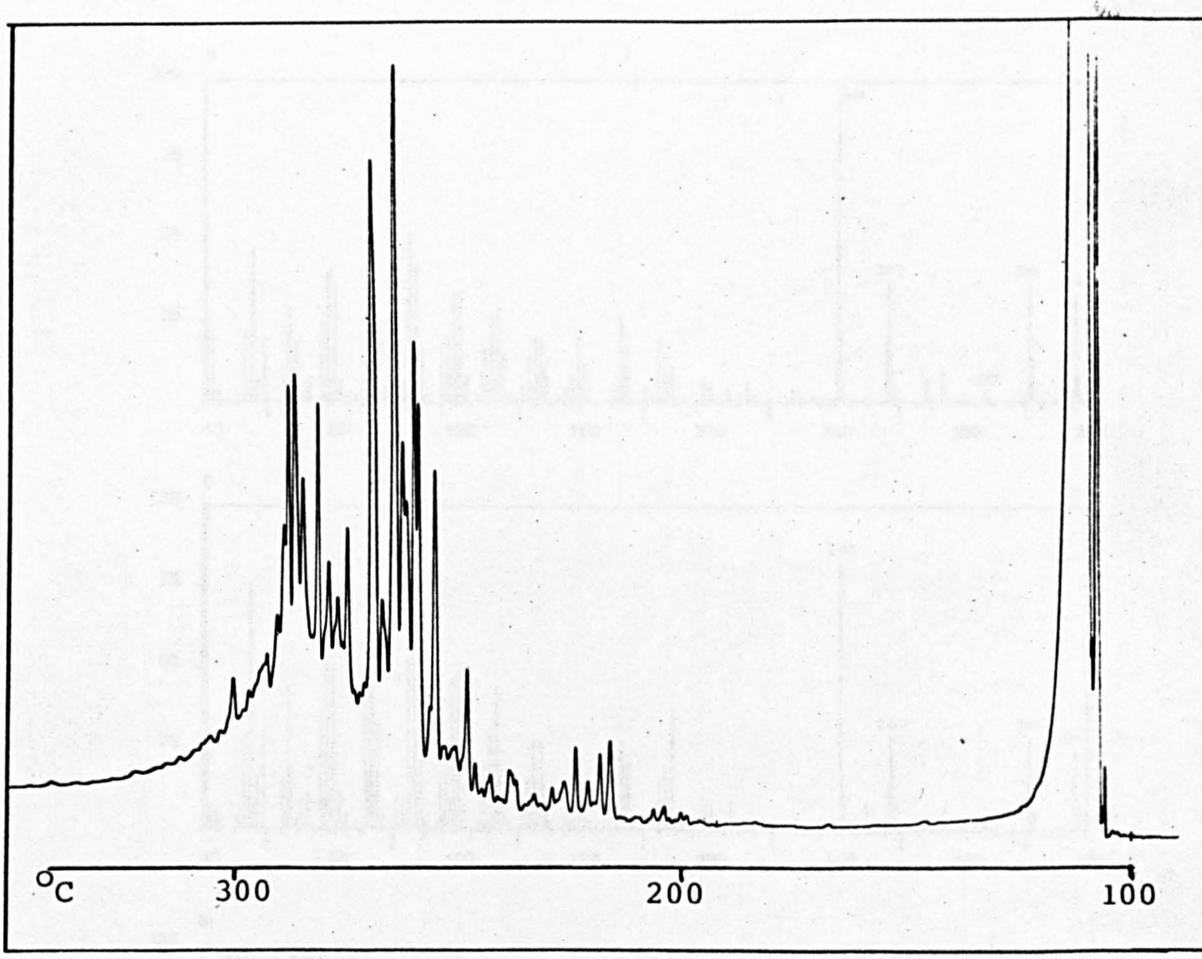

Gas chromatographic conditions as in Fig. 8.

Fig. 40. Mass spectra of methyl esters of some resin acids extracted from Yallourn resinite

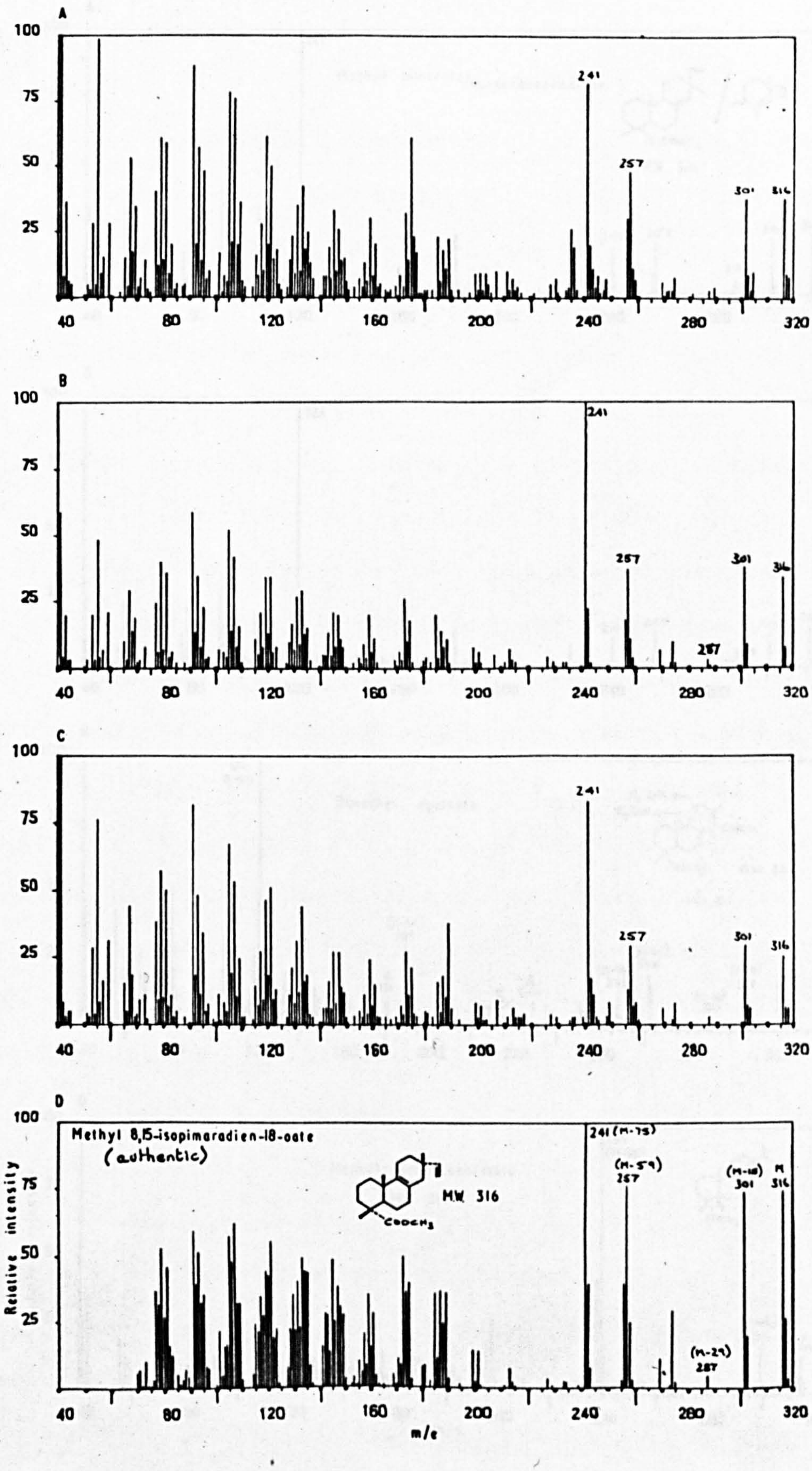

Fig. 41. Mass spectra of methyl esters of some resin acids extracted from Yallourn resinite

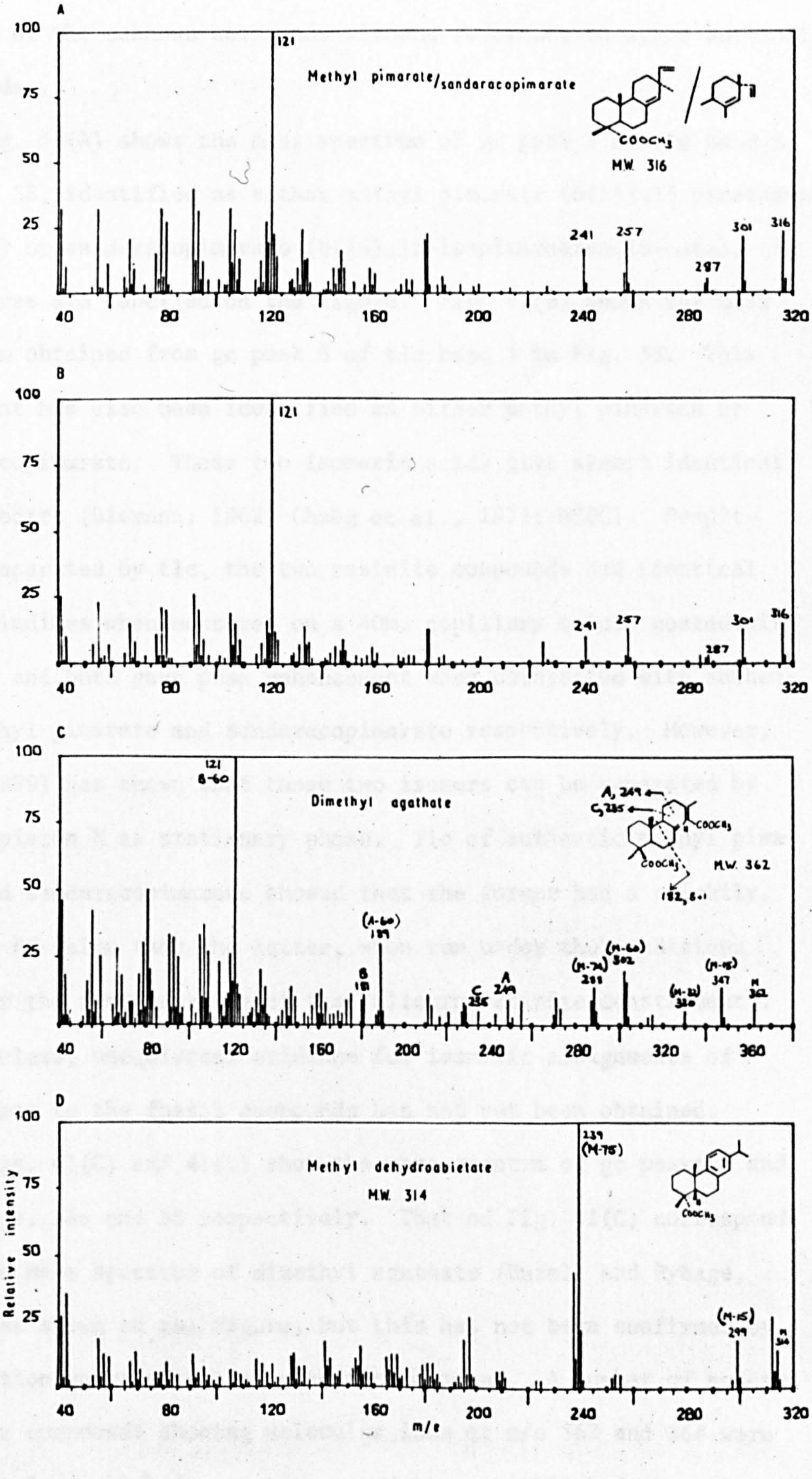

also give very similar spectra to those illustrated. The information so far available is insufficient to determine the absolute configurations of the unknown compounds without reference to other authentic standards.

Fig. 41(A) shows the mass spectrum of gc peak 4 of tlc band 3 in Fig. 38, identified as either methyl pimarate (8(14),15-pimaradien-18-oate) or sandaracopimarate (8(14),15-isopimaradien-18-oate); the structures are labelled on the figure. Fig. 41(B) shows the mass spectrum obtained from gc peak 5 of tlc band 4 in Fig. 38. This component has also been identified as either methyl pimarate or sandaracopimarate. These two isomeric acids give almost identical mass spectra (Biemann, 1962; Chang *et al.*, 1971; MSDC). Despite being separated by tlc, the two resinite compounds had identical Kovats indices when measured on a 40m. capillary column coated with OV-101, and both gave peak enhancement when coinjected with authentic methyl pimarate and sandaracopimarate respectively. However, Hudy (1959) has shown that these two isomers can be separated by using Apiezon N as stationary phase. Tlc of authentic methyl pimarate and sandaracopimarate showed that the former had a slightly greater Rf value than the latter, when run under the conditions used for the fractionation of the Yallourn resinite constituents. Nevertheless, unequivocal evidence for isomeric assignments of structures to the fossil compounds has not yet been obtained.

Figs. 41(C) and 41(D) show the mass spectra of gc peaks 6 and 7 in Figs. 38a and 38 respectively. That of Fig. 41(C) corresponds with the mass spectrum of dimethyl agathate (Enzell and Ryhage, 1965), as shown on the figure, but this has not been confirmed by coinjection on gc with the authentic compound. A number of spectra of other compounds showing molecular ions at m/e 362 and 364 were also obtained which do not correspond to any published spectra, and they may represent derivatives of agathic acid which have undergone diagenetic changes.

Fig. 41(D) shows that peak 7 in Fig. 38 is a mixture of two compounds with molecular ions at m/e 312 and 314. The predominant spectrum in the mixture is very similar to that of methyl dehydroabietate (8,11,13-abietatrien-18-oate) (Enzell and Wahlberg, 1969; Chang *et al.*, 1971; MSDC). The gc peak was enhanced when coinjected with authentic methyl dehydroabietate. The other component of the mixture, with a molecular ion at m/e 312, appears to have a similar fragmentation pattern to that of methyl dehydroabietate, and probably has the same basic configuration, but the location of the additional double bond is not known. Location in the C6-C7 position extends the conjugation, but this compound (methyl 6,8,11,13-abietatetraen-18-oate) has a rather different fragmentation pattern to that of methyl dehydroabietate and shows a base peak at m/e 141 due to a stable naphthyl ion (Chang *et al.*, 1971). Another position extending the conjugation is in the isopropyl side-chain at C13. This side-chain is retained in all the major fragment peaks above m/e 230 in the mass spectrum of methyl dehydroabietate (Enzell and Wahlberg, 1969), and so the unknown compound may have this configuration.

Experimental

Free acids in maceral extracts

Aliquots of the total extracts were fractionated by column chromatography into petroleum ether and methanol eluates. The methanol eluates were saponified with 6% methanolic KOH by boiling under reflux for 24 hrs, and the products were separated into neutral and acidic fractions. The acidic fractions were purified by preparative tlc using silica gel plates (Keiselgel G) impregnated with KOH (Douglas and Powell, 1969). The carboxylic acids were recovered from the silica gel and methylated with ethereal diazomethane. The resulting esters were fractionated by preparative tlc on silica gel (developer 90:10 petroleum ether : diethyl ether), recovered and analysed by gc. All diacid fractions were also analysed by combined gc-ms which confirmed that the dominant homology in each fraction was composed of saturated, straight chain α,ω-dicarboxylic acids. Data are given in Table 19.

Bound acids in maceral residues

Each maceral residue, after extraction, was saponified with 6% methanolic KOH to release bound acidic material. Mono- and dicarboxylic acid fractions were obtained as methyl esters by the procedure outlined above for free acids. Data are given in Table 20.

Resinite acids

Resinite extracts, and the extracted resinite residues, were examined for free and bound acids. Aliquots of the total extracts were saponified directly without prior fractionation by column chromatography. The procedure for obtaining purified acids, and preparation of their methyl esters, was the same as that outlined

Table 19: Experimental data for the isolation of free acids from macerals other than resinites

	Weight methanol eluate* (mg)	Weight acidic fraction recovered (mg)	Tlc fractionation of methylated acids: Mono-acids (mg)	Di-acids (mg)
Vitrinite				
High Hazles Gedling	267.7	23.4	0.5	-
Westfield	279.6	41.1	0.2	-
Clowne	442.1	6.2	0.1	-
Shallow	394.8	14.9	0.2	-
High Hazles Warsop	506.2	7.9	0.3	-
Deep Hard	299.4	22.1	0.2	-
High Hazles Whitwell	370.6	3.1	0.2	-
Beeston	184.5	35.9	0.2	-
Barnsley	243.1	4.2	0.2	-
Parkgate	141.3	8.6	0.2	-
Silkstone	107.3	4.7	0.3	-
Sporinite				
Donibristle	177.5	78.1	0.2	-
High Hazles Gedling	107.8	62.7	0.3	-
Clowne	350.5	28.2	0.2	-
Shallow	487.0	38.4	0.3	-
High Hazles Warsop	440.4	33.5	0.3	-
Deep Hard	282.9	36.3	0.1	-
High Hazles Whitwell	338.9	47.3	0.6	-
Beeston	166.5	57.5	0.3	-
Barnsley	231.2	19.3	0.3	-
Parkgate	109.4	15.4	0.1	-
Silkstone	113.9	11.7	0.1	-
Alginite				
Scotland	23.4	7.2	0.2	0.1
South Africa	46.0	21.2	0.8	1.1
New South Wales	115.7	61.0	1.5	4.7
Cutinite				
Indiana	267.7	31.7	0.7	0.4

* See Table 14 for isolation of methanol eluates from column chromatography.

Table 20: Experimental data for the isolation of bound acids from macerals other than resinite

	Weight maceral residue (gm)	Weight acidic fraction recovered (mg)	Tlc fractionation of methylated acids Mono-acids (mg)	Di-acids (mg)
Vitrinite				
High Hazles Gedling	21.3	23.4	0.2	-
Westfield	57.5	16.2	0.1	-
Clowne	40.5	19.3	0.2	-
Shallow	53.6	9.9	0.2	-
High Hazles Warsop	54.2	24.2	0.2	-
Deep Hard	59.7	18.0	0.1	-
High Hazles Whitwell	56.6	19.3	0.1	-
Beeston	24.2	7.7	0.1	-
Barnsley	8.6	1.6	0.1	-
Parkgate	44.2	17.0	0.2	-
Silkstone	56.1	14.1	0.1	-
Sporinite				
Donibristle	38.2	91.4	0.5	-
High Hazles Gedling	20.2	138.6	0.5	-
Clowne	21.1	8.2	0.5	-
Shallow	42.4	12.4	0.1	-
High Hazles Warsop	41.5	33.9	0.4	-
Deep Hard	57.0	31.0	0.6	-
High Hazles Whitwell	43.5	10.8	0.3	-
Beeston	49.7	10.4	0.4	-
Barnsley	42.6	6.7	0.3	-
Parkgate	11.6	3.0	0.5	-
Silkstone	38.3	8.5	0.4	-
Alginite				
Scotland	51.4	24.1	0.4	0.9
South Africa	48.9	22.9	0.1	4.4
New South Wales	48.3	22.1	3.6	5.7
Cutinite				
Indiana	10.0	64.5	0.3	9.0

for acid fractions of the other macerals. All but one of the total ester fractions (i.e. Yallourn resinite extract acids) were then fractionated by preparative tlc using hexane:acetone (70:30) as the developing solvent (Thomas, 1969). This produced separations into seven fairly distinct bands for Maghara and Bitterfeld free acid esters, and into three and four bands respectively for the residue acid esters. Yallourn extract acid esters were not fractionated cleanly into distinct bands by this solvent system, and they were consequently fractionated by developing twice in petroleum ether: diethyl ether (95:5). This produced nine separate tlc bands. Experimental data are given in Tables 21 and 22. All the fractions were recovered from the silica gel and examined by gc and combined gc-ms.

Table 21: Experimental data for the isolation of free acids from resinites

	Weight extract (mg)	Weight acidic fraction recovered (mg)	Tlc fractionation of methylated acids: Band	Wt. (mg)	Rf
Yallourn	784.0	137.6	1	0.5	0.70
			2	0.8	0.61
			3	1.0	0.55
			4	0.7	0.47
			5	0.2	0.39
			6	0.1	0.28
			7	0.4	0.21
			8	1.1	0.16
			9	18.5	0.15-0.00
			Total =	23.3	
Maghara	1104.0	50.6	1	0.2	0.86
			2	0.9	0.79
			3	1.2	0.71
			4	0.4	0.50
			5	0.5	0.35
			6	0.5	0.30
			7	0.6	0.21-0.00
			Total =	4.3	
Bitterfeld	376.4	171.3	1	3.9	0.81
			2	5.1	0.73
			3	3.7	0.68
			4	4.1	0.62
			5	6.6	0.56
			6	27.2	0.52-0.18
			7	8.5	0.16-0.00
			Total =	59.1	

Table 22: Experimental data for the isolation of bound acids from resinites

	Weight extracted residue (gm)	Weight acidic fraction recovered (mg)	Tlc fractionation of methylated acids Band	Wt. (mg)	Rf
Yallourn	2.7	108.3	1	12.6	0.70
			2	2.8	0.55
			3	4.3	0.48
			4	16.9	0.44-0.00
			Total =	36.6	
Maghara	5.4	12.7	1	2.6	0.73
			2	1.3	0.55
			3	2.8	0.50-0.00
			Total =	6.7	
Bitterfeld	10.1	465.1	1	23.6	0.70
			2	21.1	0.56
			3	26.3	0.45
			4	76.9	0.41-0.00
			Total =	147.9	

Chapter 4

Pyrolytic degradation of extracted and saponified maceral concentrates

Introduction

Pyrolysis of coal has long been of commercial interest because of the wide variety of products that can be obtained. Industrial processes are usually carried out at temperatures in excess of $500^{o}C$, i.e. above the decomposition temperature of coal. Pyrolysis in an inert atmosphere (i.e. carbonisation) at temperatures in the 450^{o} to $700^{o}C$ range has been defined as low-temperature carbonisation, the products being primary tar and semi-coke (Wilson and Clendenin, 1963). At these temperatures the aliphatic edge-groupings are cracked from the coal matrix to yield primary tar and gas, but the residue, semi-coke, retains much of its aromatic hydrogen. Semi-coke is used as a smokeless fuel, while the tars provide raw materials for the organic chemical industries. High-temperature carbonisation, at temperatures up to *ca.* $1000^{o}C$, produces coal gas, and coke from which virtually all the hydrogen has been removed. Although the petroleum and natural gas industries have been steadily undermining the economic viability of coal as a primary source material, the recent long-term predictions about the limited future of the world's petroleum reserves have already begun to revive interest in the science and technology of coal.

Pyrolysis is an important technique in the elucidation of coal structure. The basic mechanisms involved in the thermal conversion of coal to soluble products have been summarized by van Krevelen (1961), who divided the process into primary (less than $500^{o}C$) and secondary (greater than $500^{o}C$) carbonisation. The major soluble product of the primary stage is tar, and the residue is semi-coke. The controlling mechanisms are depolymerisation and disproportionation involving aliphatic hydrogen only (van Krevelen *et al.*, 1960). The hydrogen-enriched fraction produces mainly tar, with lesser quantities of gas, while the residue gives a semi-coke. During secondary carbonisation semi-coke is reduced to coke through the loss of aromatic hydrogen while primary tar is pyrolysed to gas and lighter oils. The yield and nature of the evolved products vary with the composition and rank of the coal, as well as with the conditions of carbonisation.

Berkowitz (1967) divided pyrolysis into three temperature-dependent phases. The first phase terminates between 350^{o}C and 400^{o}C, and induced structural changes in bituminous coals have been compared with those which would occur during natural coalification (Cavell and Berkowitz, 1960). These essentially involve the loss of -COOH, -OCH_3 and some -OH groups. The distribution of oxygen functions with the rank of coal has been outlined by Blom *et al.*, (1957). At ranks greater than about 80% C, oxygen in -COOH and -OCH_3 groups has largely been eliminated naturally. In agreement, pyrolysis of coals of ranks higher than *ca.* 80% C induces little elimination of oxygen below 400^{o}C (Bergman *et al.*, 1954; Brown, 1955b; Brooks and Maher, 1957). On the other hand, reactions involving -COOH and -OH groups have been noted in brown coals at temperatures below 300^{o}C (Brooks *et al.*, 1958b).

Differential thermal analysis of bituminous coals provides evidence of mild exothermic reactions taking place below 350^{o}C which, because of their independence of rank, are interpreted as involving some C-C scission (Whitehead and Breger, 1950; Glass, 1954; Berkowitz, 1957). On the other hand, Kröger and Pohl (1957) report no exothermic reactions below 410^{o}C in similar investigations of maceral concentrates. Measurement of changes in electron spin resonance (ESR) signals with pyrolysis indicate that some homolytic fission occurs below 400°C, but major changes only occur at higher temperatures (Ingram *et al.*, 1954; Smidt and van Krevelen, 1959; Austen *et al.*, 1966).

The second phase of carbonisation as defined by Berkowitz occurs between 400° and 650°C, and is characterised by the evolution of abundant volatile matter. This is the temperature range, as indicated by ESR, where the concentration of free radicals increases markedly before falling virtually to zero at the higher temperature. The origin of the evolved material is the aliphatic and hydro-aromatic bridging structures between condensed aromatic centres; by 650°C, most of these bridging structures have been cleaved. The final carbonisation phase, occurring above 650°C and terminating at about 1000°C, is marked by the loss of aromatic hydrogen, growth of condensed aromatic systems and progression towards quasi-graphitic structures.

Vahrman (1972) considers that much of the low molecular weight material, (i.e. molecular weights below 1000), which gives rise to primary tars is in fact present primarily as adsorbed material restricted within the micropores of coal and is thus not recoverable by solvent extraction at ordinary temperatures. The effect of primary carbonisation is simply to release this material through decomposition of the remainder of the structure.

Mazumdar and Chatterjee (1973) have considered the formation of pyrolysis products in relation to industrial and laboratory practice. Using a carbon balance procedure, they concluded that during primary carbonisation (below 600°C) gaseous products are formed from aliphatic carbon (mainly $-CH_3$), tar is generated from hydroaromatic carbon, while the aromatic carbon is retained in the residue. This division only occurs under ideal conditions. Observed departures from the ideal in industrial processes are thought to be due mainly to the interaction of primary tar and the residue, as gas yields are less affected. The degree of interaction is considered to be dependent mainly on the physical dimensions of the coal sample in the crucible.

Low-temperature tars are composed of many compounds, compositions varying with the type and rank of the source coal and upon the conditions of carbonisation. A short review by Karr (1963) lists many low boiling aliphatic and aromatic hydrocarbons, phenols, pyridines, thiophenes, anilines and ketones which have been identified.

Products of the rapid pyrolyses of coals have been evaluated by pyrolysis gas chromatography, the principles of the process being flash pyrolysis of small samples with immediate injection of a part of the volatilised product into a gas chromatograph (Evans and Raphaely, 1964; Bricteux, 1967; Romovacek and Kubat, 1968). Because of the high temperatures involved, the coal substance is instantly degraded to relatively small molecules, and it is claimed that secondary reactions are unimportant because the primary products are instantly removed from the coal by a carrier gas. The method appears useful in comparative work on pyrolytic oil and gas compositions, but is of more restricted value in the elucidation of the original structure of the coal.

Using a similar principle, but applying much lower temperatures which lead to a more controlled degradation, pyrolysis products have been fed directly into a mass spectrometer (Holden and Robb, 1958, 1960a, 1960b). With this technique, the temperature-dependence of evolved compounds has been investigated. Gas chromatographic analysis of evolved hydrocarbons produced by a step-wise heating of coals up to 700^{o}C has been used by Girling (1963). Evaluations were made on the temperatures of evolution of different hydrocarbons, and the pyrolysis products of vitrinites and sporinites were compared.

Exinites have been investigated by successive low-temperature pyrolyses in relation to oil and gas production (Combaz, 1971) and by progressive heating at very slow incremental rates (Macrae, 1943). Fresh spore and coalified sporinite pyrolysis products have been compared (Archari *et al.*, 1973), while Dungworth *et al.*, (1971) examined the aliphatic hydrocarbons produced by hydrogenolytic degradation of extracted and saponified sporinites.

A number of investigations have been carried out on the hydrocarbon products of low-temperature thermal degradation of coals and macerals. Boyer *et al.*, (1961), identified long-chain n-alkanes in tar produced at 550^{o}C from an unextracted exinite-rich coal. The n-alkanes had a virtually smooth distribution, but n-alkenes also identified had an even-numbered predominance in the n-C_{22} to n-C_{27} range. Kroger *et al.*, (1964), identified n- and branched/cyclic alkanes, olefins and aromatic hydrocarbons in an extensive investigation of tars produced by low-temperature pyrolysis of bituminous vitrinites and exinites. Smooth distributions of n-alkanes were reported. n-Alkanes and n-alkenes, both having smooth distributions as demonstrated by gc, were produced in relatively large quantities in a 500^{o}C pyrolysis of unextracted alginite (Henderson, 1968). Alkanes produced by temperature-programmed pyrolysis of unextracted vitrinites of various ranks have been investigated by Barker (1974), but only the shorter-chain homologues (i.e. lower than C_{10}) were identified.

Brooks and Smith (1969) demonstrated that heating both fresh and extracted brown coal at 330°C with water generated n-alkanes which showed a predominance of even-carbon-numbered chains in the n-C_{23} to n-C_{30} range, while Connan (1973) found that pyrolysis of another sample of coal from the same sequence (Yallourn lignites, Australia) produced odd-dominated n-alkane distributions in the absence of water. Palmer and Vahrman (1972a, 1972b) extended the earlier work of Spence and Vahrman (1967) to conclude that true extractable n-alkane distributions in bituminous coals at low ranks are petroleum-like, showing smooth distributions and maxima well below n-C_{20}. These conclusions were based on analyses of tars produced at 600°C. However, as has already been discussed, this temperature is sufficiently high to crack aliphatic material from the coal matrix, and it is considered by the present author that at least a part of the lower molecular weight n-alkanes observed by Palmer and Vahrman may have been derived from n-alkyl chains in the coal structure. The conditions of pyrolysis employed by Palmer and Vahrman were such that rapid condensation of the evolved tar occurred. Data presented by Mazumdar and Chatterjee (1973) indicate that this can virtually eliminate further degradation of primary molecular fragments. It seems, therefore, that pyrolysis at rather elevated temperatures can be a useful technique in structural investigations.

Volatile thermal-degradation products of recent and fossil spore exines and related substances were investigated by Combaz (1971), using successive short-term pyrolyses at 280°C. Alkanes and aromatic hydrocarbons were identified, but the published information only concerned n-alkanes up to about n-C_{20}. Hydrogenolytic degradation at 380°C and 2000 p.s.i. of both fresh pollens and Carboniferous sporinite, pre-extracted and saponified, yielded significant quantities of alkanes (Dungworth *et al.*, 1971). Total alkane fractions were of rather low molecular weight, with maxima in the C_{14} to C_{18} range, but n-alkanes up to n-C_{28} were present in the products of two fresh pollens and one Carboniferous sporinite of bituminous rank. In the n-C_{20} to n-C_{28} range they showed a marked predominance of even-numbered chain lengths.

In this investigation, selected samples of vitrinite and sporinite of ranks between 77.1% and 86.6% C (d.a.f.), together with other low-rank exinites besides sporinite, were pyrolysed at 275° and 375°C under an inert atmosphere in an autoclave. All the samples were extracted and saponified prior to pyrolysis. The conditions of pyrolysis lie within phase one of carbonisation, as defined by Berkowitz, and, as such, may simulate those reactions which occur during natural coalification.

The extractable material liberated from the macerals was removed and fractionated chromatographically into aliphatic and aromatic hydrocarbons, and asphalts. Data from the respective macerals have been compared, and alkane yields and distributions have been examined in conjunction with extractable alkanes from these macerals. Their potentials as contributors to sedimentary hydrocarbon sources has also been discussed.

Results

Vitrinite: pyrolysis at 375°C

Seven selected vitrinite residues (i.e. vitrinites that had been extracted and saponified) were pyrolysed at 375°C for 24 hrs, and then extracted with dichloromethane. The extracts were chromatographed on columns containing silica gel to give aliphatic hydrocarbons (petroleum ether eluate), aromatic hydrocarbons (benzene eluate) and asphalts (methanol eluate). Data are given in Table 23. Petroleum ether eluates were fractionated into saturated and unsaturated fractions, using argentatious tlc, and the alkanes were further separated into n- and branched/cyclic alkanes with 5A molecular sieve (Table 24).

The aliphatic hydrocarbons were examined by packed-column gc. The total alkane fractions of all the samples contained material generally in the C_{14} to *ca.* C_{30} range, the fractions being complex mixtures of both normal and branched/cyclic alkanes (Figs. 42 and 42a). The apparent distributions of n-alkanes from each sample were similar, showing maxima in the C_{17} to C_{20} region. Primary qualitative differences in the hydrocarbon products of pyrolyses at 375°C may of course be masked by secondary reactions occurring during the pyrolyses.

Alkene fractions (Fig. 43) contained compounds in the same carbon number range as the total alkanes. Despite their general complexity, an homologous series of n-alkenes occurred in all the fractions except that from High Hazles Gedling vitrinite. n-Alkenes occurred in the n-C_{15} to n-C_{28} range in general.

Gas chromatographic analyses of the n-alkanes provided evidence of some differences in distribution that were not apparent in the total alkane chromatograms. n-Alkanes were found up to about

Table 23: Quantitative extraction and chromatographic data for vitrinites pyrolysed at 375°C

	Total extract (mg/gm)	Column eluates Petroleum ether (mg/gm)	Benzene (mg/gm)	Methanol (mg/gm)	Wt. lost as volatiles (mg/gm)*
Vitrinite					
High Hazles Gedling	24.10	1.21	8.90	9.69	241.5
Clowne	12.21	0.92	3.79	7.22	277.9
Deep Hard	24.67	1.71	8.79	9.25	228.3
High Hazles Whitwell	15.40	0.91	5.18	6.54	210.7
Barnsley	11.69	0.87	4.04	5.63	133.7
Parkgate	31.18	2.19	13.46	9.58	104.6
Silkstone	33.76	2.26	15.50	12.55	76.3

* (mg/gm) refers to mg material/gm of extracted and saponified maceral.

Table 24: Alkane and alkene fractions isolated from vitrinites pyrolysed at 375°C

	Total alkanes (mg/gm)	_n_-Alkanes (mg/gm)	Branched/cyclic alkanes (mg/gm)	Alkenes (mg/gm)
Vitrinite				
High Hazles Gedling	0.30	0.12	0.18	0.12
Clowne	0.18	0.09	0.18	0.18
Deep Hard	0.97	0.30	0.55	0.29
High Hazles Whitwell	0.49	0.04	0.38	0.18
Barnsley	0.51	0.08	0.25	0.22
Parkgate	1.25	0.30	0.79	0.25
Silkstone	1.28	0.27	0.82	0.20

Fig. 42. Total alkanes of vitrinites after pyrolysis at 375°

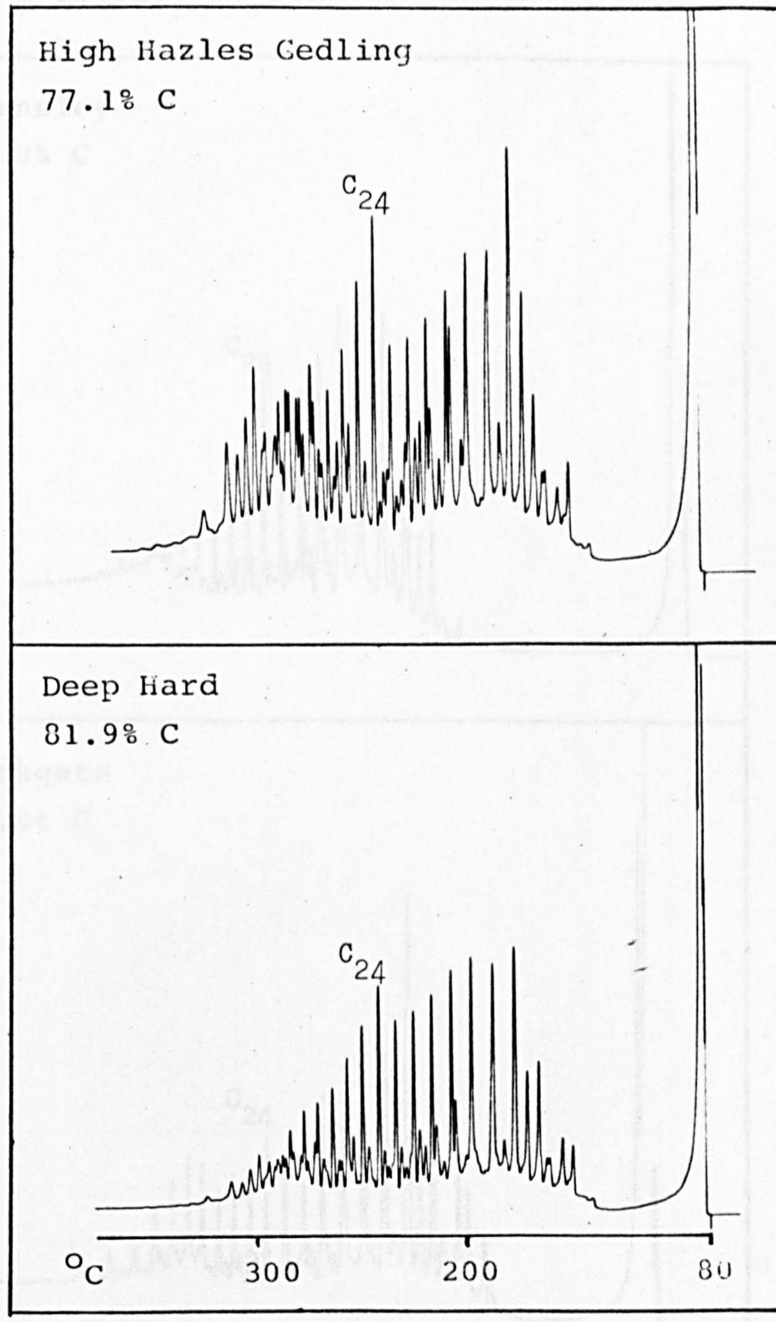

Gas chromatographic conditions: 5'x1/8" column containing 3% OV-101 on Varaport 30 (100-120 mesh); programmed 80-300°C at 6°/min; detector 300°; injector 300°; nitrogen 40 p.s.i.

Fig. 42a. Total alkanes of vitrinites after pyrolysis at 375°

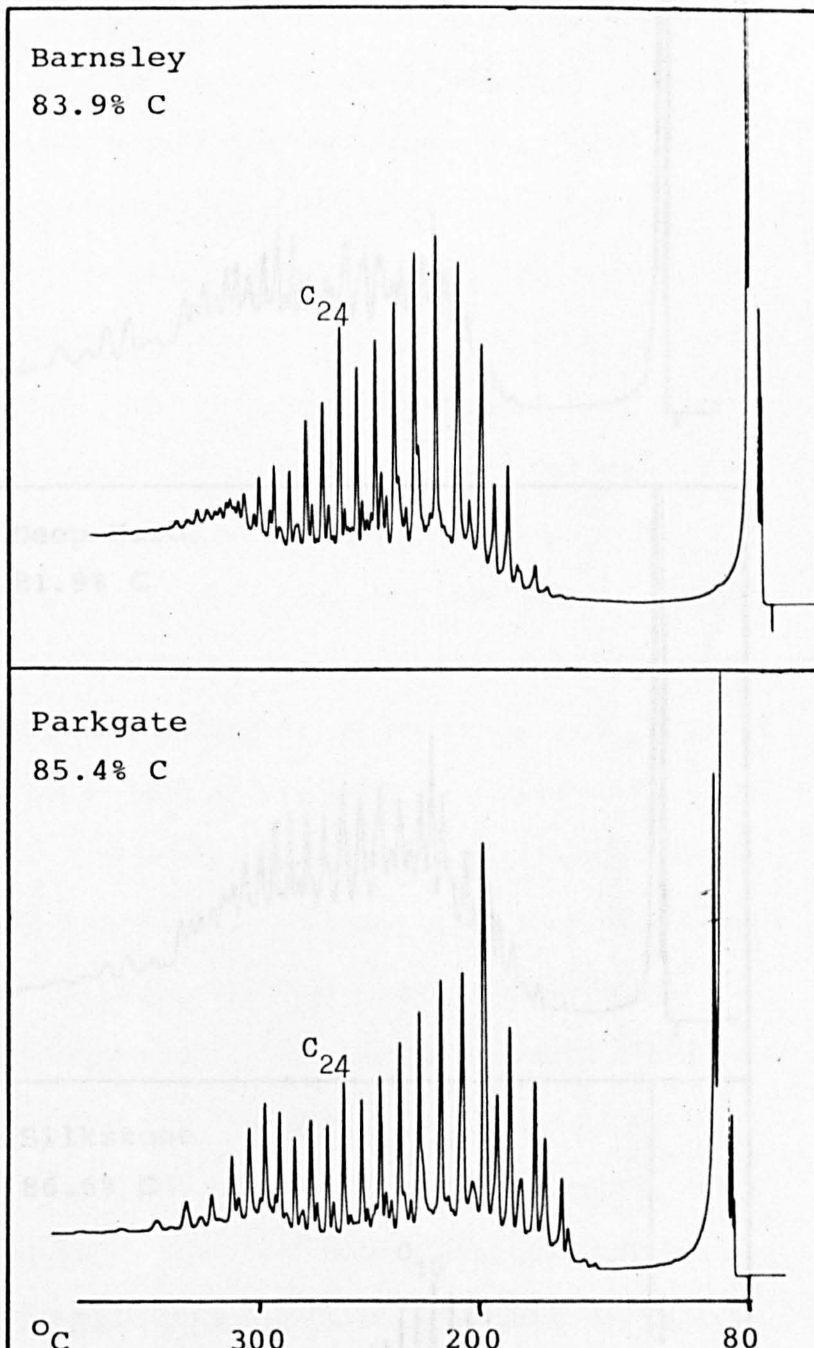

Gas chromatographic conditions: 6'x1/8"o.d. column containing 3% OV-101 on Varaport 30 (100-120 mesh); programmed 80-300°C at 6°/min; detector 300°; injector 300°; nitrogen 40 p.s.i.

Fig. 43. Alkenes of vitrinites after pyrolysis at 375^{o}

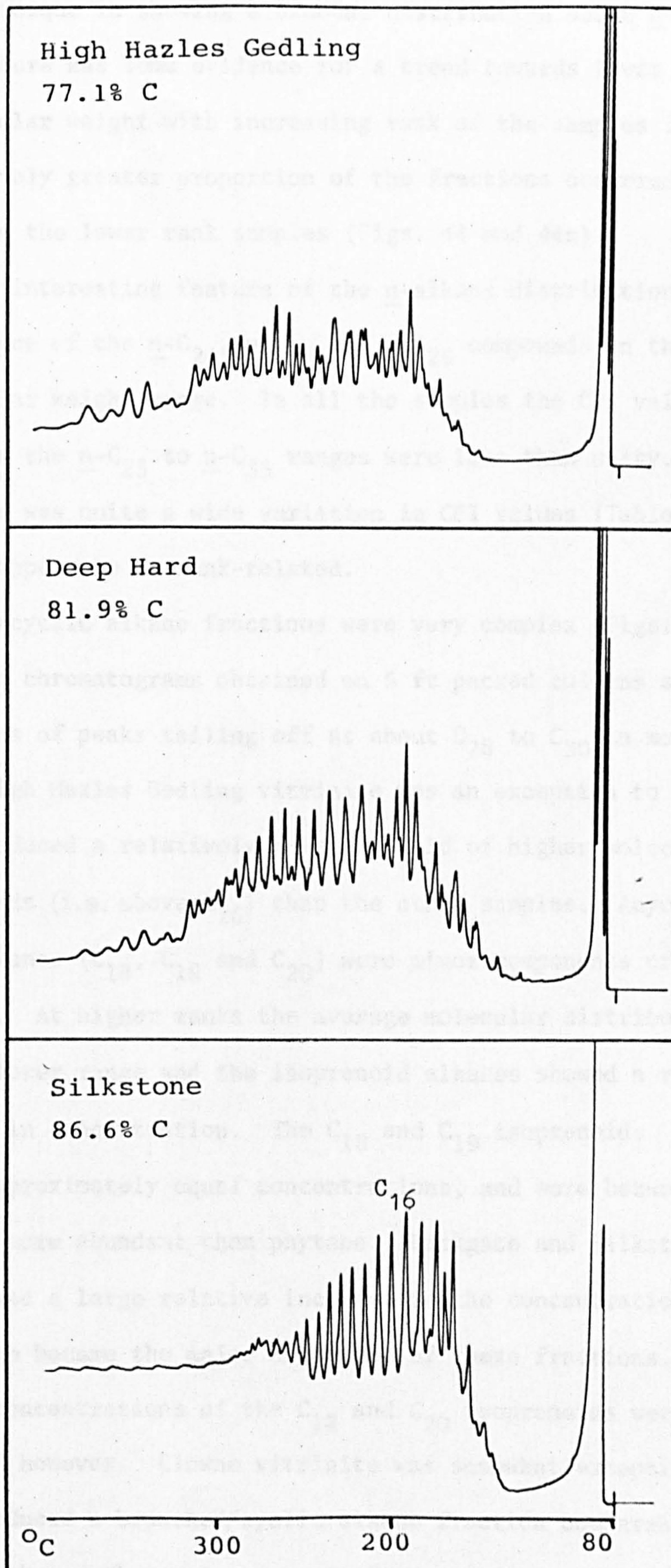

Gas chromatographic conditions as Fig. 42.

$\underline{n}$-C_{35}, mostly showing a maximum at $\underline{n}$-C_{20}. Parkgate vitrinite $\underline{n}$-alkanes were unique in showing a bimodal distribution about $\underline{n}$-C_{20} and $\underline{n}$-C_{29}. There was some evidence for a trend towards lower average molecular weight with increasing rank of the samples in that a relatively greater proportion of the fractions occurred above $\underline{n}$-C_{20} in the lower rank samples (Figs. 44 and 44a).

The most interesting feature of the $\underline{n}$-alkane distributions was the predominance of the $\underline{n}$-C_{24}, $\underline{n}$-C_{26} and $\underline{n}$-C_{28} compounds in the higher molecular weight range. In all the samples the CPI values calculated for the $\underline{n}$-C_{23} to $\underline{n}$-C_{33} ranges were less than unity. Although there was quite a wide variation in CPI values (Table 25), they did not appear to be rank-related.

Branched/cyclic alkane fractions were very complex (Figs. 45 and 45a). Gas chromatograms obtained on 5 ft packed columns showed broad envelopes of peaks tailing off at about C_{28} to C_{30} in most fractions. High Hazles Gedling vitrinite was an exception to this in that it produced a relatively greater yield of higher molecular weight compounds (i.e. above C_{26}) than the other samples. Acyclic isoprenoid alkanes (C_{18}, C_{19} and C_{20}) were minor components of this fraction. At higher ranks the average molecular distribution shifted to a lower range and the isoprenoid alkanes showed a relative increase in concentration. The C_{18} and C_{19} isoprenoids occurred in approximately equal concentrations, and were between one and two times more abundant than phytane. Parkgate and Silkstone fractions showed a large relative increase in the concentration of pristane, which became the major component of these fractions. The relative concentrations of the C_{18} and C_{20} isoprenoids were little changed however. Clowne vitrinite was somewhat exceptional in that it produced a branched/cyclic alkane fraction comparable to those of higher rank samples, except for a predominance of

Fig. 44. n-Alkanes of vitrinites after pyrolysis at 375°

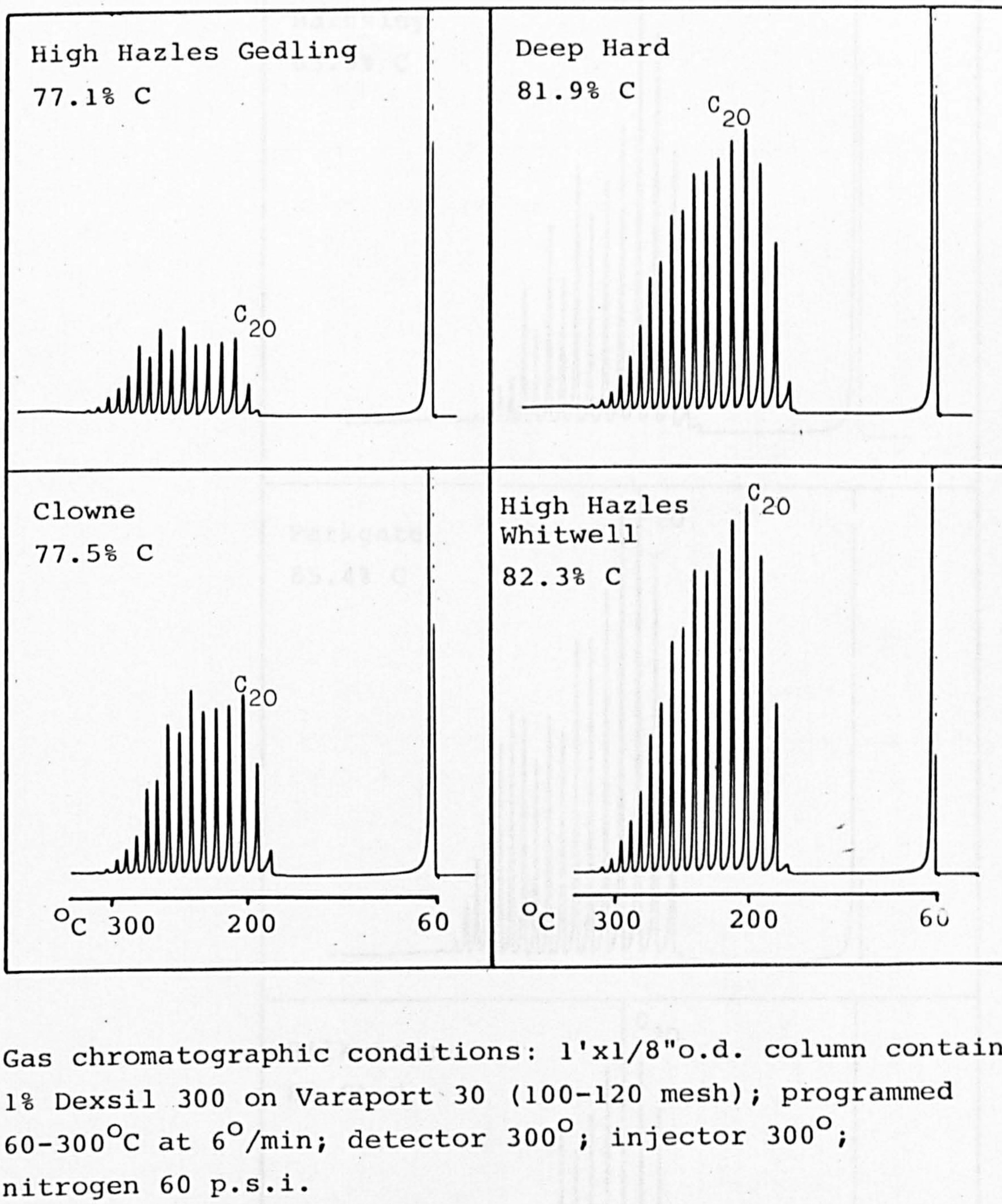

Gas chromatographic conditions: 1'x1/8"o.d. column containing 1% Dexsil 300 on Varaport 30 (100-120 mesh); programmed 60-300°C at 6°/min; detector 300°; injector 300°; nitrogen 60 p.s.i.

Fig. 44a. $\underline{n}$-Alkanes of vitrinites after pyrolysis at 375°

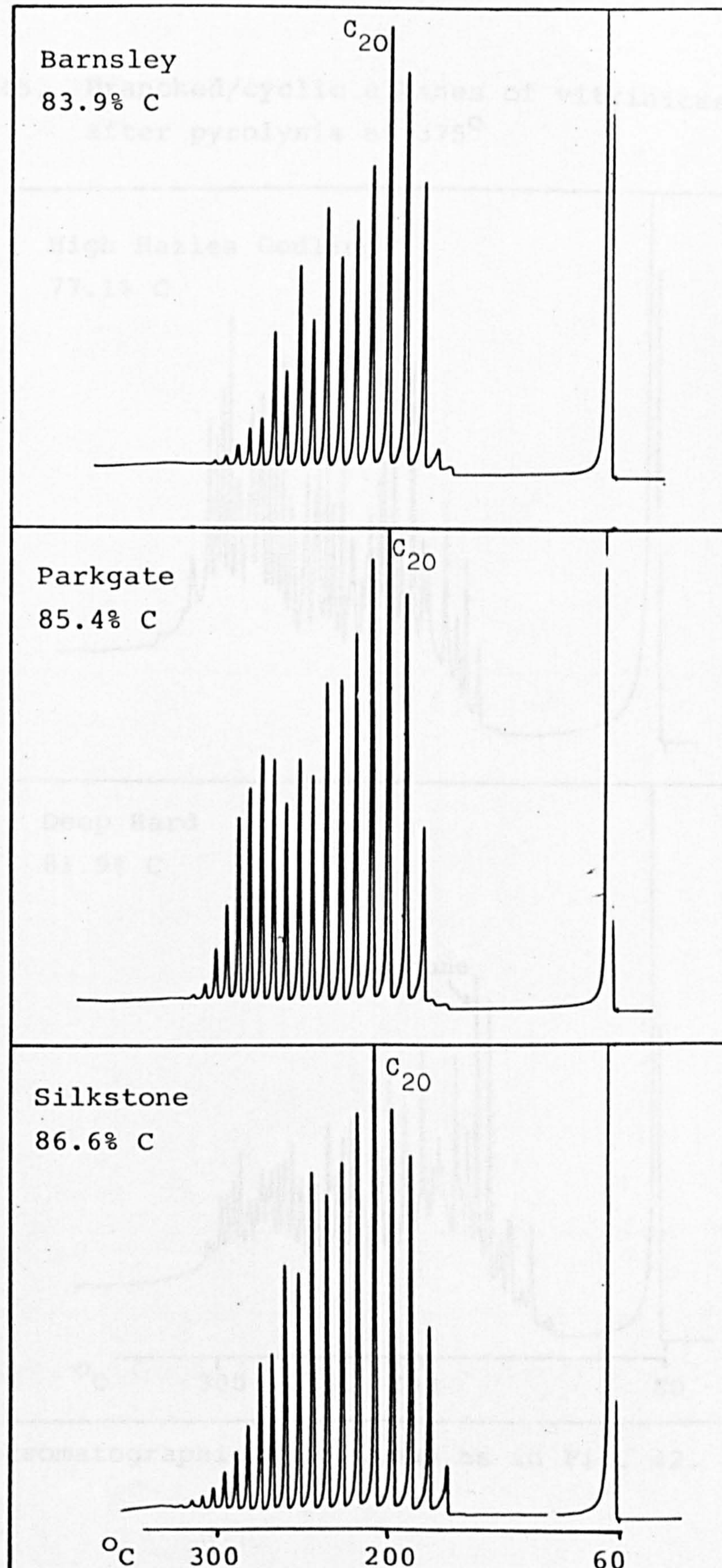

Gas chromatographic conditions as in Fig. 44.

Fig. 45. Branched/cyclic alkanes of vitrinites after pyrolysis at 375°

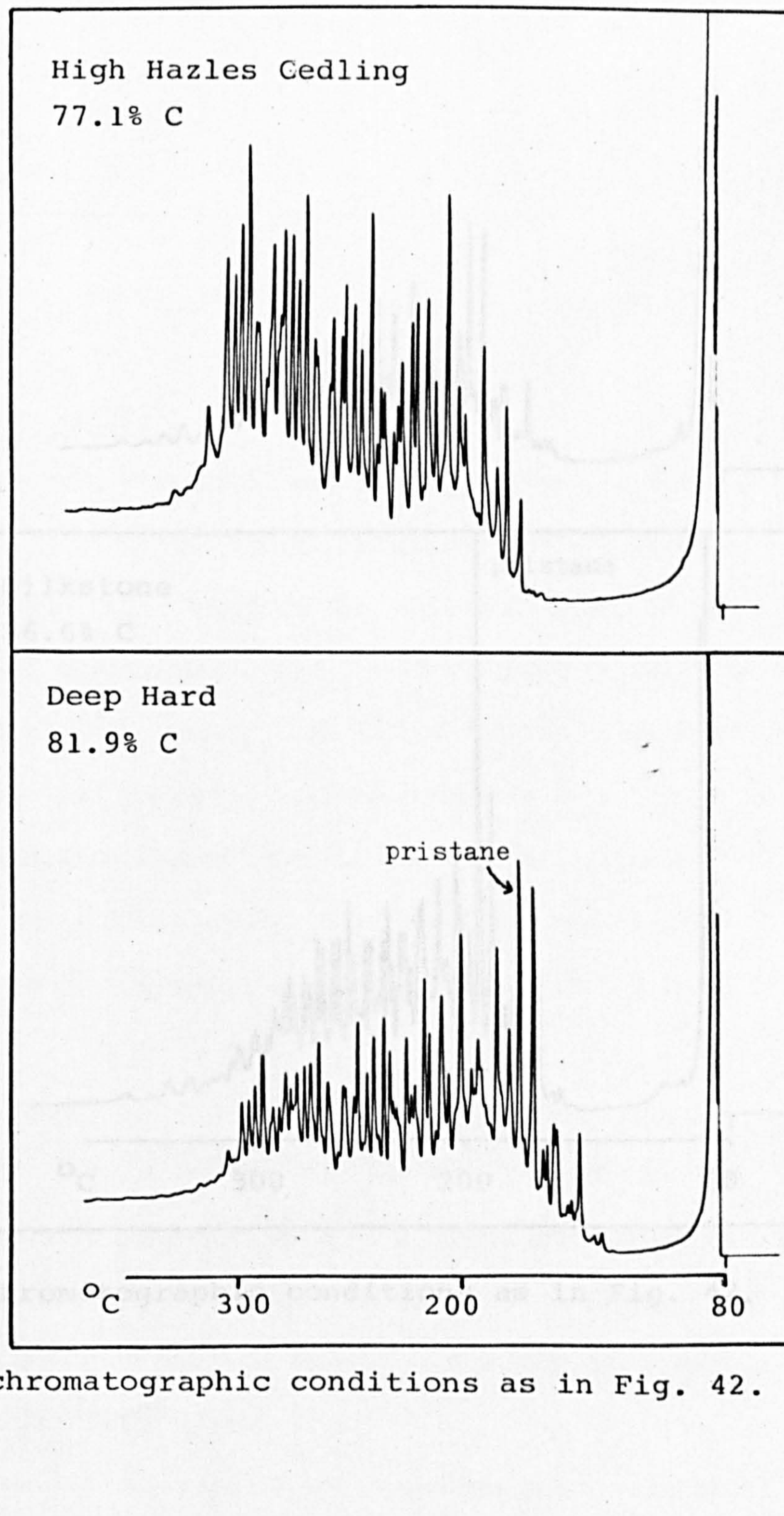

Gas chromatographic conditions as in Fig. 42.

Fig. 45a. Branched/cyclic alkanes of vitrinites after pyrolysis at 375°

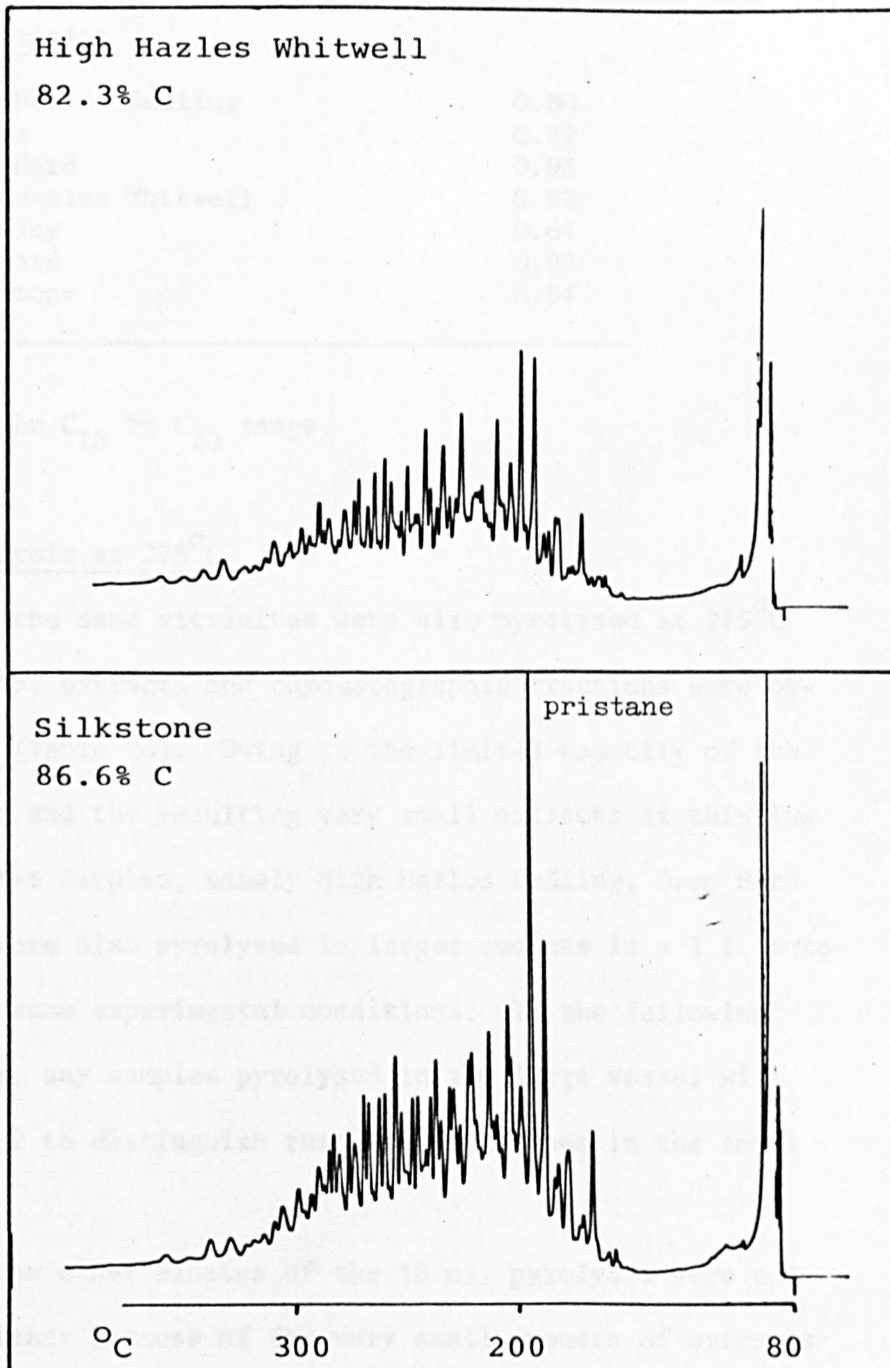

Gas chromatographic conditions as in Fig. 42.

Table 25: CPI values of n-alkanes produced by pyrolyses of vitrinites at 375°C

Vitrinite	CPI
High Hazles Gedling	0.80
Clowne	0.82
Deep Hard	0.93
High Hazles Whitwell	0.92
Barnsley	0.64
Parkgate	0.93
Silkstone	0.84

isoprenoids in the C_{18} to C_{20} range.

Vitrinite: pyrolysis at 275°C

Samples of the same vitrinites were also pyrolysed at 275°C for 24 hrs. Total extracts and chromatographic fractions were obtained as above (Table 26). Owing to the limited capacity of the 16 ml. autoclave and the resulting very small extracts at this low temperature, three samples, namely High Hazles Gedling, Deep Hard and Silkstone, were also pyrolysed in larger amounts in a 1 l. autoclave under the same experimental conditions. In the following text and figures, any samples pyrolysed in the large vessel will be suffixed by *2 to distinguish them from pyrolyses in the small vessel.

The petroleum ether eluates of the 16 ml. pyrolyses were not fractionated further because of the very small amounts of extracts involved. The aliphatic products of the 1 l. autoclave pyrolyses were separated into alkanes and alkenes by preparative argentatious tlc, and the n-alkanes were further separated from the total alkanes with 5A molecular sieve (Table 27).

Gas chromatographic analyses of the petroleum ether eluates

Table 26: Quantitative extraction and chromatographic data for vitrinites pyrolysed at 275°C

	Total extract (mg/gm)	Column eluates: Petroleum ether (mg/gm)	Benzene (mg/gm)	Methanol (mg/gm)	Wt. lost as volatiles (mg/gm)
Vitrinite					
High Hazles Gedling	0.75	0.04	0.09	0.49	129.3
Clowne	1.94	<0.05	0.46	1.26	162.4
Deep Hard	2.22	0.04	0.36	2.26	145.0
High Hazles Whitwell	2.03	<0.05	0.27	0.91	152.2
Barnsley	1.46	0.11	0.49	1.14	51.2
Parkgate	11.92	0.90	5.93	4.04	39.8
Silkstone	17.05	0.62	7.21	4.95	51.0
High Hazles Gedling*2	8.13	0.16	1.69	6.73	75.8
Deep Hard*2	4.80	0.05	1.09	3.10	25.0
Silkstone*2	19.85	0.27	3.40	15.31	29.5

Table 27: Alkane and alkene fractions isolated from vitrinites pyrolysed at 275°C

	Total alkanes (mg/gm)	n-Alkanes (mg/gm)	Branched/cyclic alkanes (mg/gm)	Alkenes (mg/gm)
Vitrinite				
High Hazles Gedling*2	0.04	0.01	0.02	0.02
Deep Hard*2	0.02	0.005	0.01	0.005
Silkstone*2	0.18	0.03	0.11	0.01

of the 16 ml. autoclave pyrolyses were of little diagnostic value in themselves as these fractions were not further fractionated. High Hazles Gedling to Barnsley samples contained material in the C_{18} to > C_{30} ranges, with relatively large amounts of material in the sterane/triterpane ranges (Fig. 46, top and middle chromatograms). Parkgate and Silkstone fractions were quantitatively greater than those obtained at lower ranks and showed distributions rather similar to their original soluble total alkane fractions. n-Alkanes occurred in the n-C_{14} to > n-C_{30} ranges and C_{16}, C_{18}, C_{19} and C_{20} acyclic isoprenoid alkanes were present, with pristane as the major component of the eluates. Sterane and triterpane constituents were also probably present in relatively large quantities, although confirmatory mass spectrometric evidence of structures has not been obtained.

n-Alkanes isolated from the larger-scale pyrolyses showed an apparently rank-related distributional change (Fig. 47). High Hazles Gedling vitrinite n-alkanes showed a predominance of even-numbered homologues in the n-C_{22} to n-C_{29} range, while above n-C_{29} odd-numbered homologues were dominant up to n-C_{34}. Deep Hard vitrinite n-alkanes showed similar characteristics, but the respective even and odd chain length predominances were reduced. Silkstone vitrinite n-alkanes had a slightly odd-dominated distribution in this range.

Alkene fractions also changed with rank. They all contained an homology of n-alkenes in the n-C_{18} to n-C_{30} range. At lower ranks even-numbered chains strongly predominated but were only slightly dominant at higher ranks (Fig. 48). All three fractions contained material in the triterpene region which was abundant only in High Hazles Gedling and Deep Hard vitrinites.

The branched/cyclic alkane fractions were all rather complex.

Fig. 46. Aliphatic hydrocarbons of vitrinites after pyrolysis at 275°

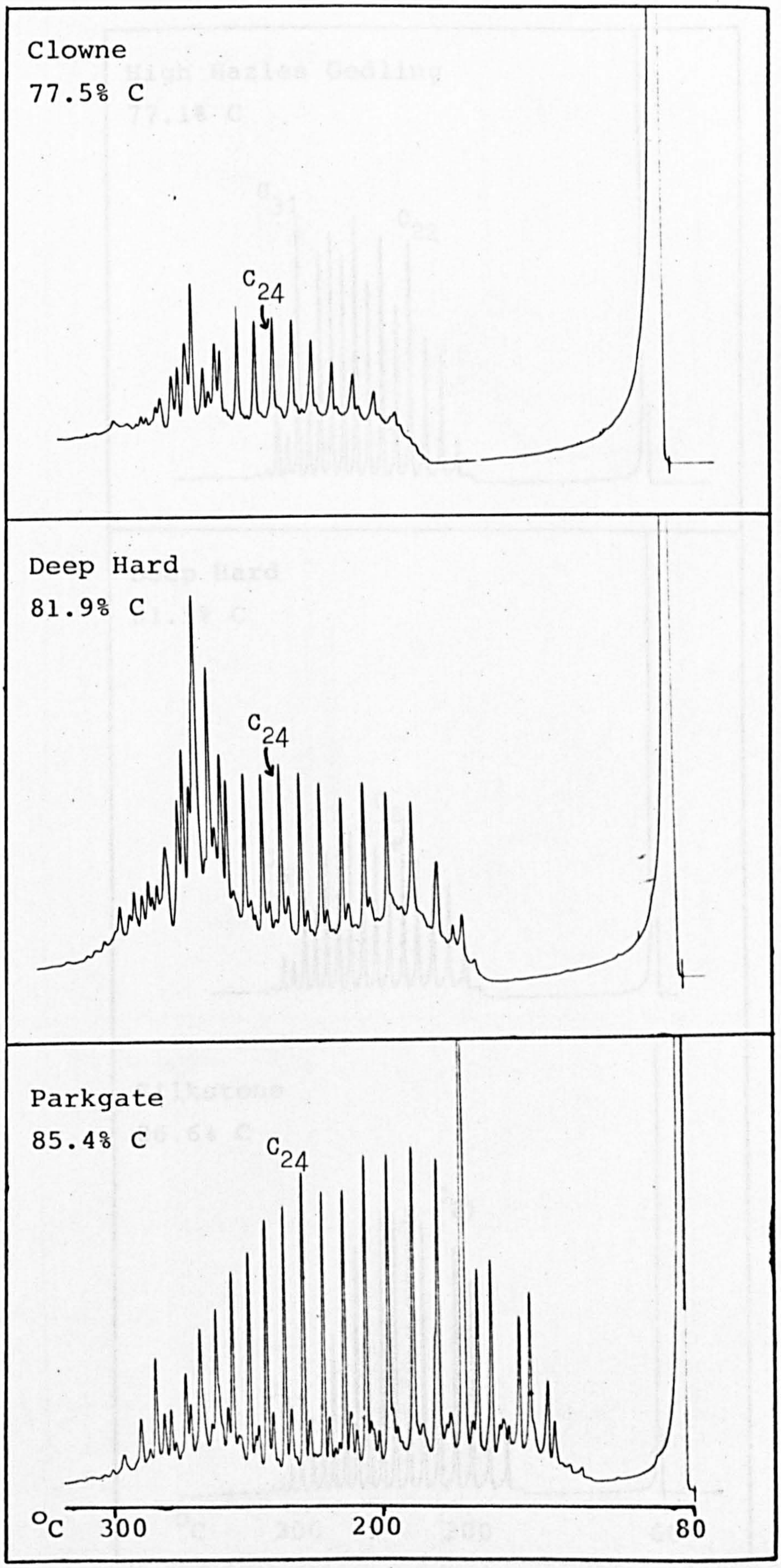

Gas chromatographic conditions as in Fig. 42 except programmed at 4°/min.

Fig. 47. n-Alkanes of vitrinites after pyrolysis at 275°

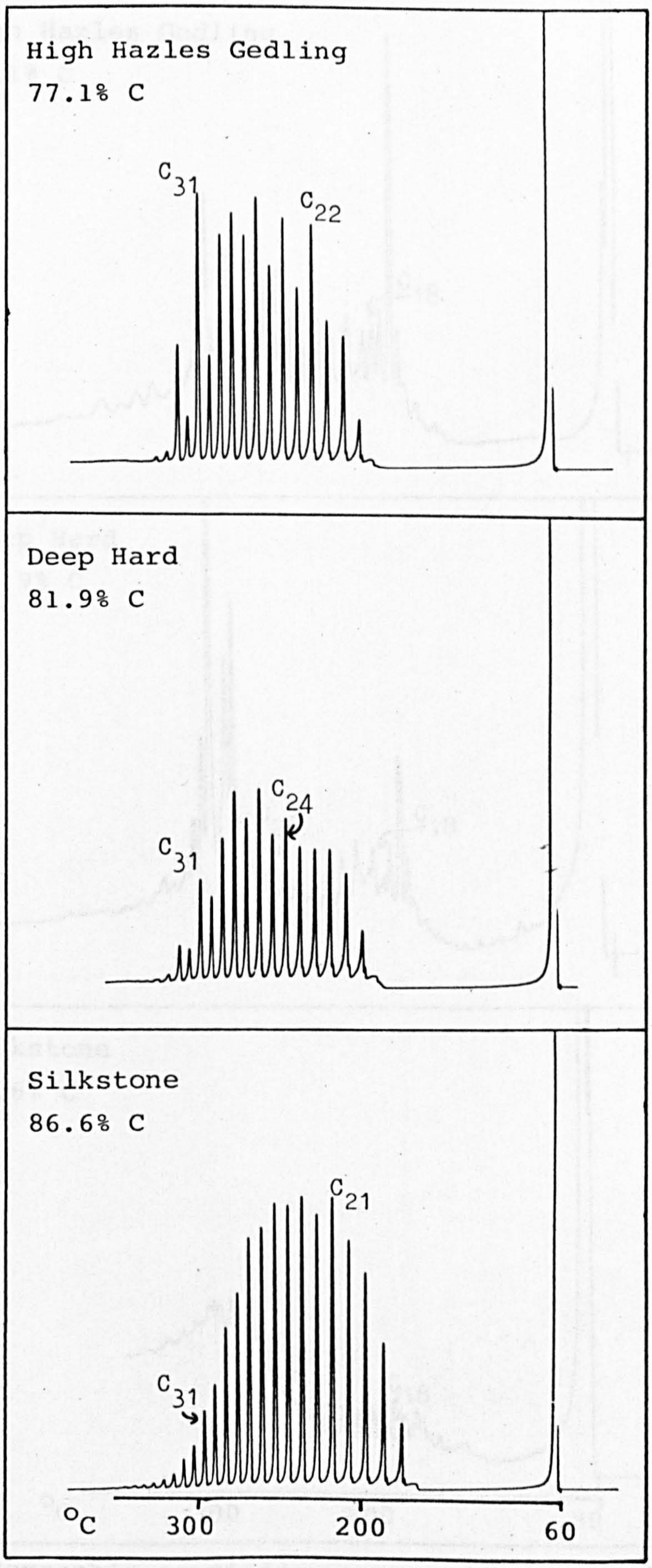

Gas chromatographic conditions as in Fig. 44.

Fig. 48. Alkenes of vitrinites after pyrolysis at 275°

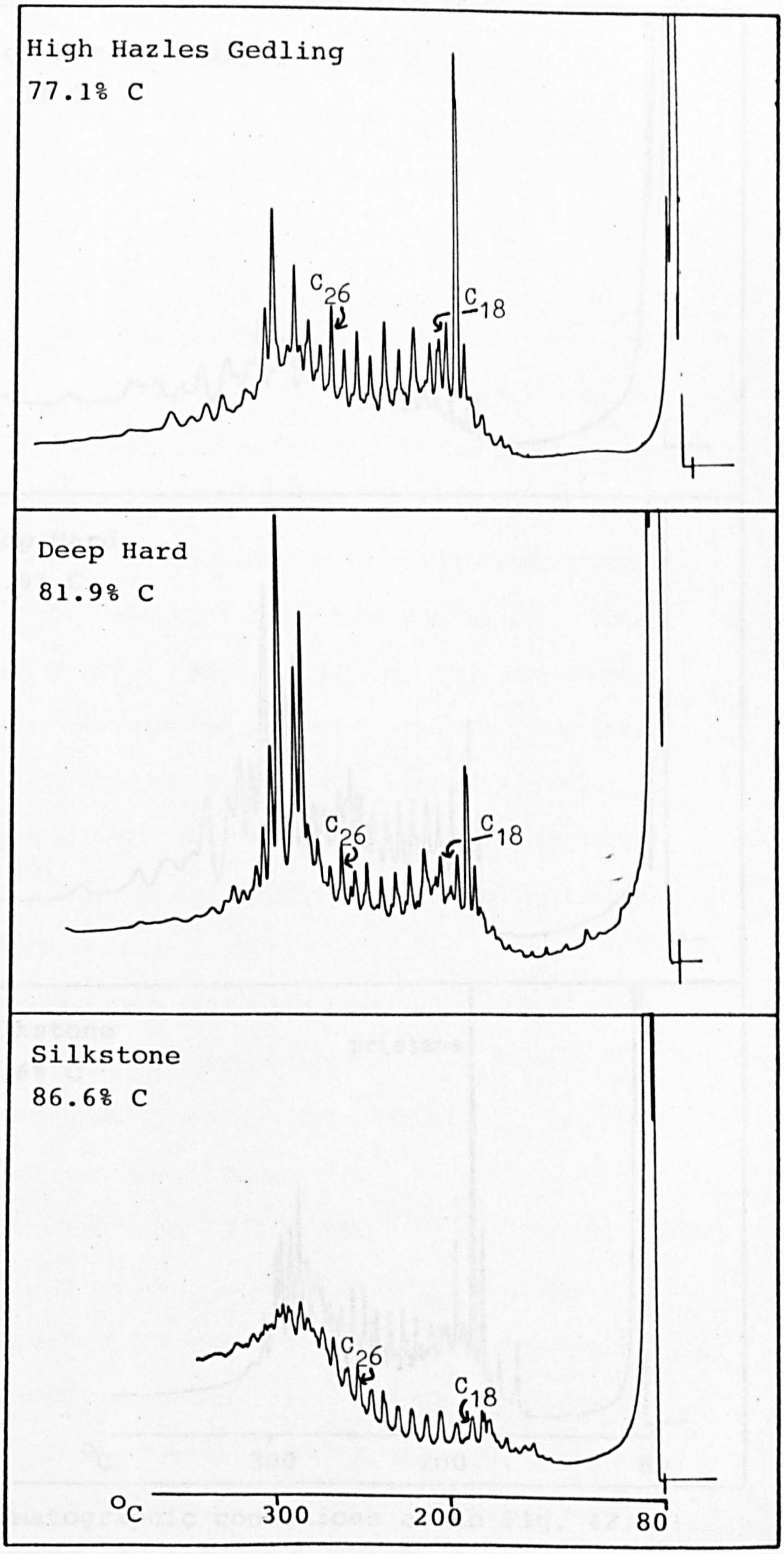

Gas chromatographic conditions as in Fig. 42.

Fig. 49. Branched/cyclic alkanes of vitrinites after pyrolysis at 275^{o}

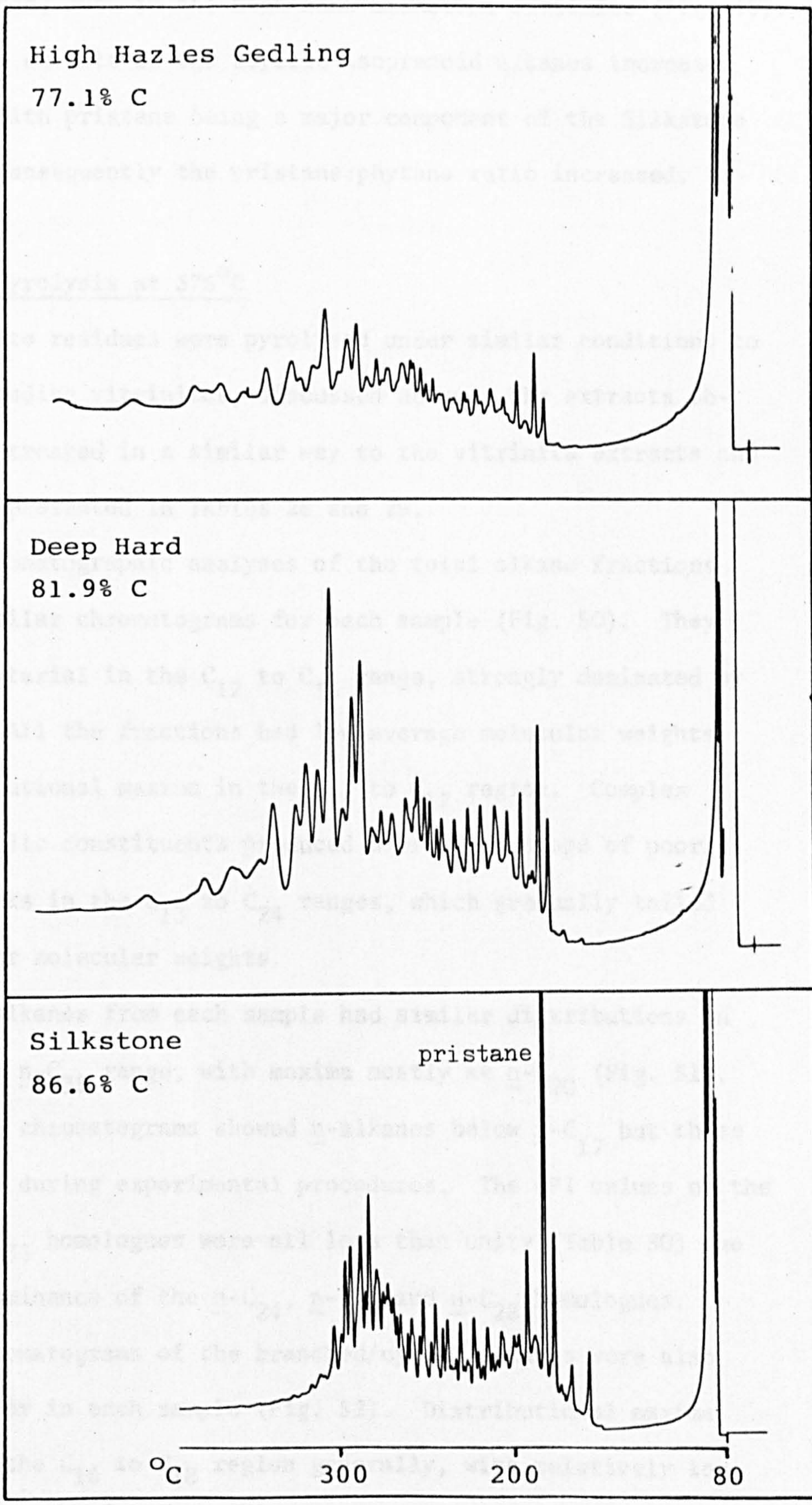

Gas chromatographic conditions as in Fig. 42.

Material in the sterane/triterpane ranges were major constituents of each sample, even in the high-rank Silkstone vitrinite (Fig. 49). The relative amounts of the acyclic isoprenoid alkanes increased with rank, with pristane being a major component of the Silkstone fraction. Consequently the pristane:phytane ratio increased.

Sporinite: pyrolysis at 375^oC

Sporinite residues were pyrolysed under similar conditions to the corresponding vitrinites, discussed above. The extracts obtained were treated in a similar way to the vitrinite extracts and results are presented in Tables 28 and 29.

Gas chromatographic analyses of the total alkane fractions produced similar chromatograms for each sample (Fig. 50). They contained material in the C_{12} to C_{35} range, strongly dominated by n-alkanes. All the fractions had low average molecular weights with distributional maxima in the C_{15} to C_{17} region. Complex branched/cyclic constituents produced a broad envelope of poorly resolved peaks in the C_{13} to C_{24} ranges, which gradually tailed off at higher molecular weights.

The n-alkanes from each sample had similar distributions in the n-C_{17} to n-C_{35} range, with maxima mostly at n-C_{20} (Fig. 51). Total alkane chromatograms showed n-alkanes below n-C_{17} but these are depleted during experimental procedures. The CPI values of the n-C_{23} to n-C_{33} homologues were all less than unity (Table 30) due to the predominance of the n-C_{24}, n-C_{26} and n-C_{28} homologues.

Gas chromatograms of the branched/cyclic alkanes were also rather similar in each sample (Fig. 52). Distributional maxima occurred in the C_{16} to C_{18} region generally, with relatively low amounts of material above about C_{28}. Acyclic isoprenoid alkanes were not predominant constituents of any sample. Although peaks

Table 28: Quantitative extraction and chromatographic data for sporinites pyrolysed at 375°C

	Total extract (mg/gm)	Column eluates Petroleum ether (mg/gm)	Benzene (mg/gm)	Methanol (mg/gm)	Wt. lost as volatiles (mg/gm)
Sporinite					
High Hazles Gedling	165.53	13.05	81.79	70.41	300.0
Clowne	207.71	10.08	107.13	49.67	270.5
Deep Hard	162.59	5.84	95.77	61.78	266.4
High Hazles Whitwell	186.32	9.26	88.34	64.04	263.7
Barnsley	110.98	10.00	55.01	31.93	271.2
Parkgate	103.81	6.17	50.48	51.28	167.8
Silkstone	96.19	3.68	59.78	33.11	213.0

Table 29: Alkane and alkene fractions isolated from sporinites pyrolysed at 375°C

	Total alkanes (mg/gm)	n-Alkanes (mg/gm	Branched/ cyclic alkanes (mg/gm)	Alkenes (mg/gm)
Sporinite				
High Hazles Gedling	6.11	1.26	3.58	1.11
Clowne	2.70	0.54	1.89	0.20
Deep Hard	2.70	0.49	1.84	0.18
High Hazles Whitwell	4.05	0.60	2.40	0.10
Barnsley	5.58	1.03	3.82	0.19
Parkgate	2.40	0.60	1.20	0.46
Silkstone	1.84	n.d.	0.92	0.37

n.d. not determined.

Fig. 50. Total alkanes of sporinites after pyrolysis at 375°

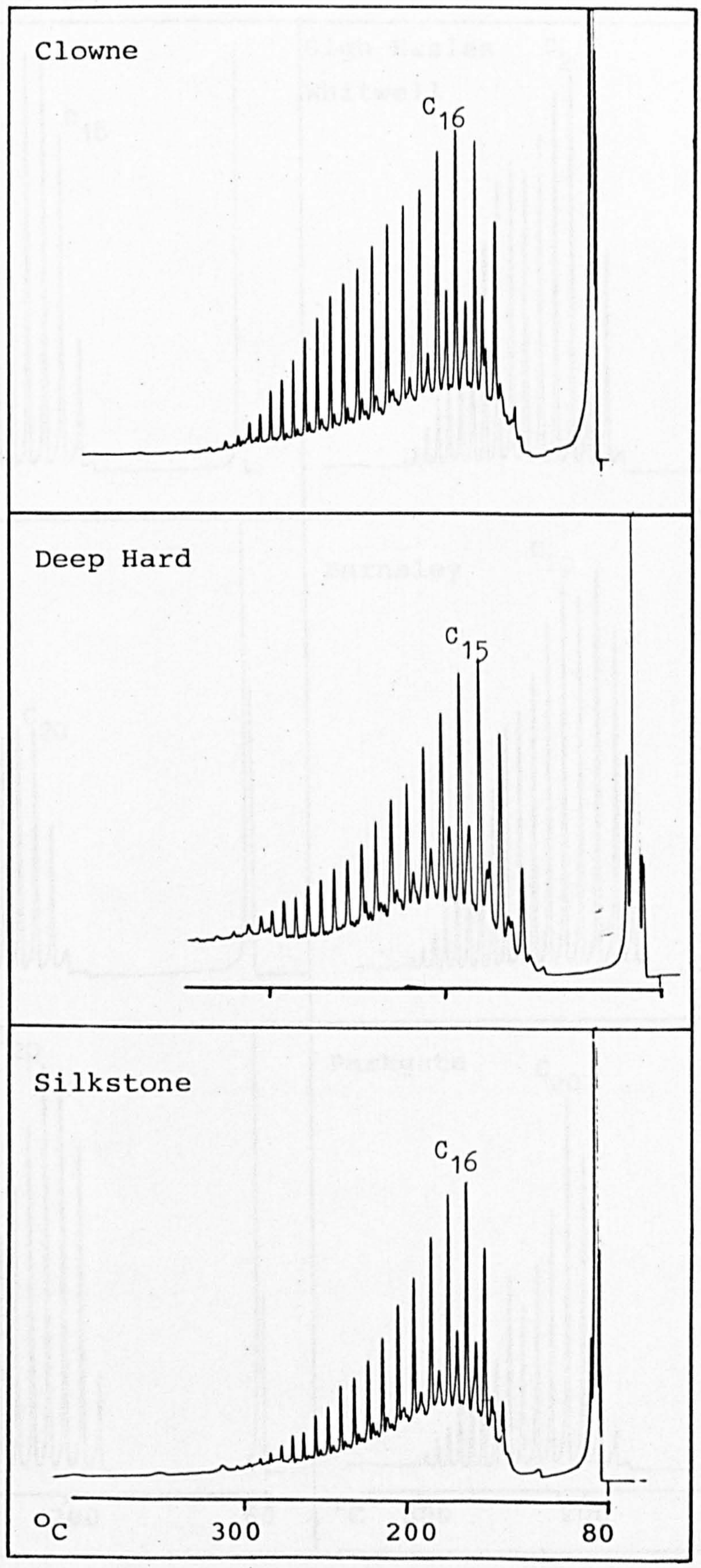

Gas chromatographic conditions as in Fig. 42.

Fig. 51. n-Alkanes of sporinites after pyrolysis at 375°

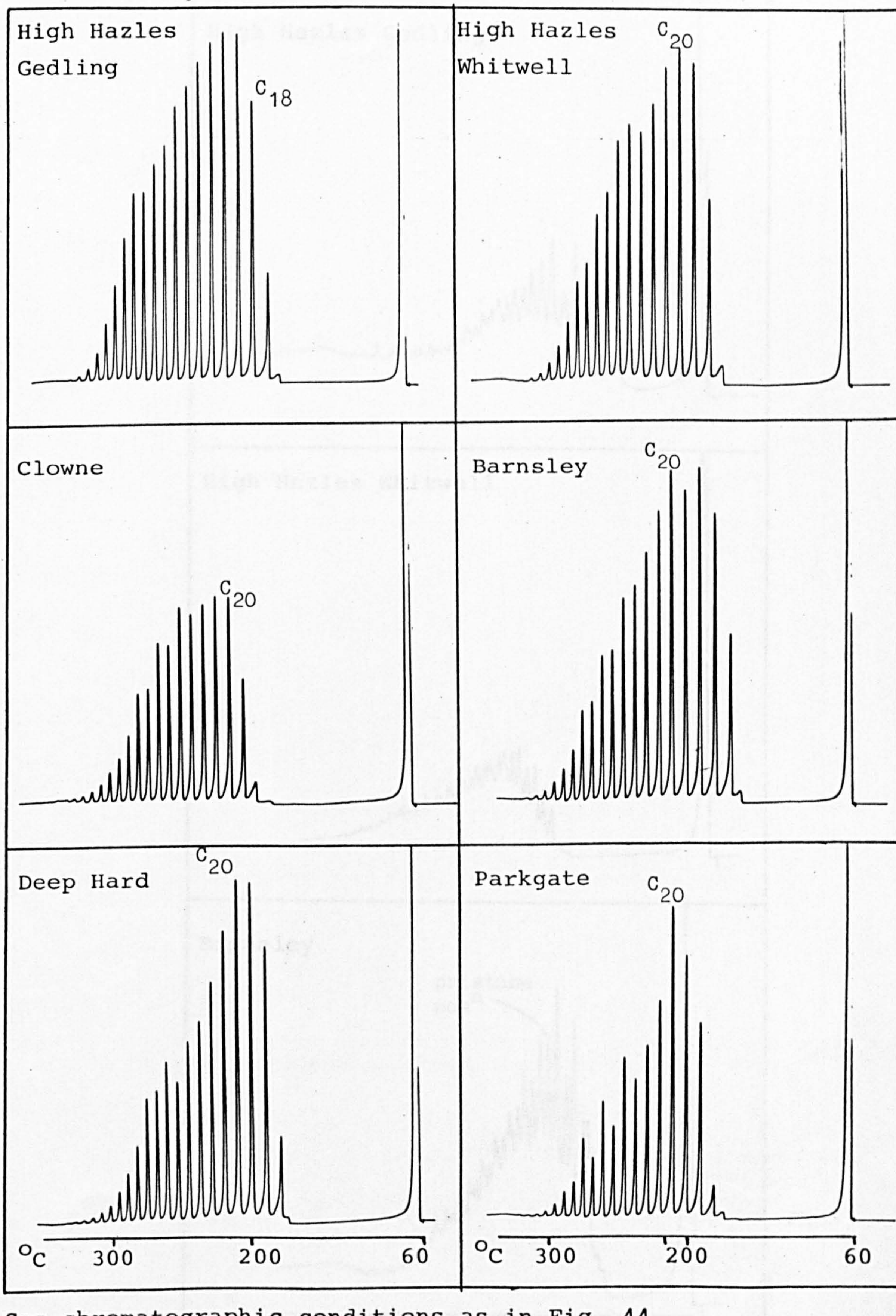

Gas chromatographic conditions as in Fig. 44.

Fig. 52. Branched/cyclic alkanes of sporinites after pyrolysis at 375^{o}

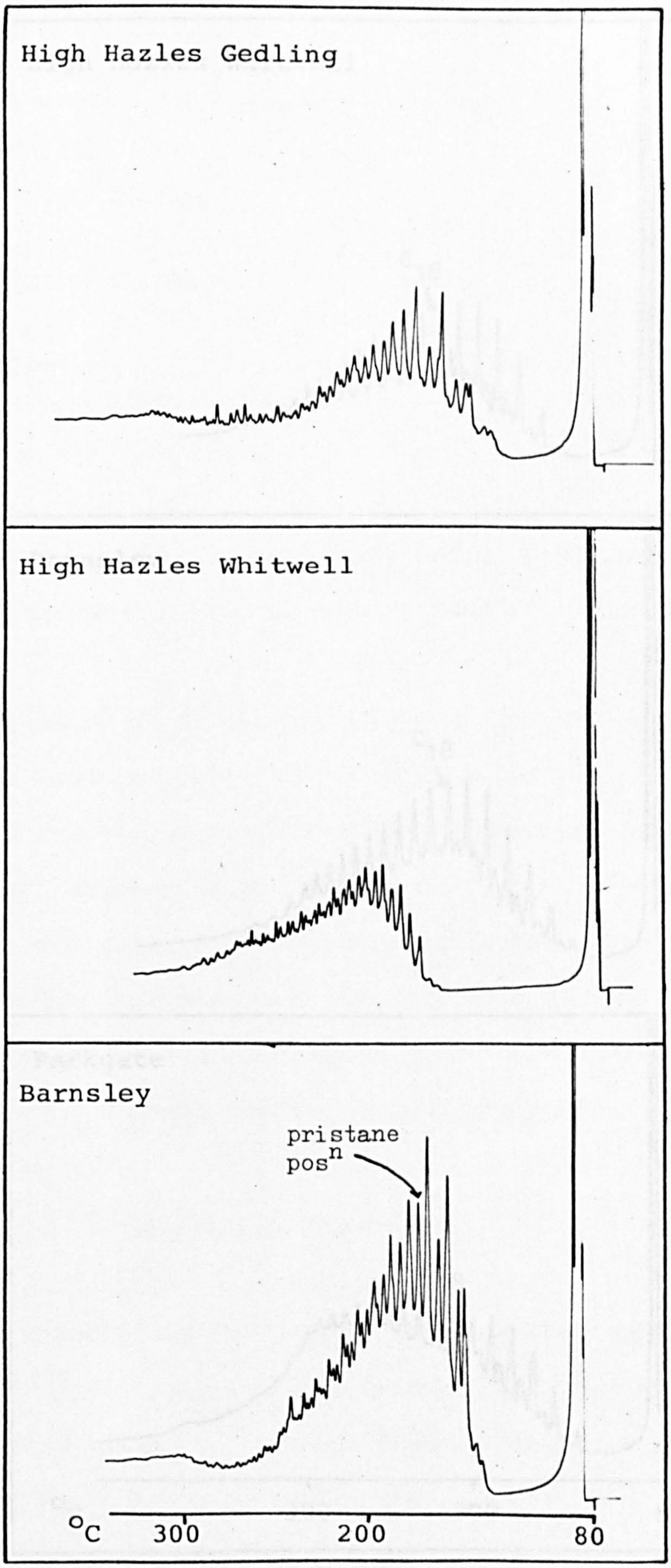

Gas chromatographic conditions as in Fig. 42a, except for H. Hazles Whitwell where as in Fig. 42.

Fig. 53. Alkenes of sporinites after pyrolysis at 375°

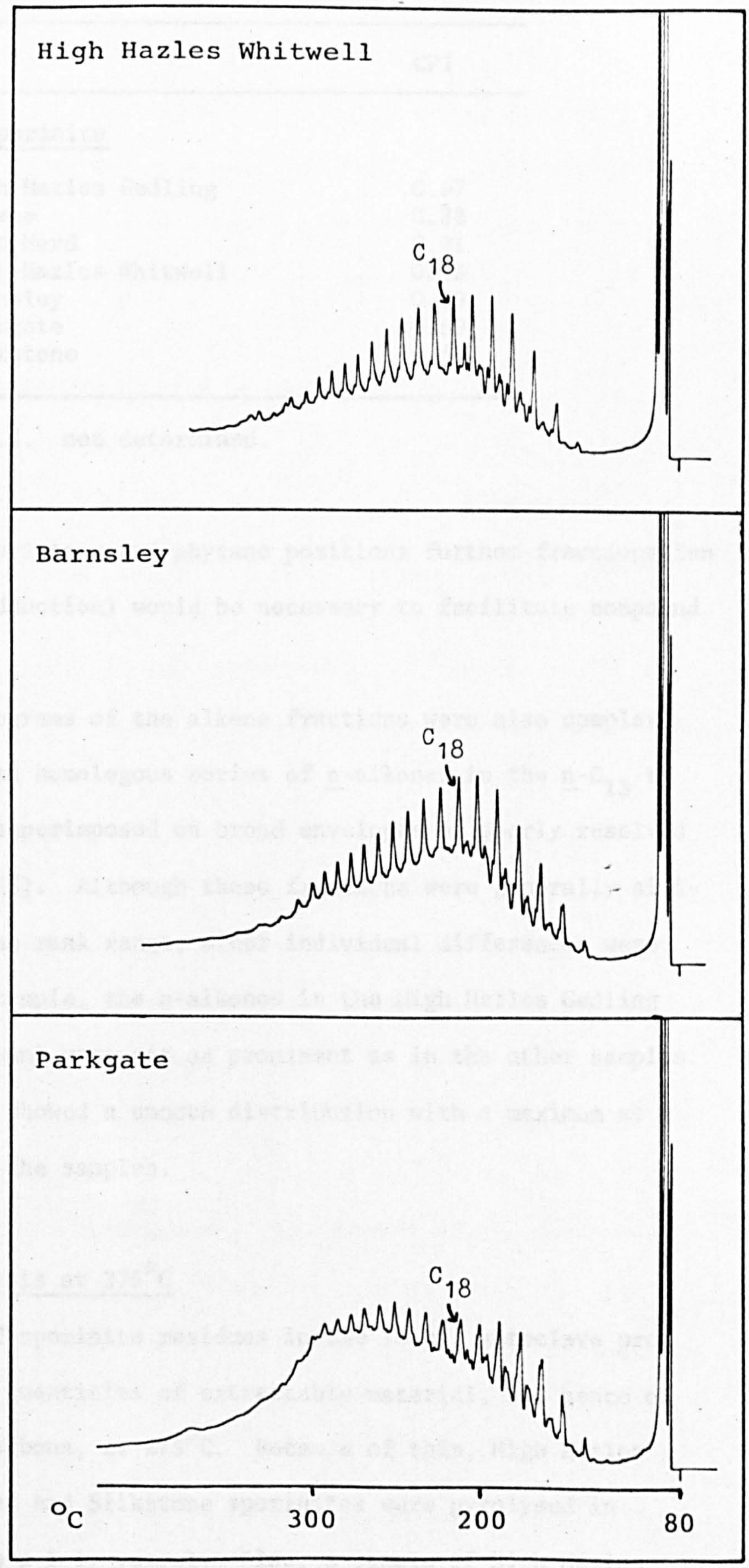

Gas chromatographic conditions as in Fig. 42.

Table 30: CPI values of n-alkanes produced by pyrolyses of sporinites at 375°C

Sporinite	CPI
High Hazles Gedling	0.97
Clowne	0.88
Deep Hard	0.91
High Hazles Whitwell	0.93
Barnsley	0.89
Parkgate	0.69
Silkstone	n.d.

n.d. not determined.

occurred in the pristane and phytane positions further fractionation (e.g. thiourea adduction) would be necessary to facilitate compound identification.

Gas chromatograms of the alkene fractions were also complex, but they showed an homologous series of n-alkenes in the n-C_{13} to *ca.* n-C_{29} range superimposed on broad envelopes of poorly resolved compounds (Fig. 53). Although these fractions were generally similar throughout the rank range, minor individual differences were apparent. For example, the n-alkenes in the High Hazles Gedling fraction (not shown) were not as prominent as in the other samples. n-Alkenes mostly showed a smooth distribution with a maximum at n-C_{18} in most of the samples.

Sporinite: pyrolysis at 275°C

Pyrolysis of sporinite residues in the 16 ml. autoclave produced very small quantities of extractable material, and hence of aliphatic hydrocarbons, at 275°C. Because of this, High Hazles Gedling, Deep Hard and Silkstone sporinites were pyrolysed in larger amounts in a 1 l. vessel. Also, a sample of High Hazles

Whitwell sporinite was pyrolysed in the 16 ml. autoclave for 287 hrs to assess the effect of time on product yield. Results are given in Table 31.

The petroleum ether eluates of the three larger pyrolyses and that of the long-term pyrolysis were separated by argentatious tlc into alkanes and alkenes; the alkanes were further separated into n- and branched/cyclic fractions. These results are given in Table 32.

The petroleum ether eluates of the sporinites showed some variations with increasing rank (Fig. 54). At lower ranks the fractions contained relatively large amounts of polycyclic hydrocarbons and n-alkanes were relatively minor components. At higher ranks n-alkanes and acyclic isoprenoid alkanes showed a relative increase, although high molecular weight polycyclic hydrocarbons were still being produced. In general, the branched/cyclic components appeared to increase in overall complexity with increasing rank.

The petroleum ether eluate of the 287 hr. pyrolysis of High Hazles Whitwell sporinite showed some differences to that of the 24 hr. pyrolysis of this sample, principally in that pristane had been generated in relatively greater amounts and the apparent distribution of the high molecular weight components had changed. n-Alkanes isolated from this fraction showed a slight dominance of even-numbered homologues above n-C_{23} and a distributional maximum at n-C_{21}. The branched/cyclic alkane fraction was dominated by triterpanes (Fig. 55), their structures being confirmed by mass spectrometry. Gas chromatographic analysis of the alkene fraction showed that high molecular weight alkenes, possibly triterpenes, had been generated during the pyrolysis.

The gc "fingerprints" of the petroleum ether eluates of the larger scale pyrolyses were generally comparable to those of the

Table 31: Quantitative extraction and chromatographic data for sporinites pyrolysed at 275°C

	Total extract (mg/gm)	Column eluates Petroleum ether (mg/gm)	Benzene (mg/gm)	Methanol (mg/gm)	Wt. lost as volatiles (mg/gm)
Sporinite					
High Hazles Gedling	56.18	< 0.15	2.63	34.38	133.6
Clowne	n.d.	< 0.07	1.45	3.80	n.d.
Deep Hard	3.88	< 0.06	0.56	2.34	16.1
High Hazles Whitwell	3.88	< 0.07	0.95	1.90	43.1
Barnsley	4.24	< 0.06	0.62	3.56	59.4
Parkgate	13.65	0.07	6.03	5.01	21.2
Silkstone	17.23	0.36	9.39	5.92	76.1
High Hazles Gedling*2	7.72	0.11	1.70	4.32	31.5
Deep Hard*2	2.60	0.06	0.69	1.69	16.3
Silkstone*2	12.07	0.36	6.36	3.73	5.4
High Hazles Whitwell*3	21.26	0.74	9.08	8.55	1.5

n.d. not determined

*3 indicates the sample pyrolysed for 287 hrs.

Table 32: Alkane and alkene fractions isolated from sporinites pyrolysed at 275°C

	Total alkanes (mg/gm)	*n*-Alkanes (mg/gm)	Branched/ cyclic alkanes (mg/gm)	Alkenes (mg/gm)
Sporinite				
High Hazles Gedling*2	0.04	0.01	0.02	0.01
Deep Hard*2	0.02	0.01	0.01	0.02
Silkstone*2	0.23	0.01	0.21	0.05
High Hazles Whitwell*3	0.40	0.14	0.14	0.14

Fig. 54. Aliphatic hydrocarbons of sporinites after pyrolysis at 275°

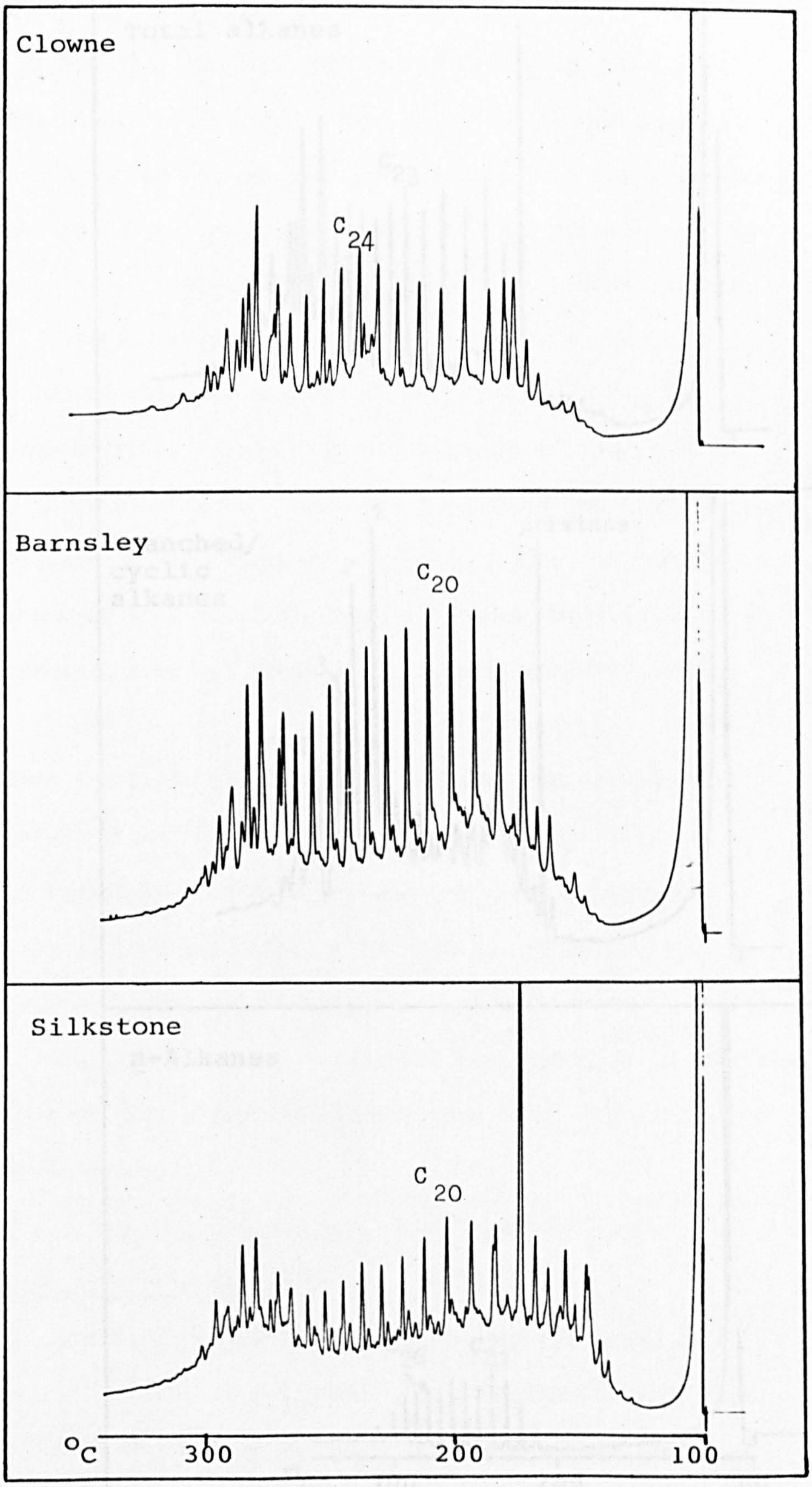

Gas chromatographic conditions: 10'x1/16"o.d. column containing 2% OV-101 on Varaport 30 (100-120 mesh); programmed 100-300°C at 4%/min; detector 300°; injector 300°; nitrogen 60 p.s.i.

Fig. 55. Alkanes of High Hazles Whitwell sporinite after pyrolysis at 275° for 287 hours

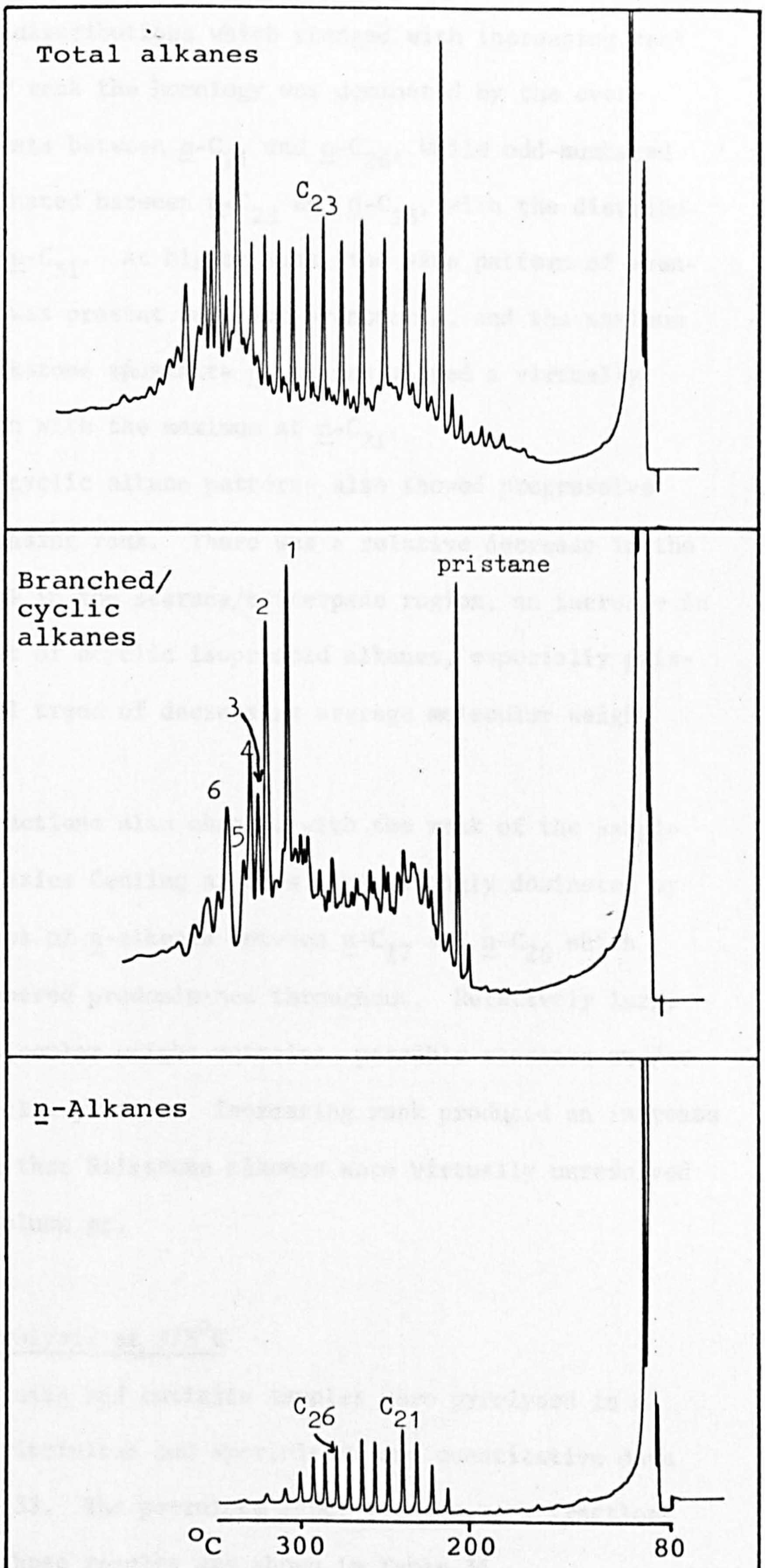

Gas chromatographic conditions as in Fig. 42, except for total alkanes where as in Fig. 42a.

smaller scale experiments. n-Alkanes isolated from the three samples exhibited distributions which changed with increasing rank (Fig. 56). At low rank the homology was dominated by the even-numbered constituents between n-C_{21} and n-C_{26}, while odd-numbered homologues predominated between n-C_{28} and n-C_{33}, with the distributional maximum at n-C_{31}. At higher rank, the same pattern of even- and odd-dominance was present but less pronounced, and the maximum was at n-C_{29}. Silkstone sporinite n-alkanes showed a virtually smooth distribution with the maximum at n-C_{21}.

The branched/cyclic alkane patterns also showed progressive changes with increasing rank. There was a relative decrease in the content of material in the sterane/triterpane region, an increase in the relative amount of acyclic isoprenoid alkanes, especially pristane, and a general trend of decreasing average molecular weight (Fig. 57).

The alkene fractions also changed with the rank of the sample (Fig. 58). High Hazles Gedling alkenes were strongly dominated by an homologous series of n-alkenes between n-C_{17} and n-C_{28} which showed an even-numbered predominance throughout. Relatively large amounts of high molecular weight material, possible sterenes and/or triterpenes, were also present. Increasing rank produced an increase in complexity such that Silkstone alkenes were virtually unresolved by short, packed-column gc.

Other exinites: pyrolysis at 375°C

Alginite, resinite and cutinite samples were pyrolysed in a similar manner to vitrinites and sporinites, and quantitative data are given in Table 33. The petroleum ether eluates were fractionated as above and these results are shown in Table 34.

Gc analyses of the petroleum ether eluates showed the alginite

Fig. 56. $\underline{n}$-Alkanes of sporinites after pyrolysis at 275°

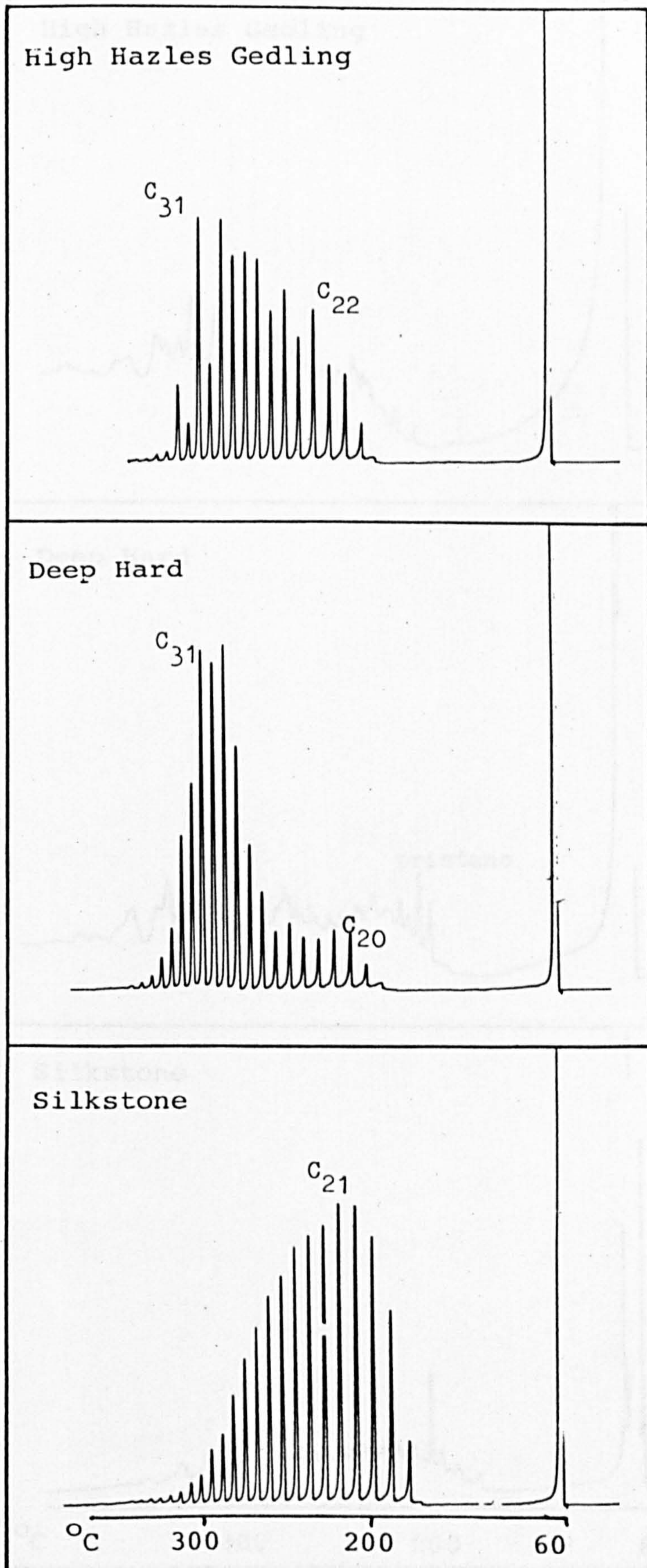

Gas chromatographic conditions as in Fig. 44.

Fig. 57. Branched/cyclic alkanes of sporinites after pyrolysis at 275°

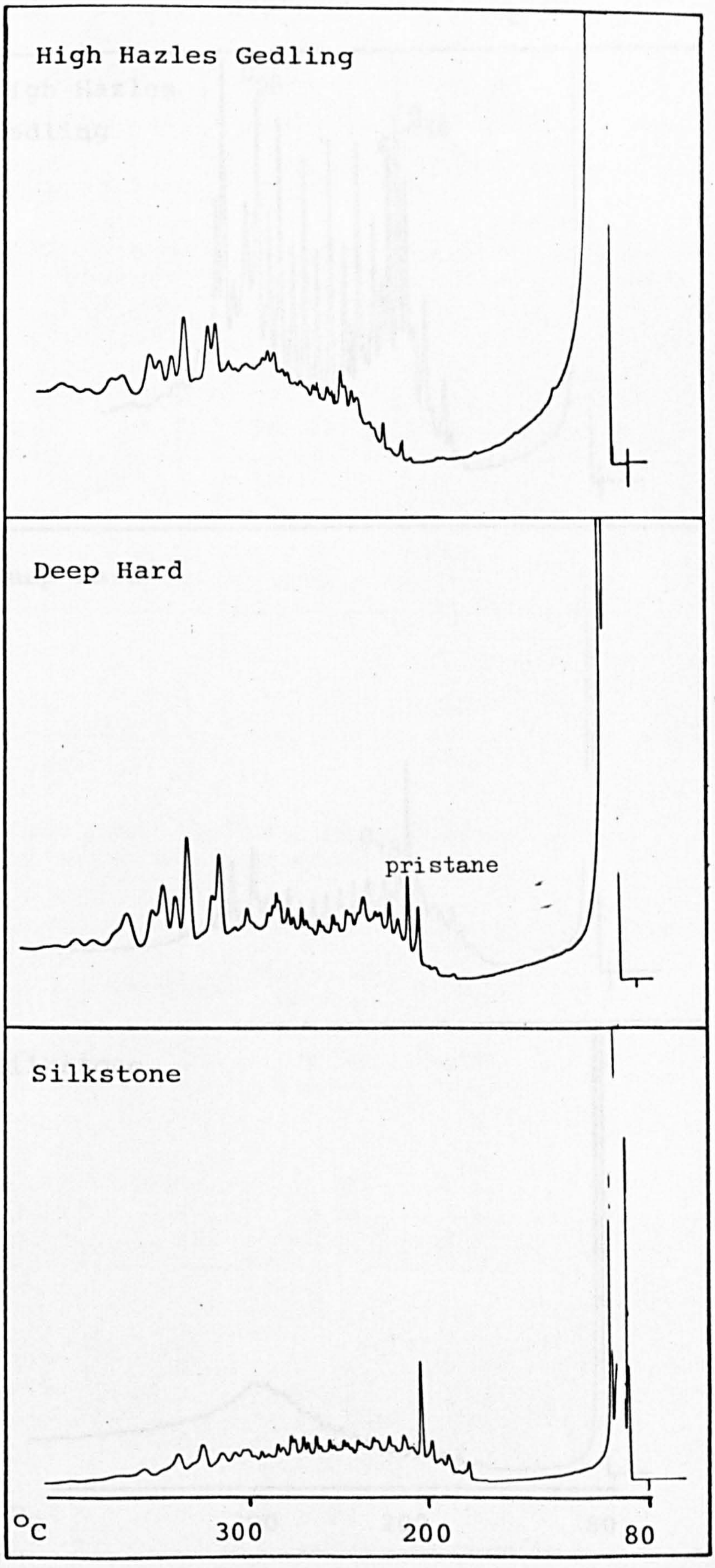

Gas chromatographic conditions as in Fig. 42.

Fig. 58. Alkenes of sporinites after pyrolysis at 275°

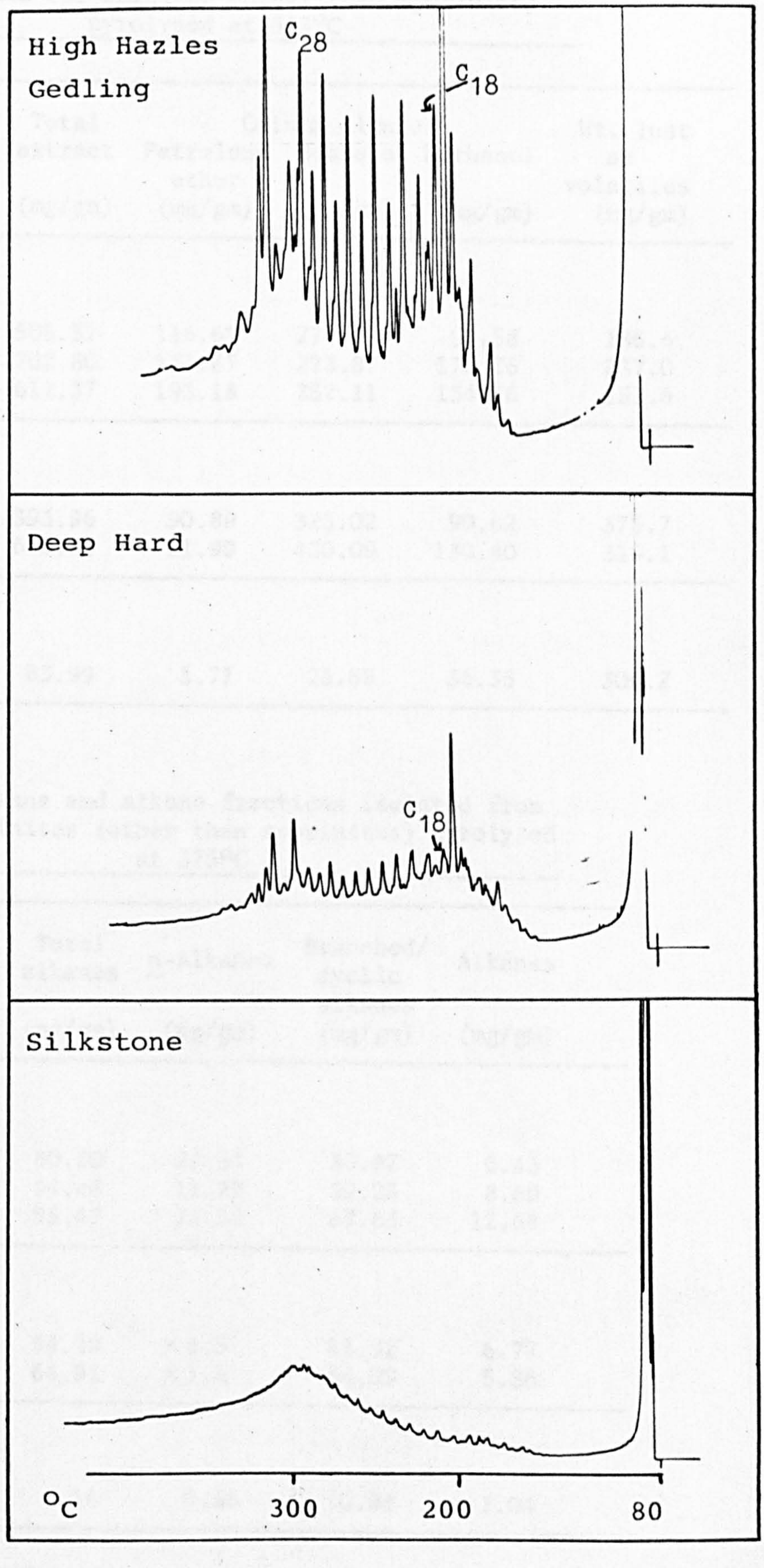

Gas chromatographic conditions as in Fig. 42.

Table 33: Quantitative extraction and chromatographic data for exinites (other than sporinite) pyrolysed at 375°C

	Total extract (mg/gm)	Column eluates: Petroleum ether (mg/gm)	Column eluates: Benzene (mg/gm)	Column eluates: Methanol (mg/gm)	Wt. lost as volatiles (mg/gm)
Alginite					
Scotland	505.37	116.69	277.05	95.58	186.6
South Africa	702.80	131.87	273.87	170.26	237.0
New South Wales	612.37	193.18	252.11	134.26	253.6
Resinite					
Bitterfeld	593.96	90.89	323.02	90.62	375.7
Maghara	680.91	91.99	430.09	130.40	319.1
Cutinite					
Indiana	83.99	5.71	26.85	36.55	306.2

Table 34: Alkane and alkene fractions isolated from exinites (other than sporinites) pyrolysed at 375°C

	Total alkanes (mg/gm)	n-Alkanes (mg/gm)	Branched/cyclic alkanes (mg/gm)	Alkenes (mg/gm)
Alginite				
Scotland	80.29	29.34	33.97	6.43
South Africa	64.48	11.22	39.25	8.69
New South Wales	95.47	23.89	67.63	12.68
Resinite				
Bitterfeld	54.28	< 0.5	51.92	6.77
Maghara	64.91	< 1.5	54.09	5.86
Cutinite				
Indiana	2.16	0.66	0.99	1.04

and cutinite products to be dominated by n-alkanes up to *ca*. n-C_{35} in the alginites and n-C_{30} in the cutinite. The fractions were complex throughout and of fairly low average molecular weights. By contrast, the two resinites produced hydrocarbons occurring mainly between C_{12} and C_{24}. These fractions were very complex but the elution patterns of the major components from the two samples were similar. n-Alkanes did not appear to be present.

n-Alkanes from the alginites were similar, with homologues occurring up to n-C_{35}, and envelope maxima at n-C_{17} and n-C_{19} (Fig. 59). The New South Wales sample showed a slight predominance of even-numbered homologues in the n-C_{23} to n-C_{33} range (Table 35) just discernible in the gc (Fig. 59). Cutinite n-alkanes also exhibited an even-dominated distribution in the higher molecular weight range (Fig. 60). Trace quantities of n-alkanes were isolated from the resinite fractions, ranging from n-C_{19} to n-C_{30} with n-C_{24}, n-C_{26} and n-C_{28} as the major components.

Alginite branched/cyclic alkane fractions (Fig. 61) showed a close resemblance to each other, and packed-column gc indicated that a number of homologous series were probably present. Capillary gc of Scottish alginite branched/cyclic alkanes (Fig. 62) on a 40 m. column (generating *ca*. 30,000 effective plates for n-hexacosane) indicated that iso- and anteiso-alkanes in the C_{15} to C_{26} range were probably present; this indication was obtained by co-injection with internal standards. The cutinite branched/cyclic alkane fraction was very complex (Fig. 60).

Bitterfeld resinite branched/cyclic alkane fraction (Fig. 63) showed very little change from the petroleum ether eluate gc elution pattern, despite the removal of alkenes. Maghara resinite branched/cyclic alkanes differed in that much of the lower molecular weight material (< C_{14}) had been removed, although this may have been an

Fig. 59. n-Alkanes of alginites after pyrolysis at 375°

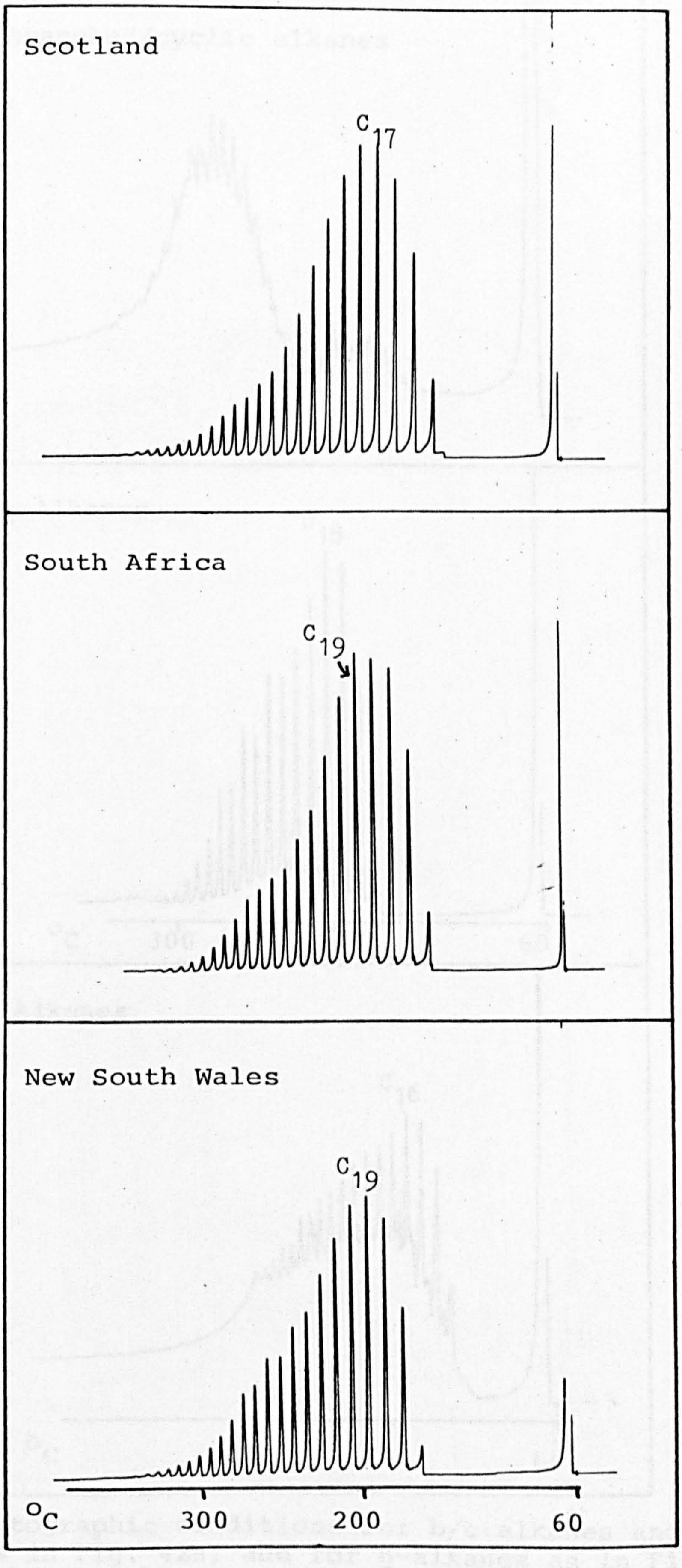

Gas chromatographic conditions as in Fig. 44.

Fig. 60. Alkanes and alkenes of cutinite after pyrolysis at 375°

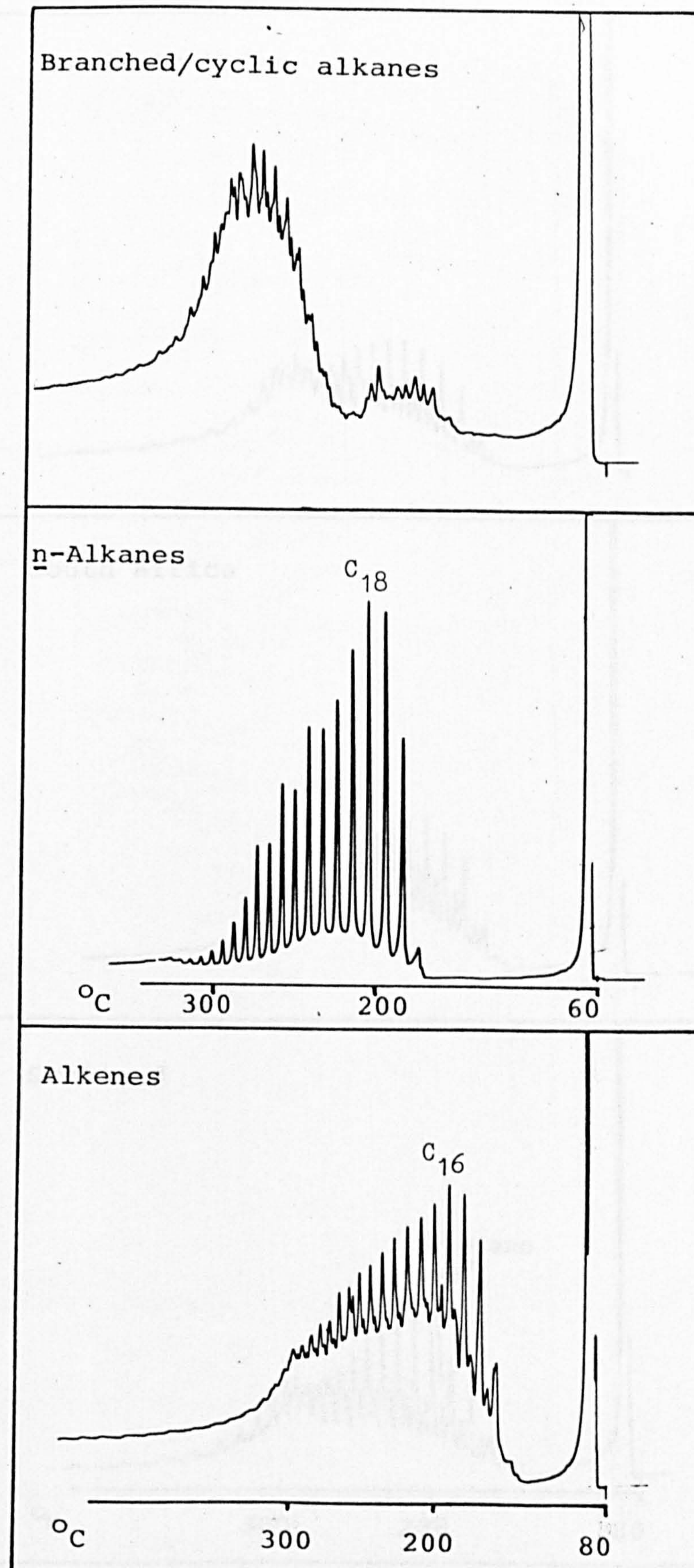

Gas chromatographic conditions for b/c alkanes and alkenes as in Fig. 42a, and for n-alkanes as in Fig. 44.

Fig. 61. Branched/cyclic alkanes of alginites after pyrolysis at 375^{o}

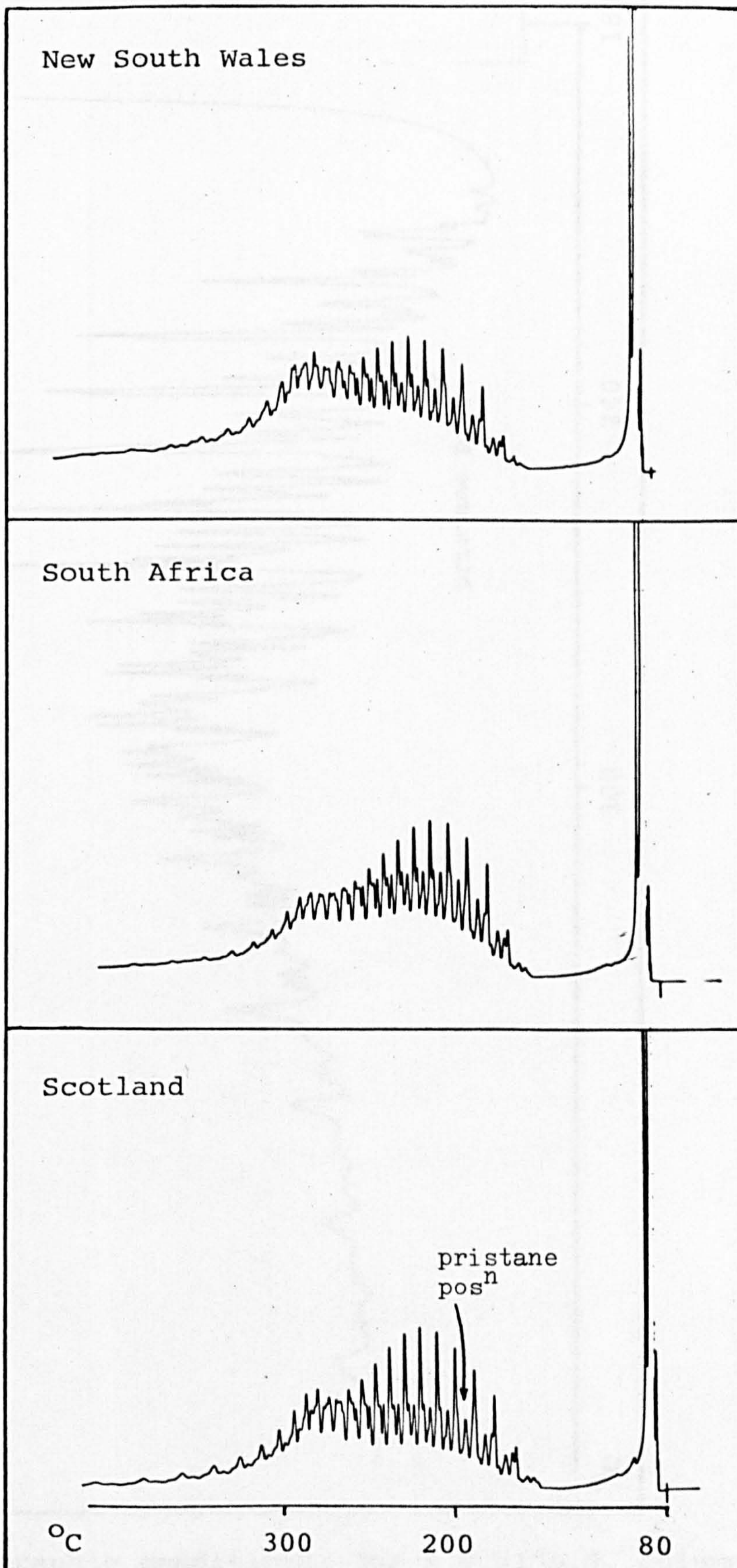

Gas chromatographic conditions as in Fig. 42.

Fig. 62. Capillary gas chromatogram of branched/cyclic alkanes of Scottish alginite after pyrolysis at 375°

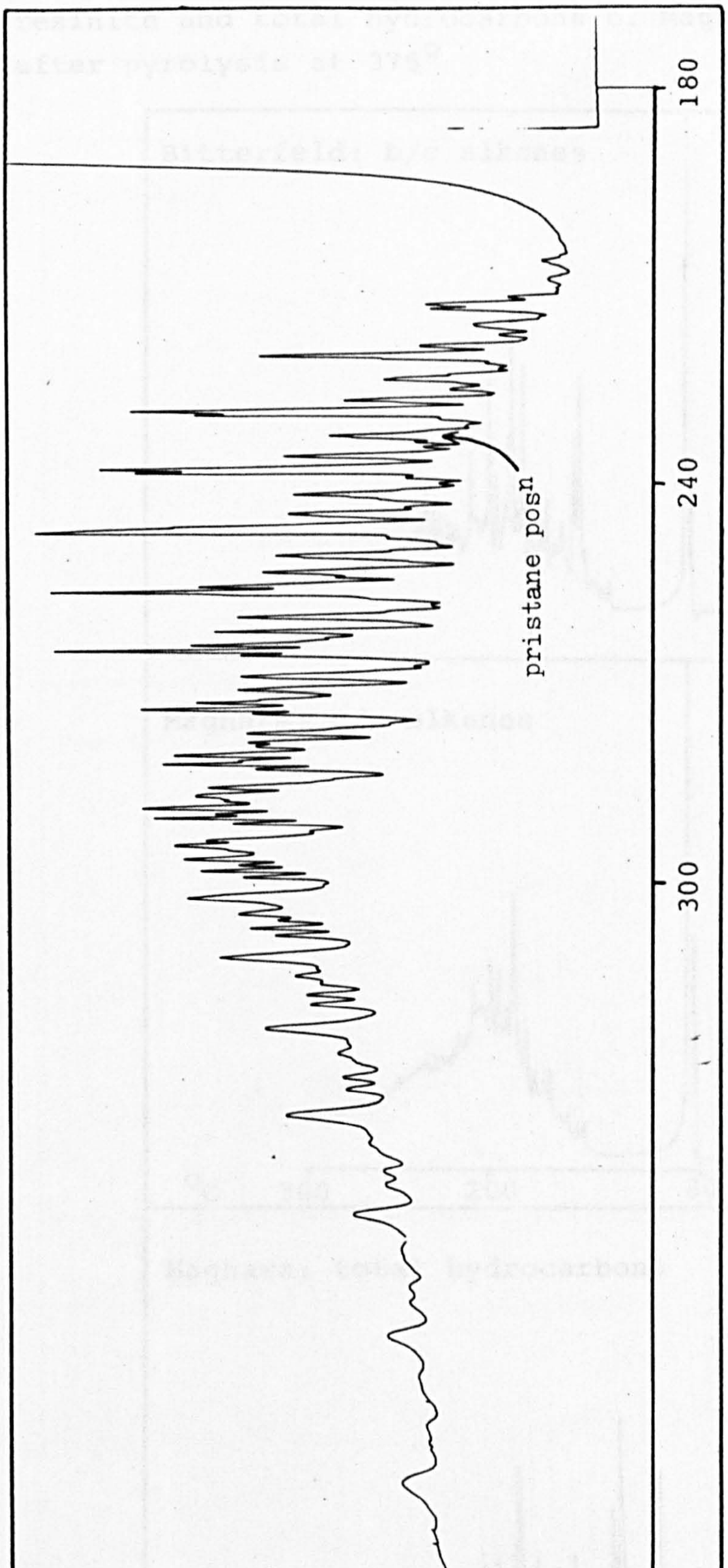

Gas chromatographic conditions: 40m x 0.01"o.d. column OV-101; programmed 180-300°C at 2°/min; detector 300°; injector 300°; nitrogen 6 p.s.i.

Fig. 63. Branched/cyclic alkanes of Bitterfeld and Maghara resinite and total hydrocarbons of Maghara resinite after pyrolysis at 375°

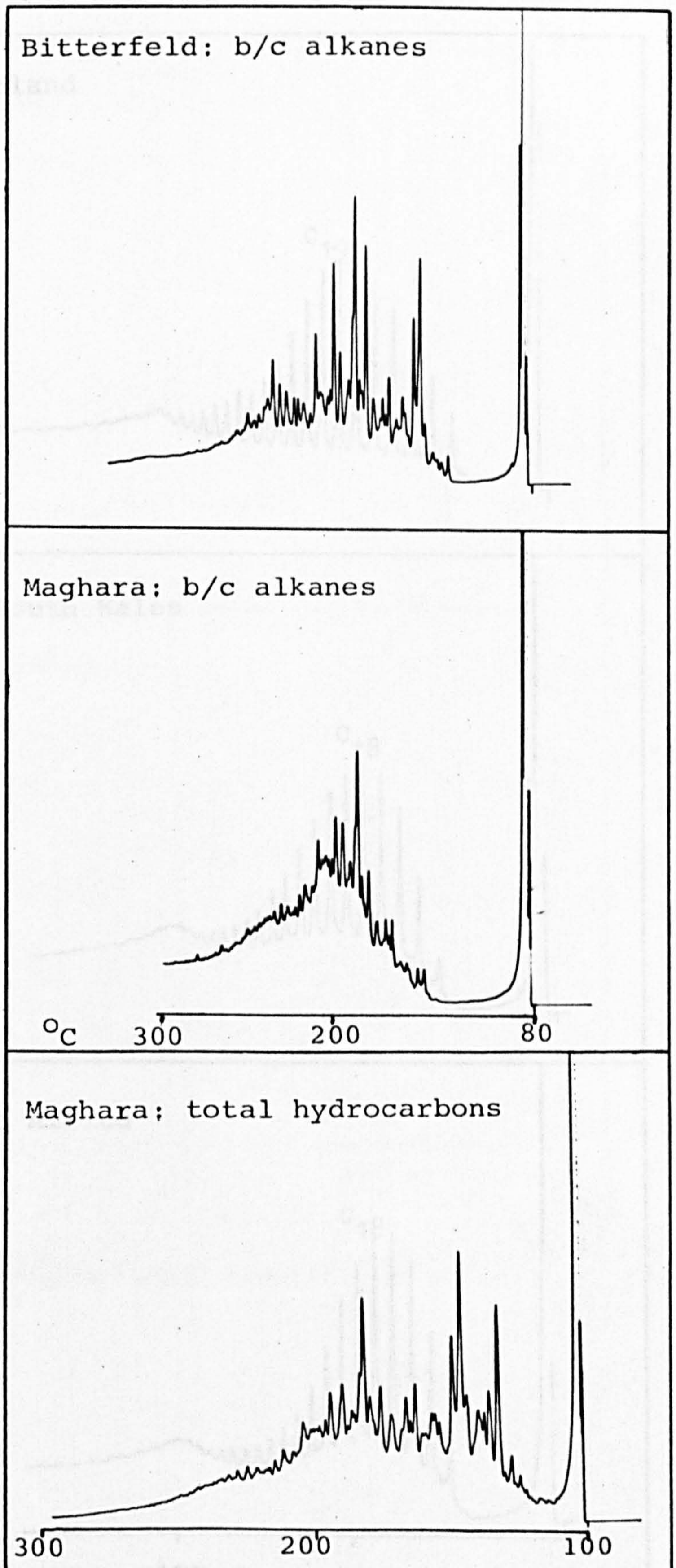

Gas chromatographic conditions as in Fig. 42 for b/c alkanes, and as in Fig.54 for total hydrocarbons

Fig. 64. Alkenes of alginites after pyrolysis at375°

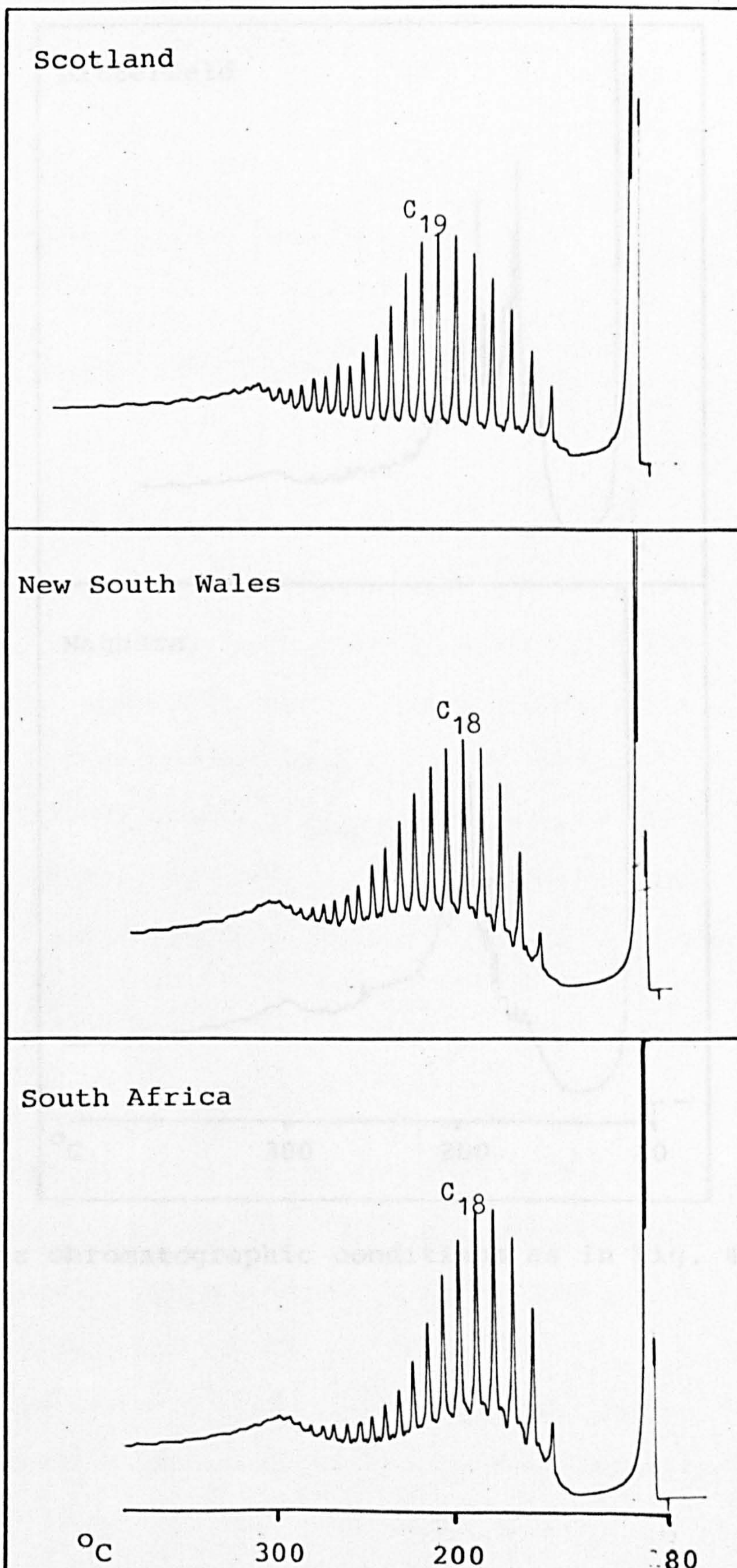

Gas chromatographic conditions as in Fig. 42a.

Fig. 65. Alkenes of resinites after pyrolysis at 375°

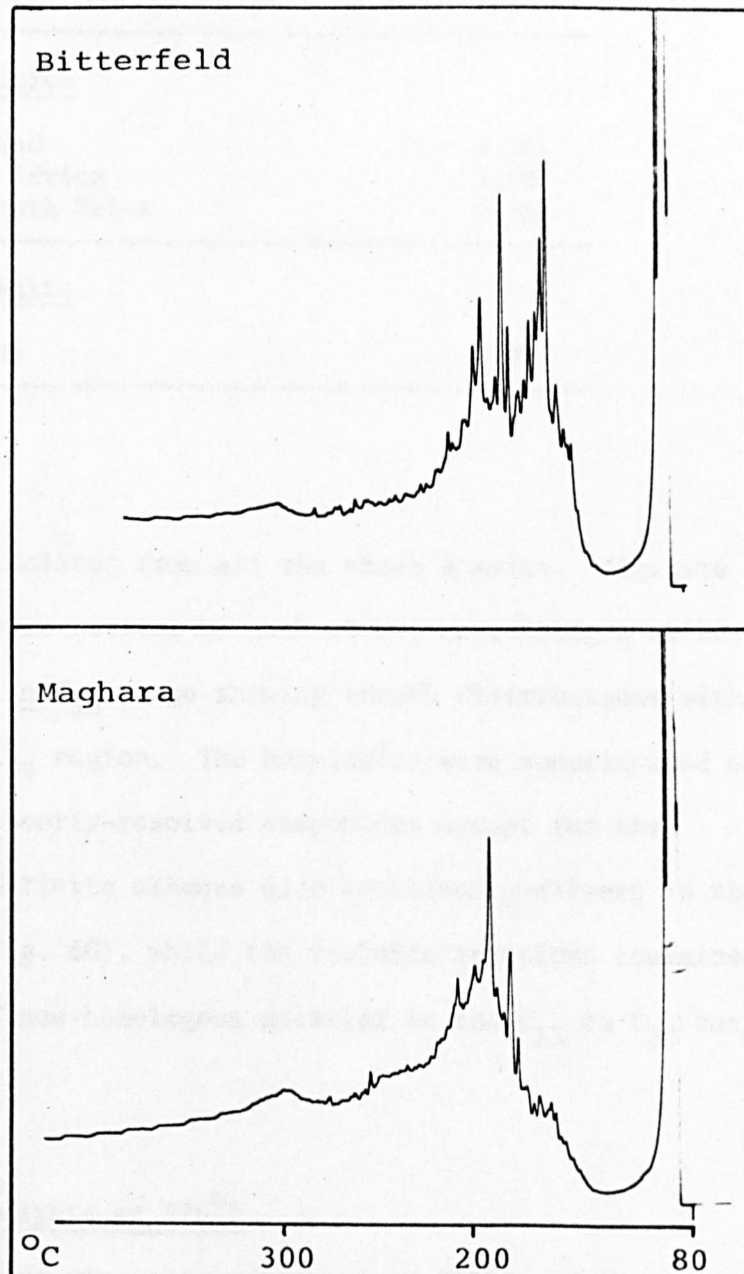

Gas chromatographic conditions as in Fig. 42a.

Table 35: CPI values of n-alkanes isolated from exinites (other than sporinites) pyrolysed at 375°C

	CPI
Alginite	
Scotland	1.01
South Africa	1.06
New South Wales	0.94
Cutinite	
Indiana	0.84

experimental loss.

Alkenes were isolated from all the above samples. Alginite alkenes (Fig. 64) were similar to each other, containing n-alkenes in the n-C_{14} to *ca.* n-C_{33} range showing smooth distributions with maxima in the C_{18}-C_{19} region. The homologies were superimposed on broad envelopes of poorly-resolved components except for the Scottish sample. Cutinite alkenes also contained n-alkenes in the C_{13} to C_{30} range (Fig. 60), while the resinite fractions contained complex mixtures of non-homologous material in the C_{13} to C_{20} range (Fig. 65).

Other exinites: pyrolysis at 275°C

The above samples were also pyrolysed at 275°C and the same experimental procedures were applied in working up the products, except that no separations using molecular sieve were carried out. Results are given in Tables 36 and 37.

The total alkane fractions of the alginites appeared qualitatively similar to those obtained at 375°C, being dominated by n-alkanes in the C_{15} to C_{35} range and showing maxima at *ca.* n-C_{19} (Fig. 66). However, New South Wales alginite alkanes showed a

Table 36: Quantitative extraction and chromatographic data for exinites (other than sporinite) pyrolysed at 275°C

	Total extract (mg/gm)	Column eluates: Petroleum ether (mg/gm)	Column eluates: Benzene (mg/gm)	Column eluates: Methanol (mg/gm)	Wt. lost as volatiles (mg/gm)
Alginite					
Scotland	1.59	0.15	0.44	0.51	69.0
South Africa	0.71	< 0.07	0.07	0.28	95.5
New South Wales	2.91	0.43	0.14	0.50	76.7
Resinite					
Bitterfeld	344.62	9.49	191.07	145.96	12.8
Maghara	20.38	2.87	7.65	7.49	76.9
Cutinite					
Indiana	3.66	1.00	0.45	1.55	38.3

Table 37: Alkane and alkene fractions isolated from exinites (other than sporinites) pyrolysed at 275°C

	Total alkanes (mg/gm)	Alkenes (mg/gm)
Alginite		
Scotland	0.15	-
South Africa	< 0.07	-
New South Wales	0.14	0.07
Resinite		
Bitterfeld	0.44	1.02
Maghara	0.16	0.16
Cutinite		
Cutinite	< 0.11	< 0.11

greater predominance of even-numbered n-alkanes between n-C_{20} and n-C_{30} than was observed in the 375°C pyrolysate. The alkene fraction of this alginite also contained a slight even-dominated distribution of n-alkenes (Fig. 66).

Cutinite produced a rather restricted range of alkanes at 275°C, dominated by n-alkanes between C_{16} and C_{20} with n-C_{17} and n-C_{18} as the major constituents. n-Alkanes above C_{20} were minor constituents (Fig. 67).

The petroleum ether eluate of Bitterfeld resinite was an apparently simple fraction with four main components in the C_{13} to C_{15} region. Fractionation by argentatious tlc confined these compounds to the alkene fraction but also indicated a highly complex alkane fraction containing compounds mostly in the C_{16} to C_{20} range, but extending up to C_{30} (Fig. 68). Apparent n-alkanes in this higher range showed a strong predominance of even-numbered homologues. Maghara resinite yielded a highly complex petroleum ether eluate containing material in the C_{14} to C_{30} range. Total alkanes isolated from this fraction also appeared to contain n-alkanes between n-C_{20} and n-C_{30} with a strongly even-dominated distribution (Fig. 68).

Fig. 66. Alkenes of New South Wales alginite and total alkanes of New South Wales and Scottish alginite after pyrolysis at 275°

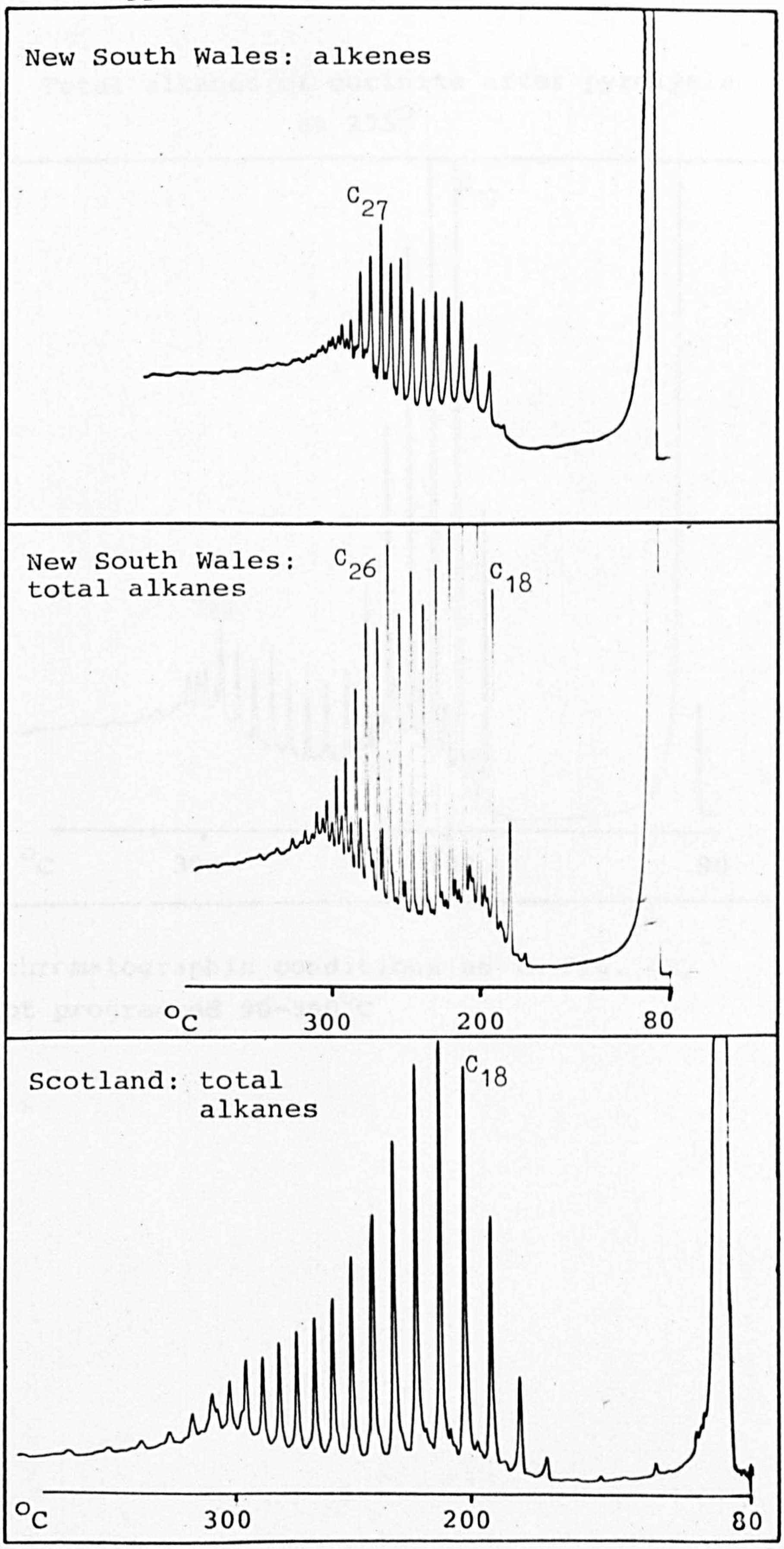

Gas chromatographic conditions as in Fig. 42a for New South Wales fractions, and as above for Scottish alginite except 20' x 1/16" o.d. column, programmed at 4 °/min.

Fig. 67. Total alkanes of cutinite after pyrolysis at 275°

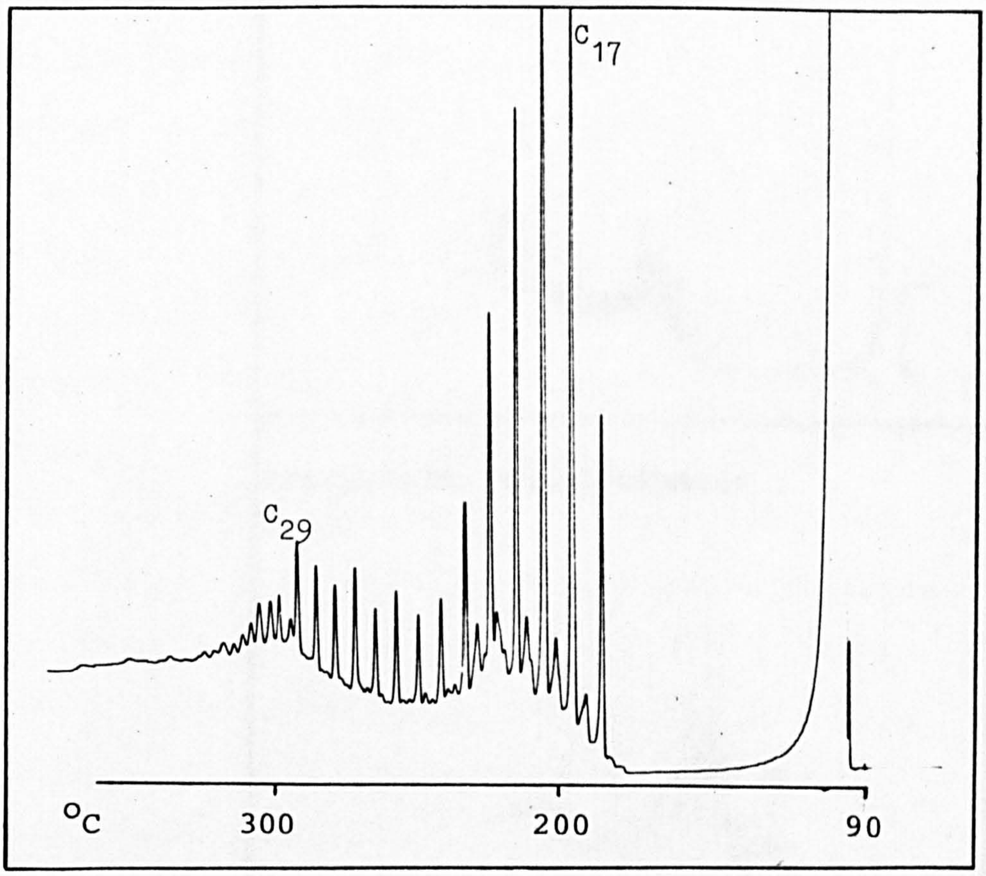

Gas chromatographic conditions as in Fig. 42, except programmed 90-300°C

Fig. 68. Total alkanes of Maghara and Bitterfeld resinites and alkenes of Bitterfeld resinite after pyrolysis at 275°

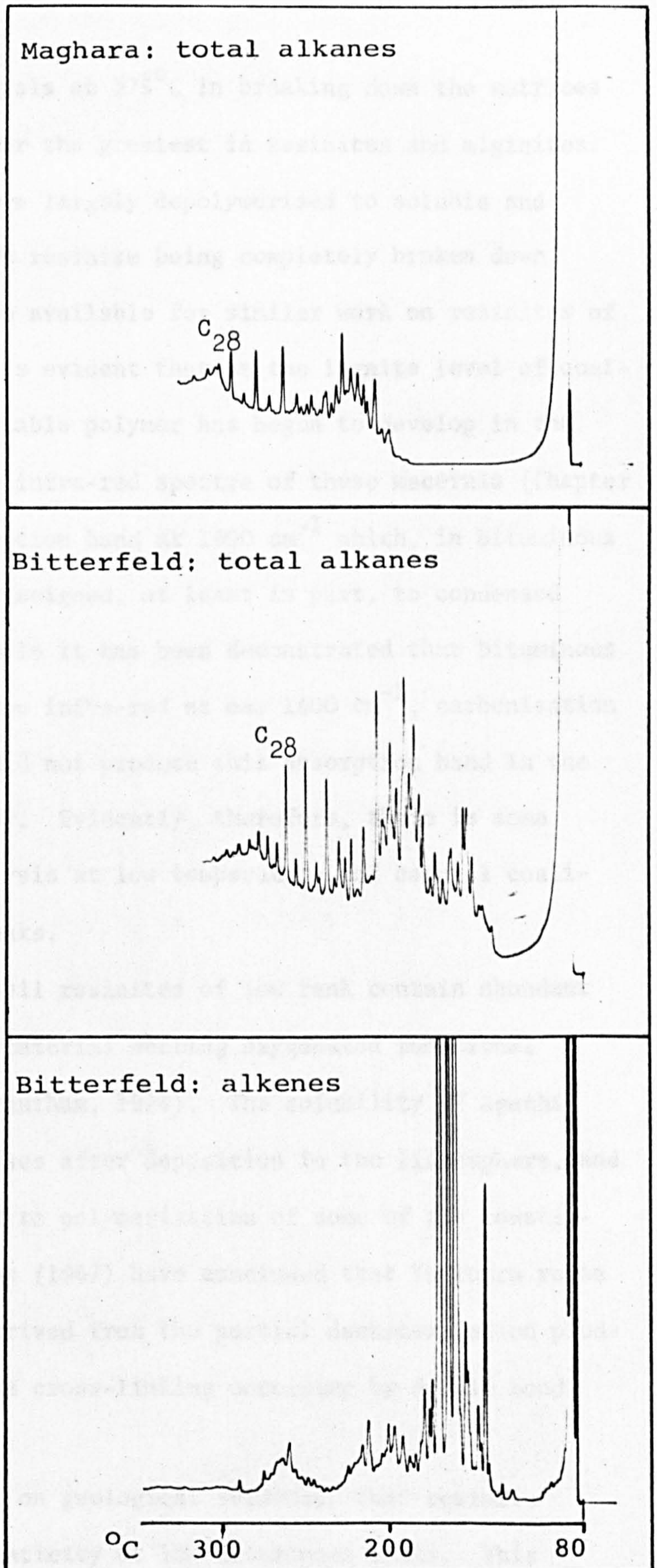

Gas chromatographic conditions as in Fig. 42.

Discussion

Pyrolysis at 375°C

The effect of pyrolysis at 375°C in breaking down the matrices of the macerals was by far the greatest in resinites and alginites. The resinite kerogens were largely depolymerised to soluble and gaseous products, Maghara resinite being completely broken down. Unfortunately no data are available for similar work on resinites of bituminous rank, but it is evident that at the lignite level of coalification no thermally stable polymer has begun to develop in the resinite structure. The infra-red spectra of these macerals (Chapter 1) did not show an absorption band at 1600 cm^{-1} which, in bituminous rank macerals, has been assigned, at least in part, to condensed aromatic structures. While it has been demonstrated that bituminous resinites do absorb in the infra-red at *ca.* 1600 cm^{-1}, carbonisation of lignitous resinites did not produce this absorption band in the residue (Murchison, 1966). Evidently, therefore, there is some difference between pyrolysis at low temperature and natural coalification at these low ranks.

Fresh resin and fossil resinites of low rank contain abundant quantities of alicyclic material bearing oxygenated functional groups (Thomas, 1969; Grantham, 1974). The solubility of *Agathis* resins in acetone decreases after deposition in the lithosphere, and this has been attributed to polymerisation of some of the constituents. Brooks and Steven (1967) have concluded that Yallourn resin consists of oligomers derived from the partial decarboxylation products of agathic acid, the cross-linking occurring by double bond condensation.

It has been stated, on geological evidence, that resinite develops a degree of plasticity at low bituminous ranks. This occurs over a very narrow rank range and resinite does not show any increase in reflectivity through this stage (Murchison and Jones, 1963). This plasticity, and subsequent flow, may be due to elimination of functional groups, the evolved products providing some lubrication leading to flow under pressure of overburden. Subsequent to the plastic stage, reflectivities of resinites increase, due to progressive condensation of the structures. Organic geochemical analyses of resinites at this critical stage would be advantageous here.

The three alginites were also of low rank, and they also underwent extensive decomposition at 375^{o}C. There was, however, a relatively wide variation between the samples. South African alginite was almost completely degraded to soluble and gaseous products, whereas 30% of the Scottish sample remained insoluble. These samples were not demineralised prior to pyrolysis and the variations can be partly attributed to ash contents. Scottish alginite, for example, contained *ca.* 18% ash. As in resinites, the infra-red spectra of the alginites provided very little evidence of aromatic material.

The mechanism and products of the pyrolysis of alginite have been investigated by Cane (1951, 1963). Broad, overlapping stages of thermal decomposition have been recognized which occur over a range of temperatures. Thermal cracking was considered to be the major controlling process of the degradation, although the possibility of limited depolymerisation occurring at lower temperatures was not ruled out.

Cane and Albion (1973), investigating the structure of alginite, postulated that the coorongite precursor is formed by oxidative polymerisation of straight-chain alkadienes. The evidence from this investigation is that aromatisation and condensation of the polymer is not significant at the rank of these samples. However, their rank has only been determined by comparing their elemental analyses with those of sporinites (Table 2, Chapter 1). Comparison of the respective carbon contents suggests that they may be of high-volatile bituminous rank, although this can only be stated in the broadest sense as quite different materials are being compared. If they are of high-volatile bituminous rank, then the validity of the identification of associated vitrinite stringers must be questioned. Reflectivity determinations on these materials (Table 3, Chapter 1), gave values of mean reflectances of 0.18% and 0.27% for the New South Wales and Scottish samples respectively. These values are much too low for high-volatile bituminous vitrinites, and the value of 0.18% is rather low for vitrinite at all. It seems probable therefore that, despite the physical similarities of this material to vitrinite, it may have a quite different, and unrelated, origin.

The decomposition of sporinite and vitrinite kerogens at 375°C varied with the rank of the samples. Each sporinite produced a greater yield of extract and volatiles than its corresponding vitrinite. In comparison with resinites and alginites, sporinites were much more resistant to pyrolysis. This was undoubtedly a function of rank as the lowest-rank sporinite used in this study was of high-volatile bituminous rank, but a further contributing factor may be the nature of the molecular matrices of the respective exinite macerals. It has been noted in Northumberland coals that resinite is apparently absent, (i.e. it is not distinguishable), in coals of ranks higher than *ca.* 86% C, whereas sporinite remains visible as such up to *ca.* 89% C, after which it too rapidly becomes indistinguishable from vitrinite. If such physical changes are related to increasing aromaticity, then clearly resinite is the more susceptible of the two to aromatisation. This may be related to the inherent cyclic nature of resinites, based on diterpenoid structures, whereas sporinite has been proposed as an oxidative polymer of carotenoids and carotenoid esters (Brooks and Shaw, 1968a). Taking exinites as a group, it is apparent that the development of a stable polymeric structure is minimal until bituminous rank is achieved, but thereafter the rate of stabilisation through aromatisation and condensation may be variable between individual members of the group.

Extracts obtained from the pyrolysed sporinites showed a marked quantitative decrease with increasing rank, while those from vitrinites showed a slight increasing trend (Fig. 69). On the other hand, the amount of volatile constituents liberated decreased in both macerals with increasing rank, the average rate of decrease being greater in vitrinite (Fig. 70). When total weight losses are compared with rank it can be seen that there is a remarkable parallelism in their respective stabilities, but with no apparent convergence up to 86.6% C (d.a.f.) (Fig. 71).

The percentage compositions of the extracts are shown in Fig. 72, where the percentage of asphalts has been calculated by the difference between the total extracts and the sum of the aliphatic and aromatic hydrocarbons. As such, these will not represent the amounts determined by column chromatography where total recoveries as low as 72% were recorded. The percentage of aliphatic hydrocarbons was similar in each extract. Between 82% and 84% C (d.a.f.) there was a relative increase in the amount of aliphatic material liberated from sporinites, which then decreased again at higher ranks. The relative amounts of aliphatic hydrocarbons in vitrinite extracts remained virtually constant. The main differences in the two extracts were the relative amounts of aromatic hydrocarbons and polar compounds (asphalts), the former always being greater for sporinites and the latter greater for vitrinites. This may be a reflection in part of the variation of heteroatoms, and in part of variable aromatic structures in the non-condencsed part of the structures.

FIG. 69. VARIATION OF TOTAL EXTRACT YIELDS WITH RANK AFTER PYROLYSIS AT 375°C

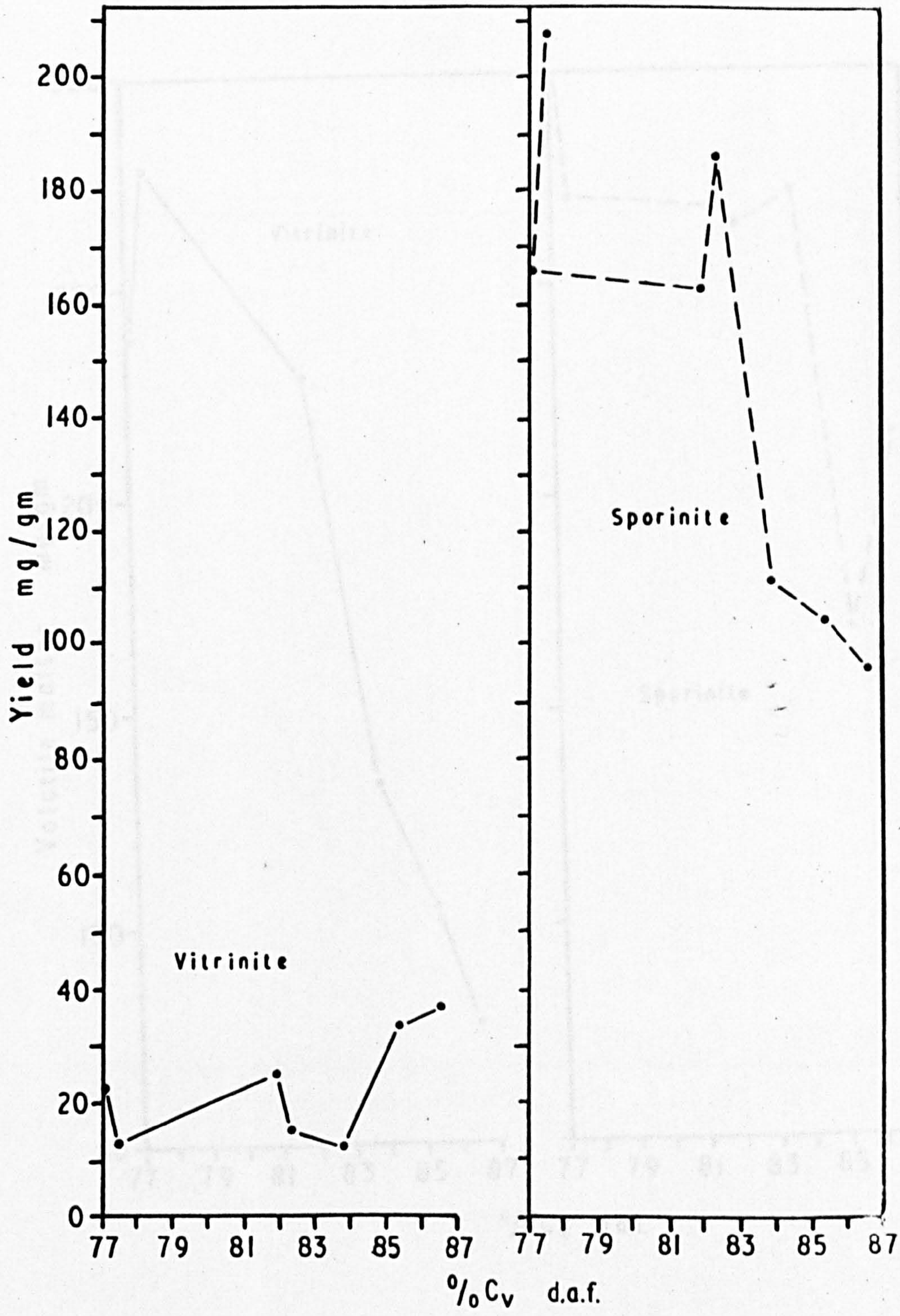

FIG. 70. VARIATION OF YIELDS OF VOLATILE MATTER FROM PYROLYSIS AT 375°C

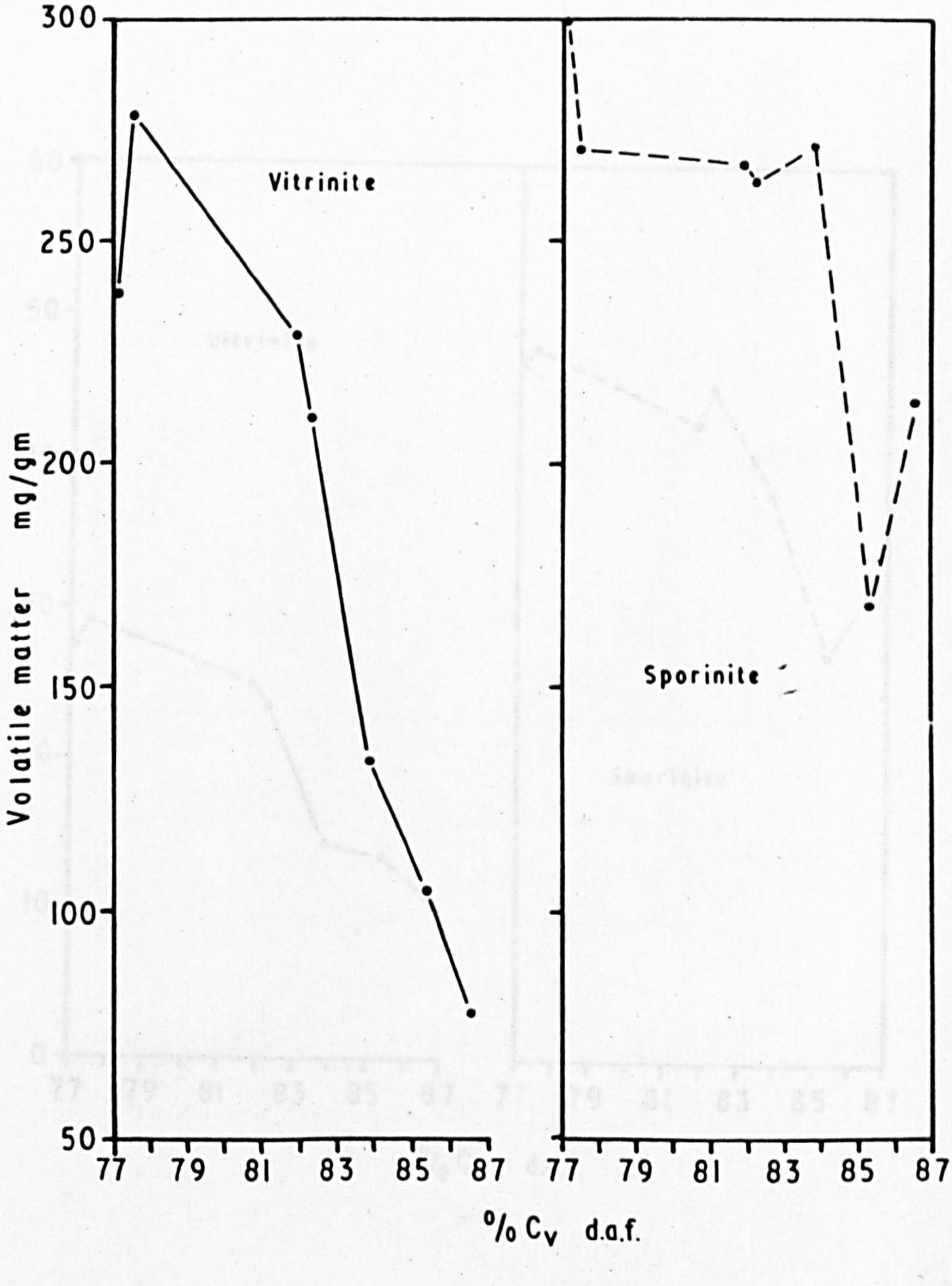

FIG. 71. WEIGHT LOSSES OF VITRINITE AND SPORINITE AFTER PYROLYSIS AT 375°C

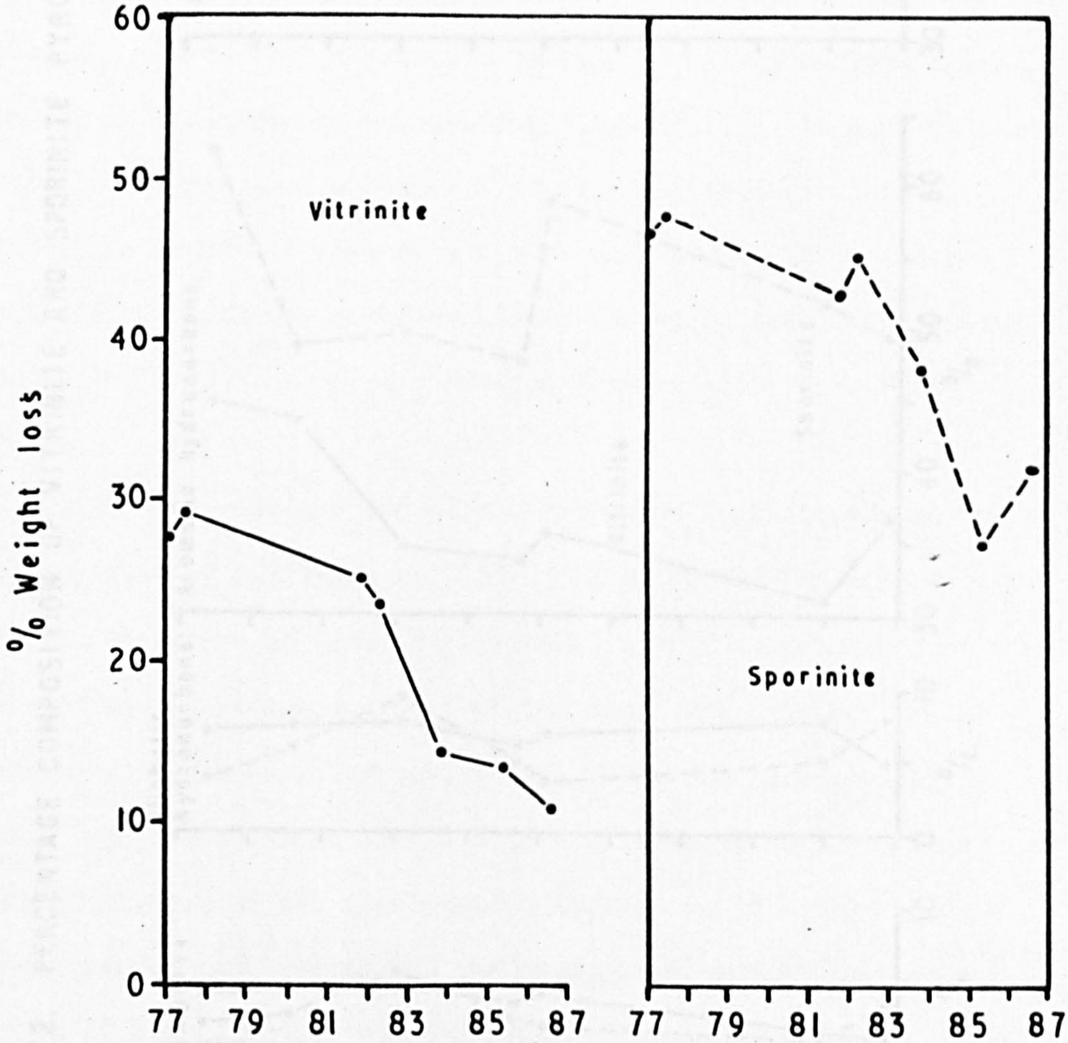

FIG. 72. PERCENTAGE COMPOSITION OF VITRINITE AND SPORINITE PYROLYSATES – 375°C

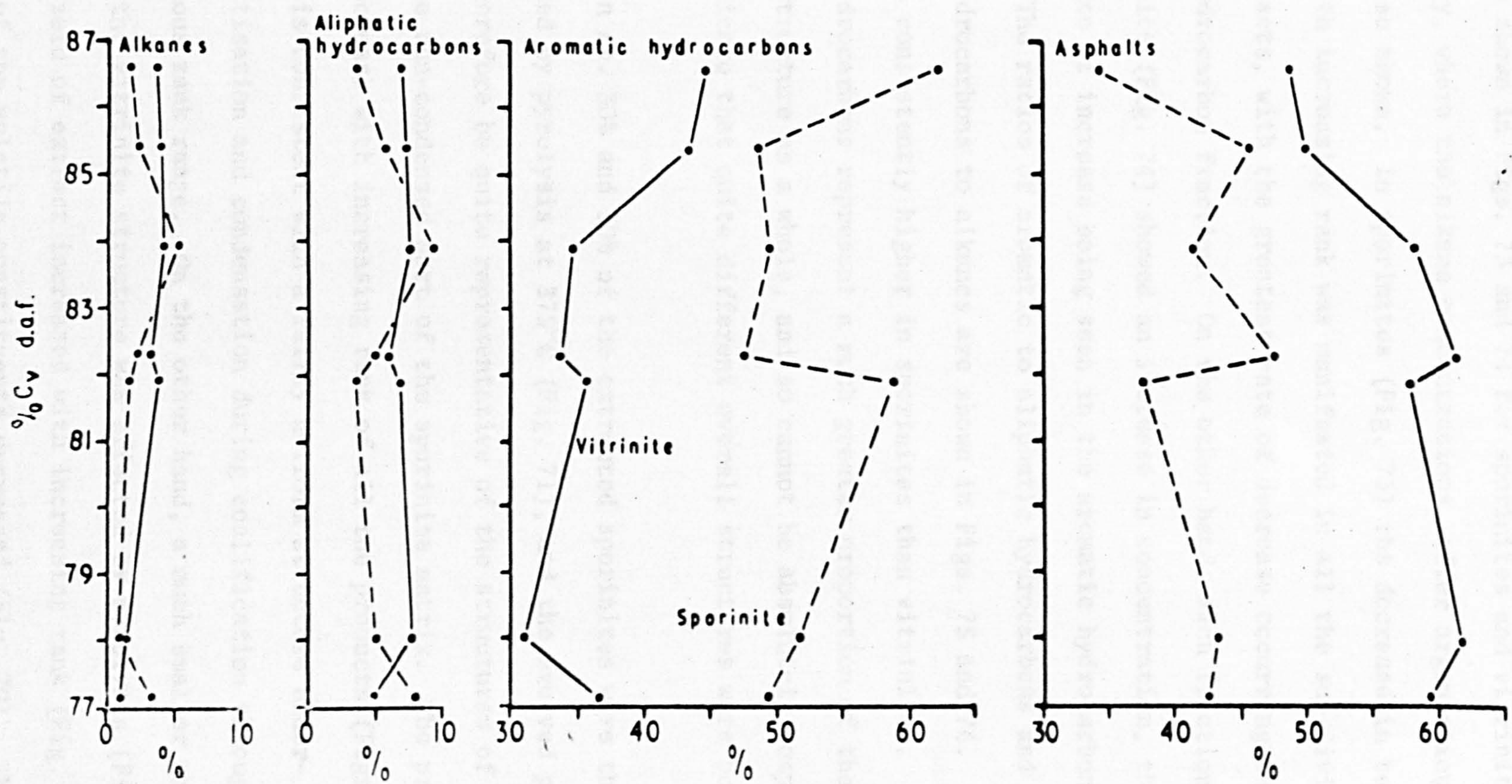

The concentrations of the extract fractions in terms of column eluates are shown in Figs. 73 and 74 for sporinites and vitrinites respectively, where the alkane concentrations, after argentatious tlc, are also shown. In sporinites (Fig. 73) the decrease in total extracts with increasing rank was manifested in all the sub-divisions of the extracts, with the greatest rate of decrease occurring in the aromatic hydrocarbon fraction. On the other hand, each fraction from vitrinite (Fig. 74) showed an increase in concentration, the greatest rate of increase being seen in the aromatic hydrocarbon fraction. The ratios of aromatic to aliphatic hydrocarbons and aromatic hydrocarbons to alkanes are shown in Figs. 75 and 76. Both ratios were consistently higher in sporinites than vitrinites. Although hydrocarbons represent a much greater proportion of the sporinite structure as a whole, and so cannot be absolutely compared, results indicate that quite different overall structures were being degraded.

Between *ca*. 30% and 50% of the extracted sporinites were thermally degraded by pyrolysis at 375°C (Fig. 71), and the evolved products may therefore be quite representative of the structures of the whole of the non-condensed part of the sporinite matrix. The progressive decrease with increasing rank of all the products (Figs. 69 and 70) is consistent with a fairly uniform structure undergoing aromatisation and condensation during coalification through the bituminous rank range. On the other hand, a much smaller proportion of the vitrinite structure was affected by pyrolysis (Fig. 71). The yield of extract increased with increasing rank (Fig. 69) while that of the volatile constituents decreased (Fig. 70). This implies that the production of tar and gas, (i.e. solvent extract and volatile constituents respectively in this context), may be independent of each other, a finding in accord with that of Mazumdar

FIG. 73. VARIATION OF CONCENTRATIONS OF HYDROCARBONS AND NON-HYDROCARBONS FROM PYROLYSIS OF SPORINITES AT 375°C

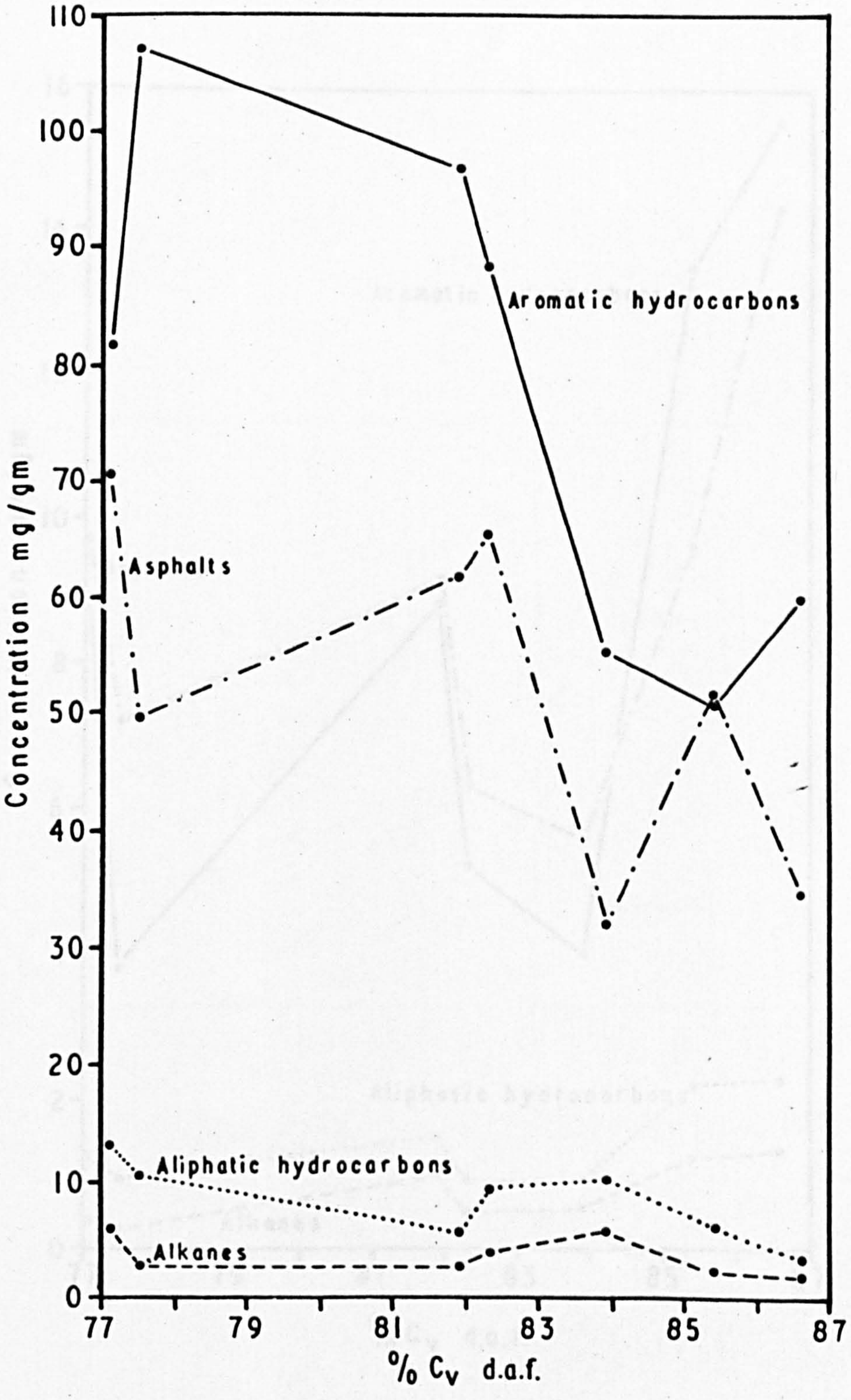

FIG. 74. VARIATION OF CONCENTRATIONS OF HYDROCARBONS AND NON-HYDROCARBONS FROM PYROLYSIS OF VITRINITES AT 375°C

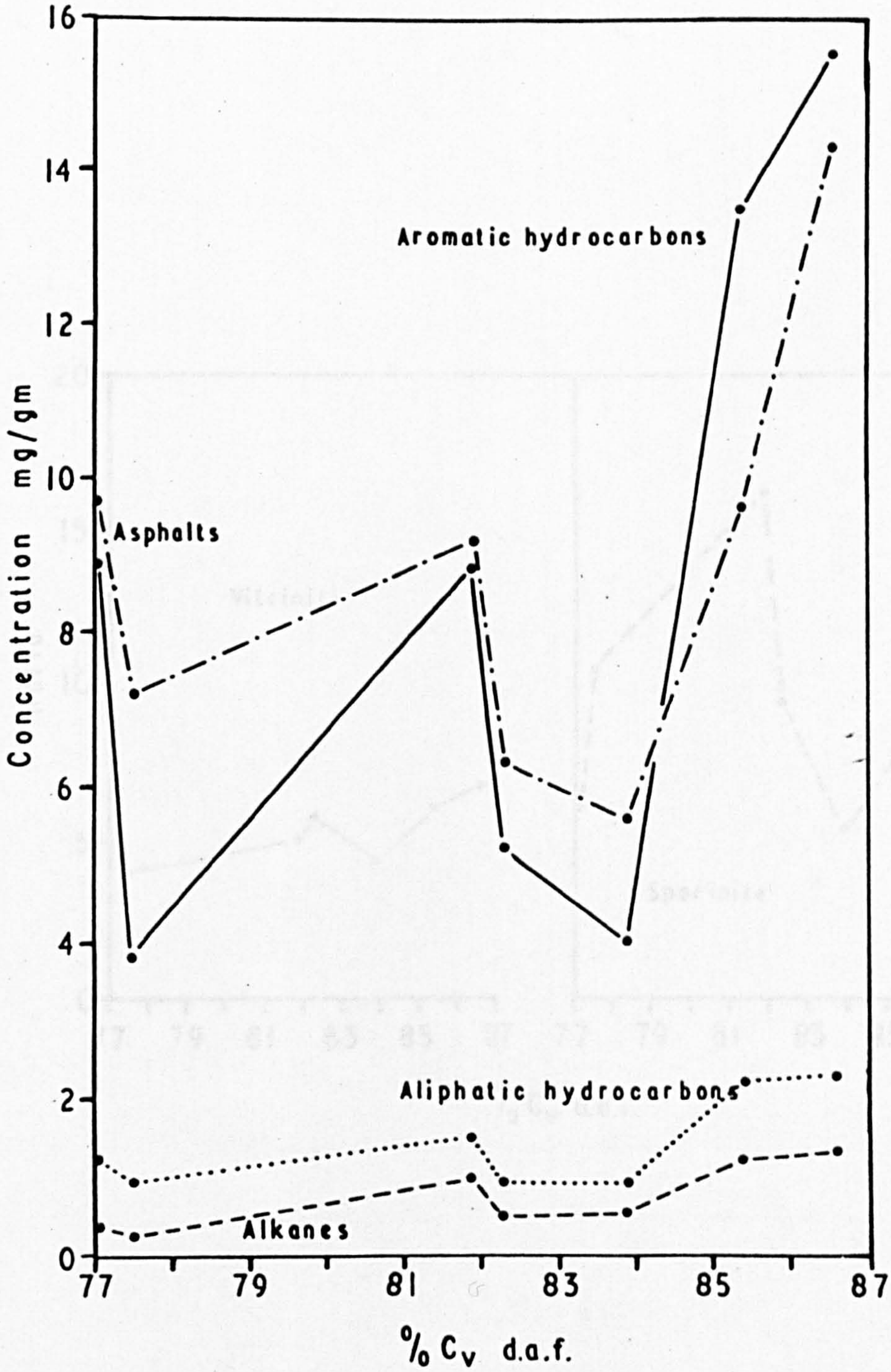

FIG. 75. AROMATIC:ALIPHATIC RATIOS OF PYROLYSIS PRODUCTS - 375°C

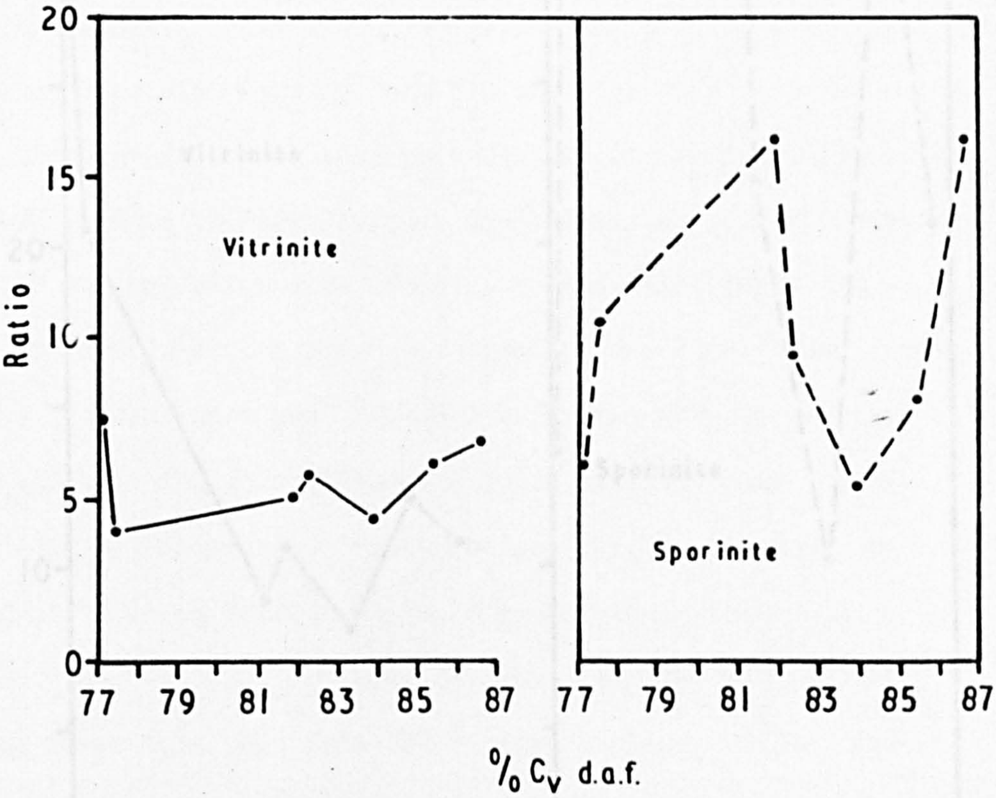

FIG. 76. RATIOS OF AROMATIC TO ALIPHATIC SATURATED HYDROCARBONS IN 375° PYROLYSATES

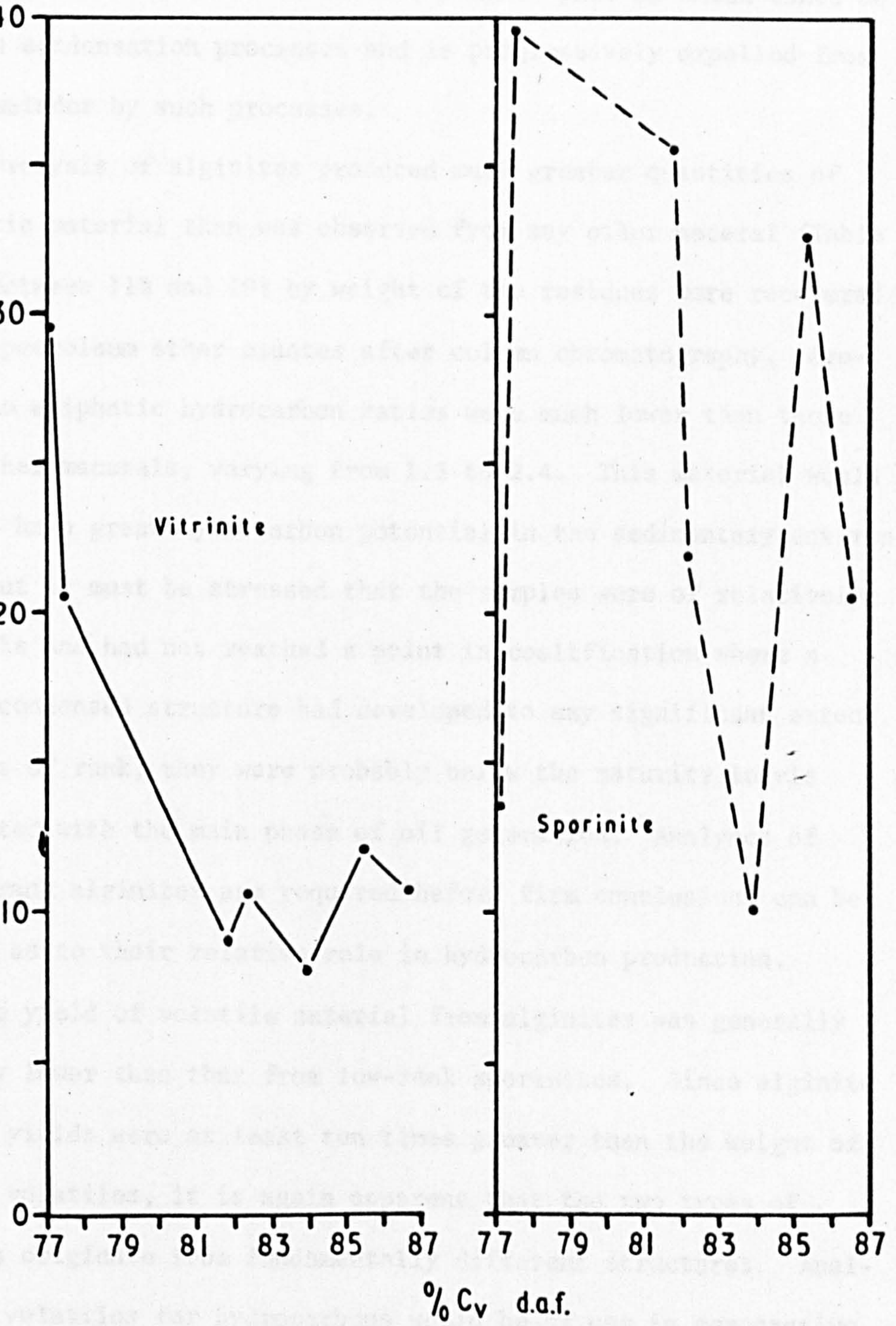

and Chatterjee (1973), and that the volatile hydrocarbon components were derived from low molecular weight edge-groups in the matrix. Analysis of volatiles will clearly be of some importance. The increasing yield of extracts is perhaps surprising, but may be indicative of a heterogeneous structure, a minor part of which takes no part in condensation processes and is progressively expelled from the remainder by such processes.

Pyrolysis of alginites produced much greater quantities of aliphatic material than was observed from any other maceral (Table 33). Between 11% and 19% by weight of the residues were recovered in the petroleum ether eluates after column chromatography. Aromatic to aliphatic hydrocarbon ratios were much lower than those from other macerals, varying from 1.3 to 2.4. This material would seem to have great hydrocarbon potential in the sedimentary environment, but it must be stressed that the samples were of relatively low ranks and had not reached a point in coalification where a stable condensed structure had developed to any significant extent. In terms of rank, they were probably below the maturity levels associated with the main phase of oil generation. Analyses of higher rank alginites are required before firm conclusions can be reached as to their relative role in hydrocarbon production.

The yield of volatile material from alginites was generally slightly lower than that from low-rank sporinites. Since alginite extract yields were at least ten times greater than the weight of evolved volatiles, it is again apparent that the two types of products originate from fundamentally different structures. Analyses of volatiles for hydrocarbons would be of use in comparative estimations of short-chain alkyl substituents and bridging structures in the macerals.

Resinites gave high hydrocarbon yields, and also very high yields of volatile constituents. It is probable that carbon dioxide and water accounted for a part of the latter, considering the low rank of the samples and the known structures occurring in resins (Carman and Cowley, 1967; Brooks and Steven, 1967; Thomas, 1969).

Figs. 73 and 74 show that the yields of total aliphatic hydrocarbons closely parallel the yields of alkanes from sporinites and vitrinites throughout the rank range investigated, indicating, possibly, a genetic relationship between the liberated alkanes and alkenes. Gas chromatographic analyses of the alkene fractions showed them to be highly complex, but in general their distributions were similar to the corresponding alkanes. Infra-red analyses of the alkene fractions showed that absorption bands due to vinyl (992 and 908 cm^{-1}) and trans-alkenes (966 cm^{-1}) were present. The generation of alkenes by pyrolysis of Green River shale and Scottish alginite has been reported (Douglas *et al.*, 1970b). Pyrolysis of brown coal esters yielded n-alkenes, derived from alkanoic moieties of wax esters (Brooks and Smith, 1969). Olefins have also been reported from whole coal pyrolysates (Boyer *et al.*, 1961; Girling, 1963; Kroger *et al.*, 1964; Spence and Vahrman, 1967), in laboratory pyrolysis studies of pure compounds, n-octacosane produced n-alkanes and n-alkenes of lower carbon number (Henderson, 1968), while similar investigations of aliphatic esters produced alkenes among the degradation products (Esnault, 1973).

Brooks and Smith (1969) demonstrated that while n-alkenes could be produced by heating straight-chain esters in the presence of water, the addition of the acetone-soluble branched/cyclic ester fraction of a brown coal promoted the reduction of alkenes to alkanes. It is to be expected, therefore, that in the lithosphere alkenes formed by homolytic scission of aliphatic chains in kerogens would be rapidly converted to alkanes by addition of protons liberated through aromatisation and condensation of other structures. In coal extracts, alkenes form only a very minor proportion of the total aliphatic constituents, and have only been detected in extracts of relatively low-rank coals.

The yields of total alkanes from sporinites decreased slightly from low to high rank, although there was a minor maximum between 82% and 84% C (d.a.f.) (Fig. 73). The overall change was small, and these alkyl substituents represent less than 1% of the whole structure which was degradable at 375^{o}C. An opposite trend was observed in vitrinites where the highest yield was found at the highest rank (Fig. 74).

The qualitative aspect of the liberated alkanes showed a number of variations between the two macerals. The distribution of sporinite branched/cyclic alkanes was virtually independent of rank, each fraction appearing very similar and showing a distributional maximum in the C_{16} to C_{18} range (Fig. 52). Coinjection of these fractions with authentic acyclic isoprenoid alkanes on a high-resolution capillary column showed that pristane and phytane were probably present, but only as minor peaks on the chromatographic trace. The complexity of the fractions can be seen in the high-resolution capillary gc (Fig. 77), which indicates that homologous compounds are present throughout the carbon number range, which has been illustrated by coinjection of n-alkanes. The similarity of the gc fingerprints of these fractions throughout the rank range may indicate that that part of the kerogen from which they were derived undergoes little structural change in this rank range, other than possible conversion to non-aliphatic constituents.

Vitrinite branched/cyclic alkanes showed a number of features indicating progressive maturation within the matrix (Figs. 45 and 45a). With increasing rank, there was a progressive decrease of

Fig. 77. Capillary gas chromatograms of branched/cyclic alkanes of Barnsley sporinite after pyrolysis at 375^{O}, and the same sample co-injected with n-alkanes

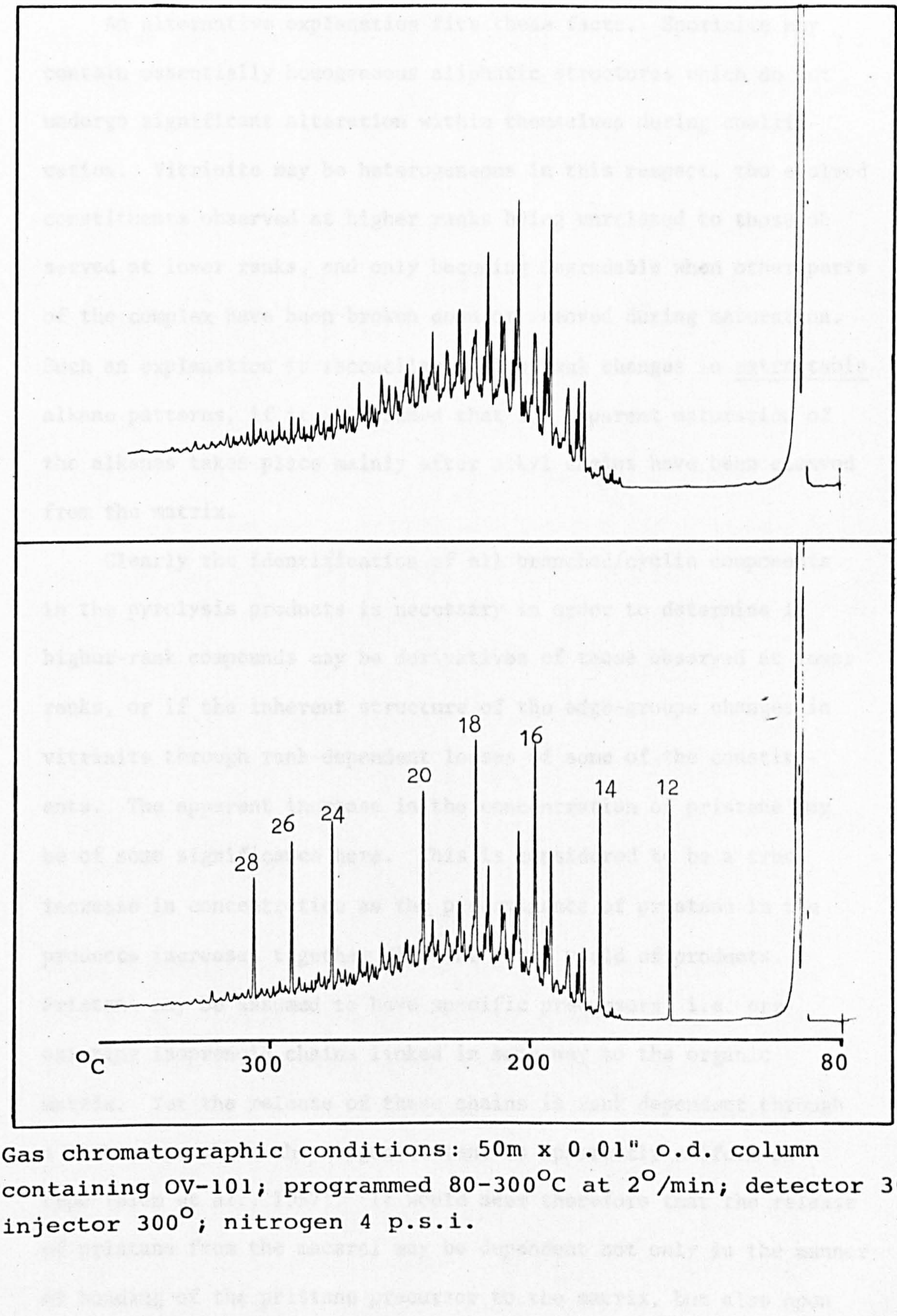

Gas chromatographic conditions: 50m x 0.01" o.d. column containing OV-101; programmed 80-300^{O}C at 2^{O}/min; detector 300^{O}; injector 300^{O}; nitrogen 4 p.s.i.

high molecular weight (i.e. higher than C_{26}) components, a relative increase of acyclic isoprenoid alkanes, especially pristane, and a trend towards lower average molecular weights.

An alternative explanation fits these facts. Sporinite may contain essentially homogeneous aliphatic structures which do not undergo significant alteration within themselves during coalification. Vitrinite may be heterogeneous in this respect, the evolved constituents observed at higher ranks being unrelated to those observed at lower ranks, and only becoming degradable when other parts of the complex have been broken down or removed during maturation. Such an explanation is reconcilable with rank changes in extractable alkane patterns, if it is assumed that the apparent maturation of the alkanes takes place mainly after alkyl chains have been cleaved from the matrix.

Clearly the identification of all branched/cyclic components in the pyrolysis products is necessary in order to determine if higher-rank compounds may be derivatives of those observed at lower ranks, or if the inherent structure of the edge-groups changes in vitrinite through rank-dependent losses of some of the constituents. The apparent increase in the concentration of pristane may be of some significance here. This is considered to be a true increase in concentration as the predominance of pristane in the products increases together with the total yield of products. Pristane may be assumed to have specific precursors, i.e. pre-existing isoprenoid chains linked in some way to the organic matrix. Yet the release of these chains is rank dependent through a rank range where the oxygen content is apparently uniform in type (Blom *et al.*, 1957). It would seem therefore that the release of pristane from the maceral may be dependent not only in the manner of bonding of the pristane precursor to the matrix, but also upon the nature of the structures within its immediate environment.

One of the problems of pyrolysis work is that of cracking of compounds after they have been fragmented from the parent structure, thus producing amounts, and distributions, of reaction products that are not directly related to the part they play in the original structures. Methods have been devised for the rapid removal of products from the pyrolysis site, (e.g. Girling, 1963), but such open systems cannot be representative of conditions in deeply-buried sedimentary sequences. On the other hand, closed pyrolytic systems will be favourable for secondary reactions, thus giving yields below theoretical maxima for any given temperature.

The thermal stability of n-alkanes has been investigated (Henderson, 1968). After heating pure n-octacosane at 375°C for 75 hrs, a 61% recovery of the starting material was obtained. After 150 hrs, almost all of the compound was degraded. Extrapolation of the full data indicated that after a 24 hr period of heating only minor degradation would occur. Addition of clay catalysts greatly accelerated thermal breakdown, but the catalytic effect of a low-ash coal residue is not known. Such effects could be investigated by addition of standard compounds to residues prior to pyrolysis. Esnault (1973) has shown that pure n-eicosane (n-C_{20}) is thermally stable for up to six months at 300°C, after which a 93% recovery of the compound was obtained. It would appear that the n-alkane patterns generated by pyrolyses of coal at 375°C may be reasonably representative of the initial structures.

The gc patterns of n-alkane fractions isolated from all sporinite and vitrinite pyrolysates showed a predominance of even-numbered homologues in the range above n-C_{23}; n-C_{24}, n-C_{26} and n-C_{28} were invariably the predominating components. CPI values (Tables 25 and 30) were always less than unity, and fell as low as

0.64 in vitrinites and 0.69 in sporinites. Variations did not appear to be rank-related, and they may reflect compositional or early environmental differences between the samples.

All macerals were fully extracted prior to pyrolysis, and the n-alkanes in the pyrolysates showed fundamentally different distributions from those in the original extracts. They undoubtedly represent n-alkyl fragments in the maceral matrices. Pyrolysis of coals below *ca.* 400^{o}C has been said to induce changes comparable to those that would occur during normal coalification (Cavell and Berkowitz, 1960), thus generally being confined to the edge-groups in bituminous coals (Berkowitz, 1967). The observed n-alkane distributions may therefore be comparable to those which are forming *in situ*, but which are a) diluted by pre-formed alkanes and b) thermally degraded over the geological time scale, to give distributions in which the CPI values are near 1.0.

It is important to note that the predominance of even-numbered chains was still found in pyrolysates of macerals with ranks above *ca.* 84% C (d.a.f.). In examining the alkane patterns in the original extracts of the macerals, it was found that above this rank the average molecular weights of the n-alkane fractions began to shift to low carbon numbers, giving petroleum-like distributions. It was postulated in Chapter 2 that the long-chain components were still being liberated and that subsequent maturation was cracking them to more petroleum-like patterns. The pyrolysate n-alkane patterns lend support to this view, although it should be noted that the maxima were usually at n-C_{20}. The contribution of these relatively greater amounts of shorter-chain homologues may be partly a function of secondary degradation in the reaction vessel and partly a function of some maturation occurring in the kerogen. That the former process occurred can be clearly seen by comparing the n-alkane patterns produced by pyrolyses at 275°C and 375°C (Figs. 56 and 51), while the latter process is demonstrated by the rank-dependence of the amount of alkanes occurring below n-C_{23} (Fig. 78).

The n-alkanes occurring above n-C_{23} are thought to be derived from wax esters originally deposited in the coal (Brooks and Smith, 1969; Connan, 1970; Connan, 1973). Brooks and Smith demonstrated that pyrolysis of both fresh and extracted Yallourn pollen coal at 330°C in the presence of water (20:1 w/v) yielded an even-dominated n-alkane distribution. Connan (1973) showed that at 300°C a sample of the same coal yielded an odd-dominated pattern when water was not added to the reaction. He concluded that the absence of water was the significance difference. The data of Esnault (1973) illustrate this point. Thermal decomposition of n-hexadecyl stearate ($CH_3(CH_2)_{14}CH_2 \cdot O \cdot COCH_2(CH_2)_{15}CH_3$) produced n-alkanes dominated by n-C_{17}, whereas the prior addition of water produced n-alkanes dominated by n-C_{16}.

Returning to Connan's work, pyrolysis of Yallourn pollen coal for 3 days at 300°C produced a hundredfold increase in n-alkane yields. If these results, presented in the original paper only as a normalised diagram, are replotted after subtraction of the unheated n-alkane distribution, it can be seen clearly that the generated n-alkanes show a preferential relative increase of the even-numbered homologues between n-C_{21} and n-C_{27} (Fig. 79B). Similarly, the products of 1 and 6 day pyrolyses show the same trend (Figs. 79A and 79C). Above n-C_{27} the n-alkanes show a slight preferential increase of the odd-numbered members. This reversal was exactly what was found in the 275°C pyrolyses of low-rank sporinites and vitrinites in this investigation, as will be discussed later. In Connan's work the relative amounts of the n-alkanes above n-C_{23} decrease with increasing time of pyrolysis,

FIG. 78. PERCENTAGE OF TOTAL n-ALKANE FRACTIONS OF 375° PYROLYSATES OCCURRING ABOVE $\underline{n}$-C_{23}

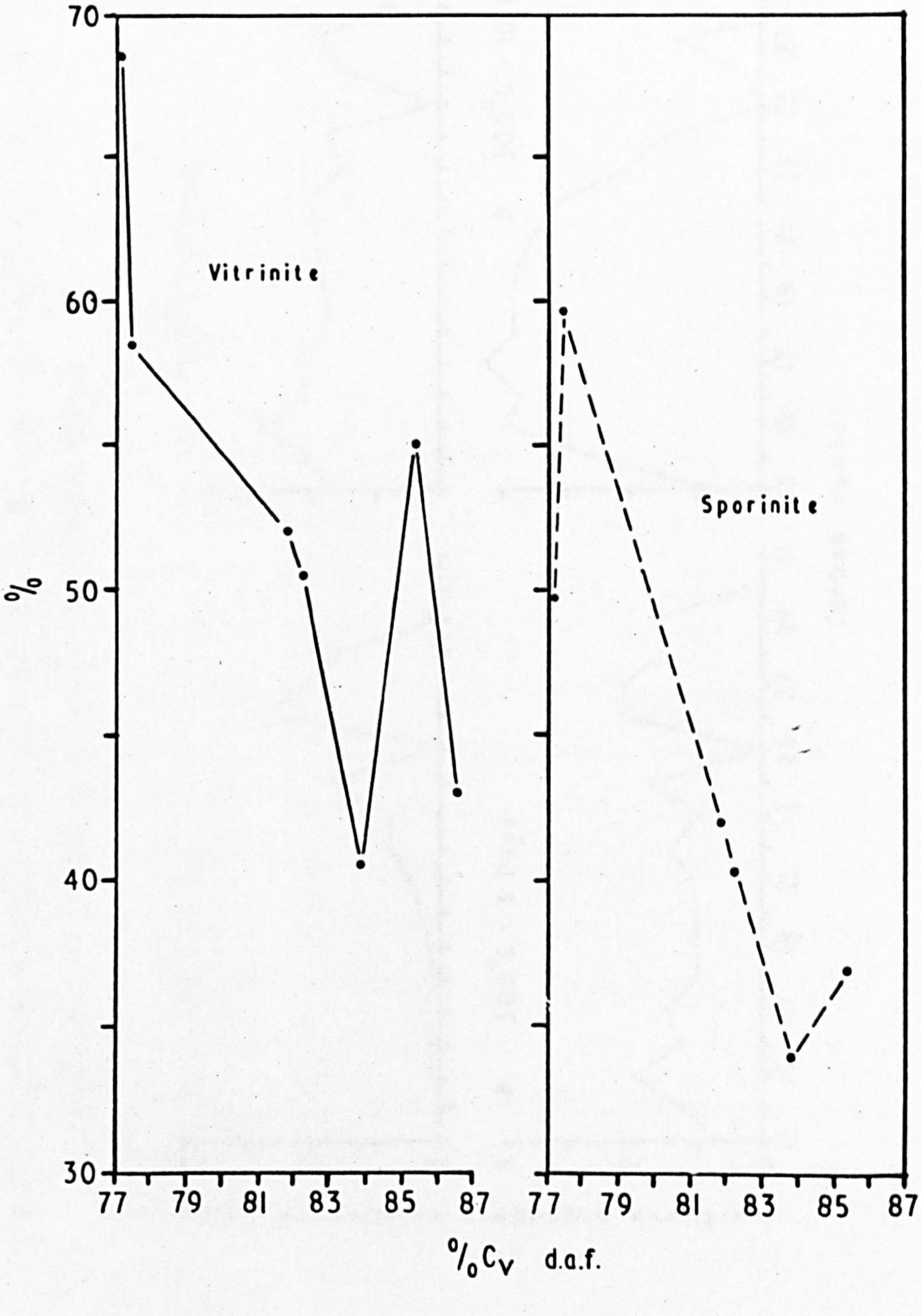

FIG. 79. RELATIVE CHANGES IN n-ALKANE DISTRIBUTIONS OF YALLOURN POLLEN COAL PRODUCED BY PYROLYSIS: DATA OF CONNAN (1973)

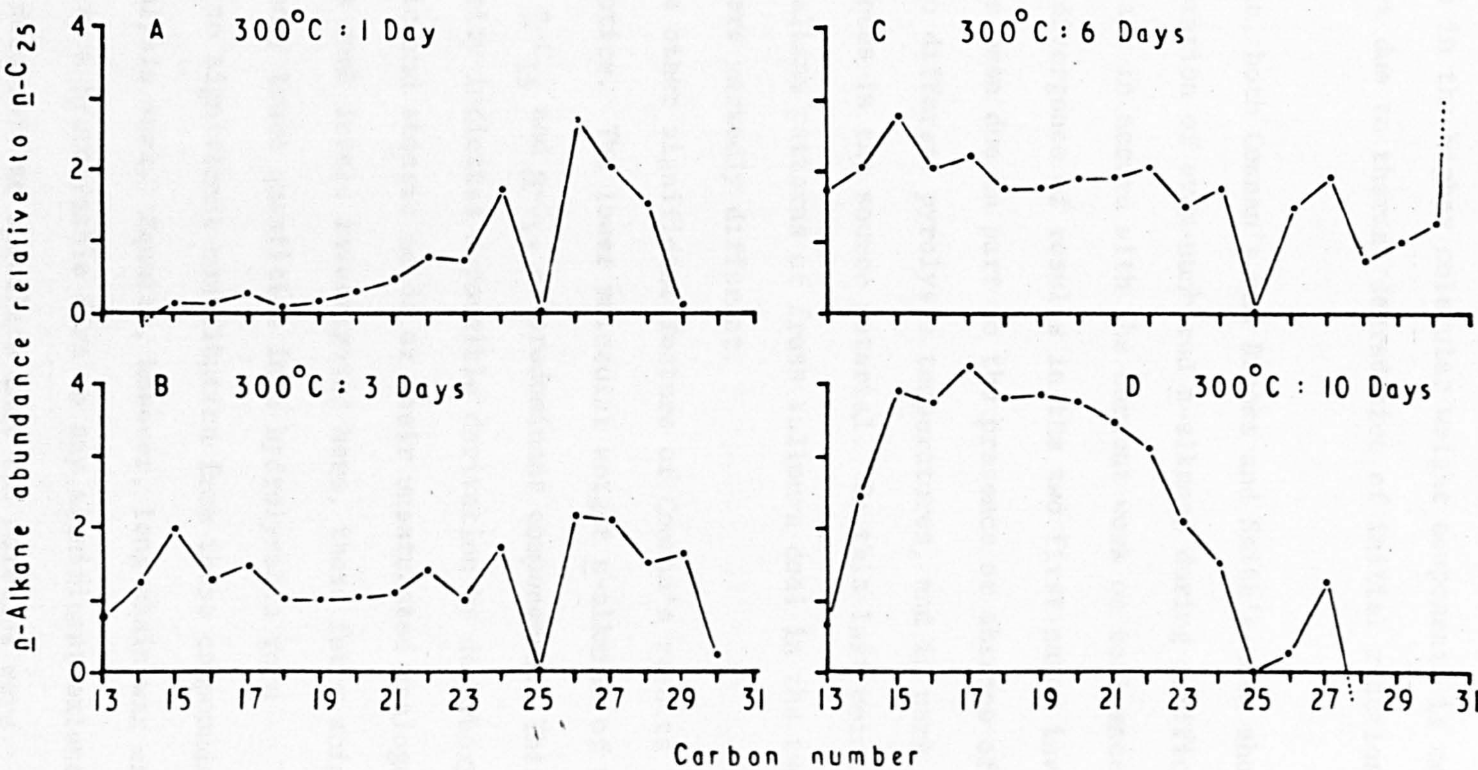

and after 10 days the major proportion of the homology lies below $\underline{n}$-C_{23} (Fig. 79D). However, unless absolute amounts of the higher homologues can be calculated, it is not possible to say whether or not the decrease in the higher molecular weight components is merely a dilution effect due to thermal degradation of initial reaction products.

To summarise, both Connan's and Brooks and Smith's work showed a preferred generation of even-numbered $\underline{n}$-alkanes during artificial diagenesis, and are in accord with the current work on coal-maceral pyrolyses. The divergence of results in the two first-named investigations may have been due in part to the presence or absence of water, in part to different pyrolysis temperatures, and in part to possible differences in the source material. On this last point, the published $\underline{n}$-alkane patterns of fresh Yallourn coal in the two investigations were markedly different.

There is one other significant feature of Connan's results which deserves notice. The lower molecular weight $\underline{n}$-alkanes of the pyrolysates show $\underline{n}$-C_{15} and $\underline{n}$-C_{17} as predominant components. This constant specificity indicates a possible derivation by decarboxylation of palmitic and stearic acids or their unsaturated analogues. At the bituminous rank levels investigated here, these fatty acids were present in only trace quantities in a hydrolysable form (Chapter 3), and no significant contribution from these compounds was noted in the pyrolysis work. Equally, however, long-chain wax esters were not present in a hydrolysable form to any significant extent either, so it is necessary to speculate that the moieties were separately combined to the matrix.

The proportion of total alkanes with chain lengths greater than $\underline{n}$-C_{23} decreased with increasing rank of the samples (Fig. 78), indicating that some depletion of precursor material takes place with increasing coalification. Closer analysis of the absolute concentrations of n-alkanes shows a striking difference between sporinites and vitrinites (Tables 38 and 39). The overall yield of n-alkanes from sporinites decreased with increasing rank, and the ratios of concentrations of the higher homologues (i.e. higher than n-C_{23}) between high- and low-rank samples were less than unity (Fig. 80). Once again, the preference for even-numbered chains is demonstrated. Thus the total amount of these n-alkyl fragments in the maceral kerogen must be decreasing with increasing rank, unless they become more stabilised against pyrolytic degradation as coalification advances.

Vitrinite n-alkanes above n-C_{23} showed a decreasing rate of generation up to a rank of 83.9% C (d.a.f.), then increased up to 85.4% C (d.a.f.) and finally decreased once more (Fig. 78). The accelerated rate of production of the n-alkanes at higher ranks was mirrored in an increased generation of total aliphatic hydrocarbons (Fig. 74). The greatest increase of n-alkanes occurred in the n-C_{28} to n-C_{33} range, showing little preference for odd- or even-dominated chain lengths (Fig. 81). The gas chromatogram of Parkgate vitrinite n-alkanes (Fig. 44a) illustrates the phenomenon.

The smooth envelope of these higher homologues possibly indicates another source of n-alkanes in vitrinite other than wax esters, but the expulsion of these compounds is critically rank-dependent and occurred over a very restricted range. A similar phenomenon has been noted by Cooper (personal communication) in a borehole depth profile, where extractable n-alkanes of vitrain-rich coals underwent an expansion in chain lengths over a narrow rank range. Leythaeuser and Welte (1969) also provided evidence of a reversal of the trend towards lower average molecular weights during coalification. Both these investigations noted that the change occurred at ranks of *ca.* 85-86% C, while it was found

Table 38: Concentrations of n-alkanes (mg/gm residue x 10^{-3}) isolated from the 375°C pyrolysates of sporinites

	High Hazles Gedling	Clowne	Deep Hard	High Hazles Whitwell	Barnsley	Parkgate
n-C_{16}	3.7	-	-	5.3	56.5	-
17	38.5	-	15.4	37.7	99.3	9.8
18	101.2	6.1	50.0	66.8	115.7	60.9
19	125.9	35.3	61.3	69.9	107.6	80.1
20	126.9	60.0	61.9	65.9	114.3	96.2
21	122.8	60.4	52.5	58.1	99.8	67.1
22	115.9	58.2	43.6	52.1	85.4	58.6
23	107.3	55.2	36.7	53.3	74.3	42.9
24	100.0	57.6	33.0	49.7	70.1	50.0
25	85.9	45.8	25.9	38.8	51.8	28.2
26	79.1	46.7	29.6	34.2	50.0	36.5
27	68.6	32.7	24.0	24.0	33.6	18.7
28	67.8	31.5	22.6	20.3	31.0	25.0
29	51.2	18.8	13.9	11.7	17.0	10.9
30	34.0	12.4	8.9	6.9	10.8	7.8
31	20.0	8.5	5.6	3.5	6.2	3.9
32	9.5	4.9	2.9	1.4	2.9	1.6
33	4.3	3.0	1.7	0.5	1.2	0.7
34	1.5	1.9	0.8	-	0.4	0.3
35	-	1.0	0.4	-	-	-
36	-	-	0.2	-	-	-

An n-alkane fraction was not isolated from the 375°C pyrolysate of Silkstone sporinite.

Table 39: Concentrations of n-alkanes (mg/gm residue x 10^{-3}) isolated from the 375°C pyrolysates of vitrinites

	High Hazles Gedling	Clowne	Deep Hard	High Hazles Whitwell	Barnsley	Parkgate	Silkstone
n-C_{16}	-	-	-	-	0.2	-	3.3
17	-	-	3.4	0.1	0.6	-	12.4
18	0.8	1.0	19.4	2.1	8.5	12.2	23.6
19	4.9	6.6	29.0	3.9	11.8	28.7	26.5
20	11.1	10.9	32.3	4.5	13.1	34.7	30.6
21	10.0	10.2	31.8	4.3	8.8	31.1	26.2
22	11.3	10.1	29.7	4.0	7.2	25.8	23.0
23	11.8	9.9	28.1	3.7	6.2	22.6	20.9
24	14.6	12.2	27.9	3.7	7.6	22.4	22.4
25	10.6	8.6	23.5	3.0	4.3	15.8	15.8
26	13.3	9.1	22.9	2.8	5.9	17.0	16.4
27	8.9	5.6	17.3	2.1	2.7	13.8	10.5
28	9.9	5.1	15.5	1.7	3.9	17.0	9.9
29	5.8	2.2	9.6	1.0	1.3	17.2	5.6
30	3.8	1.4	6.0	0.6	1.1	14.8	3.8
31	2.4	0.8	3.7	0.4	0.5	12.7	2.5
32	1.0	0.2	1.7	0.2	0.2	6.4	1.3
33	0.5	0.1	0.9	0.1	0.1	3.5	0.8
34	0.2	-	0.3	-	-	1.0	0.4
35	-	-	-	-	-	0.3	0.2

FIG. 80. RATIOS OF CONCENTRATIONS OF n-ALKANES IN 375° PYROLYSATES OF SPORINITES OF DIFFERENT RANKS

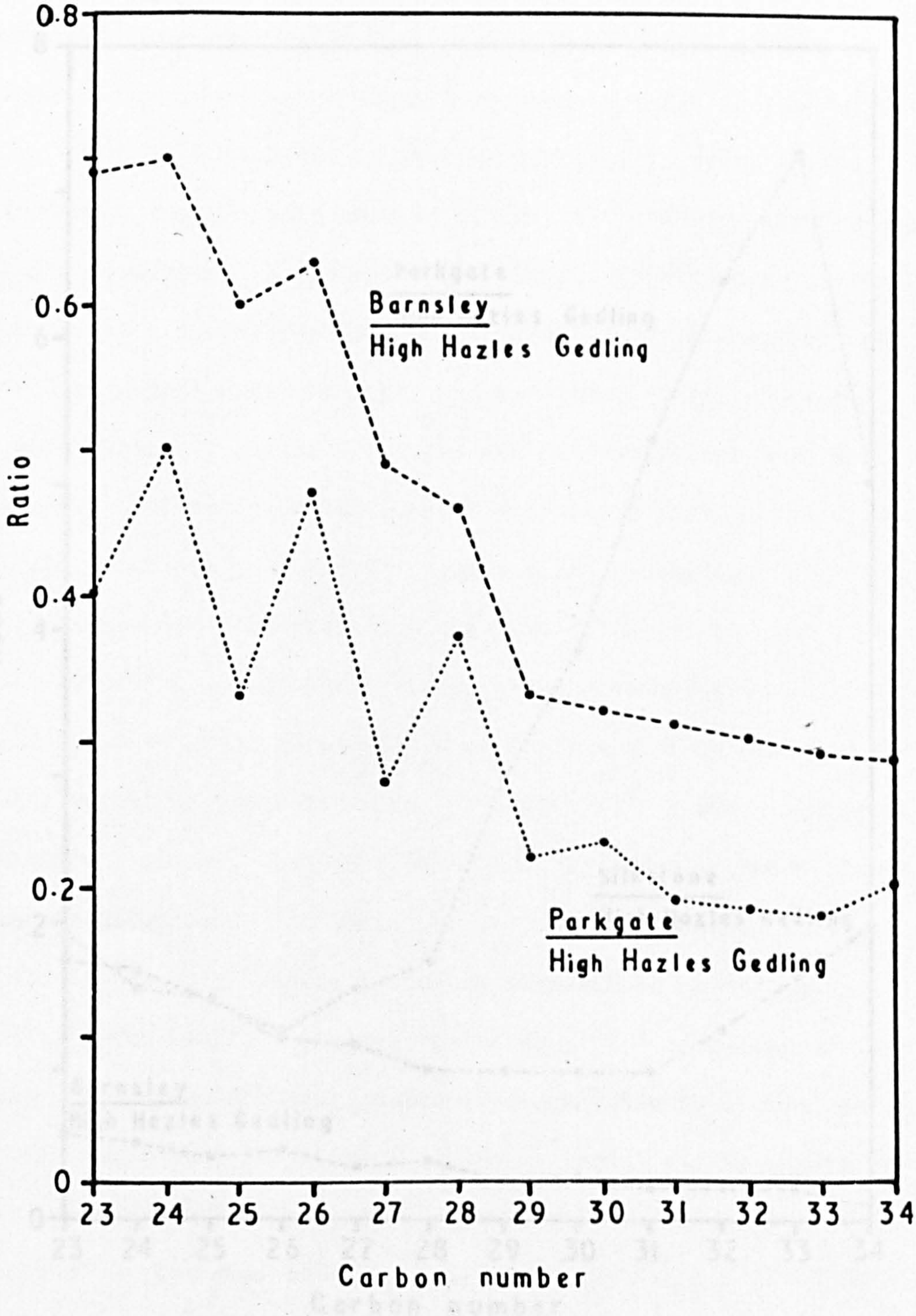

FIG. 81. RATIOS OF CONCENTRATIONS OF n-ALKANES IN 375° PYROLYSATES OF VITRINITES OF DIFFERENT RANKS

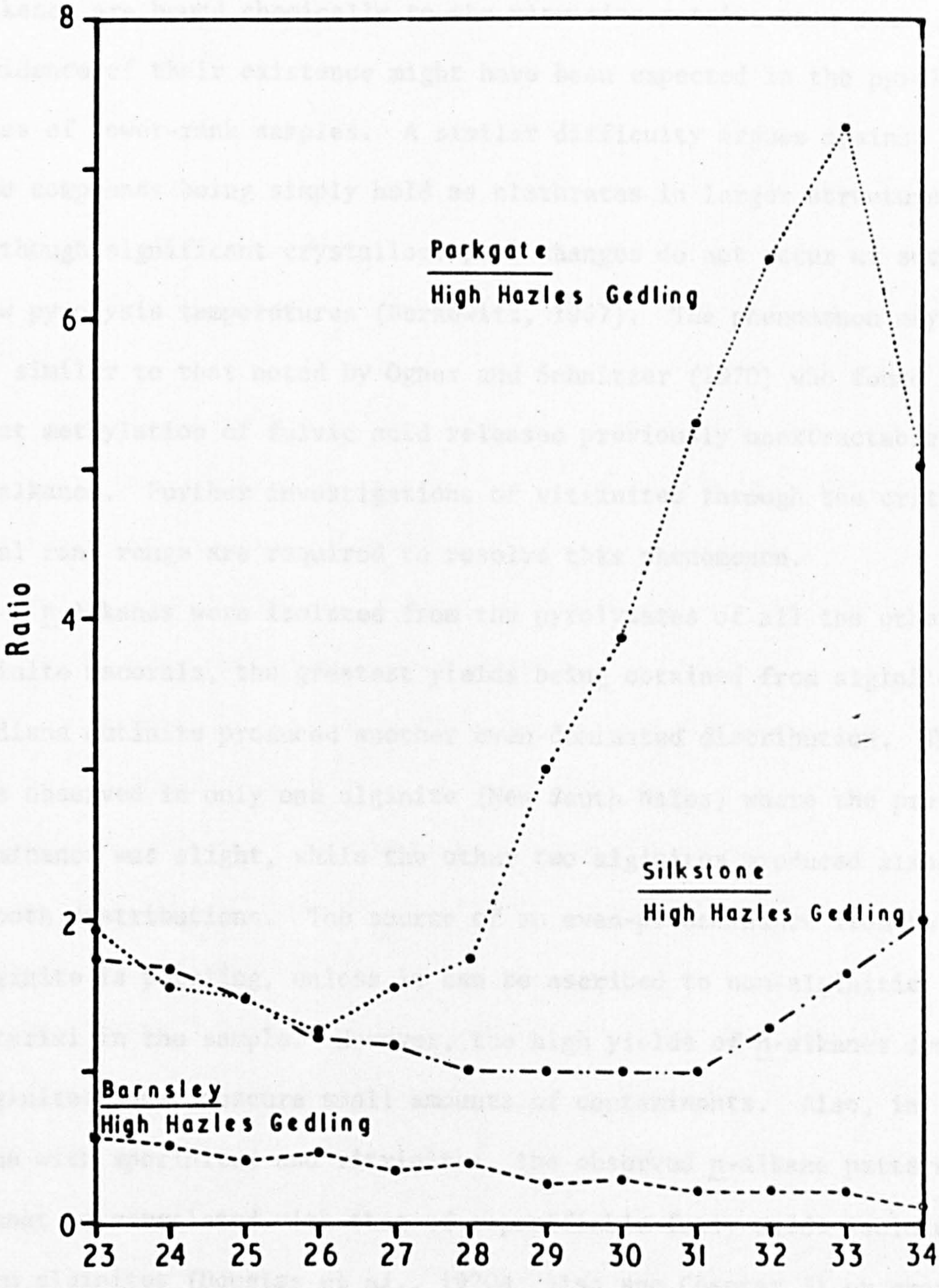

here in mild pyrolyses of vitrinites of similar rank.

It appears therefore that vitrinite structures undergo some sort of re-organization at this critical rank, which is close to one of the coalification jumps, expelling small quantities of material previously entrapped in the matrix. If these long-chain n-alkanes are bound chemically to the vitrinite matrix, then some evidence of their existence might have been expected in the pyrolyses of lower-rank samples. A similar difficulty argues against the compounds being simply held as clathrates in larger structures, although significant crystallographic changes do not occur at such low pyrolysis temperatures (Berkowitz, 1967). The phenomenon may be similar to that noted by Ogner and Schnitzer (1970) who found that methylation of fulvic acid released previously unextractable n-alkanes. Further investigations of vitrinites through the critical rank range are required to resolve this phenomenon.

n-Alkanes were isolated from the pyrolysates of all the other exinite macerals, the greatest yields being obtained from alginites. Indiana cutinite produced another even-dominated distribution. This was observed in only one alginite (New South Wales) where the predominance was slight, while the other two alginites produced almost smooth distributions. The source of an even-predominance from an alginite is puzzling, unless it can be ascribed to non-alginitic material in the sample. However, the high yields of n-alkanes from alginites would obscure small amounts of contaminants. Also, in line with sporinites and vitrinites, the observed n-alkane pattern cannot be correlated with that of saponifiable fatty acids isolated from alginites (Douglas *et al.*, 1970a; also see Chapter 3) or cooron-gite (Ramsey, 1966).

n-Alkanes were isolated from resinites in small yields, although the majority of the total alkanes were branched and cyclic components.

The major normal compounds isolated were $\underline{n}$-C_{24}, $\underline{n}$-C_{26} and $\underline{n}$-C_{28}, with smaller amounts of other homologues in the $\underline{n}$-C_{19} to $\underline{n}$-C_{30} range. It would seem that resins contain small amounts of $\underline{n}$-alkyl constituents possibly esterified to the dominantly cyclic terpenoid structures that have been recorded for these materials.

Pyrolysis at 275°C

Pyrolyses at 275°C liberated much smaller quantities of material than those at 375°C, and in many cases the distributions of alkanes and alkenes obtained showed significant differences to those obtained at the higher temperature. The yields of volatile material were also much reduced. Of all the samples investigated at this temperature, only Bitterfeld resinite showed more than a minor degree of thermal breakdown, the residual weight being *ca.* 65% of the starting material. The pyrolysate accounted for almost all of the weight loss, with only a minor loss as volatiles. Maghara resinite was much less affected and produced mainly volatile components.

The overall weight losses from the various macerals varied widely between samples, and also varied with rank in sporinites and vitrinites. The three alginites lost between 7.1% and 9.6% by weight, but the division between volatiles and extract was quite divergent, as shown in Table 40.

The degree of thermal breakdown of sporinites and vitrinites was rank-dependent, as was the nature of the products obtained (i.e. volatiles and extract). The total weight losses at the lower and higher ends of the investigated rank range were similar, but at *ca.* 82% C vitrinite produced much greater quantities of product than sporinite (Fig. 82). A wide divergence can be seen in the nature of the pyrolysis products (Fig. 83). Vitrinites showed a progressive decrease in the ratio of volatiles to extract from *ca.* 172:1 at

FIG. 82. PERCENTAGE WEIGHT LOSS OF MACERAL RESIDUES AFTER PYROLYSIS AT 275° C

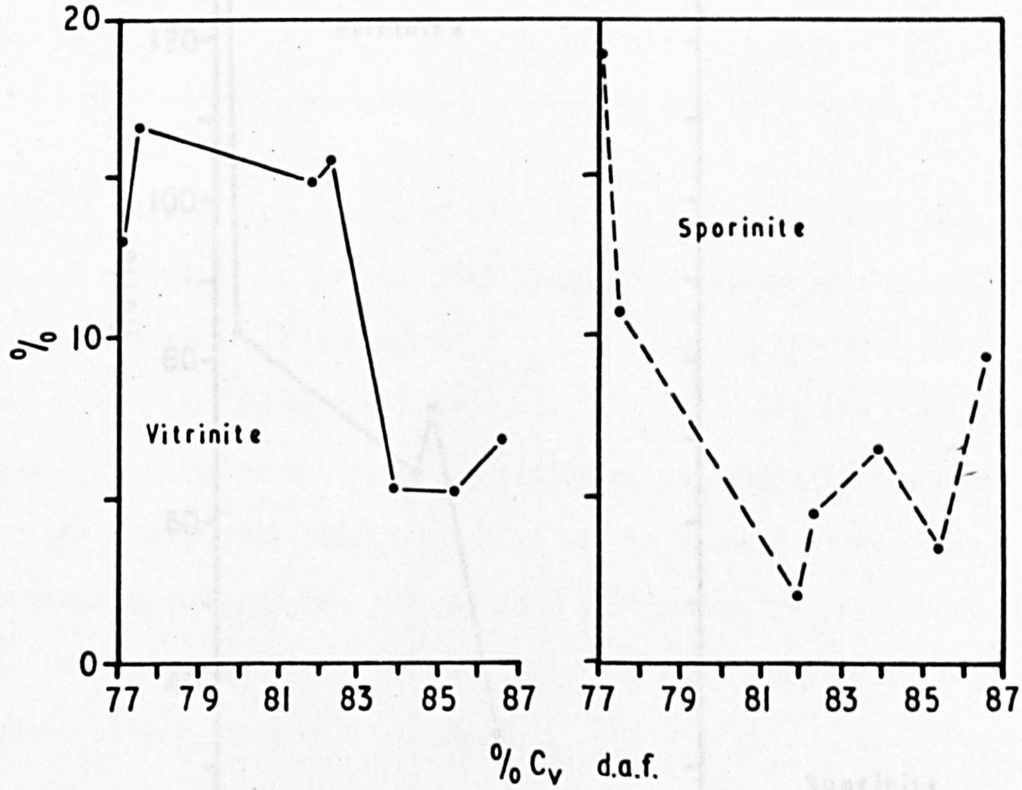

FIG. 83. RATIOS OF VOLATILES TO EXTRACT PRODUCED BY PYROLYSIS AT 275°C

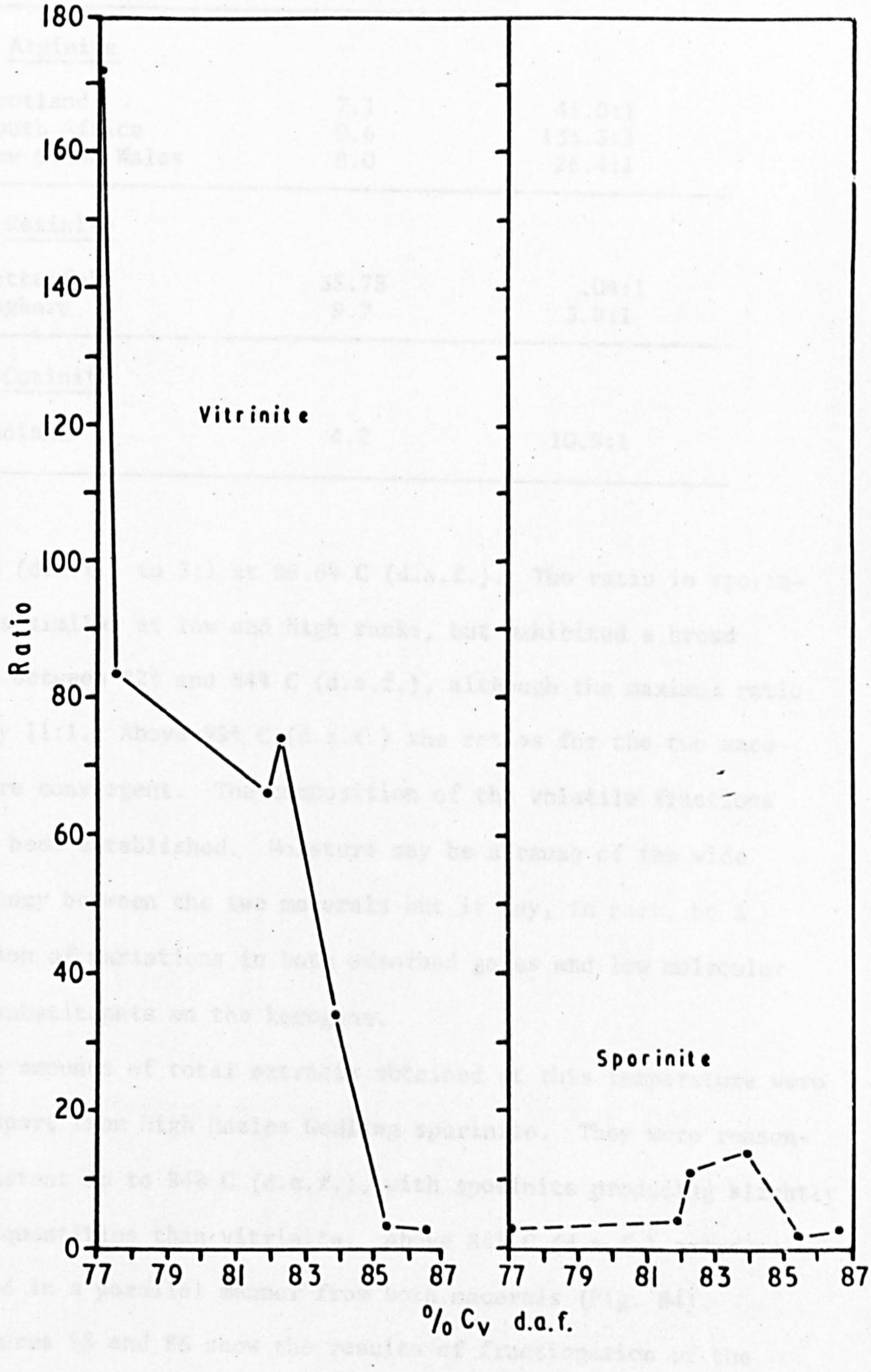

Table 40: Pyrolysis of exinites (other than sporinite) at 275°C

	Percentage wt. loss of residues	Ratio $\frac{\text{Volatiles}}{\text{Extract}}$
Alginite		
Scotland	7.1	41.0:1
South Africa	9.6	135.3:1
New South Wales	8.0	26.4:1
Resinite		
Bitterfeld	35.75	.04:1
Maghara	9.7	3.8:1
Cutinite		
Indiana	4.2	10.5:1

77.1% C (d.a.f.) to 3:1 at 86.6% C (d.a.f.). The ratio in sporinites was similar at low and high ranks, but exhibited a broad maximum between 82% and 84% C (d.a.f.), although the maximum ratio was only 11:1. Above 85% C (d.a.f.) the ratios for the two macerals were convergent. The composition of the volatile fractions has not been established. Moisture may be a cause of the wide discrepancy between the two macerals but it may, in part, be a reflection of variations in both adsorbed gases and low molecular weight substituents on the kerogens.

The amounts of total extracts obtained at this temperature were small, apart from High Hazles Gedling sporinite. They were reasonably constant up to 84% C (d.a.f.), with sporinite producing slightly greater quantities than vitrinite. Above 84% C (d.a.f.) extracts increased in a parallel manner from both macerals (Fig. 84).

Figures 85 and 86 show the results of fractionation of the extracts by column chromatography. In both cases the yields of aliphatic hydrocarbons were fairly constant and very small at low

FIG. 84. VARIATION OF TOTAL EXTRACT YIELDS WITH RANK AFTER PYROLYSIS AT 275° C

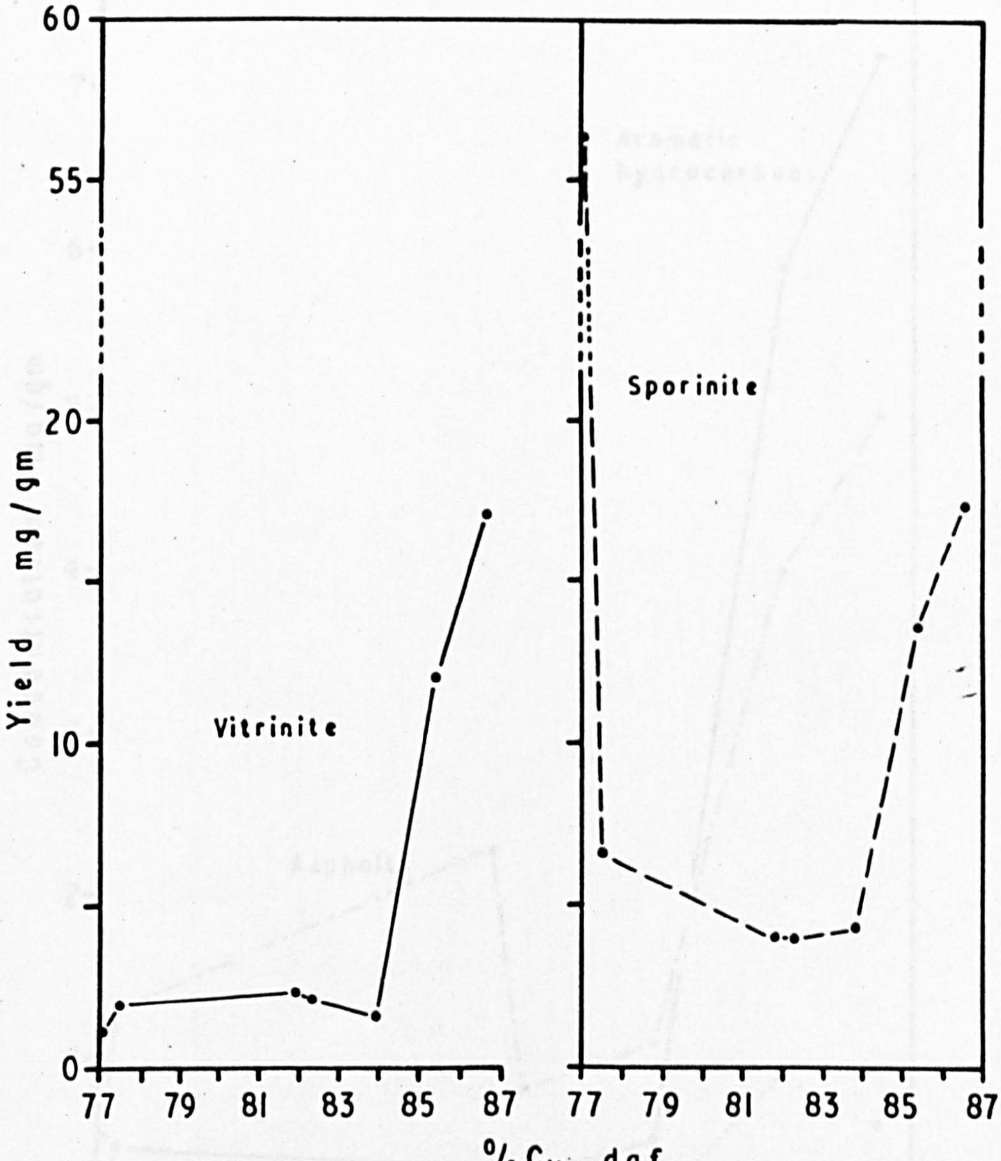

FIG. 85. VARIATION OF CONCENTRATIONS OF HYDROCARBONS AND NON HYDROCARBONS FROM PYROLYSIS OF VITRINITES AT 275° C

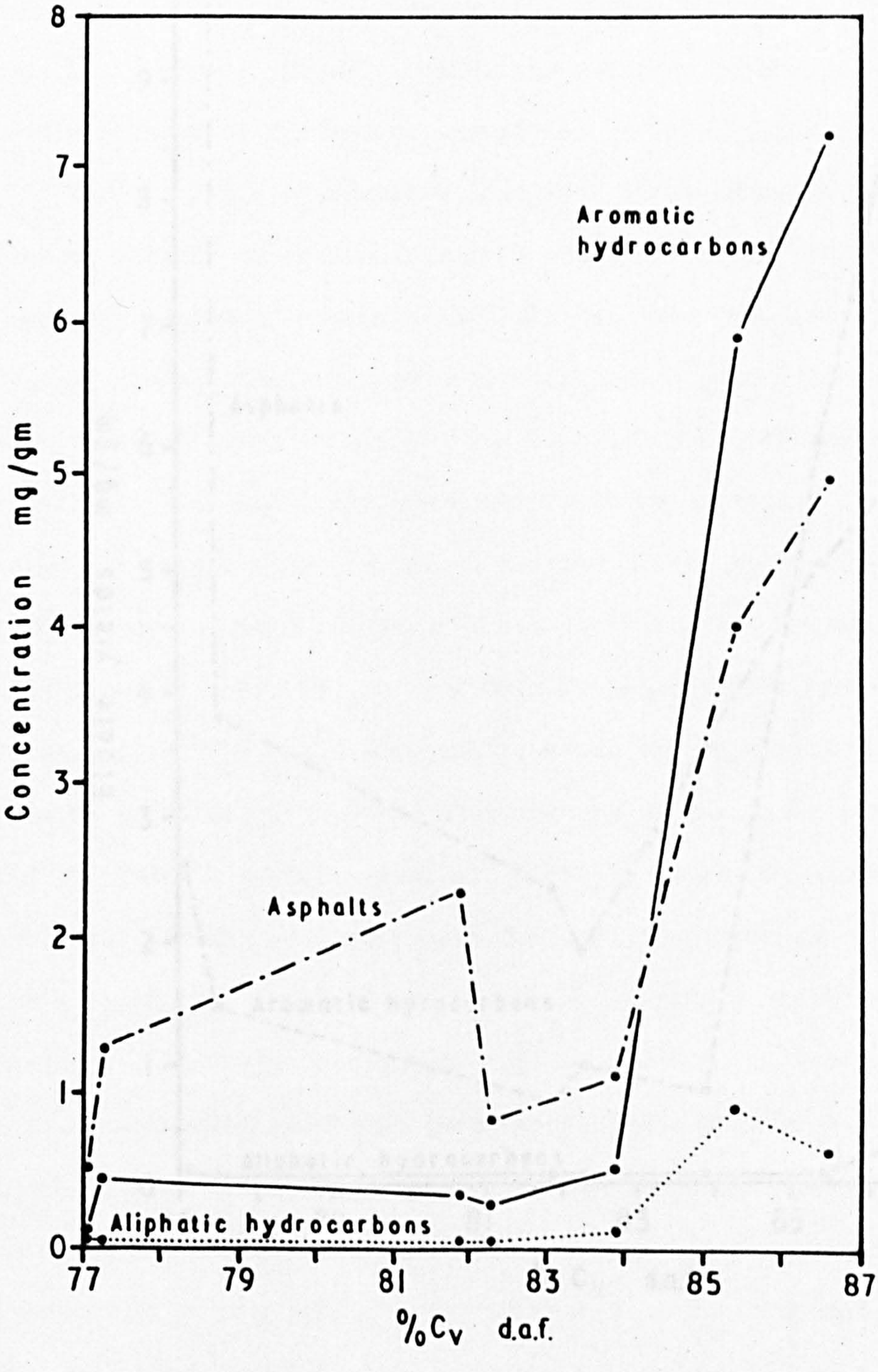

FIG. 86. VARIATION OF ELUATE YIELDS OF SPORINITES AFTER PYROLYSIS AT 275°C

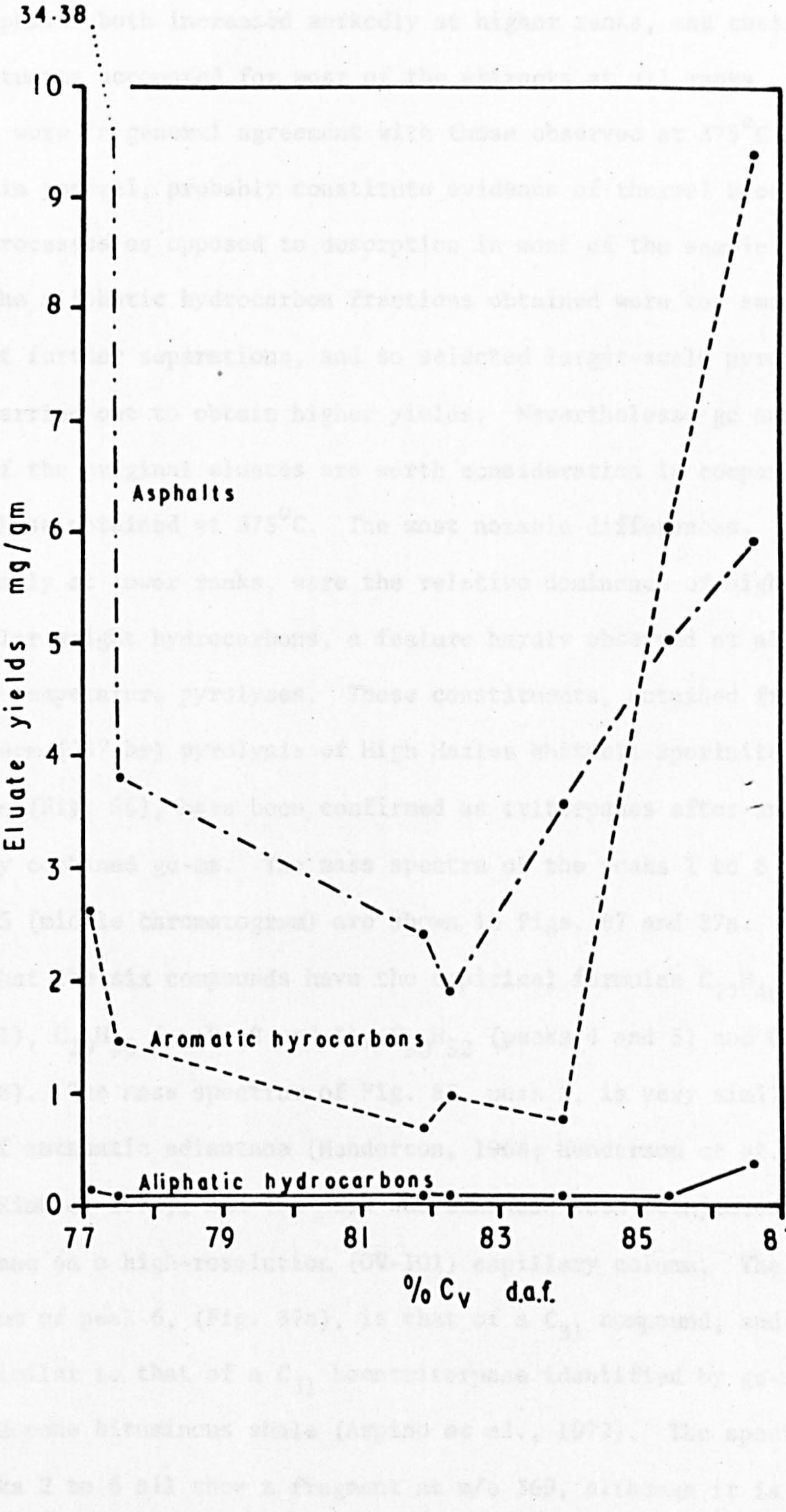

ranks. Above 84% C (d.a.f.) the yields from vitrinite increased to a maximum value of 0.9 mg/gm at 85.4% C (d.a.f.). A smaller increase was seen in sporinites. The yields of aromatic hydrocarbons and asphalts both increased markedly at higher ranks, and these constituents accounted for most of the extracts at all ranks. These trends were in general agreement with those observed at 375°C and thus, in general, probably constitute evidence of thermal breakdown processes as opposed to desorption in most of the samples.

The aliphatic hydrocarbon fractions obtained were too small to attempt further separations, and so selected larger-scale pyrolyses were carried out to obtain higher yields. Nevertheless, gc analyses of the original eluates are worth consideration in comparison with those obtained at 375°C. The most notable differences, especially at lower ranks, were the relative dominance of high molecular weight hydrocarbons, a feature hardly observed at all in higher temperature pyrolyses. These constituents, obtained from a long-term (287 hr) pyrolysis of High Hazles Whitwell sporinite residue (Fig. 55), have been confirmed as triterpanes after analysis by combined gc-ms. The mass spectra of the peaks 1 to 6 in Fig. 55 (middle chromatogram) are shown in Figs. 87 and 87a. They show that the six compounds have the empirical formulae $C_{27}H_{46}$ (peak 1), $C_{29}H_{50}$ (peaks 2 and 3), $C_{30}H_{52}$ (peaks 4 and 5) and $C_{31}H_{54}$ (peak 6). The mass spectrum of Fig. 87, peak 3, is very similar to that of authentic adiantane (Henderson, 1968; Henderson *et al.*, 1969; Kimble, 1972), and the peak was enhanced when coinjected with adiantane on a high-resolution (OV-101) capillary column. The mass spectrum of peak 6, (Fig. 87a), is that of a C_{31} compound, and is very similar to that of a C_{31} homotriterpane identified by gc-ms in an Eocene bituminous shale (Arpino *et al.*, 1972). The spectra of peaks 2 to 6 all show a fragment at m/e 369, although it is very

Fig. 87. Mass spectra of triterpanes obtained after 287 hr pyrolysis of High Hazles Whitwell sporinite at 275°

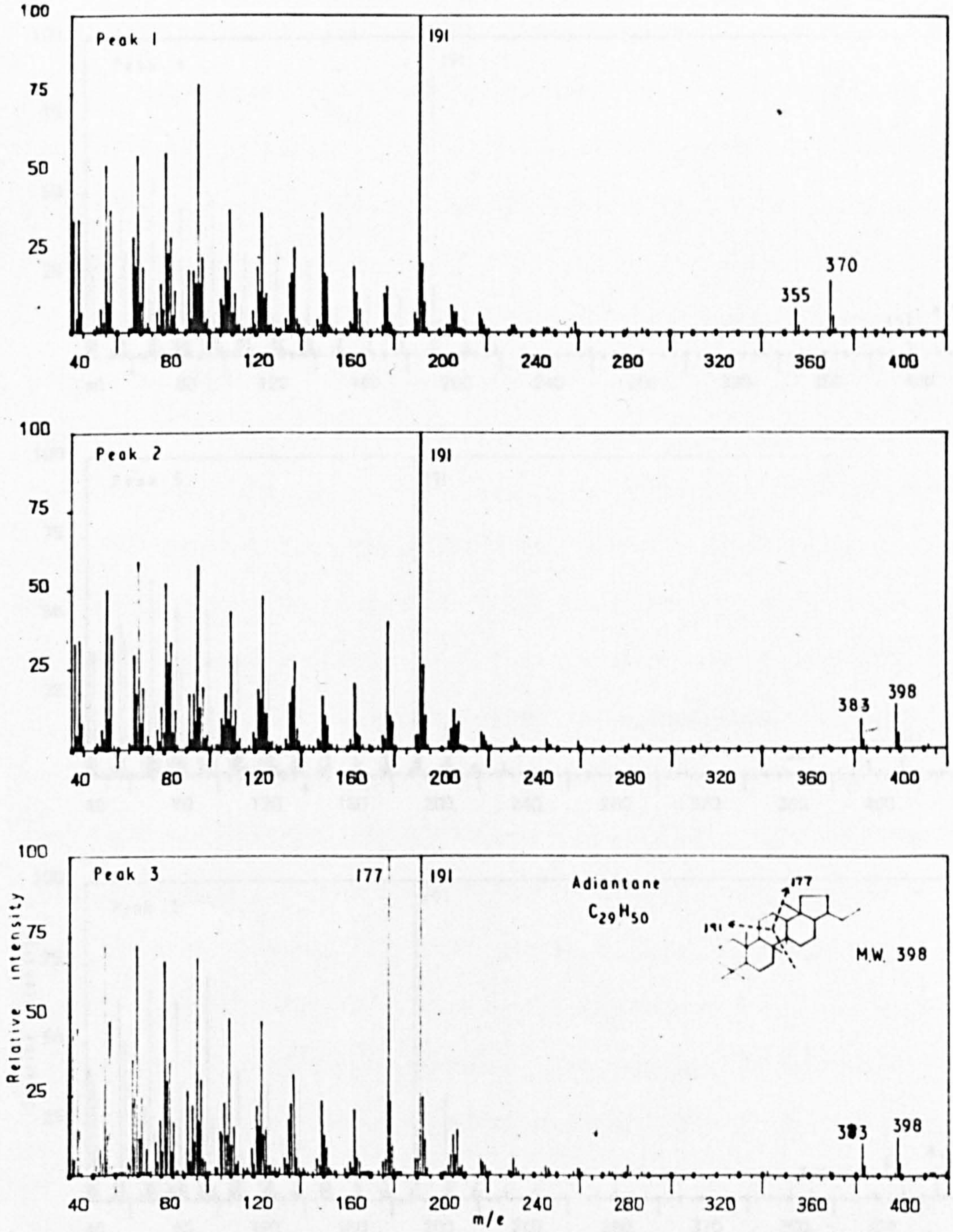

Fig. 87a. Mass spectra of triterpanes obtained after 287 hr pyrolysis of High Hazles Whitwell sporinite at 275°

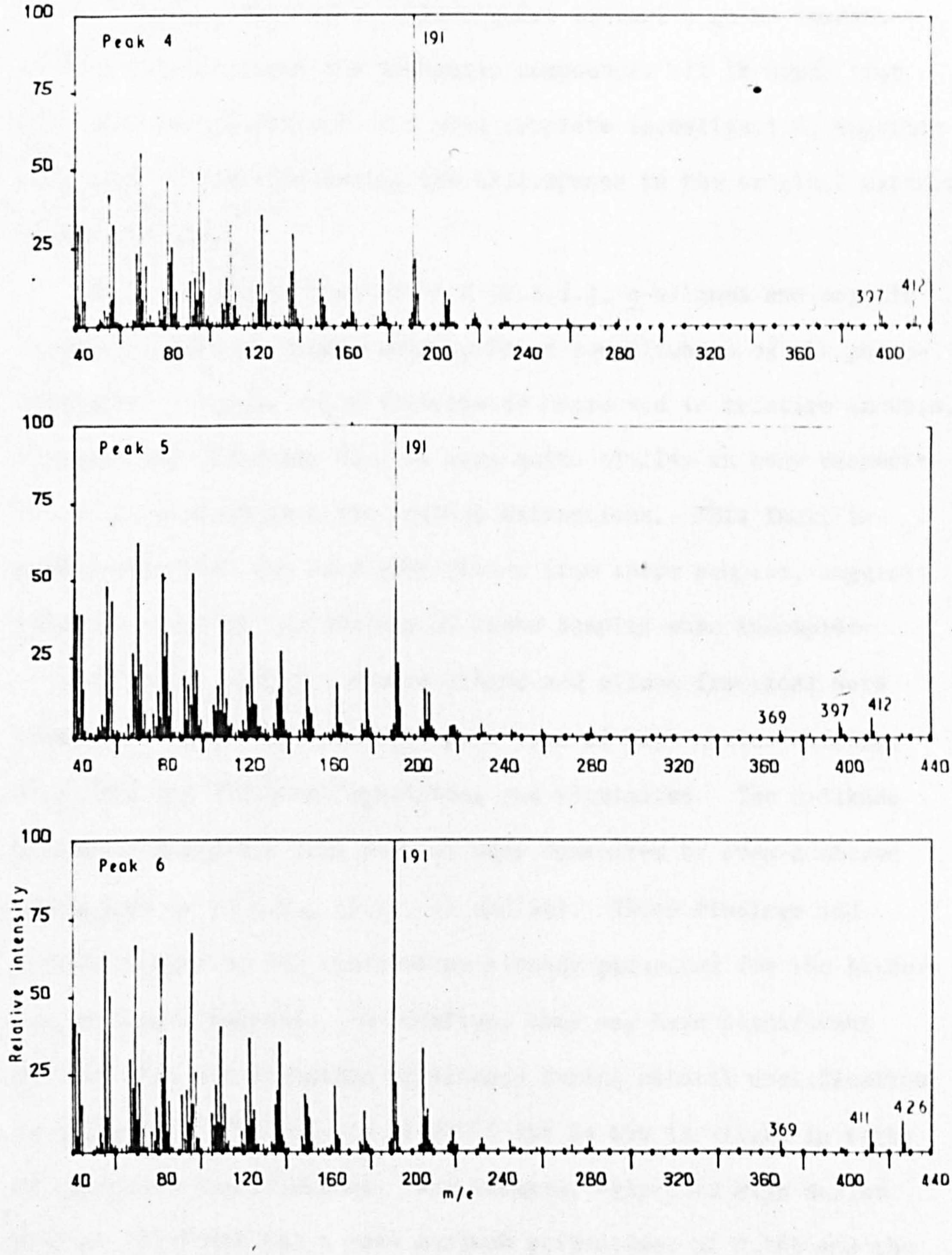

small in spectra 2 to 4. This fragment corresponds to the loss of C_2H_5 for compounds 2 and 3, C_3H_7 for compounds 4 and 5 and C_4H_9 for compound 6.

Because of the great similarities between the mass spectra of many closely-related triterpanes, full identifications of the various sporinite constituents will require extensive gc-ms investigations between these and authentic compounds. It is hoped that this will be the subject of a more complete investigation, together with similar work concerning the triterpanes in the original extracts of the macerals.

At ranks higher than 83.9% C (d.a.f.), n-alkanes and acyclic isoprenoid alkanes became more dominant constituents of the petroleum ether eluates, while triterpanes decreased in relative amounts. Parkgate and Silkstone eluates were quite similar in many respects to those obtained from the initial extractions. This fact, in combination with the increased yields from these samples, suggests that the original extractions of these samples were incomplete.

n-Alkane, branched/cyclic alkane and alkene fractions were obtained from the larger-scale pyrolyses of High Hazles Gedling, Deep Hard and Silkstone sporinites and vitrinites. The n-alkane patterns of the low-rank samples were dominated by even-numbered homologues up to n-C_{28} (Figs. 47 and 56). These findings add further weight to the conclusions already presented for the higher-temperature pyrolyses. In addition, they may have significant bearing upon the formation of alkanes during natural coalification, as the effect of pyrolysis at $275^{o}C$ for 24 hrs is slight in terms of increased coalification. For example, extracted High Hazles Gedling vitrinite had a mean maximum reflectance of 0.46% and the effect of pyrolysis and re-extraction only raised this to 0.63%. These findings indicate that even-numbered n-alkanes may be formed preferentially during natural coalification of sporinites and vitrinites.

The n-alkane patterns of these samples above n-C_{28} were dominated by the odd-numbered homologues. These higher members may in fact be derived from the initial n-alkane input, despite the samples having been extracted prior to pyrolysis. This conclusion is supported by alkene patterns produced by the pyrolyses, which, although complex, contained an homology of n-alkenes that were strongly dominated by the even-numbered members up to n-C_{28} or n-C_{30}. Presupposing that n-alkanes were formed by homolytic fission, a corresponding series of alkenes might be expected. However, no n-alkenes were found showing an odd-dominated distribution in the higher carbon number ranges.

The Silkstone macerals produced a virtually smooth distribution of n-alkanes, but the corresponding alkenes contained no dominant n-alkene homology. The fractions were so complex as to be virtually unresolved by gc on short, packed columns, but the vitrinite fraction contained traces of an homologous series. This supports the conclusion that any products that may have been formed by pyrolysis have been masked by desorption of unextracted material in these particular samples.

A similar effect was seen in the branched/cyclic alkanes which, at higher ranks, were distributionally similar to the extracted patterns. At low ranks, acyclic isoprenoid alkanes were minor constituents of the fractions, and triterpanes predominated. This was the reverse of the results from extraction where pristane was the dominant constituent of all but the lowest rank samples. A possible conclusion here is that a significant generation of pristane requires a greater temperature (or time) than that needed for n-alkane generation. High Hazles Whitwell sporinite was pyrolysed for 24 and 287 hrs at 275°C, and the major significant difference in the hydrocarbon patterns was a much greater dominance of pristane in the longer pyrolysis. It should also be remembered that the extraction data showed pristane concentrations increasing at ranks where n-alkanes were cracking to lower molecular weights.

Alkanes isolated from the 275°C pyrolyses of alginites were generally qualitatively comparable to those produced at 375°C in that they exhibited rather "mature" distributions, comparable with much higher-rank sporinites. New South Wales alginite was again exceptional in that the n-alkanes showed a minor predominance of even-numbered chain lengths in the n-C_{20} to n-C_{28} range.

Relatively high proportions of hydrocarbons, predominantly alkenes, have been isolated from *Botryococcus braunii*. During the brown resting stage of this organism, the botryococcenes, which are highly branched compounds, can account for much of the dry weight (Maxwell *et al.*, 1968). During the green growing stage, smaller, although still significant, amounts of straight-chain alkenes have been identified with chain lengths up to C_{31} (Knights *et al.*, 1970). These may be possible precursors, at least in part, of extractable n-alkanes from the fossilized material. On the other hand, a bacterial origin has been proposed for alginite and cooronite n-alkanes (Douglas *et al.*, 1969b).

Cutinite alkanes showed a very restricted range of distribution, concentrated in the C_{15} region, in marked contrast to those obtained by pyrolysis at 375°C. The different distributions of alkanes obtained at the two temperatures suggests derivation from different precursor structures showing variable stabilities to thermal degradation.

Resinites themselves yielded highly complex mixtures of hydrocarbons, probably diterpenoids, but once again minor quantities of strongly even-dominated n-alkanes were apparent in the n-C_{20} to n-C_{30} range, indicating n-alkanoic structures in the matrices.

Thus, pyrolysis of coal macerals at low temperatures has been of some value in interpreting some of the structures occurring in the peripheral groups, and changes which take place with increasing coalification. The study illustrates that significant quantities of material can be cleaved from the matrices at temperatures below those of active decomposition (Berkowitz, 1967). Because of the supposed stability of the oxygen functions in bituminous coals, much of the material liberated may have been derived by rupture of C-C bonds, perhaps indicating some depolymerisation of the structures. The implications of this work towards understanding geochemical processes of maturation have been discussed with special reference to n-alkanes.

A great deal more information would be forthcoming from detailed analyses of branched/cyclic alkanes and aromatic hydrocarbons. Aromatic and hydroaromatic substitution patterns and the nature of alkyl substituents would be of assistance in possible reconstructions of the original polymers.

The value of removing extractable material prior to pyrolysis has been shown. Step-wise pyrolysis of macerals would appear to be a promising method of analysis if the soluble products produced at each step are removed and analysed. Analysis of gaseous products will also be of significance. A step-wise procedure involving increasing temperature will enable structures of increasing stability to be examined. Such studies, made in relation to coalification, will be valuable in determining not only parent structures in the polymer, but may also aid understanding of the processes involved in aromatisation and condensation of coals. This technique would undoubtedly be useful if applied to sedimentary kerogens and would be of value in understanding differences in structures involved in the polymerisation of materials from a variety of sedimentary environments.

Experimental

Apparatus

Two autoclaves were used in this work, one of 16 ml. capacity and the other of 1 l. capacity. Most of the work was done in the 16 ml. vessel which was fitted with a T-piece head for attachment of a pressure gauge, bursting disc assembly and gas inlet/outlet port (Baskerville and Lindsay Ltd). This apparatus had a maximum working temperature of 450°C at a pressure of 150 atmospheres. The bursting discs (dual discs of silver and nickel, thickness 0.003" each) had a bursting pressure of 177 atmospheres.

The autoclave was heated in an aluminium block containing two 500 watt cartridge heating elements. Current was supplied through an 8 amp variable transformer (Variac) at a voltage of 150-180 volts, which provided a heating rate of 5 to 6°C/min., up to 300°C. Temperature regulation was provided by means of a thermocouple, control unit (Ether) and mercury switch.

A number of experiments were carried out using a 1 l. autoclave (Baskerville and Lindsay Ltd), heated by a 1 Kw. circular heating coil located beneath the vessel. Operating at mains voltage, this provided a heating rate of between ½ and 1°C/min. This apparatus was also fitted with a pressure gauge, bursting disc and gas inlet/outlet assembly.

Experimental procedure

Samples of macerals to be pyrolysed, previously extracted with an azeotropic mixture of chloroform, acetone and methanol, were preweighed into glass containers and placed in the autoclave. All experiments were carried out in a nitrogen atmosphere, achieved by triple flushing of the vessel before filling to the required pressure.

All pyrolyses were done for *ca*. 24 hrs, and one additional experiment was carried out for 287 hrs. These times included the time taken for the vessels to reach operating temperature.

In order to determine the temperatures to be used, samples of High Hazles Gedling sporinite were pyrolysed at 275^o, 325^o, 375^o and 425^{o}C respectively. The yields of total extract and aliphatic hydrocarbons obtained are shown in Fig. 88. The highest yields of hydrocarbons were found at 375^{o}C, although the greatest yield of total extract was found at 325^{o}C. At 275^{o}C, the yield of extract was low but showed an interesting hydrocarbon distribution. Consequently the maceral residues were pyrolysed at both 275^o and 375^{o}C.

After pyrolysis, the macerals were extracted with dichloromethane by boiling under reflux for 2 hrs, and the solutions were filtered, and evaporated, to give total extracts. Residues were dried and weighed to determine overall weight losses. The scheme of fractionation employed for isolation of hydrocarbon fractions is shown in Fig. 89.

Experimental data on pyrolysis conditions and extracts obtained are given in Tables 41 and 42.

<u>Column chromatography</u>

Pyrolysis extracts were chromatographed over silica gel (B.D.H., 60-120 mesh) using a sequential elution system of petroleum ether, benzene and methanol. Experimental procedures were similar to those described in the relevant experimental section of Chapter 2, and details are given in Tables 43 and 44.

<u>Thin-layer chromatography</u>

Analytical and preparative argentatious tlc were used to identify and separate saturated and unsaturated hydrocarbons in the

FIG. 88. VARIATION OF YIELDS OF TOTAL EXTRACTS AND ALIPHATIC HYDROCARBONS WITH PYROLYSIS TEMPERATURE — HIGH HAZLES GEDLING SPORINITE

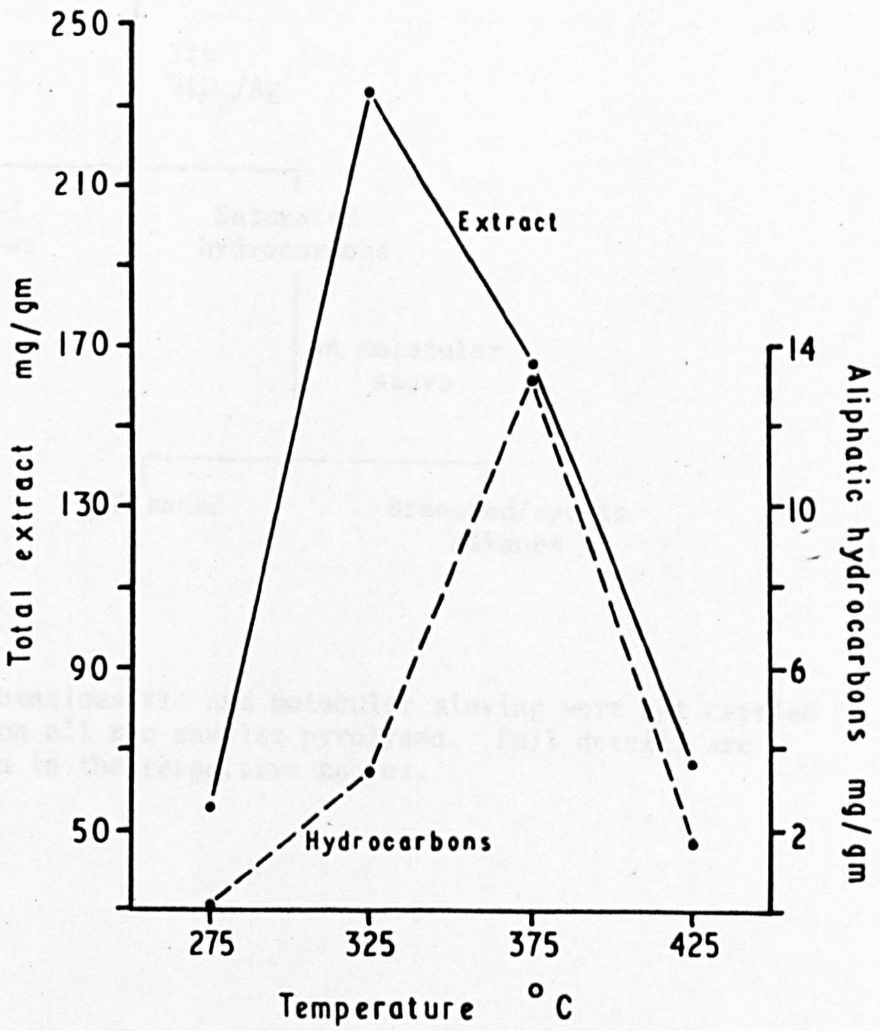

Fig. 89: Flow diagram of the pyrolysis extract fractionation scheme

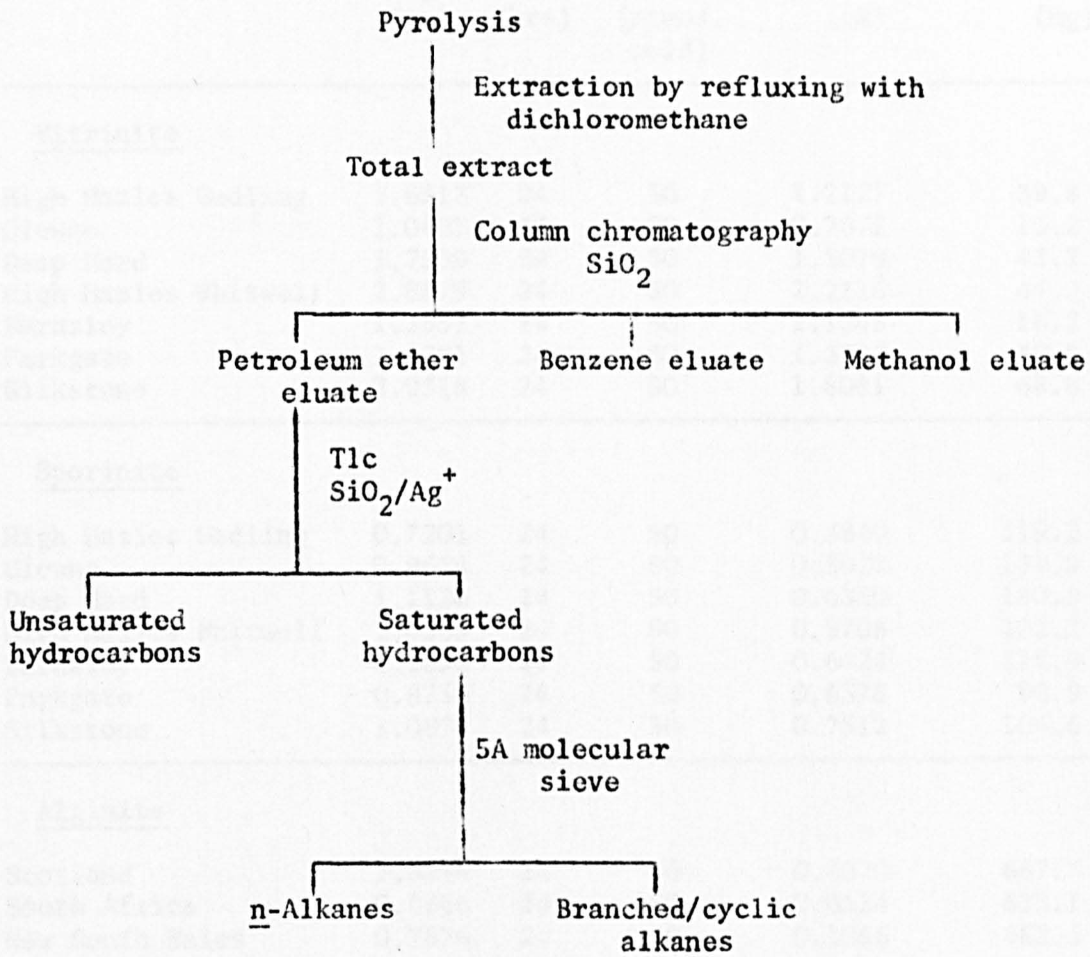

N.B. Argentatious tlc and molecular sieving were not carried out on all the samples pyrolysed. Full details are given in the respective tables.

Table 41: Experimental data for pyrolyses at 375°C

	Weight (gm)	Time (hrs)	Pressure (atmos. cold)	Residual wt. (gm)	Extract wt. (mg)
Vitrinite					
High Hazles Gedling	1.6513	24	50	1.2127	39.8
Clowne	1.0807	24	50	0.7672	13.2
Deep Hard	1.7509	24	50	1.3079	43.2
High Hazles Whitwell	2.8579	24	50	2.2116	44.0
Barnsley	1.3857	24	50	1.1843	16.2
Parkgate	1.5791	24	50	1.3803	49.8
Silkstone	2.0318	24	50	1.8081	68.6
Sporinite					
High Hazles Gedling	0.7201	24	50	0.3849	119.2
Clowne	0.9624	24	50	0.5022	199.9
Deep Hard	1.1120	24	50	0.6350	180.8
High Hazles Whitwell	1.0369	24	50	0.5703	193.2
Barnsley	1.0398	24	50	0.6424	115.4
Parkgate	0.8756	24	50	0.6378	90.9
Silkstone	1.0874	24	50	0.7512	104.6
Alginite					
Scotland	1.3214	24	50	0.4070	667.6
South Africa	0.8866	24	50	0.0534	623.1
New South Wales	0.7876	24	50	0.1056	482.3
Resinite					
Bitterfeld	1.0925	24	50	0.0331	648.9
Maghara	1.0414	24	50	zero	709.1
Cutinite					
Indiana	0.9275	24	50	0.5656	77.9

Table 42: Experimental data for pyrolyses at 275°C

	Weight (gm)	Time (hrs)	Pressure (atmos. cold)	Residual wt. (gm)	Extract wt. (mg)
Vitrinite					
High Hazles Gedling	2.2648	24	50	1.9702	1.7
Clowne	1.7478	24	50	1.4605	3.4
Deep Hard	2.2555	24	50	1.9235	5.0
High Hazles Whitwell	1.8684	24	50	1.5803	3.8
Barnsley	1.8449	24	50	1.7478	2.7
Parkgate	2.0057	24	50	1.9020	23.9
Silkstone	1.9411	24	50	1.8090	33.1
High Hazles Gedling*2	19.1736	26	32	17.5635	155.9
Deep Hard*2	41.8864	30	32	40.6402	200.9
Silkstone*2	43.4300	29.5	32	41.2854	862.1
Sporinite					
High Hazles Gedling	0.6835	24	51	0.5538	38.4
Clowne	1.4473	24	50	1.2906	n.d.
Deep Hard	1.6220	24	50	1.5896	6.3
High Hazles Whitwell	1.3651	24	50	1.3010	5.3
Barnsley	1.6026	24	50	1.5006	6.8
Parkgate	1.3777	24	50	1.3297	18.8
Silkstone	1.6712	24	50	1.5152	28.8
High Hazles Gedling*2	11.5070	27	50	11.0561	88.8
Deep Hard*2	41.8953	29	30	41.1031	108.8
Silkstone*2	27.2209	27	32	26.7455	328.6
High Hazles Whitwell*3	1.4862	287	50	1.4524	31.0
Alginite					
Scotland	1.3084	24	49	1.2159	2.2
South Africa	1.4167	24	50	1.2804	1.0
New South Wales	1.4090	24	50	1.2968	4.1
Resinite					
Bitterfeld	0.6851	24	50	0.4402	236.1
Maghara	0.6279	24	50	0.5668	12.8
Cutinite					
Indiana	0.9018	24	50	0.8640	3.3

n.d. not determined.

Table 43: Column chromatographic data for pyrolyses at 375°C

	Weight SiO_2 in column (gm)	Eluant volumes Petroleum ether (ml)	Benzene (ml)	Methanol (ml)	Eluate weights Petroleum ether (mg)	Benzene (mg)	Methanol (mg)
Vitrinite							
High Hazles Gedling	6	25	20	30	2.0	14.7	16.0
Clowne	5	25	20	30	1.0	4.1	7.8
Deep Hard	5	25	20	30	3.0	15.4	16.2
High Hazles Whitwell	5	25	20	30	2.6	14.8	18.7
Barnsley	5	25	20	30	1.2	5.6	7.8
Parkgate	5	25	20	30	3.5	21.5	15.3
Silkstone	5	25	20	30	4.6	31.5	25.5
Sporinite							
High Hazles Gedling	6	30	40	50	9.4	58.9	50.7
Clowne	10	30	40	60	9.7	103.1	47.8
Deep Hard	9	30	40	50	6.5	106.5	68.7
High Hazles Whitwell	9	30	40	50	9.6	91.6	66.4
Barnsley	9	30	40	40	10.4	57.2	33.2
Parkgate	7	30	40	40	5.4	41.2	44.9
Silkstone	6	30	40	50	4.0	65.0	36.0
Alginite							
Scotland	30	30	40	80	154.2	366.1	126.3
South Africa **	6	30	20	40	18.2	37.8	23.5
New South Wales **	10	30	20	40	25.9	33.8	18.0
Resinite							
Bitterfeld	30	40	40	80	99.3	352.9	99.0
Maghara	30	40	40	100	95.8	447.9	135.8
Cutinite							
Indiana	8	30	20	40	5.3	24.9	33.9

** Only an aliquot of the total extract was taken for chromatography for these two samples, i.e. South Africa 97.0 mgs, New South Wales 82.1 mgs.

Table 44: Column chromatographic data for pyrolyses at 275°C

	Weight SiO_2 in column (gm)	Eluant volumes Petroleum ether (ml)	Benzene (ml)	Methanol (ml)	Eluate weights Petroleum ether (mg)	Benzene (mg)	Methanol (mg)
Vitrinite							
High Hazles Gedling	4	20	15	25	0.1	0.2	1.1
Clowne	4	20	15	25	< 0.1	0.8	2.2
Deep Hard	4	20	15	25	0.1	0.8	5.1
High Hazles Whitwell	3	20	15	25	< 0.1	0.5	1.7
Barnsley	4	20	15	25	0.2	0.9	2.1
Parkgate	5	25	20	30	1.8	11.9	8.1
Silkstone	5	25	20	30	1.2	14.0	9.6
High Hazles Gedling* 2	8	30	30	50	3.0	32.5	129.1
Deep Hard* 2	8	30	30	50	2.1	45.5	129.7
Silkstone* 2	8	30	30	50	11.9	147.7	66.5
Sporinite							
High Hazles Gedling	5	30	40	40	< 0.1	1.8	23.5
Clowne	6	30	30	40	< 0.1	2.1	5.5
Deep Hard	5	30	20	40	< 0.1	0.9	3.8
High Hazles Whitwell	5	30	20	40	< 0.1	1.3	2.6
Barnsley	5	30	25	40	< 0.1	1.0	5.7
Parkgate	5	30	20	40	0.1	8.3	6.9
Silkstone	5	30	20	40	0.6	15.7	9.9
High Hazles Gedling* 2	8	30	40	50	1.3	19.6	49.7
Deep Hard* 2	8	30	30	50	2.7	29.0	70.9
Silkstone* 2	7	30	30	50	9.8	173.2	101.4
High Hazles Whitwell* 3	5	25	20	30	1.1	13.5	12.7
Alginite							
Scotland	3	15	15	20	0.2	0.6	0.7
South Africa	3	20	20	20	< 0.1	0.1	0.4
New South Wales	4	20	20	20	0.6	0.2	0.7
Resinite							
Bitterfeld	10	30	20	30	6.5	130.9	100.0
Maghara	5	25	20	30	1.8	4.8	4.7
Cutinite							
Indiana	5	25	20	30	0.9	0.4	1.4

petroleum ether column eluates. Procedures were similar to those outlined in the relevant experimental section of Chapter 2.

All the petroleum ether eluates, obtained from column chromatography of the 375°C extracts, were separated into alkane and alkene fractions. Of those from pyrolyses at 275°C, only alginites, resinites, cutinite, the long-term pyrolysis of one sporinite and the pyrolyses of vitrinite and sporinite carried out in the 1 l. autoclave were analysed. Data are given in Table 45.

Molecular sieve

Total alkane fractions from all 375°C pyrolyses, and those from the larger scale pyrolyses of vitrinites and sporinites at 275°C, were separated into n- and branched/cyclic alkane fractions by 5A molecular sieve. The method was essentially the same as that described in Chapter 2 except that cyclohexane was used instead of benzene. Data are given in Table 46.

Hydrogenation of alkenes

Several alkene fractions in ethyl acetate solution were hydrogenated over palladium charcoal catalyst (ratio catalyst to sample of 30:1). Subsequent glc of the products showed that the dominant homology in the original alkene fractions co-injected with authentic n-alkanes on a 40 m. capillary OV-101 column capable of resolving n-alkanes from their corresponding n-alk-1-enes.

Table 45: Tlc data for hydrocarbons obtained at 375°C and 275°C

	375°C Alkanes (mg)	375°C Alkenes (mg)	275°C Alkanes (mg)	275°C Alkenes (mg)
Vitrinite				
High Hazles Gedling	0.5	0.2	n.d.	n.d.
Clowne	0.2	0.2	n.d	n.d.
Deep Hard	1.7	0.5	n.d.	n.d.
High Hazles Whitwell	1.4	0.5	n.d.	n.d.
Barnsley	0.7	0.3	n.d.	n.d.
Parkgate	2.0	0.4	n.d.	n.d.
Silkstone	2.6	0.4	n.d.	n.d.
High Hazles Gedling* 2			0.7	0.4
Deep Hard* 2			0.8	0.2
Silkstone* 2			8.0	0.6
Sporinite				
High Hazles Gedling	4.4	0.8	n.d.	n.d.
Clowne	2.6	0.2	n.d.	n.d.
Deep Hard	3.0	0.2	n.d.	n.d.
High Hazles Whitwell	4.2	0.1	n.d.	n.d.
Barnsley	5.8	0.2	n.d.	n.d.
Parkgate	2.1	0.4	n.d.	n.d.
Silkstone	2.0	0.4	n.d.	n.d.
High Hazles Gedling* 2			0.4	0.1
Deep Hard* 2			0.7	0.7
Silkstone* 2			6.3	1.4
High Hazles Whitwell* 3			0.6	0.2
Alginite				
Scotland	106.1	8.5	0.2	zero
South Africa	8.9	1.2	<0.1	zero
New South Wales	12.8	1.7	0.2	<0.1
Resinite				
Bitterfeld	59.3	7.4	0.3	0.7
Maghara	67.6	6.1	0.1	0.1
Cutinite				
Indiana	2.0	1.3	<0.1	<0.1

n.d. not determined.

Table 46: Molecular sieve data for alkanes obtained from pyrolyses at 375°C and 275°C

	Wt. alkanes sieved (mg)	Yield $\underline{n}$-Alkanes (mg)	Yield Branched/cyclic alkanes (mg)
Pyrolysis at 375°C			
Vitrinite			
High Hazles Gedling	0.5	0.2	0.3
Clowne	0.2	0.1	0.2
Deep Hard	1.6	0.5	0.9
High Hazles Whitwell	1.3	0.1	1.0
Barnsley	0.6	0.1	0.3
Parkgate	1.9	0.4	1.2
Silkstone	2.5	0.5	1.6
Sporinite			
High Hazles Gedling	2.9	0.6	1.7
Clowne	2.0	0.4	1.4
Deep Hard	2.2	0.4	1.5
High Hazles Whitwell	2.7	0.4	1.6
Barnsley	3.8	0.7	2.6
Parkgate	1.6	0.4	0.8
Silkstone	1.6	n.d.	0.8
Alginite			
Scotland	5.2	1.9	2.2
South Africa	2.3	0.4	1.4
New South Wales	2.4	0.6	1.7
Resinite			
Bitterfeld	11.5	0.1	11.0
Maghara	4.2	0.1	3.5
Cutinite			
Indiana	1.3	0.4	0.6

n.d. not determined.

Table 46 cont'd.

	Wt. alkanes sieved (mg)	Yield n-Alkanes (mg)	Yield Branched/cyclic alkanes (mg)
Pyrolysis at 275°C			
Vitrinite			
High Hazles Gedling*2	0.7	0.2	0.4
Deep Hard*2	0.6	0.2	0.4
Silkstone*2	8.0	1.3	4.8
Sporinite			
High Hazles Gedling*2	0.4	0.1	0.2
Deep Hard*2	0.7	0.2	0.3
Silkstone*2	6.3	0.2	5.8
High Hazles Whitwell*3	0.6	0.2	0.2

Chapter 5

Oxidative degradation of extracted and saponified exinite concentrates

Introduction

Coal is susceptible to oxidation to the extent that spontaneous combustion presents a fire risk in coal storage. Oxidative degradation of coals has been widely applied in coal science, as a high conversion of the coal substance to lower molecular weight soluble compounds can be achieved, the identity of the products giving indications of the type of structures present in the starting materials. With certain oxidants however, mild oxidation produces high yields of insoluble acids, the so-called humic acids, which do not lend themselves to direct analytical identification. At the other extreme, severe oxidising conditions lead to a high conversion of coal to simple compounds which, in themselves, provide only very basic structural information.

Oxidation has been carried out in acidic, neutral and alkaline media, common reagents being potassium permanganate, nitric acid, chromium trioxide, hydrogen peroxide, oxygen and ozone. Oxidation with nitric acid yields acid-insoluble, black humic acids, which, upon further oxidation, are converted to acid-soluble, brown humic acids and finally to water-soluble products (Kinney and Ockert, 1956). Simple products obtained from nitric acid oxidation are short-chain aliphatic mono- and dicarboxylic acids and benzene carboxylic acids (van Duuren and Warren, 1950). Many of these latter compounds have been identified in coal oxidation products and, in particular, the yield of mellitic acid has been correlated with coal rank (van Krevelen, 1963). This is a reflection of the increasing condensation of aromatic centres in the coal matrix as the rank increases.

Humic acids from coal have been investigated by hydrogen peroxide oxidation (Brooks et al., 1956; Lawson, 1957; Hartley and Lawson, 1962). Initially, ether-insoluble sub-humic acids are produced along with volatile constituents such as formic and acetic acids. The volatile constituents are considered to be derived from peripheral groups of the humic acids. The insoluble constituents become increasingly aromatic in character, presumably by concentration of the essentially aromatic nuclei of the humic acids.

Oxidation of coals with oxygen in alkaline media is an effective degradation technique, and is usually carried out at elevated temperatures. Aliphatic acids, aromatic polycarboxylic acids and humic acids are the products. Roy (1965) considers that only aliphatic carbon is attacked after noting the greater effect of oxygen oxidation on exinite than vitrinite. Considerable amounts of aliphatic compounds (as a proportion of the total water-soluble products) were noted by Holly and Montgomery (1956) after oxidation of bituminous coal at 270^{o}C and *ca.* 900 p.s.i. pressure, while the disappearance of aliphatic carbon during aerial oxidation has been noted (Conrow *et al.*, 1963).

This view is supported by other investigations where it was found that aromatic systems are generally stable to oxygen oxidation below 220^{o}C. Such oxidation is held to take place mainly at end groups of aliphatic substituents, leading to the formation of hydroxyl, carbonyl and carboxyl groups (Mazumdar and Lahiri, 1958; Chakrabartty *et al.*, 1958; Mazumdar *et al.*, 1959). These authors concluded that the aliphatic material of coals between *ca.* 71% and 90% C is present either as alkyl chains with at least four carbon atoms or alicyclic networks with more than seven carbon atoms.

The reduction of pyrolytic coal tar yields by pre-oxidation is well established (Howard, 1963), due to the degradation of aliphatic material. Some specific assignments of the oxidative attack on aliphatic carbon in coal were made by Kinney (1947) who noted that the yield of acetic acid by nitric acid/potassium dichromate oxidation was similar to the yield of methane from low-temperature carbonisation.

Conversely, oxidation of a coal pre-carbonised to 500°C yielded no acetic acid.

Benzene polycarboxylic acids have been obtained by oxygen oxidation. A Japanese bituminous coal yielded a mixture of these acids (Kamiya, 1961a) in which the benzenetri- and benzenetetracarboxylic acids were the main constituents (Kamiya, 1961b). Benzenoid acids as a whole represented 26% by weight of the dry, ash-free coal.

The structures of some of the aromatic systems in coals have been established from the oxidation products obtained with oxygen in an alkaline medium. They include benzoic and toluic acids, alkyl-substituted benzoic acids with between one and five and seven carbon atoms in the substituent groups (but with butyl as the longest single open-chain constituent), phthalic and alkyl-substituted phthalic acids, benzenetricarboxylic acids and naphthoic acid. Further analyses of the decarboxylated oxidation products identified methylnaphthalene, indane, phenanthrene and anthracene (Holly and Montgomery, 1956; Holly *et al.*, 1956; Montgomery *et al.*, 1956).

Ozone has been used to degrade both coals and humic acids isolated from coals. The latter materials are extensively converted to carbon dioxide and oxalic acid by ozonisation (Ahmed and Kinney, 1950). The reduction of humic acids to sub-humic acids has been investigated (Dobinson *et al.*, 1956; Dobinson and Lawson, 1959). Later work concluded that the humic acids had a basic skeleton of aromatic rings interlinked by mainly short, straight-chain aliphatic bridges (Lawson and Purdie, 1966). Direct ozonolysis of bituminous coal converted a large part of the coal to water-soluble products without the formation of insoluble intermediate compounds (Kinney and Friedman, 1952). Benzene polycarboxylic acids and aliphatic hydroxy-acids have been identified as ozonisation products (Bitz and Nagy, 1966). Repeated stepwise ozonolysis produced similar compounds each time, leading to the suggestion that degradation occurred by the progressive removal of layers of similar material from the coal polymer (Bitz and Nagy, 1967).

Ozone is a particularly effective degradative agent for the conversion of sporopollenin from modern biological sources to mixtures of mainly straight-chain aliphatic mono- and dicarboxylic acids, with maximum chain lengths of eighteen carbon atoms (Shaw and Yeadon, 1966; Brooks and Shaw, 1968a). Extension of this work to the ozonolysis of various fossil materials of fungal, algal and higher plant palynomorphs produced similar distributions of degradation products, leading to the proposal that sporopollenin occurs ubiquitously in the geosphere (Brooks and Shaw, 1968b; Brooks and Shaw, 1969; Brooks, 1971; Shaw, 1971; Brooks and Shaw, 1972). However, another study of one of these "sporopollenins", *Tasmanites*, by chromic acid oxidation yielded a much wider range of aliphatic compounds up to C_{30} and a lack of isoprene structures in the products (Burlingame *et al.*, 1969; Simoneit and Burlingame, 1973). These products are incompatible with sporopollenin as defined biologically, and indicate either modification of the structure or the presence in *Tasmanites* of significant quantities of material other than sporopollenin. It is clear that the assign~~ation~~ment of a single definitive name to both an extant biological product and possible fossil counterparts can lead to some confusion owing to transitions wrought by microbial degradation, organic assimilation and maturation. It is suggested that the term sporopollenin be only applied in a biological sense to products of living organisms.

Torbanite has been studied by oxidative degradation with alkaline potassium permanganate. A South African torbanite showed a relatively high resistance to this reagent, although carbon balance oxidations yielded carbon dioxide and non-volatile, non-oxalic acids as the major products (Down and Himus, 1941). Benzenepenta- and -hexacarboxylic acids were identified in bulk oxidations. The oxidative residues gave high oil yields on distillation (Dancy and Giedroyc, 1950). Controlled stepwise oxidation of an Australian torbanite, again with alkaline permanganate, produced aliphatic straight-chain mono- and dicarboxylic acids (C_7 to C_{29} and C_2 to C_{14} respectively) and various benzene polycarboxylic acids (Djuricic *et al.*, 1972). This sample again proved rather resistant to this particular oxidising agent.

Alkaline permanganate oxidation has been widely applied to the study of coal. The yield and nature of the products can vary widely with the conditions employed. Virtually complete oxidation, especially of bright coal, can be achieved using a high permanganate:coal ratio (Bone and Quarendon, 1926; Bone *et al.*, 1930), the products being carbon dioxide, acetic acid, oxalic acid and benzenoid acids. In the original investigations the term "benzenoid acids" was used to indicate benzene polycarboxylic acids, but the validity of the identifications has since been questioned (Francis, 1961). Bone and co-workers analysed the distribution of carbon among the products in the carbon balance technique. To achieve this the ratio of $KMnO_4$ to coal had to be greater than eight, otherwise insoluble humic acids were produced as intermediate products. These compounds are themselves capable of further oxidation, principally to oxalic acid and aromatic acids.

Investigations were carried out on coals of variable rank (Bone *et al.*, 1930) and then extended to include cellulose, lignin and peat at one extreme and anthracite at the other (Bone *et al.*, 1935). The dominant carbon balance products of cellulose oxidation were carbon dioxide and oxalic acid. Lignins produced significant quantities of aromatic acids but greater amounts of carbon dioxide and oxalic acid. Acetic acid was a minor product. Increasing maturity through the peat to anthracite range showed decreasing yields of carbon dioxide, oxalic and acetic acids and increasing amounts of aromatic acids. Benzenepenta- and -hexacarboxylic acids predominated throughout. Most of the benzenoid acids were identified, except benzoic acid.

The lithotypes vitrain, durain and fusain were later compared by carbon balance oxidations (Bone and Bard, 1937). Little qualitative difference was found between the products but the resistance to oxidation increased in the order vitrain, durain and fusain.

The intermediate humic and sub-humic acids produced by the oxidation of coal have been investigated as such (Bailey *et al.*, 1954; Bailey *et al.*, 1955), and also by examination of the products of their further degradation, (Davies and Lawson, 1967a, 1967b), which included aromatic acids and short-chain aliphatic diacids. In an investigation of methylated humic acids from soils, peats and brown coals, aliphatic diacids, benzenoid diacids and methoxy-aromatic acids were identified (Maximov *et al.*, 1972). The humic acids were found to differ, according to their source, by increasing yields of benzenoid acids and decreasing yields of methoxy-aromatic acids. Derivation of the humic acids from lignin was postulated because of the presence of the methoxy-aromatic acids.

The mechanism of the alkaline permanganate oxidation of coal was investigated by Smith and Mapstone (1957). They concluded that peripheral groups were initially oxidised to carbon dioxide and oxalic acid before the aromatic structures were broken down. Boiling alkaline permanganate was employed in their investigations but it is doubtful if such general conclusions can be applied where a variety of oxidising conditions have been employed. Following oxidations of lignin, lignite and humic acids from brown and bituminous coals and a variety of model compounds with hot nitric acid and cold permanganate, Yokokawa *et al.*, (1962), concluded that alicyclic structures were the most vulnerable to degradation and that they were destroyed in the oxidative transition of coal to humic acid. The further oxidation of humic acid was held to be less selective. The authors postulated that coals in the bituminous rank range are composed of separate alicyclic and aromatic complexes. No deductions were made on the constitution of the alicyclic systems, other than that the average composition approximated to $(CH_2)_n$.

Alkaline permanganate oxidation has also been carried out on sedimentary kerogens (Down and Himus, 1941; Dancy and Giedroyc, 1950; Robinson *et al.*, 1953; Robinson *et al.*, 1956; Robinson and Lawlor, 1961; Djuricic *et al.*, 1971; Djuricic *et al.*, 1972; Vitorovic *et al.*, 1973). The relative yields of aliphatic and aromatic products have been used as an indication of the degree of aromaticity of the coaly/non-coaly nature of a given kerogen.

One of the problems of oxidative degradation is the subsequent breakdown of the initial reaction products. In permanganate oxidation both aliphatic mono- and dibasic acids may be further oxidised under sufficiently vigorous conditions, the final more stable products being acetic and oxalic acids and carbon dioxide. Benzene polycarboxylic acids are also stable, while many alkyl-, alkoxy-, hydroxy- and oxo-substituted aromatic systems are unstable. Unsubstituted aromatic hydrocarbons are very stable. Benzenoid acids are the end products of oxidation of a wide variety of structures and are not necessarily an indication of isolated aromatic rings in a given matrix (Randall *et al.*, 1938).

Stepwise oxidative degradation can be applied to minimise secondary degradation reactions. This technique was used by Bone and co-workers in their investigations, but identification of products was limited by the then-available analytical techniques. Similar oxidations of humic acids isolated from coal led to the identification of hydroxy-carboxylic aromatic acids as initial breakdown products (Ward, 1947). Recent investigations of various kerogens by stepwise oxidation with alkaline permanganate has led to the identification of many aliphatic and aromatic products (Djuricic *et al.*, 1971; Djuricic *et al.*, 1972; Vitorovic *et al.*, 1973).

In this investigation of exinite macerals the stepwise method of Djuricic and co-workers has been applied to macerals which have been previously extracted and saponified. Small quantities of permanganate were employed at each step to ensure short reaction times, except in the final steps. However, this led to the formation of relatively large amounts of insoluble humic acids from some of the samples. Only the organic-soluble fraction has been analysed to date, and in this respect the results are of a preliminary nature as they represent only a relatively small part of the total oxidation products.

Results

Stepwise oxidation with alkaline permanganate was employed, following the method of Djuricic *et al.*, (1971) for oxidative studies of Green River shale. A sample of extracted and saponified exinite residue (*ca.* 5 gm) was suspended in potassium hydroxide solution at 80°C and oxidised with an aliquot of potassium permanganate. Initially, a ratio of maceral to permanganate of 4:1 was used, but it was found that a large number of steps were required to achieve complete oxidation and so this ratio was increased to 1:1. At each step the acids that were soluble in organic solvents were recovered and converted to their methyl esters. The total ester fractions were fractionated by preparative tlc into four fractions and analysed by gc. Infra-red spectroscopy confirmed that methyl esters had been obtained (absorption bands in the 1720 to 1735 cm^{-1} region) and they were identified by gc co-injection with authentic methyl esters of n-fatty acids, saturated straight chain α,ω-dicarboxylic acids and benzene polycarboxylic acids. Oxidation steps were repeated until the aliquot of oxidant was not completely used up after a reaction time of 8 hrs. Fig. 90 shows the procedure used in a schematic form.

Quantitative data for all the oxidations carried out are given in Table 47. Qualitative information concerning the oxidation products is given below under individual sample headings. The complete experimental details of the work are presented collectively at the end of this chapter.

Sporinite

High Hazles Gedling (13 oxidation steps)

a) Monocarboxylic acid fraction (Fig. 91)

The yield of monomethyl esters showed no significant variations

Fig. 90: Flow diagram of the procedure used for the oxidation of exinites

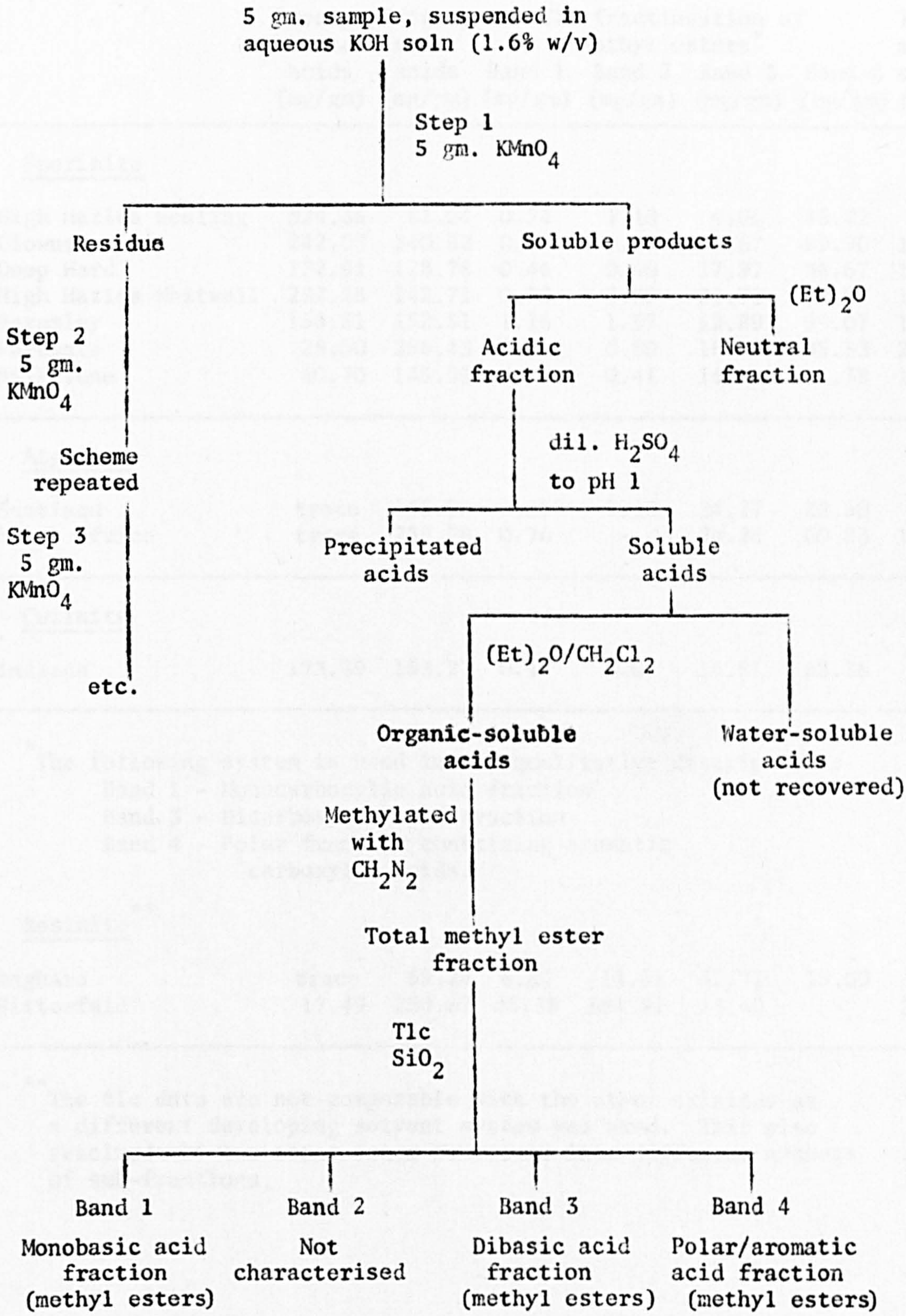

Table 47: Yields of the products obtained from the oxidation of extracted and saponified exinites

	Precipitated acids (mg/gm)	Extracted acids (mg/gm)	Tlc fractionation of methyl esters* Band 1 (mg/gm)	Band 2 (mg/gm)	Band 3 (mg/gm)	Band 4 (mg/gm)	Total methyl esters (mg/gm)
Sporinite							
High Hazles Gedling	324.36	81.94	0.74	1.18	4.06	45.22	51.20
Clowne	242.03	140.52	0.64	0.40	15.67	99.90	116.63
Deep Hard	132.91	128.78	0.46	0.40	17.97	88.67	107.50
High Hazles Whitwell	232.48	142.71	0.72	0.32	21.51	92.27	114.82
Barnsley	156.31	152.51	1.16	1.57	12.89	99.07	114.69
Parkgate	28.50	256.43	0.61	0.80	16.47	205.53	223.41
Silkstone	40.70	145.85	0.47	0.41	16.08	114.38	131.44
Alginite							
Scotland	trace	145.08	0.28	0.12	24.27	28.50	53.17
South Africa	trace	232.78	0.76	-	74.24	60.83	135.83
Cutinite							
Indiana	173.39	153.27	0.18	0.07	14.51	68.38	83.14

*The following system is used in the qualitative descriptions:
Band 1 - Monocarboxylic acid fraction
Band 3 - Dicarboxylic acid fraction
Band 4 - Polar fraction containing aromatic carboxylic acids.

	Precipitated acids (mg/gm)	Extracted acids (mg/gm)	Band 1 (mg/gm)	Band 2 (mg/gm)	Band 3 (mg/gm)	Band 4 (mg/gm)	Total methyl esters (mg/gm)
Resinite**							
Maghara	trace	69.24	6.84	14.61	32.71	15.09	69.25
Bitterfeld	17.49	250.67	45.39	164.92	13.40	-	223.71

**The tlc data are not comparable with the other exinites as a different developing solvent system was used. This also resolved the two total ester fractions into different numbers of sub-fractions.

Fig. 91. Methyl esters of monocarboxylic acids from the oxidation of High Hazles Gedling sporinite

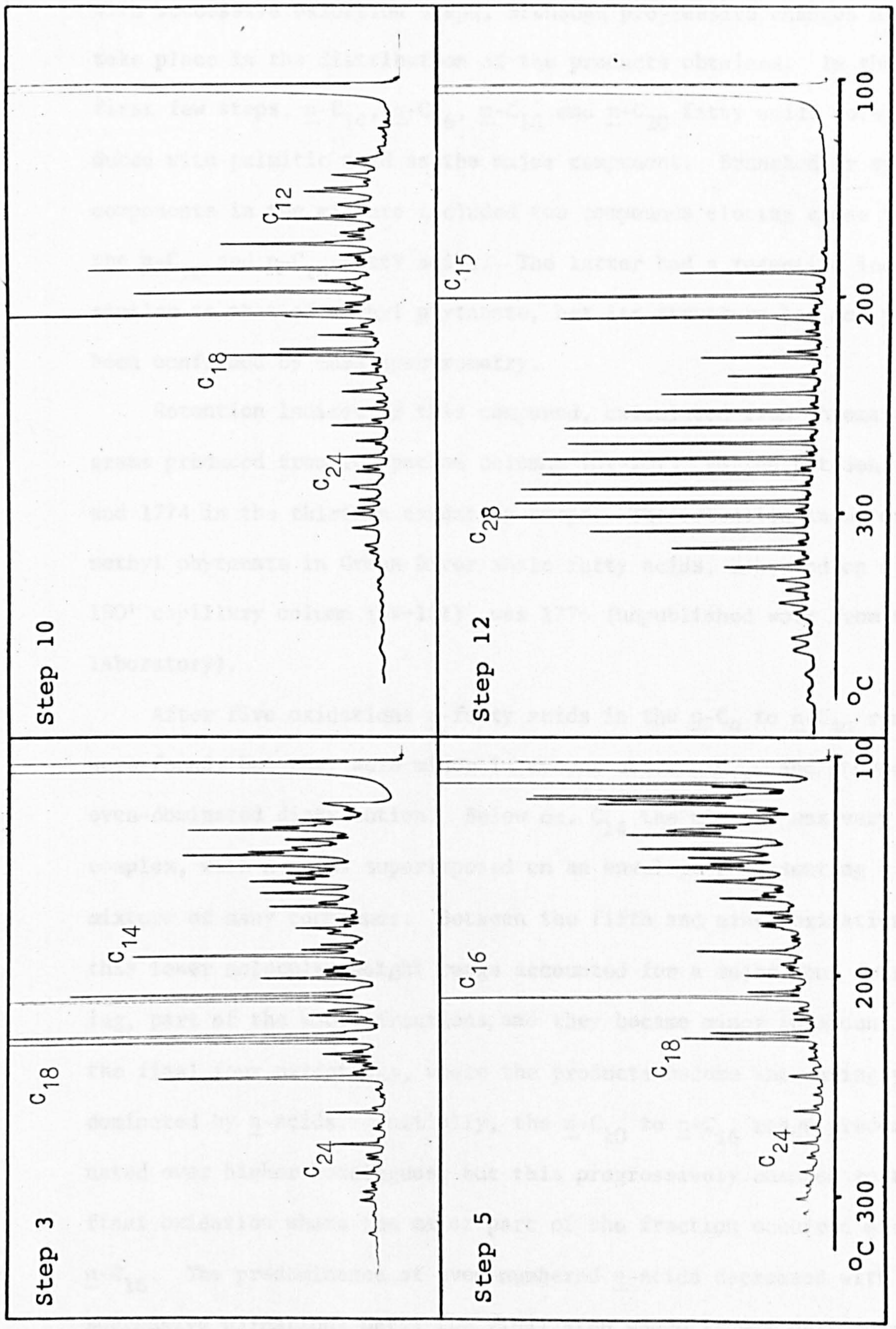

Gas chromatographic conditions: 10'x1/16" o.d. column containing 3% OV-101 on Varaport 30 (100-120 mesh); programmed 100-300°C at 4°/min; detector 300°; injector 300°; nitrogen 60 p.s.i.

with successive oxidation steps, although progressive changes did take place in the distribution of the products obtained. In the first few steps, n-C_{14}, n-C_{16}, n-C_{18} and n-C_{20} fatty acids were produced with palmitic acid as the major component. Branched or cyclic components in the mixture included two compounds eluting close to the n-C_{16} and n-C_{18} fatty acids. The latter had a retention index similar to that of methyl phytanate, but its structure has not yet been confirmed by mass spectrometry.

Retention indices of this compound, calculated from chromatograms produced from 10' packed columns (OV-101), varied between 1772 and 1774 in the thirteen oxidation steps. The retention index of methyl phytanate in Green River shale fatty acids, measured on a 150' capillary column (OV-101), was 1776 (unpublished work from this laboratory).

After five oxidations n-fatty acids in the n-C_9 to n-C_{30} range were found, but they were minor in amount above n-C_{18}, and showed an even-dominated distribution. Below *ca*. C_{14} the mixture was very complex, with n-acids superimposed on an envelope representing a mixture of many compounds. Between the fifth and ninth oxidations this lower molecular weight range accounted for a major, but decreasing, part of the whole fractions, and they became minor in amount in the final four oxidations, where the products became increasingly dominated by n-acids. Initially, the n-C_{10} to n-C_{16} range predominated over higher homologues, but this progressively changed to the final oxidation where the major part of the fraction occurred above n-C_{16}. The predominance of even-numbered n-acids decreased with successive oxidations until the final step where it was only found in the n-C_{16} to n-C_{22} range.

b) Dicarboxylic acid fraction (Fig. 92)

The yield of the di-acid fraction varied widely from step to step

Fig. 92. Dimethyl esters of dicarboxylic acids from the oxidation of High Hazles Gedling sporinite

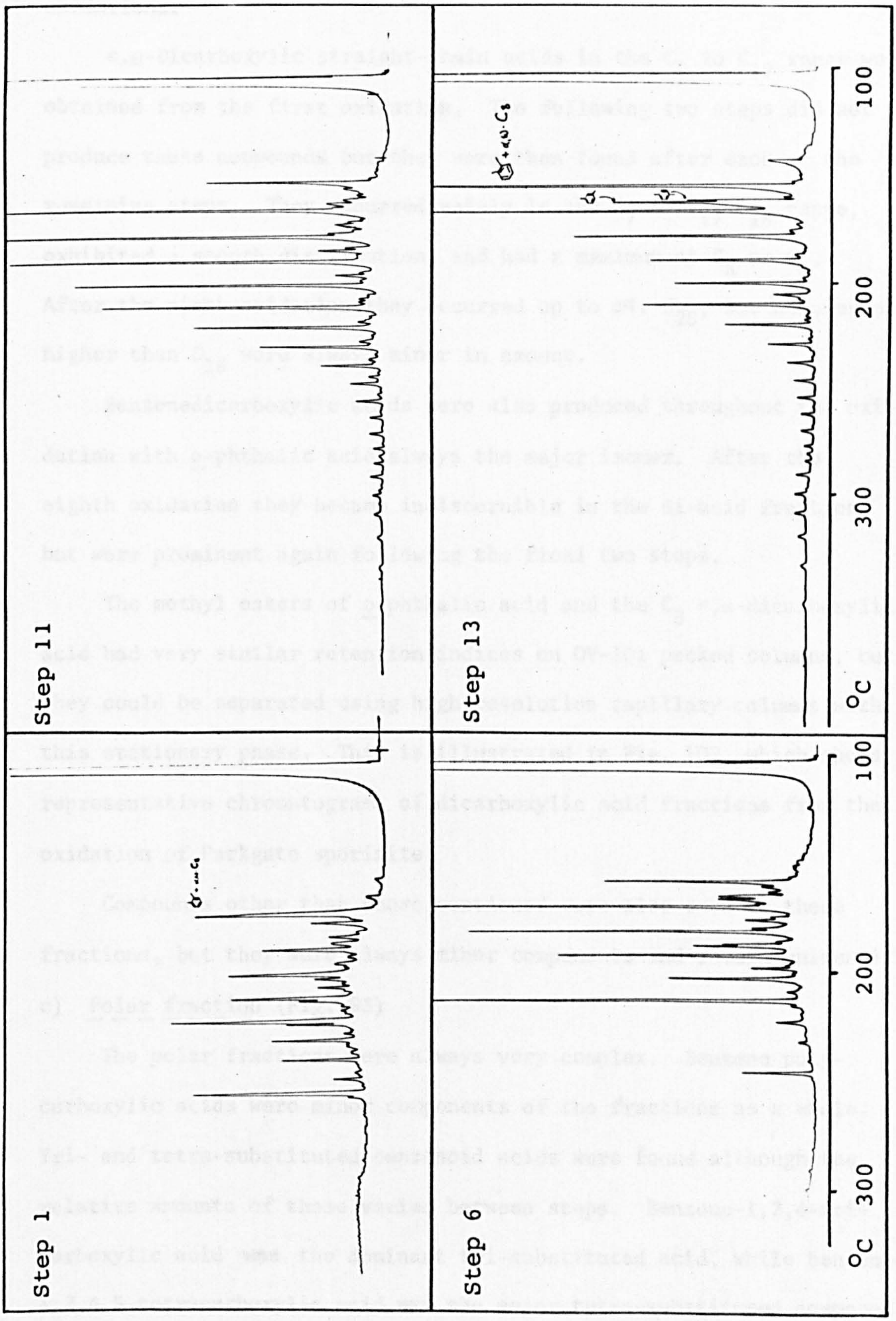

Gas chromatographic conditions as in Fig. 91.

but consistently higher yields were obtained following the final four oxidations.

α,ω-Dicarboxylic straight-chain acids in the C_9 to C_{17} range were obtained from the first oxidation. The following two steps did not produce these compounds but they were then found after each of the remaining steps. They occurred mainly in the C_7 to C_{17}-C_{18} range, exhibited a smooth distribution, and had a maximum at C_8 or C_9. After the ninth oxidation they occurred up to *ca*. C_{28}, but homologues higher than C_{18} were always minor in amount.

Benzenedicarboxylic acids were also produced throughout the oxidation with o-phthalic acid always the major isomer. After the eighth oxidation they became indiscernible in the di-acid fraction, but were prominent again following the final two steps.

The methyl esters of o-phthalic acid and the C_8 α,ω-dicarboxylic acid had very similar retention indices on OV-101 packed columns, but they could be separated using high-resolution capillary columns with this stationary phase. This is illustrated in Fig. 107, which shows representative chromatograms of dicarboxylic acid fractions from the oxidation of Parkgate sporinite.

Compounds other than those mentioned were also seen in these fractions, but they were always minor components and remain unidentified.

c) Polar fraction (Fig. 93)

The polar fractions were always very complex. Benzene polycarboxylic acids were minor components of the fractions as a whole. Tri- and tetra-substituted benzenoid acids were found although the relative amounts of these varied between steps. Benzene-1,2,4-tricarboxylic acid **was** the dominant tri-substituted acid, while benzene-1,2,4,5-tetracarboxylic acid **was** the major tetra-substituted compound. Only after the final oxidation was trimellitic acid (benzene-1,2,4-tricarboxylic acid) the major component of the whole fraction.

Fig. 93. Methyl esters of the acids of the polar fraction from the oxidation of High Hazles Gedling sporinite

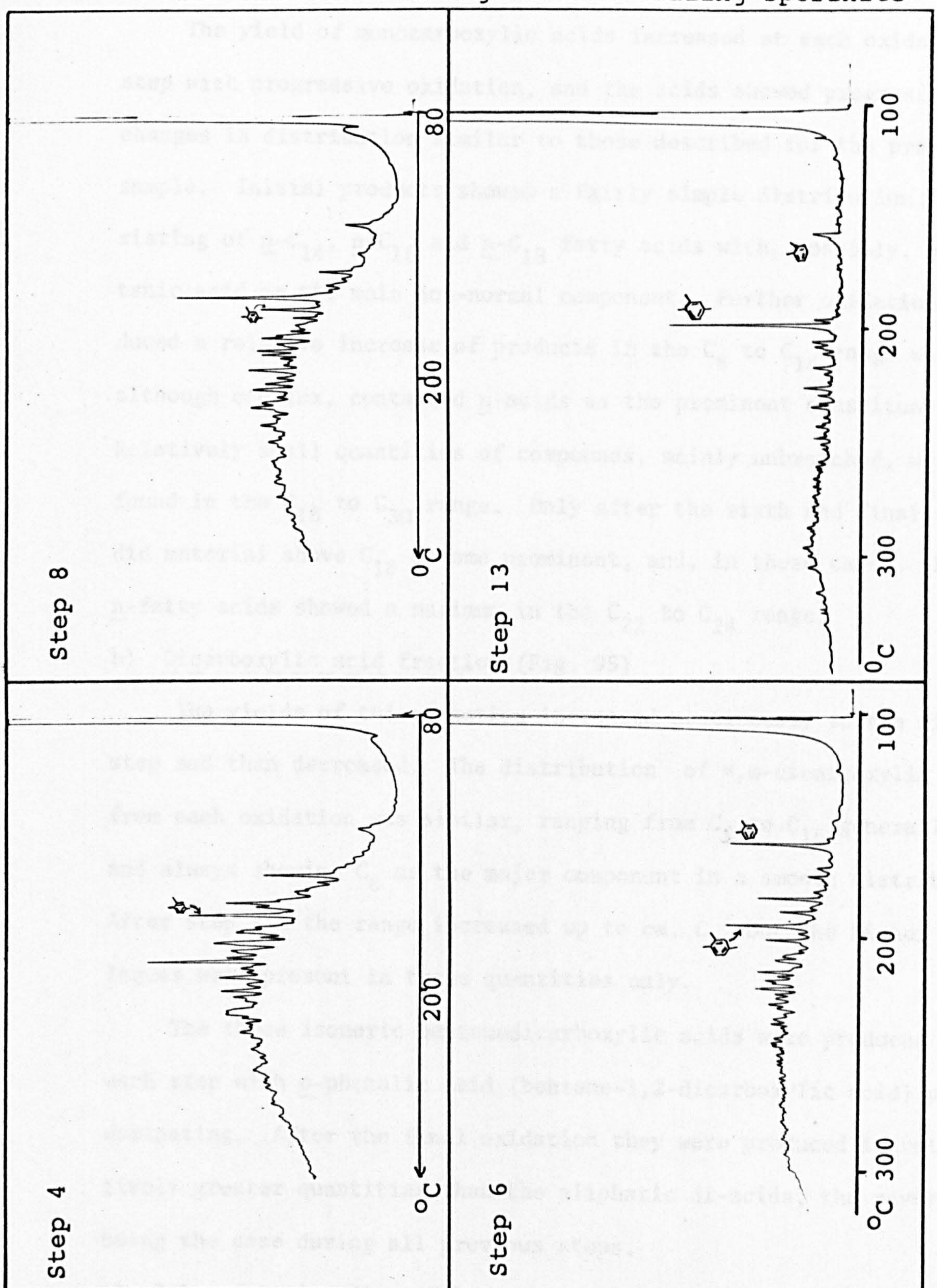

Gas chromatographic conditions as in Fig. 91 for steps 6 & 13. For steps 4 & 8: 10'x1/8" o.d. column containing 3% OV-101 on Varaport 30 (100-120 mesh); programmed 80-300^{o}C at 4^{o}/min; detector 300^{o}; injector 300^{o}; nitrogen 40 p.s.i.

Clowne (7 oxidation steps)

a) Monocarboxylic acid fraction (Fig. 94)

The yield of monocarboxylic acids increased at each oxidation step with progressive oxidation, and the acids showed progressive changes in distribution similar to those described for the previous sample. Initial products showed a fairly simple distribution, consisting of n-C_{14}, n-C_{16} and n-C_{18} fatty acids with, possibly, phytanic acid as the main non-normal component. Further oxidation produced a relative increase of products in the C_8 to C_{16} range which, although complex, contained n-acids as the prominent constituents. Relatively small quantities of compounds, mainly unbranched, were found in the C_{18} to C_{30} range. Only after the sixth and final steps did material above C_{18} become prominent, and, in these cases, the n-fatty acids showed a maximum in the C_{22} to C_{24} range.

b) Dicarboxylic acid fraction (Fig. 95)

The yields of this fraction increased continously to the fifth step and then decreased. The distribution of α,ω-dicarboxylic acids from each oxidation was similar, ranging from C_5 to C_{16} generally, and always showing C_8 as the major component in a smooth distribution. After step six the range increased up to *ca*. C_{20} but the higher homologues were present in trace quantities only.

The three isomeric benzenedicarboxylic acids were produced at each step with o-phthalic acid (benzene-1,2-dicarboxylic acid) predominating. After the final oxidation they were produced in relatively greater quantities than the aliphatic di-acids, the reverse being the case during all previous steps.

c) Polar fraction (Fig. 96)

The rate of generation of polar compounds increased from the first to the fifth step, and then decreased. Apart from the final step, the distribution of benzene polycarboxylic acids remained fairly

Fig. 94. Methyl esters of monocarboxylic acids from the oxidation of Clowne sporinite

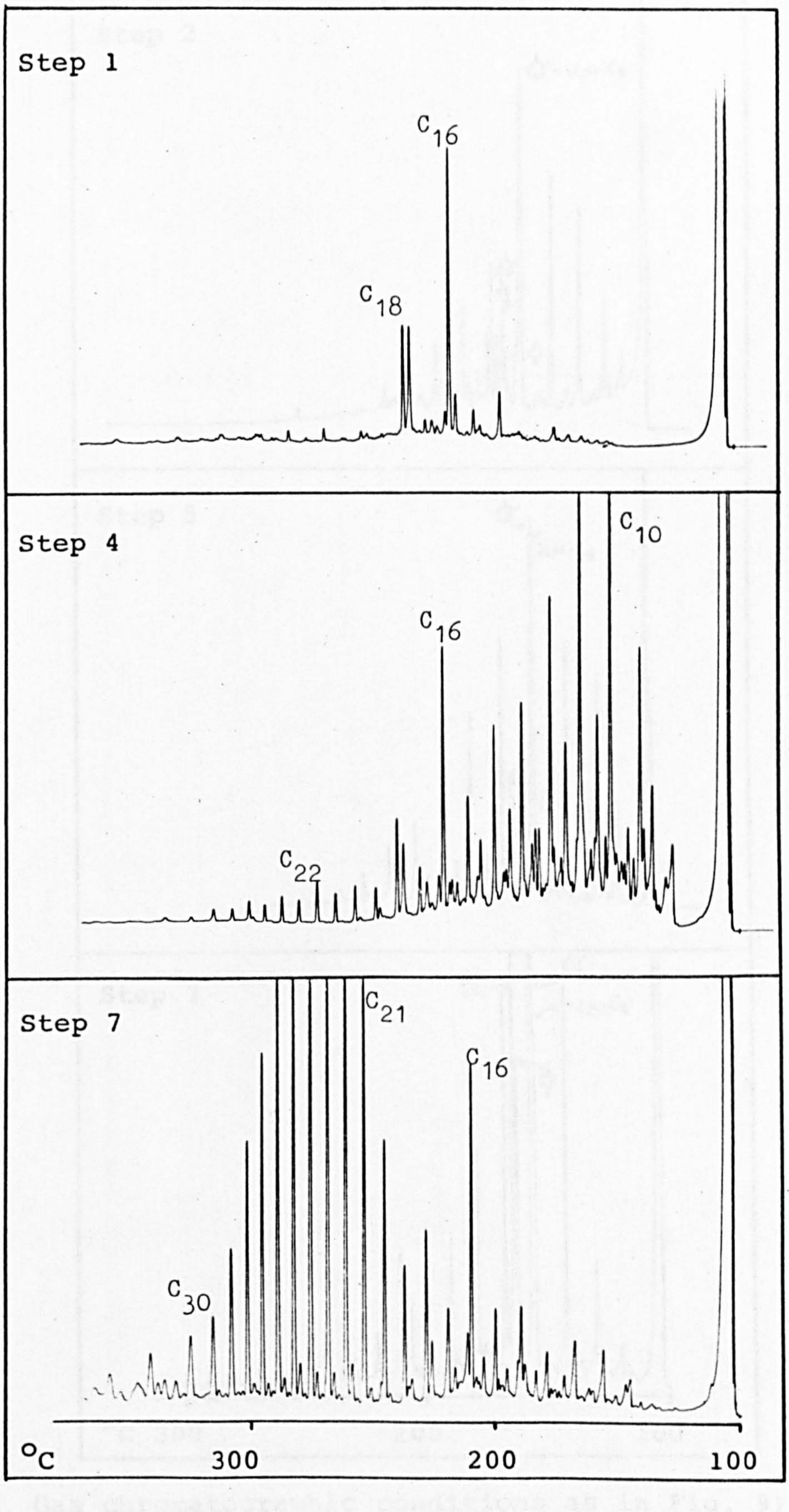

Gas chromatographic conditions as in Fig. 91.

Fig. 95. Dimethyl esters of dicarboxylic acids from the oxidation of Clowne sporinite

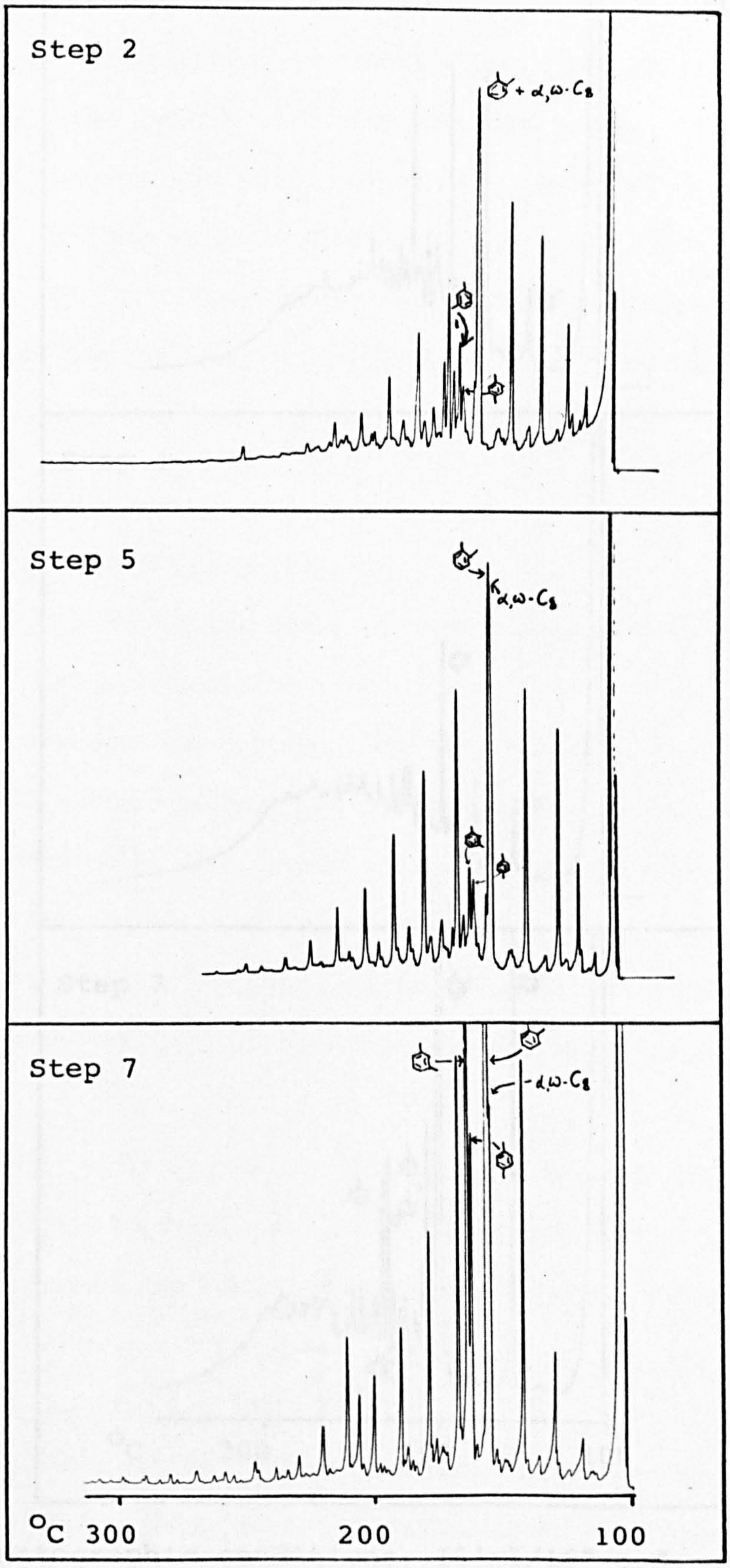

Gas chromatographic conditions as in Fig. 91.

Fig. 96. Methyl esters of the acids of the polar fraction from the oxidation of Clowne sporinite

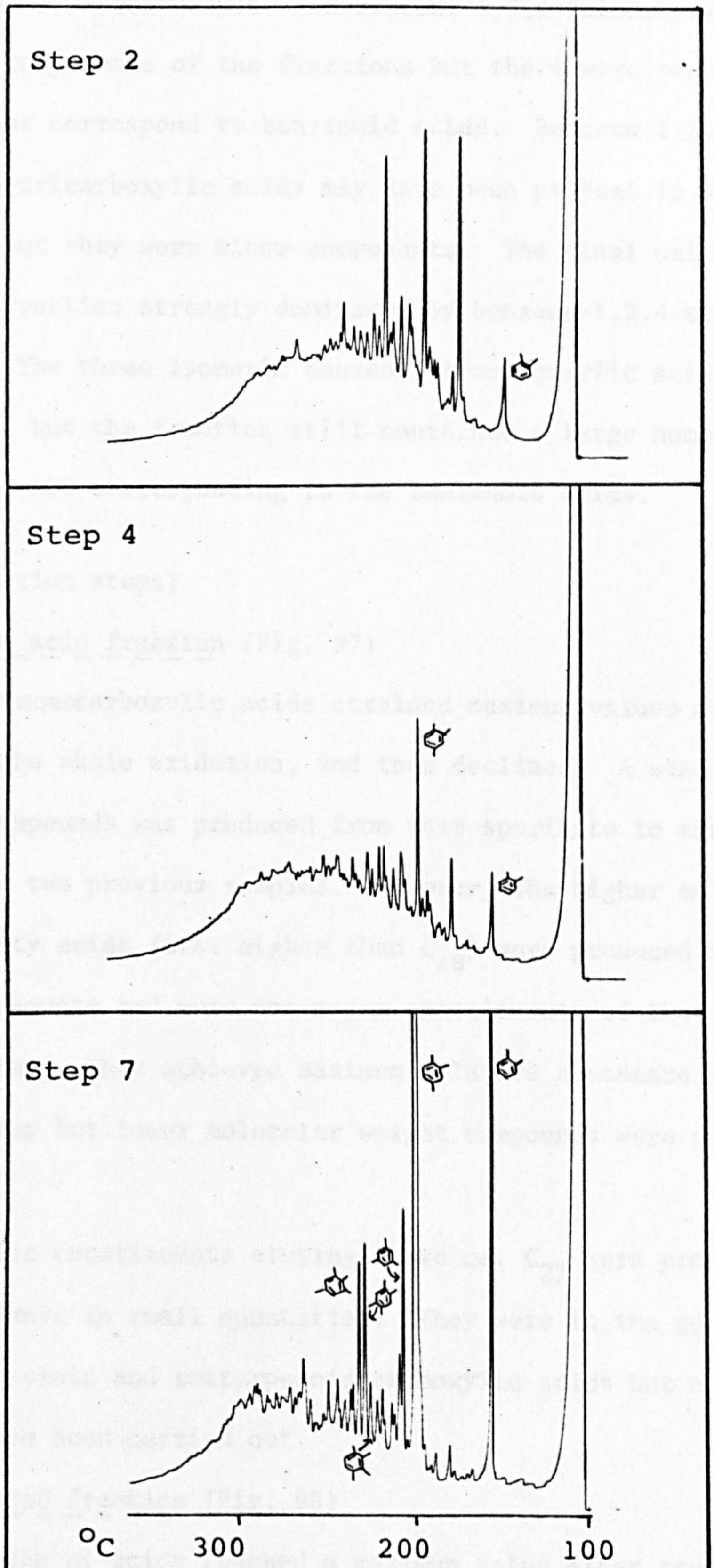

Gas chromatographic conditions: 10'x1/16" o.d. column containing 5% OV-1 on Varaport 30 (100-120 mesh); programmed 100-300°C at 6°/min; detector 300°; injector 300°; nitrogen 60 p.s.i.

constant. Benzene-1,2-dicarboxylic and benzene-1,2,4-tricarboxylic acids were major components of the fractions but there were many others that did not correspond to benzenoid acids. Benzene-1,2,3- and benzene-1,3,5-tricarboxylic acids may have been present in some of the fractions but they were minor components. The final oxidation produced a polar fraction strongly dominated by benzene-1,2,4-tricarboxylic acid. The three isomeric benzenetetracarboxylic acids were also present, but the fraction still contained a large number of other compounds not corresponding to the benzenoid acids.

Deep Hard (6 oxidation steps)

a) Monocarboxylic acid fraction (Fig. 97)

The yields of monocarboxylic acids attained maximum values near the mid-point of the whole oxidation, and then declined. A similar distribution of compounds was produced from this sporinite to those described from the two previous samples. However, the higher molecular weight *n*-fatty acids (i.e. higher than C_{18}) were produced in relatively small amounts and were not major constituents of the final oxidation step. They achieved maximum relative abundance in the penultimate step but lower molecular weight compounds were predominant.

Branched/cyclic constituents eluting above *ca.* C_{27} were produced throughout, but always in small quantities. They were in the gc elution range of steroid and triterpenoid carboxylic acids but no identifications have been carried out.

b) Dicarboxylic acid fraction (Fig. 98)

The yield of the di-acids reached a maximum value after step four and then declined. The range and distribution of α,ω-dicarboxylic acids was similar to those previously described. They were produced after each step, showing a maximum range of C_5 to *ca.* C_{25}.

Fig. 97. Methyl esters of monocarboxylic acids from the oxidation of Deep Hard sporinite

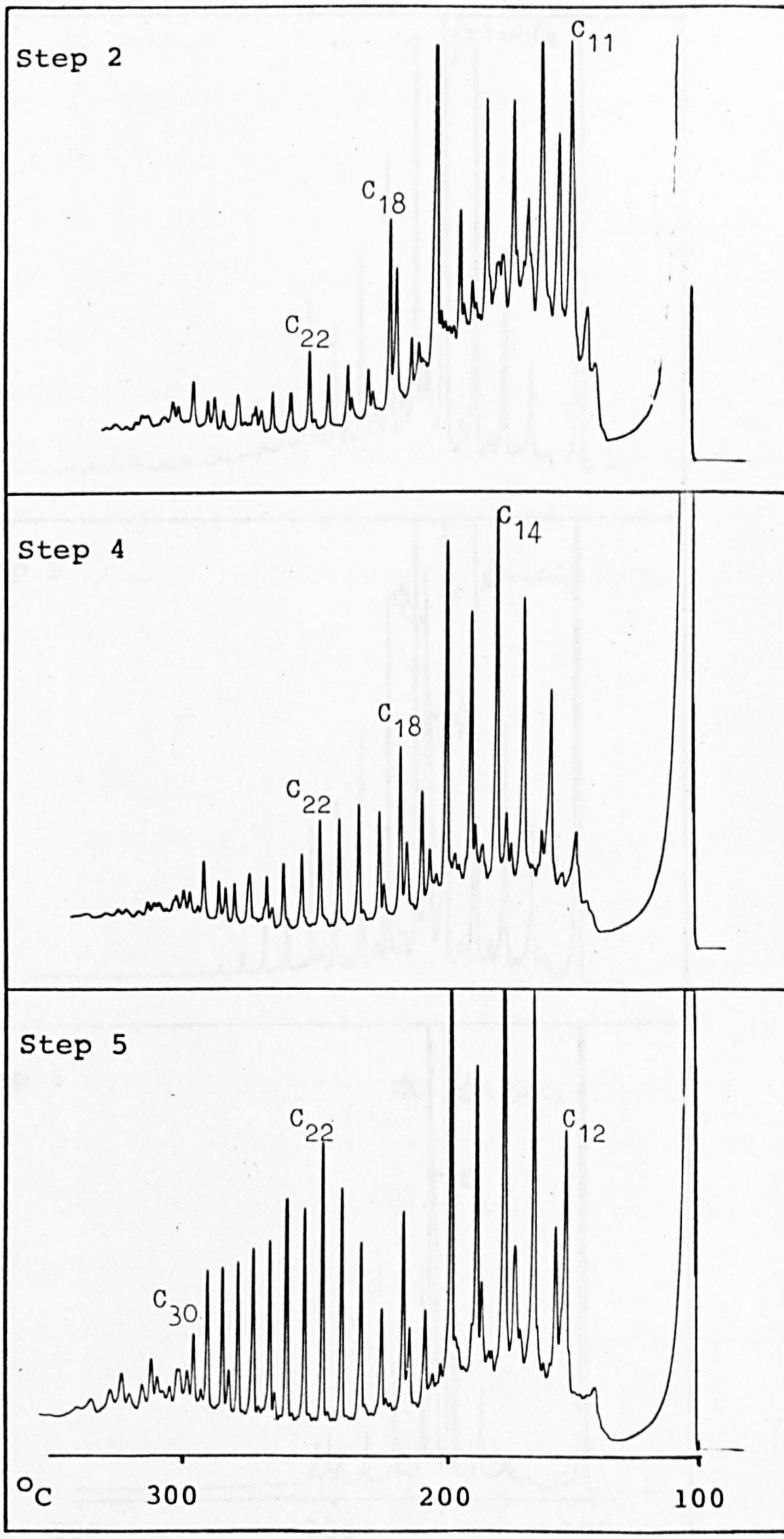

Gas chromatographic conditions as in Fig. 91, except stationary phase 2% OV-101.

Fig. 98. Dimethyl esters of dicarboxylic acids from the oxidation of Deep Hard sporinite

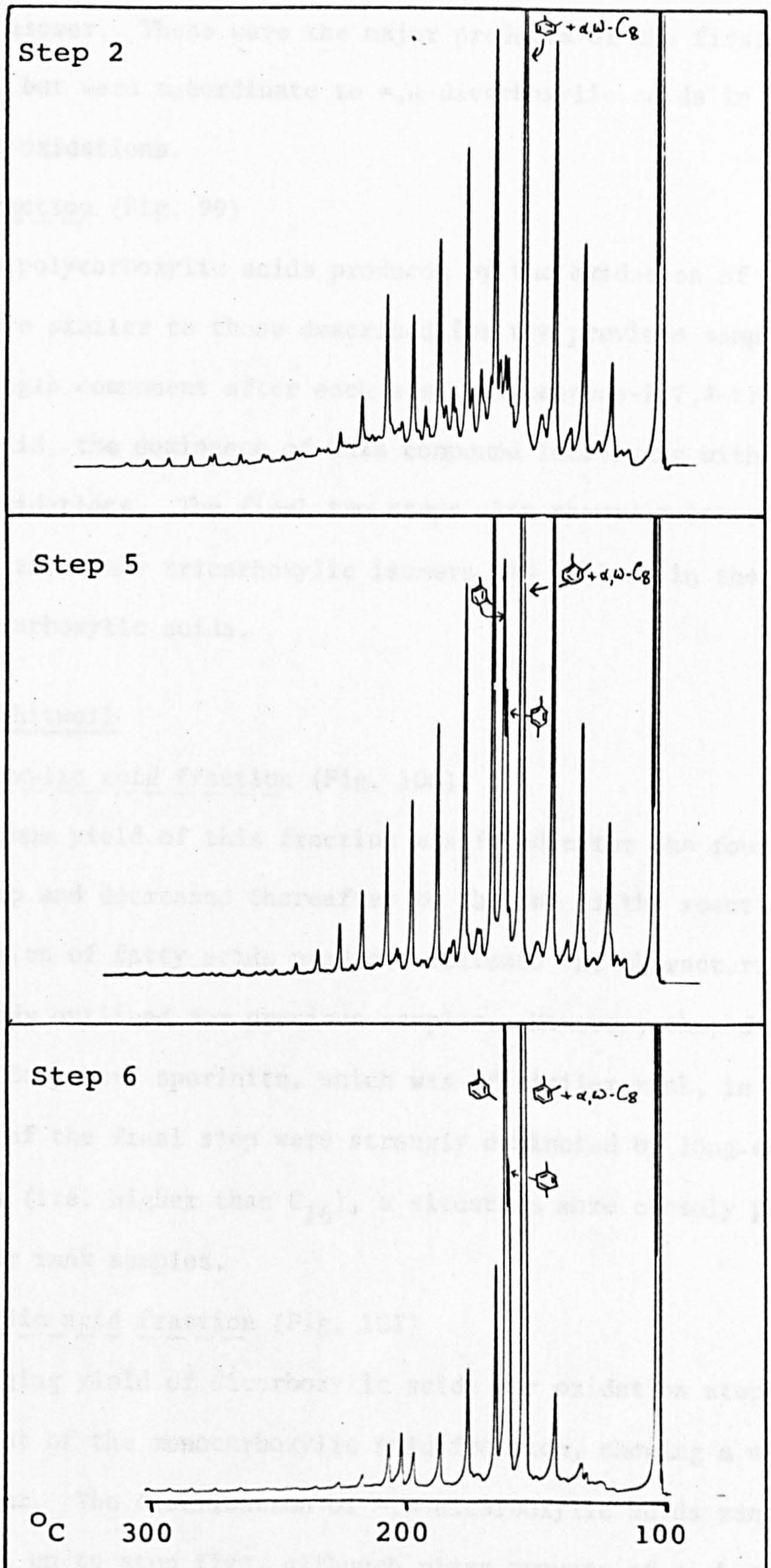

Gas chromatographic conditions as in Fig. 97.

Benzenedicarboxylic acids were also produced with o-phthalic acid as the main isomer. These were the major products of the first and final steps, but were subordinate to α,ω-dicarboxylic acids in the intermediate oxidations.

c) Polar fraction (Fig. 99)

Benzene polycarboxylic acids produced by the oxidation of this sporinite were similar to those described for the previous samples. The major single component after each step was benzene-1,2,4-tricarboxylic acid, the dominance of this compound increasing with successive oxidations. The final two steps also showed relative increases in the other tricarboxylic isomers, as well as in the three benzenetetracarboxylic acids.

High Hazles Whitwell

a) Monocarboxylic acid fraction (Fig. 100)

The maximum yield of this fraction was found after the fourth oxidation step and decreased thereafter to the end of the reaction. The distribution of fatty acids produced followed the characteristic changes already outlined for previous samples. However, they differed from that of Deep Hard sporinite, which was of similar rank, in that the products of the final step were strongly dominated by long-chain n-fatty acids (i.e. higher than C_{16}), a situation more closely paralleling lower rank samples.

b) Dicarboxylic acid fraction (Fig. 101)

The changing yield of dicarboxylic acids per oxidation step was similar to that of the monocarboxylic acid fraction, showing a maximum after step four. The distribution of α,ω-dicarboxylic acids ranged from C_5 to C_{17} up to step five, although minor amounts of higher homologues extended up to *ca.* C_{27} after the third oxidation. The C_8 di-acid was the major component throughout.

Fig. 99. Methyl esters of the acids of the polar fraction from the oxidation of Deep Hard sporinite

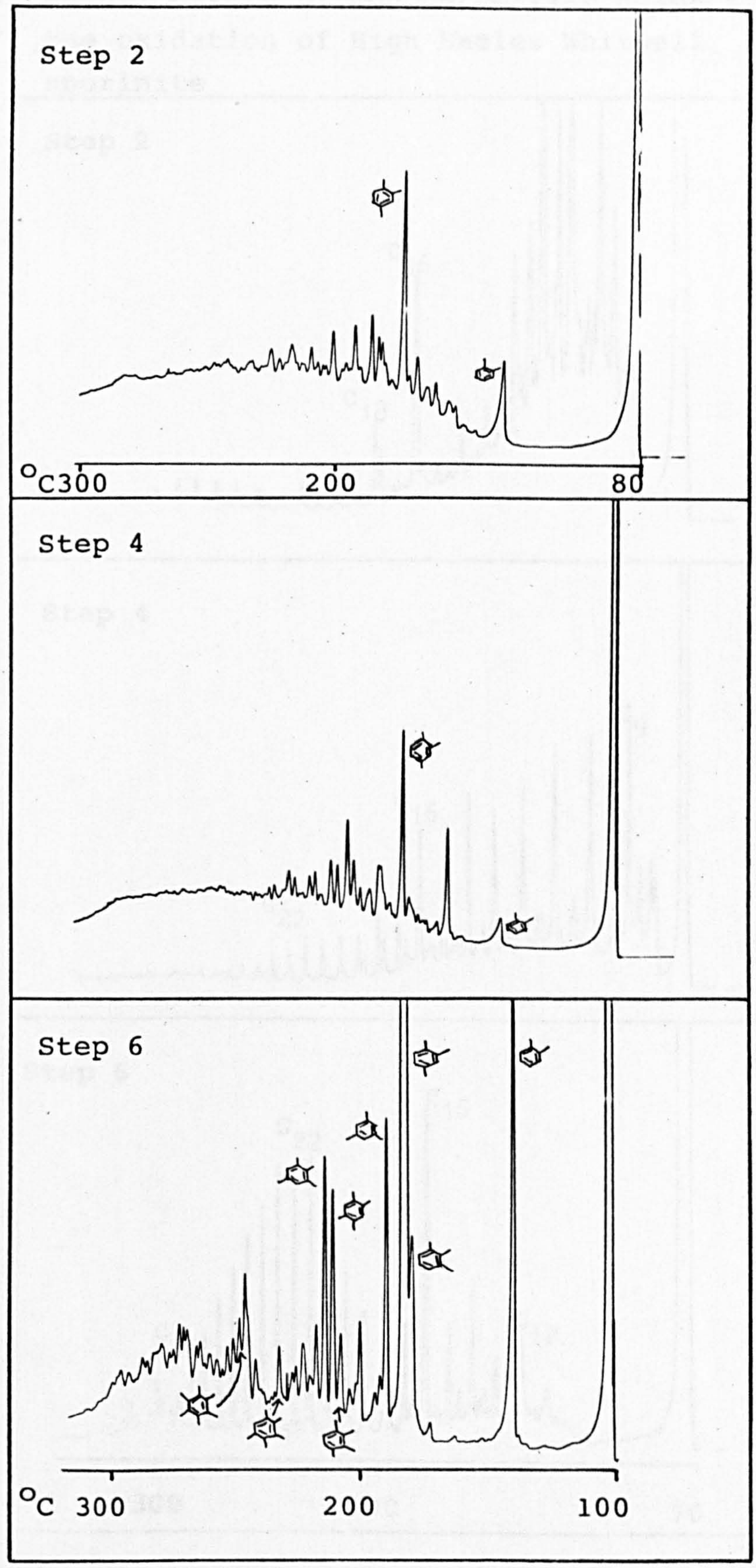

Gas chromatographic conditions for step 2: 5'x1/8" o.d. column containing 3% OV-101 on Varaport 30 (100-120 mesh); programmed 80-300°C at 4°/min; detector 300°; injector 300°; nitrogen 40 p.s.i.
For steps 4 & 6, gc conditions as in Fig. 97.

Fig. 100. Methyl esters of monocarboxylic acids from the oxidation of High Hazles Whitwell sporinite

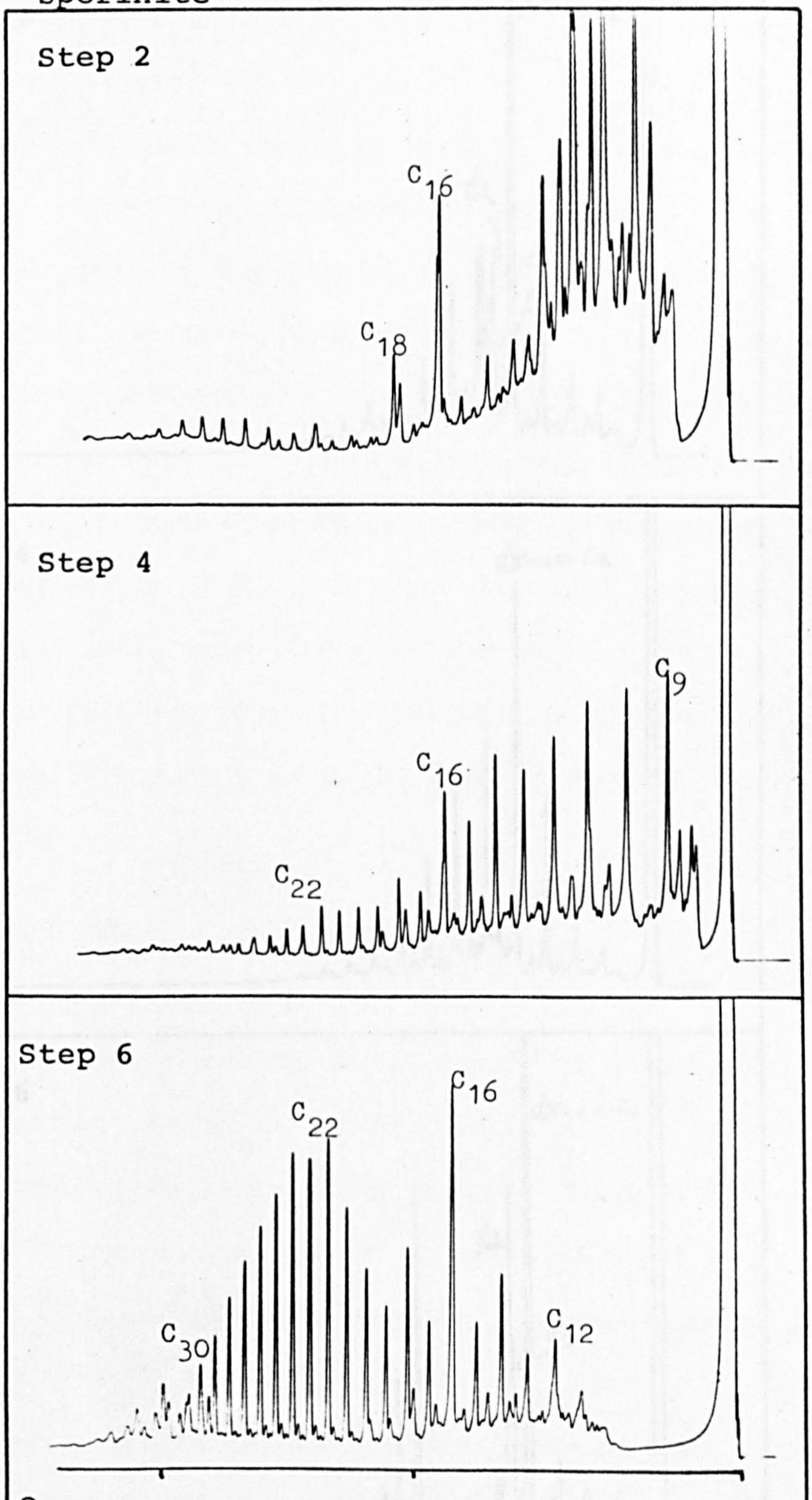

Gas chromatographic conditions as in Fig. 97, except programmed 70-300°C.

Fig. 101. Dimethyl esters of dicarboxylic acids from the oxidation of High Hazles Whitwell sporinite

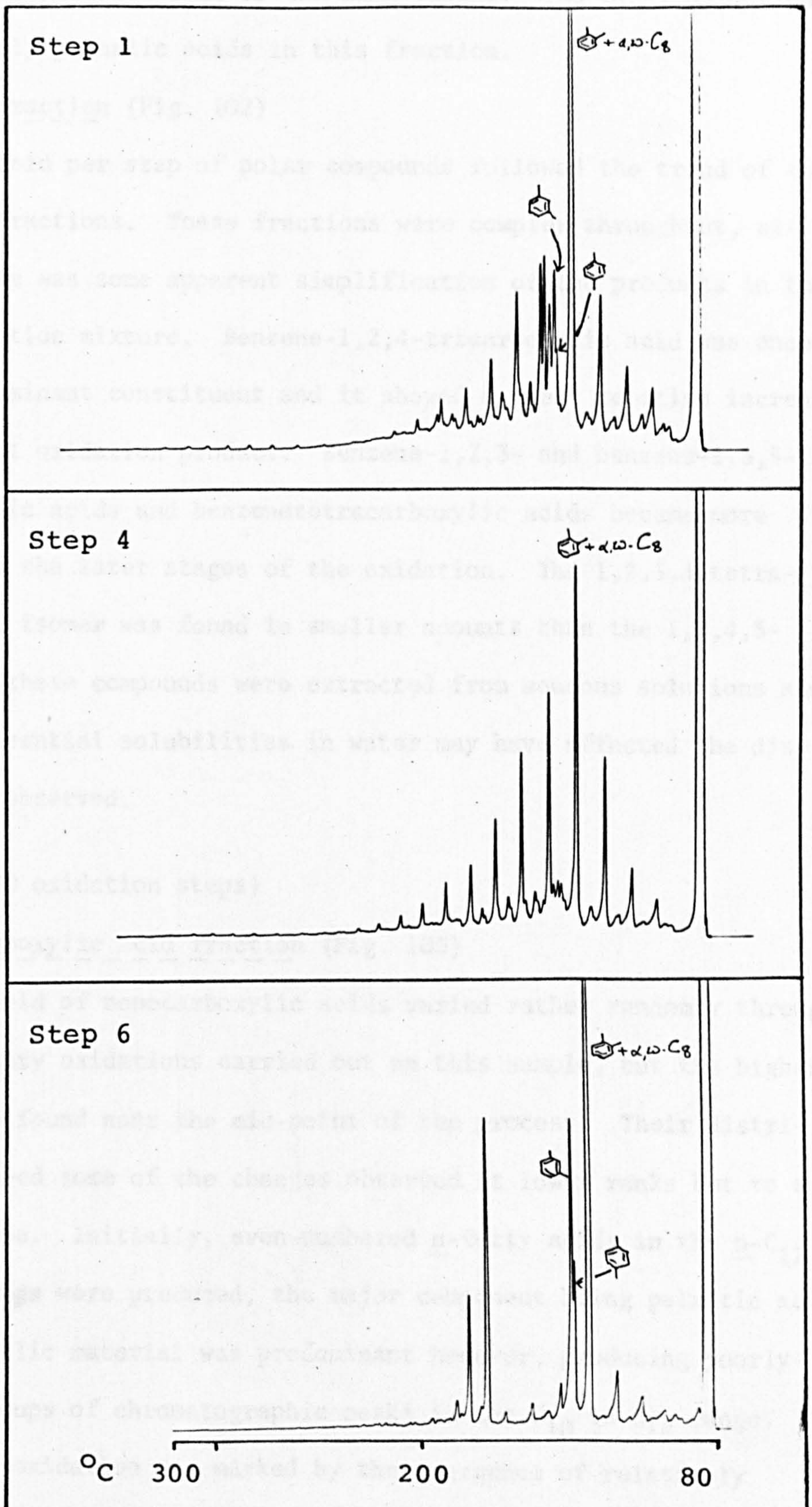

Gas chromatographic conditions as in Fig. 97, except programmed 80-300 °C.

Benzenedicarboxylic acids were also produced by each oxidation, again with o-phthalic acid as the main isomer. The final oxidation produced only phthalic acids in this fraction.

c) Polar fraction (Fig. 102)

The yield per step of polar compounds followed the trend of the other tlc fractions. These fractions were complex throughout, although there was some apparent simplification of the products in the final oxidation mixture. Benzene-1,2,4-tricarboxylic acid was once more the dominant constituent and it showed a great relative increase in the final oxidation product. Benzene-1,2,3- and benzene-1,3,5-tricarboxylic acids and benzenetetracarboxylic acids became more apparent in the later stages of the oxidation. The 1,2,3,4-tetra-substituted isomer was found in smaller amounts than the 1,2,4,5-isomer but these compounds were extracted from aqueous solutions and their differential solubilities in water may have affected the distributions observed.

Barnsley (20 oxidation steps)

a) Monocarboxylic acid fraction (Fig. 103)

The yield of monocarboxylic acids varied rather randomly throughout the twenty oxidations carried out on this sample, but the highest yields were found near the mid-point of the process. Their distributions showed some of the changes observed at lower ranks but to a lesser degree. Initially, even-numbered n-fatty acids in the n-C_{12} to n-C_{24} range were produced, the major component being palmitic acid. Branched/cyclic material was predominant however, producing poorly-resolved groups of chromatographic peaks in the C_{10} to C_{18} range. Progressive oxidation was marked by the emergence of relatively greater quantities of n-acids, especially below n-C_{16}, which itself became less conspicuous in the fractions as a whole. The lower range

Fig. 102. Methyl esters of the acids of the polar fraction from the oxidation of High Hazles Whitwell sporinite

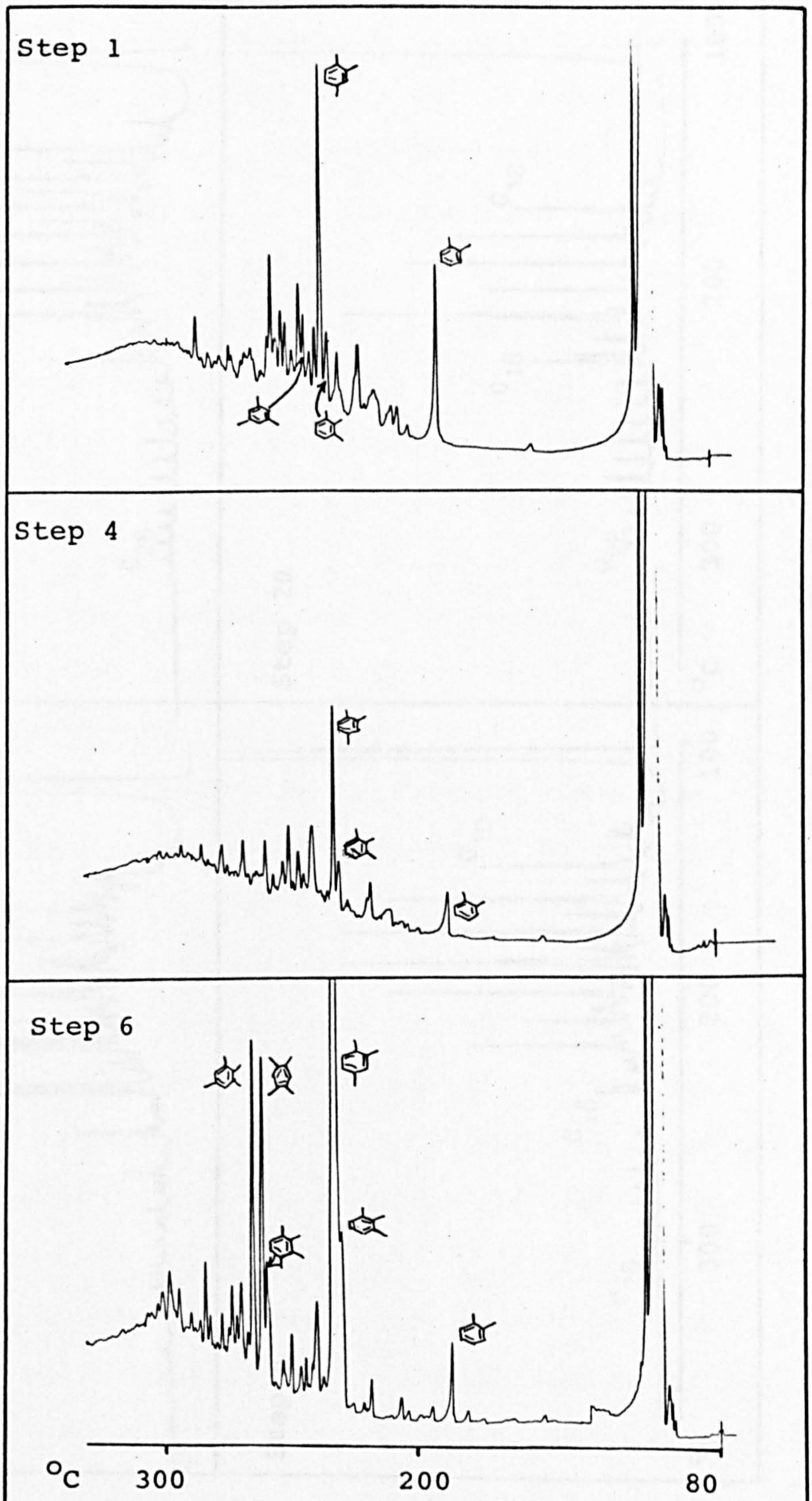

Gas chromatographic conditions: 20'x1/16" o.d. column containing 3% OV-101 on Varaport 30 (100-120 mesh); programmed 80-300°C at 4°/min; detector 300°; injector 300°; nitrogen 60 p.s.i.

Fig. 103. Methyl esters of monocarboxylic acids from the oxidation of Barnsley sporinite

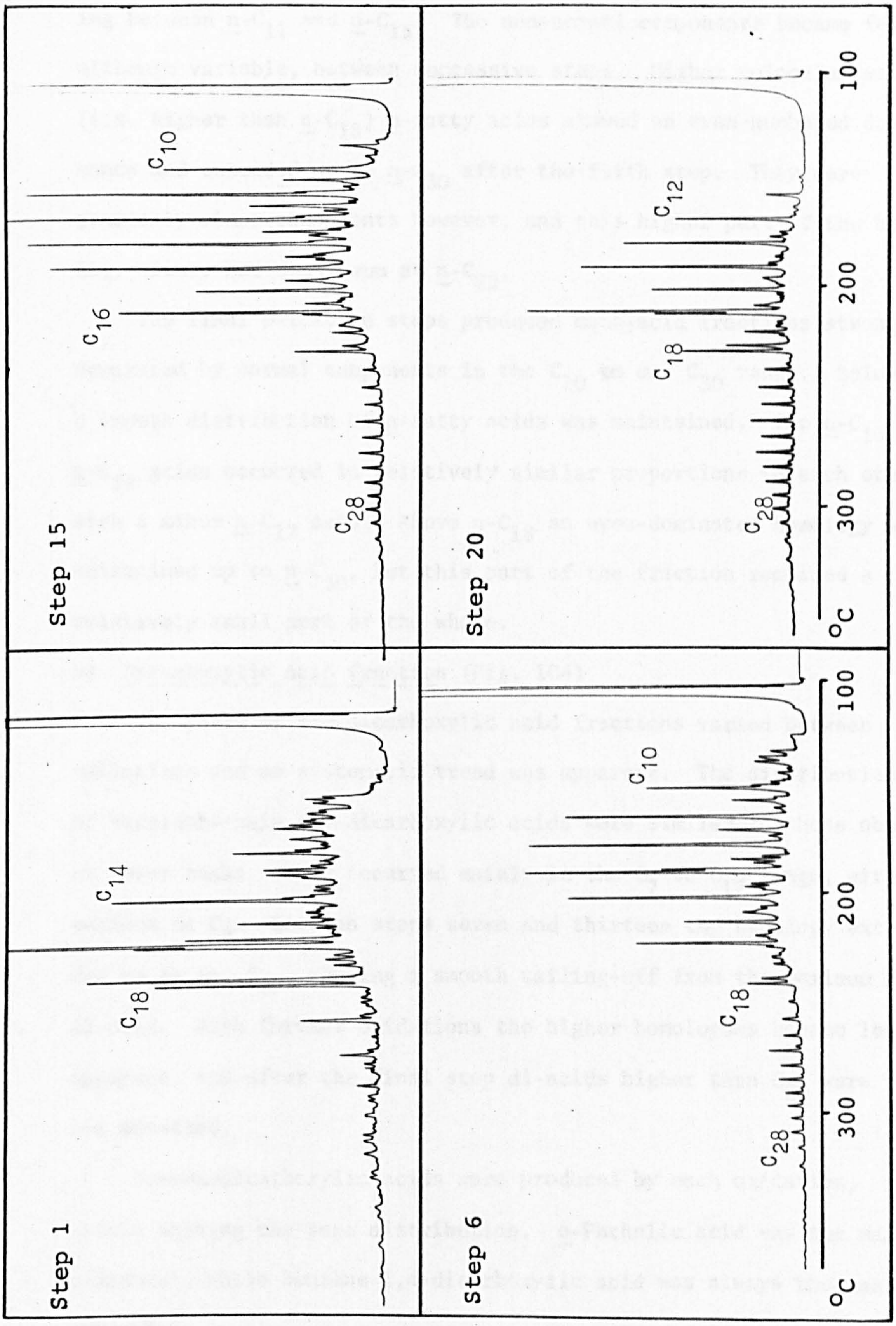

Gas chromatographic conditions as in Fig. 91.

of n-fatty acids showed a smooth distribution with the maximum varying between n-C_{11} and n-C_{13}. The non-normal components became fewer, although variable, between successive steps. Higher molecular weight (i.e. higher than n-C_{18}) n-fatty acids showed an even-numbered dominance and extended up to n-C_{30} after the fifth step. They were generally minor components however, and this higher part of the homology always had a maximum at n-C_{22}.

The final oxidative steps produced mono-acid fractions strongly dominated by normal components in the C_{10} to *ca.* C_{30} range. Below C_{16} a smooth distribution of n-fatty acids was maintained. The n-C_{16} and n-C_{18} acids occurred in relatively similar proportions to each other with a minor n-C_{17} acid. Above n-C_{18} an even-dominated homology was maintained up to n-C_{30}, but this part of the fraction remained a relatively small part of the whole.

b) Dicarboxylic acid fraction (Fig. 104)

The yield of the dicarboxylic acid fractions varied between oxidations and no systematic trend was apparent. The distributions of straight-chain α,ω-dicarboxylic acids were similar to those observed at lower ranks. They occurred mainly in the C_7 to C_{17} range, with a maximum at C_8. Between steps seven and thirteen the homology extended up to *ca.* C_{27}, showing a smooth tailing-off from the maximum C_8 di-acid. With further oxidations the higher homologues became less apparent, and after the final step di-acids higher than C_{20} were not detected.

Benzenedicarboxylic acids were produced by each oxidation, always showing the same distribution. o-Phthalic acid was the main component, while benzene-1,4-dicarboxylic acid was always the smallest component.

c) Polar fraction (Fig. 105)

The yield of polar compounds was variable between steps and

Fig. 104. Dimethyl esters of dicarboxylic acids from the oxidation of Barnsley sporinite

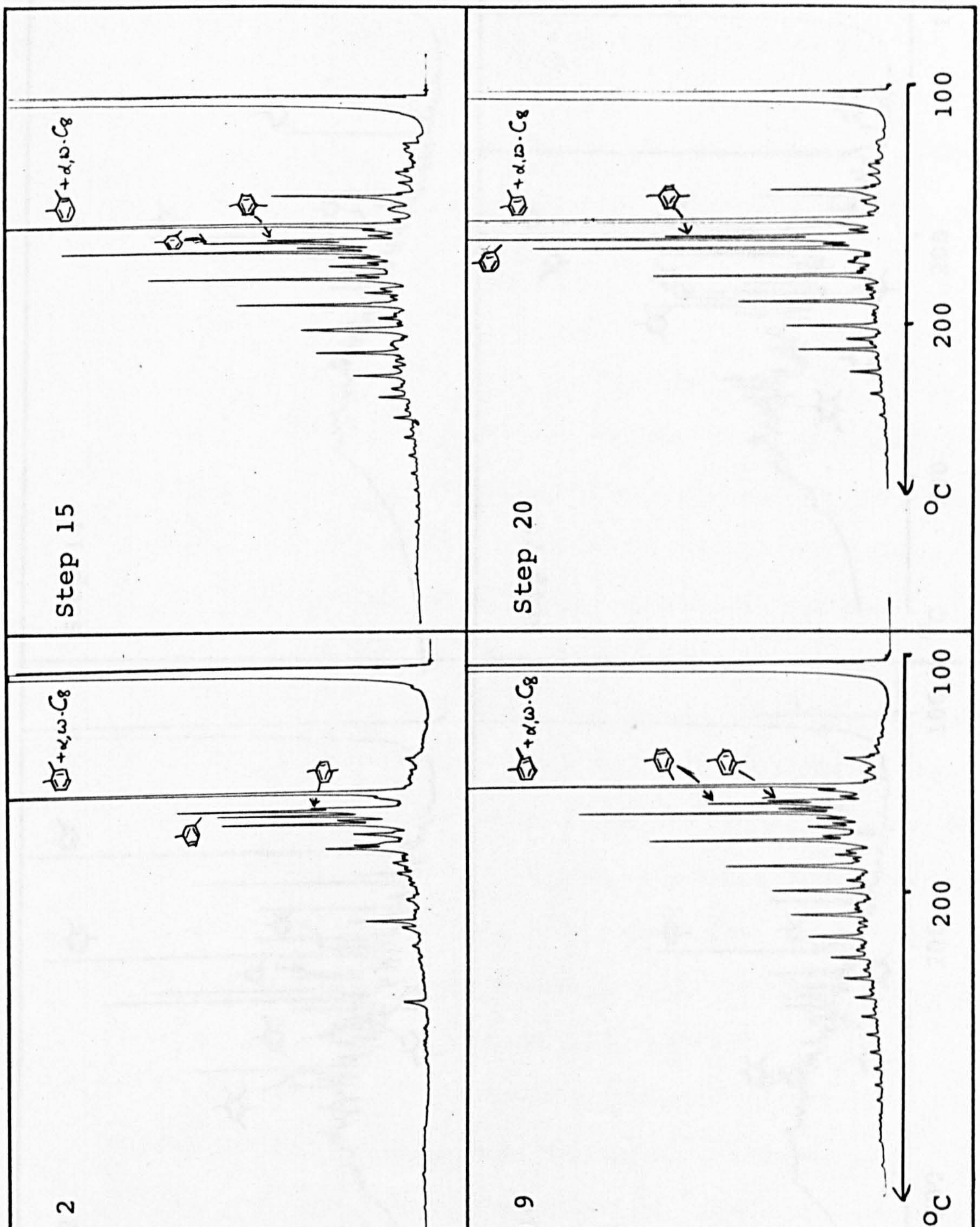

Gas chromatographic conditions as in Fig. 91.

Fig. 105. Methyl esters of the acids of the polar fraction from the oxidation of Barnsley sporinite

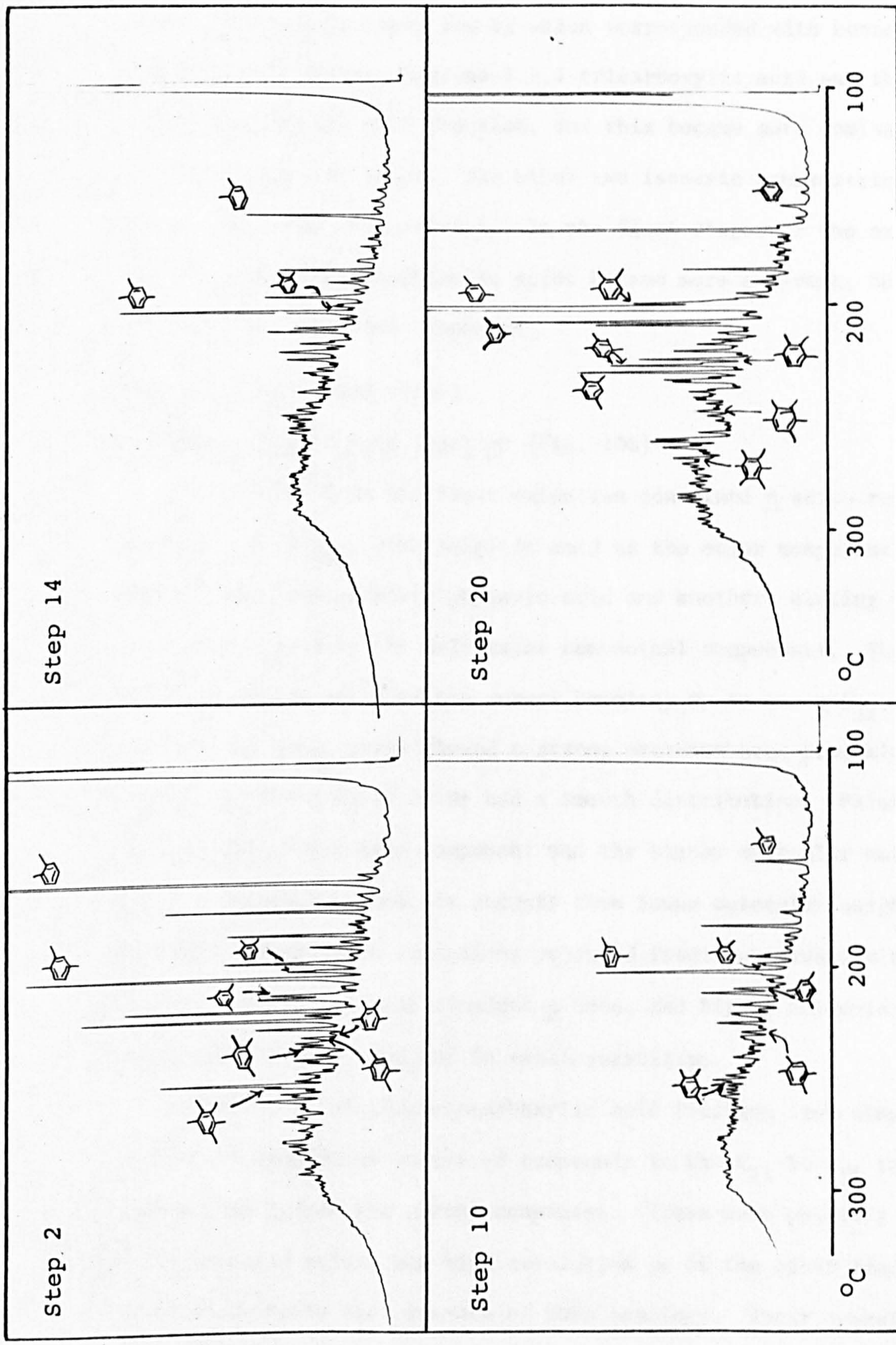

Gas chromatographic conditions as in Fig. 91.

showed no systematic variation. The fractions contained a large number of compounds, very few of which corresponded with benzene polycarboxylic acids. Benzene-1,2,4-tricarboxylic acid was the main single component in each fraction, and this became more dominant in the later oxidation steps. The other two isomeric benzenetricarboxylic acids were also present. In the final stages of the oxidation the benzenetetracarboxylic acids became more apparent, but still remained as minor components.

Parkgate (7 oxidation steps)

a) Monocarboxylic acid fraction (Fig. 106)

Fatty acids from the first oxidation contained n-acids ranging from n-C_{11} to n-C_{18}, with palmitic acid as the major component. A compound that was possibly phytanic acid and another, eluting very close to n-C_{16}, were the only major non-normal components. The second oxidation extended the normal homology up to *ca.* n-C_{31}, and the n-C_{16} to n-C_{31} range showed a strong even-numbered predominance. Below n-C_{16} the n-fatty acids had a smooth distribution. Palmitic acid was itself the main component and the higher molecular weight material occurred in smaller amounts than lower molecular weight compounds. Successive oxidations produced fractions always with palmitic acid as the most abundant n-acid, and higher molecular weight n-acids were produced in small quantities.

Capillary gc of the monocarboxylic acid fraction from step four resolved an homologous series of compounds in the C_{11} to C_{15} range, eluting just before the normal component. These were possibly monomethyl branched acids, but high resolution gc of the other fractions failed to indicate the presence of this homology. Their overall content was therefore very small.

b) Dicarboxylic acid fraction (Fig. 107)

The yield of the di-acid fraction increased initially up to

Fig. 106. Methyl esters of monocarboxylic acids from the oxidation of Parkgate sporinite

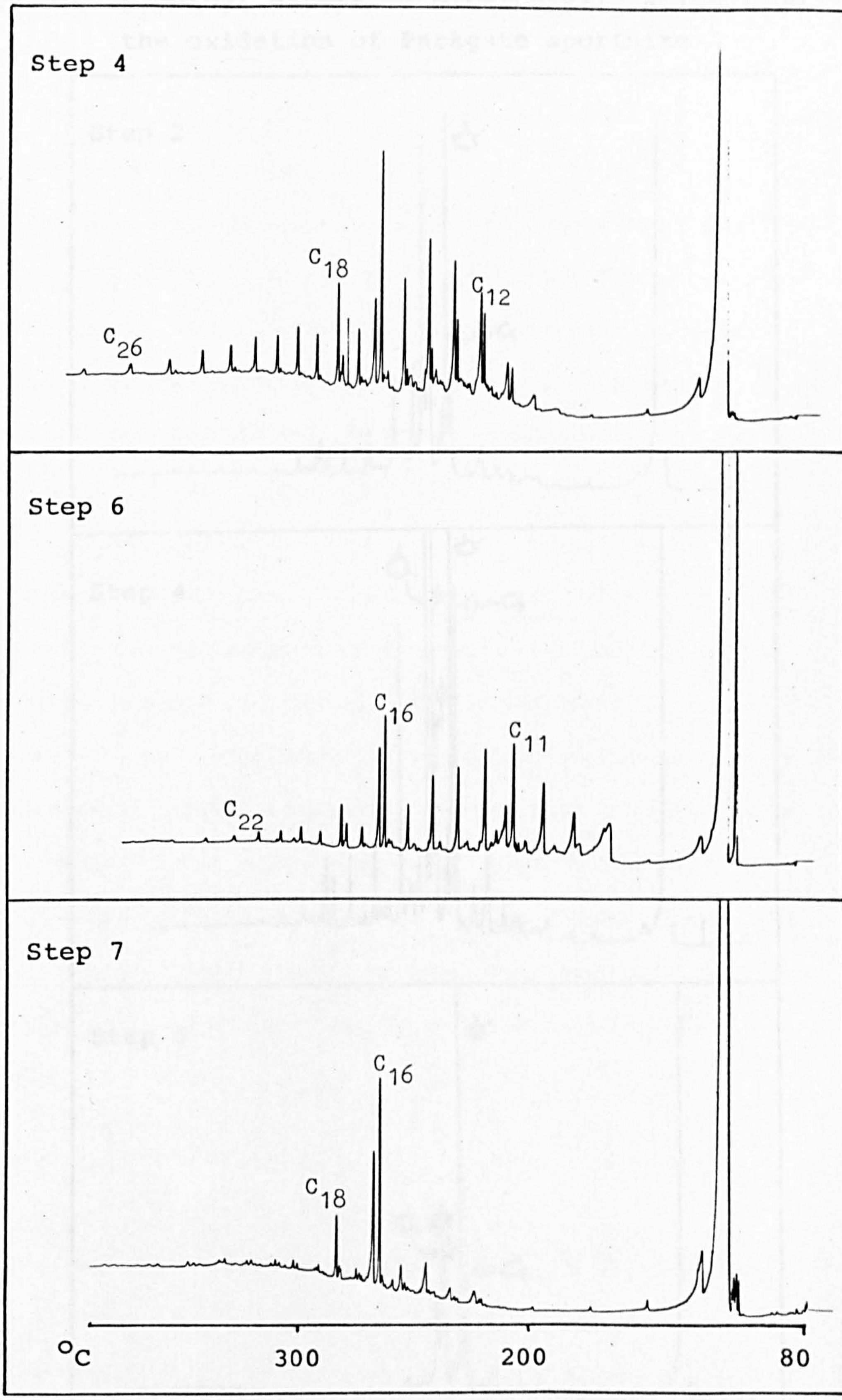

Gas chromatographic conditions: 150m. x 0.02" capillary column containing OV-101; programmed 80-300^{o}C at 4^{o}/min; detector 300^{o}; injector 300^{o}; nitrogen 4 p.s.i.

Fig. 107. Dimethyl esters of dicarboxylic acids from the oxidation of Parkgate sporinite

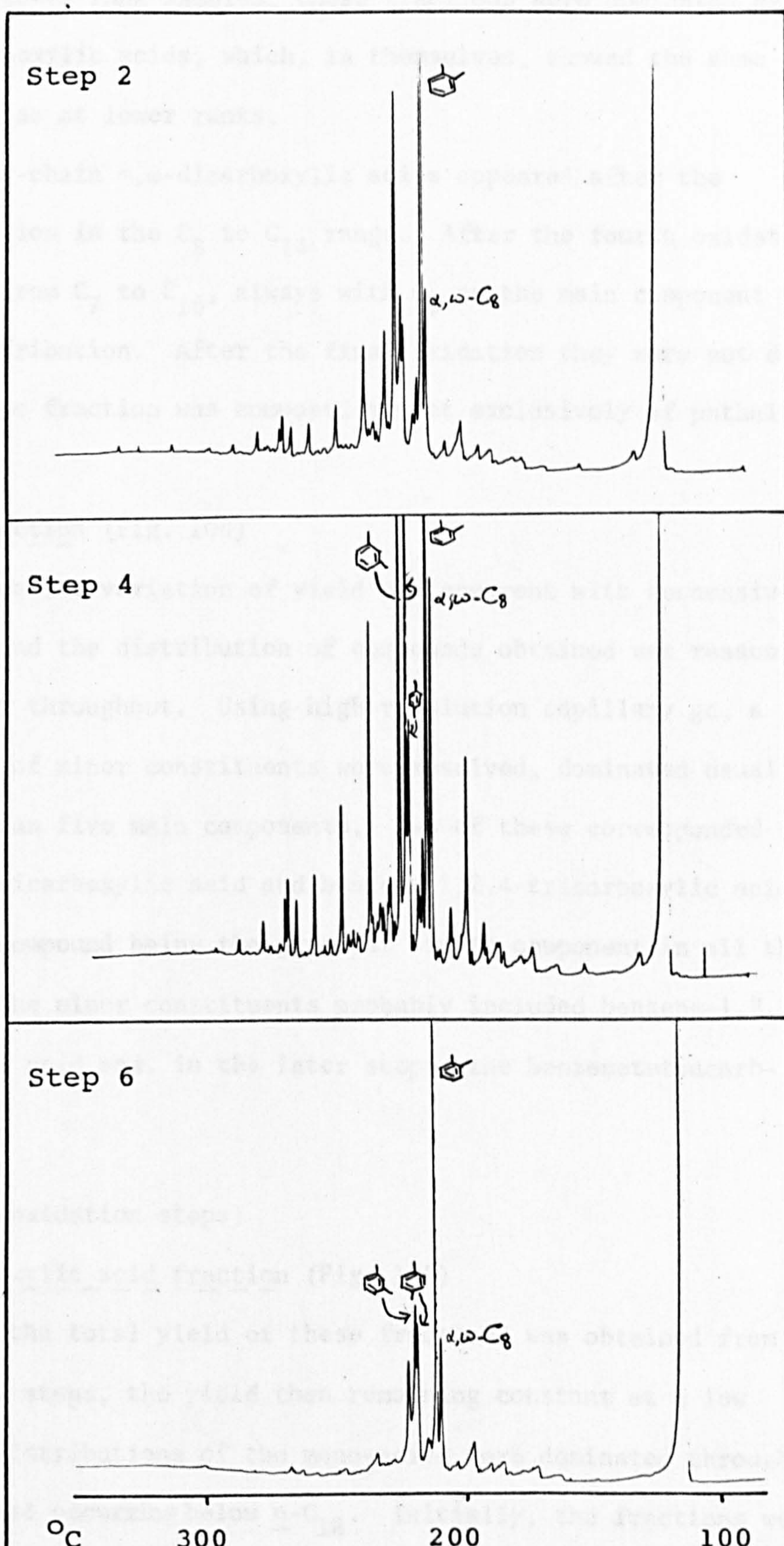

Gas chromatographic conditions as in Fig. 106.

step three, and then declined uniformly to the final step. In contrast to lower rank samples, these fractions were dominated by benzenedicarboxylic acids, which, in themselves, showed the same distribution as at lower ranks.

Straight-chain α,ω-dicarboxylic acids appeared after the second oxidation in the C_8 to C_{14} range. After the fourth oxidation they ranged from C_7 to C_{16}, always with C_9 as the main component of a smooth distribution. After the final oxidation they were not detectable, and the fraction was composed almost exclusively of phthalic acids.

c) Polar fraction (Fig. 108)

No systematic variation of yield was apparent with successive oxidations, and the distribution of compounds obtained was reasonably constant throughout. Using high-resolution capillary gc, a large number of minor constituents were resolved, dominated usually by no more than five main components. Two of these corresponded to benzene-1,2-dicarboxylic acid and benzene-1,2,4-tricarboxylic acid, this latter compound being the greatest single component in all the fractions. The minor constituents probably included benzene-1,2,3-tricarboxylic acid and, in the later steps, the benzenetetracarboxylic acids.

Silkstone (7 oxidation steps)

a) Monocarboxylic acid fraction (Fig. 109)

Half of the total yield of these fractions was obtained from the first two steps, the yield then remaining constant at a low level. The distributions of the mono-acids were dominated throughout by material occurring below n-C_{18}. Initially, the fractions were isomerically complex up to C_{16}, but n-fatty acids became more prominent with increasing oxidation. Distributional maxima varied from

Fig. 108. Methyl esters of the acids of the polar fraction from the oxidation of Parkgate sporinite

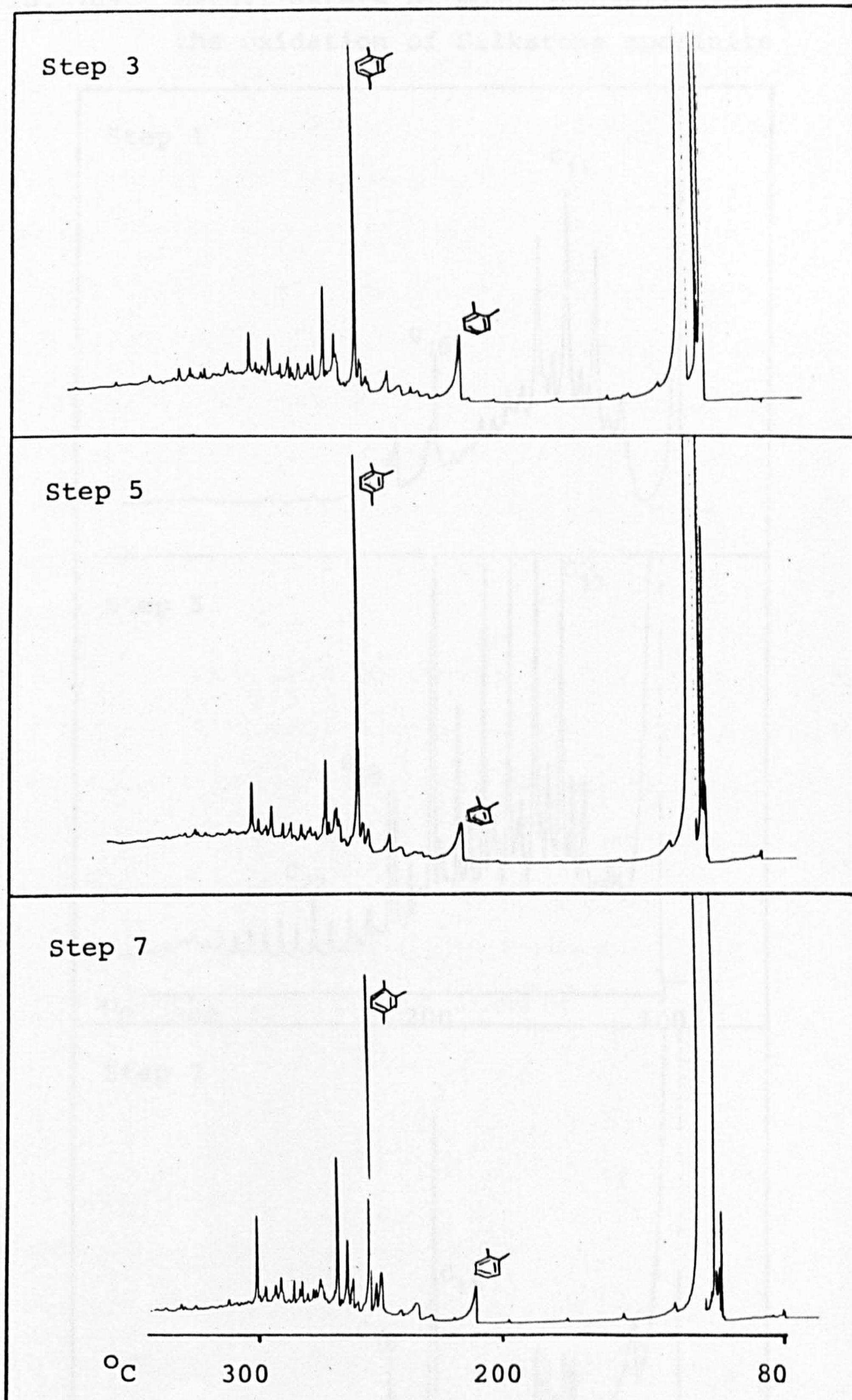

Gas chromatographic conditions as in Fig. 106.

Fig. 109. Methyl esters of monocarboxylic acids from the oxidation of Silkstone sporinite

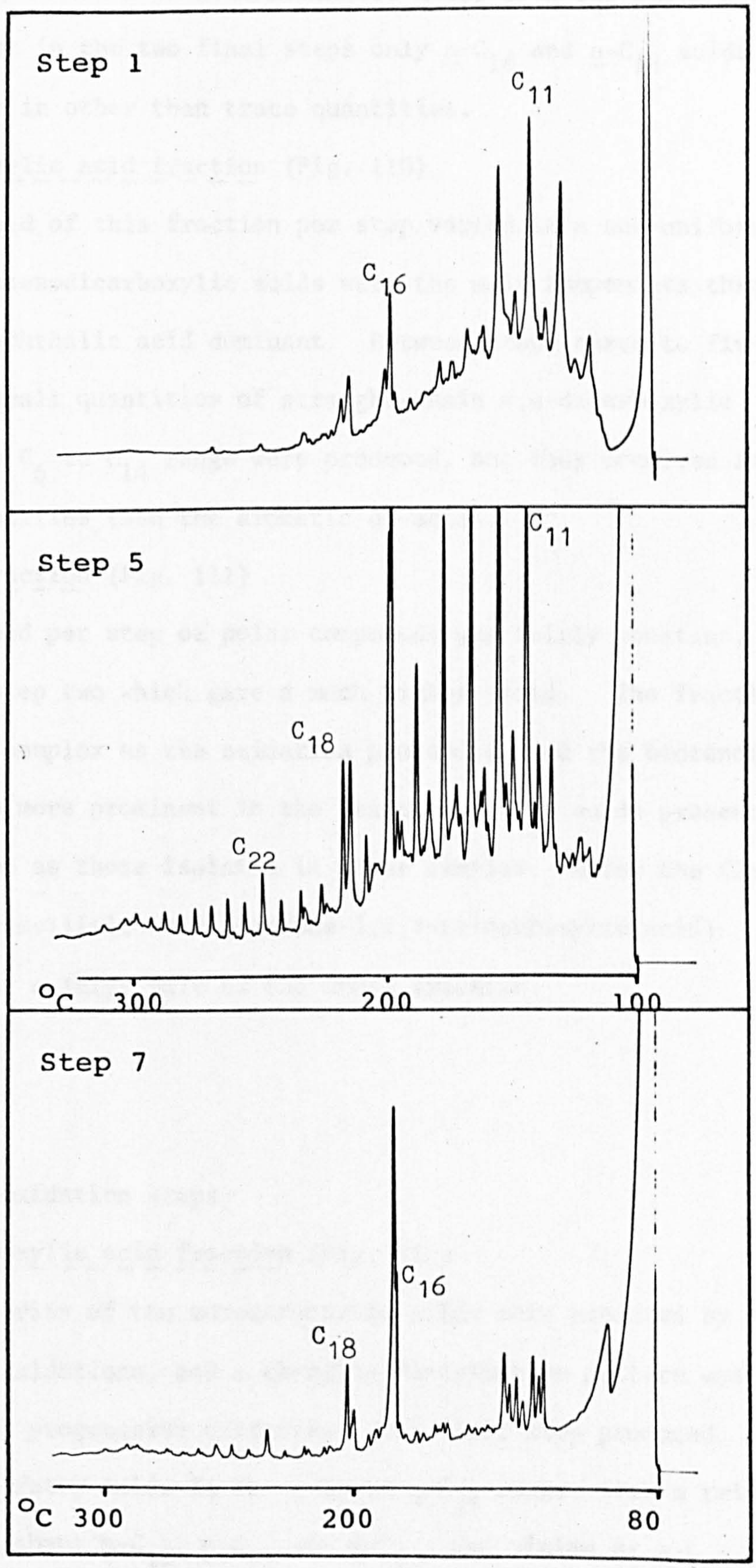

Gas chromatographic conditions for steps 1 & 7 as in Fig. 101, and for step 5 as in Fig. 97.

n-C_{16}, initially, to n-C_{10} after the second step. After the fifth step small quantities of even-dominated n-C_{18} to n-C_{30} acids were produced, but in the two final steps only n-C_{16} and n-C_{18} acids were present in other than trace quantities.

b) Dicarboxylic acid fraction (Fig. 110)

The yield of this fraction per step varied in a non-uniform manner. Benzenedicarboxylic acids were the main components throughout, with o-phthalic acid dominant. Between steps three to five inclusive, small quantities of straight-chain α,ω-dicarboxylic acids in the C_6 to C_{14} range were produced, but they occurred in smaller quantities than the aromatic di-acids.

c) Polar fraction (Fig. 111)

The yield per step of polar compounds was fairly constant, except for step two which gave a much higher yield. The fractions became less complex as the oxidation proceeded, and the benzenoid acids became more prominent in the fractions. The acids present were the same as those isolated in other samples. After the final oxidation trimellitic acid (benzene-1,2,4-tricarboxylic acid) accounted for a large part of the whole fraction.

Alginite

Scotland (5 oxidation steps)

a) Monocarboxylic acid fraction (Fig. 112)

The majority of the monocarboxylic acids were produced by the first three oxidations, and a changing distribution pattern was observed with progressive oxidation. The first step produced dominantly n-fatty acids in the n-C_7 to n-C_{34} range, with a trimodal distribution about n-C_{11}, n-C_{16} and n-C_{22}, and minima at n-C_{13} and n-C_{17}. An even-numbered predominance was present throughout. The

Fig. 110. Dimethyl esters of dicarboxylic acids from the oxidation of Silkstone sporinite

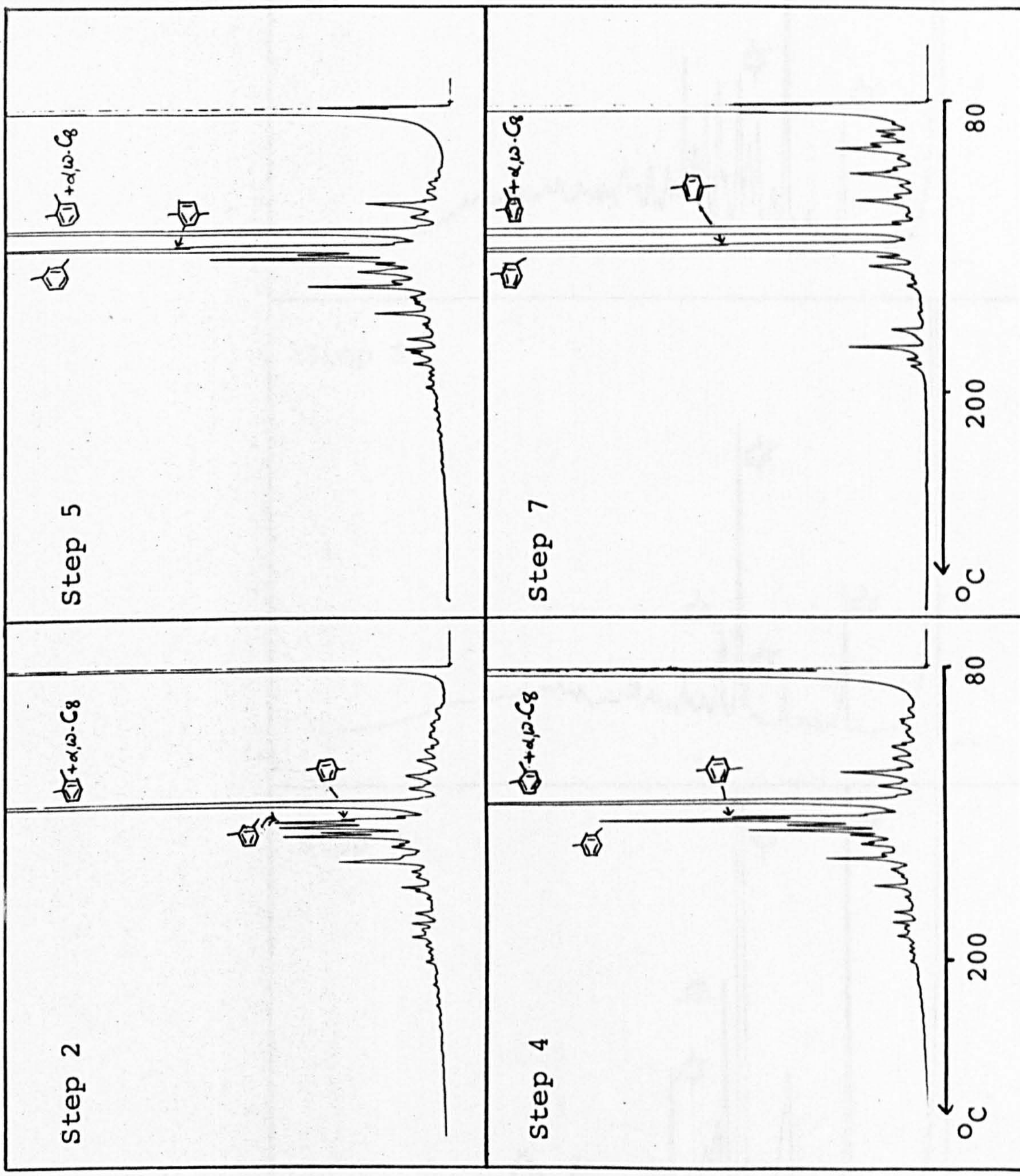

Gas chromatographic conditions as in Fig. 101.

Fig. 111. Methyl esters of the acids of the polar fraction from the oxidation of Silkstone sporinite

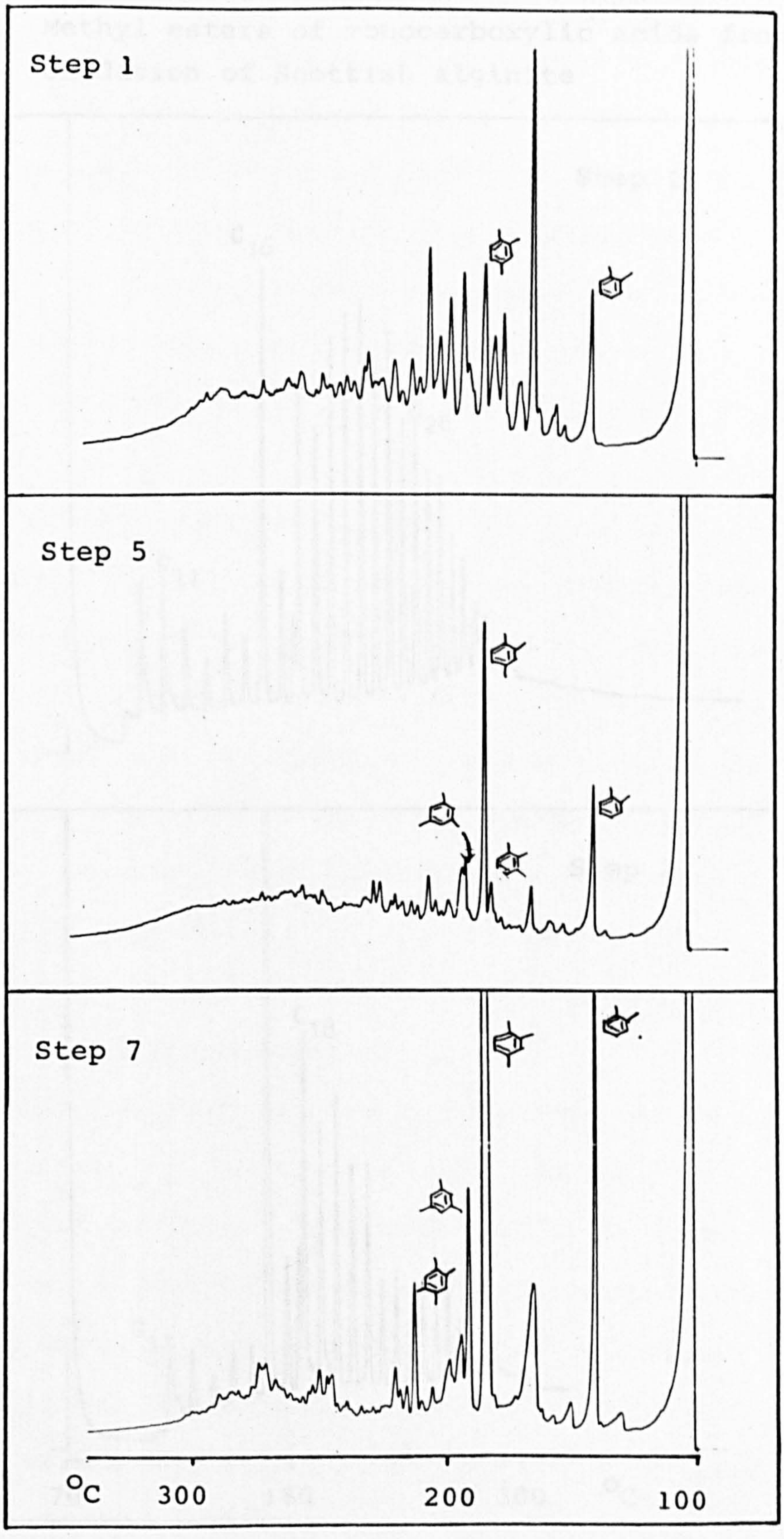

Gas chromatographic conditions as in Fig. 97.

Fig. 112. Methyl esters of monocarboxylic acids from the oxidation of Scottish alginite

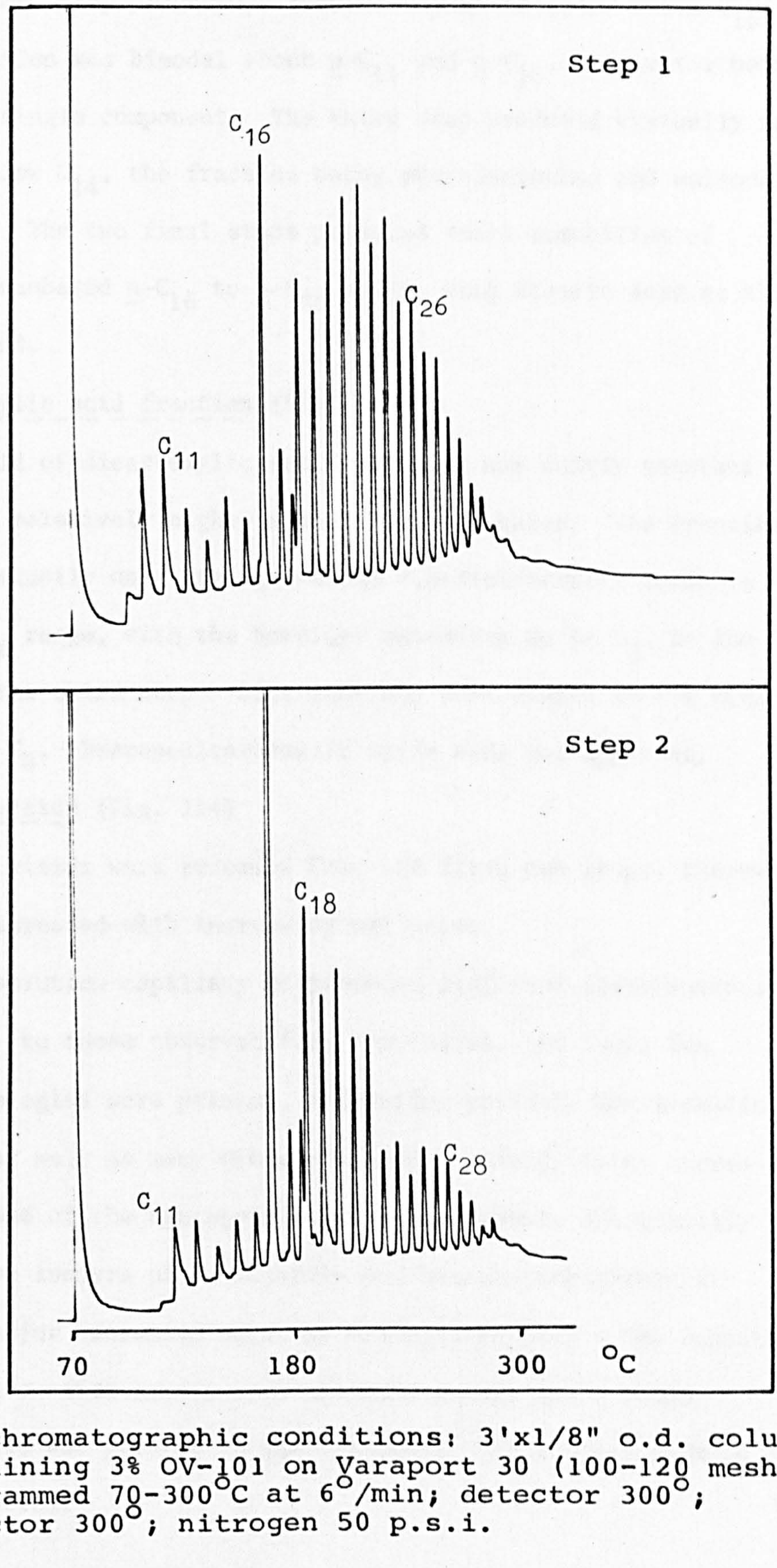

Gas chromatographic conditions: 3'x1/8" o.d. column containing 3% OV-101 on Varaport 30 (100-120 mesh); programmed 70-300°C at 6°/min; detector 300°; injector 300°; nitrogen 50 p.s.i.

only non-normal constituent had a retention index of 1775 (measured on a 150' capillary OV-101 column) and was possibly phytanic acid.

The second step produced a reduced amount of acids above C_{16}. The distribution was bimodal about n-C_{11} and n-C_{16}, the latter being the largest single component. The third step produced virtually no compounds below C_{14}, the fraction being even-dominated and unimodal about n-C_{20}. The two final steps produced small quantities of mainly even-numbered n-C_{16} to n-C_{30} acids, with stearic acid as the major compound.

b) Dicarboxylic acid fraction (Fig. 113)

The yield of dicarboxylic acids per step was fairly constant apart from a relatively higher yield from step three. The fractions contained virtually only straight-chain α,ω-dicarboxylic acids in the C_4 to C_{16} range, with the homology extending up to C_{20} in the products of the third step. Distributions were always smooth with a maximum at C_8. Benzenedicarboxylic acids were not apparent.

c) Polar fraction (Fig. 114)

Highest yields were recorded from the first two steps; thereafter they decreased with increasing oxidation.

High-resolution capillary gc produced different distributions of compounds to those observed from sporinites. At least two apparent homologies were present, indicating possibly non-aromatic structures, as well as many other compounds. Constituents corresponding to some of the benzenoid acids were present, specifically the respective isomers of benzenetri- and benzenetetracarboxylic acids. The major benzenoid acid was trimellitic acid. The benzenetetracarboxylic acids became more apparent in the later steps. o-Phthalic acid was present in small amounts, but its two isomers were not detected.

Fig. 113. Dimethyl esters of dicarboxylic acids from the oxidation of Scottish alginite

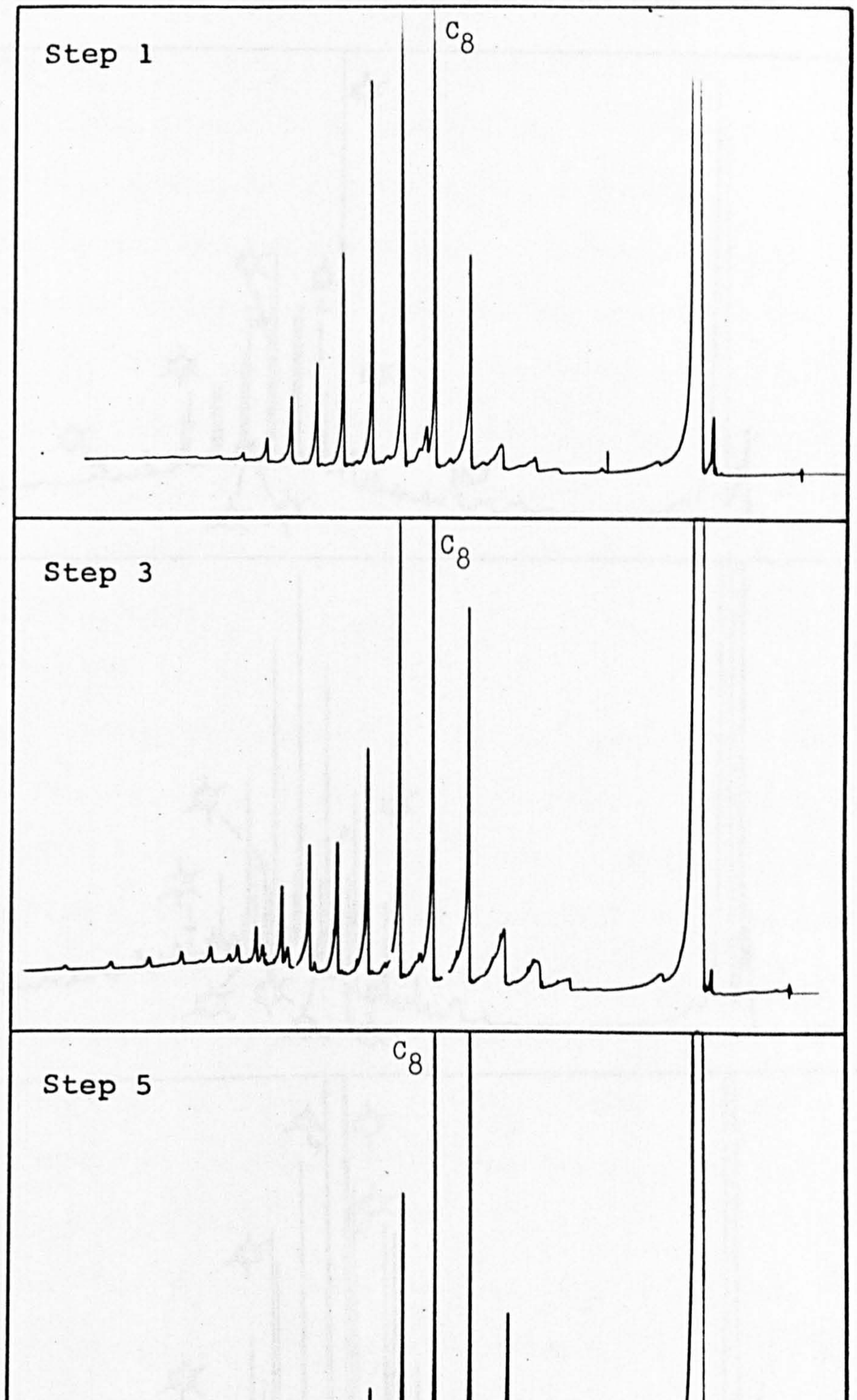

Gas chromatographic conditions as in Fig. 106.

Fig. 114. Methyl esters of the acids of the polar fraction from the oxidation of Scottish alginite

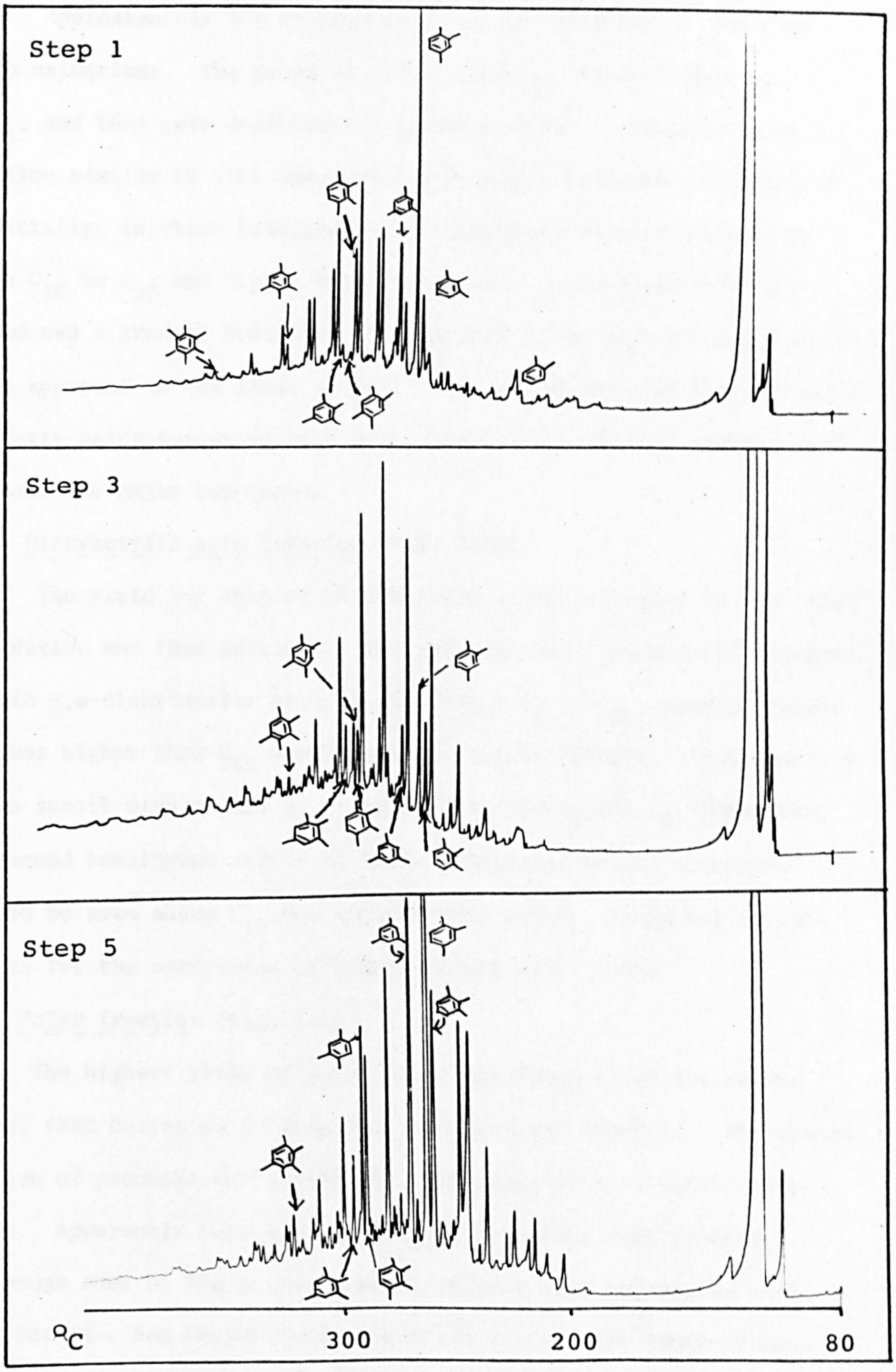

Gas chromatographic conditions as in Fig. 106.

South Africa (6 oxidation steps)

a) Monocarboxylic acid fraction (Fig. 115A)

Approximately 85% of this fraction was produced by the first two oxidations. The range of acids produced extended from C_8 to C_{31}, and they were dominated by n-fatty acids. A trimodal distribution similar to that observed for Scottish alginite was produced initially, in which branched/cyclic compounds were restricted to the C_{16} to C_{20} and higher than C_{24} ranges. Successive oxidations produced a gradual reduction of compounds below C_{16}, and these were not apparent in the final stages. The predominance of even-numbered n-fatty acids increased with progressive oxidation and stearic acid became the major component.

b) Dicarboxylic acid fraction (Fig. 115B)

The yield per step of dicarboxylic acids increased to the third oxidation and then declined. The products were essentially straight-chain α,ω-dicarboxylic acids in the range C_6 to C_{25}, although homologues higher than C_{15} were present in small amounts. Distributions were smooth with maxima at C_9 up to step three, and C_8 thereafter. A second homologous series of higher molecular weight compounds could be seen above C_{15} but amounts were small. There was no evidence for the occurrence of benzenedicarboxylic acids.

c) Polar fraction (Fig. 116)

The highest yield of polar acids was found after the second step, then decreased to step four and remained constant. The distribution of products was similar to that observed in Scottish alginite. Apparently homologous series of compounds were present, although some of the gc peaks were enhanced when coinjected with benzenetri- and benzenetetracarboxylic acids. The range of compounds varied little between steps, except for step four where a relatively greater quantity of higher molecular weight compounds

Fig. 115. A. Methyl esters of monocarboxylic acids from the oxidation of South African alginite

B. Dimethyl esters of dicarboxylic acids from the oxidation of South African alginite

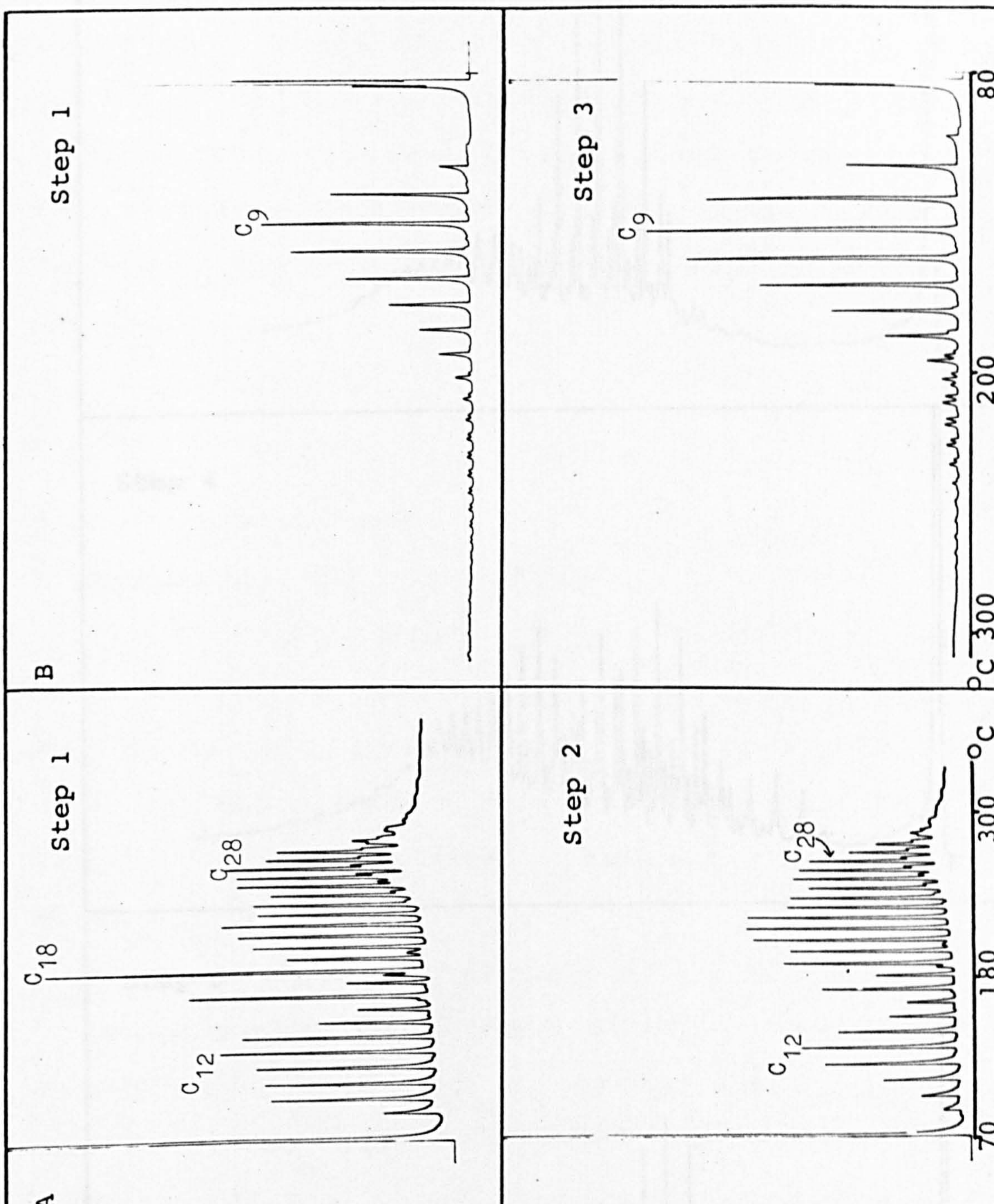

Gas chromatographic conditions for A as in Fig. 112, and for B as in Fig. 99 (step 2).

Fig. 116. Methyl esters of the acids of the polar fraction from the oxidation of S. African alginite

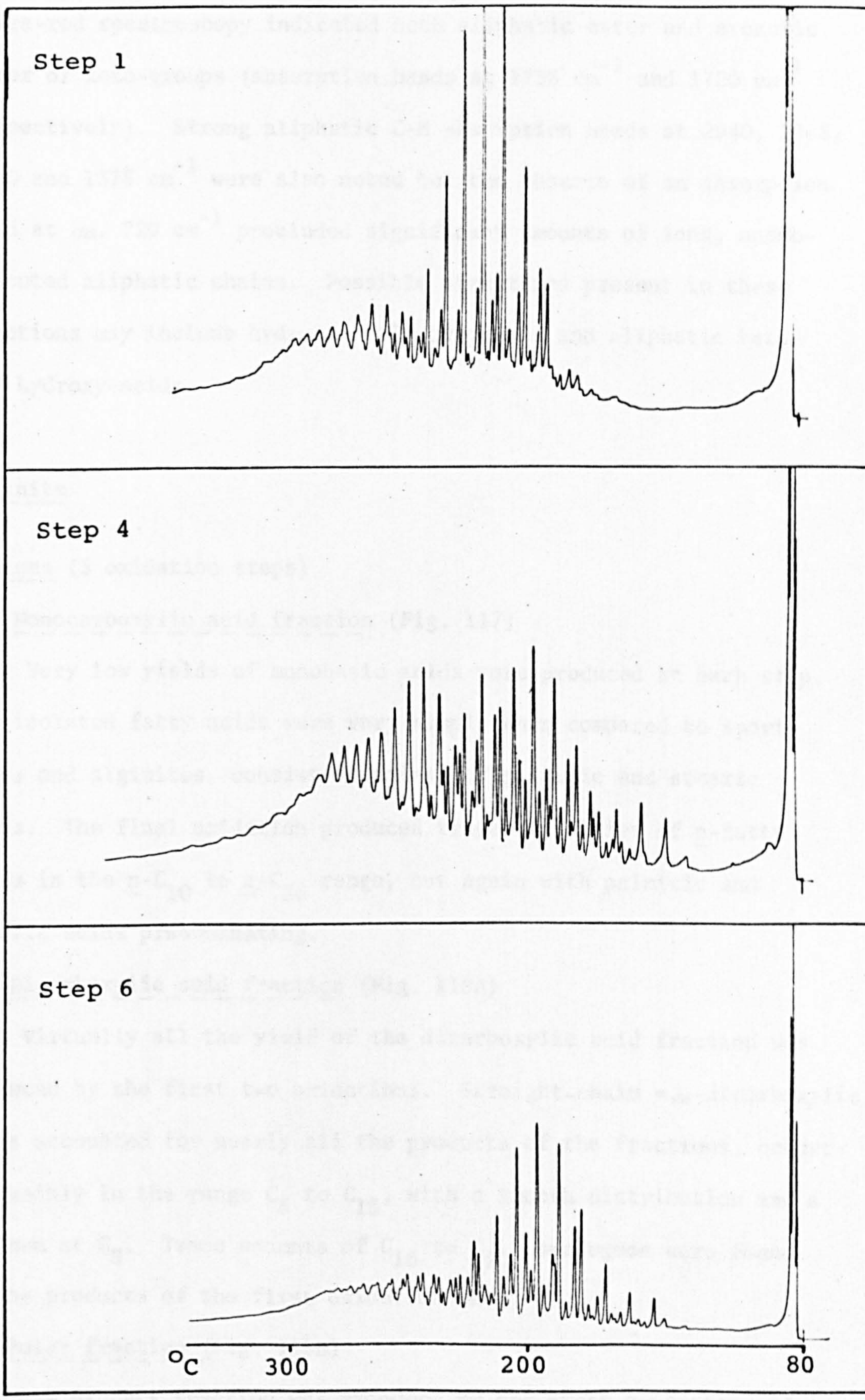

Gas chromatographic conditions as in Fig. 99 (step 2).

was produced.

The structures of most of these compounds were not determined. Infra-red spectroscopy indicated both aliphatic ester and aromatic ester or keto-groups (absorption bands at 1735 cm^{-1} and 1720 cm^{-1} respectively). Strong aliphatic C-H absorption bands at 2940, 2863, 1460 and 1375 cm^{-1} were also noted but the absence of an absorption band at *ca.* 720 cm^{-1} precluded significant amounts of long, unsubstituted aliphatic chains. Possible structures present in these fractions may include hydroaromatic compounds and aliphatic keto- and hydroxy-acids.

Cutinite

Indiana (3 oxidation steps)

a) Monocarboxylic acid fraction (Fig. 117)

Very low yields of monobasic acids were produced at each step. The isolated fatty acids were very simple when compared to sporinites and alginites, consisting mainly of palmitic and stearic acids. The final oxidation produced trace quantities of n-fatty acids in the n-C_{10} to n-C_{36} range, but again with palmitic and stearic acids predominating.

b) Dicarboxylic acid fraction (Fig. 118A)

Virtually all the yield of the dicarboxylic acid fraction was produced by the first two oxidations. Straight-chain α,ω-dicarboxylic acids accounted for nearly all the products of the fractions, occurring mainly in the range C_6 to C_{15}, with a smooth distribution and a maximum at C_8. Trace amounts of C_{16} to C_{20} homologues were found in the products of the first oxidation only.

c) Polar fraction (Fig. 118B)

65% of this fraction was produced by the first oxidation and

Fig. 117. Methyl esters of monocarboxylic acids from the oxidation of Indiana cutinite

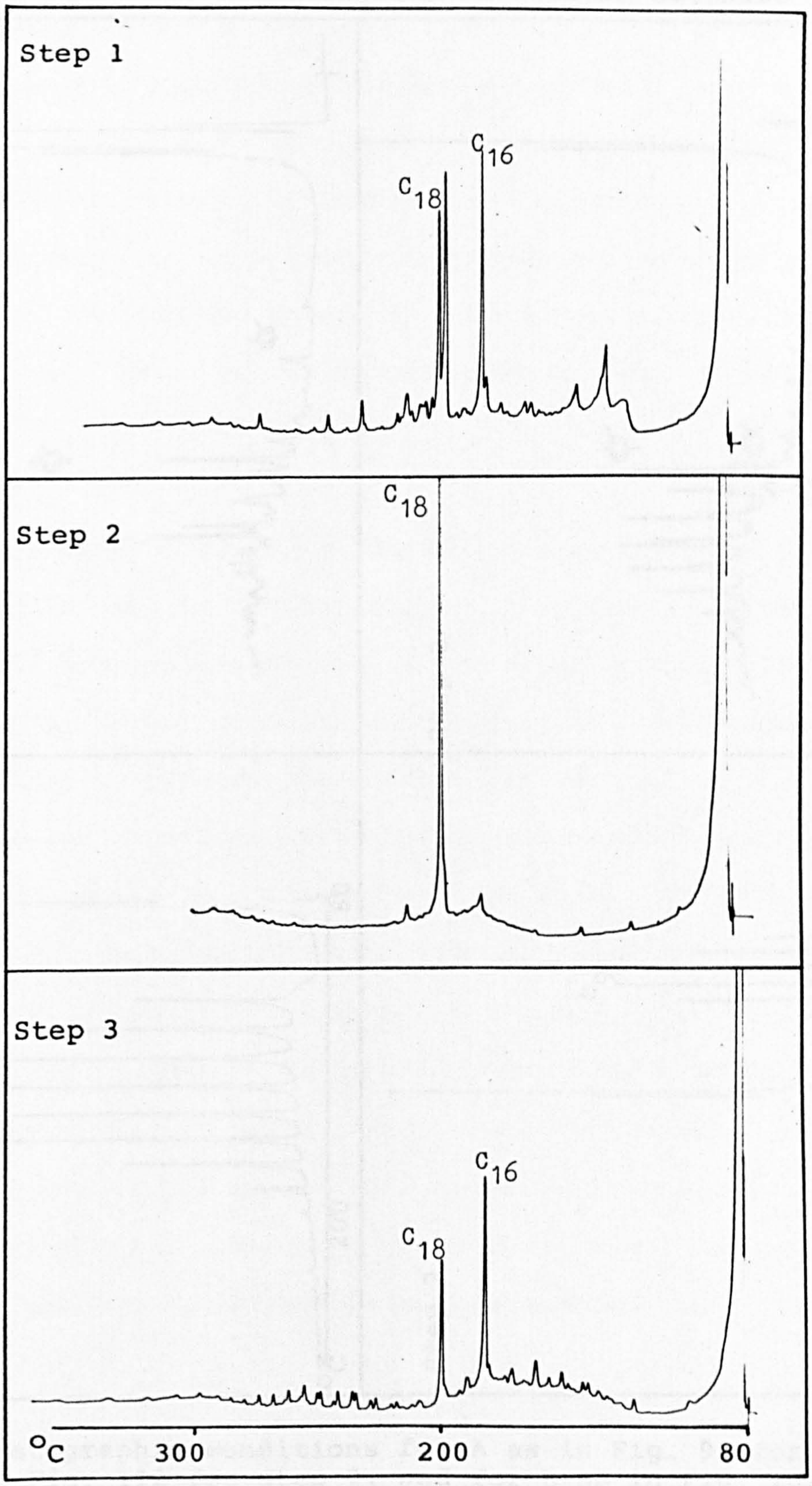

Gas chromatographic conditions as in Fig. 99 (step 2).

Fig. 118. A. Dimethyl esters of dicarboxylic acids from the oxidation of Indiana cutinite

B. Methyl esters of the acids of the polar fraction from the oxidation of Indiana cutinite

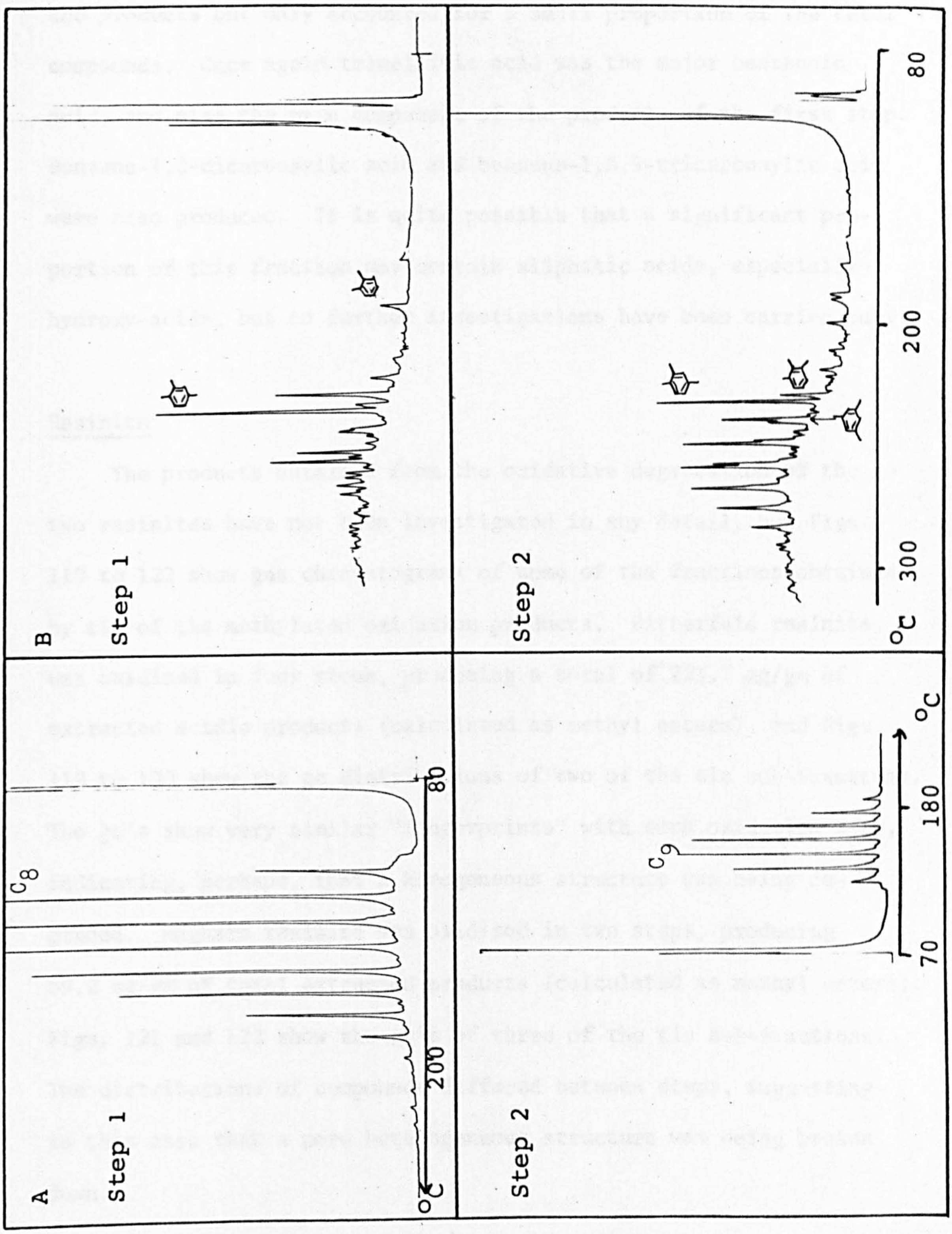

Gas chromatographic conditions for A as in Fig. 99 for step 1 and as in Fig. 112 for step 2, and for B as in Fig. 102.

a further 25% by the second step. Benzenoid acids were present in the products but only accounted for a small proportion of the total compounds. Once again trimellitic acid was the major benzenoid acid, and also the main component of the products of the first step. Benzene-1,2-dicarboxylic acid and benzene-1,3,5-tricarboxylic acid were also produced. It is quite possible that a significant proportion of this fraction may contain aliphatic acids, especially hydroxy-acids, but no further investigations have been carried out.

Resinite

The products obtained from the oxidative degradation of the two resinites have not been investigated in any detail, but Figs. 119 to 122 show gas chromatograms of some of the fractions obtained by tlc of the methylated oxidation products. Bitterfeld resinite was oxidised in four steps, producing a total of 223.7 mg/gm of extracted acidic products (calculated as methyl esters), and Figs. 119 to 120 show the gc distributions of two of the tlc sub-fractions. The gc's show very similar "fingerprints" with each oxidation step, indicating, perhaps, that a homogeneous structure was being degraded. Maghara resinite was oxidised in two steps, producing 69.2 mg/gm of total extracted products (calculated as methyl esters). Figs. 121 and 122 show the gc's of three of the tlc sub-fractions. The distributions of compounds differed between steps, suggesting in this case that a more heterogeneous structure was being broken down.

Fig. 119. Methyl esters of tlc fraction 1 from the oxidation of Bitterfeld resinite

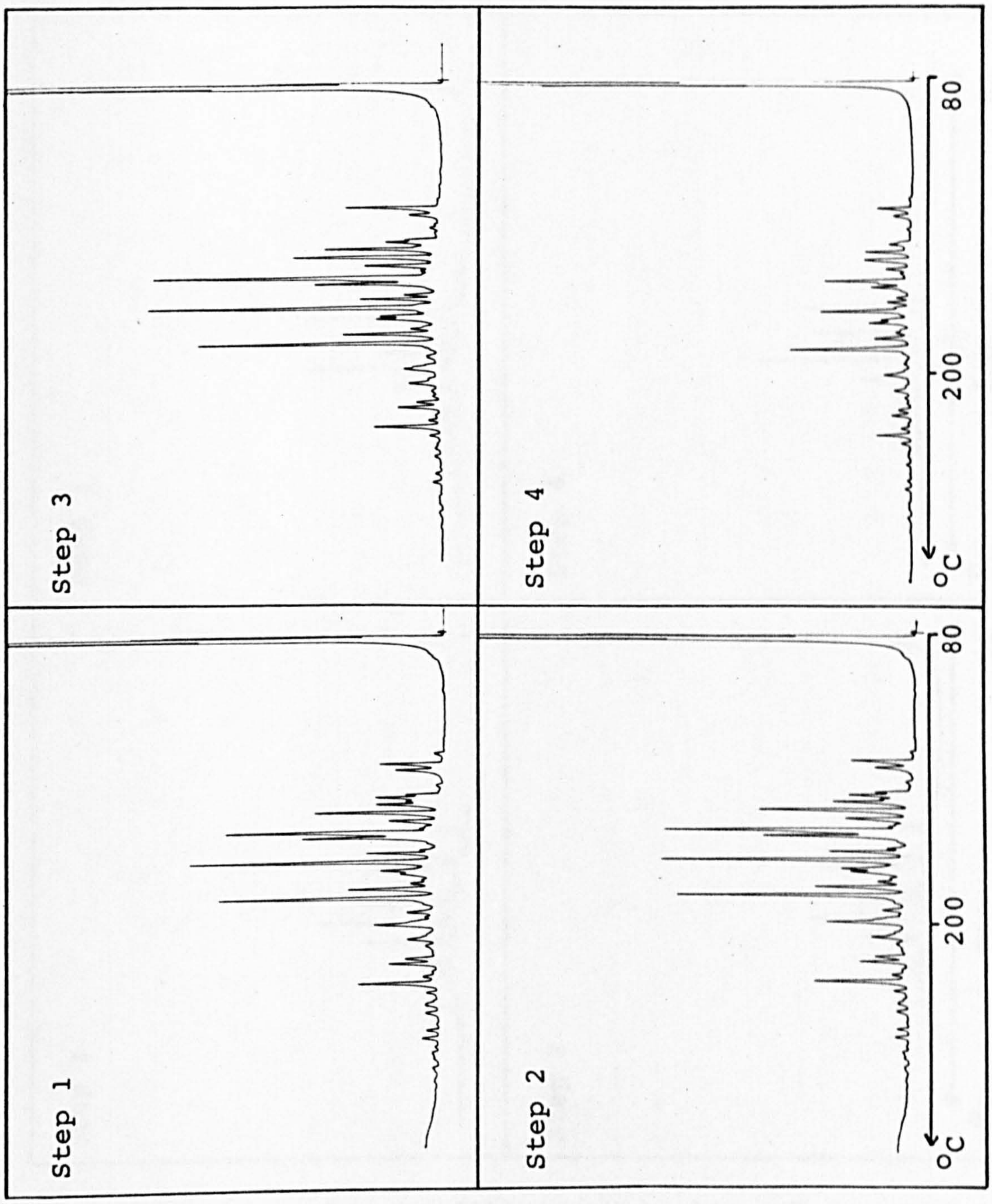

Gas chromatographic conditions as in Fig. 99 (step 2).

Fig. 120. Methyl esters of tlc fraction 2 from the oxidation of Bitterfeld resinite

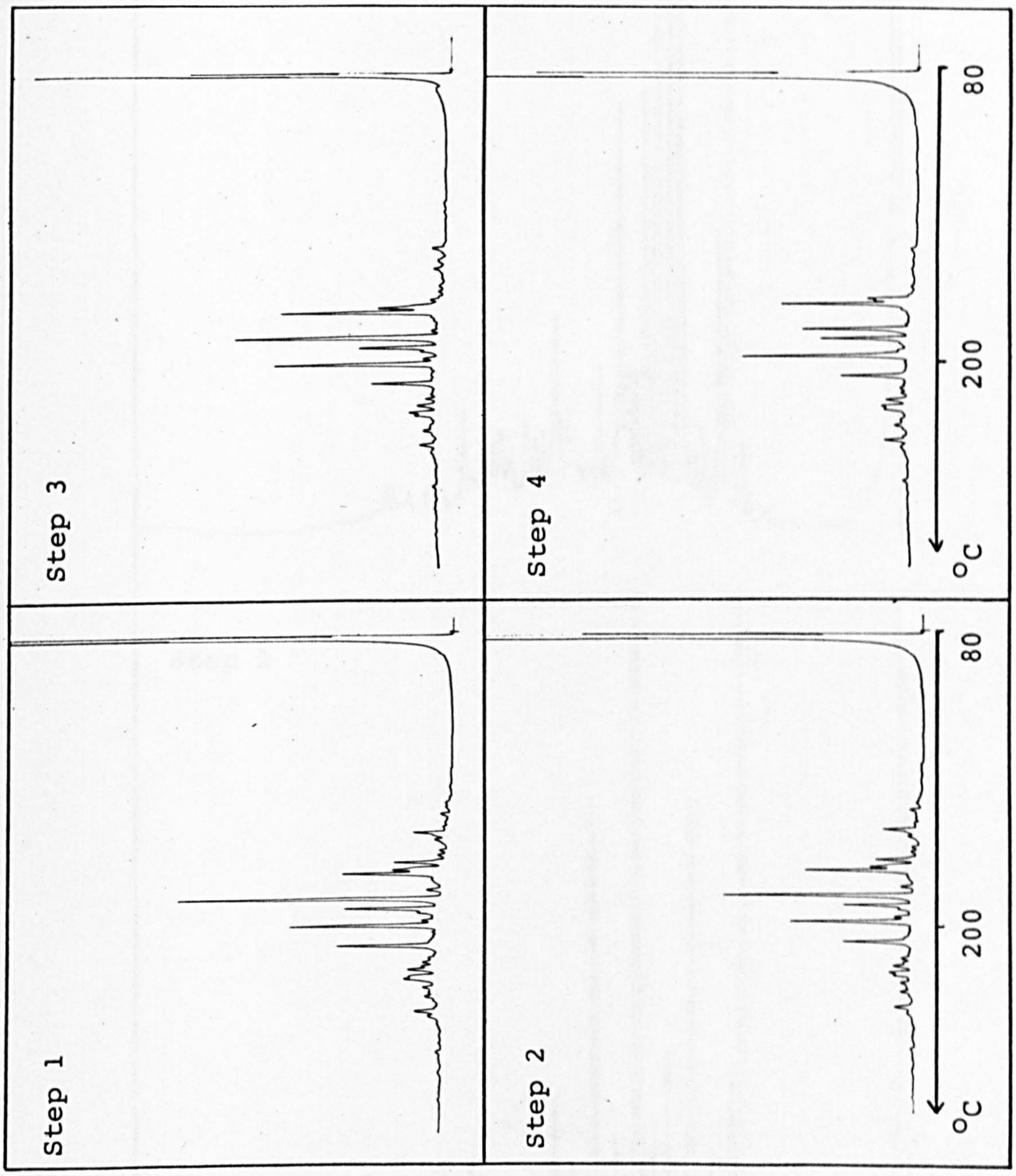

Gas chromatographic conditions as in Fig. 99 (step 2).

Fig. 121. Methyl esters of tlc fraction 1 from the oxidation of Maghara resinite

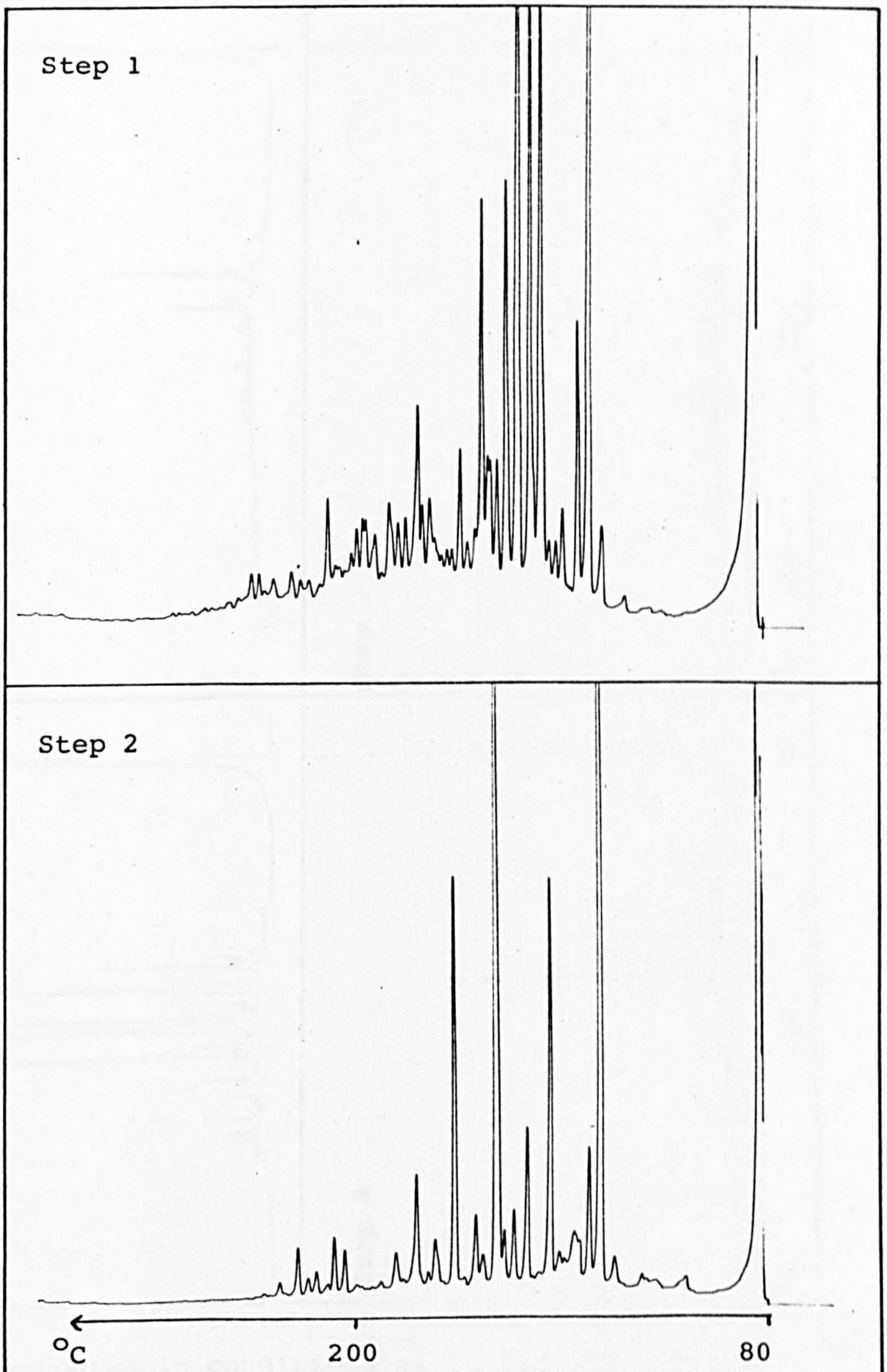

Gas chromatographic conditions as in Fig. 99 (step 2).

Fig. 122. A. Methyl esters of tlc fraction 2 from the oxidation of Maghara resinite

B. Methyl esters of tlc fraction 3 from the oxidation of Maghara resinite

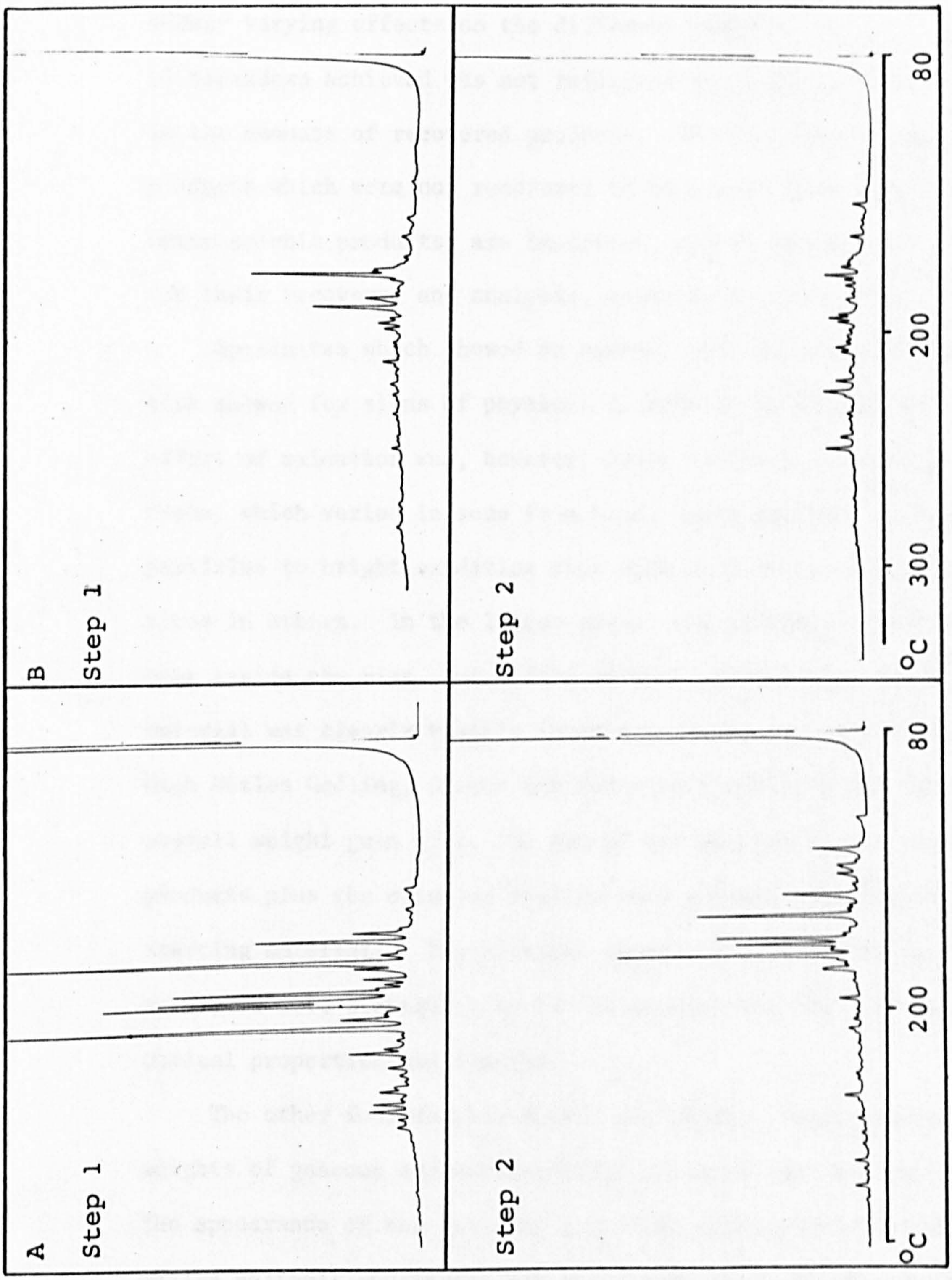

Gas chromatographic conditions as in Fig. 99 (step 2) for A and B.

Discussion

Stepwise alkaline permanganate oxidation of sporinites had widely varying effects on the different samples. However, the degree of breakdown achieved was not reflected in marked parallel variations in the amounts of recovered products. In this respect, oxidation products which were not recovered in this work (i.e. gaseous and water-soluble products) are important, and in future work methods for their recovery, and analysis, ought to be considered.

Sporinites which showed an overall gain in weight after oxidation showed few signs of physical disruption of particles. The effect of oxidation was, however, quite variable in terms of reflectance, which varied in some from being quite uniform over whole particles to bright oxidation rims with much duller interior portions in others. In the latter cases, the particles appeared granular inside the rims, but a fine network of very high reflecting material was clearly visible interlaced among the duller granules. High Hazles Gedling, Clowne and Barnsley sporinites all showed an overall weight gain (i.e. the sum of the weights of the recovered products plus the oxidised residue were greater than the weight of starting material). The physical shape and size of the oxidised particles were comparable to the unoxidised material, although the optical properties had changed.

The other four samples showed net weight losses, although the weights of gaseous and water-soluble products were not determined. The appearance of the oxidised particles of Deep Hard and High Hazles Whitwell sporinites was similar to those samples described above (i.e. retention of original spore morphology but alteration of optical appearance). Parkgate and Silkstone sporinites were much more affected and showed a high degree of disruption of individual particles, and all spore morphology was lost.

The total weight of material lost between the original samples and the residues (Table 48) was highly variable, but the differences did not appear to be directly related to the rank of the samples. On the other hand, the two highest rank samples were the ones which suffered extensive physical disruption of individual particles. This may perhaps be attributed to the attainment of a higher degree of order of the structures at these ranks, such as that proposed by Hirsch (1954), Brown and Hirsch (1955) and Cartz *et al.*, (1956) from X-ray diffraction studies.

The development of apparent granularity in some of the sporinites may in some way reflect chemical variations within the structure, with oxidation selectively attacking some at present unknown, but presumably aliphatic, structures and building up a network of pathways of oxidation through the matrix. If an extension of such a process is that by which physical disruption eventually occurs, then the possibility arises of devising a carefully-controlled oxidation, monitored throughout by microscopical examination, whereby the point of disruption is actually observed. Recovery and analysis of released products throughout may provide valuable information concerning structure, while subsequent oxidation products may be useful in delineating differences in the initially more-resistant areas.

The oxidised residues of all the sporinites were also examined microscopically under incident ultraviolet radiation, where only very faint traces of any fluorescence were occasionally seen. In contrast, the alginite residues from oxidation showed bright fluorescence, with much of the fine cellular detail preserved. Under incident ordinary light, the algal bodies appeared rather diffuse but they showed no visible signs of oxidation in the form of rims or areas of increased reflectance. The material was apparently the same as unoxidised alginite.

The yields of humic acids showed a definite rank-dependence in sporinites, decreasing with increasing rank (Fig. 123). This variation could not be related in any statistically-significant way with the breakdown of spore particles, implying independence of this process. The yields of recovered extractable acids, on the other hand, were fairly uniform, apart from two samples (Fig. 124), but this again would seem to imply independence from the process of granularity formation and disruption. The mechanisms of oxidation are obviously complex.

The generation of humic acids from sporinite is interesting in that it would seem incompatible with a material derived solely from sporopollenin. However, the term "humic acid", although conventionally applied to a specific water-insoluble fraction precipitated by acidification of the alkaline oxidation mixture, is one which can be applied in only a very general sense without connotations of chemical structure. Indeed, humic acids in general are often defined as such on their method of isolation rather than on evidence of specific structures.

Degradation of humic acids from coals yields benzene polycarboxylic acids and short-chain aliphatic di-acids (Davies and Lawson, 1967a, 1967b). Methoxy-aromatic acids are oxidation products of brown coal humic acids and this fact led Maximov *et al.*, (1972), to postulate a lignin-based precursor for these materials. Interestingly, initial investigations of sporopollenin led Shaw and Yeadon (1966) to conclude that the material contained a proportion of lignin-like material although this suggestion was later abandoned. In later work, Brooks and Shaw (1968a) stated that a small proportion of aromatic material could well be derived from the aromatisation of

FIG. 123. VARIATION OF YIELDS OF HUMIC ACIDS FROM ALKALINE PERMANGANATE OXIDATIONS OF SPORINITES OF DIFFERENT RANKS

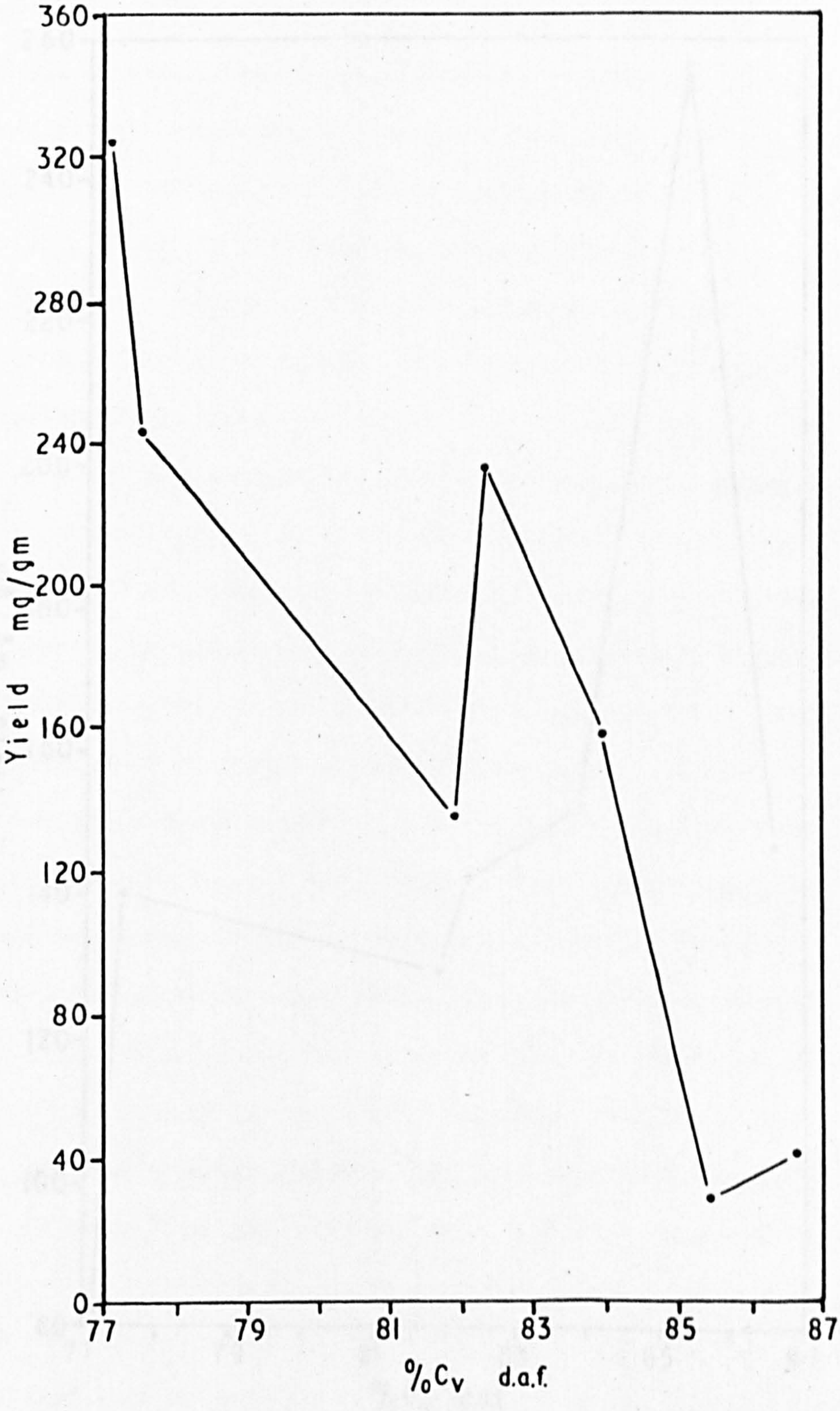

FIG.124. VARIATION OF YIELDS OF EXTRACTABLE ACIDS FROM ALKALINE PERMANGANATE OXIDATIONS OF SPORINITES OF DIFFERENT RANKS

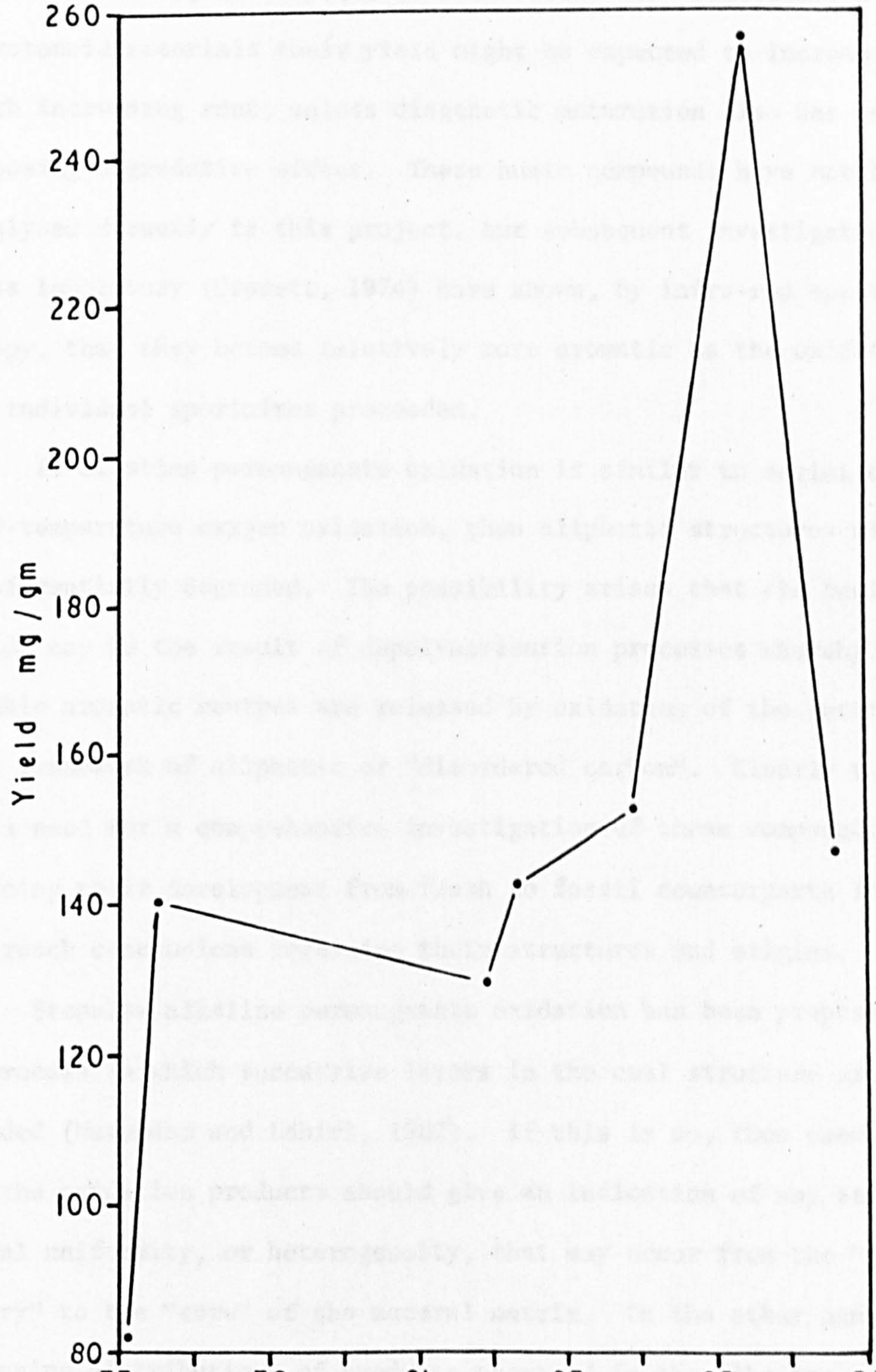

a part of the oxidative carotenoid polymer.

Sporinite humic acids appear to be an integral part of the overall structure as indicated by the rank-dependence of their yield. However, if they are derived solely via aromatisation of carotenoid materials their yield might be expected to increase with increasing rank, unless diagenetic maturation also has an opposing degradative effect. These humic compounds have not been analysed directly in this project, but subsequent investigations in this laboratory (Everett, 1974) have shown, by infra-red spectroscopy, that they become relatively more aromatic as the oxidation of individual sporinites proceeded.

If alkaline permanganate oxidation is similar to aerial or low-temperature oxygen oxidation, then aliphatic structures will be preferentially degraded. The possibility arises that the humic acids may be the result of depolymerisation processes whereby more stable aromatic centres are released by oxidation of the interlinking framework of aliphatic or "disordered carbon". Clearly there is a need for a comprehensive investigation of these compounds, tracing their development from fresh to fossil counterparts in order to reach conclusions regarding their structures and origins.

Stepwise alkaline permanganate oxidation has been proposed as a process in which successive layers in the coal structure are degraded (Mazumdar and Lahiri, 1962). If this is so, then examination of the oxidation products should give an indication of any structural uniformity, or heterogeneity, that may occur from the "periphery" to the "core" of the maceral matrix. On the other hand, the changing distributions of products observed in the alkaline permanganate oxidation of an oil-shale kerogen led to the conclusion that they were derived from structures of different biological origins exhibiting varying susceptibilities to oxidation (Vitorovic *et al.*, 1973). This would seem perfectly valid for a shale kerogen, but it would seem that such a conclusion could equally apply to a kerogen derived from a single biological source, assuming chemical heterogeneity of the structure.

The experimental procedure employed in this study involved the fractionation, by preparative tlc, of the methyl esters of the acids obtained from the oxidations. In the following discussion, the separated fractions will be considered separately.

Monocarboxylic acid fraction

A small proportion of the sporinite residues were degraded to fatty acids by oxidation. The formation of single carboxyl groups signifies cleavage of one bond only and these alkyl moieties represent components attached peripherally to the structure as a whole. Although the yields of fatty acids varied between samples, both high and low rank sporinites produced similar amounts (Fig. 125). The significantly high yield from Barnsley sporinite may be a function of the experimental conditions (see experimental section).

The constant occurrence of $\underline{n}$-C_{16} and $\underline{n}$-C_{18} fatty acids, both with successive oxidations per sample and with the rank of the samples, indicates that $\underline{n}$-C_{16} and $\underline{n}$-C_{18} alkyl chains are common, albeit minor, structures throughout the matrix. Their specificity points to a fatty acid origin. Palmitic and stearic acids were found to be the main products of saponification (Chapter 3). However, it is possible that saponification, although vigorous, may have failed to hydrolyse all the ester groups within the structures.

The changing distributions of the fatty acids observed with progressive oxidations raise a number of interesting points. Fatty acids containing less than 16 carbon atoms were common to all the

FIG.125. TLC FRACTIONATION OF METHYLATED EXTRACTABLE ACIDS OBTAINED FROM THE ALKALINE PERMANGANATE OXIDATION OF SPORINITES

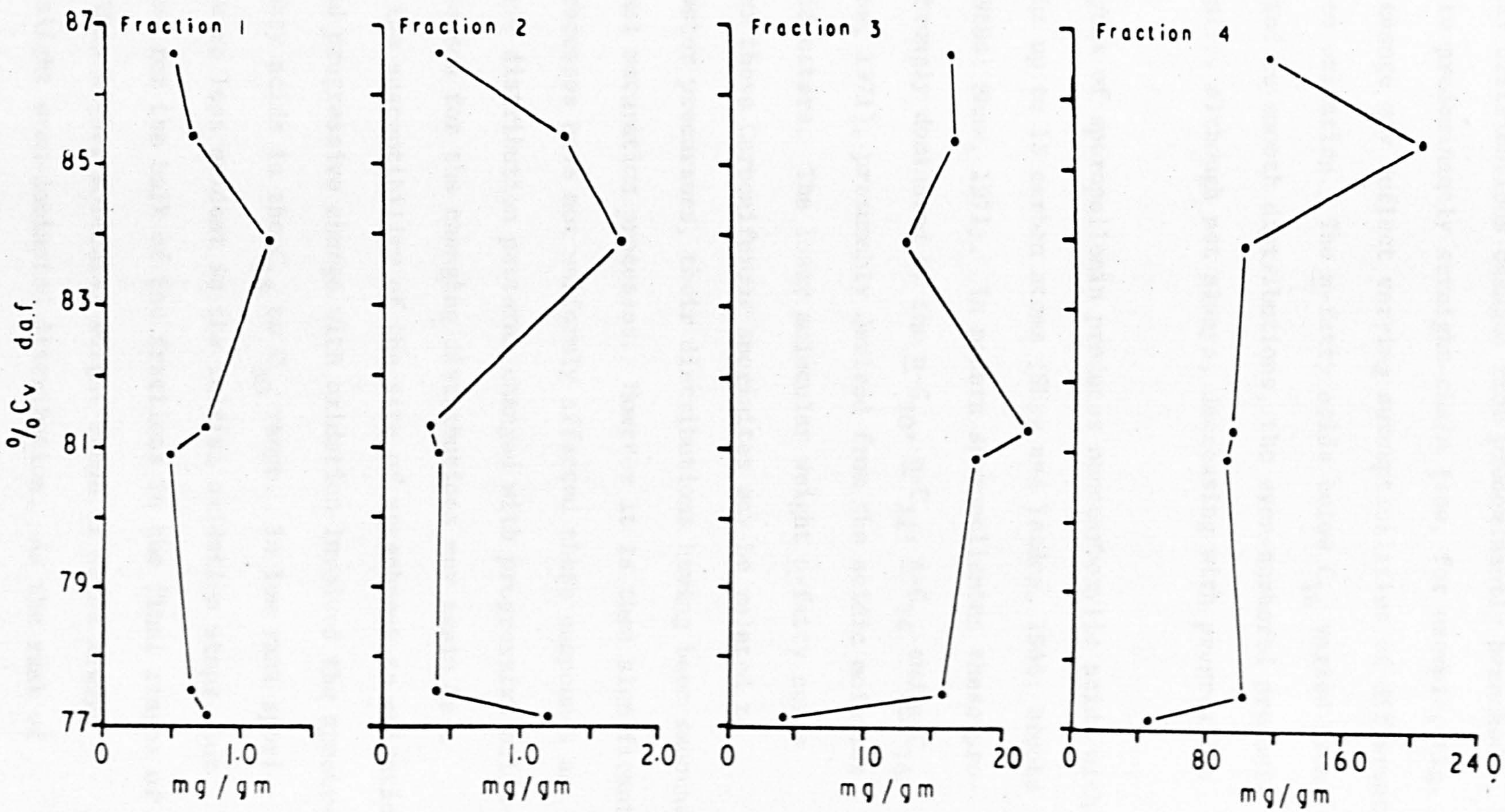

sporinite oxidations. However, with progressive oxidation of the samples their distributions changed from predominantly branched and cyclic to predominantly straight-chain (see, for example, Fig. 91). This change may reflect varying susceptibilities of different structures to oxidation. The n-fatty acids below C_{16} varied from even-dominated to smooth distributions, the even-numbered predominance generally, although not always, decreasing with progressive oxidation.

Ozonolysis of sporopollenin produces monocarboxylic acids with chain lengths up to 18 carbon atoms (Shaw and Yeadon, 1966; Brooks and Shaw, 1968a; Shaw, 1971). In modern sporopollenins these products are strongly dominated by the n-C_{10}, n-C_{12}, n-C_{14} and n-C_{16} members (Shaw, 1971), presumably derived from the acidic moieties of carotenoid esters. The lower molecular weight n-fatty acids isolated from these Carboniferous sporinites may be related to carotenoid ester precursors, their distributions having been smoothed out by thermal maturation processes. However it is then significant that such processes have not uniformly affected these compounds as their relative distribution patterns changed with progressive oxidation. The reason for the changing distributions may again be a function of the susceptibility of the site of attachment to oxidation.

A second progressive change with oxidation involved the appearance of n-fatty acids in the C_{18} to C_{30} range. In low rank sporinites these were less evident in the initial oxidation steps, but they accounted for the bulk of the fractions in the final stages of oxidation. This higher molecular weight range of acids always exhibited a slight even-dominated distribution. As the rank of the sporinites increased, the amount of C_{18} to C_{30} material decreased, and at highest ranks they were always a very minor part of the total monocarboxylic acid fractions. This range of n-fatty acids qualitatively paralleled the distributions of n-alkanes produced by the pyrolysis experiments, but there is a quantitative disparity, especially at higher ranks. For example, pyrolysis of Silkstone sporinite at 375°C produced 0.60 mg/gm of n-alkanes (see Chapter 4, Table 29), predominantly with chain lengths greater than 18 carbon atoms. The oxidation of this sporinite produced 0.47 mg/gm of monocarboxylic acids, predominantly with chain lengths less than 18 carbon atoms. This disparity may, in part, be due to the selective nature of alkaline permanganate oxidation over pyrolysis. Alkaline permanganate selectively oxidises at or next to carbon atoms bearing a functional group (Djuricic *et al.*, 1972), and aromatic rings bearing a wide variety of substituents (Randall *et al.*, 1938). The work of Djuricic *et al.*, (1971), indicates that points of branching in aliphatic networks are also attacked. On the other hand, low-temperature pyrolysis involves random C-C scission (Berkowitz, 1967).

The final oxidation residues may, therefore, be relatively enriched in long-chain aliphatic material. In this respect the residue of a South African alginite, after permanganate oxidation, still gave a very high oil yield upon distillation, although the constitution of the oil was not reported (Dancy and Giedroyc, 1950). Long-chain fatty acids have not been reported as oxidation products of autochthonous coals. Acetic acid is a minor product of carbon-balance oxidations and may be derived in part from the degradation of long alkyl chains, although the work of Kinney (1947) indicated that much of the acetic acid is derived from low molecular weight substituents. Yohe and Harris (1961) reported n-fatty acids up to n-heptanoic acid only. An Australian alginite yielded n-fatty acids up to n-C_{29} (Djuricic *et al.*, 1972), and their occurrence has been reported from various shale and Recent sediment kerogen oxidations (Robinson and Lawlor, 1961; Hoering and Abelson, 1965; Hoering, 1968; Djuricic *et al.*, 1971; Djuricic *et al.*, 1972). Chromic acid oxidation of *Tasmanites* also produced significant quantities of long-chain fatty acids (Burlingame *et al.*, 1969; Simoneit and Burlingame, 1973), as did similar degradations of kerogen from the Green River formation (Burlingame *et al.*, 1969; Burlingame and Simoneit, 1969). In this work on sporinites, extensive degradation of the n-alkanoic acids which may have initially been produced is not thought to have occurred to a great extent. For example, a sample of stearic acid was oxidised for one hour using the same conditions employed in the maceral oxidations. A 97.1% recovery of an acid product was achieved after this period, and on analysis by gc one peak was found with the retention of methyl stearate.

Another possibility is that some long-chain alkyl material may be bound in with the precipitated acid fraction, but these have not yet been studied by further oxidative degradation. Further amounts may be present in the complex polar fractions, although gc evidence did not indicate the presence of any homologous material which may be attributed to aliphatic keto or hydroxy-acids for example. Their occurrence as alkyl substituents on aromatic nuclei would not be expected because of the susceptibility of such structures to oxidation (Randall *et al.*, 1938). The dicarboxylic acid fractions, although containing relatively abundant aliphatic material, showed virtually no long-chain compounds.

Scottish and South African alginites also yielded a wide range of n-fatty acids, extending up to *ca.* n-C_{34}. However, in contrast to sporinites, the long-chain components were produced in the initial steps and tended to persist throughout. Branched/cyclic components occurred in minor amounts relative to n-acids. Djuricic *et al.*, (1972) reported no branched/cyclic monocarboxylic acids from a similar oxidation of a New South Wales alginite, but n-fatty acids in the C_7 to C_{29} range were produced. Once again the amount of long-chain aliphatic material from oxidation was less than the yield of long-chain hydrocarbons from pyrolysis. The unoxidised residues may therefore contain significant amounts of these structures, although Djuricic *et al.*, (1972), considered that the residue of oxidised New South Wales alginite was composed of highly condensed aromatic systems. Such a conclusion is not supported in this work. The alginite residues appeared physically unaffected by oxidation when examined microscopically. Cellular detail was preserved and their fluorescence seemed scarcely affected. An alternative oxidising agent will have to be used for alginite oxidations.

Indiana cutinite yielded predominantly palmitic and stearic acids in the monocarboxylic acid fractions. This is again in contrast to pyrolysis experiments where alkanes, although small in amount, were predominantly of longer chain lengths.

No simple monocarboxylic products were identified from resinite oxidations.

In general it can be concluded that although the oxidative degradation has given an indication of the nature of some of the alkyl constituents occurring in peripheral positions on the respective exinite structures, the disparities between these and the results of the pyrolytic work indicate that only a proportion of such constituents may have been removed, owing to the selectivity of the oxidising agent.

Band 2 from the tlc fractionation of total methyl esters

The oxidation products isolated in this tlc fraction have only been examined summarily, and no structural interpretations have been made. Gc analyses showed varying degrees of complexity, but the range of compounds was often rather restricted, usually eluting in a range equivalent to $\underline{n}$-C_{14} to $\underline{n}$-C_{20} fatty acids. Total yields of these compounds were small, but variable, and in some of the sporinites their yield was greater than that of the monocarboxylic acid fraction (Fig. 125).

Ultraviolet spectroscopic analysis of the combined band 2 fractions of Barnsley sporinite indicated the presence of unsaturated material. The spectrum showed a broad absorbance peak with a maximum at 246 nm and a subsidiary peak at 286 nm. The infra-red spectrum of this same sample showed absorption bands at 3050, 778, 747, 695, and 665 cm^{-1} due to unsaturated C=C bonds, aliphatic C-H absorption bands at 2950, 2921 and 2858 cm^{-1}, and strong absorption at 1723 cm^{-1} due to olefinic or aromatic esters. The tlc behaviour suggests the former rather than the latter. The 1100 to 1500 cm^{-1} region showed numerous absorption bands, probably due to C-H and C-O bending vibrations.

<u>Dicarboxylic acid fraction</u>

A dicarboxylic acid fraction was isolated by tlc from sporinites, alginites and cutinite. These fractions variously contained straight-chain α,ω-dicarboxylic acids and benzenedicarboxylic acids, with other, usually minor, unidentified components.

α,ω-Dicarboxylic acids are well documented as products of coal and humic acid oxidations. Oxidative degradation of sporopollenin and fossil counterparts always yields significant quantities of α,ω-diacids, usually in the C_3 to C_{10} range (Shaw and Yeadon, 1966; Brooks and Shaw, 1968a, 1968b; Shaw, 1971; Brooks, 1971; Brooks and Shaw, 1972). Other work on *Tasmanites*, documented as sporopollenin by the above authors, confirmed α,ω-diacids as chromic acid oxidation products, but in the C_{10} to C_{24} range (Burlingame *et al.*, 1969; Simoneit and Burlingame, 1973). Alginite (Down and Himus, 1941; Djuricic *et al.*, 1972) and cutinite (Hunneman and Eglinton, 1969) oxidations have also yielded these compounds, as have sedimentary kerogens (Down and Himus, 1941; Robinson *et al.*, 1956; Robinson and Lawlor, 1961; Hoering, 1968; Burlingame *et al.*, 1969; Burlingame and Simoneit, 1969; Djuricic *et al.*, 1971; Djuricic *et al.*, 1972; Vitorovic *et al.*, 1973). The isolated products were predominantly straight-chain and extended up to *ca.* C_{25}.

Humic acid degradations yield straight-chain α,ω-diacids. C_2 to C_9 diacids have been recorded from humic and fulvic acids (Schnitzer and Khan, 1972), while C_4 to C_{10} diacids have been isolated from humic acids derived from soils, peats and brown coals (Maximov *et al.*, 1972). Very short chain (C_2 to C_4) compounds have been reported from bituminous coal humic acids (Lawson and Purdie, 1966; Davies and Lawson, 1967a, 1967b).

The range of α,ω-dicarboxylic acids isolated from sporinites gives some indication of the chain lengths of polymethylene bridges in the structures. Although the overall quantity of the dicarboxylic acid fraction showed little reduction with increasing rank (Fig. 125), the decreasing relative predominance of α,ω-dicarboxylic acids in the fractions testifies to their decrease with increasing rank. In sporinites of ranks equivalent to 77% to 83% $C_{vit.}$ (d.a.f.), significant quantities were produced, but they declined steadily thereafter and were only minor constituents in Silkstone sporinite (86.6% C_{vit}, d.a.f.).

Certain reservations must however be made as to the true chain lengths of these compounds, as they are themselves susceptible to oxidation with alkaline permanganate. They only achieve relative stability at shorter chain lengths (Randall *et al.*, 1938).

Two standard α,ω-dicarboxylic acids (1,9-nonandioic and 1,16-hexadecandioic acid) were each oxidised for one hour under the conditions employed for the maceral oxidations. A 14% recovery of products was made from the oxidation of the C_9 diacid which were shown, by methylation, tlc and gc, to consist only of 1,9-dimethyl nonandioate. A 4.1% recovery of products was made from the other oxidation and these were shown to consist of C_8 to C_{13} diacids with a small amount of the C_{16} diacid.

In the final oxidation steps of individual samples, considerable reaction times were involved and the relatively low yields of α,ω-dicarboxylic acids may be due, in part, to their degradation to shorter chain and more water-soluble homologues. However, the fact that the distributions did not change significantly with increasing oxidation times suggests that either any degradation occurred rapidly or that the permanganate selectively oxidised other, more-easily degradable, structures.

Within the above limitations, the relative distributional constancy of the diacids in the C_5 to C_{17} range with rank indicates a certain stability of structure. High rank distributions were essentially the same as those at low rank, although quantitatively reduced. The implication is that the polymethylene structures do not degrade to progressively shorter chains with increasing coalification but are lost as complete entities, presumably by expulsion, or perhaps by cyclisation.

The appearance of longer-chain diacids in the middle or late stages of oxidation is a similar phenomenon to that noted with the monocarboxylic acid fractions. In both cases they were mostly found in the lower rank samples. This suggests that a part of the aliphatic material in the matrix has a greater resistance to oxidation than other parts, which could be indicative of a heterogeneous structure composed of predominantly aliphatic and predominantly aromatic regions. Initial short period oxidations might thus be expected to preferentially degrade the more susceptible peripheral groups attached to aromatic structures, whereas the more aliphatic regions would require more sustained oxidative conditions. The microscopical evidence from the oxidation residues indicated selective lines of oxidative attack through individual spore fragments at lower ranks, followed by particle disruption at higher ranks. Yokokawa *et al.*, (1962), have previously postulated a heterogeneous coal structure containing predominantly alicyclic and predominantly aromatic areas.

A heterogeneous structure based on these kinds of models would be expected to lose the aliphatic regions in the course of natural coalification, which is consistent with these experimental observations. It may also help to explain the discrepancies between pyrolytic hydrocarbon and oxidative acid chain lengths, remembering that the pyrolytic conditions employed are considered as simulating natural maturation (Berkowitz, 1967). Palmer and Vahrman (1972b) illustrated, however, that more severe pyrolysis to 600°C, albeit of bright coal, alters generated alkane patterns by the addition of relatively large amounts of shorter (i.e. less than C_{15}) chain alkanes. The present oxidative work suggests that these short-chain alkanes were probably derived from cross-linking polymethylene structures between aromatic clusters.

α,ω-Dicarboxylic acids were also produced by the oxidation of alginites and cutinite. The yield of the dicarboxylic acid fraction from the alginites was higher than from sporinites and they were composed entirely of aliphatic diacids with apparently no benzenedicarboxylic acids. The higher alginite yields may well reflect a more aliphatic macrostructure, but the oxidation scarcely affected the physical appearance of these macerals, even in quite fine detail. The structural nature of the residues cannot be extrapolated from these results, but the good physical comparison between these and fresh alginites would suggest retention of much of the original, and hence aliphatic, structure.

The distribution of α,ω-dicarboxylic acids isolated by oxidation was similar to those of the sporinites. The cutinite di-acids were also similar. If this di-acid pattern was not simply due to the oxidation conditions used, it implies that the nature of these polymethylene linkages may be determined in the early stages of coalification, that they are relatively stable structures, and that they develop irrespective of the type of maceral. Their source is problematical as the chain-length distributions do not correlate readily with typical biolipid distributions. Their occurrence in humic acids of very young sediments indicates formation quite quickly after deposition of source organic materials, and this possibly points to microbiological participation.

Benzenedicarboxylic acids were present in the dicarboxylic acid fractions of sporinites, but they were not detected from alginites and cutinite. Benzene-1,2-dicarboxylic acid (o-phthalic acid) was found, however, in the polar fractions from all three macerals. The occurrence of this compound in two tlc fractions was caused by the inability of the developing solvent system to confine it to a narrow chromatographic band.

o-Phthalic acid was always the major isomer of the benzenedicarboxylic acids, and at higher ranks in the sporinites the dicarboxylic acids were almost entirely composed of the benzenoid di-acids, polymethylene structures no longer being found in significant quantities. These ranks are at the beginning of the "liquid structure" stage of Hirsch and co-workers, and the change from relatively long, open-chain linkages to more planar cyclic linkages between condensed nuclei would facilitate the orientation of the nuclei into more parallel layers.

The ubiquitous predominance of o-phthalic acid over its two isomers testifies to the predominant occurrence of cyclic systems rather than isolated benzene rings. However, substituted benzene rings bearing an -OH or -OCH_3 group will not be detected as benzenoid acids, as these lead to ring disruption by alkaline permanganate oxidation (Randall *et al.*, 1938). It is not possible to postulate further about actual coal structures which could give rise to o-phthalic acid as it can be an oxidative product of a large variety of condensed aromatic compounds (Randall *et al.*, 1938).

Polar fraction

This tlc fraction accounted for the major part of the oxidation products of sporinite (Fig. 125), alginite and cutinite. In all cases, they contained a large number of compounds, and, generally, few of them corresponded to the benzenoid acids. No further fractionations were undertaken. Furthermore, the observed distributions of benzenoid acids will not be the true distributions of these compounds as the more highly substituted members become increasingly soluble in water, and will have been partially lost by partition between aqueous and organic extraction phases.

Benzene polycarboxylic acids are the end-products of oxidation of many aromatic structures and are themselves quite resistant to further oxidation with alkaline permanganate. The most prominent benzenoid acid isolated from sporinites was benzene-1,2,4-tricarboxylic acid (trimellitic acid). The other two trisubstituted isomers generally were produced in much smaller quantities. As trimellitic acid is the most water-soluble of the benzenetricarboxylic acids, and hence the one most likely to be lost by partition with an aqueous phase, this relative distribution is probably a true distribution.

The predominance of trimellitic acid increased both with successive oxidations of individual samples and also with the rank of the samples. A similar situation was observed with o-phthalic acid, and their relative increases corresponded with decreases in the yields of aliphatic dicarboxylic acids. It is possible that there may be a genetic relationship, at least in part, between o-phthalic acid and trimellitic acid, as these would be products of the oxidation of mono-substituted naphthalene or dihydronaphthalene type structures.

The many other constituents of the polar fractions would require identification before any meaningful conclusions could be drawn concerning parent coal structures. Benzenetetracarboxylic acids appeared as minor components in the later stages of many of the oxidations. This perhaps suggests that they were derived from polycyclic systems rather than highly alkly-substituted mononuclear systems, and only began to oxidise significantly when the greater part of the oxidisable aliphatic material had been degraded. Benzenepenta- and -hexacarboxylic acids were not apparent as important oxidation products, although they are well documented as coal oxidation products. The oxidative yield of benzenehexacarboxylic acid (mellitic acid) has been equated with coal rank (van Krevelen, 1963), being formed in greater amounts as condensation progresses. The apparent absence of these compounds in any significant quantities may be due to their having been removed in the water-soluble fractions. Alternatively, the oxidising conditions employed may have been insufficiently vigorous to fully degrade parent systems to these compounds.

Francis (1961) considers that the majority of aromatic acids identified in early coal oxidation work as benzene polycarboxylic acids were, in fact, heterocyclic acids, and that benzenoid acids account for only a small proportion of coal oxidation products. Under relatively mild oxidising conditions such as those employed in this work, heterocyclic acids, as well as aromatic systems not fully oxidised to simple benzenoid acids, were probably present in the polar fractions, especially in the initial, rapid oxidation steps.

Alginites yielded large amounts of polar material with gc distributional patterns very different to those of sporinites. Benzenetri- and -tetracarboxylic acids were present but only as minor constituents. The structures of most of the compounds are unknown, but infra-red spectra showed strong aliphatic C-H absorption bands at characteristic frequencies. Both aliphatic and aromatic (or possibly ketone) acids were also indicated by infra-red analyses. A similar oxidation of an Australian alginite produced benzene polycarboxylic acids, benzoic acid and a methyl-naphthalene dicarboxylic acid (Djuricic *et al.*, 1972), but no identifications of other compounds which might occur in the polar fractions were reported. Aliphatic keto-acids and numerous naphthyl acids have been reported from the chromic acid oxidation of *Tasmanites*, a material similar in origin to alginites of *Botryococcus* derivation (Burlingame *et al.*, 1969; Simoneit and Burlingame, 1973).

Benzenoid acids produced from the cutinite sample were similar to those from sporinites, and once again they only constituted a minor proportion of the total polar fractions.

Resinites

The oxidation products of Maghara and Bitterfeld resinites were of a completely different nature to those of the other exinites, probably being cyclic structures of diterpenoid origin. This has been a feature of all lines of investigation undertaken with the resinites, and it is clear that this particular maceral, at least at low ranks, requires extensive and detailed chemical investigation to elucidate the structures of the many (probably) cyclic products obtained by extraction and by degradative techniques.

Experimental

Stepwise oxidation with alkaline potassium permanganate was employed, using the method of Djuricic *et al.*, (1971), for their oxidative studies of Green River shale kerogen. The methodology did not vary much between samples but the experimental procedure will be described in full, noting any variations from the norm in this text. Full experimental data for all the samples is presented in Table 48.

Permanganate ratios

Djuricic *et al.*, used a sample to permanganate ratio of 4:1 (by weight) in their Green River shale studies. In the present study of exinites a similar ratio was used for High Hazles Gedling and Barnsley sporinites. The number of oxidations needed for these two samples was found to be large and, principally because of the time factor, the ratio was changed to 4:3 for Clowne sporinite, and then to 1:1 for all the other samples.

Oxidation procedure

The oxidation procedure was identical for all the samples. In a typical experiment the extracted and saponified maceral residue plus aqueous KOH, (1.6%, 150 ml), was vigorously stirred in a two-necked flask fitted with a condenser and stirrer. The suspension was heated to 80°C in a water bath. An aliquot of solid potassium permanganate was added (Table 48) and stirring was continued until the purple colour disappeared. The mixture was filtered and the residue was washed with aqueous KOH until a colourless filtrate was obtained. The original filtrate and washings were combined and retained. The residue, containing unoxidised maceral and manganese dioxide, was re-oxidised as above, in steps. Oxidation was considered to be complete when the reaction mixture remained purple after an 8 hr. reaction time.

Extraction of acidic products

The filtrates obtained from each oxidation step were worked up separately. Neutral components were initially extracted with chloroform but this procedure was abandoned when negligible quantities were obtained. The filtrates were acidified to pH 1 with dilute sulphuric acid (10%) and the resulting precipitates of insoluble acids were filtered off and collected, dried and then weighed, where possible (Table 48). Alginites and resinites generally produced too small a precipitate for accurate recovery. The remaining filtrates were extracted with aliquots of diethyl ether and then dichloromethane until colourless extracts were obtained. The extracts were combined to yield organic-soluble acidic fractions for each oxidative step (Table 48). The remaining water-soluble material was not recovered.

The filtrate from the last oxidation step of each sample contained the excess permanganate in solution. This was reduced by the addition of excess dilute sulphuric acid (10%) and solid sodium metabisulphite, after which the oxidation products were extracted in the usual manner.

Fractionation of methylated products

The organic-soluble acids were methylated with ethereal diazomethane and the ester fractions so obtained were fractionated by preparative tlc (SiO_2). Details of the plate preparation have been given in Chapter 2. The developing solvent system for sporinite, alginite and cutinite esters was petroleum ether: diethyl ether (90:10), and n-heptane:acetone (70:30) for resinite esters. After

Table 48: Experimental details for the exinite degradations by stepwise alkaline potassium permanganate oxidation

	Initial Weight (gm)	Weight $KMnO_4$/ step (gm)	No. of steps	Total weight extracted acids (gm)	Total weight precipitated acids (gm)	Weight oxidised residue recovered (gm)
Sporinite						
High Hazles Gedling	5.0000	1.25	13	0.4097	1.6218	4.5500
Clowne	4.9700	3.75	7	0.6984	1.2029	4.6389
Deep Hard	4.9869	5.00	6	0.6422	0.6628	0.2090
High Hazles Whitwell	4.9802	5.00	6	0.7107	1.1578	1.2181
Barnsley	5.1066	1.25	20	0.7788	0.7982	4.8760
Parkgate	4.7468	5.00	7	1.2172	0.1353	1.6309
Silkstone	4.6581	5.00	7	0.6794	0.1896	3.5471
Alginite						
Scotland	4.9475	5.00	5	0.7178	n.d.	2.0647
South Africa	4.4682	4.50	6	1.0401	n.d.	4.3969
Resinite						
Bitterfeld	4.2833	4.50	4	1.0737	0.0749	1.2810
Maghara	2.4854	2.50	2	0.2102	n.d.	1.9818
Cutinite						
Indiana	4.4241	4.50	3	0.6781	0.7671	0.4217

n.d. Weights not determined because of the very low yields and consequent difficulties in separating them from filter papers.

development the plates were sprayed with a fluorescent dye (Rhodamine G or dichlorofluorescein) and band positions were identified under an ultraviolet lamp. In general the esters were fractionated into four fractions (Table 49). Bands 3 and 4 consisted of a number of contiguous bands which were too close together for individual separations to be made.

The bands were scraped off the tlc plates and the esters were recovered by elution with dichloromethane, or dichloromethane: methanol (1:1) for the polar fractions.

Residues

The oxidation residues consisted of unoxidised maceral and the accumulated manganese dioxide from each oxidative step. The insoluble manganese dioxide was converted to soluble manganese sulphate by the addition of excess dilute sulphuric acid (10%) and solid sodium metabisulphite. The remaining insoluble organic matter was filtered, washed, dried and weighed (Table 48). Subsequent microscopical examination showed that all the inorganic matter had been removed.

Gas chromatography

All the ester fractions were analysed by gc, using both packed (3% OV-101 on Varaport 30) and capillary (OV-101) columns. Internal standards (methyl esters of n-fatty acids, straight-chain α, ω-dicarboxylic acids and the benzene polycarboxylic acids) were used to identify the acids. The presence of esters was confirmed for selected fractions by infra-red spectroscopy.

Oxidation of standard aliphatic acids

Stearic, suberic and 1,16-hexadecandioic acids were separately oxidised for 1 hr under the oxidising conditions employed in the maceral oxidations, using a sample to permanganate ratio of 1:1. The aliquot of permanganate was reduced after *ca*. 30 mins with 1,16-hexadecandioic acid but was not completely reduced in the other two experiments. Oxidation products were recovered in the same way as that described for the maceral oxidations.

Stearic acid:- 97% recovery of this compound was obtained and was shown by gc, after methylation, to be a single component with the retention of methyl stearate.

Suberic acid:- organic-extractable acids accounted for 14% of the suberic acid after a 1 hr oxidation. Gc analysis of the methylated product indicated a single component with the retention of dimethyl suberate.

1,16-hexadecandioic acid:- organic-extractable acids accounted for only 4.1% of the starting material after only a 30 min. oxidation. Gc analysis of the methylated product showed a series of dimethyl esters of α,ω-dicarboxylic acids in the C_8 to C_{13} range with 1,11-dimethyl undecandioate as the main constituent. There was also a small quantity of 1,16-dimethyl hexadecandioate remaining.

Table 49: Preparative thin-layer chromatography data: fractionation of methyl esters

High Hazles Gedling sporinite

Step	Band 1 mg	Band 1 Rf	Band 2 mg	Band 2 Rf	Band 3 mg	Band 3 Rf	Band 4 mg	Band 4 Rf
1	0.3	0.72-0.49	0.9	0.43	0.8	0.29-0.21	16.7	0.21-0.00
2	0.2	0.73-0.48	0.3	0.40	0.5	0.23-0.15	8.7	0.15-0.00
3	0.1	0.68-0.45	0.3	0.37	-	-	23.3	0.17-0.00
4	0.2	0.65-0.40	0.1	0.31	1.4	0.25-0.15	16.9	0.15-0.00
5	0.2	0.76-0.50	0.6	0.47	1.4	0.31-0.20	14.7	0.20-0.00
6	0.4	0.73-0.50	0.6	0.44	2.2	0.26-0.17	24.6	0.17-0.00
7	0.4	0.69-0.40	0.4	0.36	1.4	0.25-0.18	12.4	0.18-0.00
8	0.9	0.66-0.44	0.7	0.33	1.7	0.20-0.14	18.3	0.14-0.00
9	0.1	0.68-0.47	1.0	0.34	1.7	0.21-0.14	13.2	0.14-0.00
10	0.2	0.59-0.35	0.5	0.29	1.5	0.19-0.13	13.3	0.13-0.00
11	0.3	0.62-0.38	0.2	0.31	1.6	0.26-0.09	26.6	0.09-0.00
12	0.1	0.63-0.43	0.1	0.33	4.2	0.29-0.10	19.1	0.10-0.00
13	0.3	0.65-0.43	0.2	0.31	1.9	0.18-0.07	18.3	0.07-0.00
	3.7		5.9		20.3		226.1	

Clowne sporinite

Step	Band 1 mg	Band 1 Rf	Band 2 mg	Band 2 Rf	Band 3 mg	Band 3 Rf	Band 4 mg	Band 4 Rf
1	0.1	0.66-0.40	0.1	0.37-0.31	7.6	0.26-0.08	58.9	0.08-0.00
2	0.3	0.74-0.45	0.1	0.41-0.35	11.4	0.32-0.11	84.0	0.11-0.00
3	0.3	0.75-0.47	0.4	0.43-0.35	11.6	0.31-0.09	80.0	0.09-0.00
4	0.5	0.70-0.40	0.6	0.35-0.28	11.3	0.26-0.08	68.7	0.08-0.00
5	0.6	0.70-0.41	0.3	0.40-0.33	14.9	0.30-0.12	101.4	0.11-0.00
6	0.7	0.67-0.40	0.4	0.39-0.30	14.1	0.27-0.08	68.9	0.08-0.00
7	0.7	0.78-0.47	0.1	0.32	7.0	0.28-0.08	34.6	0.08-0.00
	3.2		2.0		77.9		496.5	

Deep Hard sporinite

Step	Band 1 mg	Band 1 Rf	Band 2 mg	Band 2 Rf	Band 3 mg	Band 3 Rf	Band 4 mg	Band 4 Rf
1	0.4	0.73-0.44	0.6	0.41-0.31	13.1	0.27-0.07	91.7	0.07-0.00
2	0.2	0.75-0.42	0.3	0.38-0.30	19.0	0.27-0.10	110.3	0.10-0.00
3	0.5	0.77-0.50	0.3	0.47-0.38	18.4	0.32-0.10	81.4	0.10-0.00
4	0.9	0.74-0.43	0.5	0.36-0.31	19.1	0.27-0.08	95.8	0.08-0.00
5	0.2	0.65-0.36	0.1	0.33-0.27	14.2	0.21-0.07	40.8	0.07-0.00
6	0.1	0.74-0.43	0.1	0.29	5.8	0.23-0.09	22.2	0.09-0.00
	2.3		1.9		89.6		442.2	

High Hazles Whitwell sporinite

Step	Band 1 mg	Band 1 Rf	Band 2 mg	Band 2 Rf	Band 3 mg	Band 3 Rf	Band 4 mg	Band 4 Rf
1	0.2	0.80-0.49	0.5	0.45-0.37	11.4	0.32-0.10	59.5	0.10-0.00
2	0.3	0.78-0.50	0.2	0.47-0.36	15.9	0.29-0.10	78.8	0.10-0.00
3	0.5	0.82-0.58	0.1	0.53-0.43	21.3	0.38-0.12	101.6	0.12-0.00
4	1.3	0.81-0.54	0.4	0.50-0.36	24.1	0.31-0.11	120.2	0.11-0.00
5	0.8	0.82-0.54	0.3	0.39	18.8	0.31-0.09	56.9	0.09-0.00
6	0.5	0.70-0.45	0.1	0.35	15.6	0.31-0.07	42.5	0.07-0.00
	3.6		1.6		107.1		459.5	

Table 49 cont'd.

Barnsley sporinite

Step	Band 1 mg	Band 1 Rf	Band 2 mg	Band 2 Rf	Band 3 mg	Band 3 Rf	Band 4 mg	Band 4 Rf
1	0.1	0.74-0.49	0.1	0.37	0.8	0.32-0.12	27.1	0.10-0.00
2	0.2	0.73-0.40	0.5	0.33	1.7	0.30-0.09	14.4	0.09-0.00
3	0.3	0.71-0.40	0.5	0.35	3.0	0.29-0.07	14.7	0.07-0.00
4	0.3	0.75-0.45	0.7	0.40	3.0	0.33-0.08	19.4	0.08-0.00
5	0.3	0.70-0.40	0.1	0.34	2.2	0.26-0.10	23.9	0.10-0.00
6	0.3	0.63-0.37	0.6	0.30	2.8	0.27-0.07	26.2	0.07-0.00
7	0.4	0.65-0.37	1.9	0.31	2.4	0.26-0.08	27.3	0.08-0.00
8	0.3	0.74-0.46	0.1	0.33	3.3	0.27-0.07	20.6	0.07-0.00
9	0.2	0.69-0.45	0.2	0.32	2.6	0.27-0.09	25.9	0.09-0.00
10	0.8	0.68-0.40	0.4	0.30	4.5	0.26-0.07	28.0	0.07-0.00
11	0.5	0.67-0.41	0.2	0.29	5.1	0.25-0.07	37.2	0.07-0.00
12	0.2	0.71-0.41	0.2	0.30	2.6	0.26-0.07	29.7	0.07-0.00
13	0.1	0.75-0.46	0.1	0.31	3.6	0.27-0.08	23.2	0.07-0.00
14	0.2	0.70-0.40	0.4	0.28	4.4	0.24-0.06	29.9	0.06-0.00
15	0.3	0.75-0.48	0.5	0.37	4.0	0.33-0.10	31.5	0.10-0.00
16	0.5	0.75-0.48	0.4	0.38	3.8	0.32-0.11	29.3	0.10-0.00
17	0.3	0.71-0.45	0.1	0.33	3.9	0.29-0.08	28.8	0.08-0.00
18	0.2	0.77-0.52	0.8	0.36	3.5	0.31-0.09	22.1	0.09-0.00
19	0.2	0.74-0.46	0.1	0.34	4.2	0.29-0.08	19.9	0.07-0.00
20	0.2	0.61-0.35	0.1	0.25	4.4	0.23-0.07	26.8	0.07-0.00
	5.9		7.0		65.8		505.9	

Parkgate sporinite

Step	Band 1 mg	Band 1 Rf	Band 2 mg	Band 2 Rf	Band 3 mg	Band 3 Rf	Band 4 mg	Band 4 Rf
1	0.2	0.69-0.42	1.0	0.38-0.29	9.9	0.24-0.10	144.1	0.10-0.00
2	0.3	0.70-0.45	0.8	0.38-0.30	13.5	0.27-0.12	190.2	0.12-0.00
3	0.1	0.70-0.45	0.2	0.40-0.32	14.1	0.28-0.11	153.1	0.11-0.00
4	0.4	0.75-0.47	0.2	0.41-0.32	13.4	0.27-0.12	174.9	0.12-0.00
5	0.2	0.68-0.45	0.3	0.40-0.33	7.7	0.25-0.10	141.3	0.10-0.00
6	1.2	0.76-0.50	0.7	0.45-0.35	12.5	0.30-0.11	86.2	0.11-0.00
7	0.5	0.65-0.44	0.6	0.39-0.30	7.1	0.27-0.09	85.8	0.09-0.00
	2.9		3.8		78.2		975.6	

Silkstone sporinite

Step	Band 1 mg	Band 1 Rf	Band 2 mg	Band 2 Rf	Band 3 mg	Band 3 Rf	Band 4 mg	Band 4 Rf
1	0.3	0.79-0.50	0.3	0.46-0.35	7.8	0.31-0.11	75.8	0.10-0.00
2	0.9	0.80-0.57	0.6	0.52-0.41	14.6	0.35-0.12	137.3	0.12-0.00
3	0.2	0.75-0.53	0.5	0.48-0.34	12.4	0.30-0.08	52.1	0.08-0.00
4	0.2	0.75-0.50	0.2	0.46-0.36	14.0	0.31-0.10	73.7	0.10-0.00
5	0.2	0.79-0.51	0.1	0.47-0.37	8.2	0.31-0.10	63.3	0.10-0.00
6	0.2	0.72-0.43	0.1	0.35	8.0	0.30-0.08	68.1	0.08-0.00
7	0.2	0.77-0.51	0.1	0.42	9.9	0.33-0.08	62.5	0.08-0.00
	2.2		1.9		74.9		532.8	

Table 49 cont'd.

Scottish alginite

Step	Band 1 mg	Band 1 Rf	Band 2 mg	Band 2 Rf	Band 3 mg	Band 3 Rf	Band 4 mg	Band 4 Rf
1	0.7	0.76-0.53	0.3	0.47-0.39	27.8	0.35-0.11	39.0	0.11-0.00
2	0.2	0.80-0.62	0.1	0.58-0.46	22.3	0.41-0.14	42.1	0.14-0.00
3	0.3	0.77-0.55	0.2	0.40	35.9	0.35-0.05	27.0	0.05-0.00
4	0.1	0.71-0.50	-	-	21.1	0.26-0.07	24.8	0.07-0.00
5	0.1	0.68-0.46	-	-	13.0	0.32-0.03	8.1	0.03-0.00
	1.5		0.6		120.1		141.0	

South African alginite

Step	Band 1 mg	Band 1 Rf	Band 2 mg	Band 2 Rf	Band 3 mg	Band 3 Rf	Band 4 mg	Band 4 Rf
1	1.2	0.75-0.47	-	-	55.0	0.45-0.09	58.5	0.07-0.00
2	1.3	0.80-0.50	-	-	71.1	0.45-0.13	86.7	0.13-0.00
3	0.5	0.70-0.45	-	-	84.6	0.32-0.06	68.7	0.06-0.00
4	0.1	0.75-0.52	-	-	40.9	0.37-0.04	17.0	0.04-0.00
5	0.1	0.75-0.57	-	-	51.2	0.33-0.04	20.4	0.04-0.00
6	0.2	0.74-0.46	-	-	28.9	0.28-0.04	20.5	0.04-0.00
	3.4				331.7		271.8	

Indiana cutinite

Step	Band 1 mg	Band 1 Rf	Band 2 mg	Band 2 Rf	Band 3 mg	Band 3 Rf	Band 4 mg	Band 4 Rf
1	0.3	0.81-0.58	0.2	0.53-0.44	25.4	0.37-0.15	185.9	0.14-0.00
2	0.3	0.77-0.55	0.1	0.40	37.7	0.36-0.12	81.7	0.11-0.00
3	0.2	0.72-0.48	-	-	1.1	0.30-0.04	34.9	0.04-0.00
	0.8		0.3		64.2		302.5	

Maghara resinite

Step	Band 1 mg	Band 1 Rf	Band 2 mg	Band 2 Rf	Band 3 mg	Band 3 Rf	Band 4 mg	Band 4 Rf
1	7.1	0.53	21.5	0.42	61.5	0.38-0.03	6.8	0.03-0.00
2	9.9	0.51, 0.42	14.8	0.36, 0.31	19.8	0.29-0.06	30.7	0.06-0.00
	17.0		36.3		81.3		37.5	

Bitterfeld resinite

Step	Band 1 mg	Band 1 Rf	Band 2 mg	Band 2 Rf	Band 3 mg	Band 3 Rf
1	59.7	0.52, 0.48	321.5	0.45-0.04	33.3	0.04-0.00
2	61.1	0.54, 0.48	212.1	0.46-0.04	11.1	0.04-0.00
3	47.7	0.56, 0.45	120.8	0.40-0.03	6.8	0.03-0.00
4	25.9	0.51, 0.41	52.0	0.39-0.04	6.2	0.04-0.00
	194.4		706.4		57.4	

References

Abelson, P.H. (1963) Organic geochemistry and the formation of petroleum. Proc. 6th World Pet. Cong., (Frankfurt), 1, A397-A407.

Adams, K.R., Bonnet, R. (1971) Long-chain α,ω-dicarboxylic acids from the spores of *Equisetum telmalei* and *E. arvense*. Phytochem., 10, 1885-1890.

Ahmed, M.D., Kinney, C.R. (1950) Ozonization of humic acids prepared from oxidised bituminous coal. J. Am. Chem. Soc., 72, 559-561.

Albaiges, J., Torradas, J.M. (1974) Significance of the even-carbon n-paraffin preference of a Spanish crude oil. Nature, 250, 567-568.

Albrecht, P., Ourisson, G. (1969) Diagenese des hydrocarbures satures dans une serie sedimentaire epaisse. Geochim. Cosmochim. Acta, 33, 138-142.

Allan, J. (1970) M.Sc. Dissertation, University of Newcastle upon Tyne.

Archari, R.G., Shaw, G., and (in part) Holleyhead, R. (1973) Identification of ionene and other carotenoid degradation products from the pyrolysis of sporopollenins derived from some pollen exines, a spore coal and the Green River shale. Chem. Geol., 12, 229-234.

Arpino, P., Albrecht, P., Ourisson, G. (1972) Studies on the organic constituents of lacustrine Eocene sediments. Possible mechanisms for the formation of some geolipids related to biologically-occurring terpenoids, in Adv. Org. Geochem., 1971, (Eds: H.R. von Gaertner, H. Wehner), Pergamon Press (Oxford), 173-187.

Austen, D.E.G., Ingram, D.J.E., Given, P.H., Binder, C.R., Hill, L.W. (1966) Electron spin resonance studies of pure macerals, in Coal Science, (Ed: R.F. Gould), Adv. Chem. Ser. No. 55, Am. Chem. Soc., (Washington D.C.), 344-362.

Bailey, A.E.W., Kimberley, I.E., Ward, S.G. (1954) Chemical constitution of coal. I - Preparation and properties of humic acids from coal. Fuel, 33, 209-221.

Bailey, A.E.W., Kimberley, I.E., Turner, L., Ward, S.G. (1955) Chemical constitution of coal. II - Preparation of sub-humic acids from humic acids by oxidation in the presence of alkali. Fuel, 34, 37-49.

Barghoorn, E.S., Schopf, J.W. (1967) Micro-organisms 3 billion years old from the Pre-Cambrian of South Africa. Science, 152, 758-762.

Barker, C. (1974) Programmed-temperature pyrolysis of vitrinites of various ranks. Fuel , 53, 176-177.

Bellamy, L.J. (1964) The Infra-red Spectra of Complex Molecules. Methuen & Co., (London).

Bent, R., Brown, J.K. (1961) The infra-red spectra of macerals. Fuel, 40, 47-56.

Bergman, G., Huck, G., Karweil, J., Luther, H. (1954) Ultrarotspektren von Kohlen. Brennst. Chem., 35, 175-176.

Berkowitz, N. (1957) On the differential thermal analysis of coal. Fuel, 36, 355-373.

Berkowitz, N. (1967) The coal-carbon transformation: basic mechanisms. Proc. Symp. Sci. Tech. Coal, Dept. Energy, Mines and Resources, Ottawa, Canada, 149-155.

Bertrand, C.E., Renault, B. (1892a) Premieres remarques sur le boghead d'Autun. Ann. Soc. Geol. Nord., 20, 213.

Bertrand, C.E., Renault, B. (1892b) ***Pila bibractensis*** et le boghead d'Autun. Bull. Soc. Hist. Nat. Autun, 5, 159-253.

Biemann, K. (1962) Mass Spectrometry. Organic Chemical Applications. McGraw-Hill Book Co., Inc., (New York).

Birkofer, L., Pauly, W. (1969) Gaschromatographische und massenspektroskopische Untersunchung von Kohlextracten. Brennst. Chem., 50, 376-382.

Bitz, M.C., Nagy, B. (1966) Ozonolysis of "polymer-type" material in coal, kerogen and the Orgeuil meteorite - a preliminary report. Proc. Nat. Acad. Sci., 56, 1383-1390.

Bitz, M.C., Nagy, B. (1967) Analysis of bituminous coal by a combined method of ozonolysis, gas chromatography and mass spectrometry. Anal. Chem., 39, 1310-1313.

Blackburn, K.B., Temperley, B.N. (1936) *Botryococcus* and the algal coals. Part II. The boghead controversy and the morphology of the boghead algae. Trans. Roy. Soc. Edin., 58, 841-868.

Blenkinsop, R. (1973) Personal communication.

Blom, L., Edelhausen, L., Krevelen, D.W. van. (1957). Chemical structure and properties of coal XVIII - Oxygen groups in coal and related products. Fuel, 36, 135-153.

Blumer, M., Mullin, M.M., Guillard, R.R.L. (1970) A polyunsaturated hydrocarbon (3,6,9,12,15,18-heneicosahexaene) in the marine food web. Mar. Biol., 6, 226-236.

Bone, W.A., Bard, B.J.A. (1937) Researches on the chemistry of coal. VIII Comparative studies of the macroconstituents of bituminous coals. Proc. Roy. Soc., Series A, 127, 480-510.

Bone, W.A., Horton, L., Ward, S.G. (1930) Researches on the chemistry of coal. VI Its benzenoid constitution as shown by its oxidation with alkaline potassium permanganate. Proc. Roy. Soc., Series A, 127, 480-510.

Bone, W.A., Parsons, L., Shapiro, R., Groocock, C.M. (1935) Researches on the chemistry of coal. VII The development of benzenoid constitution in the lignin - peat - coal series. Proc. Roy. Soc., Series A, 148, 492-522.

Bone, W.A., Quarendon, R. (1926) Researches on the chemistry of coal. IV The oxidation of the residue from the benzene pressure-extraction process. Proc. Roy. Soc., Series A, 110, 537-542.

Boyer, A.F., Ferrand, R., Ladam, A., Payen, P. (1961) Quelques indices sur la structure des charbons d'apres l'analyse de leurs produits de degradation. Chim. Ind., 86, 523-530.

Bray, E.E., Evans, E.D. (1961) Distribution of n-paraffins as a clue to the recognition of source beds. Geochim. Cosmochim. Acta, 22, 2-15.

Bricteux, J. (1967) Combination of pyrolysis and gas chromatography: a new technique of identification. Ann. Mines Belg., 761-767.

Brooks, J. (1971) Some chemical and geochemical studies on sporopollenin, in Sporopollenin, (Eds: J. Brooks, P.R. Grant, M. Muir, P. van Gijzel, G. Shaw), Academic Press (London), 351-407.

Brooks, J., Shaw, G. (1968a) Chemical structure of the exine of pollen walls and a new function for carotenoids in nature. Nature, 219, 532-533.

Brooks, J., Shaw, G. (1968b) Identity of sporopollenin with older kerogen and new evidence for the possible biological source of chemicals in sedimentary rocks. Nature, 220, 678-679.

Brooks, J., Shaw, G. (1969) Evidence for extraterrestrial life: identity of sporopollenin with the insoluble organic matter present in the Orgeuil and Murray meteorites and also in some terrestrial microfossils. Nature, 223, 754-756.

Brooks, J., Shaw, G. (1972) Geochemistry of sporopollenin. Chem. Geol., 10, 69-87.

Brooks, J.D. (1970) The use of coals as indicators of the occurrence of oil and gas. APEA Journal, 10, 35-40.

Brooks, J.D., Durie, R.A., Sternhell, S. (1958a) Chemistry of brown coals. II. Infra-red spectroscopic studies. Aust. J. Appl. Sci., 9, 63-80.

Brooks, J.D., Durie, R.A., Sternhell, S. (1958b) Chemistry of brown coals. III. Pyrolytic reactions. Aust. J. Appl. Sci., 9, 303-320.

Brooks, J.D., Gould, K., Smith, J.W. (1969) Isoprenoid hydrocarbons in coal and petroleum. Nature, 222, 257-259.

Brooks, J.D., Maher, T.P. (1957) Acidic oxygen-containing groups in coal. Fuel, 36, 51-62.

Brooks, J.D., Smith, J.W. (1967) Diagenesis of plant lipids during the formation of coal, oil and gas - I. Changes in the n-paraffin hydrocarbons. Geochim. Cosmochim. Acta, 31, 2389-2397.

Brooks, J.D., Smith, J.W. (1969) Diagenesis of plant lipids during the formation of coal, petroleum and gas - II. Coalification and formation of oil and gas in the Gippsland Basin. Geochim. Cosmochim. Acta, 33, 1183-1194.

Brooks, J.D., Steven, J.R. (1967) The constitution of an Australian brown coal resin. Fuel, 46, 13-18.

Brooks, V.T., Lawson, G.J., Ward, S.G. (1956) Chemical constitution of coal. III. Oxidation of humic acid with hydrogen peroxide in the absence of added mineral reagents. Fuel, 35, 385-397.

Brown, J.K. (1955a) The infra-red spectra of coals. J. Chem. Soc., 744-752.

Brown, J.K. (1955b) Infra-red studies of carbonized coals. J. Chem. Soc., 752-757.

Brown, J.K. (1959) Infra-red spectra of solvent extracts of coals. Fuel, 38, 55-63.

Brown, J.K., Hirsch, P.B. (1955) Recent infra-red and X-ray studies of coal. Nature, 175, 229-233.

Brown, J.K., Ladner, W.R. (1960) A study of the hydrogen distribution of coal-like materials by high resolution nuclear magnetic resonance spectroscopy. II. A comparison with infra-red measurement and the conversion to carbon structure. Fuel, 39, 87-96.

Brown, J.K., Ladner, W.R., Sheppard, N. (1960) A study of the hydrogen distribution of coal-like materials by high resolution nuclear magnetic resonance spectroscopy. I. The measurement and interpretation of the spectra. Fuel, 39, 79-86.

Burlingame, A.L., Simoneit, B.R. (1969) High resolution mass spectrometry of Green River Formation kerogen oxidations. Nature, 222, 741-747.

Burlingame, A.L., Wszolek, P.C., Simoneit, B.R. (1969) The fatty acid content of *Tasmanites*, in Adv. Org. Geochem., 1968, (Eds: P.A. Schenck, I. Havenaar), Pergamon Press (Oxford), 131-154.

Calvin, M. (1969) Chemical Evolution. Oxford University Press.

Cane, R.F. (1951) The mechanism of the pyrolysis of torbanite, in Oil Shale and Cannel Coal, Vol. 2, Inst. Petroleum (London), 592-603.

Cane, R.F. (1963) The torbanite of New South Wales and its pyrolysis. Aust. J. Sci., 26, 168-171.

Cane, R.F., Albion, P.R. (1973) Organic geochemistry of torbanite precursors. Geochim. Cosmochim. Acta, 37, 1543-1550.

Cannon, C.G. (1953) Infra-red spectra of coals and coal products. Nature, 171, 308.

Cannon, C.G., Sutherland, G.B.B.M. (1945a) Infra-red spectra of coals. Nature, 156, 240.

Cannon, C.G., Sutherland, G.B.B.M. (1945b) The infra-red absorption spectra of coals and coal extracts. Trans. Faraday Soc., 41, 279-288.

Carman, R.M., Cowley, D.E. (1967) Dundatholic acid. Aust. J. Chem., 20, 193-196.

Carman, R.M., Dennis, N. (1964) The diterpene acids of *Agathis robusta* oleoresin. Aust. J. Chem., 17, 390-392.

Cartz, L., Diamond, R., Hirsch, P.B. (1956) New X-ray data on coals. Nature, 177, 500-502.

Cavell, P.A., Berkowitz, N. (1960) Mechanisms of coal pyrolysis III - Variation of the magnetic mass susceptibility and some related parameters with carbonization temperature. Fuel, 39, 401-412.

Chakrabartty, S.K., Mazumdar, B.K., Lahiri, A. (1958) Disposition of hydrogen in coal structure. Fuel, 37, 498-501.

Chang, T.L., Mead, T.E., Zinkel, D.F. (1971) Mass spectra of diterpene resin acid methyl esters. J. Am. Oil Chem. Soc., 48, 455-461.

Clark, R.C. (1966) M.Sc. Thesis. Massachusetts Inst. Technology.

Coates, R.C. (1973) Ph.D. Thesis (in preparation). University of Newcastle upon Tyne.

Cocker, W., McMurray, T.B.H., Ntamila, M.S. (1965) Extractives from woods. Part VII. Extractives from *Cephalosphaera usambarensis warb*. J. Chem. Soc., 1692-1699.

Cocker, W., Shaw, J.S. (1963) Extractives from woods. Part III. Extractives from *Manilkara bidentata*. J. Chem. Soc., 677-680.

Combaz, A. (1971) Thermal degradation of sporopollenin and genesis of hydrocarbons, in Sporopollenin, (Eds: J. Brooks, P.R. Grant, M. Muir, P. van Gijzel, G. Shaw), Academic Press (London), 621-653.

Conacher, H.R.J. (1917) A study of oil shales and torbanites. Trans. Geol. Soc. Glasgow, 16, 164-192.

Connan, J. (1970) Essai d'interpretation geochimique de distributions de n-paraffines a predominance de molecules paires. S.N.P.A., Cent. Rech. Pau, Groupe Geologie, Note R/Geo no. 205-70.

Connan, J. (1972) Laboratory simulation and diagenesis. I. Thermal evolution of asphalts from the Aquitaine Basin (France). S.N.P.A., Cent. Rech. Pau, 6, 195-214.

Connan, J. (1973) Diagenese naturelle et diagenese artificielle de la matiere organique a elements vegetaux predominants. Paper presented at the 6th Int. Meeting on Organic Geochemistry, Paris, in press.

Conrow, R.B., Durie, R.A., Shannon, J.S., Sternhell, S. (1963) Studies in aerial oxidation I - Oxidation of the vitrain from a bituminous coal. Fuel, 42, 275-290.

Cooper, B.S. (1973) Unpublished work.

Cooper, B.S., Murchison, D.G. (1969) Organic geochemistry of coal, in Organic Geochemistry, (Eds: G. Eglinton, M.T.J. Murphy), Springer-Verlag (Berlin-Heidelberg), 699-726.

Cooper, J.E., Bray, E.E. (1963) A postulated role of fatty acids in petroleum formation. Geochim. Cosmochim. Acta, 27, 1113-1127.

Correia, M. (1969) Contribution a la recherche de zones favorables a la genese du petrole par l'observation microscopique de la matiere organique figuree. Inst. Fr. Pet. Rev., 24, 1417-1454.

Cox, R.E., Burlingame, A.L., Wilson, D.M., Eglinton, G., Maxwell, J.R. (1973) Botryococcene - a tetramethylated acyclic triterpenoid of algal origin. Chem. Comm., 284-285.

Croteau, R., Fagerson, I.S. (1972) The constituent cutin acids of cranberry cuticle. Phytochem., 11, 353-363.

Dancy, T.E., Giedroyc, V. (1950) Further investigations of the chemical constitution of the kerogen of oil shales. J. Inst. Pet., 36, 607-623.

Davies, C., Lawson, G.J. (1967a) Chemical constitution of coal XIII - The products of oxidation of humic acid with six parts of potassium permanganate at 30^{o}C. Fuel, 66, 95-108.

Davies, C., Lawson, G.J. (1967b) Chemical constitution of coal XIV - The products of oxidation of humic acid with three parts of potassium permanganate at 30^{o}C. Fuel, 66, 127-136.

Davis, J.B. (1968) Paraffinic hydrocarbons in the sulphate-reducing bacterium *Desulphovibrio desulphuricans*. Chem. Geol., 3, 155-160.

Del Castillo, J.B., Brooks, C.J.W., Cambie, R.C., Eglinton, G., Hamilton, R.J., Pellitt, P. (1967) The taxonomic distribution of some hydrocarbons in gymnosperms. Phytochem., 6, 391-398.

Djuricic, M.V., Murphy, R.C., Vitorovic, D., Biemann, K. (1971) Organic acids obtained by alkaline permanganate oxidation of kerogen from the Green River (Colorado) shale. Geochim. Cosmochim. Acta, 35, 1201-1207.

Djuricic, M.V., Vitorovic, D., Andresen, B.D., Hertz, H.S., Murphy, R.C., Preti, G., Biemann, K. (1972) Acids obtained by the oxidation of kerogens of ancient sediments of different geographic origins, in Adv. Org. Geochem., 1971, (Eds: H.R. von Gaertner, H. Wehner), Pergamon Press (Oxford), 305-322.

Dobinson, F., Lawson, G.J. (1959) Chemical constitution of coal VI - Optimum conditions for the preparation of sub-humic acids from humic acid by ozonization. Fuel, 38, 79-87.

Dobinson, F., Lawson, G.J., Ward, S.G. (1956) Chemical constitution of coal IV - Oxidation of alkaline solutions of humic acid with ozone. Fuel, 35, 398-408.

Dormans, H.N.M., Huntjens, F.J., Krevelen, D.W. van (1957) Chemical structures and properties of coal macerals (vitrinite, fusinite, micrinite and exinite). Fuel, 36, 321-339.

Douglas, A.G., Douraghi-Zadeh, K., Eglinton, G. (1969a) The fatty acids of *Botryococcus braunii*. Phytochem., 8, 285-293.

Douglas, A.G., Douraghi-Zadeh, K., Eglinton, G., Maxwell, J.R., Ramsey, J.N. (1970a) Fatty acids in sediments including the Green River shale (Eocene) and Scottish torbanite (Carboniferous), in Adv. Org. Geochem., 1966, (Eds: G.D. Hobson, G.C. Speers), Pergamon Press (Oxford), 315-334.

Douglas, A.G., Eglinton, G. (1966) The distribution of alkanes, in Comparative Phytochemistry, (Ed: T. Swain), Academic Press (London), 57-77.

Douglas, A.G., Eglinton, G., Henderson, W. (1970b) Thermal alteration of the organic matter in sediments, in Adv. Org. Geochem., 1966, (Eds: G.D. Hobson, G.C. Speers), Pergamon Press (Oxford), 369-388.

Douglas, A.G., Eglinton, G., Maxwell, J.R. (1969b) The organic geochemistry of certain samples from the Scottish Carboniferous. Geochim. Cosmochim. Acta, 33, 579-590.

Douglas, A.G., Mair, B.J. (1965) Sulphur: role in diagenesis of petroleum. Science, 147, 499-501.

Douglas, A.G., Powell, T.G. (1969) The rapid separation of fatty acids from fossil lipids by impregnated absorbent thin-layer chromatography. J. Chromatog., 43, 241-246.

Down, A.L., Himus, G.W. (1941) A preliminary study of the chemical constitution of kerogen. J. Inst. Pet., 27, 426-445.

Dryden, I.G.C. (1963) Chemical constitution and reactions of coal, in Chemistry of Coal Utilization, Suppl. Vol., (Ed: H.H. Lowry), J. Wiley & Sons Inc., (New York), 232-295.

Dulhunty, J.A. (1942) The stratigraphical arrangement and occurrence of torbanite deposits in the Upper Kamilaroi Coal Measures of New South Wales. Proc. Linn. Soc. N. S. Wales, 67, 123-141.

Dulhunty, J.A. (1944) Origin of the New South Wales torbanites. Proc. Linn. Soc. N. S. Wales, 69, 26-48.

Dungworth, G. (1972) Ph.D. Thesis. University of Newcastle upon Tyne.

Dungworth, G., McCormick, A., Powell, T.G., Douglas, A.G. (1971) Lipid components in fresh and fossil pollen and spores, in Sporopollenin, (Eds: J. Brooks, P.R. Grant, M. Muir, P. van Gijzel, G. Shaw), Academic Press (London), 512-544.

Durie, R.A., Shewchyk, Y., Friedel, R.A. (1967) The effect of mild heating on the 1600 cm^{-1} region in the infra-red spectrum of coals. Fuel, 46, 53-58.

Duuren, B.L. van, Warren, F.L. (1950) Nitric acid oxidation of coal. Part 1. Identification of some components in the ether-soluble fraction. J. S. African Chem. Inst., 111, 67-72.

Edwards, V.A., Kipping, P.J., Jeffrey, P.G. (1963) Composition of montan wax. Nature, 199, 171-172.

Eglinton, G., Hamilton, R.J. (1963) The distribution of alkanes, in Chemical Plant Taxonomy, (Ed: T. Swain), Academic Press (London), 187-217.

Eglinton, G., Hamilton, R.J. (1967) Leaf epicuticular waxes. Science, 156, 1322-1335.

Ensminger, A., Dorsselaer, A. van, Spyckerelle, C., Albrecht, P., Ourisson, G. (1973) Pentacyclic triterpanes of the hopane type as ubiquitous geochemical markers: origin and significance. Paper presented at the 6th Int. Meeting on Organic Geochemistry, Paris, in press.

Enzell, C.R., Ryhage, R. (1965) Mass spectrometric studies of diterpenes I. Carbodicyclic diterpenes. Arkiv. Kemi., 23, 367-399.

Enzell, C.R., Wahlberg, I. (1969) Mass spectrometric studies of diterpenes II. Aromatic diterpenes. Acta Chem. Scand., 23, 871-891.

Esnault, C. (1973) Ph.D. Thesis. L'Universite de Pau et des Pays de l'Adour.

Evans, W.D., Raphaely, P.B. (1964) A comparison between the petrology and pyro-chromatography of an English and a South African coal, in Adv. Org. Geochem., 1962, (Eds: U. Colombo, G.D. Hobson), Pergamon Press (Oxford), 87-95.

Everett, M.R. (1974) M.Sc. Dissertation. University of Newcastle upon Tyne.

Forsman, J.P., Hunt, J.M. (1958) Insoluble organic matter (kerogen) in sedimentary rocks of marine origin, in Habitat of Oil, (Ed: L.G. Weeks), Am. Ass. Pet. Geol., (Tulsa), 747-778.

Francis, W. (1961) Coal, 2nd Edition, E. Arnold Ltd (London).

Friedel, R.A. (1966) Infra-red in coal structure research, in Infra-red Spectroscopy, (Ed: D.N. Kendall), Reinhold Co. (New York), 312-343.

Friedel, R.A., Carlson, G.L. (1971) Laser-Raman spectral investigation of coals. Chem. Ind., 1128-1129.

Friedel, R.A., Carlson, G.L. (1972) Difficult carbonaceous materials and their infra-red and Raman spectra. Reassignments for coal spectra. Fuel, 51, 194-198.

Friedel, R.A., Pelipetz, M.G. (1953) Infra-red spectra of coal and carbohydrate chars. J. Opt. Soc. Am., 43, 1051-1052.

Friedel, R.A., Queiser, J.A. (1956) Infra-red analysis of bituminous coals and other carbonaceous substances. Anal. Chem., 28, 22-30.

Friedel, R.A., Retcofsky, H. (1963) Spectral studies of coal, in Proc. Fifth Carbon Conf., Vol. II, Pergamon Press (Oxford), 149-165.

Fujii, S. (1963) Infra-red spectra of coal: the absorption band at 1600 cm^{-1}. Fuel, 42, 17-23.

Gelpi, E., Schneider, H., Doctor, V.M., Tennison, J., Oro, J. (1969) Gas chromatographic-mass spectrometric identifications of the hydrocarbons and fatty acids of *Plantago ovata* seeds. Phytochem., 8, 2077-2081.

Girling, G.W. (1963) Evolution of volatile hydrocarbons from coal. J. Appl. Chem., 13, 77-91.

Given, P.H. (1960) The distribution of hydrogen in coals and its relation to coal structure. Fuel, 39, 147-153.

Given, P.H. (1961) Dehydrogenation of coals and its relation to coal structure. Fuel, 40, 427-431.

Given, P.H., Peover, M.E. (1958) Study of quinone groups in solvent extracts of coals by controlled potential electrolysis. Proc. Conf. on Sci. in Use of Coal (Sheffield), Inst. Fuel, 33-37.

Glass, H.D. (1954) Investigation of rank in coal by differential thermal analysis. Econ. Geol., 49, 294-308.

Gordon, R.R., Adams, W.N., Jenkins, G.I. (1952) Infra-red spectra of coals. Nature, 170, 317.

Gough, L.J. (1964) Conifer resin constituents. Chem. Ind., 2059-2060.

Grantham, P.J. (1974) Ph.D. Thesis (in preparation). University of Newcastle upon Tyne.

Grice, R.E., Locksley, H.D., Scheinmann, F. (1968) Alkane distributions as biological markers: presence and probable origin of alkanes in *Guttiferae* heartwoods. Nature, 218, 892-893.

Gruse, W.A., Stevens, D.R. (1960) Chemical Technology of Petroleum, 3rd Edition, McGraw-Hill Book Co., Inc., (New York).

Guennel, G.K., Neavel, R.C. (1959) Paper coal in Indiana. Science, 129, 1671-1672.

Hacquebard, P.A., Donaldson, R.J. (1970) Coal metamorphism and hydrocarbon potential in the Upper Palaeozoic of the Atlantic Provinces, Canada. Can. J. Earth Sci., 7, 1139-1163.

Halleux, A., Greef, H. de (1963) Extraction of a vitrinite and chemical analysis of the fractions. Fuel, 42, 185-202.

Han, J., Calvin, M. (1970) Branched alkanes from blue-green algae. Chem. Comm., 1490-1491.

Han, J., McCarthy, E.D., Calvin, M., Benn, M.H. (1968a) Hydrocarbon constituents of the blue-green algae *Nostoc muscorum, Anacystis nidulans, Phormidium luridum, Chlorogloea fritschii*. J. Chem. Soc., (C), 2785-2791.

Han, J., McCarthy, E.D., Van Hoeven, W., Calvin, M., Bradley, W.H. (1968b) Preliminary report on the distribution of aliphatic hydrocarbons in algae, in bacteria and in a Recent lake sediment. Proc. Nat. Acad. Sci., 59, 29-33.

Hardman, R., Brain, K.R. (1971) Alkanes of tubers of *Dioscorea deltoidea*. Phytochem., 10, 1115-1119.

Hardman, R., Wood, C.N., Sofowara, E.A. (1970) Isolation and characterization of seed hydrocarbons from *Balanites aegyptiaca*, *B. roxburghii* and *B. pedicellaris*. Phytochem., 9, 1087-1092

Hartley, P.D., Lawson, G.J. (1962) Chemical constitution of coal VIII. Chromatographic examination of sub-humic acids from oxidation of humic acid with hydrogen peroxide. Fuel, 41, 177-183.

Haug, P., Schnoes, H.K., Burlingame, A.L. (1967) Isoprenoid and dicarboxylic acids isolated from Colorado Green River shale (Eocene). Science, 158, 772-773.

Henderson, W. (1968) Ph.D. Thesis. University of Glasgow.

Henderson, W., Eglinton, G., Simmonds, P., Lovelock, J.E. (1968) Thermal alteration as a contributory process to the genesis of petroleum. Nature, 219, 1012-1016.

Henderson, W., Wollrab, V., Eglinton, G. (1969) Identification of steranes and triterpanes from a geological source by capillary gas liquid chromatography and mass spectrometry, in Adv. Org. Geochem., 1968, (Eds: P.A. Schenck, I. Havenaar), Pergamon Press (Oxford), 181-207.

Herbin, G.A., Robins, P.A. (1969) Patterns of variation and development in leaf wax alkanes. Phytochem., 8, 1985-1998.

Hertog, W. den, Berkowitz, N. (1958) The infra-red spectra of coal and some coal derivatives. Fuel, 37, 253-271.

Hills, I.R., Whitehead, E.V. (1966) Triterpanes in optically active petroleum distillates. Nature, 209, 977-979.

Hirsch, P.B. (1954) X-ray scattering from coals. Proc. Roy. Soc., Series A, 226, 143-169.

Hoering, T.C. (1965) The extractable organic matter in Precambrian rocks and the problem of contamination. Carn. Inst. Wash. Yearbook, 64, 215-218.

Hoering, T.C. (1967) Criteria of suitable rocks in Precambrian organic geochemistry. Carn. Inst. Wash. Yearbook, 65, 365-372.

Hoering, T.C. (1968) Organic acids from the oxidation of Recent sediments. Carn. Inst. Wash. Yearbook, 66, 515-526.

Hoering, T.C., Abelson, P.H. (1965) Fatty acids from the oxidation of kerogen. Carn. Inst. Wash. Yearbook, 64, 218-223.

Holden, H.W., Robb, J.C. (1958) Mass spectrometry of substances of low volatility. Nature, 182, 340.

Holden, H.W., Robb, J.C. (1960a) A study of coal by mass spectrometry. Fuel, 39, 39-46.

Holden, H.W., Robb, J.C. (1960b) A study of coal by mass spectrometry II - Extracts and extractable pyrolysis products. Fuel, 39, 485-494.

Holly, E.D., Montgomery, R.S. (1956) Structure of the water-soluble acids obtained by the alkali-oxygen oxidation of bituminous coal I - Chromatographic fractionation. Fuel, 35, 49-55.

Holly, E.D., Montgomery, R.S., Gohlke, R.S. (1956) Structure of the water-soluble acids obtained by the alkali-oxygen oxidation of bituminous coal II - Spectrographic studies of the methyl esters. Fuel, 35, 56-59.

Howard, H.C. (1963) Pyrolytic reactions of coal, in Chemistry of Coal Utilization, Suppl. Vol., (Ed: H.H. Lowry), J. Wiley & Sons Inc., (New York), 340-394.

Hudy, J.A. (1959) Resin acids. Gas chromatography of their methyl esters. Anal. Chem., 31, 1754-1756.

Hunneman, D.H., Eglinton, G. (1969) Gas chromatographic-mass spectrometric identification of long-chain hydroxy acids in plants and sediments, in Adv. Org. Geochem., 1968, (Eds: P.A. Schenck, I. Havenaar), Pergamon Press (Oxford), 157-166.

I.C.C.P. (1963) International Handbook of Coal Petrography, 2nd Edition, Centre National de la Recherche Scientifique (Paris).

Ikan, R., Baedecker, M.J., Kaplan, I.R. (1975) Thermal alteration experiments on organic matter in Recent marine sediment - II. Isoprenoids. Geochim. Cosmochim. Acta, 39, 187-194.

Ingram, D.J.E., Tapley, J.G., Jackson, R., Bond, R.L., Murnaghan, A.R. (1954) Paramagnetic resonance in carbonaceous solids. Nature, 174, 797-798.

Jeffrey, E.C. (1909) On the nature of the so-called algal or boghead coals. Rhodora, 9, 61-63.

Johns, R.B., Onder, O.M. (1975) Biological diagenesis: dicarboxylic acids in Recent sediments. Geochim. Cosmochim. Acta, 39, 129-136.

Jones, J.M., Cooper, B.S. (1970) Coal, in Geology of Durham County (Ed: G. Hickling), Nat. Hist. Soc. N. Durham and Newcastle (Newcastle upon Tyne), 43-65.

Jurg, J.W., Eisma, E. (1970) The mechanism of the generation of petroleum hydrocarbons from a fatty acid, in Adv. Org. Geochem., 1966, (Eds: G.D. Hobson, G.C. Speers), Pergamon Press (Oxford), 367-368.

Kamiya, Y. (1961a) Formation of aromatic polycarboxylic acids from bituminous coal by oxygen-oxidation in alkaline medium. Fuel, 40, 149-153.

Kamiya, Y. (1961b) Separation of aromatic polycarboxylic acids from oxidation of coal. Fuel, 40, 457-463.

Kaneda, T. (1969) Hydrocarbons in spinach: two distinctive carbon ranges of aliphatic hydrocarbons. Phytochem., 8, 2039-2044.

Karr, C. (1963) Low temperature tar, in Chemistry of Coal Utilization, Suppl. Vol., (Ed: H.H. Lowry), J. Wiley & Sons Inc., (New York), 539-579.

Karweil, G. (1955) Die metamorphose der Kohlen vom Standpunkt der physikalischen Chemie. Z. Deutsch. Geol. Ges., 107, 132-139.

Kester, A.S., Foster, J.W. (1963) Diterminal oxidation of long chain alkanes by bacteria. J. Bacteriol., 85, 859-869.

Kimble, B.L. (1972) Ph.D. Thesis. University of Bristol.

Kinney, C.R. (1947) The source of acetic acid obtained by the oxidation of coal. J. Am. Chem. Soc., 69, 284-289.

Kinney, C.R., Douchette, E.I. (1958) Infra-red spectra of a coalification series from cellulose and lignin to anthracite. Nature, 182, 785-786.

Kinney, C.R., Friedman, L.D. (1952) Ozonization studies of coal constitution. J. Am. Chem. Soc., 74, 57-61.

Kinney, C.R., Ockert, K.F. (1956) Nitric acid oxidation of bituminous coal. Ind. Eng. Chem., 48, 327-332.

Kirby, W.A., Lakey, W.R.A., Sarjant, R.J. (1954) A study of coal extracts by infra-red spectroscopy. Fuel, 33, 480-496.

Knights, B.A., Brown, A.C., Conway, E., Middleditch, B.S. (1970) Hydrocarbons from the green form of the freshwater alga *Botryococcus braunii*. Phytochem., 9, 1317-1324.

Kochloefl, K., Schneider, P., Rericha, R., Horak, M., Bazant, V. (1963) Isoprenoid skeleton hydrocarbons in low-temperature brown coal tar. Chem. Ind., 692.

Krevelen, D.W. van (1950) Graphical-statistical method for the study of structure and reaction processes of coal. Fuel, 29, 269-284.

Krevelen, D.W. van (1961) Coal. Elsevier Publishing Co., (Amsterdam).

Krevelen, D.W. van (1963) Geochemistry of coal, in Organic Geochemistry, (Ed: I.A. Breger), Pergamon Press (Oxford), 183-247.

Krevelen, D.W. van, Schuyer, J. (1957) Coal Science, Elsevier Publishing Co., (Amsterdam).

Krevelen, D.W. van, Wolfs, D.M.J., Waterman, H.I. (1960) Chemical structure and properties of coal XXV - The carbonisation of coal models. Fuel, 39, 25-38.

Kroger, C., Goebgen, H.G., Klusman, A. (1964) Uber die physikalischen und chemischen Eigenschaften der Steinkohlengefugebestandteile XVII. Die Teere der Hochvakuumschwelung. Brennst. Chem., 45, 170-178.

Kroger, C., Pohl, A. (1957) Die physikalischen und chemischen Eigenschaften der Steinkohlengefugebestandteile (Macerale) V. Die calorischen Effekte bei der thermischen Zersetzung. Brennst. Chem., 38, 179-183.

Kvenvolden, K.A. (1966) Molecular distributions of normal fatty acids and paraffins in some Lower Cretaceous sediments. Nature, 209, 573-577.

Kvenvolden, K.A. (1970) Evidence for transformations of normal fatty acids in sediments, in Adv. Org. Geochem., 1966, (Eds: G.D. Hobson, G.C. Speers), Pergamon Press (Oxford), 335-366.

Lamberton, J.A. (1961) The dibasic acids of Japan wax. Aust. J. Chem., 14, 323-324.

Laseter, J.L., Weete, J., Weber, D.J. (1968) Alkanes, fatty acid methyl esters and free fatty acids in surface wax of *Ustilago maydis*. Phytochem., 7, 1177-1181.

Lawson, G.J. (1957) Chemical constitution of coal V - Optimum conditions for the hydrogen peroxide oxidation of humic acid to sub-humic acids. Fuel, 36, 182-190.

Lawson, G.J., Purdie, J.W. (1966) Chemical constitution of coal XI - Examination of sub-humic acids produced by ozonization of humic acid. Fuel, 45, 115-130.

Leverson, A.I. (1967) Geology of Petroleum. W.H. Freeman & Co., (San Francisco - London).

Leythaeuser, D., Welte, D.H. (1969) Relation between distribution of heavy n-paraffins and coalification in Carboniferous coals from the Saar District, Germany, in Adv. Org. Geochem., 1968, (Eds: P.A. Schenck, I. Havenaar), Pergamon Press (Oxford), 429-442.

MacGregor, M. (1938) Conditions of deposition of the oil shales and cannel coals of Scotland, in Oil Shale and Cannel Coal, Inst. Petroleum (London), 6-17.

MacLeod, W.D. (1968) Combined GLC-MS of complex trace hydrocarbon residues in sediments. J. Gas Chromatog., 6, 591-594.

Macrae, J.C. (1943) The thermal decomposition of spore exines from bituminous coal. Fuel, 22, 117-129.

Martin, R.L., Winters, J.C., Williams, J.A. (1963) Distributions of n-paraffins in crude oils and their significance to the origin of petroleum. Nature, 199, 110-114.

Maximov, O.B., Schapovalov, V.E., Schvets, T.V. (1972) Alkaline permanganate oxidation of methylated humic acids. Fuel, 51, 185-189.

Maxwell, J.R. (1967) Ph.D. Thesis. University of Glasgow.

Maxwell, J.R., Douglas, A.G., Eglinton, G., McCormick, A. (1968) The botryococcenes - hydrocarbons of novel structure from the alga *Botryococcus braunii*, Kutzing. Phytochem., 7, 2157-2171.

Mazliak, P. (1969) Chemistry of plant cuticles, in Progress in Phytochemistry, (Eds: L. Reinhold, Y. Liwschitz), Interscience (New York), 49-111.

Mazumdar, B.K., Chakrabartty, S.K., Saha, M., Anand, K.S., Lahiri, A. (1959) Further studies on the mechanisms of the oxidation of coal. Fuel, 38, 469-482.

Mazumdar, B.K., Chatterjee, N.N. (1973) Mechanism of coal pyrolysis in relation to industrial practice. Fuel, 52, 11-19.

Mazumdar, B.K., Lahiri, A. (1958) Dimensions of side chains in coal structure. Fuel, 37, 495-498.

Mazumdar, B.K., Lahiri, A. (1962) Recent advances in the chemical constitution of coal. Am. Chem. Soc., Div. Fuel Chem., Preprints, 65-85.

McKenna, E.J., Kallio, R.E. (1964) Hydrocarbon structure: its effect on bacterial utilization of alkanes, in Principles and Applications in Aquatic Microbiology (Eds: H. Heukelekian, N.C. Dondero), J. Wiley & Sons Inc., (New York), 1-14.

McKenna, E.J., Kallio, R.E. (1965) The biology of hydrocarbons. Ann Rev. Microbiol., 19, 183-208.

Meinschein, W.G. (1961) Significance of hydrocarbons in sediments and petroleum. Geochim. Cosmochim. Acta, 22, 58-64.

Millais, R., Murchison, D.G. (1969) Properties of the coal macerals: infra-red spectra of alginites. Fuel, 48, 247-258.

Mitterer, R.M., Hoering, T.C. (1968) Production of hydrocarbons from the organic matter in a Recent sediment. Carn. Inst. Wash. Yearbook, 66, 510-514.

Mold, J.D., Stevens, R.K., Means, R.E., Ruth, J.M. (1963) The paraffin hydrocarbons of tobacco: normal, iso- and anteiso-homologues. Biochem., 2, 605-610.

Monnot, G.A., Ladam, A. (1955) Comparative physical and chemical properties of exinite and vitrinite, Compt. Rend. Acad. Sci. Paris, 241, 1939-1941.

Montgomery, R.S., Holly, E.D., Gohlke, R.S. (1956) Structures of the water-soluble acids obtained by the alkali-oxygen oxidation of bituminous coal III - Decarboxylation studies. Fuel, 35, 60-65.

Murchison, D.G. (1966) Properties of coal macerals. Infra-red spectra of resinites and their carbonized and oxidised products, in Coal Science (Ed: R.F. Gould), Adv. Chem. Ser. No. 55, Am. Chem. Soc. (Washington D.C.), 307-331.

Murchison, D.G., Jones, J.M. (1963) Properties of the coal macerals: elementary composition of resinite. Fuel, 42, 141-158.

Murray, K.E., Heulin, F.E., Davenport, J.B. (1964) Occurrence of farnesene in the natural coating of apples. Nature, 204, 80.

Nakanishi, K. (1964) Infra-red Absorption Spectroscopy, Holden-Day Inc., (San Francisco).

Neavel, R.C., Guennel, G.K. (1960) Indiana paper coal: composition and deposition. J. Sed. Pet., 30, 241-248.

Neavel, R.C., Miller, L.V. (1960) Properties of cutinite. Fuel, 39, 217-222.

Oberlin, A., Boulmier, J.L., Durand, B. (1974) Electron microscope investigation of the structure of naturally and artificially metamorphosed kerogen. Geochim. Cosmochim. Acta, 38, 647-650.

Ogner, G., Schnitzer, M. (1970) The occurrence of alkanes in fulvic acid, a soil humic acid fraction. Geochim. Cosmochim. Acta, 34, 921-928.

Orchin, M., Golumbic, C., Anderson, J.E., Storch, H.H. (1951) Studies of the extraction and coking of coal and their significance in relation to its structure. U.S. Bureau of Mines Bull. No. 505.

Oro, J., Laseter, J.L., Weber, D. (1966) Alkanes in fungal spores. Science, 154, 399-400.

Oro, J., Nooner, D.W. (1970) Aliphatic hydrocarbons from the Precambrian of North America and South Africa, in Adv. Org. Geochem., 1966, (Eds: G.D. Hobson, G.C. Speers), Pergamon Press (Oxford), 493-506.

Oro, J., Tornabene, T.G., Nooner, D.W., Gelpi, E. (1967) Aliphatic hydrocarbons and fatty acids of some marine and freshwater microorganisms. J. Bacteriol., 93, 1811-1818.

Ouchi, K., Imuta, K. (1963) The analysis of benzene extracts of a bituminous coal II - Analysis by gas chromatography. Fuel, 42, 445-456.

Ouchi, K., Imuta, K. (1973) Isolation of adamantane from coal extract. Fuel, 52, 301-302.

Palmer, T.J., Vahrman, M. (1972a) The smaller molecules obtainable from coal and their significance. Part 3. Steaming/carbonization of a weakly-caking coal at temperatures up to 600°C. Fuel, 51, 14-21.

Palmer, T.J., Vahrman, M. (1972b) The smaller molecules obtainable from coal and their significance. Part 4. Composition of low temperature tars. Fuel, 51, 22-26.

Philippi, G.T. (1965) On the depth, time and mechanism of petroleum generation. Geochim. Cosmochim. Acta, 29, 1021-1049.

Philippi, G.T. (1969) Essentials of the petroleum formation process are organic source material and a subsurface temperature-controlled chemical reaction mechanism, in Adv. Org. Geochem., 1968, (Eds: P.A. Schenck, I. Havenaar), Pergamon Press (Oxford), 25-46.

Philippi, G.T. (1974) The influence of marine and terrestrial source material on the composition of petroleum. Geochim. Cosmochim. Acta, 38, 947-966.

Powell Duffryn Technical Services Report. (1963) Petrographic examination of the coals of Ayun Musa and Maghara, United Arab Republic.

Powell, T.G. (1969) Ph.D. Thesis. University of Newcastle upon Tyne.

Powell, T.G., McKirdy, D.M. (1973) The effect of source material, rock type and diagenesis on the n-alkane content of sediments. Geochim. Cosmochim. Acta, 37, 623-633.

Pusey, W.C. (1973) The ESR-kerogen method. A new technique of estimating the organic maturity of sedimentary rocks. Petroleum Times, 21.

Ramsey, J.N. (1966) M.Sc. Thesis. University of Glasgow.

Randall, R.B., Benger, M., Groocock, C.M. (1938) The alkaline permanganate oxidation of organic substances selected for their bearing upon the chemical constitution of coal. Proc. Roy. Soc., Series A, 165, 432-452.

Ratajczak, T. (1968) Infra-red absorption spectra of coal spores. Bull. Acad. Pol. Sci., 16, 55-59.

Robinson, W.E., Cummins, J.J., Dinneen, G.V. (1965) Changes in the Green River oil shale paraffins with depth. Geochim. Cosmochim. Acta, 29, 249-258.

Robinson, W.E., Cummins , J.J., Stanfield, K.E. (1956) Constitution of organic acids prepared from Colorado oil shale - based on n-butyl esters. Ind. Eng. Chem., 48, 1134-1138.

Robinson, W.E., Heady, H.H., Hubbard, A.B. (1953) Alkaline permanganate oxidation of oil shale kerogen. Ind. Eng. Chem., 45, 788-791.

Robinson, W.E., Lawlor, D.L. (1961) Constitution of hydrocarbon-like materials derived from kerogen oxidation products. Fuel, 40, 375-388.

Romovacek, J., Kubat, J. (1968) Characterisation of coal substance by pyrolysis-gas chromatography. Anal. Chem., 40, 1119-1126.

Roy, M.M. (1957) Infra-red spectra of coal and coal extracts. Fuel, 36, 249-250.

Roy, M.M. (1965) Coal macerals III - Aerial oxidation of macerals. Econ. Geol., 60, 1213-1217.

Ryhage, R., Stenhagen, E. (1959) Mass spectrometric studies III - Esters of saturated dibasic acids. Arkiv. Kemi., 14, 497-509.

Ryhage, R., Stenhagen, E. (1965) Mass spectrometric studies XI - On the nature of the ions m/e 84 + n x 14 (n = 0, 1, 2 ....) present in the mass spectra of esters of dibasic acids. Arkiv. Kemi., 23, 167-175.

Schnitzer, M., Khan, S.U. (1972) Humic Substances in the Environment, Marcel Dekker Inc., (New York).

Shaw, G. (1971) The chemistry of sporopollenin, in Sporopollenin, (Eds: J. Brooks, P.R. Grant, M. Muir, P. van Gijzel, G. Shaw), Academic Press (London), 305-348.

Shaw, G., Yeadon, A. (1966) Chemical studies on the chemical constitution of some pollen and spore membranes. J. Chem. Soc. C, 16-22.

Shibaoka, M., Bennet, A.J.R., Gould, K.W. (1973) Diagenesis of organic matter and occurrence of hydrocarbons in some Australian sedimentary basins. APEA J., 13, 35-40.

Silverman, S.R. (1967) Carbon isotopic evidence for the role of lipids in petroleum formation. J. Am. Oil Chem. Soc., 44, 691-695.

Simoneit, B.R., Burlingame, A.L. (1973) Carboxylic acids derived from Tasmanian tasmanite by extractions and kerogen oxidations. Geochim. Cosmochim. Acta, 37, 595-610.

Smidt, J., Krevelen, D.W. van (1959) Chemical structure and properties of coal XXIII - Electron spin resonance of vitrains. Fuel, 38, 355-368.

Smith, A.H.V. (1962) The palaeoecology of Carboniferous peats based on the miospores and petrography of bituminous coals. Proc. Yorks. Geol. Soc., 33, 423-474.

Smith, J.W., Mapstone, G.E. (1957) The alkaline permanganate oxidation of coal. Fuel, 36, 191-204.

Spence, J.A., Vahrman, M. (1965) Olefins in coal. Chem. Ind., 1522.

Spence, J.A., Vahrman, M. (1967) Aliphatic hydrocarbons in a low temperature tar. J. Appl. Chem., 17, 143-146.

Spink, K., Ford, T.D. (1968) The Coal Measures, in The Geology of the East Midlands, (Eds: P.C. Sylvester-Bradley, T.D. Ford), Leicester University Press, 95-111.

Stach, E. (1953) Der Inkohlungssprung in Ruhrkarbon. Brennst. Chem., 34, 353-355.

Stach, E. (1968) Basic principles of coal petrology: macerals, microlithotypes and some effects of coalification, in Coal and Coal-Bearing Strata, (Eds: D.G. Murchison, T.S. Westoll), Oliver & Boyd (Edinburgh), 3-17.

Stanbridge, R.A. (1973) Ph.D. Thesis (in preparation). University of Newcastle upon Tyne.

Staplin, F.L. (1969) Sedimentary organic matter, organic metamorphism and oil and gas occurrence. Bull. Can. Pet. Geol., 17, 47-66.

Stransky, K., Streibl, M. (1969) On natural waxes. XII. Composition of hydrocarbons in morphologically-different plant parts. Coll. Czech. Chem. Comm., 34, 103-117.

Stransky, K., Streibl, M., Herout, V. (1967) Distribution of wax hydrocarbons in plants at different evolutionary levels. Coll. Czech. Chem. Comm., 32, 3213-3220.

Stransky, K., Streibl, M., Sorm, F. (1968) On natural waxes. VII. Lipid hydrocarbons of the alga *Scenedesmus quadricanda*. Coll. Czech. Chem. Comm., 33, 416-424.

Streibl, M., Herout, V. (1969) Terpenoids - especially oxygenated mono-, sesqui-, di- and triterpenes, in Organic Geochemistry, (Eds: G. Eglinton, M.T.J. Murphy), Springer-Verlag (Berlin-Heidelberg), 402-424.

Teichmuller, M. (1971) Anwendung kohlenpetrographischer Methoden bei der Erdol- und Erdgasprospektion. Erdol und Kohle, 24, 69-76.

Teichmuller, M., Teichmuller, R. (1968) Geological aspects of coal metamorphism, in Coal and Coal-Bearing Strata, (Eds: D.G. Murchison, T.S. Westoll), Oliver & Boyd (Edinburgh), 233-268.

Thomas, B.R. (1966) The chemistry of the order Araucariales. The bled resins of *Agathis australis*. Acta Chem. Scand., 20, 1074-1081.

Thomas, B.R. (1969) Kauri resins - modern and fossil, in Organic Geochemistry, (Eds: G. Eglinton, M.T.J. Murphy), Springer-Verlag, (Berlin-Heidelberg), 599-618.

Tissot, B., Califet-Debyser, Y., Deroo, G., Oudin, J.L. (1971) Origin and evolution of hydrocarbons in Early Toarcian shales, Paris Basin, France. Bull. Am. Ass. Pet. Geol., 55, 2177-2193.

Tornabene, T.G., Bennet, E.D., Oro, J. (1967) Fatty acid and aliphatic hydrocarbon composition of *Sarcina lutea* grown in three different media. J. Bacteriol., 94, 344-348.

Tschamler, H., Ruiter, E. de (1963) Physical properties of coals, in Chemistry of Coal Utilization, Suppl. Vol., (Ed: H.H. Lowry), J. Wiley & Sons Inc., (New York), 35-118.

Tschamler, H., Ruiter, E. de (1966) A comparative study of exinite, vitrinite and micrinite, in Coal Science, (Ed: R.F. Gould), Adv. Chem. Series No. 55, Am. Chem. Soc. (Washington D.C.), 332-341.

Vahrman, M. (1970) The smaller molecules derived from coal and their significance. Fuel, 49, 5-16.

Vahrman, M. (1972) The smaller molecules - an overlooked component of coal. Chemistry in Britain, 8, 16-24.

Vassoyevitch, N.B., Korchagina, Y.I., Lopatin, N.V., Chernysev, V.V. (1969) Principal phase of oil formation. Int. Geol. Rev., 12, 1276-1296.

Vitorovic, D., Djuricic, M.V., Ilic, B. (1973) New structural information obtained by stepwise oxidation of kerogen from the Aleksinac (Yugoslavia) shale. Preprint.

Vucht, H.A. van, Reitveld, B.J., Krevelen, D.W. van (1955) Chemical structure and properties of coal VIII - Infra-red absorption spectra. Fuel, 34, 50-59.

Ward, S.G. (1947) Coal - its constitution and utilization as a chemical raw material. J. Inst. Fuel, 21, 80-88.

Weenink, R.O. (1962) Minor constituents of the acetone-soluble lipids of red clover (*Trifolium pratense*) leaves. Biochem. J., 82, 523-527.

Weete, J.D. (1972) Aliphatic hydrocarbons of the fungi. Phytochem., 11, 1201-1205.

Welte, D.H., Waples, D.W. (1973) Uber die Bevorzugung geradzahliger n-Alkane im Sedimentgesteinen. Naturewissenschaften, 60, 516-517.

Whitehead, W.L., Breger, I.A. (1950) Vacuum differential thermal analysis. Science, 111, 279-281.

Williams, E.G., Keith, M.L. (1963) Relationship between sulphur in coals and the occurrence of marine roof beds. Econ. Geol., 58, 720-729.

Wilson, P.J., Clendenin, J.D. (1963) Low temperature carbonization, in Chemistry of Coal Utilization, Suppl. Vol., (Ed: H.H. Lowry), J. Wiley & Sons Inc., (New York), 395-460.

Winters, K., Parker, P.L., Baalen, C. van (1969) Hydrocarbons of blue-green algae: geochemical significance. Science, 163, 467-468.

Wollrab, V., Streibl, M. (1969) Earth waxes, peat, montan wax and other organic brown coal constituents, in Organic Geochemistry, (Eds: G. Eglinton, M.T.J. Murphy), Springer-Verlag (Berlin-Heidelberg), 576-598.

Wollrab, V., Streibl, M., Sorm, F. (1962) Gas chromatographic analysis of the wax components of montan wax. Chem. Ind., 1762.

Wollrab, V., Streibl, M., Sorm, F. (1967) Iso- and anteiso-alkanes in natural waxes. Chem. and Ind., 44, 1872-1873.

Yohe, G.R., Harris, J.M. (1961) Aliphatic acids from the oxidation of coal. Fuel, 40, 289-294.

Yokokawa, C., Watanabe, Y., Kajiyama, S., Takegani, Y. (1962) Studies on the chemical structure of coal I - Stepwise oxidative degradation of coal. Fuel, 41, 209-219.

Youngblood, W.W., Blumer, M., Guillard, R.L., Fiore, F. (1971) Saturated and unsaturated hydrocarbons in marine benthic algae. Mar. Biol., 8, 190-201.